## *The role of A-Type lamins and LAP2a in cellular ageing of human fibroblasts in vitro*

Peković, Vanja

# THE ROLE OF A-TYPE LAMINS AND LAP2α IN CELLULAR AGEING OF HUMAN FIBROBLASTS *IN VITRO*

by

**Vanja Peković**



**A thesis submitted at the University of Durham for the degree of Ph.D**



**School of Biological and Biomedical Sciences**

**University of Durham, October 2005**

# Table of Contents

# Index of figures

## *Chapter 1*



## *Chapter 3*

## *Chapter 4*

## *Chapter 5*

## *Chapter 6*

# Index of tables

## *Chapter 1*



## *Chapter 2*



## *Chapter 3*

## Declaration

**This thesis is my own composition, the results presented herein are produced by investigations conducted by myself, and work cited other than my own is clearly indicated by reference to the relevant workers or their publications. This work has not been presented in any previous application for a higher degree.**

**Vanja Peković**

## Statement

**I certify that Vanja Pekovic has completed thirty-six months of full time research work under my supervision and has fulfilled the conditions necessary to qualify to submit this thesis for the degree of Doctor of Philosophy.**

**Prof. C.J. Hutchison**

# Acknowledgements

I would like to warmly thank my supervisor, Prof. Chris Hutchison for his continuing guidance, encouragement and trust throughout entire period of my PhD.

I thank all work colleagues at Biology Department, Durham University and outside collaborators who have provided me with technical support, guidance and inspiring discussions: Dr Ewa Markiewicz, Dr. Artoo Maatta, Dr. Adam Benham, Prof. Richard Rzepecki, Dr Mauricio Alvarez-Reyes, Dr Rekha Rao, Dr Martin Goldberg, Prof. Roland Foisner, Dr. Jenz Harborth, Prof. Jos Broers, Mrs Pamela Ritchie, Mr. Terry Gibbon, Mrs. Christine Richardson, Dr. David Bown, Miss Georgia Salpingidou, Miss Naomi Willis, Mr Tom Cox, Dr Fida Casans, Miss Katarzyna Tilgner, Miss Magdalena Chmielewska, Dr Heather Long, Dr Vilius Pigaga, Dr Ming and Mrs Fang der Perng, Dr Frederique Tholozan, Dr Yuki Sugiyama, Dr Nkemcho Ojeh, Miss Lorna Marshall, Miss Vicky Hayes, Dr Marcel van Lith, Dr John Gatehouse, Dr Rumaisa Bashir, Dr Stephan Pzyborsky, Dr Charlie Shaw, Mr Andrew Hardisty, Mrs Jillian Lynn, Mrs Audrey Richardson, Mrs Gerry Fuller, Mrs Janet Fletcher and Mrs Gillian Baughton.

I thank all my friends who have given me their support and made my life in Durham and Newcastle my second home: Mohamed, David, Matt, Colin, Len, Neda, Vesna, Julie, Orla, Angy, Michael Webster, Richard and Hanna, Frank, Stepano, Dafi, Yasushi, Sharam, Steve Cox, Kate and Duncan, Pierre-Paolo, Healey and Martin, Chris Patton, Michael, Ryan and Marta, Vasiliki, Manja, Daniela, Gulatma, Theo, Harry, Andrew, Steve, Leah, Evelyn, Milena and Alexander, Ruki and Jelena, Alan and Eunice.

I thank my Mum Mira, my Dad Janko, my sister Sanja, my grandma Slavica and my partner Chris for their love, support and encouragement.

# Abstract

Mutations in LMNA gene have been linked to a number of age-related tissue-specific diseases and premature ageing syndromes termed laminopathies. The finding that A-type lamins affect longevity and maintenance of a number of somatic tissues makes them potential candidates in ageing of normal tissues. At the cellular level, ageing is manifested by an accumulation of irreversibly arrested senescent cells. Premature senescence is also hallmark of premature ageing syndromes. A-type lamins and lamina-associated polypeptide 2 α (LAP2α) bind to and tether retinoblastoma protein (Rb) in the nucleus, a main regulator of senescence pathway. In order to explore the role of A-type lamins and LAP2α in normal ageing and disease, I studied these proteins during ageing of wild type human fibroblasts *in vitro*. My results show that protein expression level of lamins and LAP2s does not change during ageing of wild-type fibroblasts *in vitro*. Nonetheless, fibroblasts aged *in vitro* acquire a range of nuclear morphological changes characteristic of laminopathy fibroblasts. These nuclear 'laminopathy' phenotypes are accompanied by changes in peripheral heterochromatin, accumulation of lamins A/C in the nucleoplasm, aggregation of LAP2α and decreased Rb phosphorylation. Interestingly, acquisition of such abnormal nuclear changes correlates with premature senescent arrest in five laminopathy cell lines studied. In contrast, although a down-regulation of LAP2α expression and Rb dephosphorylation accompany a reversible quiescent arrest, quiescent fibroblasts do not acquire alterations in nuclear morphology and instead show increased association of lamins at the NE. A-type and B-type lamins become more insoluble in quiescent cells, which may be a cause of a loss of nuclear anchorage of LAP2α and Rb as well as an increased solubility of LAP2β. On the contrary, during biochemical fractionation of aged fibroblasts, lamin A, but not lamin B2, becomes altered in a manner which makes it more unstable (i.e. prone to degradation) which leads to accumulation of a soluble lamin A proteolytic fragment whilst lamin C and LAP2α become lost from detergent/salt-resistant nucleoskeleton. Protein sequence analysis revealed that both lamin A and LAP2α contain a number of cysteine residues in their C-terminal specific tails. Glutathione blot assay and immunoprecipitation under non-reducing conditions showed that A-type lamins and LAP2α become S-glutathiolated in senescent cells, which may cause their decreased binding seen on immunoprecipitation. Both lamin A and LAP2α show an age-dependent accumulation of monomeric protein under non-reducing conditions, which in early passage cells leads to formation of non-native disulphide cross-links in these proteins. Interestingly, neither of the four laminopathy cell lines studied show an increased accumulation of monomeric lamin A as compared to their age-matched controls. Aged and lamin A/C-deficient laminopathy fibroblasts display a targeted loss of nucleoplasmic but not speckle-associated forms of Rb. These Rb speckles associate with sites of DNA damage in both senescent and laminopathy cells and may be involved in DNA damage signalling or post-transcriptional regulation of gene expression. sRNAi knockdown of LAP2α also leads to decreased phosphorylation and a loss of nucleoplasmic forms of Rb, which correlates with cell cycle arrest. I propose a model for ageing of human fibroblasts *in vitro* whereby oxidative modification of A-type lamin filaments induces changes in their structural conformation leading to destabilisation and a less efficient assembly at the nuclear envelope. In addition, aberrant telomere targeting of oxidatively modified LAP2α in senescent cells or aggregated LAP2α in laminopathy cells would lead to destabilised telomere structures, telomere uncapping and/or chromosome fusions which would trigger Rb-mediated DNA damage-induced senescent arrest.

# Abbreviations

| | |
|---|---|
| A | apoptotic |
| aa | amino acid |
| AD- | autosomal-dominant |
| ADP | adenosine di-phosphate |
| AE | anti-oxidant enzyme |
| AKAP | A-kinase anchoring protein |
| AML | acute myeloid leukaemia |
| AP1 | activating protein 1 |
| AR- | autosomal-recessive |
| ARE | anti-oxidant response element |
| ATP | adenosine tri-phosphate |
| AWS | atypical Werner's syndrome |
| BAF | barrier-to-auto-integration factor |
| BLAST | basic local alignment search tool |
| β-ME | beta-mercaptoethanol |
| BMP | bone morphogenetic protein |
| BOS | Buscheke-Ollendorf syndrome |
| bp | base pairs |
| BRB | blot rinse buffer |
| BSA | bovine serum albumin |
| c | cellular |
| C | confluent; carboxy- |
| CaaX | isoprenylation motif |
| CAT | catalase |

| | |
|---|---|
| CDK | cyclin dependent kinase |
| CDKI | cyclin-dependent kinase inhibitor |
| cDNA | complementary DNA |
| Ce | Caenorhabditis elegans |
| CHO | Chinese hamster ovary |
| Cip | cyclin inhibitor protein |
| cm | centimeter |
| CMT | Charcot-Marie-Tooth |
| $CO_2$ | carbon dioxide |
| CpG | cytosine guanine dinucleotide |
| CRX | cone-rod-homeobox |
| CTGF | connective tissue growth factor |
| CUT | cell-untimely-torn |
| Cys | cysteine |
| DAPI | 4,6-diamidine-2-phenylindole di-hydrochloride |
| DCM-CD | dilated cardiomyopathy with conduction system disease |
| Dm | Drosophila melanogaster |
| DMEM | Dulbecco's modified Eagle's medium |
| DMSO | dimethyl sulfoxide |
| DNA | deoxyribonucleic acid |
| DP | dimerisation protein |
| ds | double-stranded |
| DTT | dithiothreitol |
| ECL | enhanced chemiluminescence |
| EDMD | Emery-Dreyfuss muscular dystrophy |

| | |
|---|---|
| EDTA | ethylene-diamine-tetra acetic acid |
| EGFP | enhanced green fluorescent protein |
| ER | endoplasmic reticulum |
| extr | extraction |
| FACE | human prelamin A processing enzyme |
| FACS | flow cytometer |
| FITC | fluorescein isothiocyanate |
| FLIP | fluorescence loss in photo-bleaching |
| FPLD | familial partial lipodystrophy |
| FPR | footprinted region |
| FRAP | fluorescence recovery after photo-bleaching |
| FRET | fluorescence resonance energy transfer |
| FS | forward scatter |
| FT | farnesyl transferase |
| *g* | gravitational force |
| $G_0$ | gap phase (out of cycle) |
| G1 | gap phase (pre-synthetic) |
| G2 | gap phase (post-synthetic) |
| GCL | germ cell less |
| GFP | green fluorescent protein |
| GL2 | green luciferase protein |
| Gly | glycine |
| GPX | glutathione peroxidase |
| GSH | l-gamma-glutamyl-l-cysteinylglycine |
| GSSG | oxidised glutathione |

| | |
|---|---|
| GTP | guanosine tri-phosphate |
| H | histone |
| HCL | hydrochloric acid |
| HDAC | histone deacetylase complex |
| HDF | human dermal fibroblast |
| HeLa | a cancer cell line |
| HEPES | N-2-hydroxyethylpiperazine- N'-2-ethance-sulphonic acid |
| HGPS | Hutchinson-Gilford progeria syndrome |
| HNF | hepatocyte nuclear factor |
| $H_2O_2$ | hydrogen peroxide |
| HP1 | heterochromatin protein 1 |
| hr | hour |
| HRP | horse-radish peroxidase |
| IB | immuno-blotting |
| ICMT | isoprenylcysteine carboxy-methyl-transferase |
| IF | intermediate filament |
| Ig | immunoglobulin |
| IGC | inter-chromatin granule cluster |
| INK | negative kinase inhibitor |
| INM | inner nuclear membrane |
| kb | kilobase |
| kD | kilodalton |
| kip | kinase inhibitor protein |
| LAP | lamin associated polypeptide |
| LBR | lamin B receptor |

| | |
|---|---|
| LEM | common domain in LAP, emerin and MAN1 |
| LGMD | Limb-girdle muscular dystrophy |
| LMN | lamin |
| m | monoclonal |
| M | mitotic phase |
| Mb | megabase |
| mm | milimeter |
| MAD | Mandibulo-acral dysplasia |
| MAPK | mitotic activated protein kinase |
| MAR | matrix-attachment region |
| MEF | mouse embryonic fibroblasts |
| min | minute |
| MVN | mevinolin |
| µg | microgram |
| µl | microlitre |
| µM | micromolar |
| Mr | relative molecular weight |
| mRNA | messenger RNA |
| Myne | myocyte nuclear envelope |
| NaCl | sodium chloride |
| NADPH | nicotinamide adenine dinucleotide phosphate |
| NARF | nuclear prelamin A recognition factor |
| NE | nuclear envelope |
| NEM | N-ethyl-maleimide |
| NCS | new-born calf serum |

| | |
|---|---|
| NF | nuclear factor |
| NHEJ | non-homologous end-joining |
| $(NH_4)_2SO_4$ | ammonium sulphate |
| NLS | nuclear localisation signal |
| nm | nanometre |
| NPC | nuclear pore complex |
| NS | nucleosome |
| NUANCE | nucleus and actin connecting element |
| Nup | nucleoporins |
| $O_2$ | oxygen |
| Oct | octamer-binding transcription factor |
| ONM | outer nuclear membrane |
| p | passage, immuno-precipitate, pellet, polyclonal |
| P | proliferating |
| PAGE | polyacrylamide gel electrophoresis |
| PBS | phosphate buffered saline |
| PC | post-confluent |
| PCNA | proliferating nuclear antigen |
| PCR | polymerase chain reaction |
| PF | perinuclear fibril |
| PHA | Pelger-Huet anomaly |
| PI | propidium iodide |
| PK | protein kinase |
| PML | promyelocytic leukaemia |
| PP | protein phosphatase |

| | |
|---|---|
| Pr· | protein thiyl radical |
| pRb | retinoblastoma protein |
| PrSH | protein sulfhydryl group |
| PrSOH | protein sulfenic acid |
| PrS-S | protein disulphide |
| PrS-SG | protein-glutathione disulphide |
| Q | quiescent |
| R | restimulated |
| RNA | ribonucleic acid |
| rpm | revolutions per minute |
| sRNAi | small interfering RNA |
| RARE | retinoic acid response element |
| RD | Restrictive dermopathy |
| ROS | reactive oxygen species |
| RT | room temperature |
| RxR | retinoic X receptor |
| S | DNA synthesis phase |
| SA-β-gal | senescence-associated beta galactosidase |
| SAR | scaffold attachment regions |
| SDS | sodium dodecyl sulphate |
| Seip | Seip-Bordetelli syndrome |
| Ser | serine |
| SH | sulfhydryl group |
| SIPS | stress-induced premature senescence |
| SOD | superoxide dismutase |

| | |
|---|---|
| SR | sarcoplasmic reticulum |
| SREBP | sterol-response element binding protein |
| ss | single-stranded |
| SS | serum-starved |
| Syne | synaptic nuclear envelope |
| 3T3 | mouse adult fibroblasts |
| TAF | TBP-associated factor |
| TBP | transcriptional binding protein |
| TBS | Tris buffered saline |
| TEMED | N, N ,N' ,N' – tetra-methyl-ethylene-diamine |
| TGF | tumour growth factor |
| Thr | threonine |
| TM | trans-membrane |
| TRF | telomere recognition factor |
| TRITC | tetra-methyl rhodamine isothiocyanate |
| Tyr | tyrosine |
| v/v | volume per volume |
| w/v | weight per volume |
| WRN | Werner protein |
| WS | Werner syndrome |
| X | sex chromosome |
| YA | 'Young arrest' protein |

# CHAPTER 1-GENERAL INTRODUCTION

## 1.1. THE NUCLEAR ENVELOPE AND THE NUCLEAR LAMINA

The main feature of eukaryotic cells is the nucleus, which enwraps the chromosomes, and is the site of DNA replication, RNA transcription and processing and ribosome assembly. The nuclear envelope (NE) is not just a boundary to the nucleus, but is an elaborate organelle that forms an interface between the nuclear and cytoplasmic compartments during interphase, and is involved in maintaining proper NE morphology, in DNA replication and nuclear growth, in organising nuclear contents, in RNA processing and export and in protein synthesis and processing (reviewed in Goldberg and Allen 1995). The NE is composed of the inner and outer nuclear membranes (INM and ONM, respectively), which are separated by the luminal space continuous with the endoplasmic reticulum (ER) lumen (**Figure 1.1**). ONM is a cytoplasmically opposed lipid bilayer that is connected to and resembles the rough endoplasmic reticulum with functional ribosomes attached and is a site for protein translation.

Communication between the nucleoplasm and cytoplasm takes place through many thousands of large supramolecular structures, called the nuclear pores, spanning the NE, where the inner and outer membranes join (reviewed in Goldberg and Allen 1995). Within these pores are anchored nuclear pore complexes (NPCs), which mediate and regulate bidirectional nuclear transport. Nucleo-cytoplasmic transport plays a fundamental role in coordinating the functions of the nucleus and cytoplasm. The NPCs accommodate both passive diffusion of ions and small metabolites, through 10 nm diameter aqueous channels in the NPCs, and active transport of most macromolecules, through a gated channel via signal- and energy-dependent mechanisms. The membrane present in the pores is called the pore membrane, and is associated with the peripheral and integral membrane proteins of the NPCs, and may provide a route for transferring integral membrane proteins from the INM to the ONM and vice versa.

The INM is a dynamic membrane that is able to grow during S phase, vesicularise at mitosis and bud during viral infection (reviewed in Goldman *et al.,* 2002). Underneath the INM is the nuclear lamina, a term coined to describe a meshwork of near-

tetragonally oriented nuclear-specific intermediate filaments, nuclear lamins, and a growing number of integral nuclear membrane (INM) and peripheral membrane (PM) proteins. The INM proteins are type II integral membrane proteins. They contain a nucleoplasmic N-terminal domain followed by a variable number of transmembrane segments and a C-terminal domain that faces the luminal space. Although their transmembrane domain confers their ability to be inserted into the INM, binding of these proteins to the nuclear lamins ensures their efficient retention at the NE. Currently, INM proteins include lamin B receptor-LBR (Worman *et al.*, 1990), six isoforms of lamina associated polypeptide 2-LAP2 (Foisner and Gerace 1993, Harris *et al.*, 1995, Berger *et al.*, 1996), three isoforms of lamina-associated polypeptide 1-LAP1 (Martin *et al.*, 1995), emerin (Manilal *et al.*, 1996), nurim (Rolls *et al.*, 1999), MAN1 (Lin *et al.*, 2000), Lem-3 (Lee *et al.*, 2000), UNC-50/UNCL (Fitzgerald *et al.*, 2000), luma (Dreger *et al.*, 2001), UNC-84/84A (Dreger *et al.*, 2001, Lee *et al.*, 2002), Syne-1 (synaptic nuclear envelope)/Myne1 (myocyte nuclear envelope)/nesprin 1α (Apel *et al.*, 2000, Mislow *et al.*, 2002, Zhang *et al.*, 2002), and SANE (Raju *et al.*, 2003). PM proteins do not appear to contain a segment that spans the INM and are more peripherally associated with the INM. These include otefin (Padan *et al.*, 1990), Young Arrest (YA) (Lin and Wolfner 1991), LBR kinase (Simos and Georgatos 1992), p34 (RNA splicing factor 2-associated protein) (Simos and Georgatos 1994) and p18 (homologous to mitochondrial isoquinoline-binding protein) (Simos *et al.*, 1996). Near the INM is the peripheral chromatin, a large proportion of which is the heterochromatin.

Recently, a family of giant ONM proteins including NUANCE (nucleus and actin connecting element) and Enaptin have been identified (Zhen *et al.*, 2002, Padmakumar *et al.*, 2004) along with their shorter splicing isoforms, nesprins, located at the INM (Zhang *et al.*, 2002). NUANCE and Enaptin contain N-terminal α-actinin type actin-binding (ABD) domain, a central coiled-coil rod domain and a C-terminal transmembrane domain and are proposed to structurally link lamina and nucleoskeleton to actin cytoskeleton in the cytoplasm (Zhen *et al.*, 2002, Padmakumar *et al.*, 2004).

There is strong evidence that lamins are not restricted to the nuclear periphery but exist throughout the nuclear interior. It is not known whether the internal lamins form similar or different structures from peripheral lamins. Given the growing number of lamin-binding partners, it is not difficult to envisage that these might influence the assembly

and/or structural properties of lamins. Photo-bleaching of intranuclear GFP-lamin A argues for the existence of both immobile lamin A structures and a free lamin A in the nucleoplasm (Broers *et al.*, 1999). In addition, the observation of intranuclear foci of A-type lamins during G1 phase of the cell cycle (Goldman *et al.*, 1992, Bridger *et al.*, 1993, Pugh *et al.*, 1997, Broers *et al.*, 1999, Kennedy *et al.*, 2000) and B-type lamin foci during S-phase (Moir *et al.*, 1994) raised the question as to whether these foci are in direct contact with the nuclear envelope. Nuclei of many cell types contain nuclear envelope derived invaginations extending into the nucleoplasm and making contact with the nucleolus, some of which even cut all the way through the nucleus (Fricker *et al.*, 1997, Broers *et al.*, 1999). These channels are lined with nuclear pore complexes and nuclear lamins and are proposed to be involved in nucleo-cytoplasmic transport (Fricker *et al.*, 1997). However, intranuclear spots of A-type and B-type lamins are not found to colocalise with membranes (Bridger *et al.*, 1993) or with NPCs (Moir *et al.*, 1994) and are thought to be genuine intranuclear structures.

The existence of non-chromatin nuclear proteins that remain insoluble following extraction with high concentrations of salt or chaotropic agents has been defined by Coffey and Penman as the nuclear matrix or nucleoskeleton (reviewed in Stuurman *et al.*, 1998). The nuclear matrix consists of an ordered and highly compartmentalised proteinaceous network of fibres, which are linked to and include the nuclear lamina and the nucleolar matrix. Removing chromatin from the nucleus also revealed the internal lamins (otherwise buried in dense chromatin), which form a part of a diffuse skeleton that ramifies throughout the interior of human nuclei (Hozak *et al.*, 1995). In addition, internal lamins are also found in nuclear bodies called nuclear speckles, which are components of nuclear matrix (Jagatheesan *et al.*, 1999). Moreover, A-type lamins interact with nucleoplasmic proteins such as a LAP2 isoform, LAP2α, and a retinoblastoma protein (Rb) and may anchor or organise components of the nuclear matrix (Ozaki *et al.*, 1995, Mancini *et al.*, 1994, Dechat *et al.*, 2000, Markiewicz *et al.*, 2002). The nuclear matrix including lamins preferentially associates with actively transcribed genes (the euchromatin), and displays both tissue- and differentiation-stage-specific changes in its protein composition (Bidwell *et al.*, 1993). It is, thus, implicated in the regulation of tissue-specific gene expression and organisation of functional domains within the nucleus.

## 1.2. EVOLUTION OF LAMIN GENES

Vertebrates have three lamin genes: LMNA, LNB1 and LNB2. The human LMNA gene on chromosome 1q21.2-3 encodes four alternatively spliced A-type lamins (**Figure 1.2**): somatic lamins A and C (Laliberte *et al.*, 1984), lamin AΔ10, found in somatic cells and tumours (Machiels *et al.*, 1996), and male germ cell-specific C2, the only expressed lamin in meiotic stages of spermatogenesis (Furukawa *et al.*, 1994, Alsheimer and Benavente 1996). While exon 1 through 9 of the lamin A, C and lamin AΔ10 mRNAs are identical, lamin A mRNA contains the 5' 90 bases of exon 10 followed by exon 11 and 12. In contrast, lamin C mRNA contains the complete 111-bp sequence of exon 10, but not exon 11 and 12. Lamin AΔ10 mRNA is identical to lamin A but lacks exon 9 and lamin C2 is identical to lamin C except that the N-terminal head and coil 1A are replaced by a short non-helical segment (Furukawa *et al.*, 1994).

The human LNB1 gene on chromosome 5q23.2-31.3 encodes lamin B1, and the LNB2 gene on chromosome 19p13.3 encodes lamins B2 and male germ cell-specific lamin B3 (Wydner *et al.*, 1996, Brandriff *et al.*, 1994, Furukawa *et al.*, 1993) (see **Figure 2**). In amphibians, A-type lamin La and B-type lamins Li and Lii are homologs of mammalian lamins A, B1 and B2 respectively (Stick and Hausen 1985). B-type lamin LIII is expressed in Xenopus embryos and oocytes and is not homologous to mammalian germ-cell specific B3. Instead, a sperm cell specific B-type lamin LIV has been identified in Xenopus (Benavente *et al.*, 1985).

In invertebrates such as *Drosophila Melanogaster*, there are two lamin genes, *Dm0* gene which codes for two B-type lamin isoforms Dm1 and Dm2 (Gruenbaum *et al.*, 1988) and *lamin C* gene which codes for an A-type lamin DmC (Reimer *et al.*, 1994), and in *Caenorhabditis elegans,* there is one B-type lamin gene, namely *lmn-1* and no A-type lamin gene (Liu *et al.*, 2000).

Comparing the structure of LMNA and LMNB genes in the same species shows a remarkable conservation of the exon/intron patterns (Stick 1992). In both genes the last exon encodes the CaaX motif whilst the lamin A-specific tail is encoded by an additional exon (exon 11), indicating that A-type lamins derived from the insertion of

the exon with a proteolytic cleavage site into exon 10 of the LMNB gene. Therefore B-type lamins are believed to represent the ancestral type of lamins (Stick 1992, 1994).

The yeast *Saccharomyces cerevisiae* contains no identified lamin genes and lacks all other INM proteins but still has conserved NPC proteins (Cohen *et al.*, 2001). Lamina proteins appear to be absent from plants although there is some immunological evidence for lamin existence. Interestingly, chicken lamins assemble as a nuclear rim-like structure when expressed in *Shizosaccharomyces pombe*, indicating the presence of proteins that target lamins to the NE. Therefore, it is believed that proteins with homologous functions to lamins will be found in plants and yeast in the future.

## 1.3. LAMINS IN DEVELOPMENT AND TISSUE SPECIFICITY

A-type lamins are developmentally regulated whilst at least one B-type lamin is expressed in every cell type at all developmental stages (reviewed in Hutchison 2002). A-type lamins have been detected in ovulated and fertilised oocytes, but embryonic stem cells, cells of the early embryo and haematopoietic stem cells do not express LMNA gene, although derivatives of these cells do express LMNA gene during development (Stewart and Burke 1987, Paulin-Levasseur *et al.*, 1988). RNAi knockdown of either lamin B1 or lamin B2 in cultured cells inhibited cell growth and promoted apoptosis confirming that B-type lamins are essential for survival (Harborth *et al.*, 2001). In contrast, LMNA-/- mice develop normally (Sullivan *et al.*, 1999) and RNAi knockdown of A-type lamins in cultured cells had no lethal effect (Harborth *et al.*, 2001), indicating that A-type lamins are not essential for development and survival. Interestingly, inhibition of lamin B assembly in lymphoid cells, which do not express lamin A/C, triggers a signalling mechanism that depresses the LMNA gene and induces rapid synthesis and assembly of lamins A/C (Collas *et al.*, 2001). However, these cells enter apoptosis soon after, confirming the importance of B-type lamins for survival.

Immuno-localisation studies have concluded that whilst lamin B2 is expressed at relatively constant levels in all human cell types (except for hepatocytes), lamin B1 expression is more pleiotropic. Lamin B1 expression possibly correlated with the proliferation state of epithelial cells and is apparently absent from skeletal muscle, heart, kidney, connective tissues, some cell types of the prostate gland, endocrine cells of the

thyroid, parathyroid and adrenal glands, smooth muscle cells in various organs and epithelial cells with high level of differentiation (Broers *et al.*, 1997). However, recently it has been demonstrated that although human heart cardiomyocyte nuclei were negative for lamin B1 using a commercial monoclonal antibody (mAb), they were positive when using two other lamin B1 antibodies (Tunnah *et al.,* 2005), suggesting that different regions of the lamin B1 molecule may be masked in different tissues. In contrast, A-type lamins are present to variable degrees in all tissues and cell types that apparently lacked lamin B1 except for endocrine cells of parathyroid and adrenal glands (Broers *et al.,* 1997). Still, different splice variants of A-type lamins may be differently expressed in different cell types (Machiels *et al.*, 1996). In addition, a few cells of the immune system, pancreatic islets and Purkinje cells only express B-type lamins (Rober *et al.*, 1990). The differences in A-type and B-type lamin composition at the nuclear lamina seen in various tissues is thought to account for tissue specificity (Broers *et al.*, 1997) so that cells gain functional advantage from their particular lamin ratio (Schirmer and Gerace 2004).

A-type lamins are first observed at the time of organogenesis (initially in developing muscle), suggesting a role for LMNA gene in terminal differentiation (Rober *et al.*, 1990). Moreover, ectopic expression of lamin A in chicken myoblasts promotes differentiation (Lourim and Lim 1989). Since A-type lamins are not simultaneously expressed in all organs (in heart and brain, for example, expression is post-natal), it is argued that a commitment of a cell to a particular pathway of differentiation occurs before A-type lamin expression is detected (reviewed in Goldman *et al.*, 2002). This suggests that A-type lamins may be involved in maintaining a differentiated phenotype and/or limiting further developmental plasticity rather than cell fate determination. Consistent with this hypothesis, loss of A-type lamin expression is associated with dedifferentiation in some tumour cells (Broers *et al.*, 1993, Venables *et al.*, 2001).

The correlation between A-type lamin expression and cell differentiation led to speculation that A-type lamins may facilitate differential gene expression by anchoring chromatin at the NE or by sequestering inhibitors (Nigg *et al.*, 1989). Indeed, A-type lamins display a higher affinity for chromatin binding than B-type lamins (Hoger *et al.*, 1991). Further to that, expression of A-type lamins is enhanced in quiescent Swiss 3T3 fibroblasts albeit decreased mRNA levels, suggesting a role for A-type lamin protein

expression and stability in facilitating growth arrest (Pugh *et al.*, 1997). Interestingly, rearrangement of A-type lamin assembly has been seen to accompany differentiation of human promyelocytic leukaemia HL-60 cells (Collard *et al.*, 1992) and mouse myoblasts *in vitro* (Markiewicz *et al.*, 2005)

## 1.4. TRANSCRIPTIONAL REGULATION OF LAMIN GENES

The expression of LMNA gene is primarily under transcriptional control and is induced upon cell growth and differentiation (Pugh *et al.*, 1997, Reimer *et al.*, 1995). Characterisation of the proximal promoter of rat LMNA gene was reported to harbour two important motifs: a GC box that can bind to Sp1/Sp3 transcription factors, and an AP-1 motif that can bind to c-Jun and c-Fos transcription factors (Tiwari *et al.*, 1998, 1999) and these motifs are conserved in both mouse and human LMNA genes as well as in LNB1 gene (Lin and Worman 1995). Indeed, both Sp1 and AP-1 are directly found to be important in the activation of lamin A proximal promoter (Mularikrishna and Parnaik 2001).

In addition, the first intron of the LMNA gene contains two binding motifs, footprinted region A (FPRA) and FPRB (Arora *et al.*, 2004). The hepatocyte nuclear factor-3β (HNF-3β) binds to the FPRA region in somatic cells with an inhibitory effect on promoter activity. HNF-3β is a member of a Forkhead/Fox family of proteins, which are important regulators of cellular differentiation and metabolism, and act as both transcriptional activators and repressors. Interestingly, expression of Forkhead proteins has been linked to increased oxidative stress resistance in mammalian cells and increased longevity in *C.elegans* (reviewed in Finkel *et al.*, 2003). The retinoic X receptor β (RXRβ) binds to the FPRB region in both somatic and germ-line cells with an enhanced effect on promoter activity. Members of this nuclear hormone receptor superfamily are regulated during cellular differentiation. The possibility that this region harbours a retinoic-acid responsive element (RARE) has important implications since retinoic acid is a well-known inducer of differentiation and lamin A expression (Lebel *et al.*, 1987). Interestingly, the GC-rich motif that binds to the Sp1/3 family of transcription factors is also responsive to retinoic acid (Okumura *et al.*, 2000).

## 1.5. NUCLEAR LAMINA ASSEMBLY/DISASSEMBLY DURING MITOSIS

It is believed that nuclear lamina proteins first appeared around the transition between closed and open mitosis to provide functions unique to multicellular organisms (Gerace and Burke 1988). For example, *S. cerevisiae* has a 'closed' mitosis during which the NE remains intact (reviewed in Cohen *et al.*, 2001). During 'closed' mitosis, tubulin molecules are imported into the nucleus to allow mitotic spindles to assemble inside the nucleus. By contrast, the mammalian NE undergoes 'open' mitosis in which the nuclear lamina, NPCs and nucleoskeleton reversibly disassemble. In addition, physical disruption of the NE caused by spindle microtubules during mid-late prophase contributes to the release of intranuclear contents (Georgatos *et al.*, 1997). Two models of mitotic NE disassembly and reformation have emerged from studies of the NE dynamics in somatic cells and egg extracts (reviewed in Collas and Courvalin 2000). One model suggests that nuclear membranes fragment reversibly by vesiculation producing distinct NE-derived vesicles separate from the bulk ER membranes. Rapid sorting of INM proteins at the end of mitosis is thought to occur through selective targeting of distinct NE vesicles to chromosome surfaces. The second model (known as the 'diffusion-retention' model) proposes that the nuclear membranes merge into the ER and the nuclear proteins become dispersed throughout all ER membranes. At the end of mitosis, ER-derived membranes associate with chromosomes and nuclear membranes reform by diffusion of INM proteins through the ER and binding to specific sites at the chromosome surfaces.

Several studies have suggested a role for lamins in targeting membranes to chromosomes at the end of mitosis (Burke and Gerace 1986, Daubavalle *et al.*, 1991), while other work has suggested a lamin-independent mechanism for nuclear membrane targeting (Newport *et al.*, 1990, Meier *et al.*, 1991). Injection of anti-lamin antibodies in mitotic PtK2 cells arrested chromatin in a telophase-like configuration supporting the lamin-dependent nuclear envelope assembly (Benavente and Krohne 1986). The timing of nuclear membrane targeting to chromosomes coincides with the re-location of INM proteins such as LAP2, LAP1 and LBR to chromosome surfaces, which occurs before the assembly of most lamins around chromosomes (Foisner and Gerace 1993), suggesting that INM proteins are important for directing subsequent lamin assembly. The importance of INM proteins in nuclear assembly has been demonstrated by RNAi

experiments in *C.elegans, Drosophila* and mammalian cells. RNAi knockdown of BAF in both *C.elegans and Drosophila* embryos caused early mitotic lethality with chromosome misseggregation, chromatin clumping and misshapen nuclei (Zheng *et al.*, 2000, Lin *et al.*, 2000, Furukawa *et al.*, 2003). The expression of BAF missense mutant in human cells dominantly disrupted assembly of emerin, LAP2β and A-type but not B-type lamins into reforming telophase nuclei (Haraguchi *et al.*, 2001). Similarly, over-expression of the LAP2α C-terminal domain disrupted assembly of nuclear membranes, lamin A/C and endogenous LAP2α on chromosomes (Dechat *et al.*, 2001). Interestingly, in *C. elegans*, emerin RNAi had no detectible influence on NE assembly (Gruenbaum *et al.*, 2002) but a double RNAi knockdown of emerin and MAN1 caused a gross early lethality and mitotically arrested anaphase-bridged chromatin which failed to recruit Ce-lamin and Ce-BAF (Liu *et al.*, 2003). Recently, it has been shown that a subfraction of A-type lamins (previously undetected due to a high amount of unassembled lamins) associates with chromosomes at the same time as LAPs, which suggests that both INM proteins and lamins contribute to the NE and subsequent lamina assembly (Dechat *et al.*, 2004).

In vertebrates, the disassembly of the NE defines the transition between prophase and pro-metaphase (reviewed in Cohen *et al.*, 2001). Based on the timing of the NE breakdown, *C. elegans* and *Drosophila* are intermediate between yeast and vertebrates. In *C. elegans,* the nuclear membranes, NPCs and lamina remain intact (except at spindle poles) until they disassemble completely only during mid-late anaphase (Lee *et al.*, 2000). In *Drosophila,* NPCs disassemble during prophase like in vertebrates, but the nuclear membranes remain largely intact and disassemble only during mid-late anaphase (Paddy *et al.*, 1996). These observations suggest that there is a strong correlation between evolution of the NE complexity and the enhanced ability of NE disassembly early in mitosis. The relationship between the evolution of lamina complexity and 'open' mitosis is thought to relate to improvements in chromatin organisation, nuclear signalling and regulated gene expression, especially during development and differentiation (Cohen *et al.*, 2001). However, the possibility is not excluded that lamin filaments may interfere with chromosome segregation during mitosis and that 'open' mitosis co-evolved with appearance of nuclear lamins.

## 1.6. STRUCTURE OF LAMIN PROTEINS AND THE FILAMENT ASSEMBLY

With respect to sequence homology, lamins belong to the type V large family of intermediate filament (IF) proteins and, unlike types I-IV, which are located in the cytoplasm, lamins reside in the nucleus (reviewed in Hutchison 2002). Like all IF proteins, they have a tripartite structure consisting of a small N-terminal head, a 52-nm coiled-coil rod and a globular C-terminal tail. The rod domain can be divided into four α-helical segments, coils 1a, 1b, 2a and 2b, which are separated by non-helical linker sequences. In contrast to cytoplasmic IF proteins, the rod domains in lamins contain an additional six heptad repeats in coil 1B whilst the C-terminal domains include the extra nuclear localisation sequence (NLS) and the recognition sequence for isoprenylation (CaaX motif). Lamins form α-helical coiled-coil dimers, which are the building blocks for further assembly (Heitlinger *et al.*, 1991) **(Figure 1.3a)**. Lamin dimers associate longitudinally to form polar head-to-tail tetramers. This strikingly contrasts with the lateral mode of association of cytoplasmic IF dimers into anti-parallel, unstaggered or half-staggered tetramers. Lamin head-to-tail tetramers associate laterally in an anti-parallel half-staggered fashion to form IF-like assemblies that reveal distinct 24-25 nm beading filaments (Heitlinger *et al.*, 1991) **(Figure 1.3b)**. These beading filaments are not stable over time *in vitro*, and unlike cytoplasmic IF proteins, they further associate laterally into fibers and eventually form large paracrystalline arrays (Moir *et al.*, 1991, Heitlinger *et al.*, 1992, Quinlan *et al.*, 1995). Lamin paracrystal assembly occurs via other types of dimer interactions and is thus believed that lamina assembly *in vivo* must be modulated by interactions with other proteins (reviewed in Stuurman *et al.*, 1998). Generally, it is thought that the N-terminal head domain (aa 30-40) promotes lateral association of tetrameric protofilaments into octameric protofibrils and the C-terminal domain (aa 170-265) controls lateral assembly of protofilaments into 10 nm filaments as well as network formation. Interestingly, invertebrate cytoplasmic IF proteins have a distinct evolutionary relationship to vertebrate lamins since they contain the lamin-like extension within the coil 1B (Reimer *et al.*, 1998). Since cytoplasmic vertebrate IF proteins lack these regions, it is thought that they might have evolved from lamins through a combination of exon shuffling and mutation.

## 1.7. POST-TRANSLATIONAL REGULATION OF THE LAMINA PROTEINS

### *1.7.1. CAAX MOTIF MODIFICATIONS IN LAMINS*

The C-terminal ends of all lamins, except mammalian and *Drosophila* lamin C, contain a sequence motif CaaX box (C-cysteine; a-any aliphatic amino acid; X-any amino acid). This motif represents a signal for modification of proteins by an isoprenoid group and is found in many prenylated proteins, including fungal mating factors, Ras, Ras-related proteins and G-protein subunits (reviewed in Hutchison 2002). In the germ cell-specific lamin C2, this motif is myristoylated. In all other lamins, this motif is modified by farnesylation (attachment of the farnesyl moiety) of the C-terminal cysteine residue, followed by a cleavage of the final three C-terminal residues (-AAX) and methyl esterification of the newly exposed carboxyl group on the cysteine. The attached hydrophobic prenyl moiety can target and anchor lamins to the NE (Vorburger *et al.*, 1989).

It is worth mentioning that there are two types of protein prenyl modifications in living cells, farnesyl or geranylgeranyl, with geranylgeranyl group being the predominant form of isoprene attachment (reviewed in Caldwell *et al.*, 1995). Farnesyl and geranylgeranyl moieties have a common biosynthetic pathway with cholesterol and the level of prenylated proteins in the cell can regulate cholesterol metabolism.

B-type lamins remain farnesylated throughout their lifetime and locate to the NE where they become attached as peripherally associated proteins. In contrast, subsequent to the canonical CaaX box modifications, lamin A is processed further (**Figure 1.4**). The C-terminal 15 residues of lamin A and the prenyl tail are removed by proteolytic cleavage between tyrosine 646 and leucine 647 to yield mature lamin A (Sasseville and Raymond 1995). Such different processing pathway between B-type lamins and lamin A is believed to explain their different disassembly/reassembly at mitosis.

### *1.7.2. PRELAMIN A PROCESSING PATHWAY*

Lamin A is unusual amongst nuclear proteins in mammalian cells for being synthesized as an isoprenylated precursor (called prelamin A) which gets cleaved proteolytically

during the course of its assembly in the lamina in order to remove its previously isoprenylated end. The physiological role of this cleavage step is not yet understood. The only other known protein that undergoes the same processing step is the yeast mating factor α (Clarke *et al.*, 1992). An absence of this isoprenylated fragment does not impair the ability of lamin A to be reassembled at the NE after mitosis (Holtz *et al.*, 1989, Krohne *et al.*, 1989, Sasseville and Raymond 1995). Nonetheless, isoprenylation of lamin A is a prerequisite step for all other reactions to occur, including the proteolytic cleavage (Beck *et al.*, 1990, Sassevile and Raymond 1995, Kilic *et al.*, 1997). A possible candidate gene for the protease responsible for prelamin A maturation has arisen from genetic data obtained from both yeast and mice. Ste24 protease was first identified as a zinc-dependent metalloprotease in yeast which catalyses both the -aaX cleavage and the endoproteolytic cleavage of the prenylated yeast mating factor α precursor (in Kilic *et al.*, 1997). Recently, it has been shown that the mouse and human orthologue to yeast Ste24, Zmpste24/FACE, plays a role in the endoproteolytic cleavage of isoprenylated prelamin A (Corrigan *et al.*, 2005).

The half-life of the lamin A precursor is around 90-100 minutes and its processing into mature form occurs within 4 hours (Gerace *et al.*, 1984, Beck *et al.*, 1990). The subcellular sites of prelamin A processing have been a matter of controversy. Some authors concluded from kinetic studies that the lamin A processing occurred in the cytoplasm (Kitten and Nigg 1991). Others concluded from biochemical studies that lamin A precursor first assembled at the NE and only subsequently became cleaved to mature form (Gerace *et al.*, 1984) or that cleavage and assembly occurred concomitantly (Lehner *et al.*, 1986). Moreover, under conditions where isoprenylation was prevented with mevinolin (MVN), prelamin A accumulated in the nucleoplasm (Beck *et al.*, 1990, Lutz *et al.*, 1992). Kinetic evidence from microinjection studies with full-length lamin A, which resembles lamin A precursor, supported the transient passage of lamin A through intranuclear foci prior to its assembly in the lamina (Goldman *et al.*, 1992). Localisation of the farnesyl-transferase (Synesky *et al.*, 1994) and –aaX cleaving endoprotease (Jang *et al.*, 1993) in the nucleus also supported intranuclear processing of prelamin A.

Using prelamin A-specific antibodies, it was shown that prelamin A was localised in numerous intanuclear foci in the vast majority of interphase cells in culture (Sasseville

and Raymond 1995). When isoprenylation was inhibited, prelamin A was still present in foci, but also most strikingly accumulated in the peripheral lamina, where it was assembled. When isoprenylation was restored, prelamin A gradually disappeared from the lamina, but remained present in intranuclear foci. This study concluded that isoprenylation and cleavage of the lamin A precursor occur in the nucleus but that the non-isoprenylated prelamin A appears competent for assembly in the lamina. Although intranuclear localisation of A-type lamin spots during G1 phase of cell cycle had been described previously (Goldman *et al.*, 1992, Bridger *et al.*, 1993), these studies could not distinguish between localisation of prelamin A and mature forms. Whilst such lamin spots are thought to represent pools of lamins available for growth of daughter nuclei after mitosis, the precursor lamin foci detected by Sassevile and Raymond 1995 most likely represent distinct foci related to localisation of A-type lamin intermediates along the post-translational pathway, supporting the concept of distinct protein processing domains within the nucleus.

The only study that addressed the physiological role of the non-isoprenylated lamin A precursor came from Sinesky *et al.*, 1994, which showed that the accumulation of the non-isoprenylated lamin A precursor inhibited DNA replication, suggesting a link between isoprenoid metabolism and cell cycle progression. It was thus suspected that isoprenylated lamin A precursor gets transported to intranuclear foci by specific carrier molecules such as those described for other isoprenylated proteins (Clarke *et al.*, 1992), where it may play a specific role. One such prenylated prelamin A binding protein is a novel ubiquitous protein called nuclear prelamin A recognition factor (Narf) which may anchor prelamin A to organise nuclear proteins and/or heterochromatin into a higher order structure (Barton and Worman 1999). Interestingly, Narfs contain a conserved domain of iron clusters between cysteine residues found in bacterial iron-only hydrogenases, which are involved in scavenging electrons during pyruvate oxidation.

### *1.7.3. PHOSPHORYLATION*

#### 1.7.3.1 Serine/threonine phosphorylation of lamins

NE components together with lamina disassemble and reassemble during mitosis as a result of reversible phosphorylation (Collas *et al.*, 2000). Both *in vivo* and *in vitro*

assays suggest that lamins and INM proteins have mitotic CDC2 kinase, protein kinase C (PKC) and cyclic-AMP-dependent kinase (PKA) serine and threonine phosphorylation sites. Lamins and INM proteins are phosphorylated during both interphase and mitosis. Interphase phosphorylation only occurs on assembled lamina and is thought to influence nuclear envelope growth or other functions during interphase (Ottaviano and Gerace 1985, Ward and Kirschner 1990). Phosphorylation by PKA during interphase facilitates the incorporation of new lamin subunits into the assembled lamina structure as the nucleus grows (Peter *et al.*, 1990). Conversely, down-regulation of PKA has been shown to be essential for mitotic lamina disassembly (Lamb *et al.*, 1991). Phosphorylation of lamin B2 during S-phase, for example, correlates with its redistribution from NE to replication centres in the nucleus (Kill and Hutchison 1995).

Phosphorylation sites within two regions flanking the lamin rod domain are highly conserved among lamins. Mutations within these phospho-acceptor sites (Ser22 and Ser392) were shown to strongly interfere with human lamin A disassembly *in vivo* (Heald and McKeon 1990, Haas and Jost 1993). Interestingly, one of these sites, Ser22, is increasingly phosphorylated during interphase in human lamin C whereas Ser392 is a cdc2 kinase mitosis-specific phosphorylation site (Ward and Kirschner 1990, Eggert *et al.*, 1991, 1993). Phosphorylation of Ser16, Ser384 and Ser386 on chicken lamin B2 by cdc2 kinase inhibits their association into polar head-to-tail polymers and promotes lamin B2 disassembly (Heitlinger *et al.*, 1991, Peter *et al.*, 1991). In contrast, Ser395 and Ser 405 on human lamin B1 is a major site of PKC phosphorylation necessary for lamin B1 disassembly whilst phosphorylation of Ser392 by cdc2 occurs at a lower rate (Hocevar *et al.*, 1993). Phosphorylation of sites in the lamin B tail (Ser405) by PKC is also responsible for disassembly of nuclear lamins in certain cell types (Goss *et al.*, 1994, Thompson *et al.*, 1996, Collas *et al.*, 1997). Interestingly, a sequence difference between human lamin B1 and lamin C renders the analogous site Ser404 on human lamin C an interphase S6 kinase II phospho site rather than PKC site (Hocevar *et al.*, 1993, Ward and Kirschner 1990, Eggert *et al.*, 1991).

In human lamin A/C, phosphorylation by PKC is associated with interphase phosphorylation (Eggert *et al.*, 1993, Hennekes *et al.*, 1993). Interphase PKC phosphorylation of chicken lamin B2 can influence the rate of lamin entry into the nucleus (Hennekes *et al.*, 1993). PKC interphase phosphorylation has also been

identified in lamin A/C following insulin stimulation of quiescent mammalian cells in culture (Friedman *et al.*, 1988) and occurs in the N- (Ser5) and C-terminal region (Ser525 and Ser625) (Eggert *et al.*, 1993). Interestingly, the N-terminal region of human lamin A/C contains phospho sites for 3 kinases including cdc-2 kinase, PKC and PKA (Eggert *et al.*, 1991). The assembly of lamin A into the perinuclear lamina is disturbed by mutation of the carboxy-terminal Ser-525 (Haas and Jost 1993). The phenotype shows discontinuous and patch-like aggregates of the mutant protein in the nucleus, which suggests that phosphorylation of this site regulates lamina assembly and/or lamina-chromatin interaction in interphase.

Protein phosphatases have been implicated in lamina assembly (Murphy *et al.*, 1995). Protein phosphatase type 1 (PP1) has been identified as a mitotic lamin B phosphatase and the rate of dephosphorylation by PP1 at cdc-2 sites can influence the initial rate of lamin filament assembly at telophase (Thompson *et al.*, 1997). At the NE, the A-kinase anchoring protein, AKAP 149, recruits PP1 upon nuclear reassembly at the end of mitosis and during G1 phase, which correlates with the assembly of B-type lamins at the NE (Steen *et al.*, 2003). AKAP 149 interacts with A-type and B-type lamins although its interaction with the nuclear lamina does not depend on lamin A/C (Steen and Collas, 2001). AKAP149 also recruits PKA at the NE (Steen *et al.*, 2000) and the same is true for AKAP255 in differentiated myocytes (Kapiloff *et al.*, 1999). Direct binding of the C-terminal domain of lamin A to PKC is also reported (Martelli *et al.*, 2002). Disruption of the AKAP149/PP1 complex during G1 phase of cell cycle, triggers phosphorylation of lamins and their intranuclear solubilization which correlates with the inhibition of replication and G1 arrest (Steen *et al.*, 2003). These authors propose that differential binding of AKAP149, PP1 and PKA regulates phosphorylation/dephosphorylation of lamins and the NE dynamics.

### 1.7.3.2 Serine/threonine phosphorylation of the lamina proteins

INM proteins such as LBR, LAP1 and LAP2 are also phosphorylated by cdc-2 kinase during mitosis (Foisner and Gerace 1993). Emerin also shows cell-cycle dependent phosphorylation (Ellis *et al.*, 1998). Phosphorylation of LAP2 during M phase reduces its affinity for lamins and chromatin whilst mitotically modified LAP1s are still capable of binding to lamins (Foisner and Gerace 1993). Nonetheless, mitotically

phosphorylated LAP2β is retained in membrane structures whilst LAP2α becomes cytoplasmic (Dechat *et al.*, 1998). LAP2 is phosphorylated during interphase in the N-terminal common domain by both proline-directed kinases and PKC (Dreger *et al.*, 1999). LBR kinase keeps LBR phosphorylated during both interphase and mitosis and dephosphorylation of LBR on these sites decreases its affinity for lamin B (Nikolakaki *et al.*, 1996). Interestingly, LBR kinase is a serine/threonine kinase, which can phosphorylate splicing factors and influence their subnuclear localisation and RNA splicing properties (Yeakley *et al.*, 1999).

#### 1.7.3.3 Tyrosine phosphorylation of the lamina proteins

Lamins and INM proteins also become phosphorylated and dephosphorylated on tyrosine sites by as yet unidentified tyrosine kinases/phosphatases located at the NE (Otto *et al.*, 2001). Tyrosine phosphorylation is important in growth control, differentiation and control of mRNA splicing and export. One of the most characterised tyrosine kinases is a c-Abl kinase (a cellular homolog of the viral oncogene v-abl), which binds to the C-terminal pocket of retinoblastoma protein and is involved in stress-response signalling following DNA damage. Tyrosine phosphorylated lamina proteins identified so far include lamins A, B1 and B2, LAP2β, LAP2α and several less known RNA splicing factors located at the INM.

### *1.7.4. OTHER POST-TRANSLATIONAL MODIFICATIONS*

Besides isoprenylation and phosphorylation, glycosylation of lamins, particularly lamin A is another postsynthetic modification. The glycosylated form of lamin A has been shown in at least three tissues from pig and chicken (Ferraro *et al.*, 1989) but the role of this modification has not been determined.

B-type but not A type lamins undergo reversible methylation to form the methyl ester of at least two carboxyl side chains (Chelsky *et al.*, 1989). This lamin B modification is cell cycle-dependent and inversely correlates lamin phosphorylation. Maximal lamin B methylation is found in interphase cells and very little in mitotic cells. Inhibiting methylation in late mitotic cells delayed B-type lamin assembly and chromatin

decondensation demonstrating that both dephosphorylation and methylation are necessary for B-type lamin assembly.

## 1.8. A MODEL OF THE LAMINA NUCLEAR ASSEMBLY

Following disassembly, lamins A and C are soluble during mitosis in form of dimers and/or tetramers, whereas B-type lamins generally remain attached to nuclear membrane vesicles (Gerace and Blobel 1980). Based on differential lamin solubility properties during mitosis, a model was originally proposed that B-type lamins associate with membranes via hydrophobic domains and A-type lamins associate through specific protein-protein interactions with B-type lamins (Gerace and Blobel 1980). Subsequently, it was found that lamins do not have specific hydrophobic regions but that they contain C-terminal CaaX sequences which are the sites of hydrophobic modifications required for membrane association (Krohne *et al.*, 1987). Since B-type lamins remain isoprenylated during their lifetime, it was thought that this modification retains their membrane association during mitosis whereas as a result of further processing lamin A loses this sequence and is thus soluble during mitosis (Beck *et al.*, 1988). Microinjection of Xenopus B-type lamin Li lacking CaaX sequence into the cytoplasm of Xenopus oocytes resulted in soluble non-envelope associated lamin Li within the nucleus (Krohne *et al.*, 1989). Similarly, chicken lamin B2 CaaX-less mutant expressed in mouse L cells also distributed diffusely throughout nucleoplasm (Kitten and Nigg 1991). Transfecting mammalian cells with chicken lamin A mutants with a point mutation in the proteolytic cleavage site showed that preventing cleavage of prelamin A precursor conferred membrane binding properties to lamin A during mitosis (Hennekes and Nigg 1994). In contrast, mutant lamin A that lacked this motif preferentially assembled into crystalline structures in the nucleoplasm and it was therefore thought that the presence of this sequence in A-type lamins initially promotes a weak association with the NE while stable binding requires additional interactions with INM proteins (Holtz *et al.*, 1989). Indeed, in contrast to B-type lamins, microinjection of Xenopus lamin A lacking only the C-terminal cysteine of CaaX motif into mouse 3T3 cells (Holtz *et al.*, 1989) or Xenopus oocytes (Krohne *et al.*, 1989) showed that these mutants exhibited delayed but complete or partial assembly respectively suggesting that other regions in the lamin A promoted its assembly into the lamina. Transfection experiments with a deletion mutant of human lamin A lacking the

entire lamin A-specific tail (Loewinger and McKeon 1988) or a rod mutant of Xenopus lamin A (Holz *et al.*, 1989), did not properly associate with the NE and supported the above conclusions. Since lamin C does not contain the CaaX motif, it was thought that lamin C must form heterodimers with other lamins. Indeed, it was demonstrated by using yeast two hybrid system that lamin A, prelamin A, lamin B1 and lamin C were all able to form homodimers as well as heterodimers (Ye and Worman 1995). Whilst heterotypic A-B and C-B lamin interactions involved the N-terminal domain, heterotypic lamin A-C and homotypic A-A and C-C did not (Georgatos *et al.*, 1988).

Since then several studies indicated that there may be a hierarchy of lamin-lamin associations at the INM. Since A-type lamins do not become expressed until late in development (Rober *et al.*, 1989) and they are not essential for cell survival (Harborth *et al.*, 2001), they do not seem to be required for the assembly of the basic lamina (reviewed in Hutchison *et al.*, 2001). In Xenopus egg extracts, which support *in vitro* nuclear assembly, recombinant lamin A is assembled at the NE only in the presence of the endogenous lamin B3, indicating that lamin A might be incorporated into existing B-type lamina via heterotypic assembly with B-type lamins (Dyer *et al.*, 1999). These results were supported by *in vivo* observations that A-type lamins remain in the nucleoplasm until late G1 phase whilst B-type lamins assemble in the telophase nuclei (Bridger *et al.*, 1993, Broers *et al.*, 1999, Dechat *et al.*, 2001). In addition, dominant-negative lamin A and B mutants that possess altered lamina-assembly properties and form nucleoplasmic aggregates in transfected cells had distinct effects on endogenous A-type and B-type lamins in that whilst A-type lamins relocated to nucleoplasmic aggregates, B-type lamins did not (Shirmer *et al.*, 2001, Izumi *et al.*, 2000, Vaughan *et al.*, 2001), indicating that the two types of lamins incorporate into the lamina in different ways.

B-type lamins are thought to assemble at the NE by virtue of their association with INM proteins that act as specific isoprene receptors for filament assembly (reviewed in Hutchison 2002). Several INM proteins have been reported to act as isoprene receptors for B-type lamins, including LBR, LAP2β and LAP2χ. Indeed, B-type lamins remain associated with LBR during mitosis (Meier *et al.*, 1994) and lamin B1 mutants lacking CaaX motif segregate independently of LBR at mitosis (Mical and Montiero 1998). Similarly, LAP2β, which binds to the rod domain of B-type lamins, plays an essential

role in the initial assembly of the lamina (Yang *et al.*, 1997, Gant *et al.*, 1999). In contrast, A-type lamins have not been reported to have specific receptors at the NE. Instead, they show rapid association with B-type lamins after they first accumulate in the nucleoplasmic foci (Dyer *et al.*, 1999) and may also be targeted at the NE by interactions with their binding partners such as emerin and LAP1. Indeed, a subfraction of A-type lamins that gets targeted to telophase chromosomes is found in the same focal points as emerin (Dabauvalle *et al.*, 1999, Dechat *et al.*, 2004).

Lamin A and lamin C also show different assembly properties. Expression or injection of tagged lamins in mouse 3T3 cells showed that lamin A was incorporated into the lamina more rapidly than lamin C (Gerace *et al.*, 1984). In many tumour cell lines that do not express lamin A, lamin C is mislocalised to the nucleoplasm or the nucleolus (Vaughan *et al.*, 2001, Venables *et al.*, 2001) and when GFP-lamin A was overexpressed in these cells, lamin C relocated to the NE (Vaughan *et al.*, 2001). Other studies also indicate that lamin A directs lamin C to the lamina. For example, when GFP-lamin C was expressed in tissue culture cells, it formed aggregates in the nucleoplasm, however, if it was co-expressed with GFP-lamin A, it was rapidly incorporated into the lamina, indicating that lamin A may guide lamin C to the NE (Pugh *et al.*, 1997). Moreover, transfecting cells with either the rod or tail mutants of lamin A showed more compromised assembly of lamin C than that of lamin A (Raharjo *et al.*, 2001). Therefore, lamin C may require a greater number of protein-protein interactions for the NE assembly than lamin A (Hutchison *et al.*, 2001). Indeed, in emerin null cells, lamin C rather than lamin A assembly was predominantly affected and mislocalised to the nucleoplasm (Markiewicz *et al.*, 2002b). Based on these and other reports, Hutchison *et al* proposed a model for lamina assembly at the NE (Hutchison *et al.*, 2001) **(Figure 1.5)**. In this model, B-type lamins assemble via isoprene receptors at the reforming NE during telophase. Either B-type lamins or some population of pre-lamin A recruits sufficient population of emerin and LAP1C at the NE, which can then recruit lamin A-C heterodimers to the NE. Their presence at the NE may be further stabilised by interactions with their binding partners such as LAP1C (Martin *et al.*, 1995), emerin (Clements *et al.*, 2000, Vaughan *et al.*, 2001) and MAN1 (Lin *et al.*, 2000). Consistent with this model, it has been shown that emerin null human cells do assemble A-type lamins but their interactions with the lamina are unstable (Markiewicz *et al.*, 2002b).

## 1.9. ROLES OF THE NUCLEAR LAMINA

The nuclear lamina has been considered for a long time as a static exoskeleton that serves primarily to give the nucleus shape and strength. However, as one will see below, the lamina proteins appear to be true multifunctional proteins that play a role in a number of fundamental cellular processes.

### *1.9.1. THE LAMINA AND NUCLEAR SHAPE, SIZE AND STRENGTH*

Many studies have emphasized the role of the lamina in determining the shape and mechanical strength of nucleus (reviewed in Hutchison 2002). In mouse spermatocytes, nuclei are hook shaped rather than spherical due to the expression of a spermatocyte-specific lamin, lamin B3, in these cells. Exogenous expression of lamin B3 in somatic cells resulted in nuclei adopting a hook-shaped morphology (Furukawa *et al.*, 1993). A dominant-negative mutant of lamin B1, although able to self-assemble into filaments *in vitro*, when transfected into cultured cells it caused a massive deformation of the NE and highly irregular and lobulated nuclei (Schirmer *et al.*, 2001). Similarly, RNAi knock down of Ce-lamin expression in *C.elegans* altered the nuclear morphology (Lui *et al.*, 2000). Alterations in the nuclear morphology are also observed in fibroblasts from LMNA knockout mouse (Sullivan *et al.*, 1999) and patients with LMNA mutations (Capanni *et al.*, 2003).

When lamins are depleted from the nuclear assembly extracts of Xenopus eggs (Newport *et al.*, 1990, Meier *et al.*, 1991, Goldberg *et al.*, 1995), or when lamina assembly is inhibited by dominant-negative lamin mutants (Spann *et al.*, 1997, Ellis *et al.*, 1997), although NE assembly still occurred, resulting nuclei were very small and fragile. Injection of the lamin-binding fragment of LAP2β into cells or egg extracts did not inhibit lamina assembly but inhibited nuclear growth (Young *et al.*, 1997, Gant *et al.*, 1999), suggesting that LAP2-lamin interaction may be essential for the structural dynamics of the nuclear lamina and the nuclear growth.

Time-lapse studies on transfected GFP-lamin in living cells showed that the NE surface undergoes constant deformation (Broers *et al.*, 1997, Moir *et al.*, 2000) and that lamins provide constant resistance to this deformation. In contrast, after Ce-lamin RNAi in

*C.elegans*, nuclei showed little resistance to deformation, and any deformation of the NE that occurred, was maintained for the rest of the cell cycle (Lui *et al.*, 2000). Therefore, lamins may act as tensegrity elements for the nucleus (Hutchison, 2002).

### *1.9.2. LAMINS IN ORGANISATION OF THE NUCLEAR PORES*

Lamins have an important role in the correct positioning of NPCs (reviewed in Hutchison 2002). In ultrastructural studies, lamin filaments are seen to interact with the nuclear rings of the NPCs and to interconnect adjacent NPCs. In both *Drosophila* mutants null for lamin Dm0 and in *C.elegans* after Ce-lamin RNAi, the NPCs float around and eventually cluster together (Lenz *et al.*, 1997, Lui *et al.*, 2000). Therefore lamina filaments position NPCs correctly by holding them apart. When lamina assembly is prevented in Xenopus egg extracts with dominant-negative lamin mutants, a nuclear-pore protein Nup153 is not incorporated into NPCs (Smythe *et al.*, 2000). When Nup153 is depleted from the same egg extracts, the NPCs show increased mobility in the NE and cluster together (Walther *et al.*, 2001). In cells with lamin A mutations, Nup153 is mislocalised to the ER and NPCs are clustered together (Muchir *et al.*, 2003). Based on these findings, a model has been proposed in which Nup153, as a component of the nuclear ring of NPCs, directly interacts with lamin B filaments, which support lamin polymerisation between adjacent NPCs, and in turn hold them apart. In the absence of Nup153 or lamina filaments, neither lamin filaments nor Nup153 respectively will associate with the ring and in both cases NPCs will float in the NE (Hutchison 2002).

Nup153 interacts with the import/export nuclear receptors in a Ran GTP-regulated manner by shuttling between the nuclear and cytoplasmic faces of the NPCs. Nup153 and Nup214 bind Smads 2/3, the effectors of TGFβ-mediated signalling pathway, and regulate their shuttling in and out of the nucleus (Xu 2002). These results suggest that lamins can indirectly influence nuclear transport and signalling pathways by affecting the distribution of nuclear pore proteins.

### *1.9.3. LAMINS IN RECRUITMENT OF PROTEINS TO THE INM*

The current model proposes that newly synthesized INM proteins become inserted at the interphase NE via their transmembrane domains after synthesis and diffusion through the ER membrane system and are retained there by binding to relatively immobile structures such as lamins and/or chromatin (reviewed in Collas and Courvallin 2000). After targeting to the NE, lamin assembly and association may in turn be stabilised by INM proteins. Whilst members of the LAP2 family of transmembrane proteins and LBR are thought to be anchored at the INM through interactions with the lamin B rod domain, three isoforms of LAP1 and emerin are thought to be anchored mainly through interactions with A-type lamins (reviewed in Hutchison *et al.*, 2001). Emerin binds to both A-type and B-type lamins *in vitro* (Fairley *et al.*, 1999, Clements *et al.*, 2000, Vaughan *et al.*, 2001, Lee *et al.*, 2001) and in cells either null for A-type lamins (Sullivan *et al.*, 1999, Harborth *et al.*, 2001), with low levels of A-type lamins (Vaughan *et al.*, 2001) or with lamin A mutations (Fairley *et al.*, 1999, Ostlund *et al.*, 1999), emerin is mislocalised to the ER. LAP1A and LAP1B isoforms interact with both lamins as heterodimers and as such have a higher binding affinity for lamins than LAP1C, which interacts with lamins as a monomer (Martin *et al.*, 1995). LAP1C localisation at the NE is A-type lamin dependent. In undifferentiated P19 cells, LAP1C is found at both the INM and ONM, whilst upon transfection of these cells with lamin A, it is immobilised at the NE (Powell and Burke 1990). Other reports, however, showed that LAP1C specifically binds to B-type lamins (Maison *et al.*, 1997).

### *1.9.4. REGULATION OF HETEROCHROMATIN AND GENE SILENCING*

#### 1.9.4. 1. The lamina proteins and chromatin binding

In eukaryotic cells, the genome is packaged into large-scale chromatin structures giving rise to distinct functional domains or chromosome territories (reviewed in Strouboulis and Wolffe 1996). The way in which these domains are established and propagated at each cell division is still an open question. Cytological studies show that a large proportion of condensed chromatin, called constitutive heterochromatin, which includes centromeres and telomeres, borders the INM. Constitutive heterochromatin is transcriptionally repressed, highly condensed, late replicating and rich in repetitive

sequences. During interphase, heterochromatin domains are mainly located at the nuclear periphery or surrounding the nucleoli. The amount of constitutive heterochromatin is much higher in more complex organisms. Among heterochromatin domain markers conserved from mammals to yeast are under-acetylated histone H4 isoforms together with histones H3, H2A and H2B, which form a histone octamer around which DNA can wrap, to achieve the first level of chromatin organisation, the core nucleosome. Histone hypo-acetylation correlates with transcriptional repression, as it allows tighter nucleosome compaction.

A repressive heterochromatin structure can spread locally to nearby genes so the expression of genes depends on their chromosomal position and hence the term 'position effect' silencing (reviewed in Brown *et al.*, 1999). 'Facultative' heterochromatin, which also appears cytologically condensed, consists of silenced genes whose transcription is repressed at particular stages of development. Many of the genes influencing 'position effect' have been found to encode structural components of chromatin such as histones or enzymes that modify the organisation of chromatin such as histone deacetylases. Since these structural components of repressive chromatin may themselves influence the position of repressive chromatin within the nucleus, the compartmentalisation of chromosomes is thought to have a direct role in gene regulation. The euchromatin, which is rich in actively transcribed genes, and appears relatively decondensed, is predominantly found within the nuclear interior. The positioning of inactive DNA is therefore not random, and the classic example is the mammalian female inactive X chromosome, which is located near the NE, whilst the active X chromosome extends into the nuclear interior.

Early morphological studies indicated that the distribution of lamin B coincides with peripherally located chromatin (Belmont *et al.*, 1993). Lamina thickness along the NE correlated quantitatively with regions most closely associated with chromatin. *In vitro* studies showed that A-type lamins bind directly to chromatin substrates such as polynucleosomes (Yuan *et al.*, 1991). Moreover, Shoeman and Traub 1990 found a moderate-affinity binding of A-type but not B-type lamins to a double-stranded oligonucleotide telomere sequence. The extreme C-terminal end of Xenopus lamin A contains a binding site for reconstituted chromosomes (Hoger *et al.*, 1991). In addition, both the rod domain (Glass *et al.*, 1993) and the C-terminal tail domain (Taniura *et al.*,

1995) in A-type lamins bind to chromatin. There is also evidence that the rod domains of polymerised B-type lamins bind to single-stranded DNA sequences known as matrix-attachment regions (MARs) and scaffold-attachment regions (SARs) and may therefore act as anchoring sites for chromatin domains (Luderus *et al.*, 1992, 1994, Zhao *et al.*, 1996). MARs/SARs were originally defined as DNA sequences that remain bound to the nuclear matrix/nuclear scaffold and are important in organising chromatin domains. Interestingly, the C-terminal tail domain of lamin A interacts with nuclear actin, the major constituent of microfilaments involved in cell shape, movement and structure, and this binding was proposed to regulate the movement of chromatin domains and/or structural state of the chromatin (Sasseville and Langelier 1998). Recently, it was found that A-type lamins adopt an immunoglobulin (Ig) fold in the C-terminal tail (Krimm *et al.*, 2002). These Ig-like regions function as DNA binding domains in several families of transcription factors. Indeed, it was showed that the Ig fold domain of A-type lamins binds multiple DNA sites in a sequence-independent manner, which could ensure tight connection between the NE and chromatin (Stierle *et al.*, 2003). These authors also suggest that this region may interact with sequence-specific DNA binding proteins and thus interfere with the expression of targeted genes in a cell-type specific manner. This type of binding is reminiscent of dimeric Ku70, a DNA repair and telomere binding protein.

Two isoforms of LAP2, LAP2α and LAP2β also bind to chromatin (Dechat *et al.*, 2001, Shumaker *et al.*, 2001). Otefin is essential for binding of NE-derived vesicles to chromatin (Ashery Padan *et al.*, 1997). Young arrest (YA) in Drosophila binds both lamin B and chromatin (Goldberg *et al.*, 1998, Yu *et al.*, 1999). LBR binds to lamin B and DNA (Ye and Worman 1994) as well as to chromatin (Duband-Goulet and Courvalin 2000).

### 1.9.4.2 The lamina proteins and gene silencing

Many nuclear lamina proteins interact directly with chromosomal proteins and as such might affect higher-order chromatin structure at the nuclear periphery. INM proteins such as LAP2 isoforms, Emerin and MAN1 as well as otefin and Lem-3 are members of the 'LEM domain' family owing to a common 43-residue domain near their N terminus that binds to DNA-binding protein BAF (Furukawa *et al.*, 1999, Lin *et al.*, 2000, Wang

*et al.*, 2002). BAF (barrier-to-autointegration-factor) is a small highly conserved protein of diffuse nuclear localisation in interphase cells that localises on the chromosomes during mitosis (Lee and Craige 1998). BAF was discovered as a cytoplasmic factor that was acquired by retroviral preintegration complexes and prevented viral DNA from undergoing suicidal self-integration (Lee and Craige 1998, Lin and Engelman 2003). Interactions between BAF and LEM domain proteins are proposed to be frequent but transient as studies with GFP-BAF revealed BAF to be highly mobile in living cells (Shimi *et al.*, 2004). It is reported that the intermolecular bridging property of BAF compacts DNA, which results in the formation of a higher-order chromosomal structure (Zheng *et al.*, 2000). Therefore, different combinations of interactions between lamins, LEM domain proteins and BAF may influence chromatin structure and disruptions in their attachments may be functionally relevant for human diseases caused by defects in nuclear lamina proteins (Shumaker *et al.*, 2001).

Lamins bind to specific core histones H2A and H2B via their tail domain (Taniura *et al.*, 1995). LBR forms a tight complex with heterochromatin-specific protein HP1 through histone oligomers H3/H4 (Polioudaki H. *et al.*, 2001). LBR-H3/H4-HP1 interactions are inhibited by histone acetylation and have a functional significance as they maintain the association of centromeres with the NE (Ye and Worman 1996). Interestingly, LBR also interacts with a chromatin-remodelling factor, histone deacetylase (HDAC), which may be involved in the regulation of chromatin and gene expression through histone modifications. Lamin B, LAP2β and LBR interact with HA95, a chromatin-associated protein of 95 kDa (Martins *et al.*, 2000), and LAP2β-HA95 interaction has been implicated in the regulation of initiation of DNA replication (Martins *et al.*, 2003).

A growing number of transcription factors, most of which are repressors, localise at the NE. Octamer-binding transcription factor (Oct-1), for example, co-localises with B-type lamins and actively represses the aging-associated collagenase gene when present at the NE (Imai *et al.*, 1997). Collagenase is an extracellular matrix-degrading enzyme involved in tissue remodelling and repair. In aging cells, translocation of Oct-1 from the NE coincides with a loss of transcriptional silencing by Oct-1 and an increased collagenase activity, which contributes to the pathogenesis of many tissue-degenerative processes. Retinoblastoma protein (Rb) actively represses transcription factor E2F-

dependent gene transcription by binding to E2F and by recruiting histone deacetylases. The active hypophosphorylated Rb co-localises with lamins A/C at the nuclear periphery (Mancini 1994) and binds to lamins A/C and LAP2α (Ozaki *et al.*, 1995, Markiewicz *et al.*, 2002a) **(Figure 1.6)**. LMNA -/- mouse embryonic cells target Rb for proteosomal degradation (Johnson 2004). A-type lamins also bind transcriptional repressor MOK2, which is involved in the repression of CRX (cone-rod homeobox) transcription factor-dependent gene transcription (Dreuillet *et al.*, 2002). BAF also binds to lamin A and represses Crx-dependent transcription (Wang *et al.*, 2002). Further to that, LAP2β interacts with mouse germ-cell-less GCL protein, which localises at the NE and binds to E2F/DP heterodimer. Together they form a repressor complex at the NE against E2F/DP transcriptional activity (Nili *et al.*, 2001). Interestingly, C-terminal domain of Emerin binds to GCL and binding of BAF to its N-terminal LEM domain interferes with this interaction (Holaska *et al.*, 2003). Emerin also binds to a death-promoting transcriptional repressor Btf (Haraguchi *et al.*, 2004) and a splicing factor YT521-B, and the latter interaction inhibits splice site selection by YT521-B (Wilkinson *et al.*, 2003). In addition, the MAN1 C-terminal domain binds to GCL, Btf and BAF whilst the N-terminal domain binds to emerin, lamin A, lamin B1 and BAF (Liu *et al.*, 2003, Mansharammani and Wilson 2005). Such a range of evidence supports the hypothesis that the nuclear lamina plays an active role in transcriptional control and chromatin structure and silencing (Nigg *et al.*, 1989).

### *1.9.5. THE LAMINA PROTEINS AND APOPTOSIS*

Apoptosis, or programmed cell death, regulates cell numbers during tissue development, tumour growth, immune response, and eliminates damaged cells (reviewed in Earnshaw *et al.*, 1995). During apoptosis, nuclei undergo specific morphological changes, including shrinkage of the cell and dramatic reorganisation of the cell nucleus, including proteolytic cleavage of the nuclear lamina, clustering of NPCs, chromatin detachment from the NE and DNA cleavage followed by active membrane blebbing and fragmentation of the cell into membrane-enclosed vesicles called apoptotic bodies. Apoptotic bodies express surface markers (phosphatidyl-serine) that signal for rapid phagocytosis by neighbouring cells and macrophages. Eliminating cells by apoptosis avoids release of the cytoplasmic contents into the intercellular space, which is known to cause inflammation and autoimmune diseases.

Apoptosis occurs in two physiological stages: a condemned phase and an execution phase (Earnshaw *et al.*, 1995). The stochastic nature of the transition from the condemned to the execution phase results in the condemned phase being extraordinarily variable in length (hours to days) whilst the execution phase is brief (15min-1h). Caspase proteases are centrally involved in apoptotic signalling and execution. Caspases are a family of aspartate-specific cysteine proteases, which exist as latent pro-caspases, and once activated by apoptotic stimuli, they promote apoptosis by specific limited proteolysis of key intracellular substrates such as lamins and other executor caspases. A-type and B-type lamins, LAP2α and LAP2β are among the early targets for caspase degradation before detectable DNA cleavage or chromatin condensation begins. During apoptosis, lamins are hyperphosphorylated by PKCδ, which is activated by caspase 3 and in turn facilitates access of caspases to the lamina prior to their proteolysis (Cross *et al.*, 2000).

Lamins are cleaved in the α-helical rod domain by caspase 6 at a conserved aspartic acid residue at position 230 (Asp230) (Lazebnik *et al.*, 1995, Oberhammer *et al.*, 1994, Takahashi *et al.*, 1996, Rao *et al.*, 1996). Since the rod domain is important for dimerisation and chromatin binding, the cleavage at this site represents an effective mechanism of breaking down the lamina and releasing the chromatin, and thus facilitates the nuclear breakdown (Rao *et al.*, 1996). A-type and B-type lamins show a differential breakdown pattern (Broers *et al.*, 2002). Parallel to DNA condensation, A-type lamins are found diffusely dispersed within nucleoplasm and this correlates with their partial cleavage, whereas B-type lamins become completely cleaved and their fragments remain associated with the NE even after extensive DNA condensation. These results revealed that only a small fraction of A-type lamin is needed for its complete disintegration from the nuclear lamina.

LAP2α is also an early target for caspase 3 and 6 during apoptosis and is cleaved once within its chromosome binding C-terminal domain, which is thought to facilitate chromatin reorganisation during apoptosis (Gotzmann *et al.*, 2000). This cleavage releases a soluble 50 kDa N-terminal fragment and a 28 kDa C-terminal fragment that remains highly insoluble. Other INM proteins such as LBR (Duband-Goulet *et al.*, 1998), emerin (Columbaro *et al.*, 2001), LAP2β and proteins of the nuclear pore

complex (e.g. Nup153) (Buendia *et al.*, 1999) are cleaved later than lamins and LAP2α. They are also cleaved by caspases 3/6 and their cleaved fragments remain associated with the NE. It is suggested that relatively late cleavage of INM proteins may explain why lamin B fragments remain attached to the remnants of the NE and this may be important during formation of apoptotic bodies (Broers *et al.*, 2002).

Interestingly, apoptotic nuclei sometimes resemble nuclei in lamin-deficient cells, which have clustered NPCs, detached chromatin and defective nuclear shapes, which confirms that phenotypic changes during apoptosis directly result from lamina degradation (Morris *et al.*, 2000). On the other hand, it is unlikely that lamin-deficient phenotypes arise due to apoptosis (Morris *et al.*, 2000) and it is suggested that apoptosis and lamin-deficiency cause similar changes via different mechanisms and/or that lamin deficiency may trigger inappropriate apoptosis in certain cell types (Morris *et al.*, 2001).

### *1.9.6. LAMINS IN ORGANISATION OF NUCLEAR BODIES*

#### 1.9.6.1. Lamins and nuclear bodies

Lamins associate with discrete sites of DNA synthesis and RNA processing called nuclear bodies (Moir *et al.*, 1994, Jagatheesan *et al.*, 1999, Kennedy *et al.*, 2000). Just as chromosomes are revealed to occupy defined loop domains and associate with the nuclear lamina (Ma *et al.*, 1999), nuclear bodies seem to be non-randomly distributed with respect to the nuclear envelope and are associated with the nuclear matrix (Spector *et al.*, 1993). However, lamins may only have an indirect role in organisation of nuclear bodies as destabilization of DNA loop anchoring sites also leads to disruption of replication sites (Ma *et al.*, 1999).

##### 1.9.6.1.1. *Lamins in S-phase and DNA replication*

S phase is the period in the cell cycle during which DNA becomes replicated. When replication initiates, replication foci are limited to a small number surrounding nucleoli, each representing a cluster of hundreds of replication origins, but they become more diffuse as time progresses (Kennedy *et al.*, 2000). They contain accumulations of proteins necessary for replication such as DNA polymerase α, PCNA etc. In replication

foci, nascent DNA is extruded, which implies that DNA moves through a fixed nuclear architecture within the foci. Electron microscopy has revealed that replication centres become attached to the filaments of nucleoskeleton (Hozak *et al.*, 1993). In mammalian somatic nuclei, replication foci are temporally bimodal as some are used in early S phase and others in late S phase (O'Keefe *et al.*, 1992). This arrangement reflects differential replication timing between euchromatic and heterochromatic regions in the nucleus, which is an important regulatory step in maintaining local chromatin organisation and gene activity (Wolffe *et al.*, 1991) and is thought to depend on structural associations with the nucleoskeleton (Hutchison *et al.*, 1988, 1989).

It is now widely accepted that lamins have a role in DNA replication, but it is still unclear how exactly they are involved (reviewed in Hutchison 2002). The most widely used cell-free extract capable of nuclear assembly and thus exploration of mechanisms therein involved is Xenopus oocyte extract (Newport *et al.*, 1986, Hutchison *et al.*, 1988). When B-type lamins were depleted from Xenopus egg extracts, small nuclei that failed to initiate DNA replication were assembled although they had intact NE and nuclear pores (Newport *et al.*, 1990, Meier *et al.*, 1991, Jenkins *et al.*, 1993, Goldberg *et al.*, 1995), indicating that lamins might have a direct role in DNA synthesis. Interestingly, a replication protein, proliferating cell nuclear antigen (PCNA) was not assembled into insoluble structures, indicating that lamins indirectly influence replication by supporting the correct assembly of the nucleoskeleton upon which replication centres are organised.

The influence of lamins on DNA replication can be investigated using dominant negative mutant lamins that sequester depolymerised wild-type lamins and prevent them from cycling and thus prevent lamina assembly (Schmidt *et al.*, 1995). N-terminal deletion mutants of lamin A (Spann *et al.*, 1997, Moir *et al.*, 2000, Izumi *et al.*, 2000) or B1 (Ellis *et al.*, 1997, Izumi *et al.*, 2000) led to altered assembly properties and nucleoplasmic aggregation of wild-type lamins in Xenopus egg extracts or in culture cells (Izumi *et al.*, 2000). These mutants were found to inhibit the elongation phase of replication by altering the distribution of replication factor complex (RFC) and PCNA (Spann *et al.*, 1997, Moir *et al.*, 2000) but did not inhibit DNA replication after the sites of DNA replication had been established (Ellis *et al.*, 1997, Izumi *et al.*, 2000). In the latter case, lamins may be needed for some step preceding the elongation phase of

replication, by having an effect on chromatin structure or on the formation of the nuclear scaffold, which is required for the formation of elongation complexes (Sturman *et al.*, 1998). Alternatively, these findings may reflect a role for A-type and B-type lamins in different stages of replication and thus regulation of the temporal replication programme. This hypothesis is supported by the observation that in somatic cells a fraction of lamin B1 re-distributes from the NE to replication centres during mid to late S-phase (Moir *et al.*, 1994), when heterochromatin moves from a peripheral to a central nuclear location in order to replicate. In contrast, A-type lamin foci co-localise with replication proteins during early G1 and early S-phase (Kennedy *et al.*, 2000), which coincides with the organisation of G1 chromatin and the initiation of euchromatin replication, respectively.

#### 1.9.6.1.2 *Lamins in RNA transcription and silencing*

The transcriptional machinery that synthesizes pre-mRNA localises on perichromatin fibrils found at the boundaries of condensed chromatin domains (Spector *et al.*, 1990, 1993, Fakan *et al.*, 1994). These fibrils contain nuclear ribonucleoprotein complexes whose density correlates with transcriptional activity. Components of the splicing machinery are recruited to perichromatin fibrils, where they carry out RNA processing, and are also found in 20-50 interchromatin granule clusters (IGCs) or speckles together with intron-containing pre-mRNAs and mature polyadenylated mRNAs. Speckles are believed to act as splicing assembly sites closely associated with the most actively transcribing genes. Once assembled with splicing machinery and nuclear ribonucleoproteins, the processed mRNA is transported across the NE into the cytoplasm where it associates with ribosomes, indicating that speckles may also be involved in mRNA export (reviewed in Lamond and Earnshaw 1998). Dynamic recruitment or storage of splicing factors within speckles is regulated by reversible phosphorylation (Misteli *et al.*, 1996) as well as the level of RNA splicing or transcriptional activity in the cell; speckles become considerably enlarged due to reduced recruitment of splicing factors from speckles in the presence of transcriptional inhibitors (Spector *et al.*, 1993), in pathological conditions (Fakan and Puvion 1980) or upon the inhibition of splicing (O'Keefe *et al.*, 1994). The transcription sites, active pol II and splicing speckles are components of detergent/high salt insoluble nuclear matrix (Kimura *et al.*, 1999, Spector *et al.*, 1993), indicating that RNA pol II activity and

organisation of splicing speckles depends on interactions with the nucleoskeleton (Kruhlak *et al.*, 2000). Indeed, the underlying protein architecture in speckles was found to physically connect the relatively dispersed granules within the speckle (Henzdel *et al.*, 1999). Given that lamins form a part of the internal nuclear framework and can bind to both DNA and RNA in vivo (Rzepecki *et al.*, 1998), they are the main candidate proteins for the organisation of RNA transcription and splicing.

There is now increasing evidence of lamin involvement in RNA transcription, processing and transport. Using loss-of-function *Drosophila* Dm lamin mutant, it was shown that resulting oocytes had a disrupted cell polarity due to a failure to properly localise mRNA in the cytoplasm (Guillemin *et al.*, 2001). In mammalian cells, dominant-negative lamin mutants inhibited RNA polymerase II activity by influencing the distribution of splicing factors (Spann *et al.*, 2002, Kumaran *et al.*, 2002) and a TATA binding protein (TBP) (Spann *et al.*, 2002) involved in forming pre-initiation complexes on RNA pol II promoters containing a TATA box, indicating that lamins act as a scaffold upon which the basal transcription factors required for RNA pol II transcription are organised. Using specific lamin antibody, internal lamin A structures have been found to associate with splicing factor speckles in dividing cells but not in muscle cells undergoing differentiation (Jagatheesan *et al.*, 1999, Muralikrishna *et al.*, 2001). Since ectopic expression of lamin A in myoblasts promotes muscle differentiation (Lourim and Lin 1989), the association of lamin A with speckles in undifferentiated myoblasts may suppress post-transcriptional expression of muscle-specific genes (Hutchison, 2002). Indeed, reorganisation of internal lamin structures seen in differentiating muscle cells (Muralikrishna *et al.*, 2001, Markiewicz *et al.*, 2005) may release trans-acting regulatory factors required to induce expression of muscle-specific genes.

#### *1.9.6.1.3. Lamins and PML (promyelocytic leukaemia) bodies*

The PML protein is a transcription factor that contains a zinc-binding RING finger, two cysteine rich domains and a C-terminal coiled-coil domain (reviewed in Brown *et al.*, 1999). In wild-type cells, it predominantly accumulates in a novel nuclear body surrounding interchromatin granules or speckles and is associated with the nuclear matrix. PML nuclear bodies are dynamic with respect to the cell cycle and there appears

to be a correlation between their prominence and proliferative states. It has been postulated that wild-type PML functions as a tumour-suppressor by regulating histone acetylation and transcription. Viral infections disrupt PML bodies. In patients with acute myeloid leukaemia (AML), the distribution of PML into 10-30 large bodies is disrupted and a micropunctuate pattern is observed instead. Acute myeloid leukaemia (AML) is a haemopoietic malignancy associated with a chromosome translocation, which results in an in-frame fusion of the PML gene to that of the retinoic acid receptor alpha (RARα). The resultant fusion protein is thought to aberrantly recruit HDAC to target genes leading to the repression of otherwise active genes. In particular, it may interfere with the retinoic acid signalling pathway that regulates LMNA gene expression. Interestingly, cells of patients with AML lack lamin A/C expression. Treatment of cells with retinoic acid (which induces lamin A expression) facilitates the restoration of PML bodies and myeloid differentiation.

## 1.10. LAP2 FAMILY OF PROTEINS

Lamina-associated polypeptides 2 (formerly known as thymopoietins) are a family of proteins that are generated by alternative splicing from a single gene LAP2 (Foisner and Gerace 1993, Harris *et al.*, 1994, Berger *et al.*, 1996). LAPs have been primarily characterised in mammals, up to 6 isoforms exist in humans and even 7 isoforms in mice. Invertebrates such as *Drosophila* and *C. elegans* do not encode orthologs for LAP2. In non-mammalian vertebrates such as chicken and zebrafish, the LAP2 gene does not encode for an alpha isoform and it is thus believed that LAP2α is novel to mammals (Prufert *et al.*, 2004). Interestingly, the N-terminal in all LAP2 proteins is homologous to a thymic polypeptide, thymopoietin, which was found to be secreted and to affect neuromuscular transmission and T-cell differentiation (Goldstein *et al.*, 1974). However, the secreted polypeptide was thought to be artificially generated during isolation of the larger thymopoietin protein from adult thymus, one of the tissues where LAP2 proteins are most abundantly expressed (Crafford *et al.*, 1994). Interestingly, thymopentin, a synthetic peptide of N-terminal thymopoietin, had originally been used as an immunoregulatory drug in patients with rheumatoid arthritis and atopic dermatitis (in Crafford *et al.*, 1994), some of the autoimmune disorders which have been later found to produce autoantibodies against LAP2 proteins (McKeon *et al.*, 1983).

### *1.10.1. THE MEMBRANE-BOUND LAP2 ISOFORMS*

LAP2β is the best-characterised INM protein of the LAP2 family (Foisner and Gerace 1993, Furukawa *et al.*, 1995). All mammalian LAP2 isoforms have a closely related N-terminal nucleoplasmic domain of variable length with an NLS signal sequence (reviewed in Dechat *et al.*, 2000) **(Figure 1.7a)**. Except for LAP2α and LAP2ζ, they all contain a single-membrane spanning region and a short luminal domain at their C-terminus. LAP2β has the longest N-terminal domain of 408 aa. Due to alternative splicing, LAP2ε, δ and γ lack N-terminal stretches of 40, 72 and 109 aa respectively, but are otherwise identical to LAP2β. LAP2ζ is the smallest isoform that lacks the transmembrane and luminal regions. LAP2α is structurally and functionally a unique isoform. It shares only the first N-terminal 187 residues with all other LAPS and contains a unique C-terminal domain of 506 aa but not a transmembrane domain. Whilst LAP2β is restricted to the NE, LAP2α is distributed throughout the nucleus except for nucleoli (Dechat *et al.*, 1998). LAP2β, but not LAP2α, binds to B-type lamins and the LAP2β lamin-binding domain is also the NE targeting domain (Furukawa *et al.*, 1998). This region is also present in the smaller isoforms LAPζ and LAPδ, and is only partly conserved in LAPγ. LAP2 proteins share a BAF-binding LEM domain (aa 111-152) (Furukawa *et al.*, 1999) and a LEM-like domain (aa 1-85) at their N-terminus (Cai *et al.*, 2001) **(Figure 1.7b)**. The LEM-like domain binds to DNA and chromosomes directly. LAP2β associates with chromosomes in a lamin-independent manner via its LEM-like domain (Furukawa *et al.*, 1998) whilst LAP2α interacts with chromosomes via both an α-specific C-terminal domain and a N-terminal LEM-like domain (Vlcek *et al.*, 1999).

### *1.10.2. NUCLEOPLASMIC LAP2α*

LAP2α co-localises with A-type lamins in the nucleoplasm but not at the NE. LAP2α is found in stable SDS/high salt-resistant complexes with A-type lamins during interphase and nuclear reassembly (Dechat *et al.*, 1998). LAP2α specific C-terminal region associates with a C-terminal tail of lamins A/C *in vivo* and *in vitro*. Therefore, LAP2α is both a chromatin-associated protein and a component of the nuclear matrix. Disruption of endogenous lamin A structures by the expression of dominant-negative lamin B mutants in Hela cells caused LAP2α but not LAP2β to relocate to intranuclear lamin

A/C aggregates (Markiewicz *et al.*, 2002a). Interestingly, emerin null cells also have mislocalised LAP2α (Markiewicz *et al.*, 2002b).

LAP2α is the first among the lamina proteins to associate with chromosomes during nuclear reassembly before LAP2β-containing membranes enclose decondensing chromosomes (Vlcek *et al.*, 1999). LAP2α and BAF initially accumulate at telomeres during anaphase and then spread to the core regions on chromosomes (Dechat *et al.*, 2004). A subfraction of A-type lamins associates with chromosomes in early telophase and is thought to be targeted via association with LAP2α. Early association of LAP2α with chromosomes and specifically telomeres has led these authors to suggest a role for LAP2α in post-mitotic chromatin organisation and telomere positioning. LAP2α is the only LAP2 member constitutively expressed during spermiogenesis suggesting a role for LAP2α in differentiation-dependent chromatin remodelling and possibly fertilisation (Alsheimer *et al.*, 1998). Over-expression of C-terminal fragments of LAP2α inhibited assembly of membranes and A-type lamins around chromosomes and caused a cell cycle arrest (Vlcek *et al.*, 2002). RNAi knockdown of LAP2α would be necessary to establish its precise role in cell cycle progression. Vlcek *et al.*, 1999 proposed that the sequential association of LAP2α and LAP2β with chromosomes during nuclear assembly may be explained by an α-specific C-terminal nuclear targeting domain that is absent in LAP2β. Although both N- and C-terminal regions of LAP2α are essential for a timely and coordinated nuclear reassembly, the C-terminal domain co-ordinates the initial association with chromosomes whilst the N-terminal LEM-like domain mediates targeting of membranes to chromosomal surfaces. The N-terminal BAF-binding LEM domain present in both LAP2α and β interacts with BAF at the later stages of nuclear assembly, perhaps due to post-translational modifications of these proteins or due to the apparent increased affinity of LAP2 for established BAF-DNA oligomeric structures (Shumaker *et al.*, 2001).

## 1.11. RETINOBLASTOMA PROTEIN AND GROWTH REGULATION

### *1.11.1. CELL CYCLE*

The primary components of cell cycle machinery are cyclin-dependent kinases (CDKs). CDKs are a family of related serine/threonine kinases regulated by association with

regulatory cyclin subunits into cyclin-CDK complexes, whose associations are in turn regulated by a series of phosphorylations/dephosphorylations of Cdks (reviewed in Mittnacht *et al.*, 1998). A further level of CDK regulation is achieved via two families of cyclin-dependent kinase inhibitor proteins (CDKIs) that bind directly to CDKs and inactivate CDK complexes. The INK4 proteins are specific inhibitors of G1 phase-specific cyclin D/CDK4/6 complexes and the Kip/Cip inhibitors have a broader specificity. As such, cyclin-CDK complexes represent the ultimate targets among checkpoint pathways. The major checkpoint pathways include: Retinoblastoma checkpoint in late G1 phase, DNA damage checkpoint in G1 and S phase, and Anaphase checkpoint in G2/M phase. Two major cyclin-cdk complexes phosphorylate Rb during G1 phase of the cell cycle: cyclinD/CDK4/6 acts in early to mid G1, and cyclin E/CDK2 acts in late G1 (reviewed in Tamrakar *et al.*, 2000) **(Figure 1.8)**. Whilst hypophosphorylation of Rb by the former kinase activates its growth-suppressing function, the concerted activities of both kinases in late G1 hyperphosphorylate Rb and inactivate its function. Protein phosphatases PP1 and PP2A are a class of serine/threonine phosphatases implicated in the regulation of Rb dephosphorylation. PP1 dephosphorylates pRb during M phase (Durfee *et al.*, 1993) and also binds to select forms of hypophosphorylated Rb (Tamrakar *et al.*, 2000). PP1 regulates several other processes in mammalian cells including spliceosome assembly, pre-mRNA splicing, RNA II polymerase activity and mitotic exit. PP2A is found to dephosphorylate Rb after exposure to genotoxic stimuli such as DNA damage and oxidative stress (Cicchillitti *et al.*, 2003, Avni *et al.*, 2003).

### *1.11.2. RETINOBLASTOMA PROTEIN (RB)*

The human retinoblastoma gene (RB) on chromosome 13 has been isolated by molecular cloning in 1986 (Friend *et al.*, 1986, Lee *et al.*, 1987). The RB gene belongs to a growing number of tumour suppressor genes and a loss of its function is associated with malignant transformation. The RB gene is found mutated in a number of tumour cells including retinoblastomas, osteosarcomas and small cell lung carcinomas. Expression of Rb cDNA in tumour cell lines lacking Rb expression elicits a variety of responses such as morphological reversion, loss of tumorigenicity, growth inhibition and senescence (Huang *et al.*, 1988). The Rb family consists of three members: Rb and related proteins p107 and p130, collectively called pocket proteins. Rb is expressed

constitutively in most cell types regardless of their proliferation status (Furukawa *et al.*, 1990). During the cell cycle of actively proliferating cells, Rb is expressed as a population of differentially phosphorylated isoforms that migrate heterogeneously as 105 to 115 kDA species on SDS polyacrylamide gels (Buchkovich *et al.*, 1989, DeCaprio *et al.*, 1992). Hyperphosphorylation of Rb occurs in a cell-cycle dependent manner, being first detectable upon entry into S phase and lost upon emergence from M phase (Ludlow *et al.*, 1990). Processes that lead to growth arrest of cells such as the deprivation of growth factors, high cell density, genotoxic stress and induction of differentiation or senescence are associated with the disappearance of the hyperphosphorylated forms of Rb (Chen *et al.*, 1989, Avni *et al.*, 2003). Therefore, hyperphosphorylation of Rb is a regulatory event leading to inactivation of its growth-repressing functions (DeCaprio *et al.*, 1989).

The hypophosphorylated Rb species are tightly associated with the nuclear structure (Mittnacht and Weinberg 1991, Mancini *et al.*, 1994). Although Rb binds to chromatin, its association with the nucleus does not depend on the integrity of the chromatin as shown by DNAse digestion/high salt experiments. In contrast, the hyperphosphorylated Rb species, although localised in the nucleus, become eluted under low salt conditions. As such, hypophosphorylated Rb was thought to bind to components of the nuclear matrix such as lamins and/or specific transcription and replication compartments. A large body of evidence supports the notion that the tight nuclear interaction of Rb hypo-phosphorylated forms is essential for its growth-regulating functions. Most mutant forms of Rb recovered from tumours contain mutations in the binding pocket of C-terminal region (Hu *et al.*, 1990). These Rb mutants show an inability to become hyperphosphorylated but are also weakly associated with the nuclear compartment (Templeton *et al.*, 1991), which argues that underphosphorylation *per se* does not suffice to ensure tight association of Rb with the nucleus, but requires the integrity of the complex between Rb and its nuclear binding partner (Mittnacht and Weinberg 1991). This idea is supported by the findings that binding of viral oncoproteins, which occurs via C-terminal region of hypophosphorylated Rb, (Ludlow *et al.*, 1989) is also impaired (Hu *et al.*, 1990). Moreover, the binding pocket in Rb has been shown to mediate association with several cellular proteins including transcription factor E2F and related proteins (Chellappan *et al.*, 1991). Binding of Rb to E2F during G1 phase of the cell cycle is thought to sequester this transcription factor in an inactive complex and

prevent transcriptional activation of early S-phase genes (Dou *et al.*, 1992) (see **Figure 8**). Phosphorylation or oncoprotein E1A binding release Rb from this complex and in turn activate E2F (Shirodkar *et al.*, 1992, Chellappan *et al.*, 1992). Indeed, Rb was found to interact with lamin A through its C-terminal nuclear anchorage domain in vitro (Mancini *et al.*, 1994, Okazaki *et al.*, 1995). More importantly, A-type lamin/LAP2α complexes are found to interact with the hypophosphorylated Rb protein (Markiewicz *et al.*, 2002a). The anchorage of hypophosphorylated Rb correlates with the expression of LAP2α during cell cycle. Disruption of LAP2α/lamin A/C to intranuclear aggregates by dominant negative lamin mutants leads to redistribution of Rb to the same aggregates.

Although transcriptional repression of E2F genes is currently the best understood mechanism of Rb growth regulation, not all Rb activity is mediated via E2F or during G1 phase of the cycle. Rb binds to other transcription factors such as Sp1 and ATF2 (Kim *et al.*, 1992a, 1992b). Rb can also positively modulate transcription of genes involved in growth inhibition such as the gene for transforming growth factor β1 (Kim *et al.*, 1991) and this may play an important role during senescence (Kim *et al.*, 2004). Rb has also been found to localise with and bind to a nuclear matrix protein p84 in speckle compartments during early G1 (Durfee *et al.*, 1994). Rb is specifically localised in replication compartments during early S phase (Kennedy *et al.*, 2000) suggesting that it may have a function in DNA replication. Overexpression of Rb during G2 phase leads to Rb-dependent cell cycle arrest (Karantza *et al.*, 1993). Rb is phosphorylated in at least three stages during cell cycle, the last stage occurring in G2 (DeCaprio *et al.*, 1992). These reports point out that each Rb phosphorylation event independently or in combination may affect different Rb growth-suppressing activities during the cell cycle which argues against the simple model of Rb growth control whereby hyperphosphorylation of Rb during late G1 phase completely abolishes its growth-suppressing activity (Mittnacht *et al.*, 1991).

## 1.12. THE LAMINA PROTEINS AND DISEASES

### *1.12.1. LAMINOPATHIES*

The indispensable role of the lamina in diverse and fundamental cellular processes may account for a wide spectrum of human disorders being ascribed to mutations at the

LMNA locus. To date, there are at least 50 known mutations in LMNA gene (reviewed in Goldman *et al.*, 2002) causing at least eleven laminopathies **(Table 1.1)**. Although the lamina has an essential structural function in the nuclei of all cell types, the emerging evidence from human laminopathy diseases suggests that lamina proteins can have highly specialised as well as tissue-specific functions.

Laminopathies can be loosely divided into two categories: those affecting striated muscle and those affecting adipose tissue, bone and neurones. Diseases of striated muscle caused by mutations in LMNA gene include: the autosomal dominant form of Emery-Dreyfuss muscular dystrophy (AD-EDMD) (Bonne *et al.*, 1999), limb girdle muscular dystrophy with atrioventricular conduction disturbances type 1B (LGMD1B) (Muchir *et al.*, 2000) and dilated cardiomyopathy with conduction system disease (DCM-CD) (Fatkin *et al.*, 1999). A single homozygous recessive mutation has been implicated in axonal Charcot-Marie-Tooth syndrome type 2B1 (CMT2B1), a peripheral neuropathy with reduced axon density, demyelinated axons and peripheral muscle weakness and wasting (de Sandre-Giovanolli *et al.*, 2002). Dunnigan's familial lipodystrophy (FPLD) (Cao and Hegele 2000, Shackleton *et al.*, 2000) and mandibulo-acral dysplasia (MAD) (Novelli *et al.*, 2002) primarily result in loss and redistribution of white adipose tissue. Hyperlipidemia, insulin resistance and diabetes are common in FPLD (Kobberling and Dunnigan 1986) and MAD patients. FPLD is not evident until puberty, suggesting a possible endocrine involvement, at which time there is a loss of subcutaneous fat in regions such as the extremities and gluteal areas along with excess fat deposition in the neck, back and face. MAD patients also show bone defects including craniofacial abnormalities, osteolysis of teminal digits and hypoplasia of clavicles, as well as alopecia and cutaneous atrophy (Novelli *et al.*, 2002). Interestingly, mutations in ZMPSTE24, a prelamin A processing protease also cause MAD (Agarwal *et al.*, 2003).

Historically, the first genetic locus linked to EDMD was X-linked gene STA on Xq28 that encodes the INM protein. Mutations in this gene cause an X-linked recessive form of EDMD (Bione *et al.*, 1994), which is the third most common X-linked form of muscular dystrophy after Duchenne and Becker. Interestingly, it was only later that emerin was identified as an INM protein (Manilal *et al.*, 1996). Emerin mutations are dispersed all over the protein coding sequence. Non-sense mutations result in

production of truncated unstable proteins (Nagano *et al.*, 1996, Manilal *et al.*, 1997) and missense mutations result in modified proteins with reduced expression due to aberrant targeting or unstable association with the NE (Ellis *et al.*, 1998, Markiewicz *et al.*, 2002b). In any case, the clinical phenotypes of X-EDMD patients are similar and consistent with a null phenotype (Ellis *et al.*, 2000). Mutations in LMNA gene causing AD-EDMD have been first identified by Bonne *et al.*, 1999. Typically, EDMD symptoms are first detected at 4-5 years of age and the disease progresses slowly. Patients exhibit tendon contractures in the heels, elbows, and the neck, a rigid spine, wasting and weakness of the musculature of the pelvic girdle, biceps and triceps, the disappearance of deep tendon reflexes, cardiac conduction problems and facial muscle weakness. However, the first symptoms in X-EDMD are generally contractures, whereas in AD-EDMD muscle weakness appears before contractures (Mercuri and Muntoni 2001). A cardiac pacemaker is usually required by the third or fourth decade of life. Cardiomyopathy leading to ventricular dysfunction and often requiring a heart transplant is a more common feature of AD-EDMD.

In AD-EDMD, gene changes include missense point mutations, frameshift mutations, deletions and nonsense mutations (reviewed in Goldman *et al.*, 2002). Diseases caused by LMNA mutations have been found in all exons except for exon 10. Since there is a naturally occurring A-type lamin isoform without exon 10 (Machiels *et al.*, 1996), it is possible that mutations in exon 10 are not debilitating in the laminopathy context. In addition, the position of the mutation within the LMNA gene seems to sometimes determine the cell type that becomes affected. Mutations for AD-EDMD are present in all domains of LMNA gene. DCM and LGMD1B mutations are only present in the rod and carboxy-terminal domains and CMT2B1 mutations are present mainly in the rod domain. Two mutations causing DCM are also found in lamin A-specific and lamin C-specific C-terminal regions demonstrating that mutations in either lamin can cause cardiac pathology (Morris *et al.*, 2001). Interestingly, a silent polymorphism in exon 2 has been found to cause LGMD1B due to activation of a cryptic splice site and production of lamin protein containing intron sequences (Todorova *et al.*, 2003). FPLD and MAD mutations have mainly been found in the tail domain of A-type lamins, although a recent report described two patients with FPLD mutations close to the N terminus (Garg *et al.*, 2002). This suggests that particular lamin A/C domains have a

high degree of functional specificity, and opens the possibility that mutant-specific effects could underlie the phenotypic spectrum.

Surprisingly, the clinical expression of the same LMNA mutation often varies in severity among members of the same family (Fatkin *et al.*, 1999, Cao *et al.*, 2000, Brown *et al.*, 2001). A nonsense mutation in the rod domain has been reported to cause LGMD1B when in a heterozygous state but when in a homozygous state, it caused a loss of lamin A/C and a severe progeroid phenotype in the newborn child including multiple skin contractures, severe muscular dystrophy with fibrosis and an almost complete absence of muscle fibers in the diaphragm (Muchir *et al.*, 2003). Moreover, the clinical designations of laminopathies quite often overlap and patients with the most severe forms of AD-EDMD frequently have symptoms of other laminopathies such as FPLD. For example, a severe histological phenotype is seen in LMNA-knockout mice, which have both skeletal and cardiac muscle wasting, a loss of white fat, neuropathic features of peripheral axons and possibly bone defects all arising primarily from defects in mesenchymal tissue stem cells (Sullivan *et al.*, 1999). As such, these mice show a compound AD-EDMD/DCM/CMT2B1 phenotype. Additionally, these mice display impaired spermatogenesis due to a severe defect in synaptic pairing of the sex chromosomes (Alsheimer *et al.*, 2004). Laminopathies are therefore proposed to arise from alterations and/or disturbances in differentiation, maintenance, repair and regulation of mesenchymal cells with the possible exception of CMT2 (Wilson *et al.*, 2000). Differences in the individual genetic backgrounds may dictate such clinical phenotypes, and allelic variation in lamin binding and/or regulatory proteins may thus further modify the effect of a particular lamin mutation. Indeed, novel missense mutations in the head and rod domains of lamins A/C have been reported in patients with both FPLD and DCM-CD and raised the possibility of a multisystem dystrophy syndrome (Garg *et al.*, 2002). Consequently, some investigators are of the opinion that AD-EDMD, FPLD, DCM and LGMD1B represent a spectrum of related disorders rather than separate laminopathy diseases.

There are three mechanisms proposed for the autosomal dominance of LMNA mutations. One is haploinsufficiency, whereby a reduced level of functional lamins A/C is insufficient for normal lamina function (reviewed in Goldman *et al.*, 2002). A second mechanism is a gain-of-deleterious-function by the mutant protein (Goldman *et al.*, 2004). The third is the existence of a functional multimer that does not tolerate a

defective subunit so normal lamina formation becomes disrupted even if only present in 50% of lamin molecules. However the actual mechanism by which mutations in LMNA alter nuclear function and cause tissue-specific disease pathologies is as yet undetermined. Still, there are three theories put forward to explain the mechanisms behind the effects of LMNA mutations.

### 1.12.1. 1. Structural hypothesis

Mutant lamin A protein is proposed to weaken the lamin polymer, resulting in fragile nuclei that do not provide adequate structural integrity and exhibit greater susceptibility to mechanical stress (Hutchison *et al.*, 2001). Indeed, dysmorphic nuclei have been seen in fibroblasts of all laminopathy patients and LMNA knockout mice (Sullivan *et al.*, 1999, Raharjo *et al.*, 2001, Ostlund *et al.*, 2001, Vigouroux *et al.*, 2001, Muchir *et al.*, 2003). Significant redistribution of NE-associated proteins and nuclear pore components is seen in these dysmorphic nuclei. Redistribution of NE proteins is associated with the localised separation of the ONM from the INM, resulting in an increase in the intramembranous perinuclear space and a leakage of chromatin into the cytoplasm (Fidzianska *et al.*, 1998, 2003).

For cardiac and skeletal muscles and tendons, the contractile forces generated from muscle contraction might deform or rapture these fragile nuclei, resulting in cell death and muscle wasting by inducing apoptosis (Sullivan *et al.*, 1999). Direct analysis of the mechanical properties of lamin null fibroblasts in response to physical stretching revealed that nuclei were less rigid than wild type and cells were more prone to apoptosis and necrosis in response to repetitive mechanical strain (Lammerding *et al.*, 2004, Broers *et al.*, 2004). Lamin null cells showed an abnormal direction of deformation upon compression, indicating defective nucleo-cytoskeletal integrity (Broers *et al.*, 2004). All major load-bearing structures of cytoskeleton including actin, vimentin and tubulin filaments showed disturbed interactions in the perinuclear regions of lamin null cells, implying a role for lamins in maintaining cellular tensegrity. Emerin-lamin complexes bind to actin (Sassevile and Langelier 1998, Lattanzi *et al.*, 2003, Holaska *et al.*, 2004) as well as desmin in muscle cells (Nikolova *et al.*, 2004) and these disrupted stabiliser elements may in turn disrupt transmission of mechanical stimuli across the NE (Dahl *et al.*, 2004). Indeed, lamin null cells showed diminished

activation of NF-kβ mechano-transduction signalling in response to mechanical stress (Lammerding 2004).

However, this hypothesis does not explain the development of laminopathies such as FPLD and CMT2. Nonetheless, the tissues affected in laminopathies may share unique lamin binding proteins which all become disrupted (Wilson *et al.*, 2000). For example, Syne1 is required for the appropriate positioning of post-synaptic nuclei and impaired lamin/Syne-1 interaction may lead to the anomalous positioning of post-synaptic nuclei and an aberrant synapse in CMT2 (Burke *et al.*, 2002).

### 1.12.1.2. Regulatory hypothesis

Ultrastructural studies of lamin null mouse cells revealed that heterochromatin was not adjacent to the NE in the blebbed regions (Sullivan *et al.*, 1999). Therefore, changes in heterochromatin organisation and/or alterations of lamin-DNA binding needed to establish or maintain particular patterns of gene expression may play a role in the pathophysiology of some laminopathies (Stierle *et al.*, 2003). Mutant lamins may also change tissue-specific gene expression by altering assembly and/or localisation of components of transcription complexes and thus alter transcriptional processes (Wilson *et al.*, 2000). These altered interactions may involve general transcriptional regulators such as Rb and MOK2 proteins (Markiewicz *et al.*, 2005, Dreuillet *et al.*, 2002). Rb is targeted for proteosomal degradation in lamin null cells, which may lead to aberrant cell cycle control (Johnson *et al.*, 2004). Other important interactions of lamins are also reported to be impaired in laminopathies such as those with emerin, YT521-B and Myne-1. Emerin/lamin complexes regulate splicing-associated factor (YT521-B) that is directly involved in correct RNA splicing in muscle (Wilkinson *et al.*, 2003). Emerin-lamin complexes may also act as a recruitment structure for other muscle-binding partners such as Myne-1, a spectrin-repeat protein, which interacts with lamins at the NE of mature muscle cells (Mislow *et al.*, 2002b). The binding of adipocyte differentiation factor SREBP1 (sterol-response-element-binding protein 1) to lamin A was significantly reduced by FPLD mutations and was proposed that this may lead to impaired adipocyte differentiation (Lloyd *et al.*, 2002). It has been suggested that lamin A/C-LAP2α complexes may also be affected in laminopathies (Hutchison *et al.*, 2001, Goldman *et al.*, 2004) because LAP2α binds to the C-terminal tail of lamin A/C where

many different laminopathy mutations have been found. However, an involvement of LAP2α in laminopathies remains to be seen.

#### 1.12.1.3. ER hypothesis

The endoplasmic reticulum (ER) is a key organelle in all eukaryotic cells (reviewed in Mounkes *et al.*, 2001). It is a site of protein translation, folding, modification and transport of proteins to the cell membranes or their exocytosis out of the cell. This hypothesis suggests that mutations in the LMNA gene bring about changes in the NE, which in turn may lead to perturbation of the peripheral ER due to an altered distribution of emerin and other INM proteins to the ER. Since the ER is a main site of cholesterol and fatty acid synthesis, abnormal accumulation of INM proteins in the ER could alter lipogenesis or lipogenic signalling in lamin mutant cells, leading to aberrant adipocyte development and lipodystrophic disease. In skeletal and cardiac muscle, $Ca^{2+}$ release from the sarcoplasmic reticulum (SR) may be compromised during contractions by alterations in the SR, which is contiguous with the ER in muscle tissues. Alternatively, generalised ER stress resulting from the inappropriate accumulation of INM proteins in the ER could promote aberrant ER/nucleus signalling related to misfolding or ER overload with consequent downstream effects on gene expression and cell viability. For example, a loss of interaction between SREBP1 and lamin A may affect the ER/nucleus signalling related to regulation of sterol abundance in the ER. It is known that depletion of sterols in the ER leads to unregulated transcription of genes containing sterol-regulatory elements (SRE) in their promoters in order to regulate membrane biogenesis.

### *1.12.2. PROGERIAS AND PROGEROID LAMINOPATHIES*

Hutchinson-Gilford progeria syndrome (HGPS) is a rare disease, undetectable at birth, demonstrated by recent studies to be caused by mutations in LMNA gene (de Sandre-Giovanolli *et al.*, 2003, Eriksson *et al.*, 2003, Cao *et al.*, 2003). Dominant inheritance is more likely, although recessive cases appear as a result of germinal mosaicism (Chen *et al.*, 2003). Since it was first described in 1886, more than 100 cases have been reported worldwide. Patients show symptoms of premature aging (they appear to age ten times faster than normal individuals), including severe postnatal growth retardation, midface

hypoplasia, micrognathia, hypogonadism, wrinkled skin, loss of subcutaneous fat, alopecia, generalised osteodysplasia with osteolysis, poor muscle development and premature atherosclerosis. The average age of death in patients is 12-15 years, usually by myocardial infarction due to coronary artery disease or stroke (Sarkar *et al.*, 2001). Since patients with HGPS show low incidence of certain features associated with ageing including an increase in tumour susceptibility, osteoporosis, diabetes, cataract formation or cognitive degeneration, HGPS is thought to only partially reproduce the aging process and is thus classified as a segmental progeroid syndrome (Martin and Oshima 2000). Genome-scale expression profiling of HGPS cells revealed widespread transcriptional misregulation at developmental level leading to mesodermal/ mesenchymal defects and accelerated atherosclerosis (Csoka *et al.*, 2004). Interestingly, MAD shares several feature with HGPS, although life expectancy is not shortened, suggesting that the two disorders may be allelic.

A single base substitution from C to T in the LMNA gene resulting in a silent Gly to Gly change at codon 608 within exon 11 (G608G) has been found in a subset of individuals with HGPS (de Sandre-Giovanolli *et al.*, 2003). This silent mutation reveals a cryptic splice site in the LMNA gene, resulting in the lack of 50 amino acids from the C-terminal domain of lamin A (aa 609-658) before the extreme C-terminal end containing the CaaX motif (659-664), thus leaving lamin C protein unmodified (de Sandre-Giovannoli *et al.*, 2003, Eriksson *et al.*, 2003). This shortened form of lamin A has been named Progerin. The absence of 50 amino acids from the C-terminus of lamin A deletes an endoproteolytic cleavage site required for the processing of prelamin A to its mature form. The mutated prelamin A is presumed to remain with a permanently farnesylated/methylated C-terminal cysteine. In addition, mutant lamin A protein suffers from a loss of eleven serine and three tyrosine potential phosphorylation sites present in mature wild type lamin A, as well as three phospho-serine sites and one tyrosine site present in wild-type pre-lamin A. HGPS cells produce both normal and truncated transcripts by the same mutated allele, indicating that the mutation inhibits transcription of the normal allele, acting as a dominant negative mutation (de Sandre-Giovanolli *et al.*, 2003). Recently, it has been confirmed that an introduction of modified nucleotides targeted to the aberrantly activated cryptic splice site in lamin A gene reverses cellular HGPS phenotype (Scaffidi and Misteli 2005). Other rare HGPS mutations include single base pair mutations within the same exon 11 (G608S), in other exons of the

LMNA gene (R471C, R527C) and a missense mutation in exon 2 (E145K) (Cao *et al.*, 2003). A homozygous missense LMNA mutation has been reported in recessive HGPS (Plasilova *et al.*, 2004). The mutation rate of CpG nucleotides is generally 8.5 x higher than that of an average dinucleotide and *de novo* recurrence of the same point mutation in cytosine residues of most HGPS cases may be due to this nucleotide being a mutational 'hotspot' (reviewed in Novelli *et al.*, 2003).

Another premature aging syndrome is Werner's syndrome. In the majority of patients (83%), Werner's syndrome is inherited as an autosomal recessive disease due to mutations in WRN, a 3'-5' RecQ DNA helicase-exonuclease that unwinds DNA and cleaves nucleotides from DNA termini (Martin and Oshima 2000). Patients with this disease show a high incidence of early-onset cataracts, arthrosclerosis, diabetes, premature greying of hair and early death, usually in their late 40s. Werner's syndrome is also associated with an increased risk of rare mesenchymal neoplasms, although the average age of death is much later than in HGPS. Atypical cases of Werner's syndrome do not carry detectable mutations in WRN gene. A recent report revealed that 13% of these atypical cases had missense mutations in lamin A gene resulting in amino acid substitution in the N-terminal or rod domains (Chen *et al.*, 2003). Unlike typical Werner's syndrome patients who have a mean age of diagnosis at 39 years, these atypical Werner's syndrome patients have a more severe phenotype with a mean age of initial symptoms being 13 years (Chen *et al.*, 2003). The clinical pathologies of AWS include muscular atrophy, lipodystrophy, insulin-resistant diabetes mellitus, cardiovascular pathology, short stature, atrophic skin and grey or sparse hair.

The most recently described three progeroid-like laminopathies include one in a patient showing generalised lipoatrophy, insulin-resistant diabetes, hepatic steatosis, hypertrophic cardiomyopathy with valvular involvement and disseminated leukomelanodermic papules caused by the same mutation involved in AWS (Caux *et al.*, 2003). Another one is Restrictive Dermopathy (RD), which is one of the most deleterious laminopathies so far identified in humans. RD or 'tight skin contracture' syndrome is characterised by intrauterine growth retardation, tight and rigid skin with erosions and epidermal hyperkeratosis, multiple joint contractures, progeroid facial features, mineralization defects of the skull, absent eyelashes and eyebrows, pulmonary hypoplasia and early neonatal death (Navarro *et al.*, 2004). RD is caused by either

heterozygous splicing mutation in the LMNA gene found in HGPS, or heterozygous non-sense mutations in ZMPSTE-24/FACE 1 gene. The third one is a congenital Seip-Berardinelli syndrome characterised by generalized lipodystrophy, cardiomyopathy, osteosklerosis, retinopathy, anginal pectoris, pancreatic amyloidosis and variable degrees of cognitive impairment (Csoka *et al.*, 2004). The findings that lamin A mutations affect longevity offered another potential mechanism for development of laminopathies; the 'cell fate' model suggests that lamin mutations are linked to premature ageing (in Dechat *et al.*, 2004).

Immunocytological analyses with antibodies to lamins A/C showed HGPS cells to be larger than control ones, exhibiting large vacuoles and abnormal mitotic figures (de Sandre-Giovanolli *et al.*, 2003). Most cells had a strikingly altered nuclear size and shape, nuclear pore clustering and the NE interruptions accompanied by chromatin extrusion. There was almost a complete loss of peripheral and in many cases internal heterochromatin in these nuclei (Goldman *et al.*, 2004). Lamin B1 was present at the NE but also delocalised to the nucleoplasm (de Sandre-Giovanolli *et al.*, 2003). Segregated distribution of lamin A and lamin B1 was also seen in highly lobulated nuclei (Goldman *et al.*, 2004). In contrast to other laminopathies, emerin remained localised at the NE or present in nuclear lobulations rather than being redistributed to the ER (Goldman *et al.*, 2004). Western blotting showed that patients expressed only 25% of normal lamin A (de Sandre-Giovanolli *et al.*, 2003). In addition, mutant lamin A and wild type pre-lamin A significantly increased with age at the NE of HGPS cells (Goldman *et al.*, 2004) presumably due to mutated lamin A interfering with normal processing, turnover and assembly state of lamin A in the lamina.

Attempts to introduce EDMD mutation (L530P) into the LMNA gene in mice resulted in the introduction of a different splicing defect at the 3' end of the gene, but surprisingly such mice did develop a phenotype remarkably similar to HGPS (Mounkes *et al.*, 2003). However, these mice did not show any evidence of cardiovascular disease that plays a major role in the morbidity and mortality in human diseases. Also, mice homozygous null for prelamin A protease ZMPSTE24/FACE 1, which show an accumulation of prelamin A due to a loss of prelamin A processing, exhibit growth retardation, muscular dystrophy, alopecia and early death (Pendas *et al.*, 2002, Bergo *et al.*, 2002). They also show dilated cardiomyopathy and lipodystrophy (Pendas *et al.*,

2002) or multiple bone fractures (Bergo *et al.*, 2002). Knockdown of FACE1 in human cells resulted in an abrupt cell cycle arrest (Gruber *et al.*, 2005) with some cells having aberrant mitotic spindles and entering apoptosis and other cells having an extensive formation of lobulated nuclei and micronuclei. In these cells pre-lamin A accumulated at the NE as opposed to appearing in nucleoplasmic dots, presumably due to a gain of membrane anchoring properties, which dominantly interferes with nuclear disassembly. These phenotypes are remarkably similar to HGPS cells that show increased apoptosis and premature senescent arrest (Bridger and Kill 2004). Interestingly, microarray analysis of genes in HGPS patients showed misregulation of genes involved in cell cycle progression and mitotic regulation (Ly *et al.*, 2000). Findings of shortened telomeres and diminished DNA repair in HGPS fibroblasts (Allsopp *et al.*, 1991, Wang *et al.*, 1991) support the above microarray analysis and implicate HGPS as a genomic instability syndrome along with other known progerias (Martin and Oshima 2000). Interestingly, shortened telomeres have not been detected in lamin mutant mice (Mounkes *et al.*, 2003) or Zmpste24 null mice (Ly *et al.*, 2005).

### *1.12.3. OTHER LAMINA DISEASES/DISORDERS*

Mutations in B-type lamins have never been identified in humans, most likely because absence of B-type lamins is lethal in mammalian cells (Harborth *et al.*, 2001). Indeed, homozygous LNB1 mutant mice die at birth with defects in lung and bone (Vergnes *et al.*, 2004). Fibroblasts from lamin B1 mutant mouse embryos display grossly misshapen nuclei, impaired differentiation into adipocytes, increased polyploidy and premature senescence. Mutations in lamin B receptor cause dominant Pelger-Huet anomaly of white blood cell nuclear shapes with heterochromatin clumping, epilepsy, bone and cartilage disorders and developmental delay (Hoffmann *et al.*, 2002, Shultz *et al.*, 2002) as well as autosomal recessive HEM/Greenberg skeletal dysplasia (Waterham *et al.*, 2003) (**Table 1.1**). Heterozygous loss-of-function mutations in MAN1 cause syndromes characterised by increased bone density in humans including Osteopoikilosis, Buschke-Ollendorff syndrome (BOS) and Melorheostosis (Hellemans *et al.*, 2004). MAN1 has been recently found to specifically inhibit BMP, TGFβ and activin signalling (Pan *et al.*, 2005, Lin *et al.*, 2005), which is consistent with their enhanced signalling in these disorders (Hellemans *et al.*, 2004).

## 1.13. AGEING AND CELLULAR SENESCENCE

### *1.13. 1. WHY STUDY AGEING?*

Human ageing is associated with an increased chance of death mostly due to a subset of age-related diseases largely restricted in later life, including cardiovascular disorders, diabetes, neoplasms and crippling conditions such as cataract, macular degeneration auditory impairment and neurodegeneration, all of which can greatly reduce the quality of later life. It has been predicted that by the year 2015 around a fifth of the UK population will fall into the over 60 age category and generally the proportion of the elderly within the population is set to increase dramatically (Kill 2004 seminar guest speaker). Whilst living longer is a preferable alternative, it also brings distressing or fatal age-related conditions. Given that ageing may become one of the major health-care challenges of the century, understanding the normal process of human aging may give important insights into the mechanisms by which age-related diseases develop.

### *1.13.2. HOW DO WE AGE?*

Biologists have developed both evolutionary and molecular hypotheses to explain causes of aging and to date there are more than 300 theories postulated (reviewed in Martin and Oshima 2000). Most studies of human twins agree that the heritability of the life span is around 50%. Candidate genes have been screened to identify alleles that affect longevity, DNA repair, free radical scavenging, telomere shortening and heat-shock response. So how do we age? Evolutionary theorists argue that organisms age as a side effect of 'antagonistic pleiotropy' which stems from the declining force of natural selection in post-reproductive years and an accumulation of late-life deleterious effects which are not effectively selected against (Campisi *et al.*, 2001). Accordingly, any mutation that favours early reproductive success but produces detrimental effects later in life will be selected for. The result is a series of later-life emergent phenotypic changes which we call ageing. In addition, an accumulation of mutations may synergise with the accumulation of ageing cells leading to an increased rise in cancer that is seen in old age (Krtolica *et al.*, 2001). These themes were originally explored in the 'disposable soma theory' of ageing (Kirkwood *et al.*, 1996). This theory argues that, in nature, a trade-off occurs between reproduction and somatic repair/maintenance where

short-lived species invest less in durability of their somatic cells and tissues than long-lived species. Therefore, this theory predicts that the strongest candidates for longevity genes are those regulating somatic maintenance and repair, including the cellular responses to stress. Recently, lamin A gene has been linked to longevity and was proposed to be a guardian of somatic cells during its lifetime (Hutchison and Worman 2004).

### *1.13.3. AGEING AND SENESCENCE*

Once it was believed that cells could proliferate indefinitely and that the maintenance of a cell culture was just a question of finding the right conditions (reviewed in Serrano and Blasco 2001). These ideas were radically changed by the seminal work of Hayflick and Moorhead in the early 1960s, which demonstrated that for most normal cells, proliferation is limited, despite culturing conditions that appeared optimal for a significant period of time. Human fibroblasts, for example, proliferate vigorously for about 50 generations during which there is an exponential increase of cells that lose division potential and eventually reach a stage in which almost every cell has stopped division. This phenomenon is reproducible *in vitro* and is termed replicative senescence. The occurrence of replicative senescence has been demonstrated for most cell types with a few exceptions as in the case of embryonic germ cells and the large majority of tumour-derived cells. As such, Hayflick's cell hypothesis of ageing states that senescence acts as an intrinsic limit to growth in normal cells and plays a role in ageing of tissues in which senescent cells form a part (Hayflick *et al.*, 1998). However, this hypothesis does not argue that aging of tissues is caused by senescent cells *per se* but rather that ageing of regenerative tissues would have a significant impact on the ageing of an organism as a whole.

The idea that the replicative senescence of cells in culture reflects organismal aging initially rested on three bases of evidence (reviewed in Campisi *et al.*, 2001). First, it was found that there was an inverse correlation between donor age and the number of doublings at which human fibroblasts senesce, suggesting that replicative potential is progressively exhausted during organismal aging. Second, inter-species comparisons showed a correlation between species' life span and the replicative life span of fibroblast cells, suggesting an overlap in genes that control the replicative life span of

cells and organismal life span. Third, cells from premature aging syndromes senesce after fewer doublings than age-matched controls, suggesting an overlap in genes that control replicative and organismal life span (Kill *et al.*, 1994). Finally, cells expressing a senescence-associated marker enzyme are more prevalent in physiologically aged tissues as compared to young tissues (Dimri *et al.*, 1995).

Senescent cells are metabolically active yet terminally arrested cells (Goldstein *et al.*, 1990). Senescing cells display a gradual increase in the cell cycle (G0-G1 transition is lengthened) until they become irreversibly arrested in G1. As such, they are no longer sensitive to growth factor stimulation (although many genes remain mitogen-inducible) and some cell types are also resistant to apoptosis (e.g. HDF), presumably due to increased cell adhesion to the extracellular matrix. These cells have a large, flat morphology with increased granularity and acidic senescence-associated β-galactosidase (SA-β-gal) enzymatic activity, reflecting the increased lysosomal content (Garland *et al.*, 2003). They also display up-regulation of a variety of cell cycle inhibitory proteins.

Accumulation of senescent cells has been shown to be critical for compromising the function and integrity of organs like skin, arteries, retina, liver and kidney where they were seen to accumulate during ageing (reviewed in Faragher and Kipling 1998). Moreover, the altered functions of senescent cells are cell-type specific but often include the expression of genes that have long-range, pleiotropic effects including degradative enzymes, growth factors and inflammatory cytokines, which alter the tissue microenvironment. These molecules and the resulting disrupted microenvironment promote the proliferation of nearby pre-neoplastic cells *in vitro* and *in vivo*, thereby contributing to tumorigenesis in later life (Krtolica *et al.*, 2001).

### *1.13.4. MECHANISMS LEADING TO SENESCENCE*

#### 1.13.4.1 Replicative senescence

**Progressive telomere shortening** seen in cells in culture and older organisms has been proposed to be one critical determinant of replicative senescence (reviewed in Campisi *et al.*, 2001). Telomeres are GC-rich repetitive DNA structures bound by telomere-

binding proteins found at the ends of mammalian linear chromosomes (15-20 kb in length) that cap the chromosomes and provide protective function by preventing end-to-end chromosomal fusions. With each round of cell division and DNA replication, 50-100 base pairs of the telomeric DNA sequence is under-replicated (normative telomere loss) leading to progressive shortening of telomeres. Eventually the critically shortened telomeres (5-7 kb in length) may no longer be able to protect the ends of the chromosomes and the uncapped chromosomal DNA ends may release a senescence inducing signal to the cell. The most dramatic consequence of telomere dysfunction is the appearance of chromosomal fusions, which in turn lead to the gain or loss of entire chromosomes (Artandi *et al.*, 2000). This implies that critically short telomeres are 'perceived' by cells as damaged DNA and are thus attempted to be repaired resulting in telomeric fusions. In cells of germ line, the telomere lengthening mechanism is mediated by telomerase, a unique ribonucleoprotein enzyme that mediates a RNA-dependent synthesis of telomeric repeats (Blasco *et al.*, 1999). High levels of telomerase activity expressed in germ-line cells appear to be critical in maintaining stable telomere length and conserving viability of the species. However, most somatic cells do not express this enzyme and ectopic expression of the catalytic subunit of telomerase restores telomere lengths in fibroblasts and other cell types, which allows cultures to escape senescence (Bodnar *et al.*, 1998). Indeed, many tumour cell lines show high levels of telomerase activity. However, telomere shortening is not a consistent measure for the onset of senescence because cells often enter senescence before reaching critically short telomeres, and mouse cells can enter senescence in the presence of normal telomere lengths (reviewed in Serrano and Blasco 2001). Interestingly, HGPS cells are resistant to immortalisation by an ectopic expression of telomerase, and such a type of senescent arrest is known to be telomere-independent (Gorbunova *et al.*, 2002). Also, given that higher organisms have post-mitotic cells (such as nerves, muscle and fat) and mitotic cells (such as epithelial cells and stromal cells of organs like skin), these different cell types may age by different mechanisms (Campisi *et al.*, 2001). Therefore, additional signals may activate or enforce senescence programme.

### 1.13.4.2 Stress-induced premature senescence

Exposure of primary cells to certain types of stresses also triggers a permanent proliferation arrest reminiscent of replicative senescence that is referred to as **'stress-induced premature senescence'** (SIPS) (Toussaint *et al.*, 2000).

#### *1.13.4.2.1 DNA damage and telomere uncapping*

**DNA damage** is one of the mechanisms that can trigger SIPS. Irradiated human fibroblasts undergo a permanent and irreversible growth arrest (Di Leonardo *et al.*, 1994). DNA damage triggers a DNA damage checkpoint arrest in order to prevent unscheduled replication of damaged DNA (Avni *et al.*, 2003). Damaged DNA accumulates repair proteins (von Zglinicki *et al.*, 2001) and if the DNA becomes repaired, the cell cycle can continue. However, even if repaired, DNA damage can lead to chromosome abnormalities due to activation of incorrect repair systems (Campisi *et al.*, 2001). More subtle types of DNA damage such as **telomere uncapping** which results from alterations in telomere-binding proteins that maintain higher order telomere structure can also induce premature senescence. For example, Ku86 is an essential DNA repair protein of DNA breaks through a pathway known as non-homologous end joining (NHEJ). Fibroblasts deficient in this telomere-binding protein enter senescence prematurely and accumulate end-to-end telomeric fusions (Samper *et al.*, 2000). Similar observations of chromosomal fusions have been seen in cells where the function of the telomere-binding protein TRF2 has been inactivated (Yalon *et al.*, 2004). Interestingly, both shortened telomeres and uncapped telomeres can trigger the DNA damage response pathway (von Zglinicki *et al.*, 2005). Recently, HGPS cells and ZMPSTE24 null mouse cells have also been shown to accumulate chromosomal abnormalities due to increased DNA damage and NHEJ (Ly *et al.*, 2005) which directly suggests a role for lamin A in DNA damage-induced premature senescence.

#### *1.13.4.2.2 Oxidative damage and reactive oxygen species (ROS)*

**Oxidative damage** is another cellular stress that can induce premature senescence. Culturing of cells in conditions of chronic hyperoxia shortens the replicative lifespan and induces accelerated (5-10 x faster) telomere shortening (von Zglinicki *et al.*, 1995).

continue the process by converting $H_2O_2$ to water. The rate of ROS generation and the level of AE defence contribute to the overall level of oxidative stress that can exert a regulatory influence on different levels of gene expression. Interestingly, in the primary ARE defence system of progeria cells, the activities of GPX1 is reduced by 70% and the level of oxidatively modified proteins is high (Yan *et al.*, 1999). In contrast to other antioxidant enzymes, GPX is located in more than one cellular compartment including cytoplasm, mitochondria and the nucleus, and needs cofactors for its function including the glutathione system.

#### *1.13.4.2.2.2. Glutathione and oxidation of protein thiols*

A key determinant of the cellular response to oxidative stress relates to the level and form of glutathione or GSH (l-gamma-glutamyl-l-cysteinylglycine) (reviewed in Thomas and Mallis 2001). Glutathione is the predominant non-protein thiol in mammalian cells. Under physiological conditions in living cells, more than 98% of intracellular glutathione exists as the reduced thiol form GSH while the rest is present mainly as the oxidized disulfide form GSSG or mixed protein disulfide (P-SSG). The status of cellular reduction potential is essentially an index of GSH redox status and varies during the life stage of the cell. The cellular reduction potential changes whether the cell is quiescent, proliferating, confluent, differentiating, senescent or apoptotic. During normal growth conditions, GSH is involved in the reduction of toxic intermediates that accumulate during the course of normal metabolism. Therefore, GSH plays several pivotal roles including scavenging free radicals, regulation of gene expression and enzymes activities, regulation of cell death and maintenance of other antioxidants in their reduced state. Disturbed GSH status accompanies ageing and many diseases including diabetes, neurodegeneration and viral infections. During conditions of moderate oxidative stress, intracellular protein thiol groups are particularly susceptible to oxidation by free radicals. A number of reversible protein thiol oxidation states can be produced including protein disulphides, S-glutathiolated, sulfenic acid and thiyl radical (**Figure 1.9**). The reversible reaction of S-thiolation is a stress-adaptive signalling response whereas prolonged or increased oxidative stress leads to irreversible protein thiol modifications such as sulfinic and sulfonic acid. Many cellular metabolic and regulatory pathways including glycolysis, transcription, translation, protein degradation, cell cycle control and heat shock response are regulated by S-thiolation. S-

glutathiolation (a formation of mixed protein disulphide with GSH) is the most prevalent S-thiolation in biological systems. S-glutathiolation of proteins during oxidative stress protects protein thiol groups from irreversible modifications often at the expense of temporary loss in protein function and/or activity. Proteins often undergo an altered conformational state, which leads to an accumulation of inactive or heat labile proteins (Oliver *et al.*, 1987).

#### *1.13.4.2.2.3. Repair mechanisms of oxidised protein thiols*

Exposure of cells to moderate levels of oxidants causes a cell cycle arrest, which allows time for cells to detoxify. De-thiolation can occur via direct reduction by GSH **(Figure 1.9D)** or can be catalysed by enzymatic protein disulphide oxido-reductase systems such as those involving glutaredoxin, thioredoxin and protein disulphide isomerase (reviewed in Grune *et al.*, 1997). Ultimately the maintenance of cellular functions involves NADPH dependent (nicotinamide adenine dinucleotide phosphate) reduction of oxidised glutathione by glutathione reductase, which provides the reducing power for all other antioxidant enzymes systems, and is itself dependent on intracellular respiration within mitochondria. The degradation of oxidised proteins by a specific protease complex called the proteosome is a part of secondary antioxidant defence against ROS. Selective degradation of oxidatively damaged proteins prevents the accumulation of potentially toxic fragments or large aggregates of cross-linked proteins. During ageing and under the condition of chronic oxidative stress the ratio of reduced to oxidised glutathione declines and critical cysteines in a range of proteins become permanently oxidised eventually leading to the inhibition of proteosome and cell dysfunction (Friguet *et al.*, 1994).

#### *1.13.4.2.3. Epigenetic alterations and heterochromatin loss*

**The alteration of the epigenetic maintenance mechanisms** can also trigger SIPS. Short exposure of cells to histone deacetylase inhibitors, which causes loss of heterochromatin, accelerates senescence in humans, mice and yeast (reviewed in Campisi *et al.*, 2001). A significant decrease in the level and modification status of the histone deacetylases (HDAC) occurs during replicative senescence of human fibroblasts (Wagner *et al.*, 2001), which can be regulated by INM proteins (e.g. LBR) at the NE.

Recent studies in yeast suggest that heterochromatin, energy metabolism, recombinational DNA damage and aging may be linked (Lin *et al.*, 2000). The yeast SIR2 (silencing information factor) is required for the heterochromatinisation of certain loci. SIR2 also suppresses illegitimate recombination at selected loci, requires NAD (nicotinamide adenine dinucleotide) for its activity (thereby sensing energy status), and mediates the life-span extension caused by caloric restriction.

#### *1.13.4.2.4. Oncogenic Ras activation*

**Activation of oncogenic Ras** in primary cells can lead to a senescence-like state. (Serrano *et al.*, 1997). Ras-induced senescence can also be mediated by ROS. Although diverse stimuli evoke similar senescence-like states, they appear to activate distinct but not mutually exclusive biochemical effectors of the senescence programme. This has provided a strong impetus to elucidate the signalling pathways responsible for the initiation and maintenance of senescence.

### 1.13.4.3 Mediators of replicative senescence and SIPS

**The mediators of senescence** that are activated following oncogene activation are similar to the biochemical mediators of replicative and oxidative-stress induced senescence (Chen *et al.*, 2004). Prominent among these are the cdk4/6 inhibitor, p16ink4a tumour suppressor protein, which inactivates D-type cyclins, and p19/14arf. They are involved in p16/Rb and p19/p53 signalling pathways. Activation of either pathway appears to depend on the cell type and species of origin. In case of human fibroblasts, p16/Rb pathway seems to have a more prominent role than p19/p53 pathway in both Ras-induced and replicative senescence, whereas in mouse fibroblasts p19/p53 pathway is more predominant (Smogorzewska and De Lange 2002). Another biochemical mediator implicated in senescence is cdk2 inhibitor p21cip1. This protein is well characterised as a downstream effector of p53-mediated pathway following DNA damage. ROS activation of senescence can be dependent on autocrine or paracrine expression of a growth-inhibitory factor called transforming growth factor β (TGFβ), which leads to upregulation of the p15ink4B inhibitor as well as p21cip1. Rb has been directly implicated in the anti-proliferative effects of TGFβ (Frippiat *et al.*, 2001). TGFβ/Smad/Rb pathway stimulates expression of connective tissue growth factor

(CTGF), a newly identified biomarker of senescence (Kim *et al.*, 2004), and mediates p38 MAPK signalling which is a common kinase signalling cascade in all types of senescence (Iwasa *et al.*, 2003). TGFβ is involved in production of fibrotic lesions, a hallmark of aging in various organs, including heart and kidney. Interestingly, lamin A binding protein MAN1 is reported to repress TGFβ/Smad signalling-dependent cell cycle arrest (Pan *et al.*, 2005, Lin *et al.*, 2005). Another tumour-suppressor PML, known from its involvement in PML bodies, is upregulated in both mouse and human cells in both Ras-induced and replicative senescence, and is required for the activation of p53 pathway in mouse cells (Serrano and Blanco 2001) whereas it predominantly engages Rb pathway in human cells (Mallette *et al.*, 2004).

### *1.13.5. THE CONCEPT OF CELLULAR SENESCENCE*

It appears that the concept of cellular senescence has expanded to include any form of permanent and irreversible growth arrest. However, Wright and Shay 2001 argue that it is possible to minimise stress and leave telomere shortening as the only barrier to immortalisation. They propose that the concept of senescence should only be applied to the type of arrest triggered by telomere shortening or any other mechanism that counts generations (e.g. circadian cycles) but all other processes that resemble senescence should be referred to as stress. Although it is clear that different conditions can undoubtedly dramatically affect cellular lifespan, to draw this line is more difficult than it seems. The natural history of any given cell inevitably entails exposure to many types of stresses including non-telomeric DNA damage, oxidative stress, epigenetic alterations, oncogenic stress and telomere dysfunction (due to telomere shortening or uncapping). Indeed, even very old tissues generally have cells with a considerable number of remaining telomeres and yet have no division potential (reviewed in Campisi *et al.*, 2001). Thus telomere shortening may be considered as an upper limit to replicative lifespan that may only be seldom reached.

## 1.14 AIMS OF THIS THESIS

The findings that A-type lamins affect longevity and maintenance of a number of somatic tissues, implicates their role in normal ageing of tissues and in processes of cellular senescence. In hoping to understand the role of A-type lamins in premature

ageing syndromes and normal ageing, the main objective of this thesis was to study A-type lamins and their binding partners LAP2α and retinoblastoma protein (Rb) during ageing of wild type human fibroblasts *in vitro*.

In **chapter 3**, we explored whether nuclear morphology changes seen in laminopathy and progeroid fibroblasts occur as fibroblasts age *in vitro* and if so, whether these correlate with senescent arrest. We aged laminopathy fibroblasts *in vitro* in order to explore the hypothesis that lamin mutations are linked to premature senescence. We examined protein expression, distribution and solubility properties of A-type and B-type lamins and their binding partners LAP2α and LAP2β throughout cellular ageing of wild-type fibroblasts *in vitro*. These results led us to explore oxidative modifications to lamin A and LAP2α in senescent fibroblasts and their possible functional implications.

In **chapter 4**, we explored how A-type lamins and LAP2α regulate retinoblastoma protein (Rb), implicated in downstream signalling of senescence pathway. We investigated Rb protein expression, phosphorylation status, nuclear anchorage and binding to these proteins. These studies were further extended to a laminopathy cell line null for functional A-type lamins. In addition, we examined the role of LAP2α in cell proliferation and nuclear anchorage of Rb using small interfering RNA (sRNAi). These results led us to identify a senescence-associated Rb isoform and to explore functional implications of its particular distribution.

In **chapter 5**, we explored how the mechanism of transient quiescent arrest induced by either serum-starvation or contact-inhibition may differ from permanent senescent arrest. We investigated nuclear organisation and solubility properties of lamins and LAP2s in fibroblasts undergoing quiescence. In addition, we investigated how LAP2α expression and nuclear anchorage relate to expression and nuclear anchorage of hypo-phosphorylated Rb isoforms in fibroblasts undergoing quiescence or serum-restimulation. Finally, we examined expression of LAP2α and hypo-phosphorylated Rb isoforms in senescent fibroblasts grown under low serum conditions.

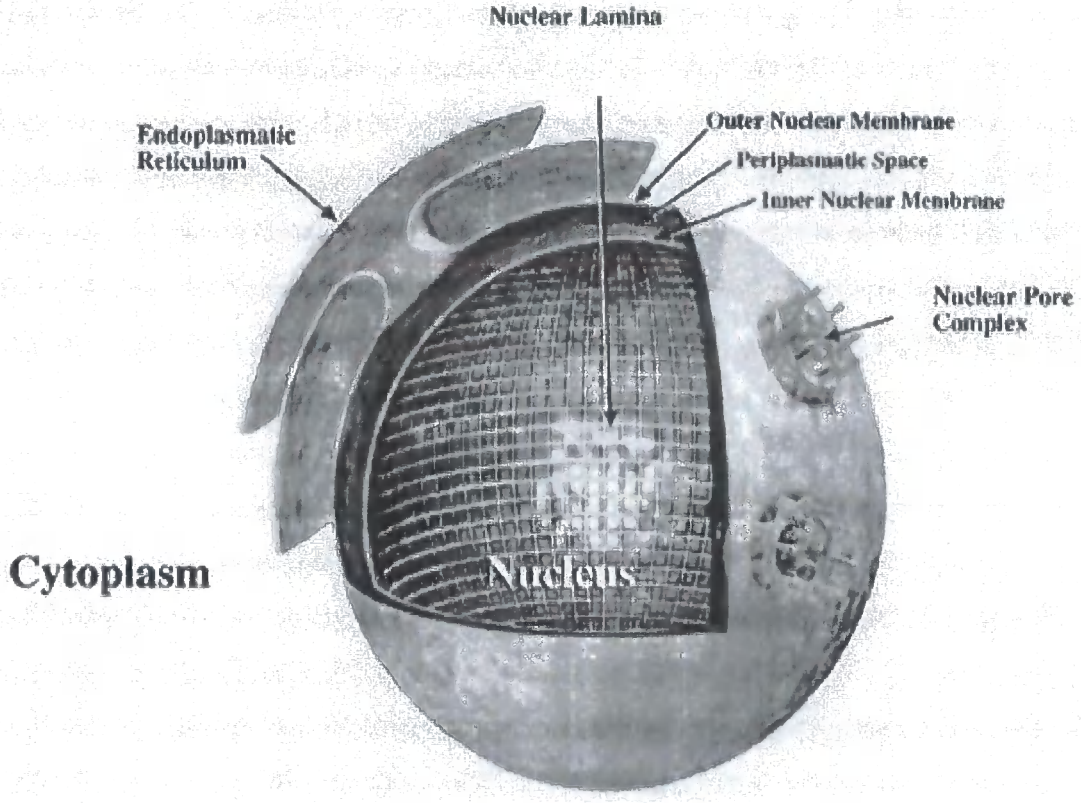


**Figure 1.1: Schematic representation of the nuclear envelope (NE) of a eukaryotic interphase cell.** Distinct NE components such as the inner and outer nuclear membrane (INM & ONM), the nuclear lamina (NL), and the nuclear pore complexes (NPCs) are indicated. Also depicted is the continuity of the outer nuclear membrane with the endoplasmatic reticulum (ER), so that the periplasmic space of the NE is contiguous with the lumen of the ER.

*(Reproduced from Stuurman et al., 1998)*

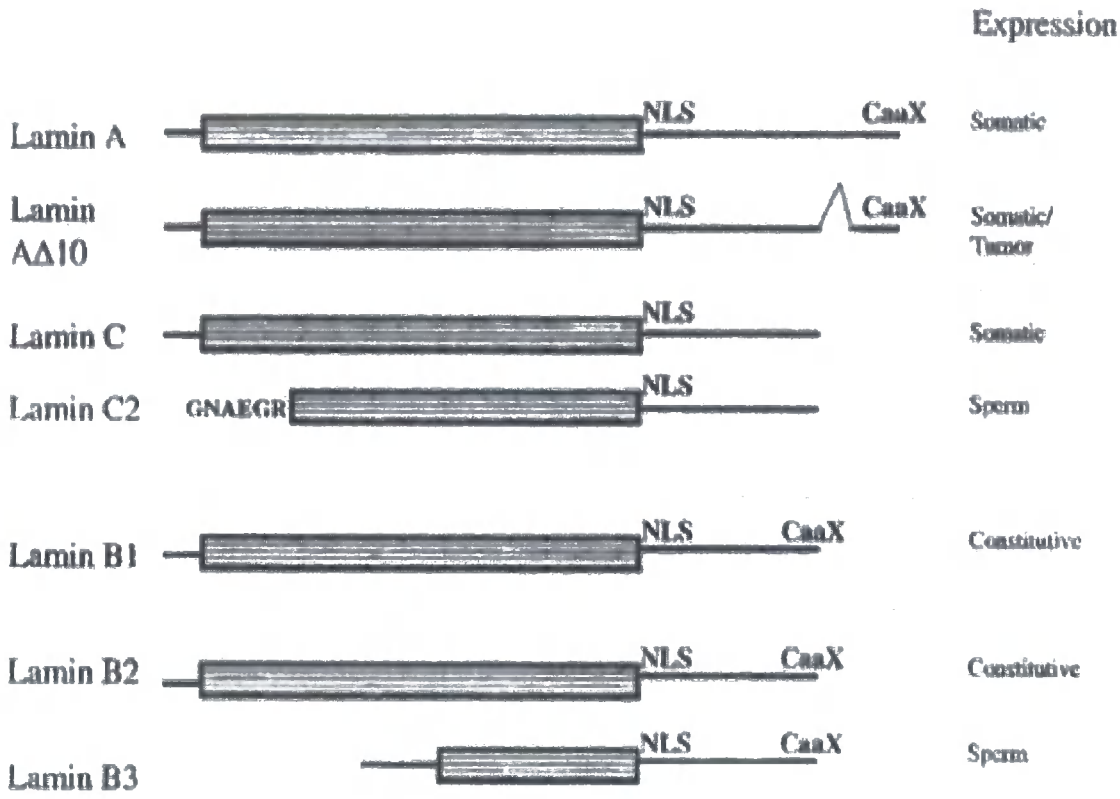


**Figure 1.2: Schematic drawing of different lamin isotypes found in mammalian tissues.** In mammals, seven different lamin proteins have been identified. Lamins A, C, A10 and C2 result from differential splicing of the lamin A gene. Only one transcript has been identified for the lamin B1 gene. Lamins B2 and B3 result from transcription of the lamin B2 gene. The rod domain is shown by a rectangle filled with horizontal lines. The N-terminal and C-terminal non-helical domains are presented as thick lines. The unique six amino acids that form the N-terminal domain of lamin C are shown using the single letter amino acid code. The nuclear localization signal (NLS) and isoprenylation motif (CaaX) are shown in the C-terminus. Lamins C and C2 lack the CaaX motif.

*(Reproduced from Moir and Spann 2000)*

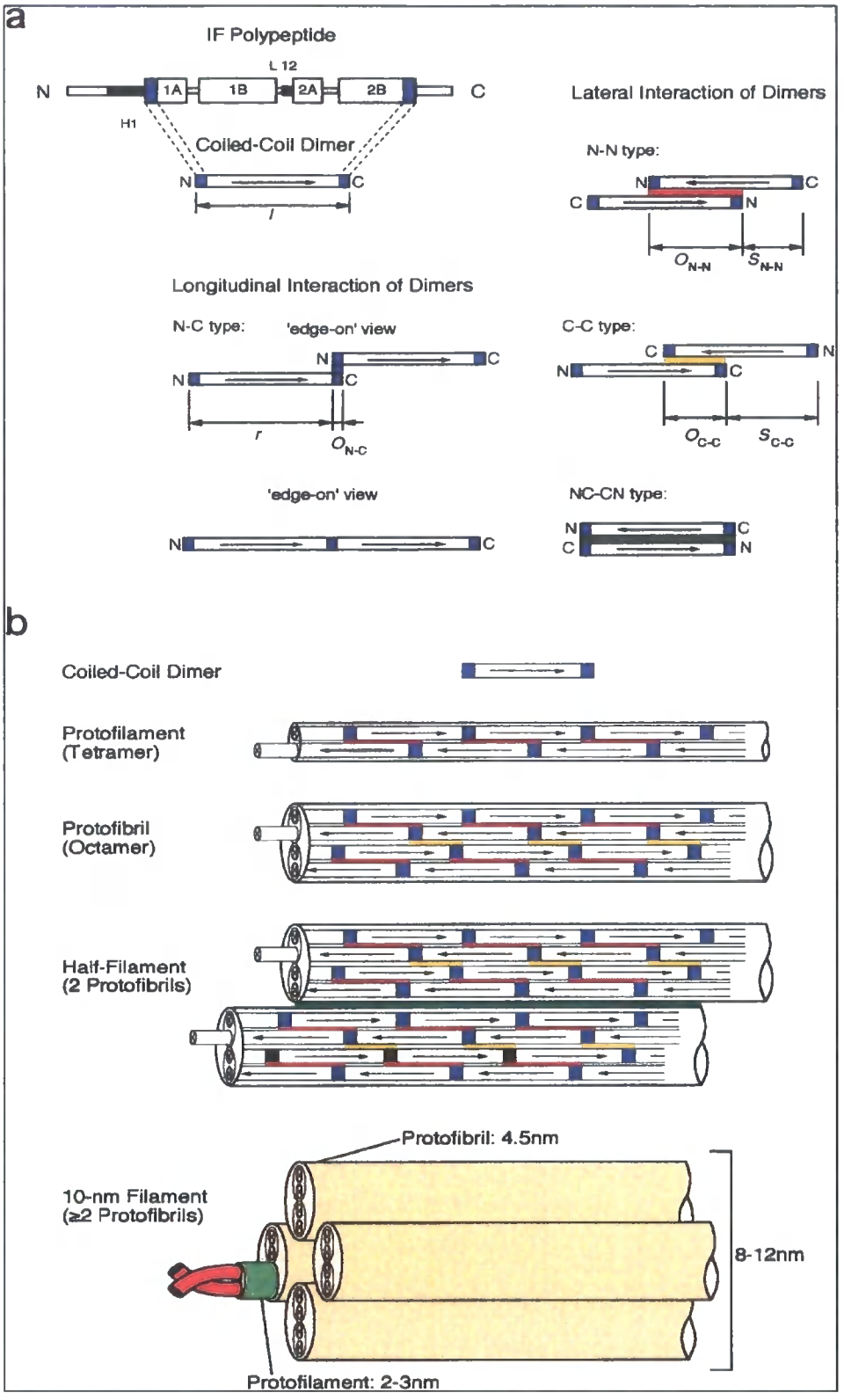


**Figure 1.3: Schematic representation of a molecular model for intermediate filament (IF) architecture. (a)** The elementary building block is a dimer consisting of a two-stranded α-helical coiled-coil rod, which associate longitudinally head-to-tail, or in three distinct lateral modes to form higher-order oligomers (N-head; C-tail). **(b)** A possible design of protofilaments, protofibrils, half-filaments, and 10-nm filaments.

*(Reproduced from Stuurman et al., 1998)*

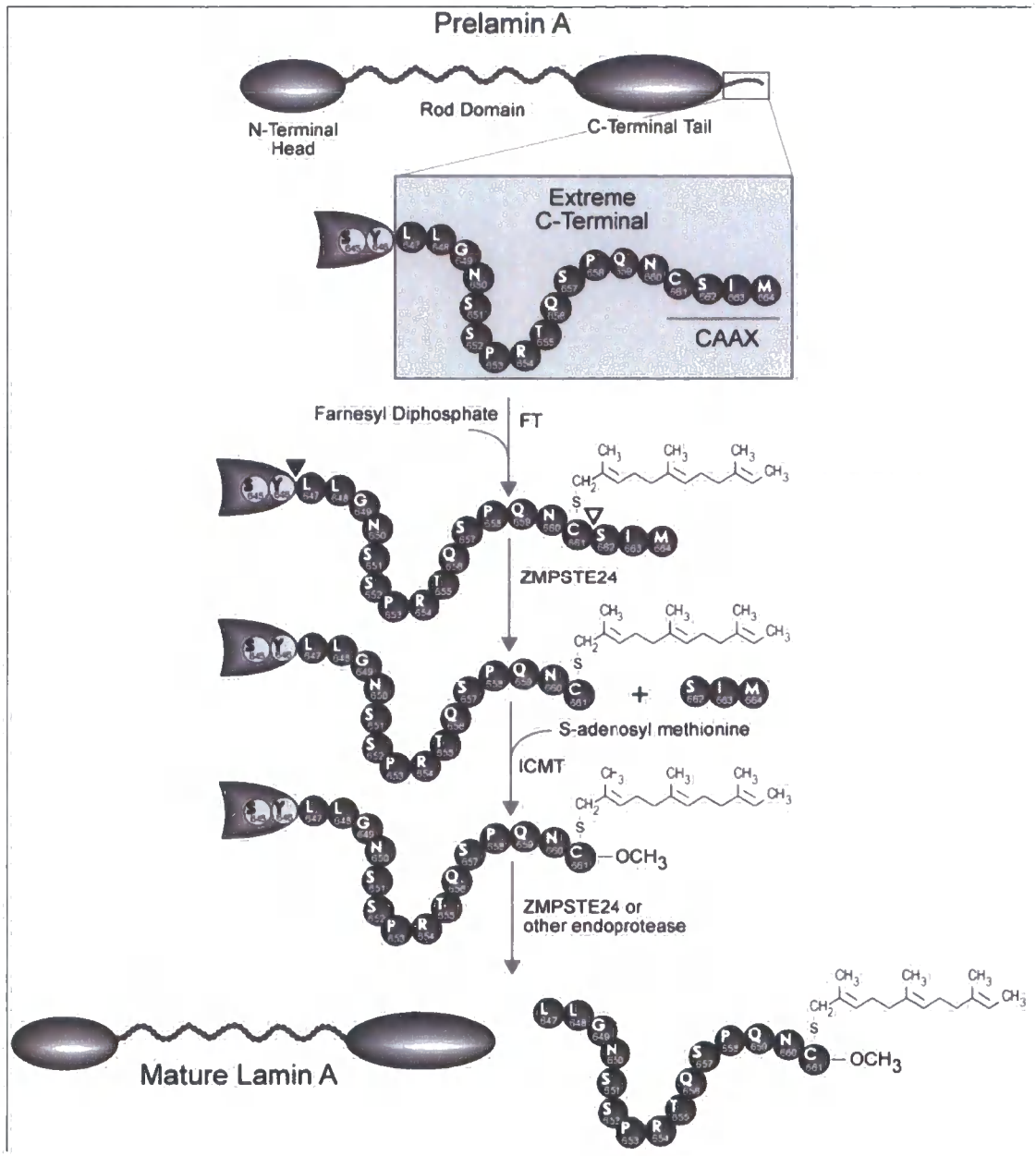


**Figure 1.4: Schema of steps involved in prelamin A processing to mature lamin A.** The post-translational processing of prelamin A involves the extreme carboxy-terminal residues. In the first step, farnesyl diphosphate is used to farnesylate the cysteine in the conserved CAAX motif at the carboxy-terminal using the enzyme farnesyl transferase (FT). During the second step, the peptide bond between the cysteine and serine residues (indicated by a triangle) is proteolytically cleaved by ZMPSTE24, resulting in removal of AAX tripeptide. This reaction is followed by methylation of the farnesylated cysteine residue by isoprenylcysteine carboxyl methyl transferase (ICMT) using S-adenosyl methionine as the methyl donor. Finally, a second proteolytic cleavage occurs between the tyrosine and leucine residues (indicated by a filled triangle), which is either catalyzed by ZMPSTE24 or by another, as yet unidentified, endoprotease, which removes 15 amino acids from the carboxy-terminal, resulting in formation of mature lamin A.

*(Reproduced from Agarwal et al, 2003)*

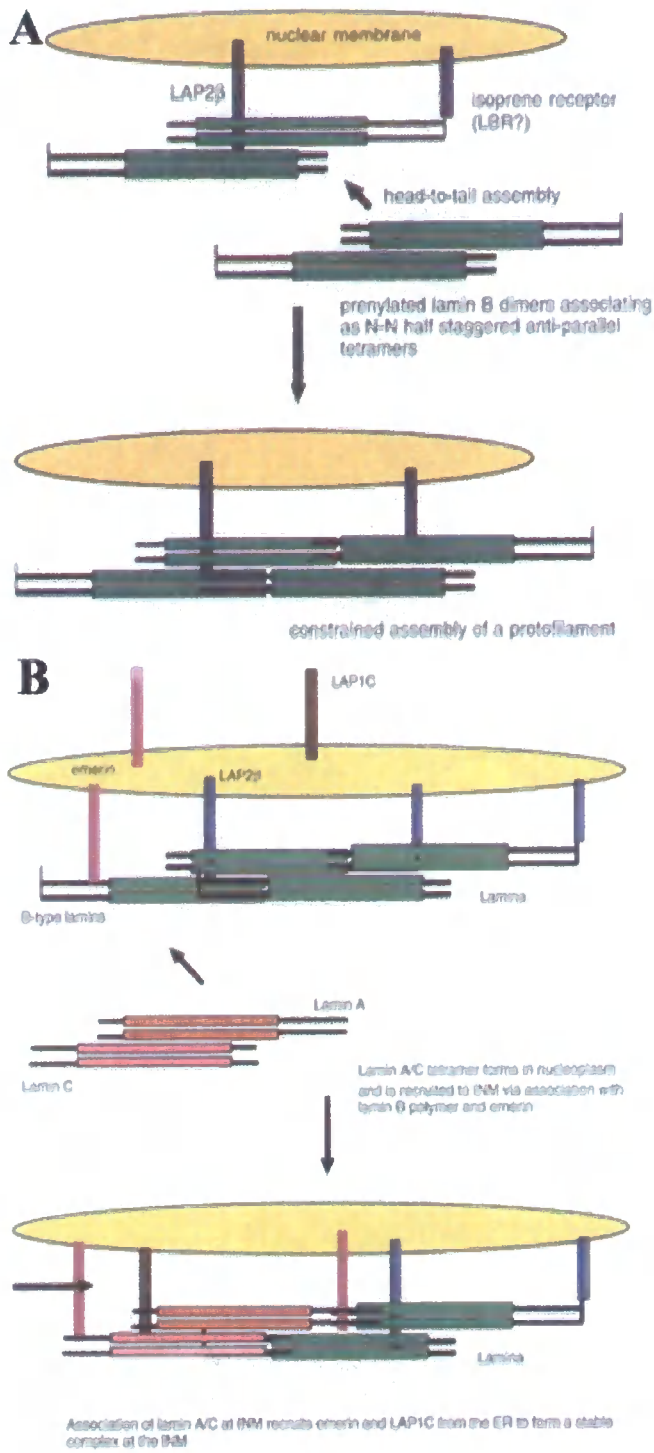


**Figure 1.5: Cartoon showing the constrained polymerisation of B-type lamin filaments and incorporation of A-type lamins at the inner nuclear membrane (INM). (A)** Tethering of B-type lamins to the INM in this model is through association with LAP2β and an isoprene receptor LBR. Lamin B dimers form N-N half-staggered anti-parallel associations to make tetramers and head-to-tail associations to form higher-order structures such as proto-filaments. **(B)** A-type lamin tetramers are incorporated into the INM by head-to-tail and anti-parallel associations with B-type lamin filaments, which leads to further recruitment of emerin and LAP1C from the outer nuclear membrane/endoplasmic reticulum (ONM/ER) to the INM, stabilising the A-type lamins.

*(Reproduced from Hutchison et al., 2001)*

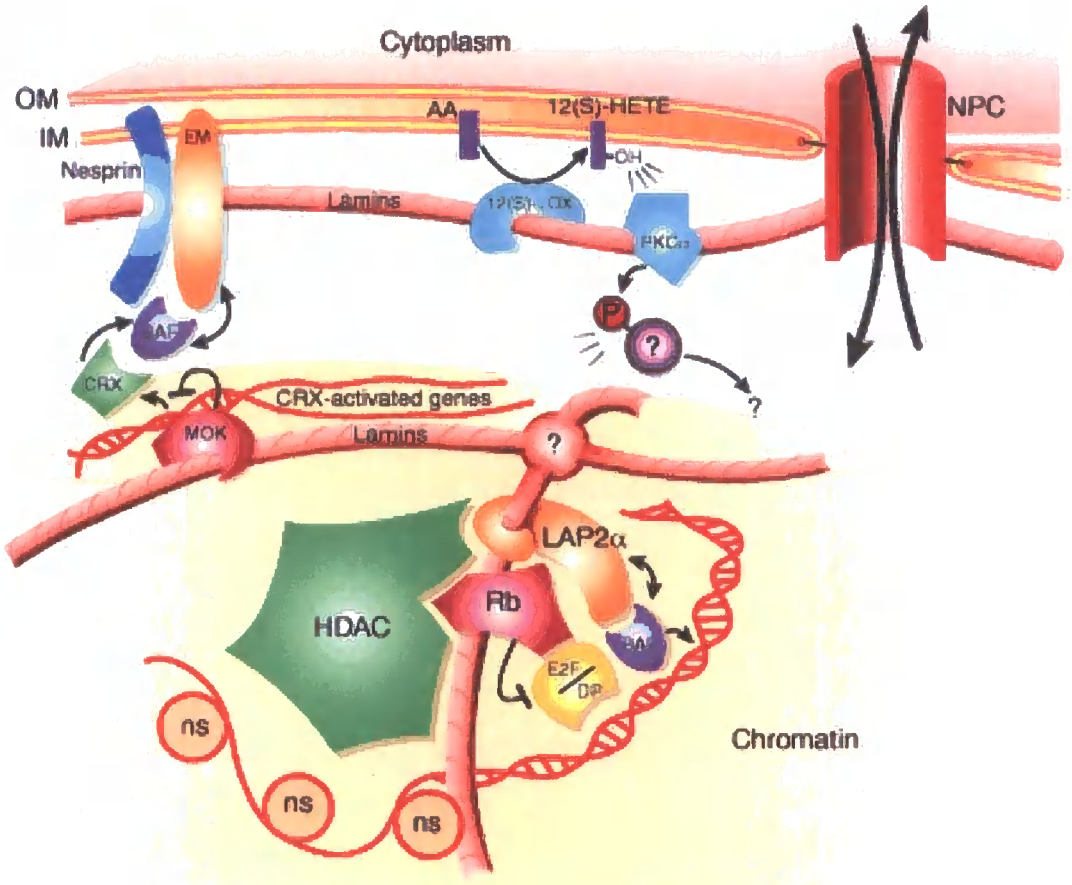


**Figure 1.6: A few interactions described for A-type lamins are illustrated.** The reader's attention is drawn to the bottom centre. Multiple oligomeric gene-regulation complexes might be formed by lamina-associated polypeptide 2α (LAP2α), A-type lamins, retinoblastoma protein (Rb), E2F/DP heterodimers (gene-specific activators), chromatin-silencing histone deacetylase complex (HDAC) and BAF (barrier-to autointegration-factor). NPCs, nuclear pore complexes; NS, nucleosome; OM, outer membrane; IM, inner membrane.

*(Reproduced from Zastrow et al., 2004)*

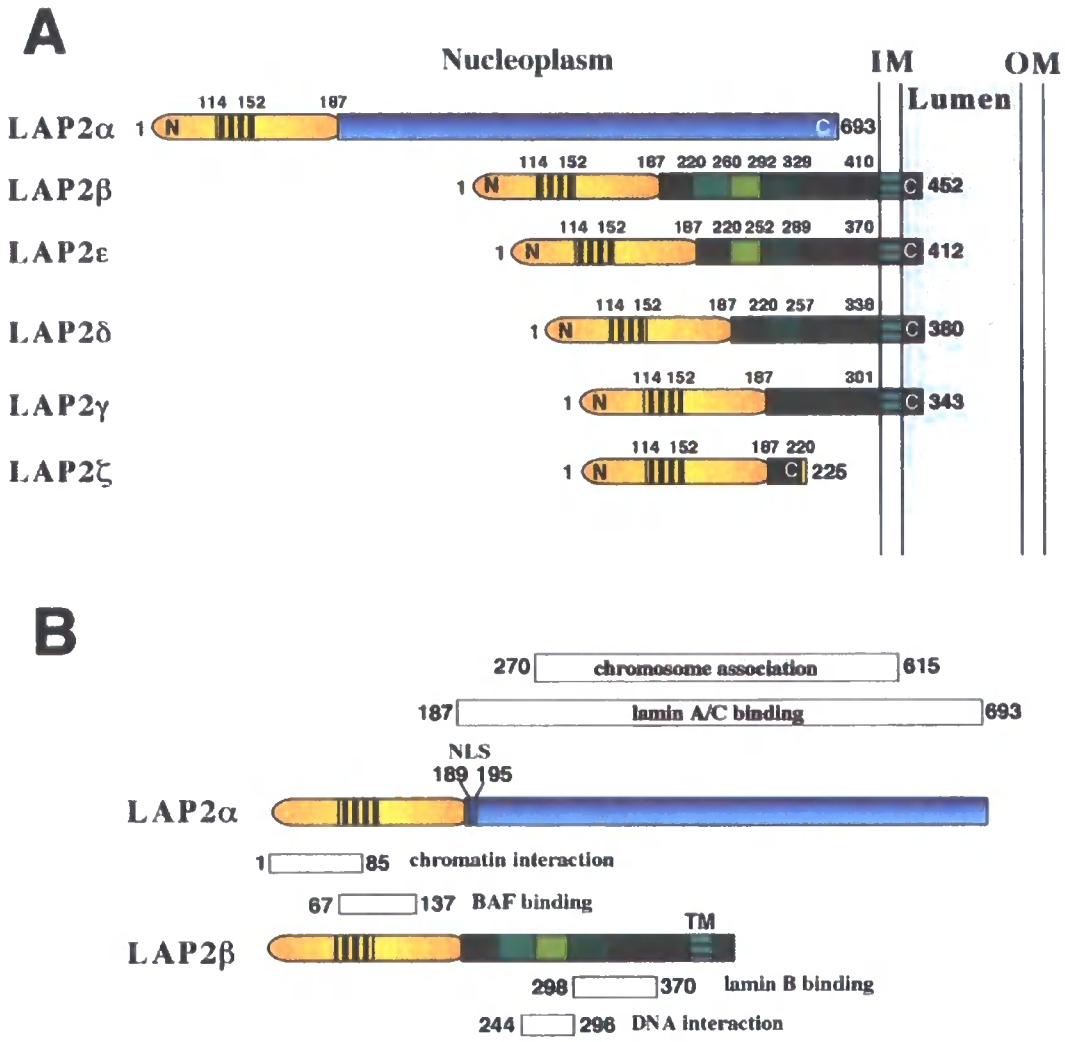


**Figure 1.7: Structural organization and functional domains of lamina-associated polypeptide 2 (LAP2) isoforms. (A)** Six alternatively spliced LAP2 isoforms have been identified in mammalian cells. **(B)** Regions in LAP2 proteins, found to contain specific interaction sites and/or functional domains. Numbers denote position of amino acids in human protein sequences; IM, inner membrane; OM, outer membrane; NLS, nuclear localization sequence; TM, transmembrane domain; N-head; C-tail.

*(Reproduced from Dechat et al., 2000)*

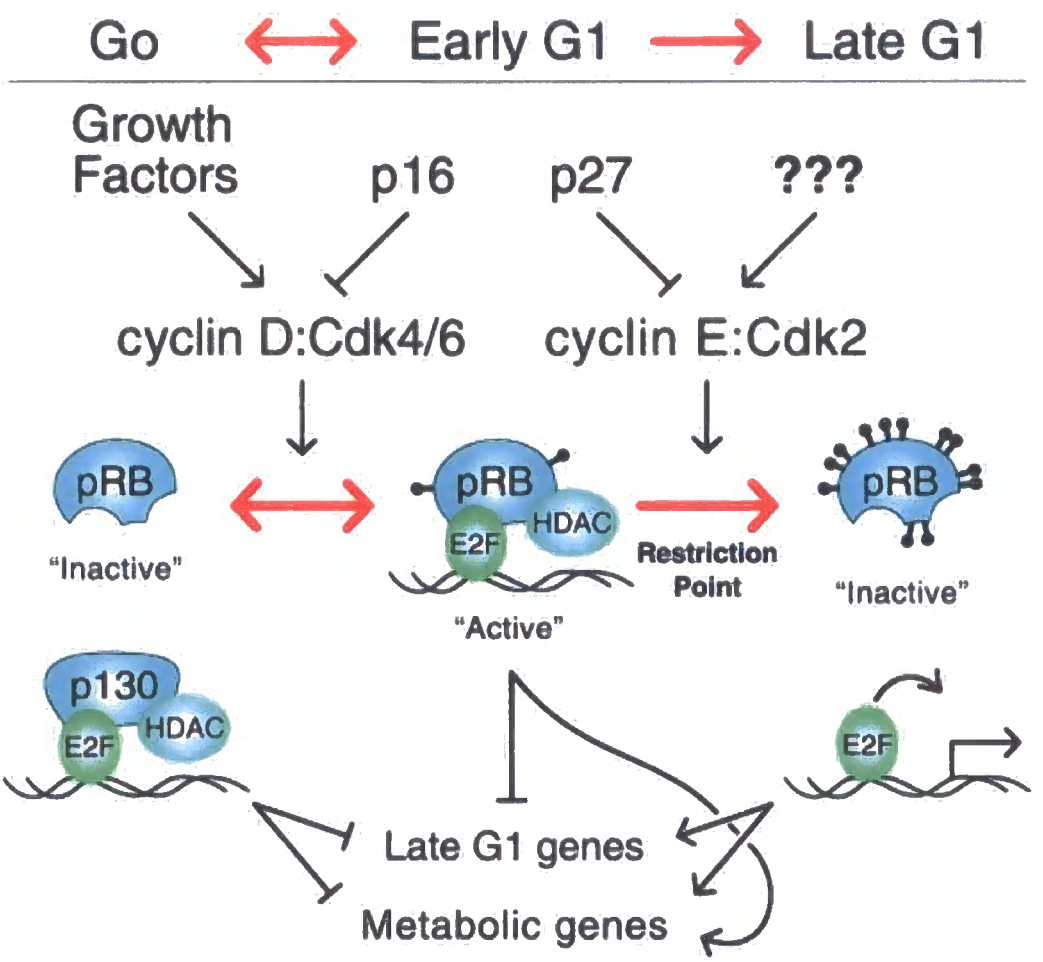


**Figure 1.8: A model of G1 cell cycle progression.** $G_0$ cells maintain E2F complexed with retinoblastoma-related protein p130. Growth factor stimulation activates cyclin D-Cdk4/6 complexes driving cells to pass through the reversible transition from $G_0$ into early G1 (Cdk- cyclin-dependent kinase). Cyclin D-Cdk4/6 hypo-phosphorylate retinoblastoma protein (Rb) and thereby increase Rb's avidity for E2Fs. Maintenance of cyclin D-Cdk4/6 activity by continuous growth factor stimulation is required during early G1. Loss of growth factor signalling or increases in cyclin inhibitor p16 drive cells back into $G_0$. Activation of cyclin E-Cdk2 in late G1 hyper-phosphorylates Rb, causing the release of E2Fs to activate transcription and drive cells across the irreversible restriction point into S phase. Histone deacetylase complex (HDAC)

*(Reproduced from Ezhevsky et al, 2001)*

**Table 1.1: A list of all diseases identified to date that are linked to altered nuclear lamina function** *(modified from Smith et al., 2005)*

| Gene mutated | Disease name | Disease abbreviation | References |
|---|---|---|---|
| *LMNA* | Emery-Dreifuss muscular dystrophy types 2 and 3 | EDMD2/3 | Bonne *et al.*, 1999 |
| *STA* (emerin) | X-linked Emery-Dreifuss muscular dystrophy type 1 | EDMD1 | Bione *et al.*, 1994 |
| *LMNA* | Cardiomyopathy, dilated, 1A | CMD1A | Fatkin *et al.*, 1999 |
| *LMNA* | Limb-girdle muscular dystrophy | LGMD1B | Muchir *et al.*, 2000 |
| *LMNA* | Dunnigan-type familial partial lipodystrophy type 2 | FPLD2 | Cao and Hegele, 2000<br>Shackleton *et al.*, 2000 |
| *LMNA* | Charcot-Marie-Tooth disease, axonal, type 2B1 | CMT2B1 | De Sandre-Giovannoli *et al.*, 2002 |
| *LMNA* | Hutchinson-Gilford progeria syndrome | HPGS | De Sandre-Giovannoli *et al.*, 2003; Eriksson *et al.*, 2003 |
| *LMNA* | Atypical Werner Syndrome | AWS | Chen *et al.*, 2003 |
| *LMNA* | Lipoatrophy with diabetes, hepatic steatosis, hypertrophic cardiomyopathy and leukomelanodermic papules | LDHCP | Caux *et al.*, 2003 |
| *LMNA* | Mandibuloacral dysplasia with type A lipodystrophy | MADA | Novelli *et al.*, 2002 |
| *ZMPST E24* | Mandibuloacral dysplasia with type B lipodystrophy | MADB | Agarwal *et al.*, 2003 |
| *LMNA* | Restrictive dermopathy | RD | Navarro *et al.*, 2004 |
| *ZMPST E24* | Restrictive dermopathy | RD | Navarro *et al.*, 2004 |
| *LMNA* | Seip syndrome | SEIP | Csoka *et al.*, 2004 |
| *LBR* | Pelger-Huët anomaly | PHA | Hoffman *et al.*, 2002<br>Schultz *et al.*, 2003 |
| *LBR* | Hydrops-ectopic calcification-moth-eaten skeletal dysplasia | HEM/Greenberg dysplasia | Waterham *et al.*, 2003 |
| *MAN1* | Osteopoikilosis, Buschke-Ollendorff syndrome and melorheostosis | BOS | Hellemans *et al.*, 2005 |

***A:*** Protein thiols respond to the decreased GSH/GSSG ratio by forming mixed disulfides with glutathione through thiol-disulfide exchange between the protein thiolate anion and oxidised glutathione (GSSG):

$$PrS^- + GSSG \rightarrow PrS\text{-}SG + GS^-$$

***B:*** The protein glutathione-mixed disulfide can be maintained as a persistently glutathiolated protein or an adjacent protein thiol can displace the GSH to form an intra-protein disulfide:

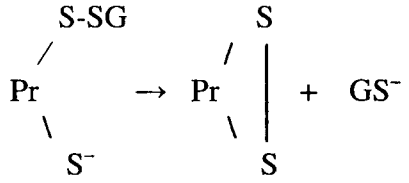

***C:*** Alternatively, reactions with ROS convert protein thiols to sulfenic acids or thiyl radicals, which can be further oxidised. To prevent this irreversible protein oxidation, GSH reacts with protein sulfenic acids or protein thiyl radicals to form mixed disulfides:

1) $PrSOH + GS^- \rightarrow PrS\text{-}SG + OH^-$

or

2) $PrS^{\cdot} + GS^- \rightarrow PrS\text{-}SG$

$\downarrow$

$O^2 \rightarrow O^{2\cdot -}$

***D:*** After the oxidative stress or redox signal has subsided, glutathione reductase will return the GSH/GSSG ratio to its resting level, enabling reversal of the protein disulphides or glutathione-mixed disulphides by reduced glutathione (GSH):

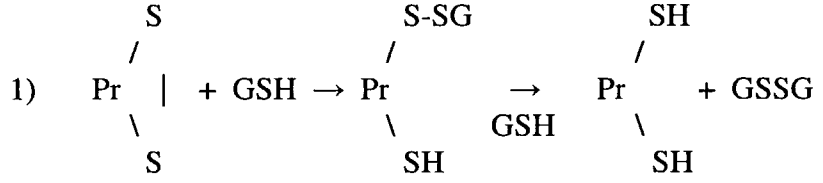

2) $PrS\text{-}SG + GSH \rightarrow PrSH + GSSG$

**Figure 1.9: A number of reversible protein thiol oxidation states can be produced including S-glutathiolated (A), protein disulphide (B), sulfenic acid and thiyl radical.** Protein sulfenic acid **(C1)** and thiyl radical **(C2)** can also become S-glutathiolated. Oxidised protein thiols **(D)** can be reversed by reduced glutathione (GSH). GSSG-oxidised glutathione; PrSH-protein sulfhydryl group; PrSOH-protein sulfenic acid; Pr·-protein thiyl radical; PrS-S-protein disulphide; PrS-SG-protein-glutathione disulphide.

*(Reproduced from Beer et al., 2004)*

# CHAPTER 2-MATERIALS AND METHODS

## 2.1 MAMMALIAN CELL CULTURE

### *2.1.1 CELL LINES AND MEDIA*

Wild-type (control) human dermal fibroblasts (HDF) were obtained from a punch biopsy of the inner forearm of the two healthy 9-year old boys following an informed consent. HDF were cultured in Dulbecco's modified Eagle's medium (DMEM, Invitrogen) supplemented with 10% newborn calf serum (NCS) and 10 units/ml penicillin plus 50 µg/ml streptomycin, at 37° C in humidified incubators containing 5% $CO_2$. In addition, human dermal fibroblasts from the patients with the following LMNA mutations were used: Y259X (progeroid foetal akinesis), E358K (multi-system lipodystrophy syndrome), R249Q (AD-EDMD), R401C (AD-EDMD) and R453Q (AD-EDMD). Patient fibroblasts with LMNA mutations were obtained from a punch biopsy of the inner forearm following an informed consent or as an autopsy sample (Y259X). Patient fibroblasts with LMNA mutations were kindly supplied by Prof. Manfred Wehnert (R249Q, R401C and R453Q), Prof. Kate Bushby (E358K) and Prof. Jos Broers (Y259X). Fibroblasts with LMNA mutations were cultures in the same media/serum with appropriate antibiotics as described for wild-type (control) human fibroblasts.

### *2.1.2 SUBCULTURE*

Cultures were grown to 70-80% confluence and sub-cultured thereafter at a seeding density of 3 x $10^5$ cells per 75 $cm^2$ flasks. Briefly, cells were washed with Versene buffer (137 mM NaCl, 2.7 mM KCl, 8 mM $Na_2HPO_4$, 1.5 mM $KH_2PO_4$, 1.5 mM EDTA pH.7.4) and detached by treatment with Versene buffer containing 10% Trypsin (Sigma) for 5 min at 37° C in a humidified incubator. Cells were neutralised with fresh DMEM (1:5 ratio) containing 10% of serum (NCS) and appropriate antibiotics. Cells were transferred to a sterile universal tube, counted by haemocytometer and centrifuged at 1000*g* for 5 min in Sigma centrifuge. Cell pellets were diluted in an appropriate

volume of fresh DMEM containing 10% serum (NSC) and antibiotics and seeded into an appropriate number of flasks.

### *2.1.3 CRYOPRESERVATION OF CULTURES*

Cells were routinely cryopreserved in liquid nitrogen. Sub-confluent cultures were detached by trypsinization and pelleted by centrifugation as described above. The cell pellets were resuspended on ice in 1ml of complete medium (10% NCS) containing 10% dimethyl sulfoxide (DMSO, Sigma) per 1x $10^6$ cells. The cell suspension was transferred to a cryovial and placed at -70° C overnight before storage in liquid nitrogen. To re-establish cultures, the cell suspensions were defrosted in 37° C water bath and cells were added slowly to medium containing 10% serum. The next day the medium was replaced by fresh medium containing 10% serum and appropriate antibiotics.

### *2.1.4 QUIESCENT AND PROLIFERATING CULTURES*

#### 2.1.4.1 Serum-starvation and re-stimulation

To induce quiescence (transient growth arrest) by serum-starvation, wild-type human dermal fibroblasts of early (p8) or late (p42) passage were seeded at 2.5 x $10^5$ cells per 90 mm dishes or 3 x $10^4$ cells per 9 mm well in 6-well plates and grown for 2 days in complete medium (10% serum) as described above. On the 3$^{rd}$ day, serum-containing media was aspirated off, cells were washed with fresh DMEM containing 0.5% NCS and maintained in the same starvation media for the next 4-5 days at 37° C in humidified incubators. To induce serum re-stimulation of quiescent cultures (re-entry into cell cycle), starvation media was aspirated off, cells were washed once in fresh DMEM supplemented with 10% serum (NCS) and thereafter growth in the same complete medium. For 24 hour serum-restimulation experiments, quiescent cultures were grown in the presence of 10% NCS for 6, 12, 18 or 24 hours and subsequently harvested or prepared for immunofluorescence microscopy at those time points. For experiments with fibroblasts undergoing quiescence, cultures were grown for 2 days in 10% NCS as described above and maintained in starvation medium (0.5% NCS) for 2 days. In these experiments as a proliferating control, cultures were serum-starved for 5

days and serum re-stimulated in 10% serum for 48 hours. To obtain proliferating cultures in all other experiments, cells were grown for 3 days in 10% NCS after serial passage to ensure exponential growth. All cultures where then processed for whole cell extraction, immunofluorescence microscopy, biochemical fractionation or immuno-precipitation as described below.

### 2.1.4.2 Quiescence by contact-inhibition

To induce quiescence by contact-inhibition (confluence), wild-type and laminopathy fibroblasts of early (p8-12) or wild-type fibroblasts of late (p42) passage were seeded at 3 x $10^5$ cells per 90 mm dishes or 3 x $10^4$ cells per 9 mm well in 6-well plates in the presence of complete medium (10% serum) and maintained thereafter for 7 days without media change to induce confluence (confluent stage) or for 10 days (post-confluent stage). Alternatively, wild-type fibroblasts of late (p42) passage were seeded at 1 x $10^5$ cells per 9 mm well in 6-well plates in the presence of complete medium (10% serum) and grown for 3 days to induce high density. All cultures were then processed for whole cell extraction, biochemical fractionation or immunofluorescence microscopy.

## *2.1.5 IN VITRO AGEING OF HUMAN DERMAL FIBROBLASTS*

Wild-type human dermal fibroblasts were aged in culture through a serial passage during which they were established at a seeding density of 3 x $10^5$ cells per 75 $cm^2$ flasks and sub-cultured thereafter at a constant density. This standard procedure was performed until cells significantly decreased their proliferative potential and reached a replicative crisis known as senescence (Hayflick and Moorhead 1961, Hayflick *et al.*, 1965). Wild-type human dermal fibroblasts reached a senescent stage within 40-50 passages as assessed by light microscopy, immunofluorescence microscopy using proliferation markers and flow cytometry. The number of population doublings a cell strain can undergo is a distinct phenotypic characteristic independent of the chronological age of the culture. As opposed to quiescent cultures (see above), senescent cultures arrested their growth in the presence of mitotic stimuli (serum). They were also resistant to apoptosis for long periods of growth in culture. Senescent cultures displayed flat characteristic appearance and showed increased resistance to detachment

from culture flasks by trypsinization during sub-culturing (15 min incubation in Versene/trypsin was required as opposed to 1 min for early passage cultures). This is most likely dependent on the formation of strong focal adhesion complexes in senescent cultures which accumulate a range of extracellular matrix proteins, some which are not expressed by early passage cultures (Campisi *et al.*, 2001).

In this study, wild-type human dermal fibroblasts of early (p7-p12), mid (p17-p27) and late (p40-44) passage were used for experiments. In the experiments below, wild-type fibroblasts between passage 40 and 45 were used at which stage less than 20% of fibroblasts were still capable of dividing (as assessed by immunofluorescence microscopy using proliferation markers). Having some cells still capable of division within senescent cultures provided a useful tool when confirming performing a comparative immunofluorescence analysis between proliferating and permanently arrested cells. Wild-type fibroblasts of late (p40-45) passage grew very slowly and needed 7-10 days to reach ~60% confluence in 75 $cm^2$ flasks as opposed to wild-type fibroblasts of early (p7-12) passage which reached 80% confluence within 4-5 days. In addition, because of the increase in cell size in late passage cultures, there is a reduction of number of cells per unit area and majority of cells are devoid of cell-cell contacts as opposed to cultures of early passage fibroblasts in which any given cell is encircled by a number of neighbouring cells. To minimise differences in their growth curves, late passage fibroblast cultures were sub-cultured at 1:2 ratio (which was found to aid their viability) whilst early passage fibroblasts were sub-cultured at 1:4 ratio and both cultures were harvested after 3 days of growth in culture for use in subsequent experiments. To circumvent of a difficulty of having significantly lower cell counts of late passage cultures for preparation of whole cell extracts and biochemical fractionation, larger number of 75 $cm^2$ flasks were seeded with late passage cultures. In experiments where a high number of cells was required (10 x $10^6$ cells for biochemical fractionation), ~30X 75 $cm^2$ flasks of late passage fibroblasts sub-cultured at a 1:2 ratio were required as compared to ~10X 75 $cm^2$ flasks of early passage fibroblasts sub-cultured at a 1:3 ratio to achieve identical cell counts.

### 2.1.5.1 In vitro ageing of fibroblasts with LMNA mutations

Early (p7) passage laminopathy fibroblasts with the following mutations Y259X, R249Q, E358K and R453Q were seeded at 3 x $10^5$ cells per 75 $cm^2$ flasks and passaged thereafter by seeding at a constant density as described for wild-type fibroblasts. Laminopathy fibroblasts reached a senescent stage within 20-25 passages as assessed by light microscopy and immunofluorescence microscopy using proliferation markers. In this study, laminopathy fibroblasts of early (p12) and mid (p18-p24) passage were used for experiments.

## 2.2 IMMUNOCYTOCHEMISTRY AND CONFOCAL MICROSCOPY

### *2.2.1 FIXATION*

Wild-type and laminopathy human dermal fibroblasts of early (p7-12), mid (p18) or wild-type fibroblasts of late (p42-44) passage were seeded at 3 x $10^4$ cells/well on sterile glass coverslips in 6-well plates in the presence of complete medium (10%) and grown for 3 days to obtain proliferating cultures as described above. For serum-starvation, re-stimulation and confluence experiments, wild type and laminopathy fibroblasts of early (p8-12) or late (p42) passage were seeded at the same density in 6-well plates and grown as described above. All cultures were washed once in PBS and either fixed with 4% formaldehyde in phosphate-buffered saline (PBS) for 15 min at room temperature and permeabilized in PBS/0.5%Triton X-100 for 5 min at 4° C, or first extracted *in situ* followed by fixation and permeabilization (see below). For antibodies LN43, phospho-H2A.X and phospho-H3, cells had to be first incubated for 5 min in ice-cold hypotonic buffer containing 0.1% Triton X-100 and then fixed and permeabilized as described above. Following fixation, cells were washed three times for 5 min each in PBS and incubated in Blocking buffer containing PBS/1%NCS for 45 min at room temperature. For phospho-histone antibodies H2A.X and H3, PBS washes, blocking buffer and primary dilution buffer contained 0.1% Triton X-100 to aid revealing of their epitopes according to the protocol by von Zglinicki *et al.*, 2001. For rabbit polyclonal antibodies, phospho-Rb780 and Rb795, blocking buffer used was PBS/1%BSA (Cell Signalling).

### *2.2.2 PRIMARY ANTIBODIES*

Primary antibodies were applied for 1 hour at room temperature in a moist chamber after which cells were washed 5X in PBS. When cells were previously extracted *in situ*, cells were incubated in primary antibodies overnight at 4° C and kept in a moist chamber. Primary antibodies used and their dilutions are described in Table 2.1. All primary antibodies were diluted in Dilution buffer containing PBS/1%NCS except for rabbit polyclonal antibodies phospho-Rb780 and Rb795 which were diluted in Tris-buffered saline TBS/1%BSA according to manufacturer's instructions (Cell signalling).

### *2.2.3 SECONDARY ANTIBODIES*

Secondary antibodies were applied for 1 hour in dark at room temperature in a moist chamber after which cells were washed 4X in PBS and 1X in deionised water. All secondary antibodies were diluted 1:50 in the same dilution buffer as their respective primary antibodies. Secondary antibodies used were donkey anti-mouse and anti-rabbit IgG conjugated to rhodamine (TRITC) or fluorescein (FITC) (Strata-tech). Secondary antibodies used and their dilutions are summarised in Table 2.2. After several washes in PBS, coverslips were mounted facedown in DNA staining mixture (12% Mowiol, 1 ng/ml 4.6-diamidino-2-phenylin-dole (DAPI), 2.5% DAPCO, 30% glycerol, 120 mM Tris ph 8.5) and used immediately for microscopy or otherwise stored at 4° C.

### *2.2.4 MICROSCOPY*

For viewing and imaging cells on coverslips a BioRad Radiance 2000 confocal microscope imaging system with LaserSharp software (Bio-Rad) was used equipped with 40X and 63X/1.40 oil immersion lens. Alternatively, for imaging DNA in cells, Zeiss LSM 510 META confocal microscope imaging system (Zeiss) was used equipped with 40X and 63X/1.10 lens. A dynamic range adjustment was set up to optimise the signal for the fluorophores and the same optimised conditions were used for comparisons of the intensity of signals between different cultures. Images were collected in Sequential Mode (BioRad) or Multi-track Mode (Zeiss). Collected images were projected as black and white or blue/red/green colour merged micrographs in which DAPI was in blue.

## 2.3 FLOW CYTOMETRY

Wild-type fibroblasts of early (p12) and late (p44) passage were seeded at 3 x $10^5$ cells per 75 $cm^2$ flasks and grown for 3 days in complete medium (10%) as described above. Cultures were trypsinised, pelleted, washed in PBS and collected by centrifugation. Cell pellets were resuspended in 0.5 ml PBS and 4.5 ml methanol pre-chilled at -20° C (1:9 ratio). Methanol was added drop-wise with constant vortexing of cells and incubated for 30 min at -20° C or overnight at 4° C. Following incubation, pellets were collected by centrifugation at 1000*g* for 5 min at 4° C and washed once in a high volume of PBS. Subsequently, cell pellets were incubated in 500 µl of PBS containing 100 µg/ml RNAse and 25 µg/ml of the fluorescent dye, propidium iodide (PI). Finally, cells were washed once in PBS, centrifuged and diluted in 1 ml of PBS for cell cycle analysis on a Becton Dickinson FACSCaliber flow cytometer. Cells were excited at 488 nm by an argon ion laser and fluorescence from PI was collected for 10,000 single cell events through 585/542 nm wavelength band-pass filter (FL2 detector). Data was collected as dot plots and DNA histograms. Dot plots measure the relative cell size and granularity by detecting forward and side scattering patterns of cells passing though laser respectively. DNA histograms measure PI fluorescence which is proportional to the DNA content of each individual cell and therefore determine cell cycle phase distribution of cells (G1, S, G2, and M).

## 2.4 *IN SITU* NUCLEAR MATRIX EXTRACTION

Wild-type and laminopathy human dermal fibroblasts of early (p7-12), mid (p18) or wild-type fibroblasts of late (p42-44) passage were seeded at 3 x $10^4$ cells/well on sterile glass coverslips in 6-well plates in the presence of complete medium (10%) and grown for 3 days to obtain proliferating cultures as described above. Alternatively, for serum-starvation and re-stimulation experiments, wild type early (p8) passage fibroblasts were seeded at the same density in 6-well plates and grown as described above. All cells were washed once in PBS and extracted by sequential treatment with detergents, nucleases and salt prior to fixation (Dyer *et al.*, 1997). Each buffer was used ice-cold and contained freshly added protease inhibitor cocktail. For phospho-Rb780 and -Rb795 antibodies, each buffer also contained phosphatase inhibitor cocktail I (inhibits serine/threonine protein phosphatases, PP-1 & PP-2A), both used at

recommended concentration (Sigma). At each stage of extraction, coverslips were removed in order to make comparisons between cells at each step of the treatment. Briefly, cells were washed three times in ice-cold CSK buffer (10 mM Pipes pH 6.8, 10 mM KCl, 300 mM sucrose, 3 mM $MgCl_2$, 1 mM EGTA pH 8.0). Cells were incubated in CSK buffer supplemented with 0.5% (v/v) Triton X-100 for 10 min at 4° C and rinsed three times in ice-cold RSB buffer (42.5 mM Tris-Cl ph 8.3, 8.5 mM NaCl, 2.6 mM $MgCl_2$). Next, cells were incubated in RSB-Magik solution (RSB buffer containing 1% (v/v) Tween 20 and 0.5% (v/v) sodium deoxycholate) for 10 min at 4° C and rinsed twice in ice-cold Digestion buffer (10 mM Pipes pH 6.8, 50 mM NaCl, 300 mM sucrose, 3 mM $MgCl_2$, 1 mM EGTA pH 8.0). To digest DNA, cells were incubated in 100 units/ml of RNAse-free DNAse I in Digestion buffer for 30 min at room temperature. To remove digested material, 1 M ammonium sulphate [$(NH_4)_2SO_4$] was added slowly to the digestion buffer to a final concentration of 0.25 M and incubated for 5 min at 4° C. Finally, cells were washed twice with ice-cold digestion buffer, formaldehyde-fixed, permeabilized with PBS/0.5% Triton and prepared for immunofluorescence microscopy as described above.

## 2.5 PREPARATION OF WHOLE CELL EXTRACTS

Wild-type and laminopathy fibroblasts of early (p7-12), mid (p17-27) or wild-type fibroblasts of late (p44) passage were seeded at 3 x $10^5$ cells per 75 $cm^2$ flasks and grown for three days in complete medium (10%) as described above. Alternatively, for serum-starvation, re-stimulation and confluence experiments, wild type fibroblasts of early (p8) or late (p42) passage were seeded at the same density in 90 mm dishes and grown as described above. All cell cultures were washed in Versene buffer, trypsinised and resuspended in fresh medium plus 10% serum. Cells were transferred to a sterile universal tube and counted using haemocytometer. Pellets of equal number of cells (2x $10^6$) were collected by centrifugation at 1000*g* for 5 min and further washed with ice-cold PBS. Cells were transferred to a 1.5 ml centrifuge tube and lysed in 0.1 ml of ice-cold Hypotonic buffer per 2 x $10^6$ cells (10 mM Tris pH 7.4, 10 mM KCl, 3 mM $MgCl_2$, 0.1% Triton X-100), containing freshly added protease inhibitor cocktail at recommended concentration (Sigma) and 100 units/ml of RNAse-free DNAse I in Hypotonic buffer for 10 min on ice. Cell lysates were resuspended in 1:1 ratio of 2X Laemmli SDS Reducing Sample buffer (125 mM Tris-HCl ph 6.8, 2% SDS, 200 mM

DTT (dithiothreitol), β-mercaptoethanol (β-ME), 5% glycerol, 0.2% bromophenol blue). Thereafter, samples were boiled for 5 min at 95° C, centrifuged in a bench-top centrifuge for 1 min at 13,000*g*, and used immediately or kept at -20° C for later use.

### *2.5.1 PREPARATION OF CELL EXTRACTS FOR DETECTION OF PROTEIN DISULPHIDE CROSS-LINKS OR PROTEIN GLUTATHIONE ADDICTS*

For detection of disulphide-cross-linked proteins or protein glutathione addicts under non-reducing conditions, wild-type and laminopathy fibroblasts of early (p12), mid (p22-24) or wild-type fibroblasts of late (p40) passage were lysed in the above Hypotonic buffer in the additional presence of sulfhydryl group blocking reagent N-ethylmaleimide (NEM, Sigma) at a final concentration of 40 mM. NEM-treated cell lysates were resuspended in 1:1 ratio of 2X SDS Non-Reducing Sample buffer (without DTT and β-ME). As a control, NEM-treated lysates were resuspended in 1:1 ratio of 2X SDS Reducing Sample buffer. Alternatively, for detection of cysteine-cross-linking under oxidising conditions, wild-type and laminopathy fibroblasts of early (p7-15), mid (p18-24) or wild-type fibroblasts of late (p40) passage were lysed in the Hypotonic buffer in the absence of NEM and resuspended in 1:1 ratio of 2X SDS Non-reducing Sample buffer. All samples were boiled for 5 min at 95° C and centrifuged in a bench-top centrifuge for 1 min at 13,000*g*.

## 2.6 BIOCHEMICAL FRACTIONATION

Wild-type fibroblasts of early (p7) or late (p44) passage were seeded at 3 x $10^5$ cells per 75 $cm^2$ flasks and grown for three days in complete medium (10%) as described above. Alternatively, for experiments with fibroblasts undergoing quiescence or serum-restimulation, wild-type fibroblasts of early (p8) passage were seeded at the same density in 90 mm dishes and grown as described above. Cells were washed once in Versene, trypsinized and counted. Five samples of equal number of cells, 2 x $10^6$ cells, (labelled 1 to 5) were collected by centrifugation per each passage. Cells were washed in ice-cold PBS and then subjected to a sequential extraction with ice-cold buffers plus freshly added protease cocktail inhibitors at recommended concentration (Sigma). Cells were extracted in 0.1 ml of each buffer per 1 x $10^6$ cell pellets. Following each extraction step, soluble material was separated from insoluble material by centrifugation

at 4000*g* for 5 min at 4° C. In brief, five cell samples were washed once in ice-cold CSK buffer, centrifuged and their supernatants discarded. The pellet from the first sample was labelled P1 (this pellet is equivalent to a whole cell extract). The other 4 pellets were incubated in ice-cold CSK buffer containing 0.5% Triton X-100 for 5 min at 4° C. The resulting 4 cell lysates were passed several times through a 21-gauge needle and their pellets collected by centrifugation. The supernatant from the second sample was kept on ice and labelled S2 while its respective pellet was labelled P2 (this pellet represents nuclei). Next, the other 3 pellets were washed in ice-cold RSB buffer and incubated in ice-cold RSB-Magik solution for 5 min at 4° C. After centrifugation, the supernatant from the third sample was saved on ice and labelled S3 while its corresponding pellet was labelled P3. The remaining 2 pellets were then washed twice with ice-cold Digestion buffer and subjected to digestion in 500 units/ml of RNAse-free DNAse I in Digestion buffer for 30 min at room temperature. The 2 digested samples were then centrifuged and the supernatant from the fourth sample was kept and labelled S4 while its pellet was labelled P4. The last pellet was then further extracted with Extraction buffer (10 mM Pipes ph 8.3, 250 mM ammonium sulfate, 300 mM sucrose, 3 mM $MgCl_2$, 1 mM EGTA pH 8.0) for 5 min at 4° C. The final nuclear shell fraction was collected by centrifugation and labelled P5 and the corresponding soluble fraction was reserved and labelled S5. All supernatants were then concentrated by methanol-acetone (1:1 vol/vol, chilled at -20°C) precipitation at -20°C for 10min. Supernatants were centrifuged at 12,000*g* for 10 min and their pellets collected and washed once in PBS. All samples (pellets and methanol-precipitated supernatants) were then incubated in ice-cold hypotonic buffer using 0.1 ml per 2 x $10^6$ cells, containing 100 units/ml of RNAse-free DNAse I in Hypotonic buffer for 10 min on ice. Finally, samples were prepared for SDS-PAGE by boiling in 2X Laemmli SDS Reducing Sample buffer (1:1 ratio) for 5 min at 95° C and centrifuged for 1 min at 13,000*g* in a bench-top centrifuge.

## 2.7 GEL ELECTROPHORESIS AND IMMUNOBLOTTING

One-dimensional SDS-PAGE was performed according to Laemmli (1970). Since all of the proteins of interest fell into 60-100 kDa range, 8-10% final concentration of acrylamide solution in resolving gels was used for higher resolution in the upper part of the gel. To ensure gel-loading equivalence, the same proportion of each sample (corresponding to the same number of cells) was loaded in each well. Prestained

molecular weight markers (BioRad) were also loaded to verify both subsequent electro-transfer and to determine molecular weights of separated proteins. Proteins in samples were resolved on SDS-PAGE in Tank buffer (25 mM Tris pH 8.3, 192 mM Glycine, 0.1% SDS) at 100 V. For immunoblotting, proteins separated on gels were electrophoretically transferred onto nitrocellulose membranes (Schleicher and Schuell bioscience) in Transfer buffer (25 mM Tris-Cl pH 9.2, 200 mM glycine, 0.1% SDS, 20% methanol) by using Mini Transblot system (Bio-Rad) at 250 mA for 1hr.

### *2.7.1 MEMBRANE BLOCKING AND ANTIBODY INCUBATION*

Following transfer, membranes were washed once in Blot Rinse buffer (BRB) (10 mM Tris pH 7.4, 150 mM NaCl and 1 mM EDTA) and incubated in Blocking buffer (BRB, 0.1% Tween-20, 5% w/v non-fat dry milk) overnight at 4° C or for 1hr at room temperature with constant agitation. Membranes were washed three times for 5 min in BRB buffer containing 0.1% Tween-20 and incubated with primary antibodies for 1 hour at room temperature with constant agitation or when rabbit polyclonal phospho-Rb780 antibody was used, overnight at 4° C with constant agitation. Primary antibodies were diluted in either Blocking buffer for all monoclonal antibodies or TBS buffer (TBS, 0.1% Tween-2) containing 5% BSA for rabbit polyclonal antibody phospho-Rb780 according to manufacturer's instructions (Cell signalling). Primary antibodies used and their dilutions are presented in Table 1. Next, membranes were washed three times for 5 min in BRB/0.1% Tween or TBS/0.1% Tween and incubated with corresponding secondary antibodies diluted 1:2000 in either Blocking buffer or TBS buffer containing 5% w/v non-fat dry milk with gentle agitation for 1 hour at room temperature. Secondary antibodies were donkey anti-mouse or donkey anti-rabbit IgG conjugated to horseradish peroxidase (HRP) (Jackson ImmunoResearch) (Table1). Membranes were washed three times for 5 min in the same wash buffers used after primary antibodies.

### *2.7.2 DETECTION OF PROTEINS*

For the immunological detection of proteins, membranes were incubated in enhanced chemiluminescence (ECL) reagents (Amersham Life Science) and exposed to x-ray film for 10 sec to 1 min. For over-exposure, immunoblots incubated in ECL reagents were

exposed to x-ray film for longer periods of time (5 min). Signals obtained for the protein bands on the autoradiograms were analysed by densitometry using Quantity One 1-D analysis software (BioRad) on the scanned autoradiograms.

### *2.7.3 STRIPPING OF BLOTS*

To remove the primary and secondary antibody from blots, membranes were washed in TBS/0.1% Tween three times for 5 min and immersed in 100 mM glycine pH 2.5 for 5 min. Membranes were neutralised in 100 mM Tris pH 8.0 for 5 min. After stripping, membranes were washed briefly in TBS/0.1% Tween and either re-blocked in Blocking buffer for 1 hour prior to subsequent antibody incubations or stored at 4° C for later re-use.

## 2.8 IMMUNOPRECIPITATION

### *2.8.1 ISOLATION AND EXTRACTION OF NUCLEI*

Wild-type human dermal fibroblasts of early passage (p8-12) or late passage (p40-42) were seeded at 3 x $10^5$ cells per 75 $cm^2$ flasks and grown in complete medium (10% NCS) as described above. Cells were washed in Versene, trypsinised and counted. Pellets of equal number of cells (1 x $10^6$) were collected by centrifugation at 1000*g* for 5 min and washed with ice-cold PBS. Cell pellets were transferred to a pre-chilled 1.5 ml centrifuge tube and lysed for 5 min on ice in ice-cold Hypotonic buffer using - 0.5 ml per 1 x $10^6$ cells, which contained freshly added protease inhibitor cocktail at recommended concentration (Sigma). For detection of disulphide bonded complexes on non-reducing gel electrophoresis, cell pellets were lysed in the same hypotonic buffer which also contained sulfhydryl group blocking reagent N-ethylmaleimide (NEM, Sigma) at a final concentration of 40 mM. Cell lysates were transferred to a Wheaton homogeniser and homogenised using tight-fitting pestle in 10 rotating strokes. Cell lysates were then transferred into a micro-centrifuge tube and the nuclear pellets were collected by centrifugation at 1000*g* for 5 min at 4° C in a bench-top centrifuge. Supernatants were discarded and pelleted nuclei extracted in 500 µl of High Salt Extraction buffer (20 mM Tris ph 7.4, 500 mM NaCl, 0.1 % Triton X-100, 1.5 mM EDTA) in the presence of freshly added protease inhibitor cocktail for 10 min on ice.

For non-reducing electrophoresis, pelleted material was extracted in the above buffer that also contained 40 mM NEM. Extracted nuclei were centrifuged at 12,000*g* for 10 min at 4° C in a bench-top centrifuge. Nuclear supernatants were transferred to a new micro-centrifuge tube whilst pelleted material was discarded. During centrifugation, dialysis tubing was prepared and supernatants were carefully transferred using glass pipette into pre-cut pieces of dialysis tubing secured with a clipper on one side. Nuclear supernatants were dialysed in large volume of ice-cold PBS/0.1% Triton buffer overnight at 4° C with constant stirring.

### *2.8.2 PREPARATION OF DYNABEADS/ANTIBODY COMPLEXES*

Sheep anti-mouse Dynabeads (Dako) were washed in PBS/1% BSA a few times using magnetic particle concentrator and incubated with the relevant primary mouse monoclonal antibodies diluted in PBS/1% BSA. JOL2 antibody diluted 1:50 or LAP15 antibody diluted 1:10 were mixed with 100 µl of Dynabeads in 1:1 ratio and incubated overnight at 4° C using Dynal rotator. Following dialysis, protein concentration in the dialysed samples was determined using Bio-Rad protein Assay and equalised by dilution in PBS/0.1% Triton. Dialysed samples were then incubated with the relevant antibody coupled to 100 µl of Dynabeads for 2 hours at 4° C. JOL2 antibody coupled to Dynabeads was used to immunoprecipitate lamins A/C and LAP15 antibody coupled to Dynabeads was used to immunoprecipitate LAP2α from dialysed nuclear supernatants. Following incubation, supernatants (labelled S) were collected using magnetic particle concentrator and beads were washed several times in PBS/ 0.1% Triton. Supernatants were methanol/acetone precipitated (1:1 vol/vol, chilled at -20° C) for 10 min at - 20° C and centrifuged at 12,000*g* for 10 min at 4° C. Lamin A/C immuno-precipitates (P) and supernatants (S) were prepared for non-reducing SDS-PAGE by boiling in 2X SDS Non-Reducing Sample buffer for 5 min at 95° C. LAP2α immuno-precipitates (P) and supernatants (S) were prepared for reducing SDS-PAGE by boiling in 2X Laemmli SDS Reducing Sample buffer (1:1 ratio) for 5 min at 95° C. Boiling disassociates the immuno-complexes from the beads and all samples were then centrifuged for 1 min at 13,000*g*.

### *2.8.3 DETERMINATION OF PROTEIN CONCENTRATION USING THE BRADFORD ASSAY*

Protein concentration in the dialysed nuclear supernatants above was determined using Bio-Rad protein Assay, which is based on differential colour response of Coomasie Brilliant Blue dye to differing protein concentrations. The dye was diluted 1:5 and 980 µl of it was vortex-mixed with either 20 µl of each supernatant or 20 µl of deionised water as a blank control. Absorbance was measured at 595 nm and protein concentration calculated according to the equation $OD_{595}$ of 0.45 = 1 mg/ml. To determine protein concentration of each extract in µg/µl, the calculated µg values were divided by 20. Subsequently, all extracts were equalised at the same protein concentration by dilution in PBS/0.1% Triton.

## 2.9 PROTEIN KNOCK-DOWN BY SMALL INTERFERING RNAs (siRNAs)

### *2.9.1 SELECTION OF siRNA SEQUENCES*

Human LAP2α specific siRNA duplexes were designed by and a kind gift from Jenz Harborth. The sequences were selected from the open reading frame of human LAP2α mRNA in order to obtain 21-nt sense and 21-nt antisense strand with symmetric 2-nt 3'overhangs of identical sequence. LAP2α-specific sequence was submitted to a BLAST search against the human genome to ensure than only LAP2α mRNA of the human genome was targeted. The siRNA specific sequence targeting LAP2α was from nucleotide position 720 to 738 relative to the start codon (accession number U09086, GeneBank). The sequence of each single-stranded LAP2α siRNA oligonucleotides was as follows: sense 5' GCUAAGAAAGUACAUACUUtt 3'

antisense 5'AAGUAUGUACUUUCUUAGCtg 3'.

As a control RNAi, siRNA oligonucleotides targeting Firefly (*Photinus Pyralis*) luciferase gene (labelled GL2) from a nucleotide position 153 to 175 was used relative to the start codon (accession number X65324, Genebank) (a gift from Jenz Harborth). The sequence of each single-stranded GL2 luciferase siRNA oligonucleotides was as follows: sense 5' ACGUACGCGGAAUACUUCGaa 3'

antisense 5' UCGAAGUAUUCCGCGUACGug 3'

### *2.9.2 CELL CULTURE AND TRANSFECTION OF siRNAs*

Wild-type human dermal fibroblasts of early (p8) passage were grown in complete medium (10% NCS, antibiotics) for 3 days in 75 $cm^2$ flasks as described before. One day before performing transfection, confluent cultures (70%) were trypsinised, diluted with fresh serum without antibiotics and counted. Cells were seeded at 5 x $10^4$ cells/well on sterile glass coverslips in 24-well plates in the presence of complete medium (532 µl/well). Transient transfection of LAP2α or control (GL2) siRNAs was carried out using Oligofectamine reagent (Life technologies). RNAi transfection procedure was modified from Harborth *et al.* (2001). 12 µl of serum-free OPTIMEM 1 medium (Life technologies) and 3 µl of Oligofectamine were pre-incubated for 5-10 min at room temperature. During this incubation time, 50 µl of OPTIMEM 1 medium were gently mixed with 3 µl siRNA. For transfection complex formation, the two mixtures were combined and incubated for 20 min at room temperature. After addition of 32 µl of OPTIMEM 1 medium to the mixture, the entire mixture was added to the cells in a drop-wise manner per one well resulting in a final concentration of 100 nM for the siRNAs. The addition of 32 µl of OPTIMEM 1 medium is used to adjust the final culture volume to 600 µl. Following transfections, cells were grown for 24 hours in culture and thereafter sub-cultured at 1:2 ratio to ensure medium density of cultures.

### *2.9.3 DETERMINATION OF TRANSFECTION EFFICIENCY*

Cells were assayed after 24-48 hours following transfection. Transfection efficiency of LAP2α RNAi was determined by immunofluorescence microscopy of LAP2α- and GL2 RNAi-transfected cultures and was estimated to be in the range of 50-60%. Specific silencing of LAP2α protein was confirmed by three independent experiments. To determine transfection efficiency of LAP2α RNAi by immunoblotting, LAP2α and GL2 RNAi transfected cells grown in 24-well plates were trypsinised, diluted in fresh medium (10% NCS) and counted. Cells were used from three wells of a 24-well plate. Pellets of equal number of cells were washed once with ice-cold PBS and resuspended in 1:1 ratio of 2X Laemmli SDS Reducing Sample buffer. Samples were boiled for 5 min at 95° C, centrifuged for 1 min at 13,000*g* and used for SDS-PAGE. To confirm equal protein loading, blots were stripped and reprobed with LAP2β (LAP17) antibody.

**Table 2.1:** Primary antibodies used in this study (IF-immunofluorescence; IB-immunoblotting; m-monoclonal; p-polyclonal).

| Antibody | Target | Antibody type | Dilution | | Source |
|---|---|---|---|---|---|
| | | | IF | IB | |
| JOL2 | Lamin A/C | Mouse/m | 1: 50 | 1: 200 | Dyer *et al.*, 1997 |
| JOL4 | Lamin A | Mouse/m | undiluted | 1: 10 | Dyer *et al.*, 1997 |
| JOL5 | Lamin A/C | Mouse/m | undiluted | | Dyer *et al.*, 1997 |
| RαLC | Lamin C | Rabbit/p | 1: 50 | 1:100 | Venables *et al.*, 2000 |
| L6 8A7 | Lamin A/C | Mouse/m | | 1: 500 | Stick *et al.*,1998 |
| LN43 | Lamin B2 | Mouse/m | 1: 25 | 1: 100 | Dyer *et al.*, 1999 |
| LAP15 | LAP2α | Mouse/m | 1: 10 | 1: 100 | Dechat *et al.*,1998 |
| LAP12 | pan-LAP2 | Mouse/m | | 1: 100 | Dechat *et al.*,1998 |
| LAP17 | LAP2β | Mouse/m | 1: 10 | 1: 100 | Dechat *et al* 1998 |
| IF8 | Pocket A of Rb | Mouse/m | 1: 10 | 1: 10 | Bartek *et al.*, 1992 |
| AB5 | Pocket A/B of Rb | Mouse/m | 1: 10 | | Cell signalling |
| Rb Ser780 | Phopho-Ser780 & | Rabbit/p | 1: 100 | 1: 1000 | Cell signalling |
| Rb Ser795 | Ser 795 of Rb | Rabbit/p | 1: 100 | | Cell signalling |
| Phospho-H3 (Ser10) | Phopsho-Ser10 of Histone3 | Mouse/m | 1: 1000 | | Upstate Biotech |
| Phospho-H2.A.X | Phopho-Histone2.A | Mouse/m | 1: 1000 | | Upstate Biotech |
| Ki67 | Ki67 | Rabbit/p, | 1: 150 | | Dako |
| | | Mouse/m | 1: 50 | | Dako |
| SC-35 | SC-35 | Mouse/m | 1: 2000 | | Sigma |
| B-actin | B-actin | Mouse/m | | 1: 2000 | Sigma |
| GSH | Protein glutathione addicts | Mouse/m | | 1: 1000 | Santa Cruz |

**Table 2.2:** Secondary antibodies used in this study (IF-immunofluorescence; IB-immunoblotting)

| Antibody | Assay | Dilution | Source |
|---|---|---|---|
| Donkey anti-mouse FITC | IF | 1:50 | Strata-tech |
| Donkey anti-rabbit TRITC | IF | 1:50 | Strata-tech |
| Donkey anti-mouse TRITC | IF | 1:50 | Strata-tech |
| Donkey anti-rabbit FITC | IF | 1:50 | Strata-tech |
| Donkey anti-mouse HRP | IB | 1:2000 | Jackson Immunoresearch |
| Donkey anti-rabbit HRP | IB | 1:2000 | Jackson Immunoresearch |

# CHAPTER 1-GENERAL INTRODUCTION

## 1.1. THE NUCLEAR ENVELOPE AND THE NUCLEAR LAMINA

The main feature of eukaryotic cells is the nucleus, which enwraps the chromosomes, and is the site of DNA replication, RNA transcription and processing and ribosome assembly. The nuclear envelope (NE) is not just a boundary to the nucleus, but is an elaborate organelle that forms an interface between the nuclear and cytoplasmic compartments during interphase, and is involved in maintaining proper NE morphology, in DNA replication and nuclear growth, in organising nuclear contents, in RNA processing and export and in protein synthesis and processing (reviewed in Goldberg and Allen 1995). The NE is composed of the inner and outer nuclear membranes (INM and ONM, respectively), which are separated by the luminal space continuous with the endoplasmic reticulum (ER) lumen (**Figure 1.1**). ONM is a cytoplasmically opposed lipid bilayer that is connected to and resembles the rough endoplasmic reticulum with functional ribosomes attached and is a site for protein translation.

Communication between the nucleoplasm and cytoplasm takes place through many thousands of large supramolecular structures, called the nuclear pores, spanning the NE, where the inner and outer membranes join (reviewed in Goldberg and Allen 1995). Within these pores are anchored nuclear pore complexes (NPCs), which mediate and regulate bidirectional nuclear transport. Nucleo-cytoplasmic transport plays a fundamental role in coordinating the functions of the nucleus and cytoplasm. The NPCs accommodate both passive diffusion of ions and small metabolites, through 10 nm diameter aqueous channels in the NPCs, and active transport of most macromolecules, through a gated channel via signal- and energy-dependent mechanisms. The membrane present in the pores is called the pore membrane, and is associated with the peripheral and integral membrane proteins of the NPCs, and may provide a route for transferring integral membrane proteins from the INM to the ONM and vice versa.

The INM is a dynamic membrane that is able to grow during S phase, vesicularise at mitosis and bud during viral infection (reviewed in Goldman *et al.*, 2002). Underneath

the INM is the nuclear lamina, a term coined to describe a meshwork of near-tetragonally oriented nuclear-specific intermediate filaments, nuclear lamins, and a growing number of integral nuclear membrane (INM) and peripheral membrane (PM) proteins. The INM proteins are type II integral membrane proteins. They contain a nucleoplasmic N-terminal domain followed by a variable number of transmembrane segments and a C-terminal domain that faces the luminal space. Although their transmembrane domain confers their ability to be inserted into the INM, binding of these proteins to the nuclear lamins ensures their efficient retention at the NE. Currently, INM proteins include lamin B receptor-LBR (Worman *et al.*, 1990), six isoforms of lamina associated polypeptide 2-LAP2 (Foisner and Gerace 1993, Harris *et al.*, 1995, Berger *et al.*, 1996), three isoforms of lamina-associated polypeptide 1-LAP1 (Martin *et al.*, 1995), emerin (Manilal *et al.*, 1996), nurim (Rolls *et al.*, 1999), MAN1 (Lin *et al.*, 2000), Lem-3 (Lee *et al.*, 2000), UNC-50/UNCL (Fitzgerald *et al.*, 2000), luma (Dreger *et al.*, 2001), UNC-84/84A (Dreger *et al.*, 2001, Lee *et al.*, 2002), Syne-1 (synaptic nuclear envelope)/Myne1 (myocyte nuclear envelope)/nesprin 1α (Apel *et al.*, 2000, Mislow *et al.*, 2002, Zhang *et al.*, 2002), and SANE (Raju *et al.*, 2003). PM proteins do not appear to contain a segment that spans the INM and are more peripherally associated with the INM. These include otefin (Padan *et al.*, 1990), Young Arrest (YA) (Lin and Wolfner 1991), LBR kinase (Simos and Georgatos 1992), p34 (RNA splicing factor 2-associated protein) (Simos and Georgatos 1994) and p18 (homologous to mitochondrial isoquinoline-binding protein) (Simos *et al.*, 1996). Near the INM is the peripheral chromatin, a large proportion of which is the heterochromatin.

Recently, a family of giant ONM proteins including NUANCE (nucleus and actin connecting element) and Enaptin have been identified (Zhen *et al.*, 2002, Padmakumar *et al.*, 2004) along with their shorter splicing isoforms, nesprins, located at the INM (Zhang *et al.*, 2002). NUANCE and Enaptin contain N-terminal α-actinin type actin-binding (ABD) domain, a central coiled-coil rod domain and a C-terminal transmembrane domain and are proposed to structurally link lamina and nucleoskeleton to actin cytoskeleton in the cytoplasm (Zhen *et al.*, 2002, Padmakumar *et al.*, 2004).

There is strong evidence that lamins are not restricted to the nuclear periphery but exist throughout the nuclear interior. It is not known whether the internal lamins form similar or different structures from peripheral lamins. Given the growing number of lamin-

binding partners, it is not difficult to envisage that these might influence the assembly and/or structural properties of lamins. Photo-bleaching of intranuclear GFP-lamin A argues for the existence of both immobile lamin A structures and a free lamin A in the nucleoplasm (Broers *et al.*, 1999). In addition, the observation of intranuclear foci of A-type lamins during G1 phase of the cell cycle (Goldman *et al.*, 1992, Bridger *et al.*, 1993, Pugh *et al.*, 1997, Broers *et al.*, 1999, Kennedy *et al.*, 2000) and B-type lamin foci during S-phase (Moir *et al.*, 1994) raised the question as to whether these foci are in direct contact with the nuclear envelope. Nuclei of many cell types contain nuclear envelope derived invaginations extending into the nucleoplasm and making contact with the nucleolus, some of which even cut all the way through the nucleus (Fricker *et al.*, 1997, Broers *et al.*, 1999). These channels are lined with nuclear pore complexes and nuclear lamins and are proposed to be involved in nucleo-cytoplasmic transport (Fricker *et al.*, 1997). However, intranuclear spots of A-type and B-type lamins are not found to colocalise with membranes (Bridger *et al.*, 1993) or with NPCs (Moir *et al.*, 1994) and are thought to be genuine intranuclear structures.

The existence of non-chromatin nuclear proteins that remain insoluble following extraction with high concentrations of salt or chaotropic agents has been defined by Coffey and Penman as the nuclear matrix or nucleoskeleton (reviewed in Stuurman *et al.*, 1998). The nuclear matrix consists of an ordered and highly compartmentalised proteinaceous network of fibres, which are linked to and include the nuclear lamina and the nucleolar matrix. Removing chromatin from the nucleus also revealed the internal lamins (otherwise buried in dense chromatin), which form a part of a diffuse skeleton that ramifies throughout the interior of human nuclei (Hozak *et al.*, 1995). In addition, internal lamins are also found in nuclear bodies called nuclear speckles, which are components of nuclear matrix (Jagatheesan *et al.*, 1999). Moreover, A-type lamins interact with nucleoplasmic proteins such as a LAP2 isoform, LAP2α, and a retinoblastoma protein (Rb) and may anchor or organise components of the nuclear matrix (Ozaki *et al.*, 1995, Mancini *et al.*, 1994, Dechat *et al.*, 2000, Markiewicz *et al.*, 2002). The nuclear matrix including lamins preferentially associates with actively transcribed genes (the euchromatin), and displays both tissue- and differentiation-stage-specific changes in its protein composition (Bidwell *et al.*, 1993). It is, thus, implicated in the regulation of tissue-specific gene expression and organisation of functional domains within the nucleus.

## 1.2. EVOLUTION OF LAMIN GENES

Vertebrates have three lamin genes: LMNA, LNB1 and LNB2. The human LMNA gene on chromosome 1q21.2-3 encodes four alternatively spliced A-type lamins (**Figure 1.2**): somatic lamins A and C (Laliberte *et al.*, 1984), lamin AΔ10, found in somatic cells and tumours (Machiels *et al.*, 1996), and male germ cell-specific C2, the only expressed lamin in meiotic stages of spermatogenesis (Furukawa *et al.*, 1994, Alsheimer and Benavente 1996). While exon 1 through 9 of the lamin A, C and lamin AΔ10 mRNAs are identical, lamin A mRNA contains the 5' 90 bases of exon 10 followed by exon 11 and 12. In contrast, lamin C mRNA contains the complete 111-bp sequence of exon 10, but not exon 11 and 12. Lamin AΔ10 mRNA is identical to lamin A but lacks exon 9 and lamin C2 is identical to lamin C except that the N-terminal head and coil 1A are replaced by a short non-helical segment (Furukawa *et al.*, 1994).

The human LNB1 gene on chromosome 5q23.2-31.3 encodes lamin B1, and the LNB2 gene on chromosome 19p13.3 encodes lamins B2 and male germ cell-specific lamin B3 (Wydner *et al.*, 1996, Brandriff *et al.*, 1994, Furukawa *et al.*, 1993) (see **Figure 2**). In amphibians, A-type lamin La and B-type lamins Li and Lii are homologs of mammalian lamins A, B1 and B2 respectively (Stick and Hausen 1985). B-type lamin LIII is expressed in Xenopus embryos and oocytes and is not homologous to mammalian germ-cell specific B3. Instead, a sperm cell specific B-type lamin LIV has been identified in Xenopus (Benavente *et al.*, 1985).

In invertebrates such as *Drosophila Melanogaster*, there are two lamin genes, *Dm0* gene which codes for two B-type lamin isoforms Dm1 and Dm2 (Gruenbaum *et al.*, 1988) and *lamin C* gene which codes for an A-type lamin DmC (Reimer *et al.*, 1994), and in *Caenorhabditis elegans,* there is one B-type lamin gene, namely *lmn-1* and no A-type lamin gene (Liu *et al.*, 2000).

Comparing the structure of LMNA and LMNB genes in the same species shows a remarkable conservation of the exon/intron patterns (Stick 1992). In both genes the last exon encodes the CaaX motif whilst the lamin A-specific tail is encoded by an additional exon (exon 11), indicating that A-type lamins derived from the insertion of

**Table 1.1: A list of all diseases identified to date that are linked to altered nuclear lamina function** *(modified from Smith et al., 2005)*

| Gene mutated | Disease name | Disease abbreviation | References |
|---|---|---|---|
| *LMNA* | Emery-Dreifuss muscular dystrophy types 2 and 3 | EDMD2/3 | Bonne *et al.*, 1999 |
| *STA* (emerin) | X-linked Emery-Dreifuss muscular dystrophy type 1 | EDMD1 | Bione *et al.*, 1994 |
| *LMNA* | Cardiomyopathy, dilated, 1A | CMD1A | Fatkin *et al.*, 1999 |
| *LMNA* | Limb-girdle muscular dystrophy | LGMD1B | Muchir *et al.*, 2000<br>Cao and Hegele, 2000 |
| *LMNA* | Dunnigan-type familial partial lipodystrophy type 2 | FPLD2 | Shackleton *et al.*, 2000 |
| *LMNA* | Charcot-Marie-Tooth disease, axonal, type 2B1 | CMT2B1 | De Sandre-Giovannoli *et al.*, 2002 |
| *LMNA* | Hutchinson-Gilford progeria syndrome | HPGS | De Sandre-Giovannoli *et al.*, 2003;<br>Eriksson *et al.*, 2003 |
| *LMNA* | Atypical Werner Syndrome | AWS | Chen *et al.*, 2003 |
| *LMNA* | Lipoatrophy with diabetes, hepatic steatosis, hypertrophic caridomyopathy and leukomelanodermic papules | LDHCP | Caux *et al.*, 2003 |
| *LMNA* | Mandibuloacral dysplasia with type A lipodystrophy | MADA | Novelli *et al.*, 2002 |
| *ZMPSTE24* | Mandibuloacral dysplasia with type B lipodystrophy | MADB | Agarwal *et al.*, 2003 |
| *LMNA* | Restrictive dermopathy | RD | Navarro *et al.*, 2004 |
| *ZMPSTE24* | Restrictive dermopathy | RD | Navarro *et al.*, 2004 |
| *LMNA* | Seip syndrome | SEIP | Csoka *et al.*, 2004<br>Hoffman *et al.*, 2002 |
| *LBR* | Pelger-Huët anomaly | PHA | Schultz *et al.*, 2003 |
| *LBR* | Hydrops-ectopic calcification-moth-eaten skeletal dysplasia | HEM/Greenberg dysplasia | Waterham *et al.*, 2003 |
| *MAN1* | Osteopoikilosis, Buschke-Ollendorff syndrome and melorheostosis | BOS | Hellemans *et al.*, 2005 |

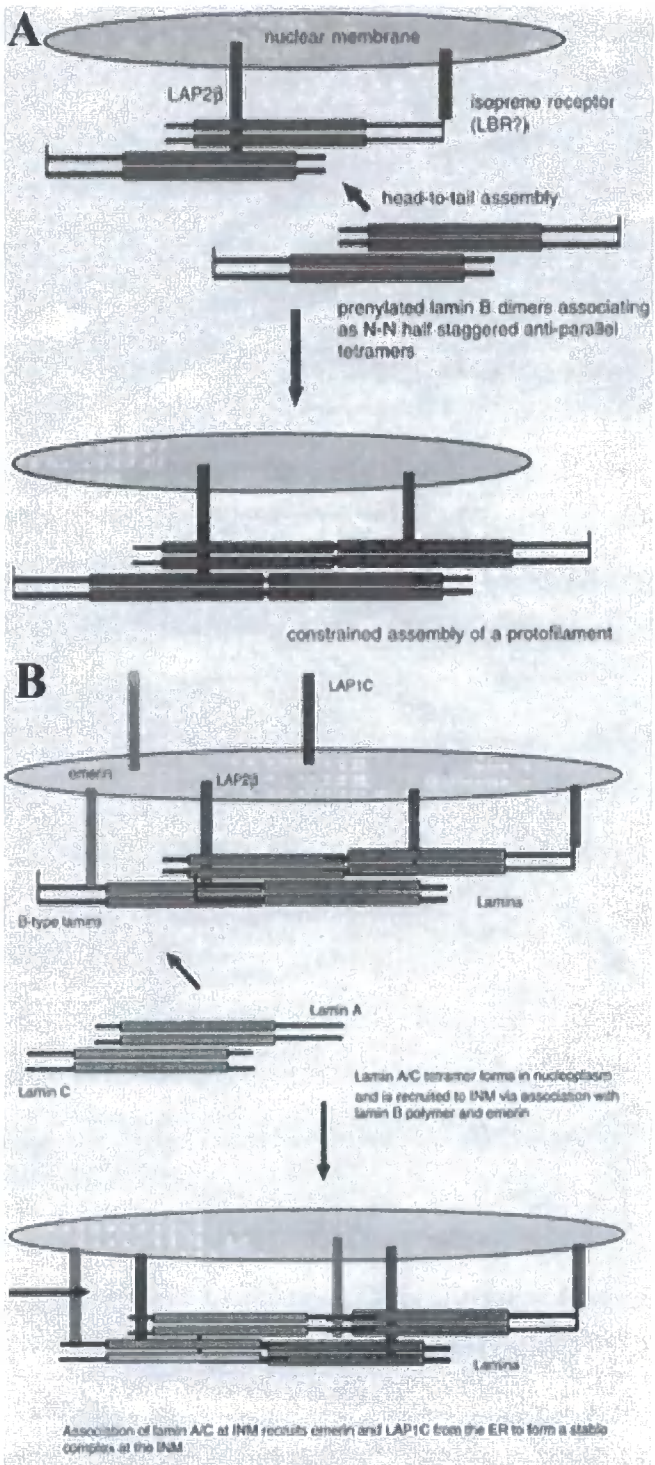


**Figure 1.5: Cartoon showing the constrained polymerisation of B-type lamin filaments and incorporation of A-type lamins at the inner nuclear membrane (INM). (A)** Tethering of B-type lamins to the INM in this model is through association with LAP2β and an isoprene receptor LBR. Lamin B dimers form N-N half-staggered anti-parallel associations to make tetramers and head-to-tail associations to form higher-order structures such as proto-filaments. **(B)** A-type lamin tetramers are incorporated into the INM by head-to-tail and anti-parallel associations with B-type lamin filaments, which leads to further recruitment of emerin and LAP1C from the outer nuclear membrane/endoplasmic reticulum (ONM/ER) to the INM, stabilising the A-type lamins.

*(Reproduced from Hutchison et al., 2001)*

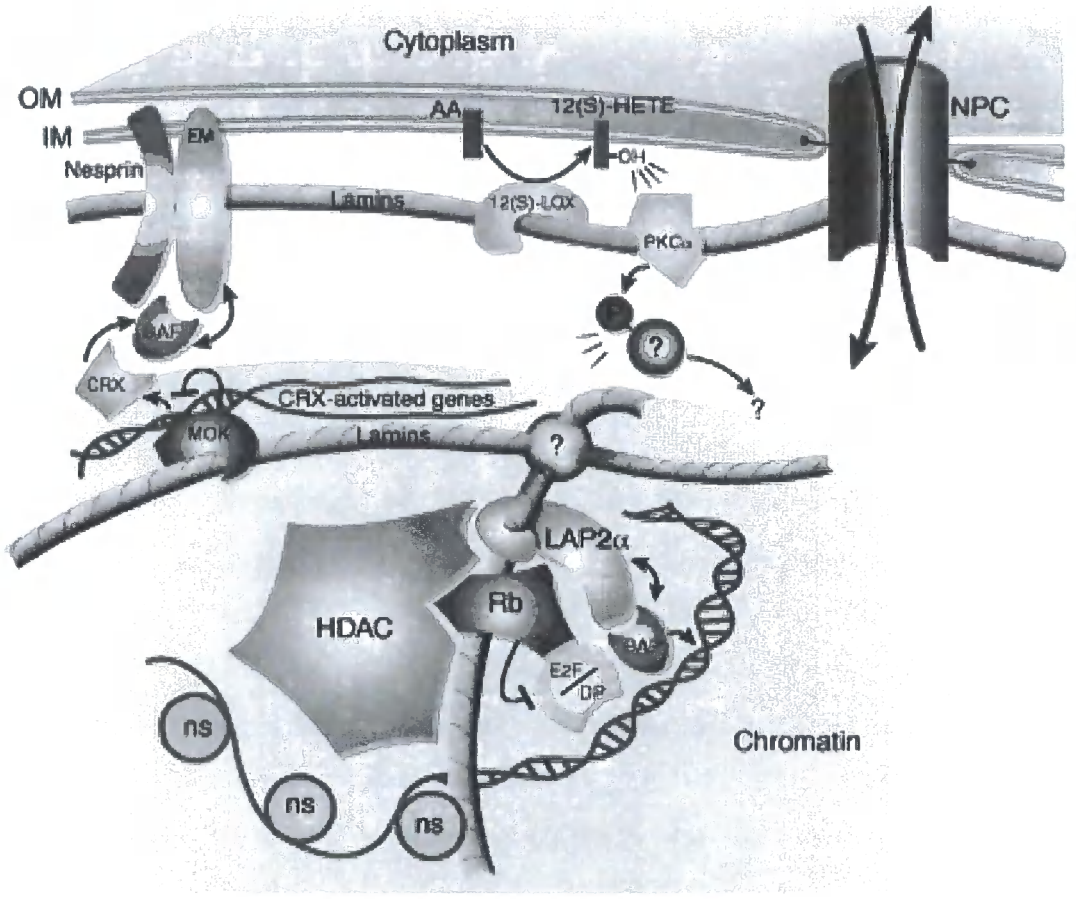


**Figure 1.6: A few interactions described for A-type lamins are illustrated.** The reader's attention is drawn to the bottom centre. Multiple oligomeric gene-regulation complexes might be formed by lamina-associated polypeptide 2α (LAP2α), A-type lamins, retinoblastoma protein (Rb), E2F/DP heterodimers (gene-specific activators), chromatin-silencing histone deacetylase complex (HDAC) and BAF (barrier-to autointegration-factor). NPCs, nuclear pore complexes; NS, nucleosome; OM, outer membrane; IM, inner membrane.

*(Reproduced from Zastrow et al., 2004)*

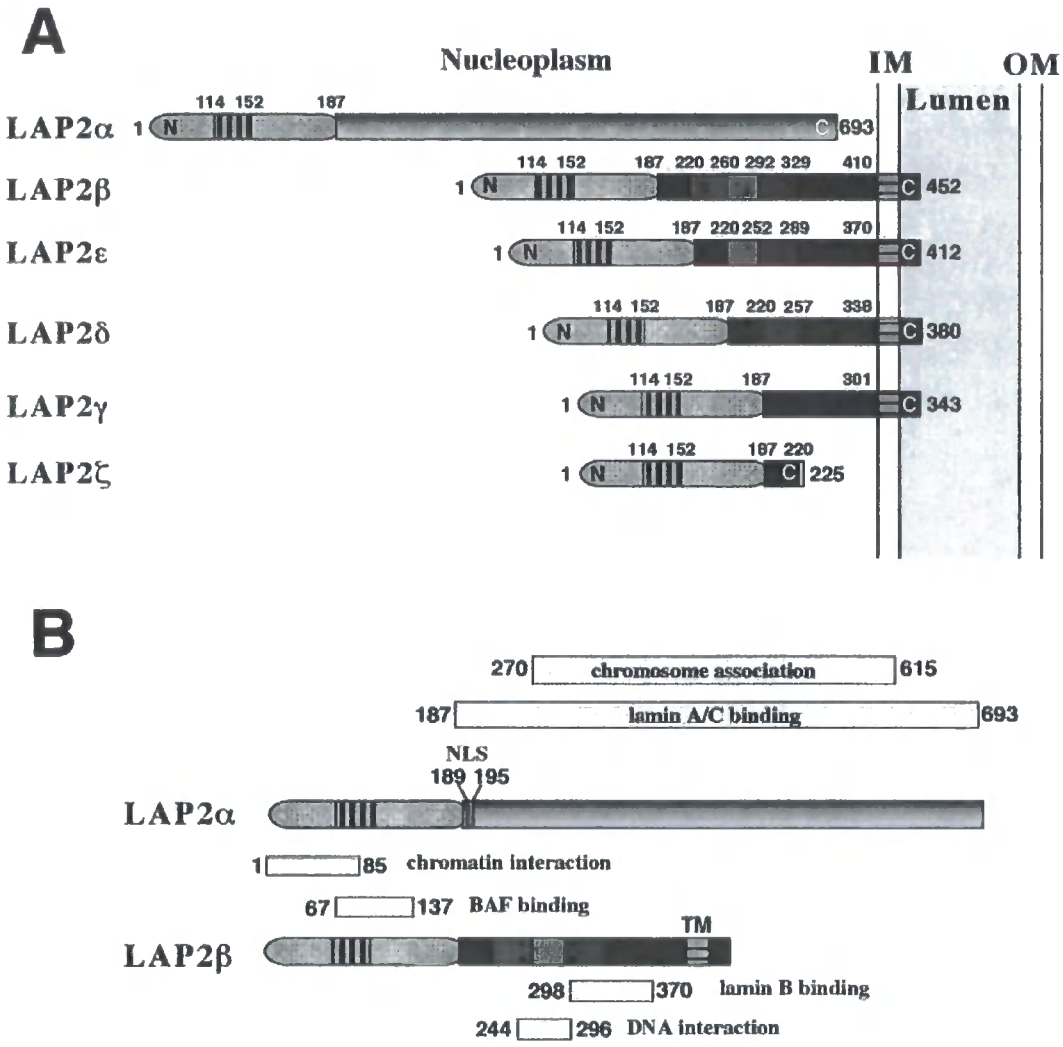


**Figure 1.7: Structural organization and functional domains of lamina-associated polypeptide 2 (LAP2) isoforms.** **(A)** Six alternatively spliced LAP2 isoforms have been identified in mammalian cells. **(B)** Regions in LAP2 proteins, found to contain specific interaction sites and/or functional domains. Numbers denote position of amino acids in human protein sequences; IM, inner membrane; OM, outer membrane; NLS, nuclear localization sequence; TM, transmembrane domain; N-head; C-tail.

*(Reproduced from Dechat et al., 2000)*

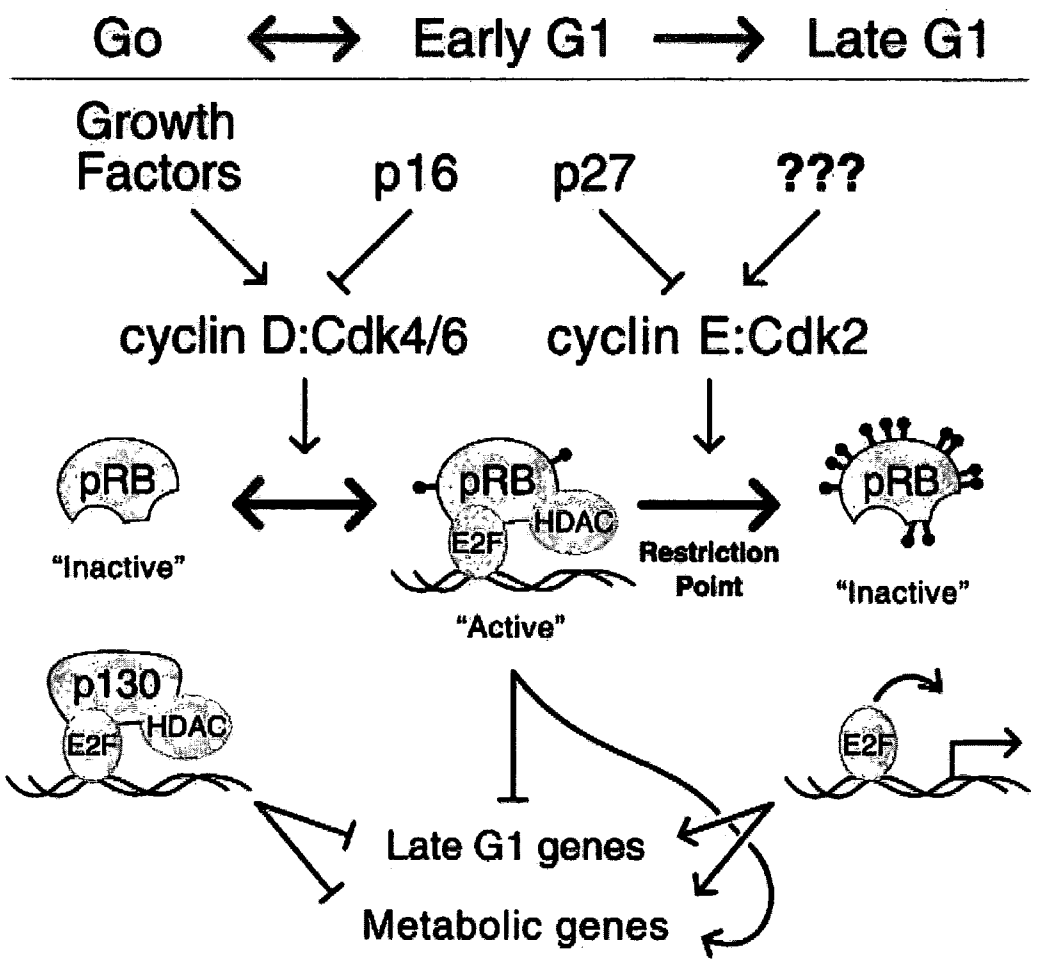


**Figure 1.8: A model of G1 cell cycle progression.** $G_0$ cells maintain E2F complexed with retinoblastoma-related protein p130. Growth factor stimulation activates cyclin D-Cdk4/6 complexes driving cells to pass through the reversible transition from $G_0$ into early G1 (Cdk- cyclin-dependent kinase). Cyclin D-Cdk4/6 hypo-phosphorylate retinoblastoma protein (Rb) and thereby increase Rb's avidity for E2Fs. Maintenance of cyclin D-Cdk4/6 activity by continuous growth factor stimulation is required during early G1. Loss of growth factor signalling or increases in cyclin inhibitor p16 drive cells back into $G_0$. Activation of cyclin E-Cdk2 in late G1 hyper-phosphorylates Rb, causing the release of E2Fs to activate transcription and drive cells across the irreversible restriction point into S phase. Histone deacetylase complex (HDAC)

*(Reproduced from Ezhevsky et al, 2001)*

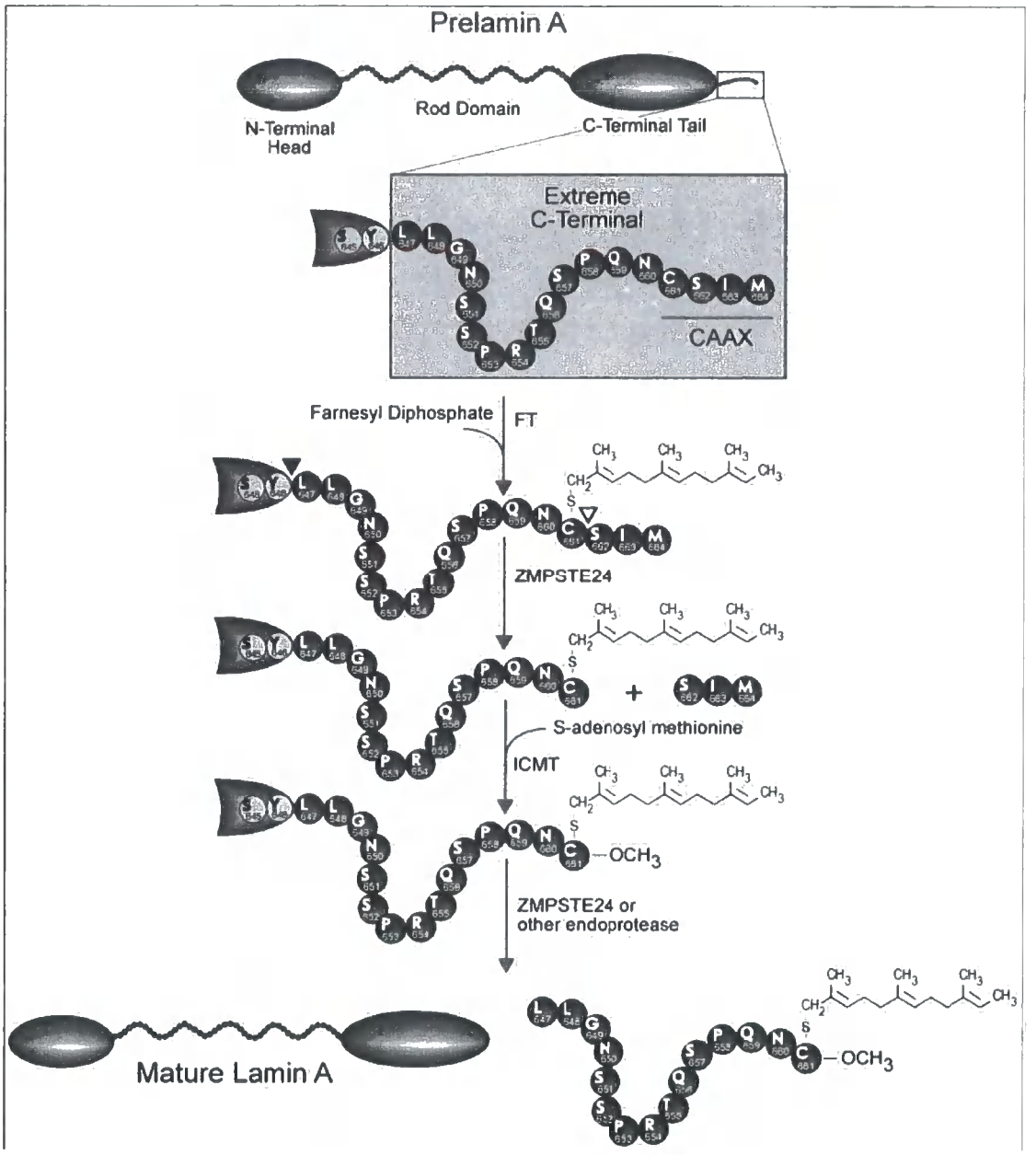


**Figure 1.4: Schema of steps involved in prelamin A processing to mature lamin A.** The post-translational processing of prelamin A involves the extreme carboxy-terminal residues. In the first step, farnesyl diphosphate is used to farnesylate the cysteine in the conserved CAAX motif at the carboxy-terminal using the enzyme farnesyl transferase (FT). During the second step, the peptide bond between the cysteine and serine residues (indicated by a triangle) is proteolytically cleaved by ZMPSTE24, resulting in removal of AAX tripeptide. This reaction is followed by methylation of the farnesylated cysteine residue by isoprenylcysteine carboxyl methyl transferase (ICMT) using S-adenosyl methionine as the methyl donor. Finally, a second proteolytic cleavage occurs between the tyrosine and leucine residues (indicated by a filled triangle), which is either catalyzed by ZMPSTE24 or by another, as yet unidentified, endoprotease, which removes 15 amino acids from the carboxy-terminal, resulting in formation of mature lamin A.

*(Reproduced from Agarwal et al, 2003)*

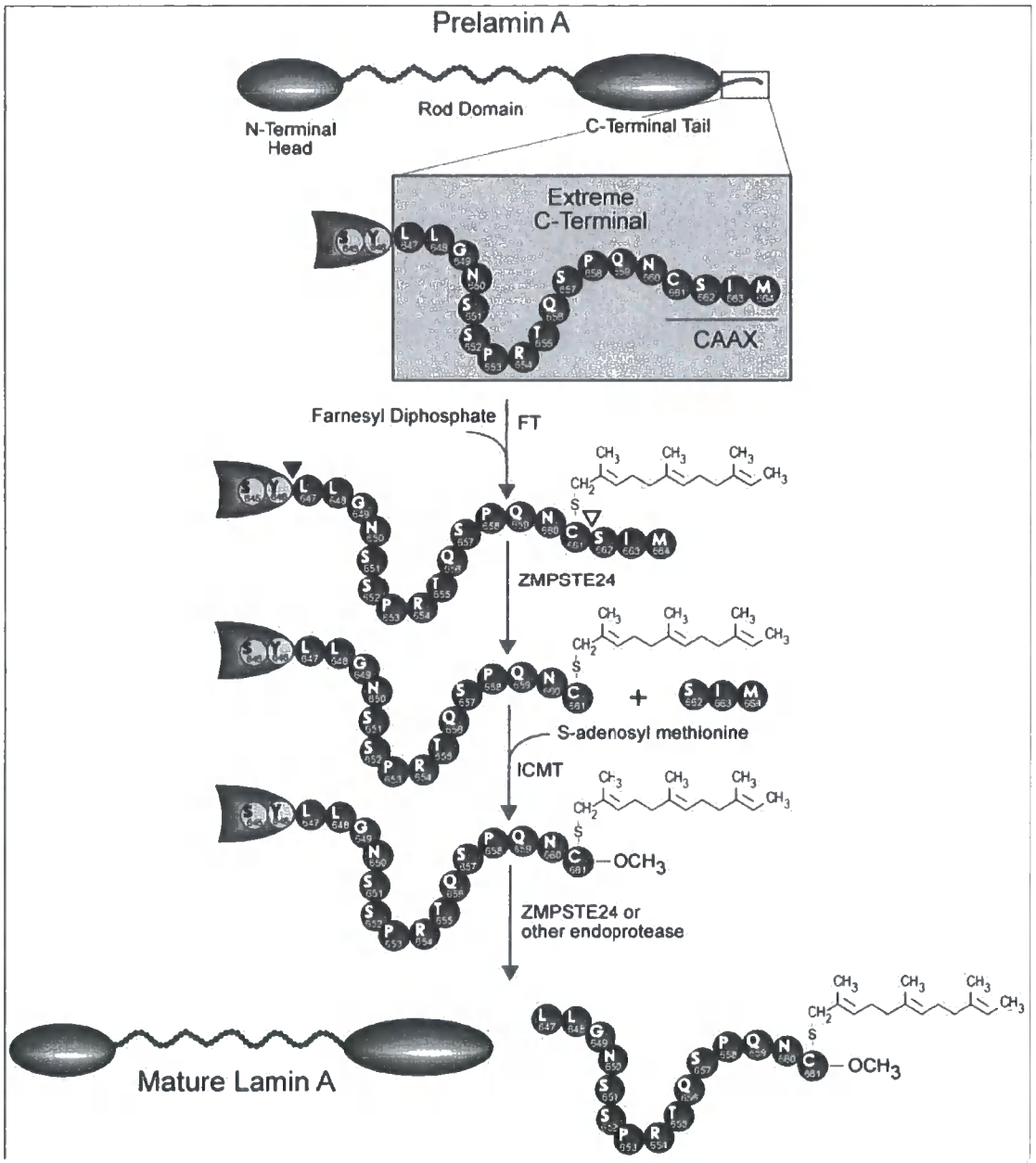


**Figure 1.4: Schema of steps involved in prelamin A processing to mature lamin A.** The post-translational processing of prelamin A involves the extreme carboxy-terminal residues. In the first step, farnesyl diphosphate is used to farnesylate the cysteine in the conserved CAAX motif at the carboxy-terminal using the enzyme farnesyl transferase (FT). During the second step, the peptide bond between the cysteine and serine residues (indicated by a triangle) is proteolytically cleaved by ZMPSTE24, resulting in removal of AAX tripeptide. This reaction is followed by methylation of the farnesylated cysteine residue by isoprenylcysteine carboxyl methyl transferase (ICMT) using S-adenosyl methionine as the methyl donor. Finally, a second proteolytic cleavage occurs between the tyrosine and leucine residues (indicated by a filled triangle), which is either catalyzed by ZMPSTE24 or by another, as yet unidentified, endoprotease, which removes 15 amino acids from the carboxy-terminal, resulting in formation of mature lamin A.

*(Reproduced from Agarwal et al, 2003)*

University of Durham
Student System

Last Name PEKOVIC

Forenames VANJA

# CONFERMENT OF DEGREE

## Higher Degree

This form should be completed by a candidate eligible to have a Higher Degree conferred. It should be forwarded to the Congregation Secretary (Secretariat), Old Shire Hall, Durham DH1 3HP, England, to arrive no later than the date stated in the Congregation pamphlet.

PLEASE CHECK THE PRE-PRINTED INFORMATION ON THIS FORM, AMEND IF NECESSARY, AND COMPLETE THE BLANK FIELDS, WRITING CLEARLY IN BLOCK CAPITALS, AND STATING WHETHER YOU WILL BE ATTENDING THE CEREMONY IN PERSON OR NOT

| | | |
|---|---|---|
| Student ID 000354204 | College/Societ USTINOV COLLEGE | |
| Name PEKOVIC | Forenames VANJA | Title MS |

My full legal name is as follows. (All names must be the same as those by which you were registered as a student. These will be the names on your degree parchment.)

**IF THIS IS INCORRECT PLEASE WRITE THE NAME CORRECTLY AND CLEARLY IN THE LOWER BOX**

**Vanja Pekovic**

| | | | |
|---|---|---|---|
| Degree Description | DOCTOR OF PHILOSOPHY | Faculty | SCIENCE |
| Programme Description | BIOLOGICAL SCIENCES | Programme Code | C1A001 |

I wish to have my degree conferred:

**IN PERSON / IN ABSENTIA (Please delete which is inapplicable)**

**Permanent (Home) Address -** Please check and correct if necessary

**NB - This is the address to which your instructions to Graduands, tickets and parchment will be sent unless you inform us otherwise.**

54 HALLGARTH STREET
DURHAM
COUNTY DURHAM
UNITED KINGDOM DH1 3AY

Telephone No 0781-5056-772

Contact E-Mail address to be used after Congregation

Signature

Date

Please note that publication of personal data in congregation programmes, videos and on the internet is regarded as a legitimate interest of the University. The names of those graduating may be released to video and photographic companies for reference purposes. By participating in this public event, graduands consent to having their name and image publicly available within the context of the ceremony.

| | | | |
|---|---|---|---|
| **OFFICE USE ONLY** | Registered by | Ack | Parchment |
| | Date | T + I | |

Conversely, cells cultured in low oxygen tension have an extended replicative lifespan and delayed senescence. Even, the routine practise of cultivating cells *in vitro* in the presence of 20% oxygen is an obvious source of oxidative stress (reviewed in von Zglinicki *et al.*, 2001). The free radical theory of ageing (Harman *et al.*, 2001) hypothesizes that the ageing process is associated with an increase in the production of oxygen-derived radicals, i.e. reactive oxygen species (ROS), together with a concurrent decrease in the ability of cells to defend against ROS which leads to the accumulation of oxidatively modified macromolecules, including DNA, RNA, proteins and lipids. In addition, a decrease in ROS buffering capacity also leads to a compromised ability to deal with the abnormal sources of ROS such as those associated with genetic predisposition and/or disease status. Abnormal levels of ROS have been implicated in the pathophysiology of several human age-related diseases including atherosclerosis, organ fibrosis, cancer and neurodegenerative disorders (reviewed in Haddad *et al.*, 2004). ROS also function as intracellular messengers in cellular signalling that modulate responses in physiological conditions such as the activation of cell cycle during $G_0$-$G_1$ transition and the activation of transcription factors such as NF-kβ, AP-1 and others, which bind to antioxidant response elements (ARE) in the gene promoters. Cellular redox changes regulate gene expression by reversible oxidative activation/inactivation of the DNA-binding capacity of these transcription factors.

#### *1.13.4.2.2.1. ROS and primary anti-oxidant enzymes (AE)*

ROS production occurs as a ubiquitous by-product of both oxidative phosphorylation and the myriad of oxidative reactions necessary to support aerobic respiration (reviewed in von Zglinicki *et al.*, 2001). In addition, ROS are generated during bacterial and viral infections, inflammatory responses, and certain environmental toxins such as UV radiation and smoking. The major and possible initiating sources of abnormal ROS during ageing are thought to be the 'leaky' mitochondria which themselves accumulate oxidative damage (Bakala *et al.*, 2003). Three primary ROS are superoxide radical $O_2^-$, hydrogen peroxide $H_2O_2$ and a very reactive hydroxyl radical $OH^-$ formed by $H_2O_2$ reacting with transition metals. One of the cellular defences against ROS damage to cellular macromolecules is a series of antioxidant enzymes (AE). The primary AE include superoxide dismutase (SOD), catalase (CAT) and glutathione peroxidase (GPX). SOD as a first line of defence reduces $O_2^-$ to $H_2O_2$ whilst CAT and GPX

# CHAPTER 3- A-TYPE LAMIN AND LAP2α EXPRESSION, SOLUBILITY PROPERTIES AND CYSTEINE MODIFICATIONS DURING CELLULAR AGEING OF HUMAN FIBROBLASTS *IN VITRO*

## Introduction

Mutations in A-type lamins cause a spectra of distinct tissue-specific diseases, and recently, a silent polymorphism in LMNA gene associated with a defect in RNA splicing has been identified in two rare premature ageing syndromes, Hutchinson-Gilford progeria syndrome (HGPS) (Ericsson *et al.*, 2003, de Sandre-Giovanolli *et al.*, 2003) and atypical Werner's syndrome (AWS) (Chen *et al.*, 2003), all affecting one or more tissues of mesenchymal origin. Since lamin A is an abundant nuclear protein, the question arose as to whether these A-type lamin diseases (collectively termed 'laminopathies') represent variable expressions of the same disease rather than separate diseases (Hutchison 2002, Mounkes *et al.*, 2004, Novelli *et al.*, 2003). Indeed, at the cytological level, patients' nuclei from a range of laminopathies studied, including HGPS and AWS, show very similar structural nuclear deformations. So far, the reported nuclear abnormalities include 'herniations', 'honeycombs', chromatin loss in the cytoplasm, and changes in association of peripheral chromatin to the nuclear membrane-lamina (Vigouroux *et al.*, 2001, Capanni *et al.*, 2003, Fidzianska *et al.*, 2003, Bridger *et al.*, 2004, Goldman *et al.*, 2004). Nuclear 'herniations' are structures that arise when the nuclear membrane blebs out or is pinched off and 'honeycombs' represent holes in the lamin/chromatin meshwork, which are often concentrated at one pole of the nucleus. In addition, abnormal anaphase chromatin bridges between nuclei in single cells were observed after knock-down of Ce-lamin in *C.elegans*, the only lamin subtype in this organism, using small interfering RNA (Liu *et al.*, 2000). Recently, aberrant mitotic spindles were observed in human cells lacking prelamin A processing protease FACE1 (Gruber *et al.*, 2005). The most severe nuclear abnormalities, including extensively lobulated nuclei and nuclear fragmentation with a subsequent formation of micronuclei have only been seen in HGPS cells (Bridger *et al.*, 2004, Goldman *et al.*, 2004) and in cells null for a prelamin A processing protease, either mouse Zmpste24 or human FACE1 (Navarro *et al.*, 2004, Gruber *et al.*, 2005). These nuclear abnormalities increase

with an increased expression of mutated A-type lamins transfected into cells (Raharjo *et al.*, 2001, Ostlund *et al.*, 2001, Favreau *et al.*, 2003) or with an age-dependent increase of mutated lamin A in HGPS cells (Goldman *et al.*, 2004), and can also be seen in mouse or human cells lacking A-type lamins (Sullivan *et al.*, 1999, Muchir *et al.*, 2003, Nikolova *et al.*, 2004).

The most consistent functional consequence of mutations in A-type lamins is that lamin C is mislocalised to the nucleoplasm (Hutchison and Worman 2004, Broers *et al.*, 2005), which is thought to lead to nuclear fragility and abnormal organisation of peripheral chromatin with a subsequent loss of gene silencing. An increased solubility of A-type lamins and lamin C redistribution to the nucleoplasm has also been reported in fibroblasts from patients with emerin mutations (Markiewicz *et al.*, 2002b). Interestingly, human fibroblasts from a patient with a non-sense Y254X LMNA mutation, which are effectively null for A-type lamins, display a poor index of growth (Muchir *et al.*, 2003). Human cells lacking FACE1 as well as *C.elegans* cells lacking Ce-lamin undergo abrupt cell cycle arrest. Moreover, premature senescent arrest is a hallmark of HGPS, AWS and ZMPSTE null cells, both clinically and in cell culture (Bridger and Kill 2004, Chen *et al.*, 2003, Liu *et al.*, 2005). In addition, three recently identified laminopathies are also progeroid-like (Caux *et al.*, 2003, Navarro *et al.*, 2004, Csoka *et al.*, 2004).

These observations raise two possibilities: 1) that lamin mutations in general are linked to premature ageing; 2) that A-type lamins play a role in aspects of normal ageing. In hoping to understand the observed close relationship between laminopathies, premature ageing syndromes and normal ageing, the protein expression, cellular distribution and protein stability of lamins and their binding partners, lamina-associated polypeptide 2 proteins, were examined throughout normal ageing of wild-type human fibroblasts in culture and their final stage of life termed senescence. These findings led me to explore *in vitro* ageing of laminopathy fibroblasts and cysteine modifications in A-type lamins and LAP2α during ageing of fibroblasts in culture.

# Results

## 3.1. Expression of A-type lamins and LAP2α during *in vitro* ageing of fibroblasts as assessed by immunoblotting

To explore how lamina expression might change as cells age in culture, initially the levels of protein expression of A-type and B-type lamins and their respective binding partners LAP2α and LAP2β were investigated throughout the life time of human dermal fibroblasts (HDF) *in vitro* using immunoblotting. Primary cultures of human dermal fibroblasts were aged through serial passage (p) and the same number of cells was harvested after 3 days of growth in culture at early **(p7-p12)**, intermediate **(p17-p27)** and late **(p44)** passages. Whole cell extracts were blotted using antibodies against lamin A/C (which recognises lamin A (70 kDa) and lamin C (65 kDa), lamin B2 (68 kDa), LAP2α (75 kDa) and LAP2β (55 kDa) **(Figure 3.1)**. The results show that neither the A-type lamin nor the B-type lamin level of protein expression changed during ageing of fibroblasts in culture. This result is consistent with constant protein expression levels of their respective binding partners LAP2α and LAP2β.

## 3.2. Cellular distribution of A-type lamins and LAP2α in aged fibroblasts as assessed by immunofluorescence microscopy

To investigate whether changes in localisation patterns of A-type and B-type lamin proteins and their binding partners LAP2α and LAP2β occur with ageing of fibroblasts in vitro, immunocytochemistry and immunofluorescence microscopy was used. Human skin cells of early **(p7)** and late **(p44)** passage were seeded at an equal density, grown in culture for 3 days and processed for double immunofluorescence microscopy using antibodies against: 1) LAP2α and a proliferation marker Ki67 (Ki67 stains a nucleolar heterochromatin-associated protein expressed only in proliferating cells and is absent in growth-arrested cells (Cheutin *et al.,* 2003)), 2) LAP2α and lamin C, 3) lamin B2 and Ki67 and 4) LAP2β and Ki67.

In p7 HDF, the majority of nuclei (75%) displayed a uniform nucleoplasmic distribution of LAP2α **(Figure 3.2A (a) and (b) p7)**. This expression of LAP2α corresponded to a bright Ki67 nucleolar staining as expected **(Figure 3.2A (a) p7)**. The remaining 25% of

p7 cells had a decreased LAP2α staining in the nucleus and were negative for Ki67, indicative of growth-arrested senescent cells (see **Chapter 5**). On the contrary, in p44 HDF, a majority of nuclei (80%) were negative for a proliferation marker Ki67 **(Figure 3.2A (a) p44)**. Under the light microscope, their nucleoli appeared compacted into one rounded structure as opposed to an 'open floret' structure seen in p7 proliferating HDF as reported before (Hannan *et al.*, 2000). The remaining 20% of p44 cells were positive for Ki67, which correlated with a positive expression of LAP2α in the nucleus, indicating that these cells were still proliferating. Surprisingly, out of the total 80% of Ki67-negative p44 cells, 56% had a positive expression of LAP2α **(Figure 3.2A (a) p44)**. In these cells, LAP2α displayed a more granular nucleoplasmic distribution, which extended into the cytoplasm **(see arrows in Figure 3.2A (a) and (b) p44)**. The remaining 44 % of Ki67-negative p44 cells had a decreased LAP2α staining in the nucleus, but still displayed a granular staining in the cytoplasm **(Table/Chart 3.1).**

In p7 HDF, lamin C staining was present at both the nuclear envelope and in the nucleoplasm **(Figure 3.2A (b) p7)**. In p44 HDF, some nuclei showed that the nuclear membrane was not ovoid or round in morphology as it was seen in p7 nuclei. The nuclei of p44 cells appeared more irregular in shape and were often larger in size **(see arrows in Figure 3.2A (b) p44)**. In addition, both p7 and p44 nuclei displayed lamin C dots and fibers indicative of G1 phase nuclei (see below).

In p7 HDF, Lamin B2 staining was present both at the nuclear envelope and in the nucleus in all cells irrespective of their Ki67 index **(Figure 3.2B (a) p7)**. In p44 cells, lamin B2 was present in the nucleoplasm at a similar intensity to p7 cells, but in contrast to p7 cells, lamin B2 staining at the nuclear envelope was often weak or absent at one pole of the nucleus and revealed large and irregularly shaped nuclei with no Ki67 staining **(see arrows in Figure 3.2B (a) p44).** In p7 HDF, LAP2β staining was present intensely both at the nuclear envelope and in the nucleoplasm **(Figure 3.2B (b) p7)**. In p44 HDF, LAP2β showed an equally intense staining in the nucleoplasm. However, similarly to the staining of lamin B2, LAP2β staining at the nuclear envelope often seemed to be reduced or absent at one pole of the nucleus and these nuclei were always Ki67 negative **(see arrows in Figure 3.2B (b) p44)**.

### 3.3. Investigation of nuclear morphology of *in vitro* aged fibroblasts by confocal microscopy

Upon closer investigation of nuclear morphology in p44 cells using confocal microscopy, a range of dysmorphic nuclei were observed, including: irregularly shaped nuclei with one or two occasional blebs/herniations **(see arrowhead in Figure 3.3 (a) MERGE)**, nuclei with holes in the lamin meshwork called honeycombs **(see arrowheads in Figure 3.3 (b) MERGE)**, irregularly shaped nuclei with a lamin detachment in the cytoplasm **(see arrowhead in Figure 3.3 (c) MERGE),** incompletely segregated nuclei, within a single cell, joined by a lamin containing bridge **(see arrowhead in Figure 3.3 (d) MERGE)**, and cells displaying formation of micronuclei **(Figure 3.3 (e) MERGE)**.

In nuclei with the least severe dysmorphic morphology **(Figures 3.3 (a)-(d))**, LAP2α displayed granular nuclear and cytoplasmic distribution with some indication of aggregation inside the nucleus **(see arrows in Figure 3.3 (a)-(d) LAP2α)**. These nuclei also showed an accumulation of intranuclear lamin C **(see arrows in Figure 3.3 (a)-(d) LAMIN C)**. In nuclei with the most severe dysmorphic morphology **(Figure 3.3 (e))**, LAP2α was found in bright aggregates, which also contained lamin C **(see arrows in Figure 3.3 (e) LAP2α and LAMIN C)**. Interestingly, in cells with a bridge between incompletely segregated nuclei within a single cell, lamin C was present on the bridges **(see arrowhead in Figure 3.3 (d) LAMIN C)**. In contrast, LAP2α was not present on the bridges but was found in cytoplasmic granules around lamin C bridges **(see arrowhead in Figure 3.3 (d) LAP2α)**.

The proportions of each type of these abnormally shaped nuclei are presented in **Table 3.2** for p12 and p44 HDF. There were less than 10% of dysmorphic nuclei in p12 cultures and only the least severe type was seen (herniations). In contrast, aged fibroblasts (p44) displayed 59.25% of nuclei with all three types of abnormalities, including 44% of nuclei with herniations/honeycombs, 8% with lamin detachments, 6% with lamin bridges and 1.25% of cells that formed micronuclei (note that some nuclei had both herniations and honeycombs present and these abnormalities were counted as one type). These results suggest that nuclei of aged cells accumulate structural changes in nuclear morphology reminiscent of cells that harbour lamin A mutations (Bridger and

Kill 2004, Goldman *et al.*, 2004) or cells that do not express A-type lamins (Sullivan *et al.*, 1999, Muchir *et al.*, 2003).

### 3.4. Chromatin distribution in dysmorphic nuclei of aged fibroblasts as assessed by confocal microscopy

Dysmorphic nuclear phenotypes seen in late passage (p44) cells were not a result of apoptosis since these cells did not display hyper-condensed distribution of chromatin characteristic of apoptotic cells as revealed by the DNA-intercalating dye DAPI. This observation was confirmed by FACS analysis of p44 cells (see **Section 3.6**).

**Figure 3.4A (a)-(e)** shows the same five dysmorphic nuclear phenotypes in p44 cells as shown in **Figure 3.3 (a)-(e)**, except that these cells were imaged with DAPI and lamin C. In all dysmorphic nuclei chromatin was not always stained by DAPI at the nuclear periphery and in such areas only lamin C staining was present **(see arrows in Figure 3.4A (a)-(e) MERGE)**. This is in contrast to p7 nuclei were chromatin and lamin C staining overlapped all along the NE periphery **(see arrow in Figure 3.4B MERGE)**. Dysmorphic nuclei had condensed regions of chromatin located centrally in the nucleus. These condensed chromatin regions often correlated with lamin C accumulation in the nucleoplasm and LAP2α aggregation **(see arrows in Figure 3.3 (a)-(e) LAP2α and lamin C)**.

In dysmorphic nuclei containing lamin C herniations **(see arrowhead in Figure 3.4A (a) LAMIN C)** DAPI staining was also seen in these herniations **(see arrowhead in Figure 3.4A (a) DAPI).** In dysmorphic nuclei containing lamin honeycombs, chromatin holes were observed, which sometimes concentrated at one pole of the nucleus but more often all along the nuclear periphery **(see arrowhead in Figure 3.4A (b) DAPI).** These chromatin holes corresponded to a lack of lamin C staining in those areas **(see arrowhead in Figure 3.4A (b) LAMIN C). Figure 3.4A (c) DAPI (see arrowhead),** shows a chromatin detachment located in the cytoplasm. Lamin C was present on detached chromatin **(see arrowhead in Figure 3.4A (c) LAMIN C).** Another unusual location of chromatin was seen in the bridge between incompletely segregated nuclei within a single cell, which also stained with lamin C **(Figure 3.4A (d) lamin C marked by arrowhead)**. Unfortunately, due to the limitations of confocal microscopy, DAPI

bridge is not seen on the image **(see arrowhead in Figure 3.4A (d) DAPI)**. As shown earlier, LAP2α was not present on these chromatin bridges **(see arrowhead in Figure 3.3 (d) LAPα)** but accumulated in cytoplasmic granules around chromatin bridges. In the most severe dysmorphic nuclei, micronuclei, which display distinct lamin C **(see arrow in Figure 3.4A (e) LAMIN C)** and LAP2α aggregates, chromatin holes were also seen in these areas **(see arrow in Figure 3.4A (e) DAPI).**

### 3.5. Investigation of intranuclear distribution of A-type lamin in aged fibroblasts by confocal microscopy

Intranuclear A-type lamin dots and fibers, which are present in early G1 nuclei of human fibroblasts and associate with condensed chromatin, have been reported before (Bridger *et al.,* 1993). Assembly of A-type lamins at the nuclear envelope during late G1 was proposed to promote the relocation of heterochromatin to the nuclear periphery. In order to investigate whether an increased accumulation of condensed chromatin inside the nucleus correlates with an intranuclear accumulation of lamin C, early **(p7)** and late-passage **(p44)** cells were processed for double confocal microscopy using antibodies against lamin C and Ki67 as well as a DNA-intercalating dye DAPI.

In 75% of p7 cells, lamin C antibody showed an intense staining at the nuclear envelope and in the nucleoplasm **(see arrowhead in Figure 3.4B LAMIN C p7)**, while ~25% of cells showed intranuclear lamin C dots and fibers and variable staining at the nuclear envelope **(Table/Chart 3.3).** In **Figure 3.4B LAMIN C p7,** a nucleus is shown which contained an intense lamin C staining at the nuclear envelope **(see arrowhead)** and very few lamin C dots in the nucleoplasm **(marked by arrow).** In contrast, in p44 cells **(Figure 3.4B LAMIN C p44)**, ~50% of nuclei showed an accumulation of nucleoplasmic lamin C staining with intanuclear lamin dots **(see arrow)** and lacked the intense staining at the nuclear envelope **(see arrowhead)**. In the other ~50% of p44 nuclei, lamin C antibody showed variable intensity at the nuclear envelope with or without intranuclear dots **(Table 3.3).**

It was then investigated how the presence of lamin C intranuclear dots correlates with the proliferation status of cells **(Table /Chart 3.3).** In p7 cells, 49.1% of nuclei displayed an intense staining at the nuclear envelope and a positive staining for

proliferation marker Ki67. 26.2% of p7 cells displayed intranuclear lamin C dots and were positive for Ki67. Another 26.7% of p7 nuclei stained intensely for lamin C staining at the nuclear envelope and were negative for Ki67. In p44 cells, 49.7% of nuclei stained variably for lamin C at the nuclear envelope and 25.7% of these nuclei were negative for Ki67. In p44 cells, 51.1% of nuclei stained intranuclear lamin C dots and 84.5% of these nuclei were negative for Ki67 **(Figure 3.4B Ki67 p44).** Interestingly, a majority of p44 nuclei with intranuclear dots were also dysmorphic. This is in contrast to p7 nuclei with intranuclear dots that stained positive for Ki67 and were ovoid **(Figure 3.4B Ki67 p7)**. This result suggests that an accumulation of intranuclear A-type lamin correlates with a proliferation arrest in aged cells.

## 3.6 Investigation of proliferation rates of dysmorphic nuclei in wild type and laminopathy fibroblasts and of laminopathy fibroblasts during ageing *in vitro*

Since a majority of p44 nuclei that accumulated nucleoplasmic lamin C were also dysmorphic, it is possible that a decreased assembly of A-type lamins at the nuclear envelope leads to dysmorphic nuclei, which in turn leads to proliferation arrest. To investigate the possibility that dysmorphic nuclei correlate with proliferation arrest, immuno-staining was performed with antibodies against lamin A/C (JOL2) and Ki67 using early **(p12)** and late passage **(p44)** HDF. Four early passage **(p12)** laminopathy fibroblasts with the following LMNA mutations: Y259X, R249Q, E358K and R459W were also used as they are known to generate dysmorphic nuclear phenotypes. **Table 3.4** shows that in p12 HDF, 77% of ovoid nuclei were Ki67-positive whereas only 54.4 % of dysmorphic nuclei were Ki67 positive. In p44 HDF, 37.35% of ovoid nuclei were Ki67-positive whereas only 3.33% of dysmorphic nuclei were Ki67-positive. In Y259X cells, 45.4% of ovoid nuclei were Ki67-positive whereas only 9.7% of dysmorphic nuclei were Ki67-positive. In R249Q cells, 62.25% of ovoid cells were Ki67-positive and only 25.25% of dysmorphic nuclei were Ki67-positive. In E358K cells, 86.14% of ovoid nuclei were Ki67-positive whereas only 32.32% of dysmorphic nuclei were Ki67-positive. In R453W cells, 67.24% of ovoid cells were Ki67-positive and only 6.24% of dysmorphic nuclei were Ki67-positive. These results indicate that generation of dysmorphic nuclei in late passage wild type and early passage laminopathy fibroblasts correlates with an increased incidence in proliferation arrest.

Early passage (p12) laminopathy fibroblasts had a significantly higher percentage of dysmorphic nuclei in comparison to early passage (p12) wild-type cells (29% in Y259X cells and 49.55% in E358K cells) and they showed lower proliferation rates as assessed by the total number of cells that were Ki67-positive (35.0% in Y259X, 40.59% in R249Q, 59.5% in E358K and 42.23% in R453Q). To assess the possibility that laminopathy fibroblasts exhaust their proliferative potential at a faster rate, early (p7) passage wild type and laminopathy fibroblasts (Y259X, R249Q, E358K and R453Q) were aged in culture until they significantly exhausted their proliferative potential. Cells of early **(p7-12)**, intermediate **(20-26)** or late **(p44)** passage were grown for three days in culture and prepared for immunofluorescence microscopy using antibodies against lamin A/C (JOL2) and Ki67. **Table 3.5** shows that although the proliferation rates of early passage (p7) laminopathy fibroblasts were not significantly different from early passage (p7) wild-type cells, mid passage (p20-24) laminopathy fibroblasts showed 2-7 times lower proliferation rates than mid passage (p24) wild-type cells. In fact, their proliferation rates were similar (E358K) or even lower (Y259X, R249Q and R453Q) than those of late passage (p44) wild-type cells. These results show that laminopathy fibroblasts enter premature senescence independently of the position of the lamin mutation and support the hypothesis that lamin mutations are linked to premature ageing.

### 3.7. Immuno-fluorescent localisation of phospho-histone H3 in CUT phenotypes of aged fibroblasts

The dysmorphic nuclear phenotype in p44 cells with lamin/chromatin bridges is reminiscent of a CUT ('cell untimely torn') phenotype observed after RNAi knockdown of CeLamin in *C. Elegans* (Liu *et al.*, 2000). These cells display abnormal segregation of chromatin during mitosis as indicated by the presence of a chromatin bridge between nuclei of the same cell. These cells also show dysmorphic nuclear morphology, loss of chromosomes, abnormal condensation of chromatin, large polyploid nuclei and an inability to complete the cell cycle. A striking feature of the CUT phenotype in *C. Elegans* is that the two nuclei connected by a chromatin bridge in the same cell display de-phosphorylated histone H3, whilst the bridge contains mitotically phosphorylated histone H3 (Liu *et al.*, 2003). This pattern indicates that incompletely segregated chromatin in bridges remains mitotically arrested whilst the segregated nuclei in the

same cell progresses to G1 phase of the cycle. These chromatin bridges can eventually break and cells continue to cycle forming more anaphase bridges.

It is important to note that site-specific phosphorylation of histone H3 on serine 10 (H3-10) is a mitotic marker which initiates during G2 phase of the cell cycle, is maximal during mitosis and diminishes during late anaphase and early telophase (Hooser *et al.*, 1998). H3-10 phosphorylation also occurs during interphase but the staining pattern is exclusively punctuated as opposed to the bright staining of large blocks of chromatin during G2/M phase (Hendzel 2003 at www.cellnucleus.com).

In order to investigate whether incompletely segregated nuclei connected via lamin bridges in p44 cells, also retain phosphorylated histone H3, early **(p7)** and late passage **(p44)** HDF were co-stained with antibodies against phosphorylated histone H3 and lamin C. In p7 cells, 83% of nuclei were either weakly stained or negative for phospho-histone H3 indicating that cells were in G1/S phase of cell cycle **(Figure 3.5 (a) p7 G1/S)** or in $G_0$ respectively. 17% of p7 nuclei stained strongly for phospho-histone H3 indicating that cells were in G2/M phase of the cycle **(Figure 3.5 (a) p7 G2/M)**. In contrast, 40% of p44 nuclei stained strongly for phospho-histone H3 including all nuclei with lamin-containing bridges **(see arrow in Figure 3.5 (b) p44 G2/M pattern)**. This indicated that those cells may be arrested in G2/M phase of cell cycle, or in the case of cells with lamin-containing bridges, may have failed to completely exit mitosis. 60% of p44 nuclei stained weakly or negatively for phospho-histone H3 indicating that cells were in G1 **(Figure 3.5 (b) p44 G1 pattern)** or $G_0$ respectively. Interestingly, 10% of p44 cells with lamin bridges contained nuclei with broken lamin bridges **(see arrow in Figure 3.5 (b) p44 G1 pattern)**. In these cells, nuclei showed a weak phospho-histone H3 staining whilst broken chromatin bridges stained intensely for phospho-histone H3, indicating that chromatin in nuclei entered G1 phase whilst chromatin in broken bridges remained mitotically arrested **(Table /Chart 3.5).**

The above results confirm the resemblance between cut phenotypes of aged and Celamin knockout cells of C.elegans. Interestingly, p44 cells accumulated twice as many nuclei with G2/M pattern of H3-10 phosphorylation than p7 cells. This may indicate altered cell cycle behaviour in p44 cells, as growth-arrested cells (such as quiescent $G_0$ cells) do not stain for H3-10 marker. In order to confirm that

phosphorylated H3 histone is normally a marker of mitotic cells, early (**p7**) and late (**p44**) HDF were co-stained for antibodies against phospho-histone H3 and a proliferation marker Ki67. In p7 cells, both weak and intense staining for phospho-histone H3 (75%) correlated with a positive Ki67 staining as expected (**Figure 3.6A p7**). Surprisingly, in p44 cells, over 92.5% of nuclei that stained intensely for phospho-histone H3, were Ki67 negative (**Figure 3.6A p44**). 72.66% of p44 nuclei that stained weakly for phospho-histone H3 were also negative for Ki67 (**Table /Chart 3.5**). These results indicate that G1 or G2/M pattern of histone H3 phosphorylation in p44 cells does not correlate with proliferation, as is the case in p7 cells.

### 3.8. FACS analysis of cell size and cell cycle phase distribution in aged fibroblasts

In order to explore the possibility that a proportion of p44 cells arrest in G2 phase of cell cycle, FACS analysis was performed. Exponentially growing early passage (**p12**) and late passage (**p44**) fibroblasts were harvested, prepared for FACS analysis and compared using flow cytometer. In these respective cell populations, we compared cell size and distribution of cells in G0/G1, S, G2/M phase and apoptosis.

**Figure 3.6B** shows side (SS) versus forward (FS) scattering patterns in the left panels (**marked A**) for p12 and p44 cells. Side scattering is proportional to the complexity of intracellular structures and forward scattering is proportional to the cell size. From **A** panels, we can see that the cell size and complexity of intracellular structures is proportionally increased in p44 cells as compared to p12 cells. This is consistent with the light microscopy observations of larger cell sizes in p44 cultures.

The right panels (**marked B**) in **Figure 3.6B** show the histograms of the DNA content (FL3) versus cell number (count) for p12 and p44 cells. The highest peak (E) in the upper **B** panel represents the position of 67.1% G1/G0 p12 cells with 2N DNA content. The shoulder (F) in upper **B** panel represents the position of 5.3% S-phase p12 cells and the second smaller peak (G) represents the position of 15.6% G2/M phase p12 cells with 4N DNA content. In the lower **B** panel, the highest peak (E) shows 73.8% of G1/G0 p44 cells with 2N DNA content and the large tail (F+G) represents 24.7% of p44 cells in G1/G0 phase with 4N to 8N DNA contents. The extra peak marked by the arrow in the lower **B** panel shows 1% p44 cells with 32N DNA content. These data are consistent

with immunofluorescent observations of larger nuclei accommodating more chromatin in p44 cells. This result does not show that senescent cells arrest in G2 phase of the cell cycle as suggested by a G2 pattern of histone H3 phosphorylation. Nonetheless, an altered histone H3 phosphorylation in conjunction with a larger proportion of senescent cells having higher than 2N DNA content does suggest that an altered cell cycle behaviour occurred in senescent cells prior to their permanent cell cycle arrest.

In **Figure 3.6B**, the **B** panels also show the position of apoptotic cells (A) to the left of G1 peak (E). In p12 cell population, the percentage of apoptotic cells reached ~12% whilst in p44 cell population, the percentage of apoptotic cells was below 1%. This result supports earlier published observations that late passage cells show a higher resistance to apoptosis than early passage proliferating cells. The cell size and intracellular structure complexity of apoptotic cells (A) is shown in the **A** panels. Apoptotic cells are smaller in size and of lower intracellular complexity as expected.

### 3.9. Solubility/stability properties of A-type lamins and LAP2α in aged fibroblasts as assessed by biochemical fractionation and immunoblotting

In laminopathy cells, dysmorphic nuclei are thought to arise due to a weak association of mutated lamins with the lamina at the nuclear envelope (reviewed in Hutchison 2002). In aged fibroblasts, decreased assembly of lamin C at the nuclear envelope in dysmorphic nuclei may also arise due to unstable associations with the nuclear lamina. Since lamin C depends on lamin A for its localisation at the nuclear envelope (Vaughan *et al.*, 2001), an altered assembly of A-type lamins at the NE may be expected in aged cells. In addition, LAP2α nuclear distribution depends on proper assembly of A-type lamins in the nucleus (Markiewicz *et al.*, 2002a) and LAP2α aggregation seen in aged dysmorphic cells may be expected from the altered assembly in the nucleus. To investigate this possibility, solubility/stability patterns of A-type lamins and their binding partner LAP2α were investigated by a nuclear matrix extraction protocol modified from Dyer *et al.*, (1997). Early **(p7)** and late passage **(p44)** HDF were grown for three days in culture and the same number of cells were subjected to sequential extraction by CSK-Triton X100, RSB-Magic, followed by chromatin digestion by DNAse1 and a final extraction by 0.25M ammonium sulphate. The insoluble pellets P2, P3, P4 and P5 and the nuclear material solubilized after each step S2, S3, S4 and S5

were then analysed by immunoblotting. Whole cell pellets (labelled P1) were prepared as a control for both p7 and p44 cells.

**Figure 3.7A Lamin A/C p7** shows that in p7 HDF, A-type lamins (stained by JOL2 antibody) were present in the insoluble pellets after each step of extraction as expected. Lamin A never appeared in any of the soluble fractions, whilst only small amounts of lamin C appeared in the soluble fractions after DNAse1 treatment (S4) and ammonium sulphate extraction (S5).

In contrast, in p44 HDF, dramatic changes in solubility and stability properties of A-type lamins were detected by immunoblotting with an antibody directed against lamins A/C (JOL2) **(Figure 3.7A Lamin A/C p44)**. Lamin A was readily detected at an expected molecular weight of 70 kDa in the whole cell pellet (P1) **(marked by thick arrow in Figure 3.7A Lamin A/C p44)**, however, after extraction with CSK-Triton X100, the intensity of this band dramatically decreased in the insoluble fraction P2. In the rest of the insoluble fractions, lamin A band of 70 kDa was not detected. Instead, a more rapidly migrating band (67 kDa) appeared increasingly in each soluble fraction and in the final insoluble fraction P5 **(marked by thin arrows in Figure 3.7A lamin A/C p44)** and was similar in size to the expected size of lamin C (65 kDa) **(marked by arrowhead in Figure 3.7A Lamin A/C p44)**.

Since 70 kDa lamin A band was not found in any of the soluble fractions of p44 nuclei, it was reasoned that this band might represent partially degraded lamin A rather than soluble fractions of lamin C protein. To investigate this possibility, immunoblotting was performed on the same fractions of p44 cells using an antibody specific for lamin C **(Figure 3.7A Lamin C p44)**. Using this antibody, lamin C protein was found throughout the insoluble fractions P1-P4 and not in the soluble fractions S2-S4. However, a majority of lamin C was found in the soluble fraction S5 and a very small amount was still present in the final insoluble fraction P5.

Since lamin C remained intact during nuclear extraction of p44 cells, it was reasoned that lamin A may become partially degraded in its extended C-terminal tail. To investigate this possibility, we immunoblotted the fractions from p44 cells with a lamin A tail-specific antibody (JOL4) **(Figure 3.7A Lamin A p44)**. Using this antibody, a

lamin A band of 70 kDa was only detected in the whole cell extract P1 and was subsequently not found in either insoluble or soluble fractions. This result suggests that lamin A becomes partially proteolysed in its C-terminal tail, which consequently abolished the epitope recognition by JOL4 antibody. This interpretation is also consistent with an observed size (67 kDa) of its solubilized proteolytic fragment.

A-type lamins' binding partner, LAP2α, was only found in insoluble fractions of p7 HDF throughout the extraction procedure albeit at decreasing levels **(Figure 3.7B LAP2α p7)**. This result confirms that A-type lamins and LAP2α are highly insoluble proteins in early passage cells and form a stable detergent/DNAse/salt-resistant nucleoskeleton as expected. I also immunoblotted the fractions of p44 cells with a LAP2α-specific antibody **(Figure 3.7B LAP2α p44)**. LAP2α was detected at an expected molecular weight of 75 kDa in the whole cells pellet of p44 cells (P1). However, after extraction with CSK-Triton X100, the intensity of this band decreased dramatically in the insoluble fractions P2 and P3, and was undetectable in fractions P4 and P5 following DNAse1 treatment and ammonium sulphate extraction, respectively. Since 75kDa LAP2α band was not found in any of the soluble fractions of p44 nuclei, LAP2α may also be subject to proteolysis.

The solubility properties of lamin B2 and its binding partner LAP2β were assessed. Lamin B2 was only found in the insoluble fractions throughout extraction in p7 HDF **(Figure 3.7B Lamin B2 p7).** In p44 HDF, lamin B2 was present in all the insoluble fractions during extraction and a very small amount was present in soluble fraction S5 after treatment with ammonium sulphate **(Figure 3.7B Lamin B2 p44)**. In p7 HDF, LAP2β was found in all insoluble fractions throughout extraction and a small amount was found in the soluble fraction S2 after CSK/Triton extraction **(Figure 3.7B LAP2β p7)**. In p44 HDF, LAP2β was found in all the insoluble fractions throughout extraction, except for tiny amounts found in the soluble fractions S3 and S5 **(Figure 3.7B LAP2β p44)**. In p44 HDF, a slight increase in solubility of lamin B2 observed after ammonium sulphate treatment is consistent with a slight increase in solubility of its binding partner LAP2β. Since, LAP2β remained intact in p44 nuclear extracts, the absence of LAP2α from the last two stages of nuclear extraction may result from a partial proteolysis in its C-terminal-specific domain.

In summary, these results suggest that upon detergent/DNAse1/salt extraction of p44 nuclei, lamin A and its binding partner LAP2α may be specifically targeted to a limited proteolysis in their C-terminal-specific domains, which resulted in an increased solubility of lamin A proteolytic fragment and a loss of LAP2α from the nucleoskeleton. In addition, lamin C was rendered almost completely soluble after ammonium sulphate extraction resulting in its loss from the nucleoskeleton. On the other hand, B-type lamin, lamin B2 and its binding partner LAP2β remained primarily insoluble during extraction.

### 3.10. Solubility/stability properties of A-type lamins and LAP2α in aged fibroblasts as assessed by *in situ* nuclear matrix extraction and confocal microscopy

In order to confirm that old nuclei display an unstable nucleoskeleton due to an increased solubility/instability of A-type lamins and their binding protein LAP2α, the resistance of early **(p7)** and late passage **(p44)** cells was tested using a nuclear matrix extraction *in situ* following 5 sequential treatments with CSK, CSK-Triton X100, RSB-Magic, chromatin digestion by DNAse1 and 0.25 M ammonium sulphate. Following each step of extraction, cells were fixed and processed for double confocal microscopy using antibodies against: a) lamin A/C and a proliferation marker Ki67, b) LAP2α and lamin C, c) lamin B2 and Ki67 and d) LAP2β and Ki67.

In p7 HDF, a majority of nuclei (75%) were Ki67 positive and all cells retained an intense nuclear lamin A/C staining following V stage of extraction irrespective of their Ki67 staining **(Figure 3.8A (a) p7, note a nucleus marked by *)**. In p44 HDF, the majority of nuclei (80%) were negative for a proliferation marker Ki67 and these nuclei displayed a weak staining of lamin A/C after V stage extraction **(see arrows in Figure 3.8A (a) p44)**. A minority of nuclei that were still Ki67 positive (20%) retained an intense staining with lamin A/C after V stage extraction **(see arrowheads in Figure 3.8A (a) p44)** and those nuclei that stained weakly for Ki67 showed an intermediate level of lamin A/C staining after V stage extraction **(unmarked nuclei in Figure 3.8A (a) p44)**.

Lamin A/C staining was also examined in p44 HDF after II stage of extraction with CSK/Triton and found that some nuclei showed a decreased staining of lamin A/C in the nucleus and a tendency of lamin A/C to aggregate **(Figure 3.8A (b) p44)**.

To confirm that a weak staining of lamin A/C staining in p44 nuclei after V stage extraction resulted from an increased A-type lamin solubility rather than epitope masking of lamin A/C, p44 cells were processed for double confocal microscopy using lamin A/C and Ki67 antibodies without performing nuclear extraction. Ki67 positive and negative p44 cells were found in the same area of the coverslip and imaged. Both Ki67-negative p44 nuclei **(see arrow)** and Ki67-positive p44 nuclei **(see arrowheads)** showed an equal intensity of lamin A/C staining before extraction **(Figure 3.8A (c) p44)**. This result confirms that following V stage nuclear extraction *in situ*, lamin A/C remains insoluble in p7 nuclei, whilst a significant fraction of A-type lamins becomes soluble in p44 nuclei.

It was then preceded with assessing the solubility properties of lamin C and A-type lamin binding partner LAP2α. In p7 HDF after V stage extraction, 75% of nuclei retained LAP2α weakly in the nucleoplasm and all nuclei retained an intense nuclear lamin C staining **(Figure 3.8B (a) p7)**. 25% of p7 cells did not retain LAP2α but showed an intense lamin C staining indicative of growth-arrested quiescent cells (see **Chapter 5**). In contrast, in p44 HDF upon V stage extraction, >65% of nuclei did not retain any nucleoplasmic LAP2α, which corresponded to a weak retention of lamin C in the nucleus **(Figure 3.8B (a) p44)**. Interestingly, 15% of p44 nuclei that did not retain LAP2α in the nucleoplasm showed unusual insoluble structures of LAP2α. These included small LAP2α caps at one or both poles of the nucleus, bright LAP2α aggregates scattered in the nucleus **(Figure 3.8B (a) p44)** or very few tiny LAP2α nuclear dots. P44 nuclei that retained LAP2α aggregates sometimes contained lamin C within them **(see arrows in Figure 3.8B (a) MERGE p44)**. In addition, 20% of p44 cells retained LAP2α and lamin C similarly to p7 cells upon V stage nuclear extraction.

In p44 HDF, after II stage of extraction with CSK/Triton, some old nuclei already showed a weaker retention of LAP2α in the nucleoplasm accompanied by aggregation in the nucleus. In these nuclei, lamin C was also found to aggregate in the nucleus **(see arrows in Figure 3.8B (b) p44)**.

In p7 HDF, lamin B2 retained a bright nuclear staining after V stage extraction in all nuclei **(Figure 3.8C (a) p7)**. Similarly, in p44 nuclei, Lamin B2 staining was retained at a similar intensity to p7 nuclei after V stage extraction **(Figure 3.8C (a) p44)**. In p7

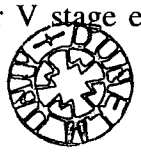

HDF, LAP2β showed a strong nuclear retention in all Ki67+ nuclei after V stage extraction **(Figure 3.8C (b) p7)**. Similarly, in p44 HDF, LAP2β staining remained intense in all cells after V stage nuclear extraction **(Figure 3.8C (b) p44).**

In summary, the above results indicate that upon extraction of p7 cells *in situ* the retention of a stable pool of LAP2α in the nucleus was correlated with the retention of A-type lamins in the nucleus. Upon *in situ* nuclear extraction in p44 cells, A-type lamins and LAP2α were significantly soluble which led to their decreased presence in the nucleus. The finding that LAP2α and A-type lamins aggregate in some p44 nuclei upon extraction indicates that these proteins were not correctly assembled in the nucleoskeleton. In contrast, lamin B2 and its binding partner LAP2β remained primarily insoluble during nuclear extraction in both p7 and p44 cells confirming previous biochemical fractionation data.

### 3.11. Investigation of C-terminal amino acid sequences in lamins and LAPs using multiple sequence alignment software

Enhanced susceptibility of proteins to degradation by intracellular proteases is often indicative of protein unfolding which occurs in oxidised proteins (Dean *et al.*, 1997, Grune *et al.*, 1997). Unfolding in proteins as a result of oxidation exposes hydrophobic residues on the surface of proteins and provides peptide bonds that serve as a recognition and proteolytic cleavage site for cysteine proteases. To investigate whether lamin A and LAP2α instability during nuclear extraction (i.e. prone to degradation) resulted from the unfolding in their specific C-terminal tails, their C-terminal amino acid sequences were examined for cysteine resides using 'T-Coffee', a specialised software for multiple sequence alignments (Notrdam *et al.*, 2000).

**Figure 3.9A** shows multiple amino acid sequence alignments for C-terminal domains of human A-type lamins (lamin A and lamin C) and B-type lamins (lamin B1 and lamin B2) starting from the amino acid 501 through to the end of their protein sequence. Lamin A sequence shows the highest number of cysteine residues; lamin A has three cysteines in lamin A-specific C-terminal tail (marked in red) at positions 570, 588 and 591, and shares one cysteine residue with lamin C in the common C-terminal domain at position 522 (marked in purple). A single cysteine residue in the extreme C-terminus of

lamin A, lamin B1 and lamin B2 (marked in yellow) shows a cysteine residue in the CaaX motif that undergoes isoprenylation and carboxymethylation in B-type lamins. In mature lamin A, this motif is cleaved along with another 14 amino acids upstream of its position during prelamin A processing (see **Chapter 1** on 'Prelamin A processing').

**Figure 3.9B** shows multiple amino acid sequence alignments for C-terminal domains of three human LAP2 isoforms, namely LAP2α, LAP2β and LAP2γ, starting from the amino acid 251 through to the end of their protein sequence. Surprisingly, LAP2α-specific C-terminal sequence shows ten cysteine residues (marked in red) at positions 280, 287, 330, 341, 518, 561, 570, 629, 658 and 684. In contrast, LAP2β-specific C-terminal domain has only one cysteine residue that it shares with LAP2γ at position 384 (marked in blue) but not with LAP2α. Interestingly, the N-terminal common domain in LAPs (aa 1-187) does not contain any cysteine residues (not shown).

## 3.12. C-terminal cysteine modifications of A-type lamins and LAP2α in aged fibroblasts as assessed by NEM/non-reducing SDS-PAGE and immunoblotting for protein glutathione adducts

Cysteine residues in some proteins are highly sensitive to changes in oxidative stress levels (Eaton, *et al.*, 2002). In living cells, the cytoplasm and nucleus are kept under reducing conditions due to a large pool of reduced glutathione. During ageing, increased levels of oxidative stress lead to an increased level of oxidised glutathione, which in turn leads to formation of protein disulphide cross-links or S-thiolation of proteins. The presence of a high number of cysteine residues specific to C-terminal domains of lamin A and LAP2α prompted to investigate whether A-type lamins and LAP2α form protein disulphides or become S-glutathiolated during ageing of human dermal fibroblasts. For this purpose, early **(p12)**, intermediate **(p24)** and late **(p40)** passages of human dermal fibroblasts as well as early **(p12)** and intermediate **(p24)** passages of laminopathy fibroblasts with E354K mutation were grown in culture for three days and the same number of cells was harvested for whole cell extracts. Whole cell extracts were prepared in the presence of 40mM sulfhydryl group-blocking reagent N-ethylmaleimide (NEM). NEM irreversibly binds to free cysteines in proteins and prevents *de novo* dimerisation or isomerisation of cysteine sulfhydryl groups during preparation of cell extracts. This treatment thus allows for the genuine assessment of protein cysteines' status in intact

cells. NEM-treated cell extracts were run on gels under both non-reducing conditions (i.e. in the absence of cysteine-reducing agents such as β-mercaptoethanol- β-ME and dithiothreitol- DTT in the SDS sample buffer) and reducing conditions (in the presence of β-ME and DTT in the SDS sample buffer). NEM-treated extracts were blotted using antibodies against lamin A/C, LAP2α and an antibody that recognizes protein glutathione addicts under non-reducing conditions. Protein glutathione addicts are mixed protein disulphides formed between protein cysteines and glutathione, and under reducing conditions, they become reduced leaving protein cysteines free. The resultant reduced glutathione is not seen following immunoblotting as it is too small in size to be retained on the gel (305 Da).

**Figure 3.10A (a)** shows NEM-treated extracts run under non-reducing conditions. Immunoblotting with lamin A/C antibody showed an equal level of protein in all extracts and no protein disulphides were detected in either early (P12) or late (P40) passage cells. When the same extracts, run on the second half of the gel, were immunoblotted with glutathione antibody, late passage (p40) cells revealed six prominent protein-glutathione bands in the range between 55-150 kDa. Two of these six prominent bands, were aligned to expected mobility of lamin A/C bands detected on the first half of the immunoblot (shown by arrowheads). Densitometry analysis of the six glutathiolated proteins in late passage (p40) cells showed that lamin A is the third and lamin C is the fifth most prominent glutathiolated protein in late passage cells (p40), thus the amount of glutathiolated lamin A is somewhat higher than that of glutathiolated lamin C. Both lamin A and C showed an age-dependent increase in glutathiolation from early (p12) to late (p40) passage cells.

**Figure 3.10A (b)** shows NEM-treated extracts run under reducing conditions. Immunoblotting with lamin A/C was performed and showed an equal amount of protein in all extracts. When the same extracts were immunoblotted with anti-glutathione antibody on the second half of the gel, the bands representing glutathiolated lamin A and lamin C seen under non-reducing conditions were absent in all extracts (marked by arrowheads), demonstrating that A-type lamins are indeed glutathiolated during the ageing of human fibroblasts as this process is reversible by reducing agents.

Next, it was investigated whether LAP2α protein becomes glutathiolated during the ageing of fibroblasts *in vitro* using the same NEM-treated extracts. **Figure 3.10B (a)** shows NEM-treated extracts run under non-reducing conditions. Immunoblotting with a LAP2α specific antibody showed an equal level of protein in all extracts and no detectible protein disulphides were formed in either early (p12) or late (p40) passage cells. When the same extracts were immunoblotted with glutathione antibody on the second half of the gel, late passage (p40) cells revealed that one of the six prominent protein-glutathione bands aligns perfectly to a molecular weight of LAP2α bands detected on the first half of the immunoblot (shown by arrowheads). Densitometry analysis of the six prominent glutathiolated proteins in late passage (p40) cells showed that LAP2α is the sixth most prominent glutathiolated protein. In contrast, no glutathiolated LAP2α was detected in early (p12) or mid (p24) passage extracts (see * in late (p44) extract).

**Figure 3.10B (b)** shows the NEM extracts run under reducing conditions. Immunoblotting with LAP2α was performed and showed an equal amount of protein in all extracts. When the same extracts were immunoblotted with anti-glutathione antibody on the second half of the gel, the protein band representing glutathiolated LAP2α protein seen under non-reducing conditions in late passage (p40) cells was reversibly reduced (marked by arrowheads) demonstrating that LAP2α is indeed glutathiolated in late passage cells.

### 3.13. Investigation of A-type lamin-glutathione complexes in aged fibroblasts by immunoprecipitation under NEM/non-reducing conditions and immunoblotting

In order to confirm the result that A-type lamins become glutathiolated during ageing of fibroblasts in vitro, early **(p12)** and late passage **(p40)** cells were grown for three days in culture and the same number of cells harvested for immunoprecipitation analysis. In brief, early (p12) and late (p40) passage cells were homogenised in an ice-cold hypotonic buffer in the presence of NEM and the nuclear pellets were collected and treated with 500 mM salt buffer in the presence of NEM. The nuclear supernatants were collected and incubated with Dynabeads pre-incubated with lamin A/C antibody. The supernatants S (not bound to Dynabeads) and immuno-precipitates P (bound to Dynabeads) of early and late passage cells were run on the gel under non-reducing

conditions and immunoblotted against lamin A/C and anti-glutathione antibodies. Under non-reducing conditions, heavy and light chains of IgGs form disulphide-linked complexes of ~160 kDa (marked by arrowhead in Ps).

**Figure 3.11** shows NEM-treated supernatants (S) and immuno-precipitates (P) for early (p12) and late (p40) passage cells run under non-reducing conditions. Immunoblotting with lamin A/C antibody (JOL2) showed that an equal level of lamin A/C protein was immunoprecipitated (P) from both early (p12) and late (p40) passage extracts (marked by thin arrows). No lamin A/C protein was present in the supernatants (S) of either early (p12) or late (p40) passage extracts indicating that all lamin A/C protein from NEM-treated nuclear extracts was immunoprecipitated successfully. When the same supernatants and immuno-precipitates of early (p12) and late (p40) passage cells were immunoblotted against glutathione antibody, the staining showed a protein glutathione addict on immunoprecipitated lamin A/C (P) in late (p40) passage cells (marked by thick arrows) whilst only a tiny amount of lamin A-glutathione addict was found in the immuno-precipitate (P) of early (p12) passage cells (marked by *). Any glutathione which is not present on lamin A/C would not be detected in the supernatants as free glutathione is too small to be retained in the gel. Interestingly, glutathione formed addicts on almost the entire amount of immuno-precipitated lamin A/C (P) in late passage cells. Since lamins A/C share a cysteine Cys 522 in the common C-terminal region, Cys 522 must be involved in the formation of lamin A/C-glutathione addicts. However, glutathione may also form addicts with other cysteine residues in lamin A specific C-terminal tail.

### 3.14. Investigation of cross-linking properties of cysteine residues in A-type lamins of aged fibroblasts by non-reducing electrophoresis and immunoblotting

It has been reported before (Kaufmann *et al.*, 1983) that during nuclear envelope isolation in the absence of reducing agents such as DTT, lamin A and to a lesser extent lamin C form non-native disulphide bonds between their juxtaposed cysteine sulfhydryl groups. The formation of these bonds can be prevented when nuclei are isolated in the presence of hydrophobic sulfhydryl-binding reagent NEM. Although these results showed that disulphide bonds were not naturally present between lamin A monomers under the conditions in which these intact cells were found, the ability to form these

intermolecular cross-links reflects the regular order in the arrangement of lamin A polymeric arrays. In order to investigate some functional consequences of cysteine-glutathiolation in A-type lamins in aged fibroblasts, non-reducing electrophoresis was employed in both the absence and presence of NEM. It was hypothesized that in aged fibroblasts glutathiolated cysteine residues in lamins A/C would not be able to engage in these intermolecular disulphide cross-links. If this was true, it would suggest that glutathiolation of cysteine residues in lamins A/C contributes to a more disordered arrangement of lamin A/C polymeric arrays in intact cells.

Early **(p12)**, intermediate **(p24)** and late **(p40)** passages of wild-type human dermal fibroblasts and early **(p12)** and intermediate **(p24)** passages of laminopathy fibroblasts with E354K mutation (labelled F02) were grown in culture for three days and the same number of cells was harvested for whole cell extracts. Whole cell extracts were prepared in the absence of NEM to allow post-lysis oxidation of proteins cysteines and in the presence of 40mM NEM to prevent cysteine oxidation. Cell extracts without NEM and NEM-treated cell extracts were run under non-reducing electrophoresis (i.e. in the absence of cysteine-reducing agents such as β-ME and DTT in the SDS sample buffer). All extracts were blotted using two antibodies against lamin A/C (JOL2 and L6 8A7) and lamin C.

**Figure 3.12A (a)** shows cell extracts prepared without NEM and run under non-reducing conditions. Immunoblotting with JOL2 antibody, which recognises an epitope in C-terminal common domain of lamins A/C (aa 464-566), showed a dramatic disappearance of lamin A band in both wild type and F02 early passage (p12) fibroblasts (see thick arrow). Mid passage (p24) fibroblasts of both wild type and F02 cells showed reduced lamin A protein in the extracts. In contrast, late passage (p40) fibroblasts showed a significantly higher amount of lamin A protein in the extract. In addition, a protein band ~1 kDa higher than molecular weight of lamin C (~66 kDa) appeared in all extracts but was hardly visible in the extract of late passage (p40) fibroblasts (see thin arrow). On non-reducing gels, proteins exhibit a faster electrophoretic mobility due to formation of an intra-molecular disulphide bond between their adjacent cysteines. Since at least two cysteine residues are required for formation of the intra-molecular disulphide bonds, we predicted that the 66 kDa band represents a lamin A conformer with an intra-molecular disulphide bond.

In order to ensure that the observed lamin A protein behaviour under non-reducing conditions is not only specific after staining with JOL2 antibody, the same cell extracts were immunoblotted with L6 8A7 antibody which recognises an epitope in the rod domain common to lamins A/C (aa 171-319). Lamin A showed the same behaviour in these extracts as seen with JOL2 antibody. The thick arrow points to a disappearance of lamin A in early passage (p12) cell extracts of both wild-type and F02 fibroblasts and an accumulation of lamin A monomer in mid (p24) and significantly in late passage (p40) extracts. The thin arrow points out to an appearance of 64 kDa band, which most likely represents lamin A protein with an intra-molecular disulphide bond, in early and mid passage extracts and only weakly in late passage (p40) extract. In addition to lamins A/C, L6 8A7 antibody cross-reacts with an unknown protein of 58-60 kDa marked by asterisk (Kill and Hutchison 1995).

Immunoblotting with JOL2 and L6 8A7 antibodies did not show dramatic differences in lamin C behaviour in these extracts under non-reducing conditions, although these antibodies showed reduced lamin C protein in early (p12) and mid (p24) passage extracts as compared to the late passage (p40) extract (see arrowheads). To further investigate lamin C behaviour under non-reducing conditions and to ensure that a 64 kDa band is not a lamin C conformer, the same extracts were immunoblotted with lamin C-specific antibody. Lamin C protein was present in lesser amounts in early (p12) and mid (p24) passage extracts of both wild type and F02 fibroblasts as compared to the late passage (p40) extracts. However, as shown by JOL2 and L6 8A7 antibodies, lamin C antibody did not show a dramatic disappearance of lamin C protein in early (p12) passage extracts as was seen for lamin A protein. In addition, lamin C antibody revealed only one band (65 kDa) for lamin C in all extracts, confirming that a 64 kDa band represents a lamin A intra-disulphide conformer with a faster electrophoretic mobility.

**Figure 3.12A (b)** shows cell extracts prepared in the presence of NEM and run under non-reducing conditions. Immunoblotting with JOL2 antibody showed a dramatic reappearance of lamin A band in both wild type and F02 early (p12) and mid passage (p24) fibroblasts (see thick arrow). The protein level of lamins A/C (see arrowhead for lamin C) was equal in all NEM-treated cell extracts, confirming that the lamin A behaviour seen in early passage extracts prepared without NEM was not caused by differences in the protein levels between the extracts. In addition, a 64 kDa band

corresponding to an intra-molecular disulphide conformer of lamin A is no longer seen in any of the cell extracts.

Immunoblotting of the same NEM-treated extracts with L6 8A7 antibody showed the same behaviour of lamin A in these extracts as seen with JOL2 antibody. The thick arrow points to a reappearance of lamin A in early (p12) and mid passage (p24) cell extracts for both wild-type and F02 fibroblasts. L6 8A7 antibody revealed an equal amount of lamin A/C protein (see arrowhead for lamin C) in all the extracts and a disappearance of 64 kDa intra-molecular disulphide of lamin A from the extracts. The asterisk shows an unknown protein of 58-60 kDa that cross-reacts with L6 8A7 antibody.

Immunoblotting of the same NEM-treated extracts with a lamin C-specific antibody showed the same amount of protein in all the cell extracts, confirming that a reduced lamin C protein seen in early (p12) and mid (p24) passage extracts treated without NEM is not caused by the differences in lamin C protein levels between the extracts.

These results show that the changes in lamin A/C behaviour seen in early passage fibroblasts depend on their free reactive cysteine sulfhydryl groups. The oxidatively modified cysteine residues in lamins A/C of aged fibroblasts (via S-glutathiolation) do not engage in inter- or intra-molecular disulphide cross-links which supports the hypothesis that such oxidative modifications may contribute to a more disordered arrangement of lamin A/C polymeric arrays in ageing fibroblasts.

### 3.15. Cross-linking properties of cysteine residues in A-type lamins throughout *in vitro* ageing of fibroblasts as assessed by non-reducing electrophoresis and immunoblotting

The finding that early and late passage cells show different cross-linking properties of A-type lamin cysteines led us to examine whether A-type lamin cysteines show an age-dependent change in their cross-linking potential across a wider range of passages. Early **(p7-p15)**, intermediate **(p18-24)** and late **(p40)** passages of human dermal fibroblasts were grown in culture for three days and the same number of cells were harvested for whole cell extracts. Whole cell extracts were prepared in the absence of

NEM to allow post-lysis oxidation of protein cysteine residues. Cell extracts without NEM were run on gels under non-reducing conditions (i.e. in the absence of cysteine-reducing agents such as β-ME and DTT in the SDS sample buffer) and blotted using antibodies against lamin A/C (JOL2) and β-actin.

**Figure 3.12B** shows early to late passage (p7-p40) cell extracts of human dermal fibroblasts prepared without NEM and run under non-reducing conditions. Immunoblotting with JOL2 antibody showed a dramatic disappearance of the lamin A band in early passage (p7-p15) and in mid passage p18 extracts (see thick arrow). Mid passage extracts p21 and p24 showed a gradual increase in monomeric lamin A protein. The late (p40) extract showed the highest accumulation of lamin A monomeric protein. These results indicate that monomeric lamin A first appears around middle passage p21 and primarily accumulates between mid passage 24 and late passage 40 as would be expected for an age-dependent trait. Immunoblotting with β-actin antibody showed that the level of β-actin was the same in all cell extracts, confirming that the changes in lamin A behaviour seen between passages under non-reducing conditions were specific and not caused by the differences in protein level between passages.

JOL2 antibody also showed an appearance of a faster-migrating 64 kDa lamin A intra-molecular disulphide conformer in early passage (p7-p15) and mid passage (p18-p24) extracts, which were absent in the late passage (p40) extract (see thin arrow). This result indicates that lamin A-specific cysteine residues involved in intra-molecular disulphide bonds become targets to age-dependent changes in later passages between p24 to p40 and are most likely not involved in the initial accumulation of monomeric lamin A protein during mid passages p21-p24. The lamin A-specific tail contains two cysteine residues, Cys 588 and Cys 591, which are in close proximity to each other and are thus most likely involved in formation of an intra-molecular disulphide bond.

Lamin C is almost absent in early (p7-10) passage extracts and significantly reduced in early (p12-p15) passage extracts (follow arrowhead). Lamin C monomer shows a somewhat increased amount in mid passage p18 extract. Mid passage extracts p21 and p24 show a rapid increase in accumulation of lamin C monomeric protein with the highest amount present in the late passage (p40) extract. These results indicate that in contrast to lamin A, monomeric lamin C first start to accumulate at mid passage (p18)

and then more rapidly in mid passages p21-p24. Lamin A accumulation of monomeric protein begins when a significant amount of lamin C monomeric protein has already been accumulated at mid passages p21-p24 and accelerates in later passages between p24 to p40. In summary, these results show that during ageing of fibroblasts in vitro, lamins A/C show age-dependent changes in their cysteine cross-linking potential and that in lamin A these changes may occur sequentially on different cysteines.

### 3.16. Investigation of cross-linking properties of cysteine residues in mutant lamins of laminopathy fibroblasts by non-reducing electrophoresis and immunoblotting

It can be seen in section 3.6 that four laminopathy cell lines studied entered irreversible senescent arrest prematurely between passages p20 and p26. Premature senescence can result from increased oxidative stress levels in cells (von Zglinicki, *et al.*, 1995). Since aged fibroblasts show an increased level of oxidatively modified lamins A/C, we investigated whether mutant lamins from laminopathy cells undergo increased oxidative modifications on their cysteine residues. The preliminary results using laminopathy fibroblasts from a patient with E358K mutation (labelled F02) did not show an increased level of protein disulphides or glutathiolated lamins A/C (or LAP2α) in early (p12) and mid (p24) passage extracts under NEM/non-reducing conditions as compared to age-matched wild-type extracts **(see Figure 3.10A and 3.10B)**. In addition, mutant lamin A cysteines from early (p12) passage E358K cells showed the same level of cross-linking ability under non-reducing conditions as the lamin A cysteines from early (p12) passage wild-type cells. Although mid (p24) passage E358K cells showed an age-dependent accumulation of monomeric mutant lamins under non-reducing conditions, the level of monomeric protein was not increased as compared to mid (p24) passage wild type cells. In order to extend these findings, three other laminopathy cell lines were tested for the ability of their mutant lamins to form cysteine disulphide cross-links under non-reducing conditions. The same number of wild-type (HDF) and laminopathy fibroblasts with the following mutations R249Q, R401C and R453Q (249 is R249Q, 401 is R401C and 453 is R453W) were harvested at early **(p12)** and intermediate **(p22)** passage. Whole cell extracts were prepared in the absence **(a)** or presence **(b)** of NEM and resolved on non-reducing gels. Cell extracts were immunoblotted using lamin A/C (JOL2) antibody.

**Figure 3.13 (a)** shows cell extracts prepared without NEM and run under non-reducing conditions. Immunoblotting with JOL2 antibody showed a disappearance of lamin A band in both wild-type and 249 early passage (p12) extracts (see thick arrow). Mid passage (p22) extracts of wild type and 249, 401 and 453 cells showed the same level of monomeric lamin A protein. Lamin C protein level was reduced in early (p12) passage wild type and 249 extracts as compared to all mid passage (p22) extracts (see arrowhead). Mid passage (p22) extracts of wild type and 249, 401 453 cells showed the same level of monomeric lamin C.

**Figure 3.13 (b)** shows cell extracts prepared in the presence of NEM and run under non-reducing conditions. Immunoblotting with JOL2 antibody showed a reappearance of lamin A band in both wild type and 249 early (p12) passage extracts (see thick arrow). The level of lamin A protein was equal in all NEM-treated extracts, confirming that the lamin A behaviour seen in early passage (p12) extracts prepared without NEM was not caused by differences in the protein level between extracts. Lamin C also showed the same amount of protein in all extracts (see arrowhead), confirming that a reduced lamin C protein seen in early (p12) passage extracts treated without NEM was not caused by differences in lamin C protein level between extracts.

These results show that lamin mutations do not prevent mutant lamins from forming disulphide cross-links in early passage laminopathy cells nor do they prevent the ability of mutant lamins to respond to mid-passage changes in oxidative stress levels. Moreover, a lack of increased accumulation of monomeric mutant lamin in mid passage laminopathy cells under complete non-reducing conditions shows that laminopathy cells do not enter premature senescence as a result of increased oxidative modifications to cysteine residues in mutant lamins. However, it is still possible that mutant lamins predispose cells to a lower threshold of resistance to oxidative stress increases during mid passages which may trigger premature senescence.

### 3.17. Investigation of cross-linking properties of cysteine residues in LAP2α in aged fibroblasts by non-reducing electrophoresis and immunoblotting

As it can be seen earlier, immunoblotting of NEM-treated cell extracts for protein glutathione addicts revealed that LAP2α protein becomes glutathiolated in late passage

(p40) fibroblasts, which was reversed upon treatment of the extract with reducing agents. It was hypothesized that in early passage cells, LAP2α cysteine residues may also become reactive under non-reducing conditions and that in aged fibroblasts glutathiolated cysteine residues in LAP2α protein would not be able to engage in these intermolecular disulphide cross-links. Therefore LAP2α protein behaviour was investigated under non-reducing conditions in both the absence and presence of NEM. Early **(p12)**, intermediate **(p24)** and late **(p40)** passages of human dermal fibroblasts were grown in culture for three days and the same number of cells was harvested for whole cell extracts. Whole cell extracts were prepared in the absence of NEM to allow post-lysis oxidation of proteins cysteines and in the presence of 40mM NEM to prevent cysteine oxidation. Cell extracts without NEM and NEM-treated cell extracts were run under non-reducing conditions. Both types of extracts were blotted using Pan-LAP2 antibody that recognises an epitope in the common N-terminal region of three distinct LAP2 isoforms, LAP2α (75 kDa), LAP2β (55 kDa) and LAP2γ (39 kDa).

**Figure 3.14A (a)** shows cell extracts prepared without NEM and run under non-reducing conditions. As we predicted, immunoblotting with Pan-LAP2 antibody showed a dramatic disappearance of 75 kDa band of LAP2α in early passage (p12) extract (see thick arrow). Mid passage (p24) cells showed some LAP2α protein in the extract. In contrast, late passage (p40) fibroblasts showed a significantly higher amount of monomeric LAP2α protein in the extract. On the other hand, LAP2β and LAP2γ protein levels did not show any significant differences between early (p12), mid (p24) and late (p40) passage cells under these conditions.

**Figure 3.14A (b)** shows cell extracts prepared in the presence of NEM and run under non-reducing conditions. Immunoblotting with Pan-LAP2 antibody showed a dramatic reappearance of the LAP2α band in early (p12) and mid passage (p24) fibroblasts (see thick arrow). The protein level of LAP2α was equal in all cell extracts, confirming that LAP2α behaviour in early and mid passage extracts prepared without NEM was not caused by the differences in protein levels between the extracts. The protein levels of LAP2β and LAP2γ were also equal across passages under these conditions. This result suggests that the single cysteine residues present in LAP2β and LAP2γ-specific C-terminal domains do not undergo cross-links between their respective monomers in the absence or presence of NEM.

In summary, changes in LAP2α behaviour in early passage fibroblasts depended on their free reactive cysteine sulfhydryl groups. These results support the hypothesis that the oxidatively modified cysteine residues in LAP2α of aged fibroblasts (via S-glutathiolation) do not engage in disulphide cross-links and may contribute to a more disordered arrangement of LAP2α in the nucleus.

In order to investigate lamin B2 behaviour under non-reducing conditions, the same early **(p12)**, intermediate **(p24)** and late **(p40)** passage extracts prepared in the absence (a) or presence (b) of NEM were run under non-reducing conditions and immunoblotted using Lamin B2 (LN43) antibody.

**Figure 3.14B (a)** shows cell extracts prepared without NEM and run under non-reducing conditions. Immunoblotting with lamin B2 antibody did not show any significant differences in the lamin B2 protein level between extracts (see thick arrow).

**Figure 3.14B (b)** shows cell extracts prepared in the presence of NEM and run under non-reducing conditions. Immunoblotting with lamin B2 antibody showed the same level of protein in all extracts (see thick arrow). The protein level of lamin B2 was somewhat reduced in all extracts prepared in the absence of NEM as compared to the extracts prepared in the presence of NEM. This result suggests that lamin B2 is able to engage in disulphide cross-links to some extent independently of increasing passage number in the extracts. Indeed, lamin B2 protein sequence shows a single cysteine residue in its rod domain at the position 192. However, the lack of lamin B2 monomer accumulation in late passage (p40) extract prepared in the absence of NEM demonstrates that a cysteine residue in lamin B2 rod domain does not become oxidatively modified during ageing of fibroblasts in vitro.

### 3.18. Detection of inter-molecular disulphide complexes of LAP2α and lamin A in early passage fibroblasts by non-reducing electrophoresis and immunoblotting

A dramatic disappearance of lamin A and LAP2α was seen in early passage extracts prepared in the absence of NEM under non-reducing conditions which is dependent on cross-linking properties of their reactive cysteines. It was hypothesized that lamin A and LAP2α formed high molecular weight disulphide cross-linked complexes in early

passage cells but not in late passage cells. As these complexes are expected to exhibit slower migration during non-reducing electrophoresis, the immunoblot in Figure 12A (a) (stained by JOL2 antibody) and the immunoblot in Figure 14A (a) (stained by Pan-LAP2 antibody) were developed again following longer exposure in ECL detection reagent. The immunoblots showed extracts from early **(p12)**, intermediate **(p24)** and late passage **(p40)** wild-type fibroblasts (HDF) prepared in the absence of NEM and resolved on non-reducing gels.

**Figure 3.15 (a)** shows the over-exposed upper part of Pan-LAP2 immunoblot. Longer exposure in ECL reagent revealed two high molecular weight disulphide cross-linked complexes of LAP2α in early passage (p12) extract that migrated slowly on the gel (see arrowheads). In mid (p24) and late (p40) passage cells, no high molecular weight disulphide cross-liked complexes of LAP2α were detected. The high molecular weight complex of LAP2α with a faster mobility had a molecular weight of ~ 150 kDa which indicates that this complex represents LAP2α homo-dimer. The second high molecular weight complex of LAP2α had a slower mobility than the slowest-migrating molecular weight marker (> 210 kDa). Although, the molecular weight of this slow-mobility LAP2α complex could not be determined more precisely, we speculate that this complex represents at least a trimer or a tetramer of LAP2α linked by disulphide bonds.

**Figure 3.15 (b)** shows the overexposed upper part of JOL2 immunoblot. Longer exposure in ECL reagent revealed a slow-migrating high molecular weight disulphide cross-linked complex of lamin A in the early passage (p12) extract, which was present at a decreased level in a mid (p24) passage extract and was completely absent in a late (p40) passage extract (follow arrowhead). The high molecular weight complex of lamin A present in early (p12) passage cells and at a lower level in mid (p24) passage cells had a molecular weight of ~ 140 kDa which indicates that this complex represents a lamin A homo-dimer.

In summary, these results confirm the hypothesis that a dramatic disappearance of lamin A and LAP2α seen in early passage cells under complete non-reducing conditions occurs as a result of lamin A and LAP2α forming high molecular weight disulphide cross-linked complexes in early passage cells. It is shown that an age-dependent accumulation of monomeric LAP2α and lamin A in late passage cells occurs due to an

age-dependent inability of LAP2α and lamin A cysteines to form these high molecular disulphide-linked complexes at later passages.

## Discussion

In this chapter it was set out to address the question of whether A-type lamins and LAP2α play a role in normal ageing of cells and whether lamin mutations in general are linked to premature ageing. Initially I examined the protein expression of A-type lamins and LAP2α throughout normal ageing of wild-type human fibroblasts in culture, including their final stage of life termed senescence.

### Senescent fibroblasts show laminopathy-like nuclear dysmorphic phenotypes and laminopathy fibroblasts enter senescence prematurely

My results show that neither A-type lamin nor B-type lamin level of protein expression changes during ageing of fibroblasts in culture, which is consistent with a stable level of protein expression of their binding partners LAP2α and LAP2β, respectively. Nonetheless, fibroblasts aged in culture acquire nuclear morphological changes characteristic of laminopathy and progeroid fibroblasts. Several transfection studies have shown that these nuclear phenotypes arise due to a poor and/or aberrant assembly of mutant A-type lamins at the nuclear envelope which leads to a disruption of underlying peripheral heterochromatin and a loss of correct localisation among their binding partners (Raharjo *et al.*, 2001, Favreau *et al.*, 2003, Ostlund *et al.*, 2001, Benchers *et al.*, 2003). In senescent cells, these nuclear 'laminopathy' phenotypes are accompanied by a loss of peripheral heterochromatin distribution and aberrant nuclear localisation of lamin C and LAPα. Accumulation of these nuclear dysmorphic phenotypes in senescent cells implied that these structural nuclear alterations impede cell cycle progression. Indeed, my results show that acquisition of these nuclear abnormalities correlates with a loss of proliferative potential in both ageing fibroblasts and in four laminopathy cell lines. Interestingly, laminopathy cell lines show an increased generation of these dysmorphic nuclear phenotypes compared to their age-matched controls, which suggested that laminopathy cells lose their proliferative potential at an earlier age. Subsequently, four laminopathy cell lines were aged in culture until they exhausted their proliferative potential and entered a permanent growth arrest (senescence). All laminopathy cell lines, irrespective of the position of their lamin mutation, entered senescence prematurely between passages 20 and 26, demonstrating that lamin mutations are linked to premature ageing in vitro.

**Dysmorphic nuclei of senescent fibroblasts display LAP2α aggregation**

The unchanged protein level of LAP2α in senescent fibroblasts was a surprising result. This is because in early passage fibroblasts LAP2α protein expression is exclusively cell cycle dependent (Markiewicz *et al.*, 2002a). However, in senescent fibroblasts, LAP2α showed a more granular nuclear distribution that often extended into the cytoplasm and a tendency to aggregate in dysmorphic senescent cells. Since senescent cells are cultured in the presence of mitotic factors (serum), LAP2α expression may still be induced in senescent cells upon induction of mitogenic signalling. Certainly, LAP2α protein expression depends on the presence of mitogenic factors. Dramatic upregulation of LAP2α protein expression is seen during serum-restimulation of quiescent fibroblasts, which have a low level of LAP2α protein (Markiewicz *et al.*, 2002a). In further support to this argument, other authors have demonstrated that the upstream mitogenic signalling still occurs in senescent cultures but it appears blocked at the downstream pathways (Seshadri and Campisi 1990, Kim *et al.*, 2003) and many genes remain mitogen-inducible (Campisi *et al.*, 2001). Moreover, it has been proposed that permanent cell cycle arrest in senescent cells depends on strong and/or sustained 'hyper-mitogenic' stimuli and is different from a 'hypo-mitogenic' arrest of quiescent cells (Blagosklonny *et al.*, 2003). In light of these findings, it is possible to envisage that in senescent cells, LAP2α protein expression is still induced upon mitogenic signalling but that its expression becomes uncoupled from the cell cycle due to alterations in downstream signalling. Indeed, the aberrant distribution of LAP2α in dysmorphic senescent cells correlates with cell cycle arrest and may itself interfere with cell cycle progression and downstream signalling (see Chapter 4).

**Accumulation of lamin C in the nucleoplasm and altered distribution of heterochromatin in dysmorphic senescent fibroblasts**

Dysmorphic senescent nuclei that contained aggregated LAP2α also accumulated lamin C in the nucleoplasm. In laminopathy cells, lamin C is consistently mislocalised to the nucleoplasm (Hutchison 2002). Decreased assembly of lamin C at the nuclear envelope of senescent nuclei was correlated with a loss of heterochromatin at the nuclear periphery. During interphase, heterochromatin domains are mainly located at the nuclear periphery or surrounding the nucleoli (Taddei *et al.*, 1999). Distribution of

lamins coincides with a peripherally located chromatin (Belmont *et al.*, 1993) and polymerised lamins can act as anchoring sites for heterochromatin domains at the nuclear periphery (Zhao *et al.*, 1996). This suggests that the lamina in senescent nuclei no longer ensure the tight connections between the chromatin and the nuclear envelope. Interestingly, senescent fibroblasts have been shown to undergo a relocation of heterochromatin from the nuclear periphery to more internal sites in the nucleus (Bridger *et al.*, 2000) and to exhibit loss of silencing of peripheral heterochromatin (Imai *et al.*, 1997). I also observed an accumulation of condensed chromatin inside senescent nuclei. Therefore, since the lamina of senescent nuclei does not appear to effectively anchor heterochromatin domains at the nuclear envelope, it would be expected that unanchored heterochromatin accumulates inside the nucleus, where lamin C accumulation and LAP2α aggregation is also seen. Intranuclear A-type lamin structures present during early G1 are also proposed to help relocate heterochromatin from the nucleus to the NE during their assembly at the nuclear envelope during late G1 (Bridger, *et al.*, 1993). Thus, accumulation of lamin C in the nucleoplasm of senescent cells may also prevent heterochromatin relocation to the nuclear periphery. As such, senescent cells would not be able to progress beyond G1 phase to S phase as the proper lamina assembly is essential for initiation of DNA replication (Meier *et al.*, 1991, Goldberg *et al.*, 1995, Moir *et al.*, 2000).

**Senescent fibroblasts show large nuclei with distinct nuclear dysmorphic phenotypes**

Senescent fibroblasts show a broad range of nuclear dysmorphic phenotypes, some of which were only reported in progeria cells, including herniations, honeycombs, chromatin detachments, aberrant chromatin bridges and micronuclei. Herniations and honeycombs are structures most commonly described in laminopathy cells. Senescent cells contain 44% of herniations and honeycombs. Interestingly, these nuclear abnormalities often show selective loss of some and aggregation of other lamina proteins. B-type lamins and LAP2β become absent from large areas of these lobules in lamin null (Muchir *et al.*, 2003, Sullivan *et al.*, 1999) or lamin mutant cells (Vigouroux *et al.*, 2001, Goldman *et al.*, 2004). Indeed, in senescent nuclei with herniations and honeycombs, lamin B and LAP2β were often missing from one pole of the nucleus, whilst lamin C and LAP2α were still present. Chromatin/lamin detachments were seen

in 8% of senescent cells, indicating that chromosome losses occur in aged cells. These chromatin detachments sometimes stained for Ki67, which is a nucleolar marker, indicating that chromatin detachments may sometimes come from nucleolar heterochromatin. Loss of nucleolar heterochromatin and chromosomes is common in aged cells (Burkle *et al.*, 2002).

FACS analysis revealed that a considerable proportion of cells in senescent populations have higher than 2N DNA content. This is in accordance with the immunofluorescence observations that 25% of senescent nuclei are similar or larger in size than early passage G2 nuclei. Other reports have also shown that senescent cells accumulate high DNA contents and that karyotypic changes occur in ageing cells including aneuploid and polyploid nuclei, chromosome aberrations and micronuclei. Indeed, I also show the formation of micronuclei in senescent cells although this severe nuclear phenotype was present at a very low frequency (1%). Interestingly, such chromosome changes are present at high levels in human cells with premature ageing syndromes (Mukherjee and Costello 1998) and mitotic misregulation of dividing cells has been implicated in chromosomal pathologies associated with the ageing process (Ly *et al.*, 2000).

One of the most striking nuclear phenotypes in senescent cells are chromatin/lamin bridges called cut phenotype although they are found at relatively low frequency (6%) and some become broken. RNAi knockdown of Ce-lamin in *C.elegans* cells also produced this phenotype at a low frequency (1%) (Liu *et al.*, 2000). Interestingly, a similar phenotype was reported after microinjection of lamin antibodies during mitosis, which caused a cell cycle arrest in a telophase-like configuration with highly condensed chromatin and irregularly shaped nuclei (Benavente and Krohne 1986). The clue to the nature of these structures comes from studies in different fields. Many mitotic mutants of the fission yeast *Schizosaccharomyces pombe* have been originally found to produce a so-called cut phenotype (Funabiki *et al.*, 1996). Cut1 mutants fail to separate sister chromatids in anaphase producing lagging chromatin between daughter nuclei (cut phenotype), and if cells continue to divide, it leads to abnormal bisection of the undivided nucleus and subsequent G1 arrest (broken bridges). In addition, the abnormally divided nucleus is either reformed with extrusion of the lagging chromatin and subsequent chromosome loss (chromatin detachments) or it reforms with the lagging chromatin inside the nucleus giving rise to bud-like projections (herniations). If

cytokinesis is blocked, the duplicated genome is held in a single nucleus but still undergoes replication for a few cycles and a giant nucleus with polyploid chromosomes is formed (micronuclei). In these yeast mutants, the lagging chromatin was found to contain predominantly telomeric DNA. Interestingly, in pre-senescent cells, telomere end-to-end fusions are found to produce cut phenotype. These structures arise due to shortened or uncapped telomeres that are highly unstable, become 'sticky' and interfere with chromosome segregation (Yalon *et al.*, 2004). The presence of lamin C in these bridges in senescent nuclei is intriguing as A-type lamins have been reported to bind to telomeric sequences *in vitro* (Shoeman and Traub 1990). Interestingly, persistent telomere fusions are associated with attempted DNA repair in pre-senescent cells (Yalon *et al.*, 2004). Since shortened or uncapped telomeres often cannot be repaired, they permanently signal a DNA damage response pathway (von Zglinicki *et al.*, 2005). However, uncapped or shortened telomeres can also be incorrectly repaired leading to chromosome abnormalities (Campisi *et al.*, 2001). Some of these abnormalities include chromosomes with long arms, which are seen in bud-like projections. These reports suggest that telomere instability may be associated with abnormal nuclear phenotypes in senescent cells and that the presence of A-type lamins on these abnormal structures may be an important aspect of telomere (in)stability, DNA repair and chromosome (mis)segregation. Interestingly, LAP2α was recently shown to transiently bind to telomeres and subtelomeric 'core' chromatin regions on chromosomes during anaphase/telophase and was proposed to be involved in telomere positioning during interphase (Dechat *et al.*, 2004). Recently, a link has been shown between telomere instability and a cut-like phenotype induced by a loss of telomere-binding proteins (Veldman *et al.*, 2004, van Steensel *et al.*, 1998). The absence of the telomere-binding protein LAP2α from lagging chromatin in senescent cells may be linked to telomere instability and cut-like phenotypes in senescent cells.

**'Mitotic' histone phosphorylation in senescent fibroblasts may indicate mitotic misregulation prior to their irreversible arrest**

FACS analysis of senescent fibroblasts shows that most senescent cells accumulated in G1 phase of the cell cycle. However, a majority of aged cells accumulate nuclei that arrest cell cycle with either G1 or G2/M pattern of histone H3 (ser 10) phosphorylation. Senescent cells with chromatin bridges show a mitotic (G2/M) pattern of histone

phosphorylation both in nuclei and on bridges whilst cells with broken bridges show G1 pattern of histone phosphorylation within the nuclei and mitotic pattern on the bridges. This suggests that senescent cells with chromatin bridges are mitotically arrested and that cells with broken bridges arrest in G1 phase with mitotic chromatin in the bridges. Therefore, a high proportion of old cells show altered cell cycle behaviour prior to their arrest and may contain mitotic-like chromatin. Indeed, histone H3 can be abnormally phosphorylated even in the absence of normal mitosis and mitotic chromosome morphology (van Hooser *et al.*, 1998). Histone 3 phosphorylation has also been linked to maintenance of ploidy (Allison and Milner 2003). Alternatively, histone 3 phosphorylation may be important for chromatin remodelling during oxidative stress (Li *et al.*, 2001).

**Increased solubility/instability of A-type lamins and LAP2α in ageing fibroblasts**

Intranuclear lamin C can be both mobile and immobile in cells (Broers *et al.*, 2005). Mislocalisation of lamin C in the nucleoplasm in laminopathy cells results in increased mobility and solubility upon nuclear extraction (Broers *et al.*, 2005, Markiewicz *et al.*, 2002b). In senescent fibroblasts, lamin C and LAP2α are aberrantly organised in the nucleus. Upon nuclear extraction, senescent fibroblasts show increased solubility of lamin C, and LAP2α was more unstable/soluble leading to its loss from the nucleoskeleton. Lamin A (and possibly LAP2α), but not lamin B2 or LAP2β, becomes altered in a manner that makes them more unstable (i.e. prone to degradation) and soluble during nuclear extraction. Both lamin C (Vaughan *et al.*, 2001) and LAP2α (Markiewicz *et al.*, 2002a) depend on lamin A for their proper assembly in the nucleus, which indicates that the increased solubility of these proteins reflects some modifications to lamin A.

Lamin A shows an apparent partial proteolysis within its specific C-terminal tail, which generated a product only detectible by an antibody that recognises a common region in lamin A/C protein. Since an expected size of lamin A is present in whole cell extracts, this indicates that in living cells the interacting components which led to apparent proteolysis are not in close contact, which would allow the proteolysis to take place in vivo. Hence I cannot at this time speculate on the biological significance of this phenomenon *in vivo*. However, it is interesting to note that a mild proteolysis of lamin

A has been observed to yield polypeptides of the size of lamin C in vitro (Shelton *et al.*, 1980). In addition, in vitro, $Ca^{2+}$-activated neutral cysteine protease calpain can partially degrade lamin A leaving lamin C intact (Traub *et al.*, 1988). Calpain activity is increased during ageing and high oxidative stress is known to increase calpain activity (Nixon *et al.*, 2003). Since senescent cells contain high levels of oxidative stress these activated proteases may be loosely associated to the nuclear membrane but then gain access inside the nucleus following disruption of the nuclear envelope during isolation. Interestingly, other authors have reported a cysteine protease-dependent proteolytic activity to be elevated during extraction preparation of senescent cells, which resulted in a limited cleavage of proteins such as telomere-binding protein Ku86 and epidermal growth factor receptor (Jeng *et al.*, 1999, Carlin *et al.*, 1994).

**Lamin A and LAP2α show oxidative modifications to their C-terminal cysteines in senescent fibroblasts**

*In vitro* studies have shown that enhanced susceptibility to degradation by intracellular cysteine proteases is often employed as a criterion of unfolding (Grune *et al.*, 1997). Protein unfolding and subsequent fragmentation occurs in oxidised proteins. Lamin A protein contains three cysteines in its C-terminal-specific tail and shares one cysteine residue with lamin C in the common C-terminal domain. LAP2α protein contains ten cysteines in an α-specific C-terminal domain whilst LAP2β and LAP2γ have one cysteine in their specific C-terminal domains. Interestingly, cleavage of lamin A around Cys 588-590 would generate a proteolytic product 2 kDa larger than the size of lamins C. Thus, we believe that the observed proteolytic product of lamin A, 2kDa larger than lamin C, was generated due to unfolding of hydrophobic regions and subsequent cleavage of peptide bonds exposed by oxidation of lamin A-specific Cys588/590 residues.

Glutathione is the most abundant cellular thiol that is essential for normal regeneration of oxidized protein sulfhydryl groups. During ageing, changes in reduced glutathione levels increase the rate of formation of S-glutathiolated proteins and protein disulphides (Thomas and Mallis 2001). Interestingly, lamin A/C has been found to undergo S-glutathiolation as a result of oxidative stress during renal ischemia (Eaton *et al.*, 2003). This prompted me to examine whether A-type lamins and LAP2α form protein

disulphides or become S-glutathiolated in senescent cells. I show that lamins A/C and LAP2α do not form protein disulphides but become significantly S-glutathiolated in senescent cells. However, this does not exclude the possibility that lamin A and LAP2α undergo irreversible cysteine oxidation on some of their cysteines. Oxidation of protein thiols can have a variety of effects. Since S-glutathiolation can be a reversible process during recovery of cellular redox, it can be regarded as a protective mechanism that guards against irreversible protein thiol oxidation. The protein thiol groups therefore act as a radical sink and protect the protein by accepting the oxidative damage and preventing an accumulation of secondary irreversible modifications on other amino acids such as protein carbonylation (Dean *et al.*, 1986, Davies *et al.*, 1993). However, if the glutathiolated cysteine residues are functionally critical, S-glutathiolation will render the protein inactive and compromise cellular function (Eaton *et al.*, 2002). This, on the other hand, may cause permanent loss of replicative or divisional competence (Davies *et al.*, 1999).

**S-glutathiolation of cysteine residues in Lamin A and LAP2α prevents formation of higher order disulphide structures**

S-glutathiolation of proteins can inhibit disulphide bonding within or between protein cysteines (Cumming *et al.*, 2004). Lamina A and to a lesser extent lamin C can form non-native disulphide cross-links upon nuclear isolation during non-reducing conditions (Kaufmann *et al.*, 1983). Indeed, whilst lamin A readily forms both intra- and inter-molecular disulphides in early passage cells under non-reducing conditions, lamin A accumulates as a monomer in senescent cells. Lamin C does not form detectible disulphides in early passage cells under non-reducing conditions, although early passage cells show a reduced amount of monomer as compared to senescent cells. In contrast, lamin B2 shows a reduced amount of monomer independently of age under non-reducing conditions. My results show for the first time that LAP2α, but not LAP2β or LAP2γ, forms inter-molecular disulphides in early passage cells under non-reducing conditions. Similarly to lamin A, LAP2α accumulates as a monomer in senescent cells under the same conditions. In addition, both lamins A/C and LAP2α show an age-dependent accumulation of monomeric protein with an increasing passage number under non-reducing conditions. Blocking of these reactive cysteines with an irreversible sulfhydryl group blocking reagent NEM prevents formation of these proteins disulphide

cross-links in early passage cells and causes a reappearance of monomeric forms of lamin A and LAP2α. This confirms that formation of disulphide cross-links in lamin A and LAP2α depends on their free reactive cysteine sulfhydryl groups and that glutathiolation of these proteins in senescent cells prevents their formation.

The ability of lamin A and LAP2α to form these intermolecular cross-links in vitro suggests a regular order in the arrangement of lamin A polymeric arrays and LAP2α complexes in early passage fibroblasts, the monomers of which contain juxtaposed sulfhydryl groups within intact cells. On the other hand, cysteine oxidation produces protein destabilization and denaturation, which in turn exposes hydrophobic domains of the denatured protein (Freeman *et al.*, 1995, McDufee *et al.*, 1997). The term protein denaturation refers to a process involving a conformational rearrangement by which the ordered native structure of a protein changes to a more disordered structure. Proteolytic cleavage of lamin A during nuclear extraction also suggests that cysteine oxidation in its C-terminal tail leads to a change in conformational structure. Therefore, the inability of lamin A and LAP2α to form higher-order disulphide structures *in vitro* suggests a disordered arrangement of lamin A polymeric arrays and LAP2α complexes in senescent fibroblasts, whereby their glutathiolated monomers do not form close inter-stand contacts to support such stable structures. Interestingly, glutathiolation of actin cysteine 374 has been shown to induce changes in the structural conformation of actin monomer which leads to slower and less efficient assembly of GS-actin monomers (Dalle-Donne *et al.*, 1999, 2003). In addition, removal of the last three C-terminal actin cysteines destabilised actin filaments by weakening of the interstrand contacts generated by an allosteric conformational change in the actin filament (Mosakowska *et al.*, 1993).

**A possible mechanism of sequential targeting of A-type lamin cysteines for oxidative modifications during ageing of fibroblasts in vitro**

Lamin A and C share Cys522 in their C-terminal common domain. Since both proteins show a similar extent of glutathiolation, they are presumably both modified at this cysteine in aged fibroblasts. However, lamin C shows a more rapid accumulation of monomeric protein in mid passage cells before extensive lamin A accumulation appears indicating that modification of this cysteine may not have as profound a structural effect on lamin A as it does on lamin C. Indeed, lamin A can still form, albeit at a lower level,

both intra- and inter-disulphide cross-links in mid passage cells whilst lamin C accumulates as a monomer. This suggests that there may be age-dependent sequential targeting of lamins A/C cysteine residues to oxidative modifications during in vitro ageing of human fibroblasts. Particularly, in lamin A, cysteine 588 and 591 may be oxidatively modified at a later age in human fibroblasts. This may be an important biological difference between these lamin isoforms. During oxidative stress, it is important to have a protein isoform (lamin A) that is not completely inactivated by oxidative modifications and would provide function in survival while a different protein isoform (lamin C) may be inactivated during oxidative stress. When oxidative stress is too high or persistent, a critical amount of cysteine modifications in both protein isoforms would render the protein completely inactive and impair cell survival and function. Such a mechanism has been observed during oxidative stress in different protein isoforms (in Eaton *et al.*, 2002).

**Laminopathy fibroblasts enter premature senescence in the absence of increased oxidative modifications to lamin A/C cysteines**

Accumulation of genetic and protein damage has long been suggested as one of the major forms of damage contributing to the ageing of cells and organisms (von Zglinicki *et al.*, 2001). In senescent cells, persistently high levels of oxidative stress would prevent recovery of the cellular redox and subsequent reversal of S-glutathiolation of proteins. Therefore, although S-glutathiolation is a reversible reaction, it can only be reversed when adequate anti-oxidant enzymes systems are activated to counter-act the oxidative stress. In two early passage laminopathy cell lines tested (E358K and R249Q), A-type lamins are able to form disulphide cross-links under non-reducing conditions. In addition, all four mid passage laminopathy cell lines tested (E358K, R249Q, R453W and R401C) show an age-dependent accumulation of monomeric lamin A protein, which is not increased as compared to the age-matched wild-type fibroblasts. One laminopathy cell line tested (E358K) shows S-glutathiolation of A-type lamins in early and mid passage cells comparable to levels in age-matched fibroblasts. Also, none of the four laminopathy cells lines tested (E358K, R249Q, R453W and R401C) shows formation of protein disulphides as a result of oxidative stress. Therefore, accumulation of monomeric lamin A under non-reducing conditions as a result of S-glutathiolation is an age-dependent trait and is not impaired by lamin mutations. Yet all five laminopathy

cell lines tested (including Y259X) entered premature senescence at mid passages 20-26. This suggests that laminopathy cells do not enter premature senescence as a result of abnormally increased oxidative stress or an inability of lamin cysteines to accept oxidative damage. Therefore, lamin mutations may cause premature senescence via different types of mechanisms that can lead to premature senescence such as DNA damage, abnormal activation of hyper-proliferative signalling pathways and epigenetic alterations. Interestingly, a recent report has shown that Zmpste24 null mouse cells and HGPS accumulate increased DNA damage and chromosome aberrations due to compromised DNA repair and that these cells do not have shortened telomeres (Liu *et al.*, 2005). As it can be seen in chapter 1, DNA damage to telomeres as a result of alterations in telomere-binding proteins can also trigger premature senescence in the presence of normal telomere lengths. Uncapped telomeres undergo end-to-end fusions (cut phenotype) and lead to defects in chromosome segregation and DNA repair (Veldman *et al.*, 2004, van Steensel *et al.*, 1998). Therefore lamin mutations may cause premature senescence by altering a higher order telomere structure.

**Structural/functional implications of lamins A/C and LAP2α cysteine modifications in ageing and lamin A/C mutations in premature ageing**

Cysteine residues are known to serve at least three structural functions in proteins: formation of disulphide bonds, hydrogen bonding and the coordination of bonds formation with metal ions (McDuffee *et al.*, 1997). In lamins, the first level of filament assembly involves dimer formation via hydrophobic interactions between rod domains of lamin monomers (in Stuurman *et al.*, 1998). Lamin dimers associate into head-to-tail polymers, and lateral association of head-to-tail polymers forms filament structures, which can assemble into protofilaments and higher order filament structures. The formation of disulphide bonds between lamin A monomers in a non-reducing assay does not reflect dimer formation between lamin monomers in vivo, although in vitro conditions (which are more oxidising due to exposure to air) seem to favour their formation. Instead, these cysteine residues may serve as direct contact points between lamin A/C protofilaments during higher order filament assembly. The way to test this is to use native high-gradient gel electrophoresis under NEM/non-reducing and, as a control, reducing conditions. In addition, since binding of other proteins to lamins is believed to significantly affect the mode of lamin filament assembly in vivo (in

Stuurman *et al.*, 1998), these cysteine residues may serve as contact sites between lamin A/C and other proteins as well as DNA and thus help to form or maintain the proper conformation needed to bind other proteins which in turn may affect higher order filament assembly.

These suggestions are not without a precedent. Deletion mutants of human lamin A lacking the last 110 C-terminal amino acids are not properly associated with the nuclear envelope (Loewinger and McKeon 1988), indicating that the C-terminal tail in lamin A plays a role in lamin A assembly. Furthermore, a Xenopus lamin A mutant lacking C-terminal cysteine shows a delayed but partial assembly, indicating that other domains in lamin A contribute to filament assembly (Krohne *et al.*, 1989). These lamin A domains were attributed to the lamin A-specific C-terminal tail. Recently, it has been shown that removal of four fifths of the rod domain in lamin A did not affect its binding interactions whereas binding interactions of lamin B1 and lamin C were strongly destabilised (Schirmer and Gerace 2004). These authors attributed these unusually strong lamin A interactions to additional lamin A binding sites in its C-terminal tail and suggest that lamin A may assemble in a distinct manner. Moreover, the common C-terminal domain of A-type lamins adopts an Ig-like fold (Krimm *et al.*, 2002). Although, A-type lamins behave primarily as monomers in solution, these authors note that the presence of solvent-exposed cysteine residue 522 in this region causes large chemical fluctuations due to dimerisation of the protein through the formation of transient disulphide bonds. Interestingly, molecular modelization favours the occurrence of these disulphide bonds between anti-parallel dimers and it was therefore proposed that disulphide bonds via these cysteines may form between distant lamin molecules from anti-parallel protofilaments of adjacent protofibrils (Stierle *et al.*, 2003).

Interestingly, the C-terminal tail of lamins A/C, which is important for lamin assembly and binds DNA, also binds to LAP2α. LAP2α interaction with lamins A/C occurs via its C-terminal specific domain (aa 615-993) (Dechat *et al.*, 1998) and this binding region in LAP2α contains three cysteine residues. The C-terminal domain in LAP2α is also a nuclear targeting domain essential for its binding to telomeres and chromosomes (aa 270-615) (Vlcek *et al.*, 1999) and this chromosome binding region contains seven cysteine residues. Therefore, S-glutathiolation of LAP2α and lamins A/C could directly affect their interactions with each other as well as their binding to chromatin. Following

nuclear extraction of senescent cells, LAP2α was significantly reduced in the insoluble fraction prior to DNAse I digestion, indicating that LAP2α does not bind to either DNA or lamins correctly.

LAP2α binds to telomeres during anaphase whilst it also self-associates via its C-terminal domain forming high molecular weight complexes (~220 kDa), which is proposed to regulate telomere positioning in interphase nuclei (Dechat *et al.*, 1998, 2004). Since in early passage cells, LAP2α forms similar high molecular weight disulphide complexes in the non-reducing assay, it is very likely that the observed self-association of LAP2α during mitosis occurs via cysteine residues in the C-terminal domain. I did not detect LAP2α disulphide complexes in early passage cells *in vivo*. However, in our experiments we used exponentially growing unsynchronised cells which contained less than 15% of cells in G2/M phase as assessed by FACS analysis. Performing these experiments on synchronised mitotic cells would be needed to confirm whether these mitotic LAP2α complexes form via disulphide bonds. Interestingly, transfection of cells with dominant-negative C-terminal LAP2α mutants caused cell cycle arrest in G1 phase by dominantly inhibiting distribution of endogenous LAP2α on chromosomes and subsequent nuclear assembly, indicating that LAP2α binding to telomeres and chromosomes is essential for cell cycle progression. The finding that LAP2α aggregates in dysmorphic senescent nuclei and is found in cytoplasmic granules around chromatin bridges of senescent cells with cut phenotype, suggests that aberrant assembly of LAP2α in the nucleus may lead to telomere instability and senescent arrest.

Lamin mutations, on the other hand, have been directly shown to affect higher order filament assembly. Krimm *et al.*, 2002 have found that ADMD mutations in the C-terminal domain of lamins A/C destabilise the three-dimensional structure whereas FPLD mutations in the same region lead to suppression of positively charged character sites and may therefore decrease protein-protein interactions or protein-DNA interactions. Indeed, the C-terminal tail of A-type lamins contains a chromatin-binding region and lamin tail mutations show a 5-fold decrease in affinity to chromatin (Stierle *et al.*, 2003). Moreover, it has been recently shown that mutations in the rod domain affect head-to-tail association and later stages of lamin filament assembly (Strelkov *et al.*, 2004). As mentioned earlier, lamin mutations may cause premature senescence by affecting higher order telomere structure through a loss of telomere binding proteins.

Since LAP2α binds to telomeres and chromosomes, which is essential for cell cycle progression, lamin mutations may impair correct assembly of LAP2α in the nucleus either by loss of protein-protein interactions (C-terminal FPLD mutations) or by sequestering LAP2α in the nucleus (C-terminal and rod ADMD mutations), thus leading to telomere instability and premature senescent arrest. Indeed, the expression of dominant negative lamin mutants that disrupt proper assembly of lamin A/C led to the sequestering of LAP2α to intranuclear aggregates in which lamins A/C were also found (Markiewicz *et al.*, 2002a).

**A model for in vitro ageing of human dermal fibroblasts**

I propose a model for ageing of human dermal fibroblasts whereby S-glutathiolation of critical cysteines in A-type lamins during ageing induces changes in the structural conformation of A-type lamin C-terminal domain which leads to a destabilisation of existing A-type lamin filaments and a less efficient assembly of glutathiolated-lamin A/C monomers at the nuclear envelope. Consequently, this would translate to a nuclear fragility, changes in association with peripheral chromatin and generation of nuclear 'laminopathy' phenotypes in senescent cells. Similarly, S-glutathiolation of LAP2α-specific cysteines would induce structural conformation changes in α-C-terminal domain which would impair an effective assembly of homo-oligomeric LAP2α complexes essential for binding to telomeres and core chromatin structures during the post-mitotic establishment of nuclear envelope assembly and higher order chromatin structure. Aberrant targeting of LAP2α complexes at telomeres would lead to telomere instability and chromosome segregation defects seen in ageing cells and trigger a signal for arrest of cell cycle progression. This model also suggests that changes in positive/negative charge often brought out by S-glutathiolation of cysteines residues may affect particular sites in the C-terminal domain of lamins A/C and LAP2α, which could impair their interactions with chromatin or other proteins known to bind to C-terminal domain of A-type lamins, including LAP2α, or to C-terminal domain of LAP2α. Therefore, this model of ageing parallels the structural/gene hypotheses (Hutchison *et al.*, 2001, Wilson *et al.*, 2001) postulated for laminopathies. However, it emphasizes that LAP2α and lamin A may play an important role in premature ageing of laminopathy cells.

**Figure 3.1: Expression of A-type and B-type lamins and their binding partners LAP2α and LAP2β does not change during *in vitro* ageing of human dermal fibroblasts (HDF).** The same number of cells was harvested after three days in culture at early **(p7-12)**, intermediate **(p17-p27)** and late **(p44)** passages. Whole cell extracts were prepared for immunoblotting with antibodies against lamin A/C (JOL2), lamin B2 (LN43), LAP2α (LAP15) and LAP2β (LAP17). Molecular weight markers showed the expected mobility for the above proteins: lamin A & C (70 & 65 kDa), lamin B2 (68 kDa), LAP2α (75 kDa) and LAP2β (55 kDa).

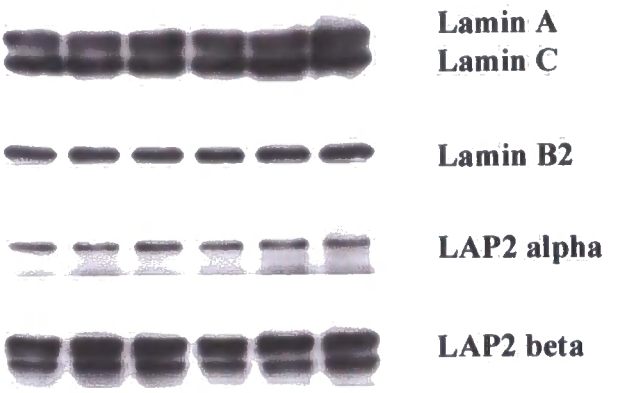
Lamin A
Lamin C
Lamin B2
LAP2 alpha
LAP2 beta
HDF
passages
p7 p12 p17 p22 p27 p44

**Figure 3.1**

**Figure 3.2A: Late passage fibroblasts show granular nuclear distribution of LAP2α which often extends into cytoplasm and lamin C reveals large and irregular nuclei.** Early **(p7)** and late **(p44)** passage HDF were prepared for immunofluorescence microscopy with antibodies against **(a)** LAP2α and Ki67, **(b)** LAP2α and lamin C. Images are projected as individual black and white or red/green colour merged micrographs in which LAP2α is in red, and Ki67 and lamin C are in green. Arrows in **LAP2α** micrographs show cytoplasmic LAP2α. Arrows in **Lamin C** micrograph show irregular nuclear shapes. Magnification 120x.

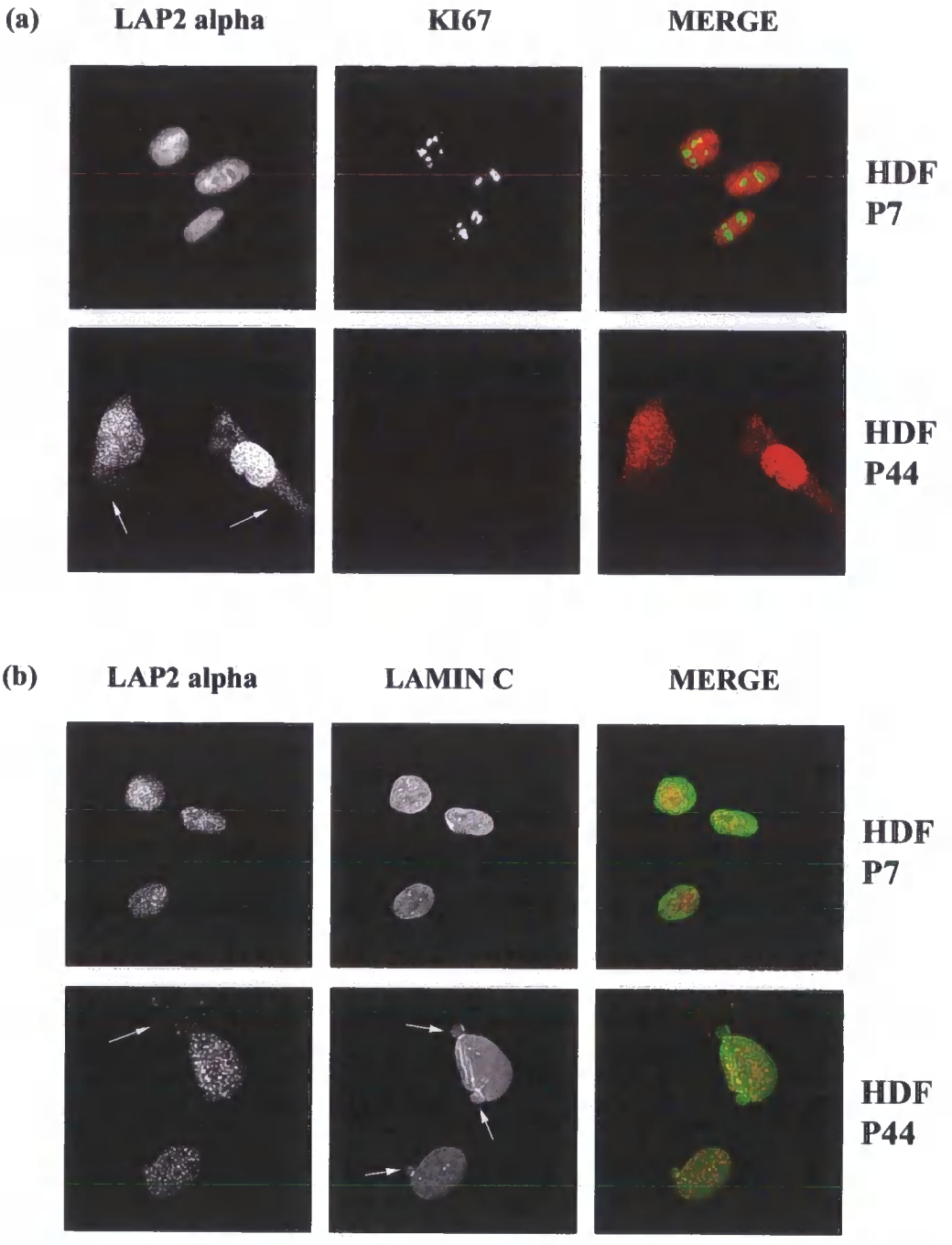
(a)
LAP2 alpha
KI67
MERGE
HDF P7
HDF P44
(b)
LAP2 alpha
LAMIN C
MERGE
HDF P7
HDF P44

# Figure 3.2A

**Table 3.1**

| Cell strain & passage number | LAP2α+ Ki67+ | LAP2α- Ki67- | LAP2α+ Ki67- |
|---|---|---|---|
| HDF p7 | 74.8 % ± 6.7 | 25.2 % ± 7.2 | 0.0 % |
| HDF p44 | 20.1 % ± 3.4 | 34.7 % ± 4.1 | 45.2 % ± 4.7 |

**Chart 3.1**

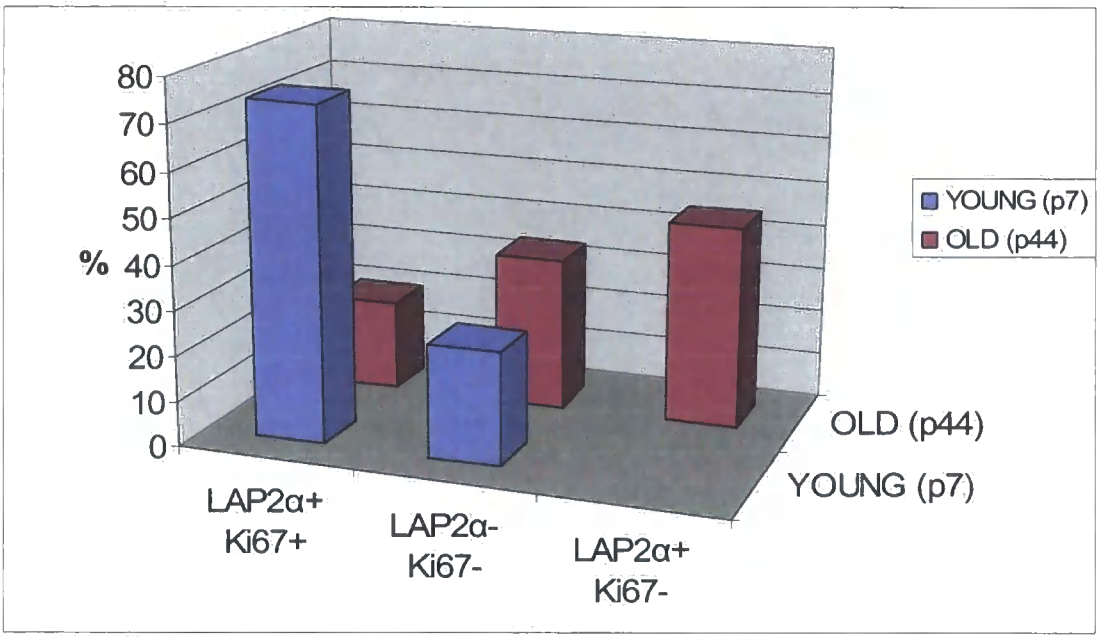


**Table 3.1: LAP2α expression correlates with proliferative status of early passage but not late passage fibroblasts.** Human dermal fibroblasts (HDF) of early (p7) and late (p44) passage were seeded at an initial density of 3 x $10^4$ cells per 9 $mm^2$ culture well, each containing 3 glass coverslips. After 72 hours in culture, triplicate coverslips were fixed and stained with LAP2α and anti-Ki67 antibodies. 300 cells on each coverslip were scored for the presence of LAP2α and Ki67, the absence of both, or the presence of LAP2α in the absence of Ki67. Table 1 shows the mean percentage of cells scored for each of the three categories described and the +/- standard deviation in triplicate experiments. **Chart 3.1** is a visual representation of the mean percentages in Table 1.

**Figure 3.2B: Lamin B2 and LAP2β show absent distribution from one pole of the nucleus and reveal irregularly shaped nuclei in late passage fibroblasts.** Early **(p7)** and late **(p44)** passage HDF were prepared for immunofluorescence microscopy with antibodies against **(a)** lamin B2 and Ki67, **(b)** LAP2β and Ki67. Images are projected as individual black and white or red/green colour merged micrographs in which Lamin B and LAP2β are in red and Ki67 is in green. In **Lamin B** micrograph, the arrow shows absence of lamin B2 from one pole of the nucleus and arrowhead shows irregular nuclear shape. In **LAP2β** micrograph, arrows show absence of LAP2β from one pole of the nucleus. Magnification 120x.

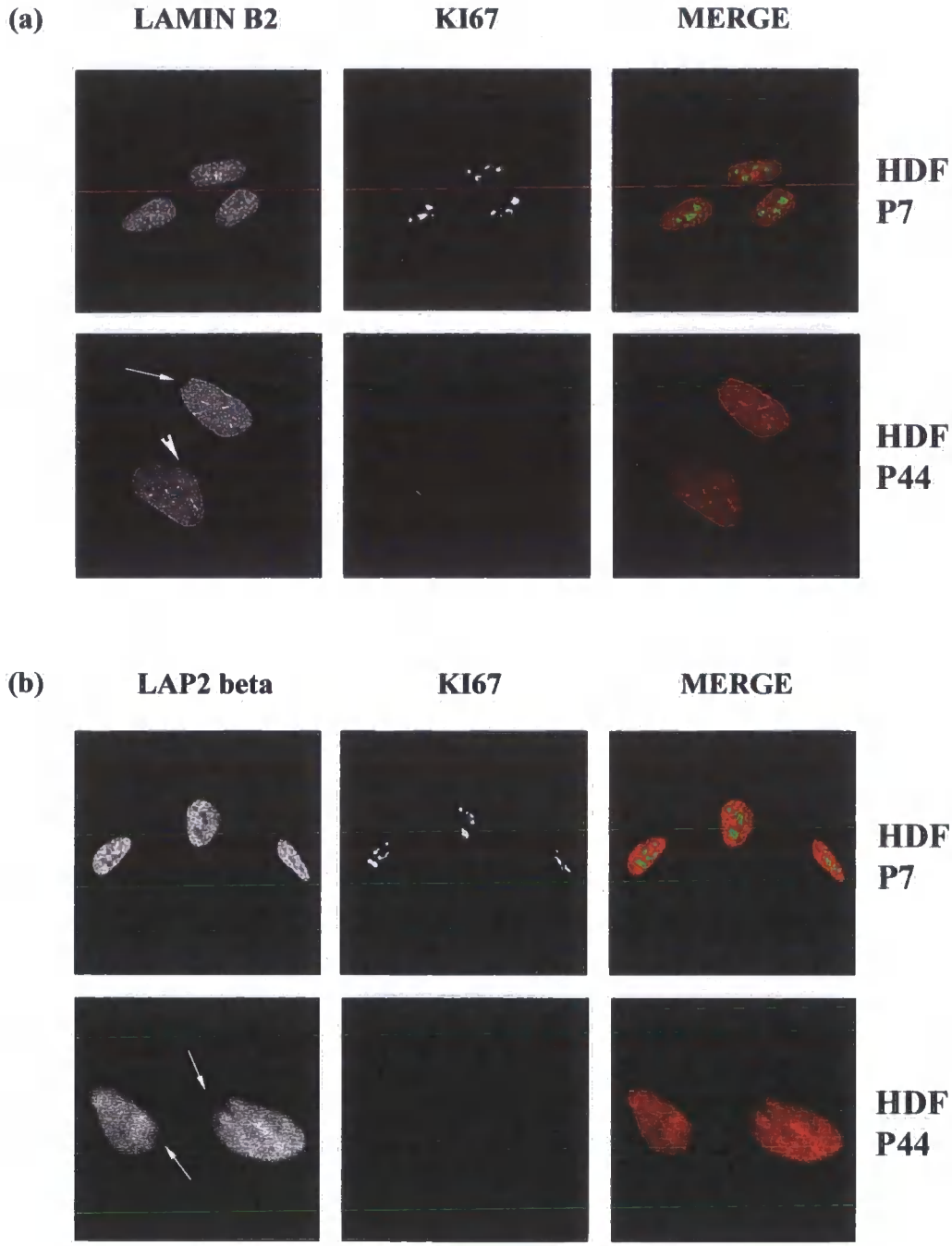
(a)
LAMIN B2
KI67
MERGE
HDF P7
HDF P44
(b)
LAP2 beta
KI67
MERGE
HDF P7
HDF P44

# Figure 3.2B

**Figure 3.3: Late passage fibroblasts show laminopathy-like nuclear dysmorphic phenotypes.** Late **(p44)** passage fibroblasts were prepared for immunofluorescence microscopy and stained with antibodies against LAP2α and lamin C. Late passage HDF display a range of nuclear dysmorphic morphologies including: **(a)** nuclei with a single herniation; **(b)** nuclei with honeycombs; **(c)** nuclei with chromatin detachments; **(d)** incompletely segregated nuclei with a lamin-containing bridge and **(e)** micronuclei. Images were collected on a Zeiss confocal microscope and projected as black and white or red/green colour merged micrographs in which LAP2α is in red and Lamin C is in green. In **LAP2α** micrographs, arrows indicate the positions of LAP2α aggregates and arrowhead indicates cytoplasmic granules of LAP2α surrounding lamin bridges between incompletely segregated nuclei. In **Lamin C** micrographs, arrows indicate intranuclear accumulation or aggregation of lamin C and arrowhead indicates the presence of lamin C bridge between incompletely segregated nuclei within a single cell. In **MERGE** micrographs, arrowheads indicate particular nuclear abnormality. Magnification 360x.

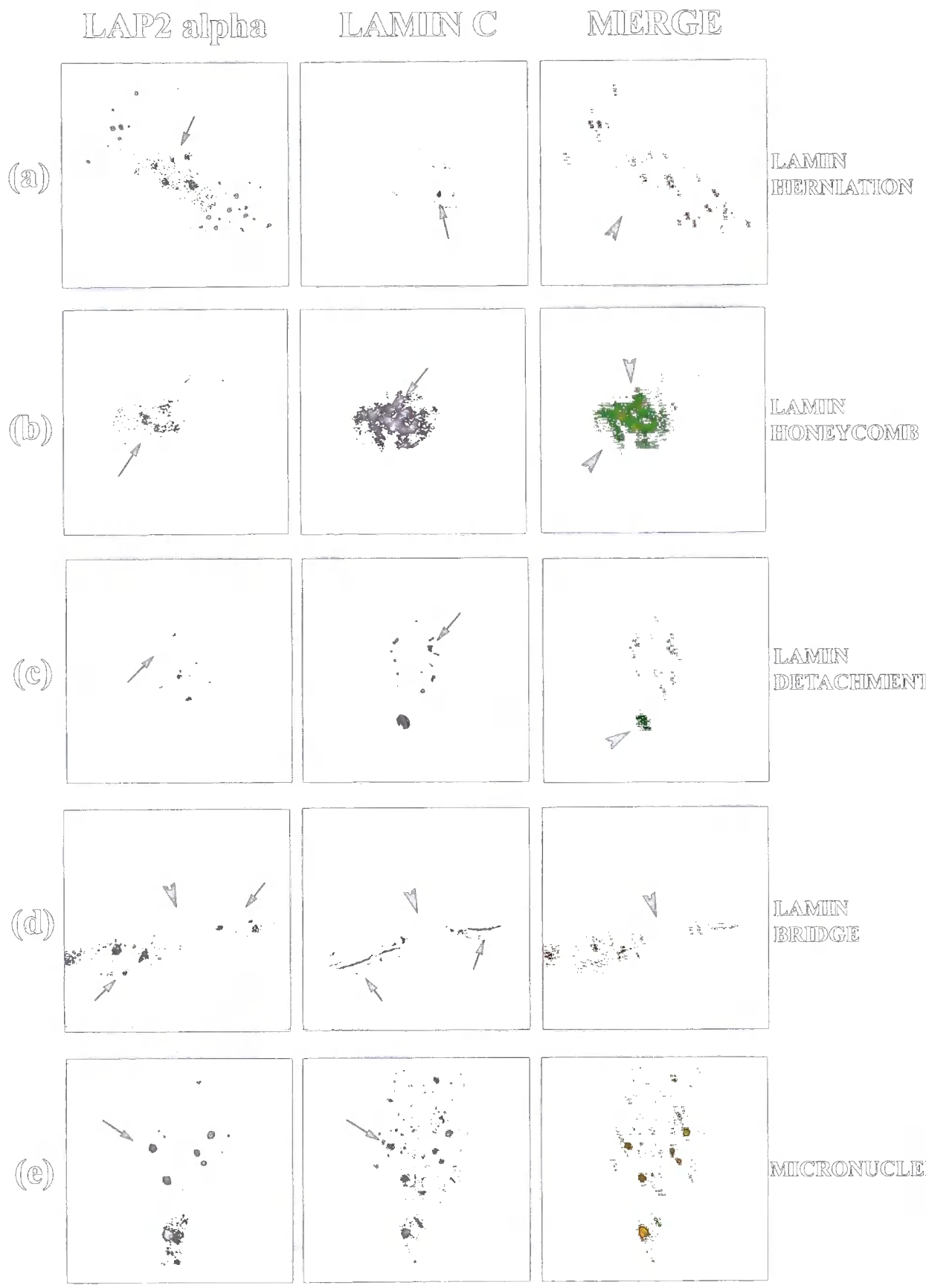
LAP2 alpha
LAMIN C
MERGE
(a)
LAMIN HERNIATION
(b)
LAMIN HONEYCOMB
(c)
LAMIN DETACHMENT
(d)
LAMIN BRIDGE
(e)
MICRONUCLEI

Figure 3.3

**Table 3.2**

| HDF | herniations | honeycombs | Chromatin Detachments | lamin bridges | micronuclei | Total dysmorphic |
|---|---|---|---|---|---|---|
| p12 | 9.0 % | 0.0 % | 0.0 % | 0.0 % | 0.00 % | 9.00 % |
| p44 | 29.0 % | 15.0 % | 8.0 % | 6.0 % | 1.25 % | 59.25 % |

**Table 3.2: The proportions of dysmorphic nuclei in early and late passage fibroblasts.** Human dermal fibroblasts (HDF) of early (p12) and late (p44) passage were seeded at an initial density of 3 x $10^4$ cells per 9 $mm^2$ culture well, each containing 3 glass coverslips. After 72 hours in culture, triplicate coverslips were fixed and stained with Lamin A/C and anti-Ki67 antibodies. 300 cells on each coverslip were scored for the presence of dysmorphic nuclei including nuclei with herniations, honeycombs, chromatin detachments, lamin bridges and micronuclei. Table 2 shows the mean percentage of cells scored for each of the five dysmorphic nuclear types and the total percentage of cells scored for dysmorphic nuclei in four independent experiments.

**Figure 3.4A: Chromatin distribution at the nuclear envelope is altered in dysmorphic nuclei of late passage fibroblasts.** Late passage **(44)** dysmorphic nuclei shown in Figure 3 were also stained with chromatin-staining dye DAPI, which confirmed that dysmorphic nuclei were not apoptotic. Chromatin distribution is shown as follows: **(a)** chromatin in single herniations; **(b)** chromatin holes in nuclei with honeycombs; **(c)** chromatin detachment in the cytoplasm; **(d)** chromatin bridge between incompletely segregated nuclei, and **(e)** chromatin in micronuclei. Images were collected on a Zeiss confocal microscope and projected as individual black and white micrographs or blue/green colour merged micrographs in which DAPI is in blue and lamin C is in green. In **DAPI** micrographs, the arrowhead indicates the presence or absence of chromatin in particular nuclear abnormality and the arrow indicates chromatin holes in micronuclei. In **Lamin C** micrographs, the arrowhead indicates the presence or absence of lamin C in particular nuclear abnormality and arrowhead indicates lamin C aggregates in micronuclei. In **MERGE** micrographs arrows indicate an absence of peripheral chromatin at the nuclear envelope. Magnification 360x.


DAPI
LAMIN C
MERGE
(a)
SINGLE HERNIATION
(b)
CHROMATIN HOLES
(c)
CHROMATIN DETACHMENT
(d)
CHROMATIN BRIDGE
(e)
MICRONUCLEI

Figure 3.4A

**Figure 3.4B: Dysmorphic nuclei of late passage fibroblasts accumulate intranuclear lamin C, which correlates with a lack of proliferative potential.** Early **(p7)** and late **(p44)** passage HDF were prepared for confocal microscopy with antibodies against Lamin C and Ki67 and stained with chromatin-staining dye DAPI. Images were collected on a Zeiss confocal microscope and projected as individual black and white micrographs or blue/green/red colour merged micrographs in which DAPI is in blue, lamin C is in green, and Ki67 is in red. In **Lamin C** micrographs, arrows point out intranuclear lamin C structures and arrowheads point out distribution of lamin C at the nuclear envelope. In **MERGE** micrographs arrows point out co-distribution of lamin C and chromatin (p7) or lack of it (p44) at the nuclear envelope. Magnification 360x.

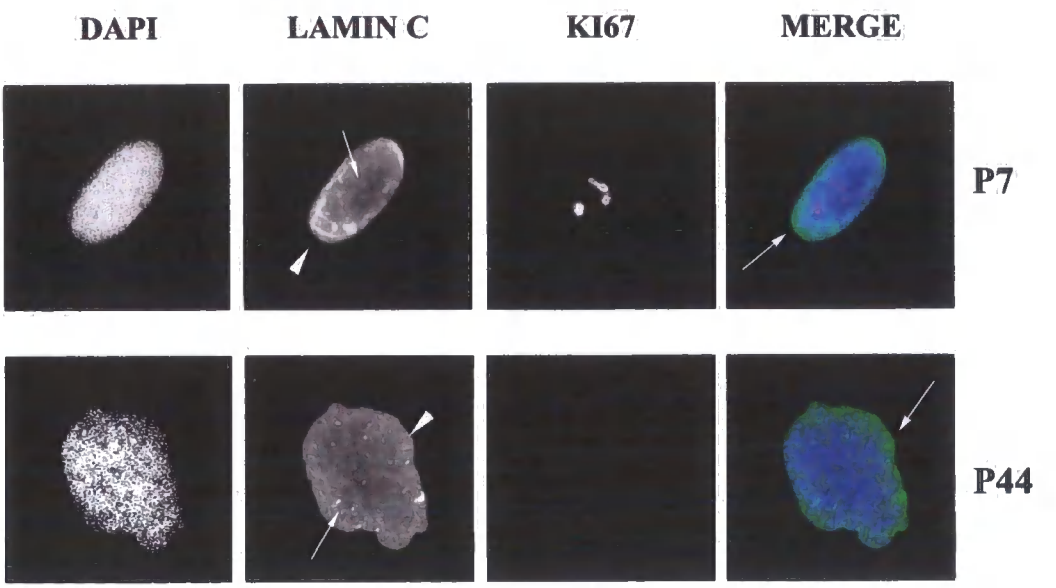


Figure 3.4B

**Table 3.3**

| Cell strain & passage n° | LNC NE Ki67+ | LNC dots Ki67+ | LNC NE Ki67- | LNC dots Ki67- |
|---|---|---|---|---|
| HDF p7 | 49.1 % ± 5.3 | 26.2 % ± 3.4 | 24.7 % ± 4.1 | 0.0 % |
| HDF p44 | 12.8 % ± 3.0 | 6.9 % ± 2.2 | 36.9 % ± 4.7 | 43.2 % ± 7.2 |

**Chart 3.3**

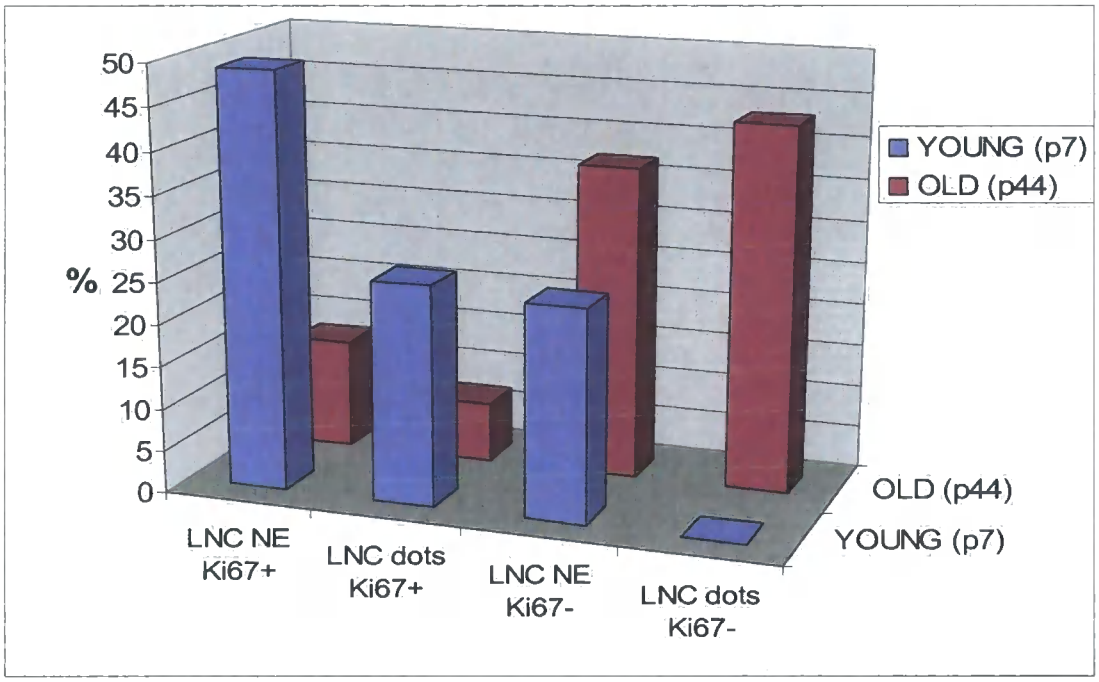


**Table 3.3: The accumulation of intranuclear lamin C structures correlates with proliferation arrest in late passage fibroblasts.** Human dermal fibroblasts (HDF) of early (p7) and late (p44) passage were seeded at an initial density of 3 x $10^4$ cells per 9 $mm^2$ culture well, each containing 3 glass coverslips. After 72 hours in culture, triplicate coverslips were fixed and stained with Lamin C and anti-Ki67 antibodies. 300 cells on each coverslip were scored for the presence of an intense lamin C staining at the nuclear envelope in the presence or absence of Ki67. Alternatively, cells were scored for the presence of lamin C dots and fibers in the presence or absence of Ki67. Table 3 shows the mean percentage of cells scored for each of the four categories described and the +/- standard deviation in triplicate experiments. **Chart 3** is a visual representation of the mean percentages in Table 3.

**Table 3.4**

| Cell strain & passage number | Ki67+ Total nuclei | Ki67+ Ovoid nuclei | Ki67+ Dysmorphic nuclei |
|---|---|---|---|
| HDF p12 | 72.00 % | 77.00 % | 54.40 % |
| HDF p44 | 20.00 % | 37.35 % | 3.33 % |
| Y259X p12 | 35.00 % | 45.40 % | 9.70 % |
| R249Q p12 | 40.59 % | 62.50 % | 25.25 % |
| E358K p12 | 59.50 % | 86.14 % | 32.32 % |
| R453Q p12 | 42.23 % | 67.24 % | 6.24 % |

**Table 3.4: Late passage wild-type fibroblasts and early passage laminopathy fibroblasts accumulate dysmorphic nuclei that correlate with cell cycle arrest.** Early (p12) and late (p44) passage wild type fibroblasts (HDF) and early passage (p12) laminopathy fibroblasts with the following mutations Y259X, R249Q, E358K and R453Q were seeded at an initial density of 3 x $10^4$ cells per 9 $mm^2$ culture well, each containing 3 glass coverslips. After 72 hours in culture, triplicate coverslips were fixed and stained with lamin C and anti-Ki67 antibodies. 300 cells on each coverslip were scored for the presence of Ki67 proliferation marker in either ovoid or dysmorphic nuclei in three independent experiments. Table 4 shows the fraction of nuclei (expressed as a mean percentage) that scored positive for Ki67 from the total proportion of cells with ovoid nuclei or from the total proportion of cells with dysmorphic nuclei. In addition, the total proportion of cells (with both ovoid and dysmorphic nuclei) positive for Ki67 marker is also displayed as a mean percentage.

**Table 3.5**

| HDF | E358K | R453W | R249Q | Y259X |
|---|---|---|---|---|
| p7 75.0 % | p7 75.00 % | p7 70.50 % | p7 68.20 % | p7 71.10 % |
| p12 72.0 % | p12 59.50 % | p12 42.23 % | p12 40.59 % | p12 35.00 % |
| p24 49.0 % | p24 28.00 % | p20 10.11 % | p20 11.67 % | p20 6.87 % |
| p40 25.0 % | p26 20.19 % | | | |
| p44 20.0 % | | | | |

**Table 3.5: Laminopathy fibroblasts enter premature senescent arrest independently of the position of the lamin mutation.** Early (p7) passage wild type and laminopathy fibroblasts with the following mutations Y259X, R249Q, E358K and R453Q were aged in culture until they significantly exhausted their proliferative potential. Cells of early (p7-12), intermediate (20-26) and late (p44) passage were seeded at an initial density of 3 x $10^4$ cells per 9 $mm^2$ culture well, each containing 3 glass coverslips. After 72 hours in culture, triplicate coverslips were fixed and stained with lamin A/C and anti-Ki67 antibodies. 300 cells on each coverslip were scored for the presence of Ki67 proliferation marker. Table 5 shows the fraction of nuclei (expressed as a mean percentage) that scored positive for Ki67 in two independent experiments.

**Figure 3.5: Late passage fibroblasts with a CUT phenotype show a mitotic (G2/M) pattern of phospho-histone H3 phosphorylation on both enclosed chromatin and chromatin bridges.** Early **(p7)** and late **(p44)** passage cells were prepared for confocal microscopy and co-stained with antibodies against phospho histone H3 and lamin C. **(a)** shows a p7 cell with G1 pattern of phospho-histone H3 phosphorylation (upper panel) and p7 cells with G2/M pattern of phospho-histone H3 phosphorylation; **(b)** shows a p44 cell with G1 pattern of phospho-histone H3 phosphorylation (upper panel) and a p44 cell with G2/M pattern of phospho-histone phosphorylation (lower panel). The arrow in the upper panel points out a broken lamin bridge with G2/M pattern of phospho-histone phosphorylation attached to nucleus with G1 pattern of phospho-histone phosphorylation. The arrow in the lower panel points out a lamin bridge with G/M pattern of phospho-histone phosphorylation between incompletely segregated nuclei within a single cell. Images were collected on a BioRad Radiance 2000 confocal microscope and projected as black and white or red/green colour merged micrographs in which histone H3 is in red and lamin C is in green. Magnification 360x.

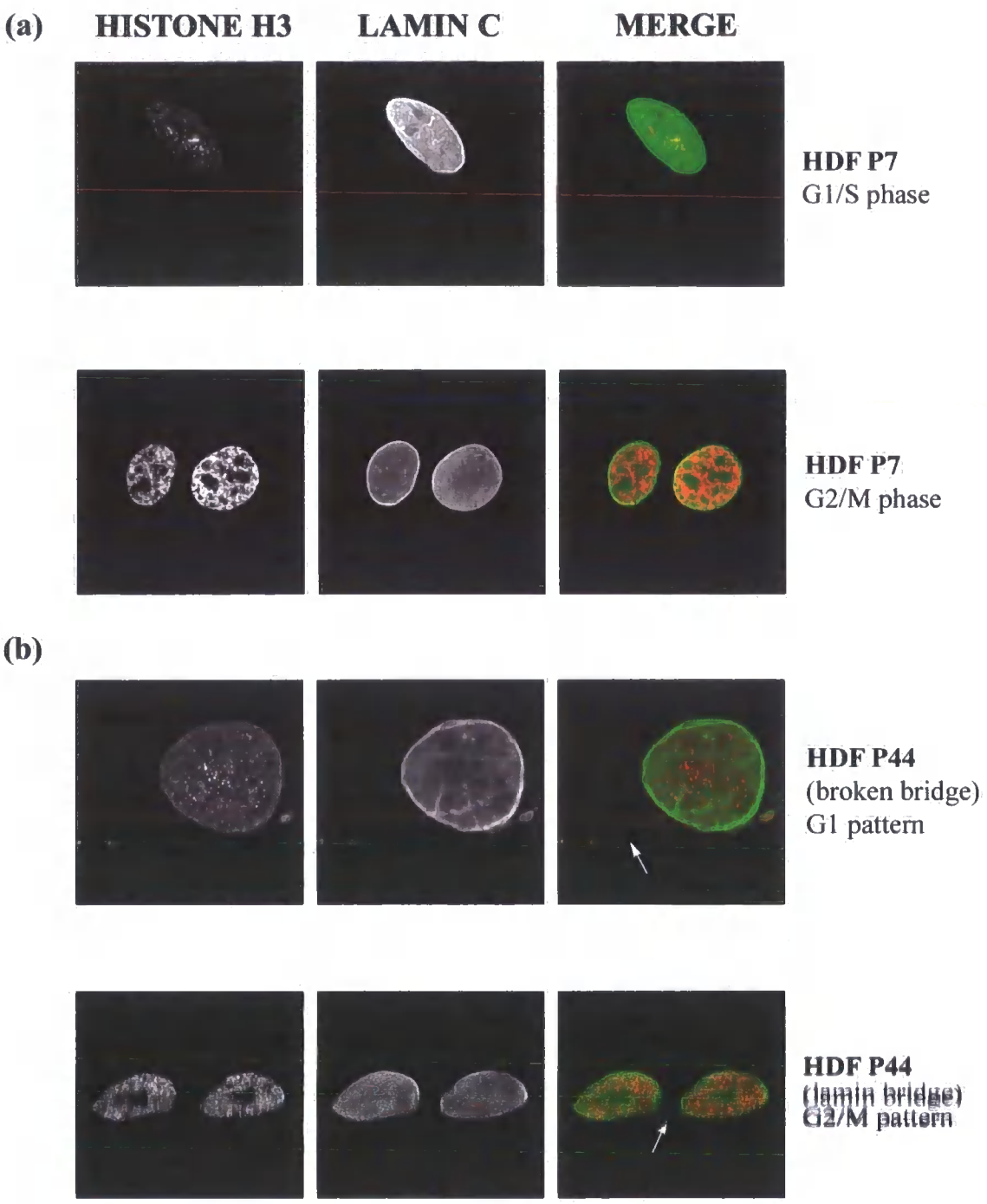
(a)
HISTONE H3
LAMIN C
MERGE
HDF P7
G1/S phase
HDF P7
G2/M phase
(b)
HDF P44
(broken bridge)
G1 pattern
HDF P44
(lamin bridge)
G2/M pattern

**Figure 3.5**

**Figure 3.6A: Mitotic phospho-histone H3 chromatin phosphorylation in late passage fibroblasts does not correlate with proliferation.** Early **(p7)** and late **(p44)** passage cells were prepared for confocal microscopy and stained for phospho histone H3 and the proliferation marker Ki67. Images were collected on a BioRad Radiance 2000 confocal microscope and projected as black and white or red/green colour merged micrographs in which histone H3 is in reed and Ki67 is in green. Magnification 360x.

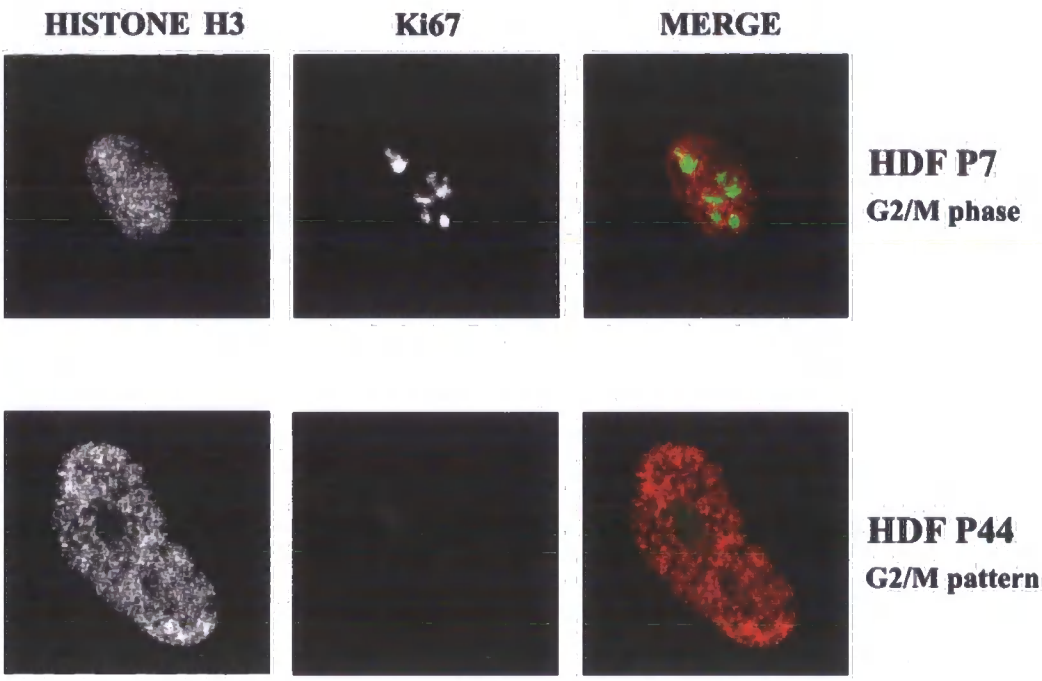


**Figure 3.6A**

**Table 3.6**

| HDF | His3 weak Ki67+ | His3 strong Ki67+ | His3- Ki67- | His3 weak Ki67- | His3 strong Ki67- |
|---|---|---|---|---|---|
| p7 | 58.3% ± 7.2 | 16.9% ± 2.2 | 24.8% ± 4.7 | 0.0% | 0.0% |
| p44 | 17.1% ± 3.3 | 2.9% ± 1.7 | 18.7% ± 2.8 | 23.6% ± 4.1 | 37.7% ± 6.1 |

**Chart 3.6**

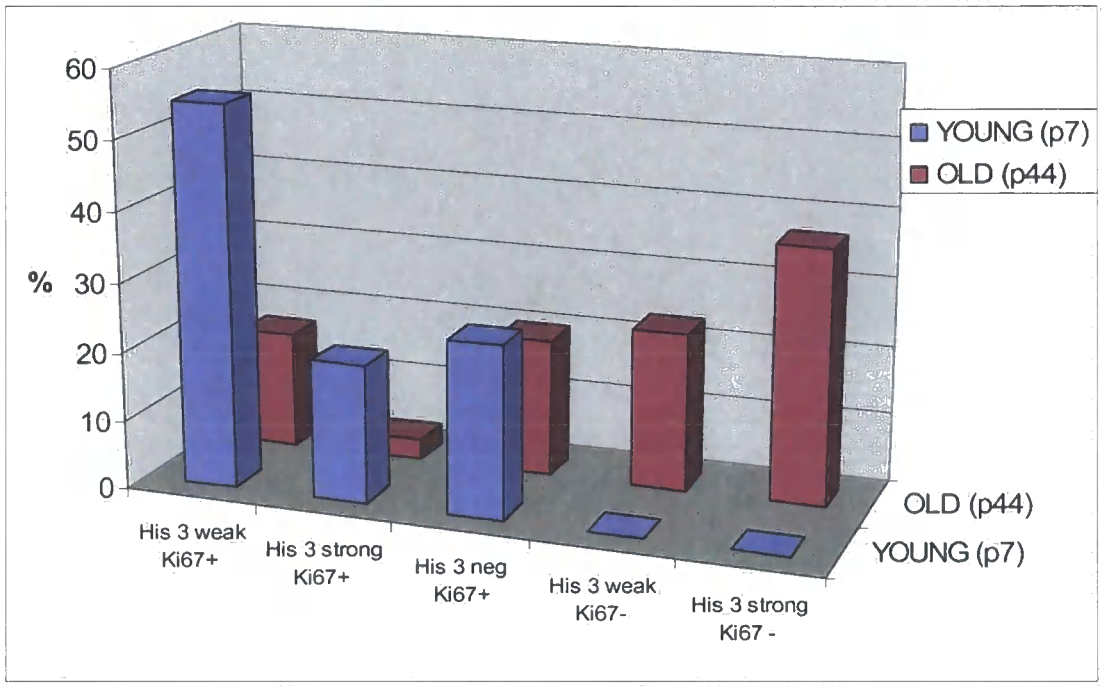


**Table 3.6: Late passage fibroblasts show histone H3 phosphorylation despite their lack of proliferation.** Human dermal fibroblasts (HDF) of early (p7) and late (p44) passage were seeded at an initial density of 3 x $10^4$ cells per 9 $mm^2$ culture well, each containing 3 glass coverslips. After 72 hours in culture, triplicate coverslips were fixed and stained with phospho-histone H3 and anti-Ki67 antibodies. 300 cells on each coverslip were scored for the presence of weak or strong phospho-histone H3 staining both in the presence and absence of Ki67, or for the absence of both. Table 6 shows the mean percentage of cells scored for each of the five categories described and the +/- standard deviation in triplicate experiments. **Chart 6** is a visual representation of the mean percentages in Table 6.

**Figure 3.6B: Late passage fibroblasts accumulate in G1 phase of cell cycle and show large cells with higher than 2N DNA contents.** Early (**p7**) and late (**p44**) passage cells were digested with RNAse and stained with the fluorescent dye, propidium iodide (PI). Cell cycle analysis was performed on Becton Dickinson FACSCaliber flow cytometer and data was collected as dot plots (**A** panels) and DNA histograms (**B** panels). The panels marked **A** show side (SS) versus forward (FS) scattering patterns. SS is proportional to the complexity of intracellular structures and FS is proportional to the cell size. In A panels, the position of apoptotic cells is marked by A. **B** panels show histograms of DNA content (FL3) versus cell number (count). In **B** panels, the highest peak (**E**) represents the position of G1/G0 cells with 2N DNA content, the shoulder (**F**) represents the position of S-phase cells, the smaller peak (**G**) represents the position of G2/M phase cells with 4N DNA content and (**A**) represents the position of apoptotic cells. In the lower **B** panel, the large tail (**F+G**) represents cells in G1/G0 phase with 4N to 8N DNA contents. The arrow in the lower **B** panel indicates p44 cells with 32N DNA content.

HDF P12

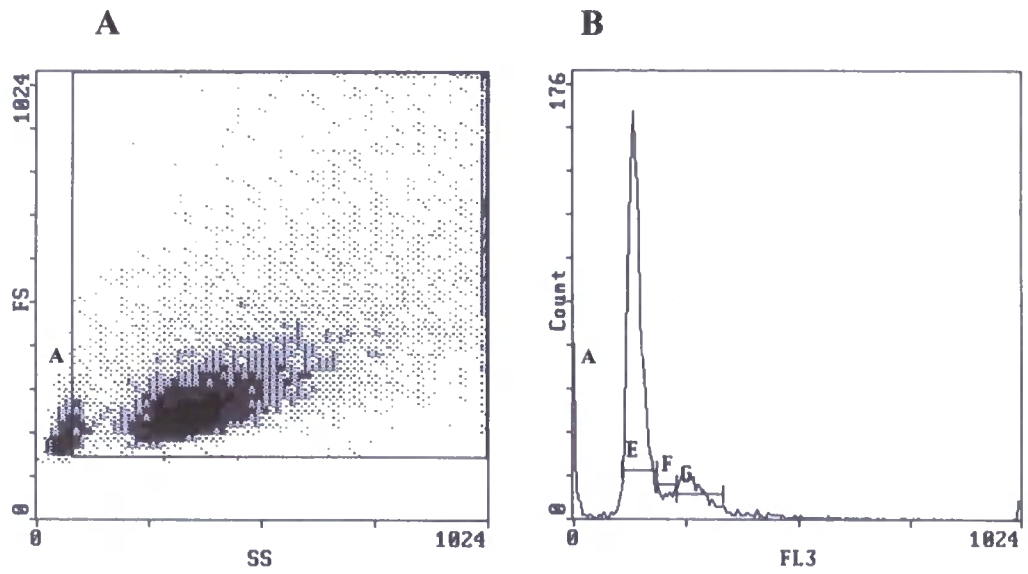


HDF P44

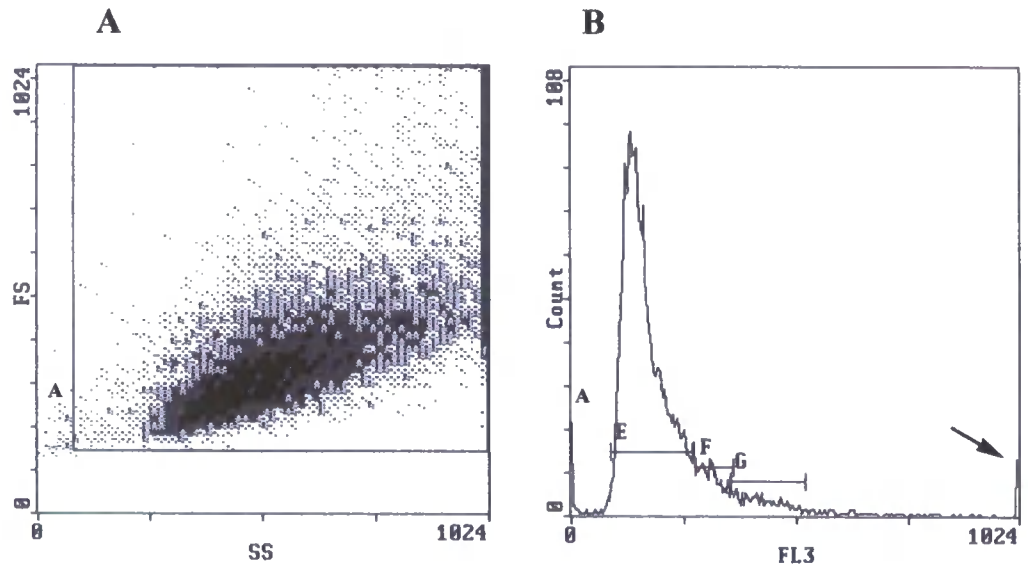


**Figure 3.6B**

**Figure 3.7A: Lamin A shows limited proteolysis in its C-terminal tail and lamin C is highly soluble during nuclear matrix extraction of late passage fibroblasts.** The same number of cells was harvested after three days in culture at early **(p7)** and late **(p44)** passages. Whole cell extracts were prepared (P1) and soluble (S2, S3, S4, S5) and pellet (P2, P3, P4, P5) fractions were obtained by sequential extraction with CSK/Triton X100, RSB-Magik, DNAse digestion and 0.25M ammonium sulphate elution. S and P fractions were immunoblotted with antibodies against lamin A/C (JOL2), lamin C (RaLC) and lamin A (JOL4). The thick arrow indicates 70 kDa lamin A band, the arrowhead indicates 65 kDa lamin C band and thin arrows indicate the presence of soluble ~67 kDa proteolytic fragment of lamin A as detected by JOL2 antibody in late passage extracts.

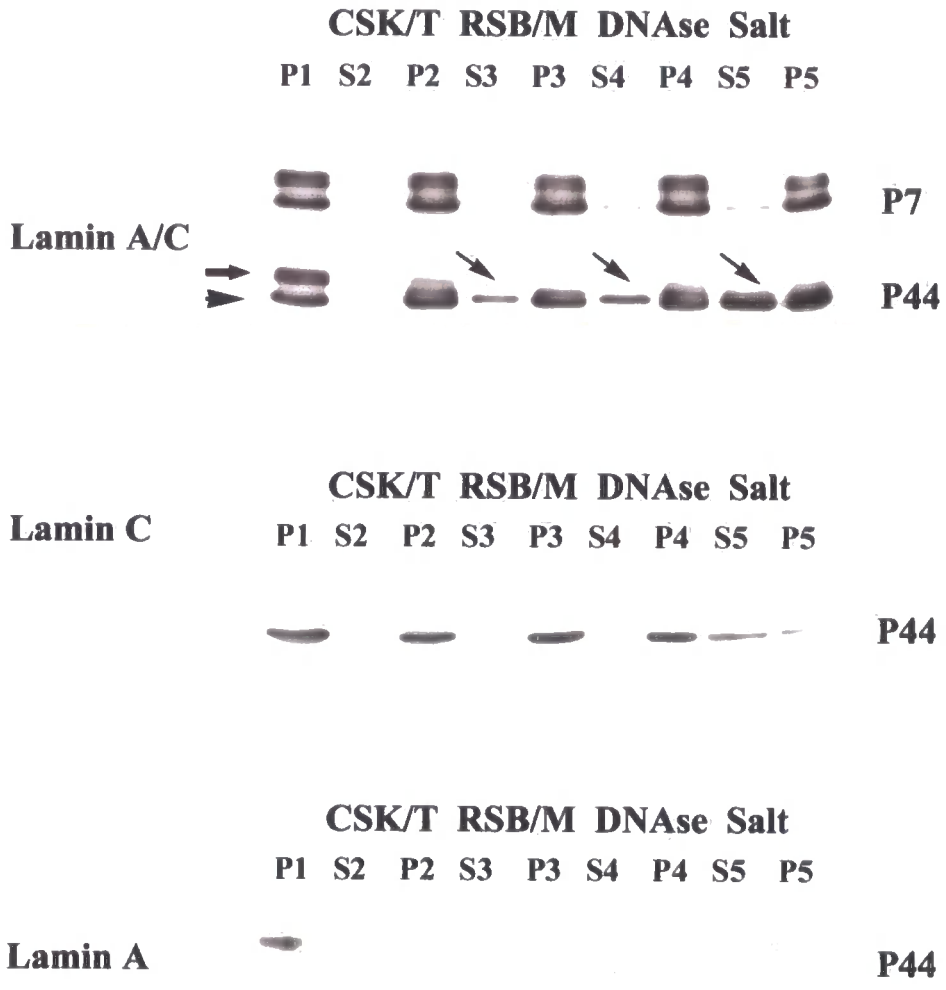
CSK/T RSB/M DNAse Salt
P1 S2 P2 S3 P3 S4 P4 S5 P5
Lamin A/C
P7
P44
CSK/T RSB/M DNAse Salt
Lamin C
P1 S2 P2 S3 P3 S4 P4 S5 P5
P44
CSK/T RSB/M DNAse Salt
P1 S2 P2 S3 P3 S4 P4 S5 P5
Lamin A
P44

# Figure 3.7A

**Figure 3.7B: LAP2α is lost from detergent/high salt-resistant nucleoskeleton during nuclear matrix extraction of late passage fibroblasts while lamin B and LAP2β remain insoluble.** Early **(p7)** and late **(p44)** passage cells were extracted sequentially as described in Figure 7A. S and P fractions were immunoblotted with antibodies against LAP2α (LAP15), lamin B2 (LN43) and LAP2β (LAP17). Molecular weight markers showed the expected mobility for the above proteins: LAP2α as 75 kDa, lamin B2 as 68 kDa and LAP2β as 55 kDa.

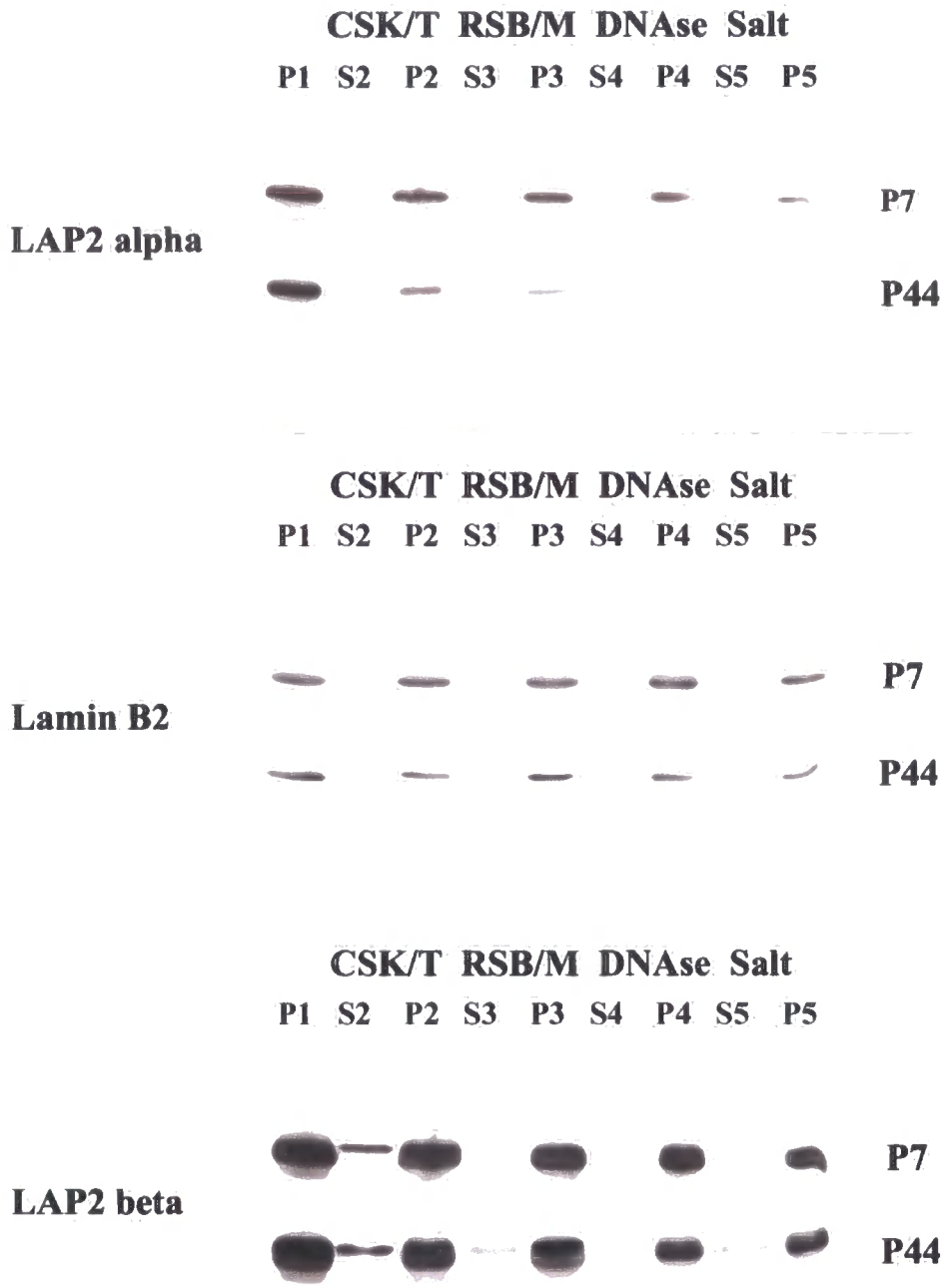
CSK/T RSB/M DNAse Salt
P1 S2 P2 S3 P3 S4 P4 S5 P5
LAP2 alpha
P7
P44
CSK/T RSB/M DNAse Salt
P1 S2 P2 S3 P3 S4 P4 S5 P5
Lamin B2
P7
P44
CSK/T RSB/M DNAse Salt
P1 S2 P2 S3 P3 S4 P4 S5 P5
LAP2 beta
P7
P44

# Figure 3.7B

**Figure 3.8A: A-type lamins show decreased resistance properties in late passage fibroblasts upon nuclear extraction *in situ*.** Early **(p7)** and late **(p44)** passage HDF were extracted sequentially *in situ* as described in Figure 7A, fixed and processed for immunofluorescence microscopy with antibodies against lamin A/C and Ki67. **(a)** shows p7 and p44 cells after V stage extraction. Arrows show lamin A/C staining in Ki67 negative p44 cells. Arrowheads show lamin A/C staining in Ki67 positive p44 cells. Unmarked cells show lamin A/C staining in p44 cells weakly positive for Ki67. * shows lamin A/C staining in a Ki67 negative p7 cell. **(b)** shows a tendency of lamin A/C to aggregate in Ki67 negative p44 cell after II stage (CSK/Triton X100) extraction. **(c)** shows p44 cells without extraction. The arrow shows lamin A/C staining in Ki67-negative p44 cell and arrowheads show lamin A/C staining in Ki67-positive p44 cells. Images were collected on a BioRad Radiance 2000 confocal microscope and projected as black and white or red/green colour merged micrographs in which lamin A/C is in red and Ki67 is in green. Magnification: **(a)** & **(c)** 80x; **(b)** 320x.

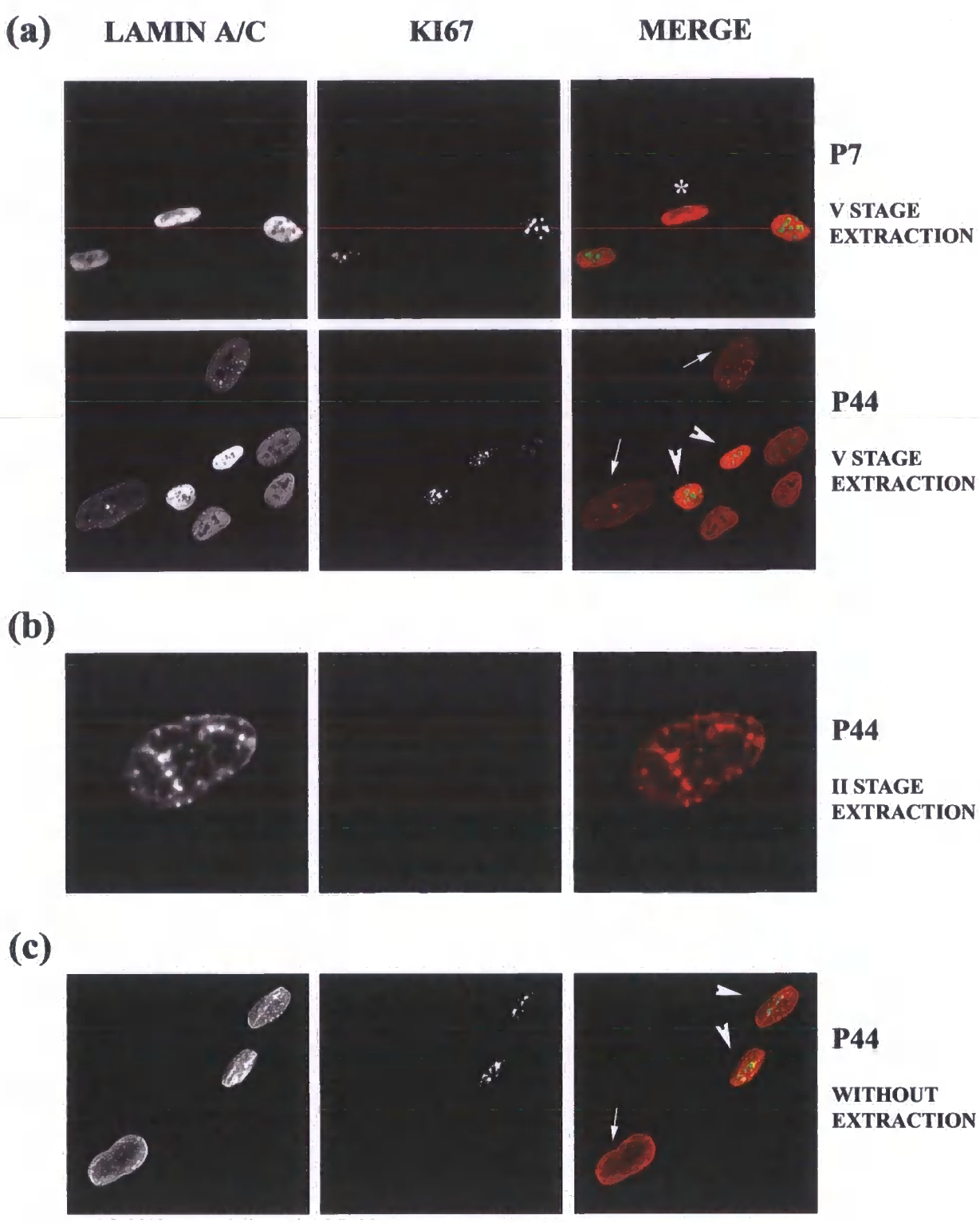
(a)
LAMIN A/C
KI67
MERGE
P7
V STAGE
EXTRACTION
P44
V STAGE
EXTRACTION
(b)
P44
II STAGE
EXTRACTION
(c)
P44
WITHOUT
EXTRACTION

**Figure 3.8A**

**Figure 3.8B: LAP2α has a tendency to aggregate in late passage fibroblasts upon nuclear extraction *in situ* and lamin C is often found within the same aggregates.** Early (**p7**) and late (**p44**) passage HDF were extracted sequentially *in situ* as described in Figure 7A and processed for immunofluorescence microscopy with antibodies against LAP2α and lamin C. (**a**) shows p7 and p44 cells after V stage extraction. Arrows show LAP2α and lamin C within the same aggregates in p44 cells. (**b**) shows a p44 cell after II stage (CSK/Triton X100) extraction. Arrows indicate a tendency of LAP2α and lamin C to aggregate within the same and individual aggregates. Images were collected on a BioRad Radiance 2000 confocal microscope and projected as black and white or red/green colour merged micrographs in which LAP2α is in red and lamin C is in green. Magnification: (**a**) 120x; (**b**) 320x.

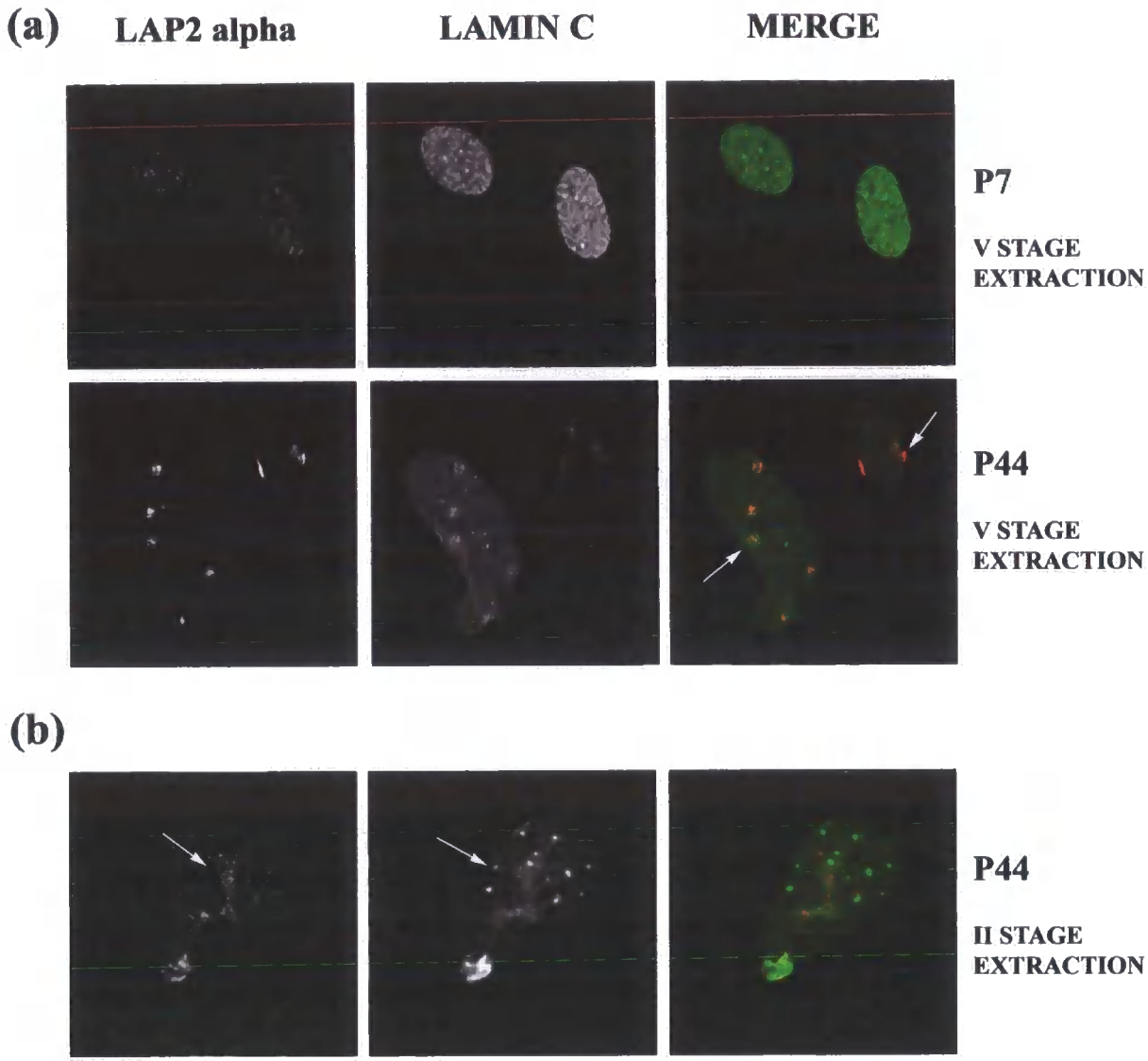
(a)
LAP2 alpha
LAMIN C
MERGE
P7
V STAGE
EXTRACTION
P44
V STAGE
EXTRACTION
(b)
P44
II STAGE
EXTRACTION

**Figure 3.8B**

**Figure 3.8C: Lamin B2 and LAP2β remain resistant to nuclear extraction *in situ* in late passage fibroblasts.** Early **(p7)** and late **(p44)** passage HDF were extracted sequentially *in situ* as described in Figure 7A and processed for immunofluorescence microscopy with antibodies against **(a)** lamin B2 and Ki67, and **(b)** LAP2β and Ki67. p7 and p44 cells were imaged after V stage extraction. Images were collected on a BioRad Radiance 2000 confocal microscope and projected as black and white or red/green colour merged micrographs in which lamin B2 and LAP2β are in red, and Ki67 is in green. Magnification 120x.

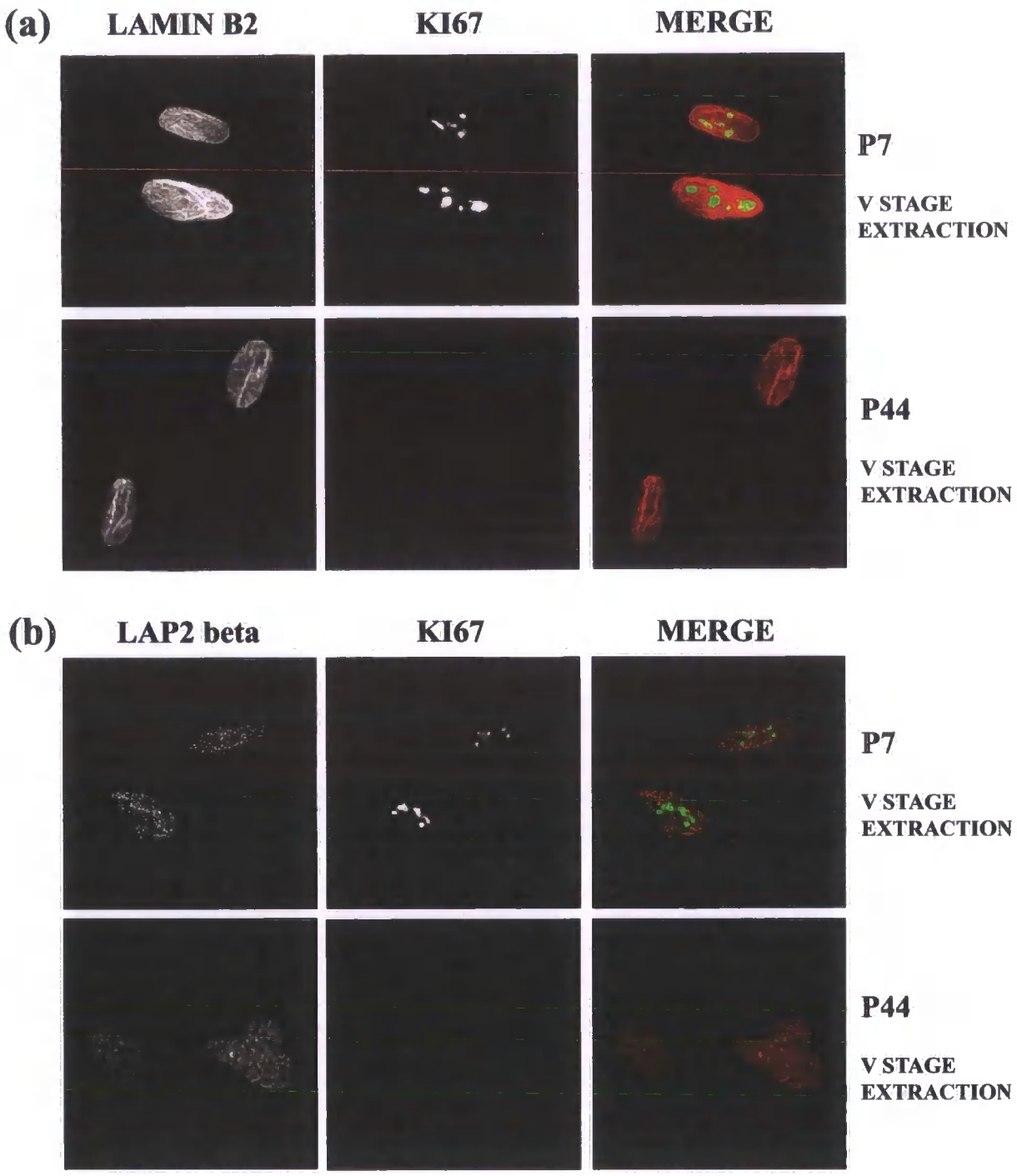
(a)
LAMIN B2
KI67
MERGE
P7
V STAGE EXTRACTION
P44
V STAGE EXTRACTION
(b)
LAP2 beta
KI67
MERGE
P7
V STAGE EXTRACTION
P44
V STAGE EXTRACTION

**Figure 3.8C**

**Figure 3.9: Lamin A and LAP2α protein sequences show a high number of cysteine residues in their specific C-terminal domains.** **(A)** Protein sequences corresponding to C-terminal domains of human lamins A (LN A), C (LN C), B1 (LNB1) and B2 (LNB2), starting from residue 501 to the end of the C-terminus were aligned. Cysteine residues are highlighted as follows: C-terminal cysteines in CaaX motifs are highlighted in yellow, lamin A specific cysteine residues are highlighted in red and a cysteine residue common to lamin A and C is highlighted in purple. **(B)** Protein sequences corresponding to C-terminal domains of human LAPs, including LAP2α, LAP2β and LAP2γ were aligned. Cysteine residues specific to LAP2α are highlighted in red and a cysteine residue common to LAP2β and LAP2γ is highlighted in blue. Sequence alignments were performed using multiple sequence alignment software 'T-Coffee' (Notrdam, *et al.*, 2000).

```
          501                                                  550
LN A =    TYRFPPKFTL KAGQVVTIWA AGAGATHSPP TDLVWKAQNT WGCGNSLRTA
LN C =    TYRFPPKFTL KAGQVVTIWA AGAGATHSPP TDLVWKAQNT WGCGNSLRTA
LNB1 =    SYKYTSRYVL KAGQTVTIWA ANAGVTASPP TDLIWKNQNS WGTGEDVKVI
LNB2 =    AYKFTPKYIL RAGQMVTVWA AGAGVAHSPP STLVWKGQSS WGTGESFRTV
          551                                                  600
LN A =    LINSTGEEVA MRKLVRSVTV V.EDDEDEDG DDLLHHHHGS HCSSSGDPAE
LN C =    LINSTGEEVA MRKLVRSVTV V.EDDEDEDG DDLLHHHHVS GSRR......
LNB1 =    LKNSQGEEVA QRSTVFKTTI P.EEEEEEE. EAAGVVVEEE LFHQQGTP..
LNB2 =    LVNADGEEVA MRTVKKSSVM R.ENENGEEE EEEAEFGEED LFHQQGDP..
          601                                                  650
LN A =    YNLRSRTVLC GTCGQPADKA SASGSGAQVG GPISSGSSAS SVTVTRSYRS
LN C =    .......... .......... .......... .......... ..........
LNB1 =    .......... .......... .......... .......... ..........
LNB2 =    .......... .......... .......... .......... ..........
          651                                       685
LN A =    VGGSGGGSFG DNLVTRSYLL GNSSPRTQSP QNCSIM
LN C =    .......... .......... .......... ......
LNB1 =    .......... .......... ......RASN RSCAIM
LNB2 =    .......... .......... ......RTTS RGCYVM
```

# Figure 3.9A

```
          251                                                  300
LAPα  = LPREPLVATN LPGRGQLQKL ASERNLFISC KSSHDRCLEK SSSSSSQPEH
LAPβ  = GPLQALTRES TRGSRRTPRK RVETSEHFRI .......... DGPVISESTP
LAPχ  = .......... .......... .......... .......... ..........
          301                                                  350
LAPα  = SAMLVSTAAS PSLIKETTTG YYKDIVENIC GREKSGIQPL CPERSHISDQ
LAPβ  = IAETIMASSN ESLVVNRVTG NFKHASPILP ITEFSDIPRR APKKPLTRAE
LAPχ  = .......... .......... .......... .......... ..........
          351                                                  400
LAPα  = SPLSSKRKAL EESESSQLIS PPLAQAIRDY VNSLLVQGGV GSLPGTSNSM
LAPβ  = VGEKTEERRV ERDILKEMF. .PYEASTPTG ISASERR... ...PIKGAAG
LAPχ  = VGEKTEERRV ERDILKEMF. .PYEASTPTG ISASERR... ...PIKGAAG
          401                                                  450
LAPα  = PPLDVENIQK RIDQSKFQET EFLSPPRKVP RLSEKSVEER DSGSFVAFQN
LAPβ  = RPLELSDF.. RMEESFSSKY V....PKYVP LADVKSEKTK KGRSIPVWIK
LAPχ  = RPLELSDF.. RMEESFSSKY V....PKYVP LADVKSEKTK KGRSIPVWIK
          451                                                  500
LAPα  = IPGSELMSSF AKTVVSHSLT TLGLEVAKQS QHDKIDASEL SFPFHESILK
LAPβ  = ILLFVVVAVF LFLVYQAMET N...QVNPFS NFLHVDPRKS N.........
LAPχ  = ILLFVVVAVF LFLVYQAMET N...QVNPFS NFLHVDPRKS N.........
          501                                                  550
LAPα  = VIEEEWQQVD RQLPSLACKY PVSSREATQI LSVPKVDDEI LGFISEATPL
LAPβ  = .......... .......... .......... .......... ..........
LAPχ  = .......... .......... .......... .......... ..........
          551                                                  600
LAPα  = GGIQAASTES CNQQLDLALC RAYEAAASAL QIATHTAFVA KAMQADISQA
LAPβ  = .......... .......... .......... .......... ..........
LAPχ  = .......... .......... .......... .......... ..........
          601                                                  650
LAPα  = AQILSSDPSR THQALGILSK TYDAASYICE AAFDEVKMAA HTMGNATVGR
LAPβ  = .......... .......... .......... .......... ..........
LAPχ  = .......... .......... .......... .......... ..........
          651                                             694
LAPα  = RYLWLKDCKI NLASKNKLAS TPFKGGTLFG GEVCKVIKKR GNKH
LAPβ  = .......... .......... .......... .......... ....
LAPχ  = .......... .......... .......... .......... ....
```

# Figure 3.9B

**Figure 3.10A: Lamins A/C are among the six most prominent S-glutathiolated proteins in late passage fibroblasts.** The same number of wild-type (HDF) and laminopathy (F02-denotes E354K mutation) fibroblasts were harvested at early **(p12)**, intermediate **(p24)** and late passage **(p40)**. Whole cell extracts were prepared in the presence of NEM and resolved on either **(a)** non-reducing or **(b)** reducing gels. Cell extracts were immunoblotted using antibodies against lamin A/C (JOL2) and glutathione. **(a)** * shows the mobility of the six most prominent S-glutathiolated protein bands in late (p44) passage HDF. Arrowheads show the two most prominent glutathione protein bands align to the expected mobility of lamins A and C (70 & 65 kDa). Note the absence of protein disulphides on the non-reducing Lamin A/C blot. **(b)** Arrowheads show that two glutathiolated protein bands (aligned to expected mobility of lamins A and C) become absent on reducing gel. M shows mobility of molecular weight markers starting from the top: 208, 119, 94 and 51 (kDa).

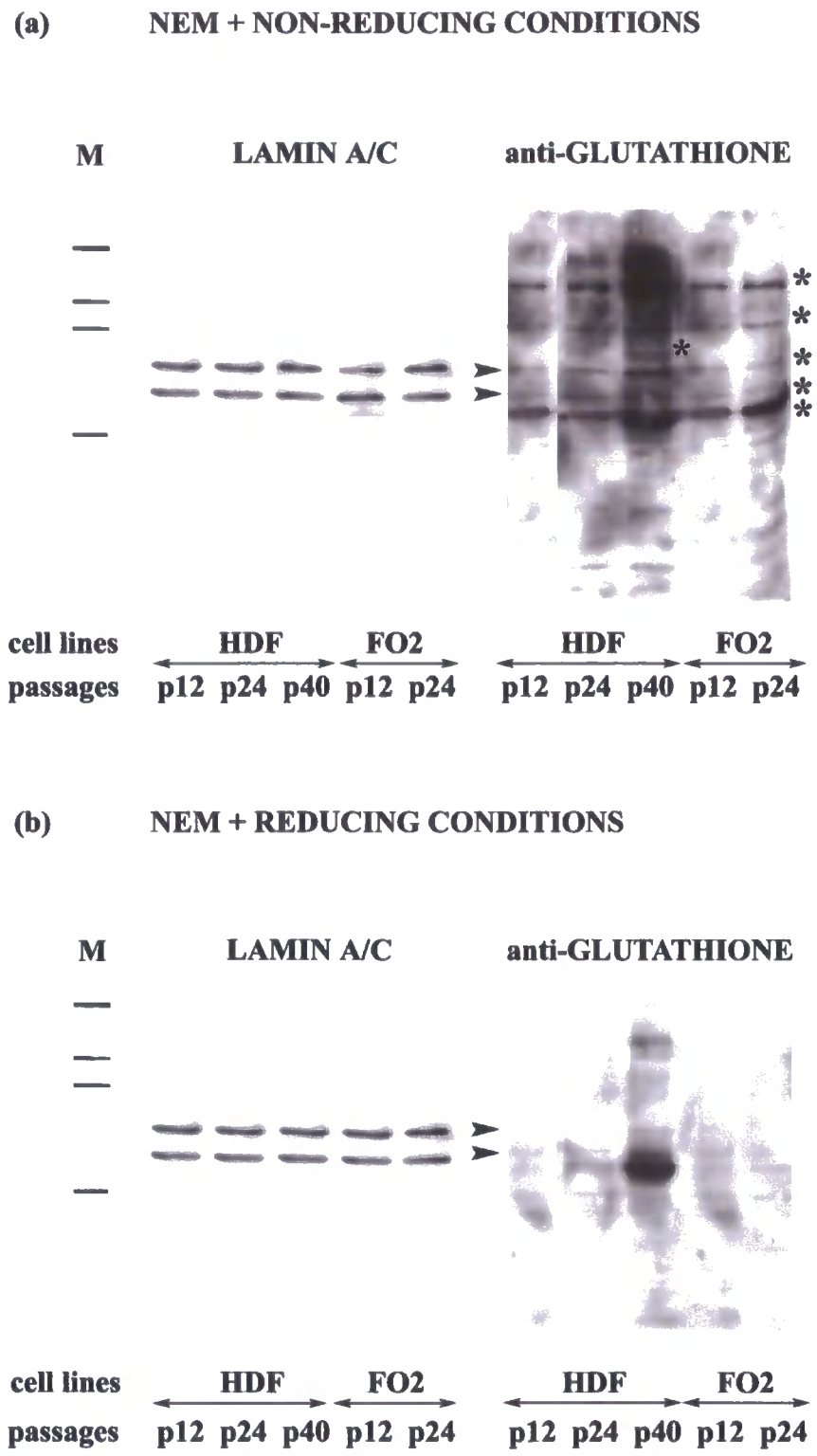
(a)
NEM + NON-REDUCING CONDITIONS
M
LAMIN A/C
anti-GLUTATHIONE
cell lines
HDF
FO2
HDF
FO2
passages
p12 p24 p40 p12 p24
p12 p24 p40 p12 p24
(b)
NEM + REDUCING CONDITIONS
M
LAMIN A/C
anti-GLUTATHIONE
cell lines
HDF
FO2
HDF
FO2
passages
p12 p24 p40 p12 p24
p12 p24 p40 p12 p24

# Figure 3.10A

**Figure 3.10B: LAP2α is one of the six S-glutathiolated proteins in late passage fibroblasts.** The same number of wild-type (HDF) and laminopathy (F02-denotes E354K mutation) fibroblasts were harvested at early **(p12)**, intermediate **(p24)** and late passage **(p40)**. Whole cell extracts were prepared in the presence of NEM and resolved on either **(a)** non-reducing or **(b)** reducing gels. Cell extracts were immunoblotted using antibodies against LAP2α (LAP15) and glutathione. **(a)** Arrowhead shows that one of the most prominent glutathiolated proteins bands aligns to the expected mobility of LAP2α (75 kDa). * shows that glutathiolated protein band (aligned to the expected mobility of LAP2α) is only present in late passage (p44) HDF. Note the absence of protein disulphides on non-reducing LAP2α immunoblot. **(b)** Arrowhead shows that the glutathiolated protein band (aligned to the expected mobility of LAP2α) becomes absent on reducing gel. M shows mobility of molecular weight markers starting from the top: 208, 119, 94 and 51 (kDa).

(a) NEM + NON-REDUCING CONDITIONS

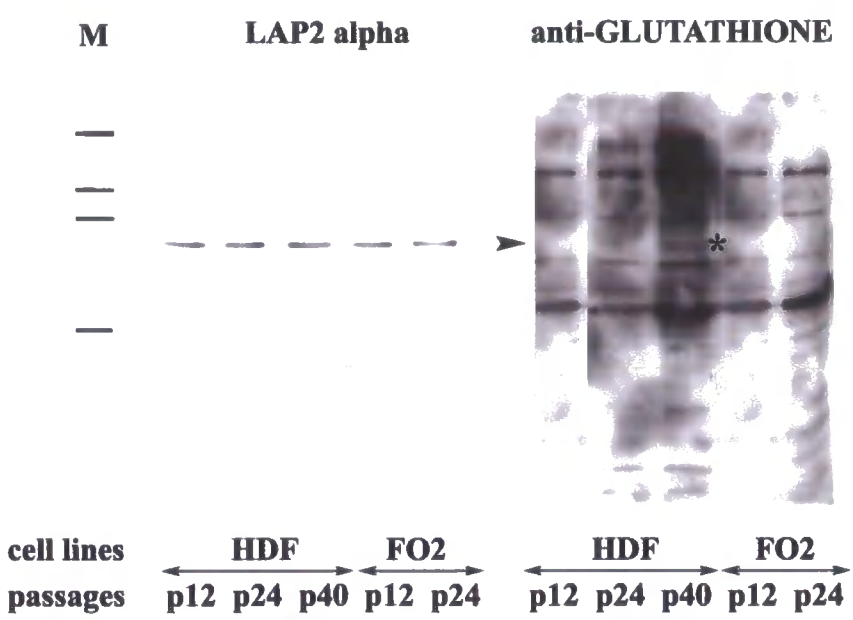


(b) NEM + REDUCING CONDITIONS

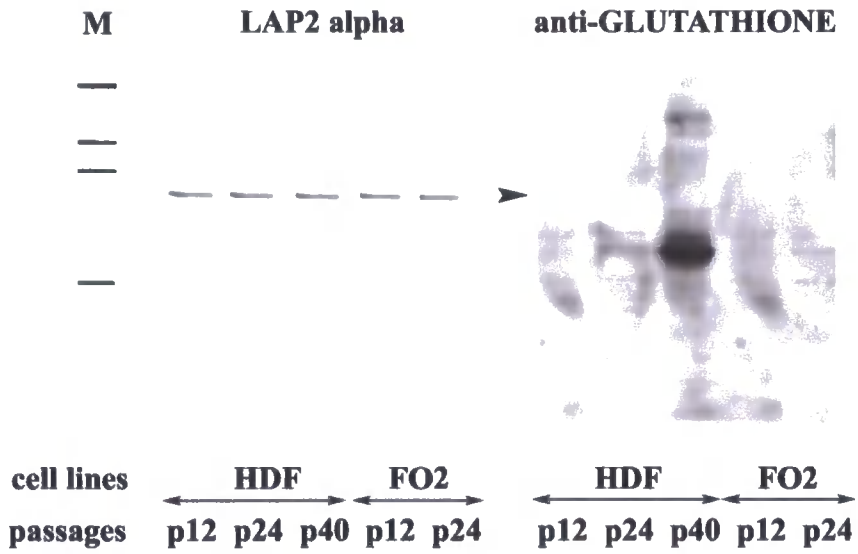


**Figure 3.10B**

**Figure 3.11: Glutathione forms protein addicts on A-type lamins in late passage fibroblasts.** The same number of cells were harvested at early **(p12)** and late **(p40)** passage HDF and nuclear pellets were prepared in the presence of NEM. Lamins A/C were immunoprecipitated using anti-lamin A/C antibody (JOL2) coupled to Dynabeads. Supernatants (S) and immuno-precipitates (P) were resolved on non-reducing gels and immunoblotted with antibodies against lamin A/C or glutathione. Arrowheads show ~160 kDa disulphide-linked IgGs found in immuno-precipitates (P). + shows a ~140 kDa band detected with lamin A/C antibody following immunoprecipitation. Thin arrows show the expected mobility of lamins A & C (75 kDa) in immuno-precipitates (P) of early and late passage HDF. Thick arrows show protein glutathione addict between lamins A/C and glutathione in late (p40) passage HDF. * shows the weak presence of lamin A glutathione addict in early (p12) passage HDF. M shows mobility of molecular weight markers starting from the top: 208, 119, 94 and 51 (kDa).

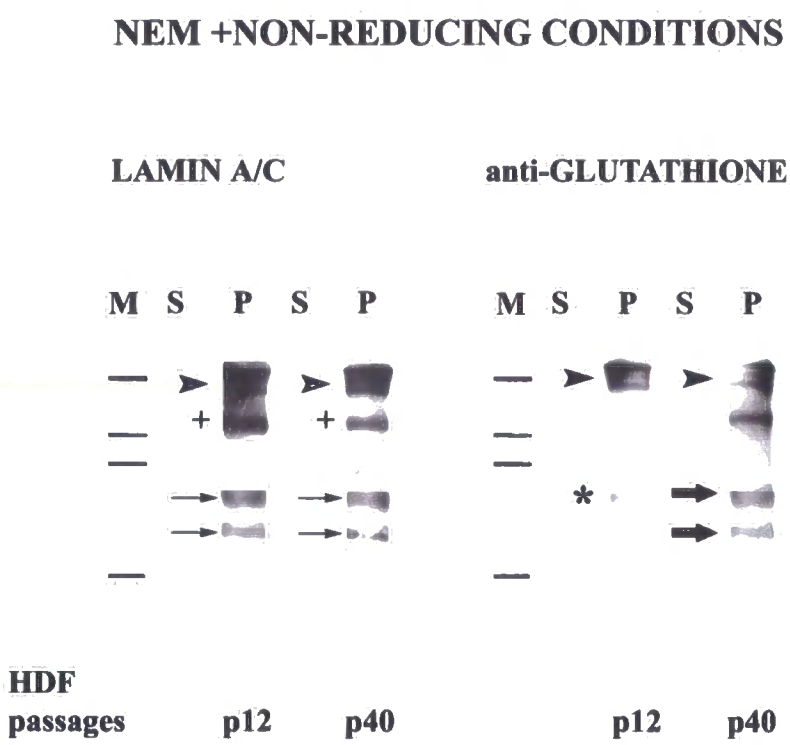
NEM +NON-REDUCING CONDITIONS
LAMIN A/C
anti-GLUTATHIONE
M S P S P
M S P S P
+
+
*
HDF
passages
p12
p40
p12
p40

# Figure 3.11

**Figure 3.12A: Glutathiolated A-type lamins accumulate in a monomeric form in late passage fibroblasts.** The same number of wild-type (HDF) and laminopathy (F02- denotes E354K mutation) fibroblasts were harvested at early **(p12)**, intermediate **(p24)** and late passage **(p40)**. Whole cell extracts were prepared in the absence **(a)** or presence **(b)** of NEM and resolved on non-reducing gels. Cell extracts were immunoblotted using two different antibodies against lamin A/C (JOL2 and L6 8A7) and an antibody specific to lamin C (RaLC). Thick arrows and arrowheads show bands with the expected mobility of lamins A (70 kDa) and C (65 kDa) respectively. **(a)** Note the complete absence of lamin A band (70 kDa) with either lamin A/C antibody in early (p12) passage extracts prepared in the absence of NEM. Thin arrows show a 66 kDa band to represent a faster migrating lamin A conformer with intra-disulphide bonds present in early (p12) and mid (p24) passage HDF and F02 prepared in the absence of NEM. **(b)** Note the absence of 66 kDa band with either lamin A/C antibody in early (p12) and mid (p24) passage HDF and F02 prepared in the presence of NEM. * shows a protein band of 58-60 kDa that cross-reacts with L6 8A7 antibody (Kill and Hutchison 1995).

(a) NON-REDUCING CONDITIONS WITHOUT NEM

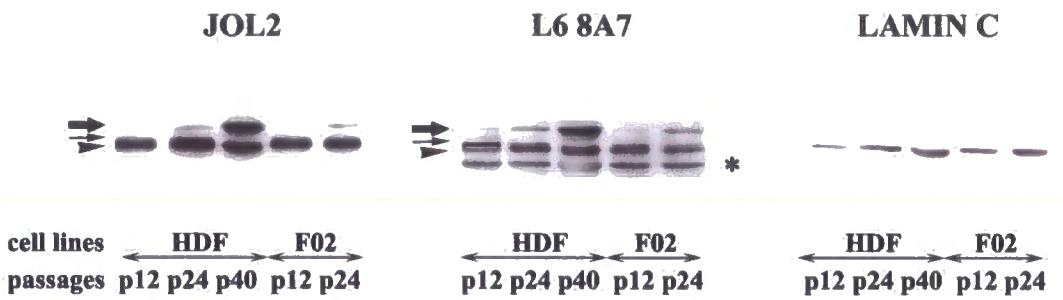


(b) NEM + NON-REDUCING CONDITIONS

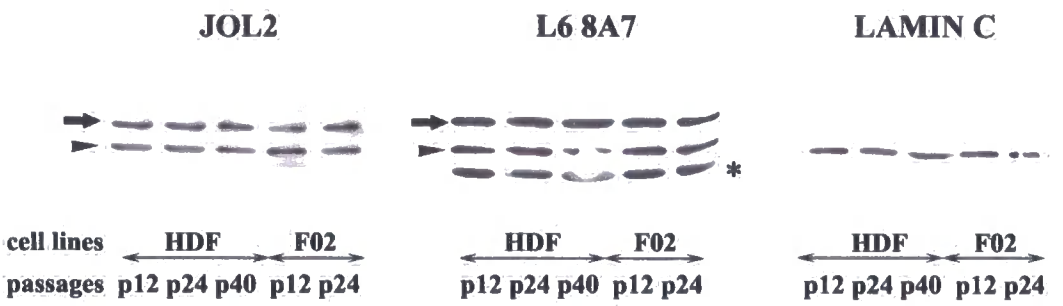


**Figure 3.12A**

**Figure 3.12B: Lamins A and C show age-dependent changes in their cysteine cross-linking potential during ageing of fibroblasts *in vitro*.** The same number of wild-type (HDF) fibroblasts was harvested at early **(p7-15)**, intermediate **(p18-24)** and late passages **(p40)**. Whole cell extracts were prepared in the absence of NEM and resolved on non-reducing gels. Cell extracts were immunoblotted using an antibody against lamin A/C (JOL2) and an antibody against β actin as a loading control. Thick arrows and arrowheads show bands with the expected mobility of lamins A (70 kDa) and C (65 kDa) respectively. Note the appearance of some lamin A monomer at mid passage (p21-24). Note the accumulation of lamin C monomer at mid passage (p18-p24). Thin arrows show a 66 kDa band to represent a faster migrating lamin A conformer with intra-disulphide bond. Note the absence of 66 kDa band at late passage (p40).

**NEM + NON-REDUCING CONDITIONS**


**HDF**
**passages** **p7 p10 p12 p15 p18 p21 p24 p40**

# Figure 3.12B

**Figure 3.13: Cysteine residues in A-type lamins from laminopathy fibroblasts do not show decreased cross-linking potential during ageing *in vitro*.** The same number of wild-type (HDF) and laminopathy fibroblasts with the following mutations (249 is R249Q, 401 is R401C, and 453 is R453W) was harvested at early **(p12)** and intermediate **(p22)** passage. Whole cell extracts were prepared in the absence **(a)** or presence **(b)** of NEM and resolved on non-reducing gels. Cell extracts were immunoblotted using lamin A/C (JOL2) antibody. Thick arrows and arrowheads show bands with the expected mobility of lamins A (70 kDa) and C (65 kDa) respectively. **(a)** Note the complete absence of lamin A band (70 kDa) and reduced amount of lamin C band (65 kDa) in early passage (p12) HDF and 249 prepared in the absence of NEM. **(b)** Note the absence of protein disulphides in mid passage (p22) laminopathy extracts in the presence of NEM.

(a) NON-REDUCING CONDITIONS WITHOUT NEM

JOL2

| cell lines | HDF | 249 | HDF | 249 | 401 | 453 |
|---|---|---|---|---|---|---|
| passages | p12 | p12 | p22 | p22 | p22 | p22 |

(b) NEM + NON-REDUCING CONDITIONS

JOL2

| cell lines | HDF | 249 | HDF | 249 | 401 | 453 |
|---|---|---|---|---|---|---|
| passages | p12 | p12 | p22 | p22 | p22 | p22 |

**Figure 3.13**

**Figure 3.14A: Glutathiolated LAP2α accumulates in a monomeric form in late passage fibroblasts.** The same number of wild-type fibroblasts (HDF) was harvested at early **(p12)**, intermediate **(p24)** and late passage **(p40)**. Whole cell extracts were prepared in the absence **(a)** or presence **(b)** of NEM and resolved on non-reducing gels. Cell extracts were immunoblotted using a pan-LAP2 antibody that recognises an epitope in the common N-terminal region of three distinct LAP2 isoforms, LAP2α (75 kDa), LAP2β (55 kDa) and LAP2γ (39 kDa). Thick arrows show bands with the expected mobility of LAP2α (75 kDa). **(a)** Note the complete absence of LAP2α band (75 kDa) in early (p12) passage extracts prepared in the absence of NEM. **(b)** Note the absence of protein disulphides in late passage (p40) extract in the presence of NEM. M shows the mobility of molecular weight markers in kDa starting from the top: 208, 119, 94 and 51 and 37.

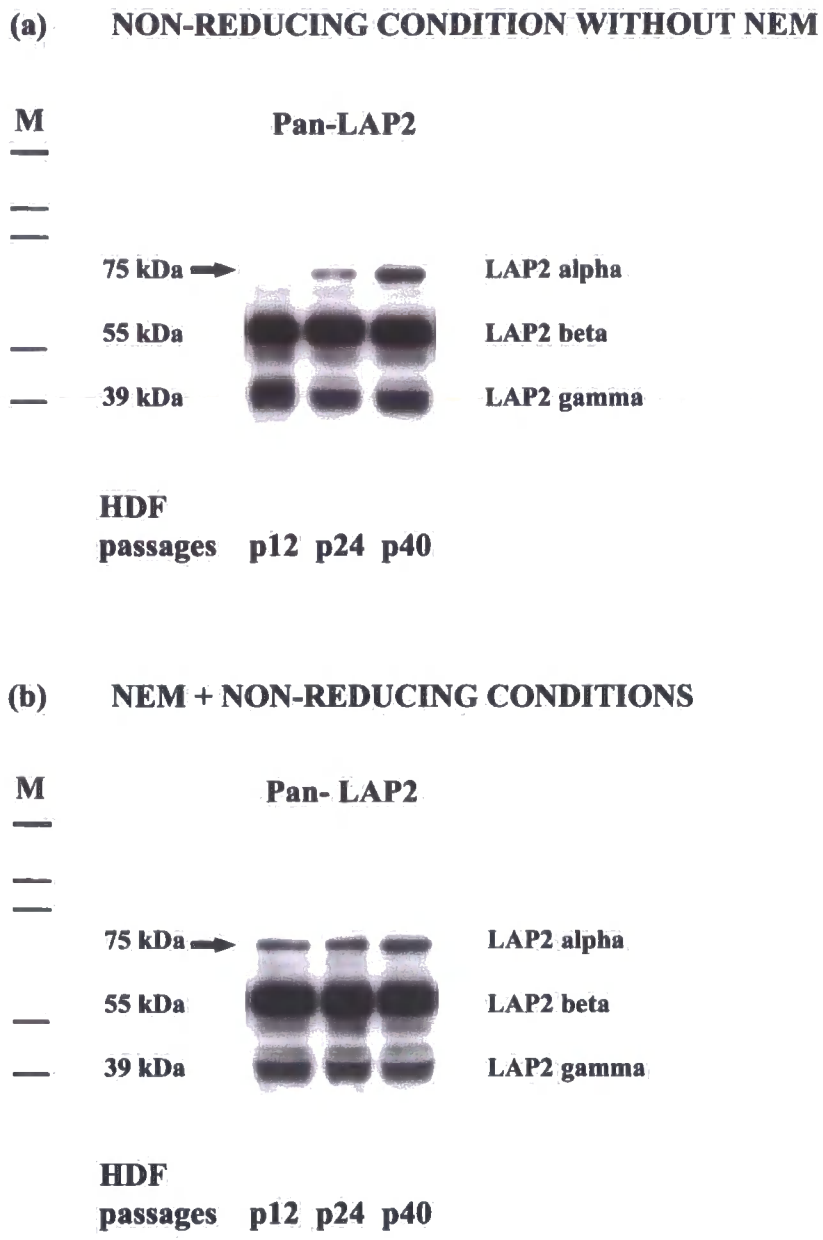
(a) NON-REDUCING CONDITION WITHOUT NEM
M
Pan-LAP2
75 kDa
55 kDa
39 kDa
LAP2 alpha
LAP2 beta
LAP2 gamma
HDF
passages p12 p24 p40
(b) NEM + NON-REDUCING CONDITIONS
M
Pan- LAP2
75 kDa
55 kDa
39 kDa
LAP2 alpha
LAP2 beta
LAP2 gamma
HDF
passages p12 p24 p40

# Figure 3.14A

**Figure 3.14B: Lamin B2 does not accumulate in a monomeric form in late passage fibroblasts.** The same number of wild-type fibroblasts (HDF) was harvested at early **(p12)**, intermediate **(p24)** and late passage **(p40)**. Whole cell extracts were prepared in the absence **(a)** or presence **(b)** of NEM and resolved on non-reducing gels. Cell extracts were immunoblotted using antibody against lamin B2 (LN43). Thick arrows show bands with the expected mobility of lamin B2 (68 kDa). **(a)** Note the reduced amount of Lamin B2 band in the extracts prepared in the absence of NEM is independent of passage number. **(b)** Note the absence of protein disulphides in the late passage (p40) extract in the presence of NEM. M shows mobility of molecular weight markers in kDa starting from the top: 208, 119, 94 and 51 and 37.

(a) NON-REDUCING CONDITION WITHOUT NEM

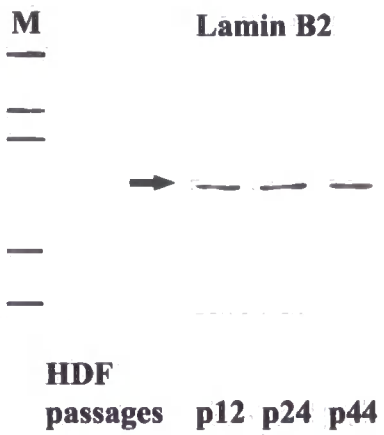


(b) NEM + NON-REDUCING CONDITIONS

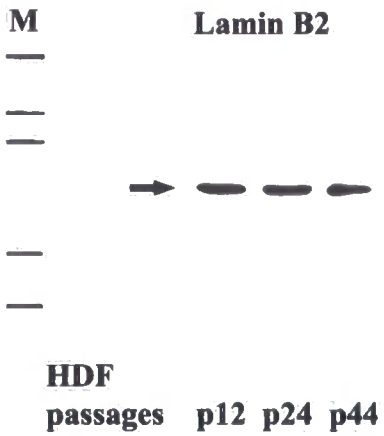


# Figure 3.14B

**Figure 3.15: Glutathiolated cysteine residues in Lamin A and LAP2α do not form higher order disulphide complexes in late passage fibroblasts.** The immunoblot in Figure 12A (a) (stained by JOL2 antibody) and the immunoblot in Figure 14A (a) (stained by pan-LAP2 antibody) were developed again following higher exposure in ECL detection reagent. The immunoblots show extracts from early **(p12)**, intermediate **(p24)** and late passage **(p40)** wild-type fibroblasts (HDF) prepared in the absence of NEM and resolved on non-reducing gels. **(a)** shows the over-exposed upper part of pan-LAP2 immunoblot. The thick arrow shows bands with the expected mobility of LAP2α (75 kDa). Note the complete absence of the LAP2α band (75 kDa) in early (p12) passage extracts. Arrowheads show two high molecular weight bands representing inter-molecular disulphide complexes of LAP2α, a >210 kDa band (LAP2α trimer or tetramer) and ~150 kDa band (LAP2α dimer), only present in early passage (p12) extract. **(b)** shows the overexposed upper part of the JOL2 immunoblot. The thick arrow shows bands with the expected mobility of Lamin A (70 kDa). Note the complete absence of Lamin A band (70 kDa) in early (p12) passage extracts. The arrowhead shows a high molecular weight band (~140 kDa) representing inter-molecular disulphide complex of Lamin A (dimer) present in the highest amount in early passage (p12) extract. The thin arrow show a 66 kDa band representing a faster migrating lamin A conformer with intra-disulphide bond present in early (p12) and mid (p24) passage HDF.

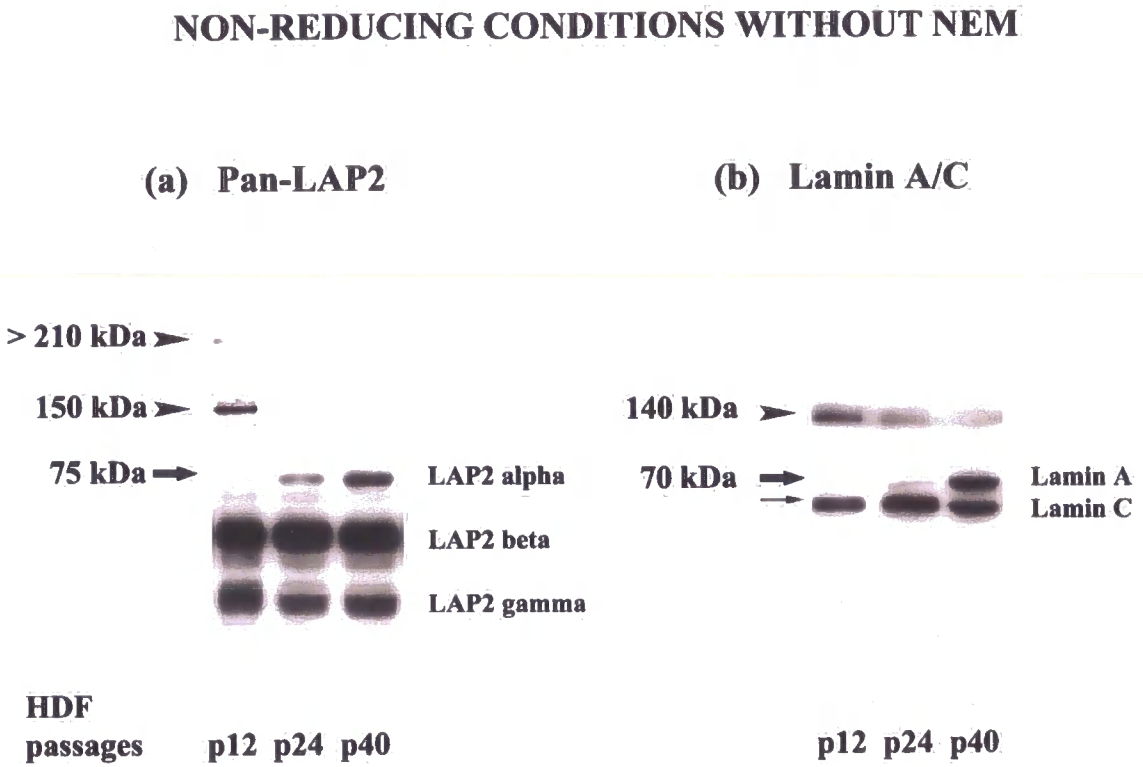
NON-REDUCING CONDITIONS WITHOUT NEM
(a) Pan-LAP2
(b) Lamin A/C
> 210 kDa
150 kDa
75 kDa
LAP2 alpha
LAP2 beta
LAP2 gamma
140 kDa
70 kDa
Lamin A
Lamin C
HDF passages
p12 p24 p40
p12 p24 p40

# Figure 3.15

# CHAPTER 4-EXPRESSION, NUCLEAR ANCHORAGE AND PHOSPHORYLATION OF RETINOBLASTOMA PROTEIN IN SENESCENT AND LAMINOPATHY FIBROBLASTS

## Introduction

Retinoblastoma protein (Rb) is a nuclear phosphoprotein that exhibits cell cycle dependent changes in its phosphorylation state (reviewed in Mittnacht *et al.*, 1998). Differential phosphorylation of Rb protein plays a pivotal role in cell cycle regulation. Rb is specifically phosphorylated on serine and threonine residues during cell cycle by cyclin-dependent kinase complexes, which intersect with many cellular signalling networks. A key pathway initiated by these kinase complexes modulates the transition from G1 into S phase through Rb/E2F signalling. In early G1, Rb protein exists in a hypo-phosphorylated state capable of binding several S-phase dependent regulatory proteins such as the transcription factor E2F-1, which prevents the transcriptional activation of S-phase-specific genes and traverse to S phase. Hyper-phosphorylation of Rb during late G1 phase by cyclin-dependent kinase complexes inactivates growth-suppressing activity of Rb by its release from nuclear tethers, which causes a release of E2F and subsequent activation of S-phase specific genes. Therefore, the tight nuclear interaction is essential for growth-regulating functions of Rb. Regulation of nuclear affinity of Rb protein is also regulated through Rb dephosphorylation which is activated from M phase to G1 phase by protein phosphatases such as PP1.

Rb growth-suppressing activity is dependent on the interactions with cellular proteins through its C-terminal domains that are affected by most naturally occurring tumour-promoting mutations and prevent its nuclear tethering (Lundberg and Weinberg 1999). Interestingly mutant forms of Rb that cannot become tethered in the nucleus are also unable to become hyper-phosphorylated (Mittnacht and Weinberg 1991), implying that Rb becomes a substrate for phosphorylation only when bound to its nuclear binding partners. Rb interacts with lamin A through its C-terminal nuclear anchorage domain (Mancini *et al.*, 1994, Okazaki *et al.*, 1995) and hyper-phosphorylation of Rb during late G1 phase causes weaker lamin A binding (Mancini *et al.*, 1994). Moreover, A-type lamin/LAP2α complexes interact with hypo-phosphorylated Rb protein and anchorage

of hypo-phosphorylated Rb during G1 phase correlates with cell-cycle dependent LAP2α expression (Markiewicz *et al.*, 2002a). Dominant negative lamin mutants that lead to intranuclear aggregation of lamin A/C and LAP2α also cause Rb protein to redistribute to the same aggregates. Thus, A-type lamin/LAP2α complexes may be important in nuclear anchorage, phosphorylation and subcellular localisation of Rb protein.

The regulation of Rb by A-type lamins is of particular interest in the context of laminopathies. Studies of Rb null embryos have established a role for Rb in muscle and fat cell differentiation and in co-ordinating proliferation and differentiation during muscle regeneration (reviewed in Smith *et al.*, 2005). Since Rb phosphorylation reflects growth conditions of cells, the status of Rb phosphorylation can serve as a stress indicator in cells. Rb protein dephosphorylation is an early event known to precede arrest of cellular growth during various processes such as quiescence, differentiation, senescence and stress-related premature senescence (Esposito *et al.*, 2000). Furthermore, A-type lamins mutations are linked to premature senescence (Chapter 3). Laminopathy fibroblasts show reduced proliferative capacity and enter early senescence, which implies alteration of the lamin/Rb pathway. Recently, it has been shown that lamin A/C null mouse fibroblasts which show premature senescence target Rb for abnormal degradation (Johnson *et al.*, 2004). Although this may explain a lack of proliferative potential in these cells, it suggests that Rb is not actively involved in maintaining senescent arrest in these cells. Indeed, it has been shown that in mouse fibroblasts a lack of Rb triggers p53-dependent senescent arrest (Smogorzewska and De Lange 2001). This is in contrast to human fibroblasts in which Rb plays a major role in all forms of cellular senescence. Such species-specific differences may lead to different regulation of Rb by A-type lamins in human fibroblasts.

Senescent cells lack hyper-phosphorylated Rb as judged by a lack of phosphorylation-dependent mobility shift on SDS-PAGE (Stein *et al.*, 1990), which led to conclusions that Rb exist in un-phosphorylated form during senescence. Recently, it has been shown that during early G1, cdk/cyclin D complexes hypo-phosphorylate Rb in a manner that does not cause an expected mobility shift (Ezhevsky *et al.*, 1997), which raises the possibility that a lack of mobility shift of Rb protein in senescent cells may be due to co-migration of un- and hypo-phosphorylated Rb on SDS-PAGE. However, it has not

been investigated as to which hypo-phosphorylated Rb isoforms, if any, may be mediating senescent arrest.

In this chapter, the protein expression and phosphorylation status of retinoblastoma protein were investigated in senescent and laminopathy Y259X human fibroblasts null for functional A-type lamins. In particular, a distribution and nuclear anchorage were examined of two hypo-phosphorylated Rb isoforms phosphorylated on either serine 780 or 795 known to occur during early G1 by cdk4/D1 complexes (Zarkowska and Mittnacht 1997, Connell-Crowley *et al.*, 1997). In addition, the role of LAP2α in cell cycle progression and nuclear anchorage of Rb was examined using small interfering RNA (siRNA). These results led to an identification of the senescence-associated Rb isoform and an exploration of functional implications of its particular distribution.

# Results

## 4.1. Protein expression and phosphorylation status of retinoblastoma protein (Rb) during *in vitro* ageing of fibroblasts as assessed by immunoblotting

In order to assess expression and phosphorylation status of retinoblastoma protein (Rb) during *in vitro* ageing of human dermal fibroblasts (HDF) and their final life stage senescence, firstly the total protein level of Rb was examined using immunoblotting. Primary cultures of human dermal fibroblasts were grown through serial passage (p) and the same number of cells was harvested after 3 days of growth in culture at early **(p7-p12)**, intermediate **(p17-p27)** and late **(p44)** passages. Whole cell extracts were blotted using two Rb antibodies: 1) IF8 which recognises an epitope in the C-terminal A-pocket of Rb protein. This antibody detects both under- and hyper-phosphorylated Rb species; and 2) phospho-Rb antibody specific for Rb phosphorylated on ser 780 (Rb780). Rb780 is a hypo-phosphorylated Rb isoform.

**Figure 4.1** shows that early (p7) passage fibroblasts had two populations of Rb protein: a slightly faster migrating band of 110 kDa which represents un- and under-phosphorylated Rb species (see arrowhead) and a slower migrating band of 115 kDa which represents hyper-phosphorylated Rb species (see arrow). In early (p7-p17) passage extracts, both under- and hyper-phosphorylated Rb species were present at the similar level. With an increasing passage number in extracts (p22-p44), the slower-migrating hyper-phosphorylated Rb population progressively decreased and was completely absent in late (p44) passage extract. This gradual decrease in the level of hyper-phosphorylated Rb in p22-p44 extracts was accompanied by an increase in the level of faster-migrating under-phosphorylated Rb whose expression was highest in late (p44) passage extract. Densitometry analysis of Rb protein bands in extracts showed that late (p44) passage cells accumulated twice as much of under-phosphorylated Rb protein than early passage (p7) cells and that the total level of Rb protein did not change with an increasing passage number in cells. Therefore, during ageing of fibroblasts *in vitro* Rb protein becomes progressively de-phosphorylated with a subsequent accumulation of faster-migrating under-phosphorylated Rb in late-passage cells as expected (Stein *et al.*, 1990).

An accumulation of faster migrating Rb species in late passage (p44) cells can represent both un-phosphorylated and hypo-phosphorylated Rb species (Ezhevsky *et al.*, 2000). This prompted me to examine the protein expression of hypo-phosphorylated Rb isoform phosphorylated on serine 780 in the same extracts. Rb becomes phosphorylated on serine 780 during early G1 phase (Boylan *et al.*, 1999, Markiewicz *et al.*, 2002a). Surprisingly, the results show that the protein expression of Rb780 gradually decreased with an increasing passage number in cell extracts **(Figure 4.1)**. Densitometry analysis of Rb780 bands across passages showed that the protein level of Rb780 in late passage (p44) cells was three times lower than that of early (p7) passage cells. This result was not expected because the accumulation of faster-migrating Rb detected by IF8 antibody in late passage cells leads one to speculate an increase in the level of Rb780 in late passage cells. Consequently, it was decided to investigate the protein expression of another hypo-phosphorylated Rb isoform phosphorylated on serine 795 (Rb795) across passages. Rb795 is also phosphorylated during early G1 phase (Boylan *et al.*, 1999). However, at the time this antibody was only produced for immunocytochemistry analysis and indeed, it did not work for immunoblotting.

## 4.2. Cellular localisation of total Rb protein and hypo-phosphorylated Rb isoforms in late passage fibroblasts as assessed by immunofluorescence microscopy

To investigate cellular localisation pattern of total Rb protein and hypo-phosphorylated Rb isoforms in late passage fibroblasts, the immunocytochemistry and confocal microscopy were used. Human fibroblasts of early **(p7)** and late passage **(p44)** were seeded at an equal density, grown in culture for 3 days and processed for double immunofluorescence microscopy using antibodies against: a) IF8 (total Rb) and a proliferation marker Ki67, b) IF8 and Rb780, and c) IF8 and Rb795.

In early (p7) passage HDF, IF8 antibody showed a bright granular nucleoplasmic distribution of Rb protein in 75% of nuclei **(Figure 4.2 (a) p7)**. This expression of Rb protein in early (p7) passage nuclei corresponded to a bright nucleolar staining of Ki67 as expected. The remaining 25% of early (p7) passage cells had a decreased IF8 staining in the nucleus and stained negatively for Ki67 marker indicative of growth-arrested quiescent cells (not shown, see Chapter 5). In late (p44) passage HDF, a majority of nuclei (80%) were negative for a proliferation marker Ki67. IF8 antibody showed a

bright granular nucleoplasmic distribution of Rb in 45% of late (p44) passage nuclei and was weakly detected in 55% of late (p44) passage nuclei **(Figure 4.2 (a) p44)**. 25% of late (p44) passage nuclei that stained brightly for IF8 were negative for Ki67 whilst the other 20% of late (p44) passage nuclei that stained brightly for IF8 were positive for Ki67 marker. 55% of late passage (p44) nuclei that stained weakly for IF8 were negative for Ki67.

Although IF8 antibody showed stable level of Rb protein in late passage cells by immunoblotting, IF8 staining *in situ* distinguished two populations of late passage cells. IF8 antibody shows epitope masking in non-proliferating quiescent cells, which becomes reversed in proliferating cells coincident with cell cycle-dependent Rb phosphorylation (see **Chapter 5**). Since 55% of late passage cells stained weakly for IF8, this indicates that this population of late passage cells may contain un-phosphorylated Rb and/or Rb with lower level of phosphorylation than late passage cell population that stained more brightly for IF8 (45%). In order to examine phosphorylation status of Rb in these two populations of late passage cells, early (p7) and late (p44) passage HDF were co-stained with IF8 and two phospho-specific Rb antibodies: one specific for Rb phosphorylated on serine 780 (Rb780) and the other specific for Rb phosphorylated on serine 795 (Rb795).

In early (p7) passage HDF, Rb780 antibody showed a bright and somewhat granular nucleoplasmic staining in 75% of nuclei and these nuclei stained brightly for IF8 **(Figure 4.2 (b) p7)**. 25% of early (p7) passage HDF showed weak or absent Rb780 staining in the nucleus and these nuclei displayed weak staining for IF8 **(see * in Figure 4.2 (b) p7)**. In late (p44) passage HDF, 45% of nuclei showed a bright nucleoplasmic expression of Rb780 and these nuclei stained brightly for IF8 whilst 55% of late (p44) passage nuclei showed weak or absent Rb780 staining and these nuclei stained weakly for IF8 **(Figure 4.2 (b) p44)**.

In early (p7) passage HDF, Rb795 antibody showed intense granular nucleoplasmic staining (except for nucleoli) in 75% of nuclei and these nuclei displayed bright IF8 staining **(Figure 4.2 (c) p7)**. 25% of early (p7) passage HDF showed weak or absent Rb795 staining in nuclei and these nuclei displayed weak IF8 staining **(see * in Figure 4.2 (c) p7)**. Surprisingly, in late (p44) passage HDF, Rb795 showed bright granular

nuclear distribution (except for nucleoli) in 75% of cells **(Figure 4.2 (c) p44).** 45% of late (p44) passage nuclei displayed bright nucleoplasmic distribution of Rb795 with prominent nuclear dots and these nuclei stained brightly for IF8. 30% of late (p44) passage nuclei had a distinct morphology to Rb795 distribution and these nuclei stained weakly for IF8. In these cells, Rb795 appeared as round nuclear foci and significantly lacked nucleoplasmic staining around the foci. The remaining 25% of late passage nuclei stained weakly for IF8 and these nuclei stained weakly for Rb795 (not shown).

These results confirm the above immunoblotting data that late passage cells contain significantly reduced level of Rb780 as compared to early passage cells. Late passage cells that stained brightly for IF8 (45%) contained both Rb780 and Rb795 species whilst 30% of late passage cells that stained weakly for IF8 did not contain Rb780 but remained phosphorylated on serine 795 in distinct nuclear foci. In contrast, early passage cells that stained weakly for IF8 did not contain Rb780 or Rb795. Since 30% of late passage cells showed bright nuclear foci of Rb795 but lacked bright nucleoplasmic distribution around the foci, it suggests that nucleoplasmic population of Rb795 in these cells becomes dephosphorylated. However, the presence of Rb795 in 75% of late passage cells indicates that late passage cells contain a distinct population of hypo-phosphorylated Rb which contributes to accumulation of faster migrating Rb species on SDS-PAGE.

## 4.3. Cellular distribution of hypo-phosphorylated Rb isoforms in relation to A-type lamins and LAP2α in late passage fibroblasts as assessed by immunofluorescence microscopy

In late passage fibroblasts, LAP2α and A-type lamins are aberrantly organised in the nucleus (chapter 3). Since these proteins bind to hypophosphorylated Rb and can influence its cellular distribution (Markiewicz *et al.*, 2002a), it was investigated how the observed changes in their nuclear organisation in late passage cells impact on the distribution of hypo-phosphorylated Rb isoforms. Human fibroblasts of early **(p7)** and late passage **(p44)** were seeded at an equal density, grown in culture for 3 days and processed for double immunofluorescence microscopy using antibodies against: 1) LAP2α and 780; 2) LAP2α and Rb795; 3) lamin A/C and 780, and 4) lamin A/C and Rb795.

In early (p7) passage HDF, LAP2α displayed bright homogenous nucleoplasmic distribution in 75% of cells. In these cells Rb780 showed bright and somewhat granular nucleoplasmic distribution that greatly co-localised with LAP2α in the nucleoplasm **(Figure 4.3 (a) p7)**. 25% of early (p7) passage HDF showed a weak or absent LAP2α nuclear staining which corresponded to a weak or absent staining of Rb780 (not shown). In late (p44) passage HDF **(Figure 4.3 (a) p44)**, 45% of nuclei showed a bright and somewhat granular Rb780 distribution that co-localised with a bright and granular LAP2α nucleoplasmic distribution **(see arrow)**. Another 20% of late passage (p44) nuclei showed heavily granulated LAP2α distribution in the nucleus and these nuclei had dramatically reduced or absent Rb780 staining **(see arrowheads).** In addition, 35% of late (p44) passage cells lacked nucleoplasmic LAP2α staining, of which 10% contained aggregates of LAP2α at one pole of the nucleus and these cells did not stain for Rb780 in the nucleus but showed a few aggregated granules within LAP2α aggregates **(see *)**.

In early (p7) passage HDF, Rb795 showed a bright, granular nucleoplasmic distribution in 75% nuclei and in these cells LAP2α showed a bright homogenous nucleoplasmic distribution that co-localised with Rb795 **(Figure 4.3 (b) p7)**. 25% of early (p7) passage cells had a decreased or absent Rb795 nuclear staining and these nuclei had a weak or absent LAP2α staining. Surprisingly, in late (p44) passage cells, 65% of nuclei that showed bright and granular LAP2α distribution also displayed bright (although distinct) distribution of Rb795 **(Figure 4.3 (b) p44)**. In 45% of late (p44) passage cells which contained granular distribution of LAP2α with some indication of aggregation, Rb795 was not present in LAP2α aggregates but showed many prominent dots in addition to nucleoplasmic distribution **(see arrow)**. In 20% of late (p44) passage cells that contained heavily granulated LAP2α distribution, Rb795 had a more distinct morphology to its distribution and appeared as rounder and larger nuclear foci with decreased nucleoplasmic staining around the foci **(see arrowhead)**. In 10% of late (p44) passage cells, LAP2α nucleoplasmic staining was completely absent and Rb795 was present in bright nuclear foci without nucleoplasmic staining around the foci **(see *).** These results show that early passage fibroblasts display a 100% co-localisation between LAP2α and Rb780/Rb795 nucleoplasmic expression. In late passage fibroblasts, Rb780 expression was absent in nuclei that contained heavily granulated or

aggregated LAP2α. In contrast, Rb795 was present in distinct nuclear foci in late passage nuclei that contained heavily granulated or aggregated LAP2α.

Next, the distribution of hypo-phosphorylated Rb isoforms was examined in relation to A-type lamin nuclear organisation. In early (p7) passage HDF **(Figure 4.4 (a) & (b) p7)**, 77% of nuclei showed intense distribution of lamins A/C at the nuclear envelope **(see arrowheads)** and in the nucleoplasm, while 23% of nuclei showed intranuclear lamin A/C dots **(see arrows)** and variable distribution at the nuclear envelope. In early (p7) passage HDF, Rb780 showed a bright and somewhat granular nucleoplasmic distribution in 75% of nuclei including 52% of nuclei which showed intense lamin A/C distribution at the nuclear envelope and 23% of nuclei which displayed intranuclear lamin A/C dots **(Figure 4.4 (a) p7)**. In contrast, in late (p44) passage HDF **(Figure 4.4 (a) & (b) p44)**, 59.5% of nuclei were dysmorphic including nuclei which showed lamin A/C herniations and honeycombs **(see arrowheads)** with an accumulation of intanuclear lamin aggregates **(see arrows)** whilst 40.5% of nuclei ovoid and showed variable intensity of lamin A/C at the nuclear envelope **(see *).** In late (p44) passage HDF, 55% of nuclei had a decreased or absent Rb780 nucleoplasmic staining, including 35% of nuclei which showed lamin A/C herniations and/or honeycombs **(Figure 4.4 (a) p44)**. In these nuclei, Rb780 tended to aggregate in a few granules around lamin A/C nucleoplasmic aggregates. In late (p44) passage HDF, Rb780 was present in 45% of nuclei, including 20% of ovoid nuclei that showed variable intensity of lamin A/C at the nuclear envelope **(Figure 4.4 (a) p44)**.

In early (p7) passage HDF, Rb795 showed a bright and granular nucleoplasmic distribution in 75% of nuclei, including 52% of nuclei which showed intense lamin A/C distribution at the nuclear envelope and 23% of nuclei which showed intranuclear lamin A/C dots **(Figure 4.4 (b) p7)**. In contrast, in late (p44) passage HDF, Rb795 was present in 75% of nuclei, including 55% of dysmorphic and 20% of ovoid nuclei. In 30% of late passage nuclei which contained lamin A/C herniations and/or honeycombs, the usual nucleoplasmic distribution of Rb795 was significantly decreased but unlike Rb780, Rb795 was not found to aggregate around lamin A/C intranuclear aggregates **(Figure 4.4 (b) p44)**. Instead, Rb795 was present in distinct bright nuclear foci. In contrast, in 20% of ovoid-shaped nuclei that showed variable intensity of lamin A/C at the nuclear envelope, Rb795 displayed nucleoplasmic distribution in addition to

prominent nuclear dots **(Figure 4.4 (b) p44)**. DNA staining dye DAPI revealed that peripheral chromatin was absent from the regions depleted of lamin A/C staining and that internal chromatin accumulates focal regions of condensed chromatin in late (p44) passage nuclei **(Figure 4.4 (a) & (b) DAPI p44)**.

These results show that late passage dysmorphic nuclei which contain lamin A/C herniations and/or honeycombs and accumulate intranuclear lamin A/C aggregates had a decreased or absent Rb780 expression. These dysmorphic nuclei also showed a tendency of LAP2α to become heavily granulated and/or to aggregate (Chapter 3). In contrast, Rb795 lacked nucleoplasmic distribution in dysmorphic nuclei with lamin A/C herniations and/or honeycombs that show heavily granulated or aggregated LAP2α but remained present in distinct nuclear foci.

## 4.4. Cellular distribution of LAP2α and lamin B2 in laminopathy Y259X fibroblasts as assessed by immunofluorescence microscopy

The above results suggest that aberrant assembly of A-type lamins in late passage cells affects distribution of LAP2α and hypo-phosphorylated Rb in the nucleus. To test this possibility more directly, laminopathy fibroblasts were employed with a homozygous non-sense Y259X mutation, which are functionally null for A-type lamins. Y259X laminopathy fibroblasts accumulate nuclear abnormalities and show premature senescence (Chapter 3). It was thus hypothesized that in the absence of functional A-type lamins, LAP2α would not be correctly organised in the nucleus. Early **(p12)** and mid passage **(p18)** Y259X fibroblasts were seeded at an equal density, grown in culture for 3 days and processed for double immunofluorescence microscopy using antibodies against: a) lamin B2 and Ki67 and b) LAP2α and Ki67.

In early (p12) passage Y259X fibroblasts, 35% of nuclei stained positively for Ki67 and 92% of these nuclei showed bright lamin B2 staining at the nuclear envelope and in the nucleoplasm **(Figure 4.5 (a) p12).** 29% of nuclei showed weak or absent lamin B2 distribution at one pole of the nucleus and 90% of these nuclei stained negatively for Ki67 **(see arrow)**. In addition, 36% of nuclei stained negatively for Ki67 in the absence of any detectible abnormal lamin B2 distribution (not shown). By mid passage 18, this abnormal nuclear envelope distribution of lamin B2 increased to 54% and all these

nuclei stained negatively for Ki67 marker **(see arrow in Figure 4.5 (a) p18)**. Only 13.8% of p18 Y259X nuclei were positive for Ki67 and these cells displayed expected lamin B2 distribution whilst 32.2% of cells were negative for Ki67 in the absence of detectible abnormal lamin B2 distribution. DNA staining dye DAPI revealed that peripheral chromatin was absent from the regions depleted of lamin B2 staining in both early (p12) and mid (p18) passage Y259X nuclei **(see arrowheads in Figure 4.5 (a))**.

In early (p12) passage Y259X fibroblasts **(Figure 4.5 (b) LAP2α p12)**, 36.8% of nuclei displayed very unusual LAP2α distribution including 16.8% of nuclei which showed nucleoplasmic LAP2α distribution with some indication of aggregation **(see arrow)** and 20% of nuclei which lacked nucleoplasmic LAP2α distribution but contained aggregates at one pole of the nucleus **(see arrowheads)**. Nuclei that still showed nucleoplasmic LAP2α with a tendency to aggregation stained positively for Ki67 and nuclei that only contained LAP2α aggregates stained negatively for Ki67 **(Figure 4.5 (b) p12)**. In addition, 18.2% of Y259X p12 nuclei displayed bright nucleoplasmic LAP2α distribution and positive Ki67 staining and 45% of nuclei lacked LAP2α expression and Ki67 staining (not shown). In mid passage (p18) Y259X fibroblasts, this unusual pattern of LAP2α distribution increased to 53% and a significantly higher proportion of such cells (39.2%) only contained LAP2α aggregates **(see arrowheads in Figure 4.5 (b) LAP2α p18)** whilst 13.8% of cells displayed nucleoplasmic LAP2α distribution with some indication of aggregation (not shown). All Y259X p18 nuclei with LAP2α aggregates stained negatively for Ki67 proliferation marker **(Figure 4.5 (b) p18)** whilst nuclei in which LAP2α tended to aggregate showed bright Ki67 staining. In addition, 47% of cells lacked LAP2α expression and Ki67 staining (not shown). DAPI staining of chromatin revealed that peripheral chromatin was often absent from one pole of the nuclei, which contained LAP2α aggregates in both early (p12) and mid (p18) passage Y259X cells **(see arrowheads in Figure 4.5 (b) DAPI)**.

These results show in the absence of functional A-type lamins in Y259X laminopathy fibroblasts, LAP2α was aberrantly mislocalised in the nucleus and tended to form aggregates. In addition, cells that showed LAP2α aggregates underwent cell cycle arrest. Such cells displayed abnormal nuclear shapes and lacked peripheral chromatin, which was also seen in cells that showed abnormal distribution of lamin B2 at one pole of the nucleus. Since nuclear abnormalities and LAP2α aggregation increased with age

in laminopathy fibroblasts when they enter premature senescence, these results indicate that LAP2α aggregation correlates with premature senescent arrest.

### 4.5. Cellular distribution of LAP2α and hypo-phosphorylated Rb isoforms in laminopathy Y259X fibroblasts as assessed by immunofluorescence microscopy

LAP2α aggregation in laminopathy Y259X fibroblasts is reminiscent of abnormal distribution of LAP2α in senescent fibroblasts. It has been seen that distribution of hypo-phosphorylated Rb is significantly affected in late passage cells which show heavily granulated or aggregated LAP2α. Therefore it was hypothesized that LAP2α mislocalisation induced by the absence of functional A-type lamins in Y259X fibroblasts would disrupt distribution of hypo-phosphorylated Rb in the nucleus which would in turn trigger cell cycle arrest. In order to investigate this hypothesis, early **(p12)** and mid passage **(p18)** Y259X fibroblasts were seeded at an equal density, grown in culture for 3 days and processed for double immunofluorescence microscopy using antibodies against: a) LAP2α and Rb780, b) LAP2α and Rb795, c) IF8 Ki67, d) Rb780 and Ki67.

In early (p12) passage Y259X fibroblasts **(Figure 4.6A (a) p12)**, cells which showed bright nucleoplasmic distribution and some tendency of LAP2α to aggregate **(see arrow)**, displayed bright nucleoplasmic distribution of Rb780 which often tended to aggregate within LAP2α aggregations. Cells which only showed LAP2α aggregates **(see arrowhead)** completely lacked nucleoplasmic distribution of Rb780 which was sometimes found within LAP2α aggregates. In addition, cells that displayed expected nucleoplasmic distribution of LAP2α **(see *)** showed bright nucleoplasmic expression of Rb780 and cells that completely lacked LAP2α expression also lacked Rb780 expression (not shown). In mid passage (p18) Y259X cells, majority of cells either showed LAP2α aggregates or completely lacked LAP2α expression and these cells also lacked Rb780 expression **(Figure 4.6A (a) p18).** A minority of cells that showed a tendency of LAP2α to aggregate in the presence of nucleoplasmic distribution still showed Rb780 brightly in the nucleus (not shown).

In early (p12) passage Y259X fibroblasts, Rb795 was brightly present in 55% of nuclei **(Figure 4.6A (b) p12)**. Cells that showed nucleoplasmic LAP2α distribution with some

aggregation (**see arrow**) displayed bright nucleoplasmic distribution of Rb795 in addition to prominent nuclear dots. Cells that only showed LAP2α aggregates (**see arrowhead**) displayed an unusual distribution Rb795. In these cells Rb795 was present in distinct bright nuclear foci and lacked nucleoplasmic distribution around the foci. Rb795 was not seen within LAP2α aggregates. Cells that showed expected LAP2α nucleoplasmic distribution (**see ***) displayed bright nucleoplasmic Rb795 distribution and cells that completely lacked LAP2α expression also lacked Rb795 expression (not shown). In mid passage (p18) Y259X cells, cells that showed LAP2α aggregates displayed distinct nuclear foci of Rb795 (**Figure 4.6A (b) p18**). A minority of cells that showed a tendency of LAP2α to aggregate in the presence of nucleoplasmic distribution still showed bright nucleoplasmic distribution of Rb795 in addition to prominent dots (not shown).

Next, the nuclear distribution of total Rb was examined using IF8 antibody, which shows epitope masking in non-proliferating cells. Also the proliferation status of cells stained with either IF8 or Rb780 antibody was examined. In early (p12) passage Y259X fibroblasts (**Figure 4.6B (c) p12**), 35% of nuclei displayed bright and granular nucleoplasmic staining of IF8 and these nuclei stained positively for Ki67 marker. 65% of nuclei displayed weak IF8 staining and these nuclei stained negatively for Ki67 marker. In mid (p18) passage Y259X cells (**Figure 4.6B (c) p18**), 13.8% of nuclei stained brightly for IF8 and these nuclei were positive for Ki67 marker. 86.2% of nuclei stained weakly for IF8 and these nuclei were negative for Ki67 marker. Similarly to IF8, in early (p12) passage Y259X cells (**Figure 4.6B (d) p12**), Rb780 displayed bright and somewhat granular nucleoplasmic distribution in 35% of nuclei and these cells stained positively for Ki67. 65% of nuclei displayed weak Rb780 staining and these nuclei stained negatively for Ki67 marker. In mid (p18) passage Y259X cells (**Figure 4.6B (d) p18**), 86.2% of nuclei stained weakly for Rb780 and these nuclei were negative for Ki67 marker. In addition, 13.8% of nuclei stained brightly for Rb780 and these nuclei were positive for Ki67 marker (not shown). Therefore, a lack of Rb780 expression and a weak IF8 staining correlate with cell cycle arrest in Y259X laminopathy cells.

These results show that in the absence of functional A-type lamins in Y259X fibroblasts, LAP2α mislocalisation in the nucleus affected distribution of hypo-

phosphorylated Rb isoforms in the nucleus. In cells that showed LAP2α aggregates and lacked expected LAP2α distribution in the nucleus, expression of Rb780 was completely lost, whilst expression of Rb795 became limited to distinct nuclear foci. The abnormal LAP2α distribution and changes in expression of Rb isoforms in Y259X laminopathy fibroblasts are reminiscent of wild-type senescent fibroblasts. These results support the above hypothesis that abnormal LAP2α distribution disrupts normal distribution of hypo-phosphorylated Rb780, which leads to cell cycle arrest.

### 4.6. Protein expression of total Rb and hypo-phosphorylated Rb780 isoform in early and mid passage Y259X fibroblasts as assessed by immunoblotting

Loss of Rb780 expression and weak IF8 staining in situ in laminopathy Y259X fibroblasts is reminiscent of changes in Rb expression seen in senescent fibroblasts. In addition, weak IF8 staining in situ reflects decreased level of Rb phosphorylation in general. Therefore the total level of Rb protein was examined using immunoblotting. Early (p12) and mid (p18) passage Y259X laminopathy fibroblasts were grown in culture for 3 days and harvested. As a control, early (p12) and mid passage (p18) wild-type fibroblasts grown in culture for 3 days were harvested for the same number of cells. Whole cell extracts were blotted using two Rb antibodies: 1) IF8 which recognises both under- and hyper-phosphorylated Rb, and 2) phospho-Rb antibody specific for Rb isoform phosphorylated on ser 780 (Rb780).

The results show **(Figure 4.7)** that early (p12) and mid passage (p18) wild-type HDF have two populations of Rb protein- a slightly faster migrating band of 110 kDa which represents under-phosphorylated Rb and a slower migrating band of 115 kDa which represents hyperphosphorylated Rb. In p12 and p18 wild-type HDF, both under- and hyper-phosphorylated Rb populations are present at the similar level. In Y259X laminopathy cells the protein level of hyper-phosphorylated Rb gradually decreased from early p12 to mid passage p18 whilst the protein level of under-phosphorylated Rb gradually increased. Densitometry analysis of IF8 bands across passages showed that the level of under-phosphorylated Rb in mid passage p18 Y259X cells is increased two times as compared to the level of under-phosphorylated Rb in mid passage p18 wild-type HDF. On the other hand, the protein level of hyper-phosphorylated Rb in mid

passage p18 Y259X cells decreased two times as compared to that of mid passage p18 wild-type HDF.

Immunoblotting the same extracts with Rb780 antibody showed that whilst the protein level of Rb780 remained constant from early passage p12 to mid passage p18 in wild-type HDF, Rb780 protein level gradually decreased from early passage p12 to mid passage p18 in Y259X laminopathy cells (**Figure 4.7**). Densitometry analysis of Rb780 bands across passages showed that the level of Rb780 in early passage p12 Y259X cells is two times lower than that of early passage p12 wild-type HDF whilst the level of Rb780 in mid passage p18 Y259X cells is four times lower than that of mid passage p18 wild-type HDF. These results confirm the immunofluorescent observations that Rb780 expression becomes increasingly absent from Y259X laminopathy nuclei. On the other hand, a significant decrease of expression of hyper-phosphorylated Rb in mid passage Y259X cells is consistent with immunofluorescent observations that majority of mid passage laminopathy cells are non-proliferating. In addition, an accumulation of faster-migrating Rb species in mid passage Y259X cells is consistent with the presence of distinct foci of hypo-phosphorylated Rb isoform Rb795 in majority of cells.

## 4.7. Solubility properties of total Rb and hypo-phosphorylated Rb780 in late passage fibroblasts as assessed by biochemical fractionation and immunoblotting

Senescent fibroblasts show increased solubility/instability of A-type lamins, which led to a loss of LAP2α from nucleoskeleton upon nuclear matrix extraction (Chapter3). Since an aberrant assembly of A-type lamins and LAP2α correlates with a loss of expression of hypo-phosphorylated Rb780, it was hypothesized these proteins would not stably anchor Rb780 in the nucleus which would lead to its decreased expression in late passage fibroblasts. To investigate this possibility, the solubility properties of both total Rb protein and a hypo-phosphorylated Rb isoform 780 were examined in late passage cells. Early (p7) and late passage (p44) fibroblasts were submitted to a sequential extraction by CSK-Triton X100, RSB-Magic, followed by chromatin digestion by DNAse1 and a final extraction by 0.25M ammonium sulphate. The insoluble pellets P2, P3, P4 and P5 and the nuclear material solubilized after each step S2, S3, S4 and S5 were then analysed by immunoblotting. The whole cell pellet P1 was prepared as a control for both early and late passage HDF.

**Figure 4.8 Rb780 p7** shows that in early (p7) passage cells, hypo-phosphorylated isoform Rb780 was present in the insoluble pellets after each step of extraction whilst some amount of Rb780 appeared in the soluble fraction after ammonium sulphate extraction (S5) resulting in a retention of a significant amount of Rb780 in a final insoluble pellet (P5). This result is consistent with the biochemical fractionation data presented in Chapter 3 which showed that in early (p7) passage HDF, A-type lamins and their binding partner, LAP2α, were found in the insoluble fractions throughout the extraction procedure. These results altogether confirm that A-type lamins and LAP2α form a strong detergent/salt-resistant nucleoskeleton that stably anchors RB780 in the nucleus.

In contrast, in late (p44) passage HDF, changes in solubility properties of hypo-phosphorylated isoform Rb780 were detected by immunoblotting of late passage extracts **(Figure 4.8 Rb780 p44)**. Whilst Rb780 was readily detected in the whole cell extract (P1), following extraction with CSK-Triton X100 and RSB/Magik, some amount of Rb780 found in the soluble fractions S2 and S3 which led to a decreased amount of Rb780 in the insoluble fractions P2-P4. Following ammonium sulphate treatment, the entire amount of Rb780 present in the insoluble fraction P4 was found in the soluble fraction S5 which resulted in a loss of Rb780 in the final insoluble fraction P5. This result is consistent with the previous biochemical fractionation data demonstrating that upon nuclear matrix extraction, late passage cells show increased solubility/instability of A-type lamins and their binding partner LAP2α. Therefore A-type lamins and LAP2α would not support stable anchorage of Rb780 in the nucleus and consequently Rb780 is lost from the nucleoskeleton upon extraction.

Next, the solubility property of total Rb protein was examined. In early (p7) passage HDF **(Figure 4.8 IF8 p7)**, immunoblotting of the extracts with IF8 antibody showed three Rb bands in the whole cell pellet P1: one slower migrating (hyper-phosphorylated Rb), one faster migrating band (hypo-phosphorylated Rb) and one band migrating at the intermediate level between the other two bands. Following CSK/Triton extraction, some amount of all three Rb bands were found in the soluble fraction S2 resulting in a loss of slower-migrating Rb band and retention of both faster and intermediate Rb bands in the insoluble fractions P2-P4. Following ammonium sulphate extraction, some amount of intermediate Rb band was found in the soluble fraction S5 resulting in the retention of a

significant amount of both Rb bands in the final insoluble pellet P5. This result confirms that a significant amount of total Rb is stably anchored in nucleoskeleton in early passage cells. The intermediate Rb band most likely represents hypo-phosphorylated Rb species that can introduce a shift in Rb migration pattern (Ezhevsky *et al.*, 2000). One such shift can occur upon hypo-phosphorylation of Rb on serine 780 (Markiewicz *et al.*, 2002a).

In contrast, in late (p44) passage HDF **(Figure 4.8 IF8 p44)** only one faster-migrating band was present in whole cell pellet P1 at an increased level. The intensity of this Rb band gradually decreased during sequential extraction of late passage cells and some amount of Rb was found in all soluble fractions S2-S5. However, unlike Rb780, following ammonium sulphate extraction, small amount of Rb was retained in the final insoluble pellet P5. This result shows that late passage cells accumulate faster-migrating Rb species, which show increased solubility properties upon nuclear matrix extraction. Nonetheless, some Rb protein did remain stably anchored in nucleoskeleton. Since Rb780 became completely lost from nucleoskeleton upon extraction, this hypo-phosphorylated isoform did not contribute to retention of Rb in late passage cells.

## 4.8 Investigation of nuclear anchorage of total Rb and hypo-phosphorylated Rb isoforms by *in situ* nuclear matrix extraction of late passage fibroblasts

The retention some Rb in nucleoskeleton of late passage cells prompted us to investigate the nuclear anchorage of hypo-phosphorylated isoforms Rb780 and Rb795 in relation to nuclear anchorage of total Rb. Since IF8 antibody shows epitope masking in majority of late passage fibroblasts *in situ*, another Rb antibody (AB5), which recognises total Rb, was utilised. Early **(p7)** and late passage **(p44)** fibroblasts were submitted to a nuclear matrix extraction *in situ* via five sequential treatments with CSK-Triton X100, RSB-Magic, DNAse1 digestion and 0.25M ammonium sulphate extraction and processed for double immunofluorescence microscopy using antibodies against: a) AB5 and Rb780 and, b) AB5 and Rb795.

In early (p7) passage HDF after V stage extraction, 55% of nuclei retained AB5 strongly in the nucleus and these cells retained Rb780 strongly in the nucleus **(Figure 4.9 (a) p7)**. 45% of cells did not retain AB5 in the nucleus and these cells did not retain

Rb780 in the nucleus. In contrast, in late (p44) passage HDF upon V stage extraction, 75% of cells retained AB5 weakly in the nucleus and these cells did not retain any Rb780 in the nucleus **(Figure 4.9 (a) p44)**. In addition, 20% of late passage cells retained both AB5 and Rb780 strongly in the nucleus upon V stage extraction.

In early (p7) passage HDF after V stage extraction, 55% of nuclei retained AB5 strongly in the nucleus and these cells also retained Rb795 strongly in the nucleus. 45% of nuclei did not retain either AB5 or Rb795 in the nucleus **(Figure 4.9 (b) p7)**. Surprisingly, in late (p44) passage HDF after V stage extraction, 75% of cells retained AB5 weakly in the nucleus and these cells retained bright nuclear foci of Rb795 and lacked nucleoplasmic staining **(Figure 4.9 (b) p44)**. In addition, 20% of late passage cells retained both AB5 and Rb795 strongly in the nucleus following V stage extraction. These results show that hypo-phosphorylated isoform Rb795 remained anchored in the nucleus of late passage cells within distinct nuclear foci and would therefore contribute to nuclear anchorage of faster-migrating Rb protein detected by immunoblotting.

It was then investigated nuclear anchorage of hypo-phosphorylated isoforms in relation to nuclear anchorage of LAP2α upon extraction *in situ*. Early **(p7)** and late passage **(p44)** fibroblasts were submitted to a nuclear matrix extraction *in situ* as described above and processed for double immunofluorescence microscopy using antibodies against: a) LAP2α and Ki67, b) LAP2α and Rb780 and, c) LAP2α and Rb795.

In early (p7) passage HDF, a majority of nuclei (>65%) retained LAP2α weakly in the nucleus following V stage of extraction and these cells were positive for Ki67 **(Figure 4.10 (a) p7)**. In late (p44) passage HDF, a majority of nuclei (80%) were Ki67 negative and these cells did not retain LAP2α in the nucleus after V stage extraction but often showed a tendency of LAP2α to aggregate **(Figure 4.10 (a) p44)**. In addition, a minority of late (p44) passage cells (20%) were still Ki67 positive and these cells retained LAP2α weakly in the nucleus after V stage extraction.

In early (p7) passage HDF after III stage extraction, 55% of cells retained LAP2α strongly in the nucleus and these cells retained Rb780 strongly in the nucleus **(Figure 4.10 (b) p7)**. In addition, 10% of cells retained LAP2α but not Rb780 in the nucleus indicative of cells beyond G1 phase (see **Chapter 5**). In contrast, in late (p44) passage

HDF upon III stage extraction, 80% of cells did not retain LAP2α in the nucleus but often contained aggregates and these cells did not retain Rb780 in the nucleus **(Figure 4.10 (b) p44)**. In addition, 20% of late passage cells retained both LAP2α and Rb780 strongly in the nucleus upon III stage extraction.

In early (p7) passage HDF after V stage extraction, 55% of cells that retained LAP2α weakly in the nucleus also retained Rb795 strongly in the nucleus **(Figure 4.10 (c) p7)**. In addition, 10% of cells retained LAP2α weakly in the nucleus but did not retain Rb795 indicative of cells beyond G1 phase of cell cycle (see Chapter 5). In contrast, in late (p44) passage HDF after V stage extraction, 75% of cells did not retain LAP2α in the nucleus but often contained aggregates and these cells retained bright nuclear foci of Rb795 and lacked nucleoplasmic staining **(Figure 4.10 (c) p44)**. In addition, 20% of late passage cells retained LAP2α weakly in the nucleus and these cells retained Rb795 strongly in the nucleus. These results show that upon extraction of early passage cells *in situ*, stable retention of LAP2α in nucleoskeleton was correlated with a stable retention of both hypo-phosphorylated isoforms Rb780 and Rb795 in the nucleoplasm. In contrast, in late passage cells a loss of retention and aggregation of nucleoskeletal LAP2α upon extraction in situ was correlated with a loss of Rb780 from nucleoskeleton and a loss of Rb795 from the nucleoplasm but not from distinct nuclear foci.

## 4.9. Investigation of LAP2α/lamin C/Rb780 binding in late passage fibroblasts by immunoprecipitation and immunoblotting

The above results have shown that increased solubility/instability of A-type lamins in late passage fibroblasts leads to a loss of nuclear anchorage of LAP2α and hypo-phosphorylated isoform Rb780 upon nuclear matrix extraction. Since A-type lamins and LAP2α bind to Rb780 in early passage fibroblasts (Markiewicz *et al.*, 2002a), it was hypothesized that a loss of nuclear anchorage of Rb780 in late passage fibroblasts stems from decreased binding of this Rb isoform to A-type lamin/LAP2α complexes in the nucleus. To test this possibility, early **(p8)** and late passage **(p42)** HDF were grown for 3 days in culture and the same number of cells was harvested for immunoprecipitation analysis. In brief, early (p8) and late (p42) passage cells were homogenised in ice-cold hypotonic buffer and the resultant nuclear pellets treated with 500mM salt buffer. Following dialysis in PBS/0.1% Triton, nuclear supernatants were incubated with

LAP2α-specific antibody (LAP15) pre-incubated with Dynabeads. LAP2α immuno-precipitates were washed in PBS/0.1% Triton and both early and late passage immuno-precipitates (P) were run on reducing SDS-PAGE and immunoblotted with antibodies against LAP2α (LAP15), lamin C (RαLC) and Rb phosphorylated on serine 780 (Rb780). Under reducing conditions, heavy and light chains of IgGs are separated and heavy chains run at ~50 kDa (labelled IgG (h) in the immuno-precipitate fractions).

**Figure 4.11** shows LAP2α immuno-precipitate (P) fractions for early (p8) and late (p42) passage cells run under reducing conditions. Immunoblotting with LAP2α antibody (LAP15) detected the same level of LAP2α protein in both early (p8) and late (p42) passage immuno-precipitate fractions indicating that the same amount of LAP2α protein was immuno-precipitated from both early (p8) and late (p42) passage cells. When the same immuno-precipitate fractions were immunoblotted with lamin C antibody, the staining showed an immuno-precipitated complex between LAP2α and lamin C in both early (p8) and late (p42) passage immuno-precipitated fractions (P). Significantly less amount of lamin C protein was detected in the immuno-precipitate fraction (P) of late (p40) passage cells indicating that in late passage cells only small amount of LAP2α is only bound to lamin C protein. Immunoblotting of same immuno-precipitate fractions with Rb780 antibody showed that Rb780 protein was strongly detected in the early (p8) passage immuno-precipitate fraction and was weakly detected in the late (p42) passage immuno-precipitate fraction. This result indicates that significantly higher amount of Rb780 protein was bound in the complex with LAP2α in early (p7) passage cells whilst only a very small amount of Rb780 protein was bound to LAP2α in late passage cells. These results demonstrate that Rb780 shows a decreased binding to LAP2α in late passage cells, which is consistent with a loss of Rb780 nuclear tethering in late passage cells. In addition, a decreased binding of LAP2α to lamin C in late passage cells is also consistent with a loss of nuclear anchorage of LAP2α upon extraction. This is contrast to early passage cells that show a strong binding of Rb780 to LAP2α/lamin C complexes and retain a stable pool of both LAP2α and Rb780 in the nucleus upon extraction.

**4.10 Nuclear anchorage of LAP2α, total Rb and hypo-phosphorylated Rb isoforms as assessed by *in situ* nuclear matrix extraction of Y259X laminopathy fibroblasts**

The above results show that in the absence of functional A-type lamins in Y259X fibroblasts, LAP2α tends to aggregate in the nucleus, which correlates with altered distribution and expression patterns of hypo-phosphorylated Rb in the nucleus. In late passage fibroblasts, decreased binding of A-type lamins to LAP2α and Rb780 led to their loss of nuclear anchorage upon extraction. It was hypothesized in the absence of functional A-type lamins in Y259X fibroblasts, LAP2α and hypo-phosphorylated Rb780 would show decreased nuclear anchorage upon extraction. To test this possibility, early **(p12)** passage Y259X fibroblasts were submitted to nuclear matrix extraction *in situ* via five sequential treatments with CSK, CSK-Triton X100, RSB-Magic, chromatin digestion by DNAse1 and 0.25 M ammonium sulphate and processed for double immunofluorescence microscopy using antibodies against: a) Lamin B2 and Ki67, b) LAP2α and Ki67, c) LAP2α and Rb780, and d) LAP2α and Rb795.

In early (p12) passage Y259X cells after V stage extraction **(Figure 4.12A (a) p12)**, a majority of nuclei (71%) retained lamin B2 strongly in the nucleus including 32% of ovoid shaped Ki67 positive nuclei **(see arrow)** and 39% of ovoid shaped Ki67 negative nuclei **(see arrowhead)**. 26% of dysmorphic Ki67 negative nuclei **(see *)** retained lamin B2 weakly in the nucleus. In early (p12) passage Y259X cells after V stage extraction **(Figure 4.12A (b) p12)**, 20% of cells did not retain LAP2α in the nucleus but retained aggregates at one pole of the nucleus and these cells were Ki67 negative. 15% of cells retained LAP2α relatively strongly in the nucleus and these cells were Ki67 positive. Another 20% of cells retained LAP2α weakly in the nucleus in addition to aggregates and these cells showed decreased Ki67 staining.

In early (p12) passage Y259X cells after III stage extraction **(Figure 4.12B (c) p12)**, cells which did not retain LAP2α strongly in the nucleus but retained LAP2α aggregates, did not retain Rb780 in the nucleus. In these cells, Rb780 was sometimes present in LAP2α aggregates. A minority of cells that retained LAP2α strongly in the nucleus also retained Rb780 strongly in the nucleus.

In early (p12) passage Y259X cells after V stage extraction **(Figure 4.12B (d) p12),** cells which did not retain LAP2α strongly in the nucleus and contained aggregates, did not retain nucleoplasmic Rb795 staining but retained Rb795 in distinct bright nuclear foci. In these cells, Rb795 was not present in LAP2α aggregates. A minority of cells that retained LAP2α relatively strongly following V stage extraction retained Rb795 strongly in the nucleoplasm. We then investigated nuclear anchorage of Rb795 in mid (p18) passage Y259X cells as majority of these cells only showed expression of Rb795 but not Rb780 in nuclei. In mid (p18) passage Y259X cells after V stage extraction **(Figure 4.12B (d) p18),** cells which did not retain LAP2α in the nucleus but displayed LAP2α aggregates still retained bright nuclear foci of Rb795. A minority of cells that retained LAP2α relatively strongly in the nucleus retained Rb795 strongly in the nucleoplasm.

Next, the nuclear anchorage of total Rb was assessed in relation to hypo-phosphorylated isoforms Rb780 and Rb795. Early **(p12)** and mid passage **(p18)** Y259X fibroblasts were submitted to a nuclear matrix extraction *in situ* and processed for double immunofluorescence microscopy using antibodies against: a) AB5 and Rb780 and, b) AB5 and Rb795. In early (p12) passage Y259X cells after V stage extraction **(Figure 4.13 (a) p12),** 40% of cells retained AB5 weakly in the nucleus and these cells did not retain Rb780 in the nucleus. A minority of cells (15%) retained AB5 strongly in the nucleus and these cells retained Rb780 strongly in the nucleus. In early (p12) passage Y259X cells after V stage extraction **(Figure 4.13 (b) p12),** cells that retained AB5 weakly in the nucleus retained Rb795 in bright nuclear foci but not in the nucleoplasm. A minority of cells that retained AB5 strongly in the nucleus retained Rb795 strongly in the nucleoplasm. In mid (p18) passage Y259X cells after V stage extraction **(Figure 4.13 (b) p18),** cells which retained AB5 weakly in the nucleus still retained bright nuclear foci of Rb795. A minority of cells that retained AB5 strongly in the nucleus retained Rb795 strongly in the nucleoplasm.

In summary, the above results show that upon extraction of Y259X laminopathy fibroblasts cells *in situ*, LAP2α tended to aggregate and showed a decreased retention in the nucleoskeleton, which is correlated with a loss nuclear anchorage of hypo-phosphorylated Rb780. In contrast, although hypo-phosphorylated Rb795 showed a decreased retention in the nucleoplasm, it was retained in distinct nuclear foci. Rb795

foci were also retained in mid passage Y259X cultures which show premature senescent arrest. The retention of Rb795 foci is consistent with some retention of total Rb in nuclei of Y259X fibroblasts.

### 4.11. Investigating the role of LAP2α in cell proliferation and nuclear anchorage of hypo-phosphorylated Rb in early passage fibroblasts using small interfering RNA

It can be seen that in the absence of functional A-type lamins in Y259X fibroblasts, LAP2α and hypo-phosphorylated Rb780 were not properly anchored in the nucleus. In addition, Y259X fibroblasts that show aggregation and/or loss of LAP2α in the nucleus underwent cell cycle arrest. Previous published work has shown that increasing LAP2α expression in serum re-stimulated early passage quiescent fibroblasts correlates with an increased anchorage of hypo-phosphorylated Rb in the nucleus (Markiewicz *et al.*, 2002a). In order to directly investigate the role of LAP2α in cell proliferation and nuclear anchorage of hypo-phosphorylated Rb, small interfering RNA (sRNAi) was used to knock-down LAP2α expression in early passage fibroblasts. sRNAi is a sequence-specific post-transcriptional gene silencing mechanism, which is triggered by double-stranded RNA (dsRNA) transfected into cells that causes degradation of mRNAs homologous in sequence to dsRNA (Harborth *et al.*, 2001).

For this purpose, early passage (p8) fibroblasts were seeded at a medium density and grown in complete medium for 24 hours after which cells were transfected with either small RNA oligonucleotides designed to interfere against LAP2α-specific mRNA or control RNAi oligonucleotides (GL2) targeting Firefly luciferase. Following transfection of LAP2α or GL2 RNAi into cells, cells were grown in culture for another 24 hours in the presence of serum and thereafter sub-cultured at 1:2 ratio and grown for further 24 hours in the presence of fresh serum. Sub-culturing of transfected cells was performed in order to decrease density of cells to a medium density at which we could readily assess the effect of LAP2α RNAi knockdown on cell proliferation. LAP2α protein is expressed in a cell cycle-dependent manner (Markiewicz *et al.*, 2002a), thus assessing the effect of LAP2α knockdown in transfected cells grown to a medium density and in the presence of serum allowed us to exclude the possibility that LAP2α became down-regulated in cells due to a lack of serum stimulation or growth of cells to a high density which normally trigger transient quiescent arrest in early passage cells.

LAP2α RNAi- and GL2 RNAi-transfected early passage (p8) fibroblasts grown to a medium density were then processed for double immunofluorescence microscopy using antibodies against: a) LAP2α and Ki67, b) LAP2β and Ki67, c) LAP2α and Rb780, and d) LAP2α and Rb795.

Firstly, the effect of LAP2α knock-down was assessed on cell proliferation using proliferation marker Ki67. In GL2 RNAi-transfected early (p8) passage fibroblasts **(Figure 4.14A (a) GL2 RNAi)**, a majority of nuclei (70%) displayed strong nucleoplasmic expression of LAP2α which correlated with a bright nucleolar expression of proliferation marker Ki67. The remaining 30% of cells had a decreased or absent LAP2α expression in the nucleus and these cells stained negatively for Ki67 marker (not shown). In LAP2α RNAi-transfected early (p8) passage fibroblasts **(Figure 4.14A (a) LAP2α RNAi)**, 80% of cells had a decreased nucleoplasmic expression of LAP2α indicating that LAP2α knockdown successfully occurred in those transfected cells. >70% of cells that showed knockdown of LAP2α expression in the nucleus displayed negative expression for proliferation marker Ki67. In addition, 20% of LAP2α RNAi-transfected cells still showed strong nucleoplasmic expression of LAP2α and these cells stained brightly for Ki67 marker. This result demonstrates that knock-down of LAP2α expression in early passage proliferating human fibroblasts triggers cell cycle arrest.

To confirm that the RNAi oligonucleotides used to knock-down LAP2α expression in transfected cells are specific for LAP2α, cells were stained for another LAP2 isoform, LAP2β, whose expression level is constant in proliferating and non-proliferating cells (Chapter 3). In GL2 RNAi-transfected early (p8) passage fibroblasts **(Figure 4.14A (b) GL2 RNAi)**, all cells displayed strong LAP2β expression in the nucleus whether they stained positively or negatively for Ki67. In LAP2α RNAi transfected early (p8) passage fibroblasts **(Figure 4.14A (b) LAP2α RNAi)**, ~60% of cells stained negatively for proliferation marker Ki67 and all these cells showed bright LAP2β expression in the nucleus. In addition, ~40% of cells which stained positively for Ki67 marker displayed strong LAP2β expression in the nucleus as equally strongly as cells which stained negatively for Ki67 marker. This result demonstrates that LAP2α RNAi oligonucleotides transfected into cells specifically knocked-down LAP2α expression in transfected cells and that cell cycle arrest triggered by knockdown of LAP2α expression in transfected cells is specific for this LAP2 isoform.

Next, the effect of LAP2α knock-down was assessed on expression and/or distribution of two hypo-phosphorylated Rb isoforms Rb780 and Rb795 in transfected cells. In GL2 RNAi-transfected fibroblasts (**Figure 4.14B (c) GL2 RNAi**), Rb780 showed a bright and somewhat granular nucleoplasmic expression in 70% of cells, which corresponded to a bright nucleoplasmic expression of LAP2α. 30% of cells showed a decreased or absent LAP2α expression in the nucleus, which corresponded to a decreased or absent Rb780 expression in the nucleus (not shown). In LAP2α RNAi-transfected fibroblasts (**Figure 4.14B (c) LAP2α RNAi**) 80% of cells showed a decreased expression of LAP2α in the nucleus, which corresponded to a decreased expression of Rb780 in the nucleus. In addition, 20% of LAP2α RNAi-transfected cells still showed strong nucleoplasmic expression of LAP2α, which corresponded to a bright and somewhat granular expression of Rb780 in the nucleus. This result demonstrates that knock-down of LAP2α expression in early passage proliferating fibroblasts causes down-regulation of hypo-phosphorylated Rb780 protein expression in the nucleus.

Furthermore, in GL2 RNAi-transfected fibroblasts (**Figure 4.14B (d) GL2 RNAi**), Rb795 showed a bright and granular nucleoplasmic expression in 70% of cells, which corresponded to a bright nucleoplasmic expression of LAP2α. 30% of cells showed a decreased or absent LAP2α expression in the nucleus, which corresponded to a decreased or absent Rb795 expression in the nucleus (not shown). In LAP2α RNAi-transfected fibroblasts (**Figure 4.14B (d) LAP2α RNAi**), 80% of cells showed a decreased expression of LAP2α in the nucleus and these cells showed decreased nucleoplasmic expression of Rb795 although Rb795 often showed either bright or weak small nuclear dots. In addition, 20% of LAP2α RNAi-transfected cells still showed strong nucleoplasmic expression of LAP2α, which corresponded to a bright and granular expression of Rb795 in the nucleus. This result demonstrates that knock-down of LAP2α expression in early passage proliferating fibroblasts causes down-regulation of hypo-phosphorylated Rb795 expression in the nucleoplasm with exception of small nuclear dots. All together these results show that a loss of expression of LAP2α in early passage proliferating fibroblasts induced cell cycle arrest that was accompanied by a decreased expression of nucleoplasmic forms of hypo-phosphorylated Rb.

## 4.12. Immunoblot analysis of protein expression of LAP2α and Rb780 in early passage fibroblasts following LAP2α knockdown by sRNAi

To confirm immunofluorescence results obtained for early passage fibroblasts following LAP2α knockdown by sRNAi, the immunoblot analysis of LAP2α protein expression was performed in LAP2α RNAi-transfected fibroblasts. For this purpose, early passage (p8) fibroblasts seeded at a medium density were grown in culture for one day and transfected with either RNA oligonucleotides designed to interfere against LAP2α-specific mRNA or control RNAi (GL2) oligonucleotides targeting Firefly luciferase as described above. After 24 hours, transfected cultures were sub-cultured, grown in culture for another 24 hours and harvested. Whole cell extracts were prepared from the same number of cells for both transfected cultures and immunoblotted using antibodies against LAP2α (LAP15), LAP2β (LAP17), lamin A/C (JOL2) and Rb phosphorylated on serine 780 (Rb780).

**Figure 4.15** shows that early (p8) passage cell extract prepared from fibroblasts transfected with LAP2α RNAi showed a significantly decreased expression of LAP2α protein as compared to that in early (p8) passage cell extract prepared from fibroblasts transfected with control (GL2) RNAi. Densitometry analysis of LAP2α protein bands in the extracts showed that the protein level of LAP2α was three times lower in the LAP2α RNAi cell extract as compared to that in the GL2 cells extract. To confirm equal protein loading, the above immunoblot was stripped and immunoblotted with LAP2β antibody. The protein expression of LAP2β was equal in both extracts confirming that a decreased protein expression of LAP2α in the LAP2α RNAi extract was caused by LAP2α-specific knockdown. The same extracts were immunoblotted with lamin A/C antibody which showed the same protein level of lamin C and slightly reduced level of lamin A in LAP2α extract indicating that LAP2α knock-down in early passage fibroblasts does not dramatically affect the protein expression of A-type lamins. Finally, the same extracts were immunoblotted with Rb780 antibody, which showed a significantly decreased expression of Rb780 protein in the LAP2α RNAi extract as compared to that in the GL2 RNAi extract. Densitometry analysis of Rb780 protein bands in the extracts showed that the protein level of Rb780 was three times lower in the LAP2α RNAi extract as compared to that in the GL2 RNAi extract. These results confirm earlier immunofluorescent analysis of LAP2α knock-down in early passage fibroblasts.

## 4.13. Distribution and nuclear anchorage of splicing factor compartments and Rb795 foci in late passage and Y259X laminopathy fibroblasts

30% of late passage fibroblasts showed bright nuclear foci of hypo-phosphorylated isoform Rb795, which were often rounder in shape and larger in size that Rb795 nuclear dots seen in 45% of late passage fibroblasts which also contained granular nucleoplasmic expression of Rb795 around these dots. Such a distinct localisation pattern and a detergent/high salt-resistant nuclear anchorage of Rb795 foci in late passage fibroblasts are highly reminiscent of the nuclear splicing factor compartments. Splicing factor compartments correspond to interchromatin granule clusters and are also dispersed in the nucleoplasm on perichromatin fibrils, which contain nascent transcripts (Spector *et al.,* 1993, Fakan *et al.,* 1994). Therefore a distribution of Rb795 foci was investigated in relation to splicing factor compartments in late passage nuclei. Early passage **(p7)** and late-passage **(p44)** fibroblasts were processed for double immunofluorescence microscopy using antibodies against splicing factor SC-35 (spliceosome component of 35 kDa) which is a component of splicing factor compartments and hypo-phosphorylated isoform Rb795.

In early (p7) passage HDF **(Figure 4.16A (a) p7)**, a majority of cells showed distinct speckled pattern of splicing factor SC-35 and a broad nucleoplasmic meshwork around the speckles. In these cells, Rb795 showed granular nucleoplasmic distribution that was broader than that of SC-35 and partially co-localised with SC-35 in the nucleoplasm and less so with SC-35 speckles. In late (p44) passage HDF **(Figure 4.16A (a) p44)**, a majority of cells showed larger and more pronounced SC-35 speckles which completely co-localised with Rb795 in cells which displayed distinct large Rb795 foci. In these cells both SC-35 and Rb795 showed a decreased nucleoplasmic distribution. In cells that contained brighter nucleoplasmic distribution of Rb795 in addition to foci, SC-35 co-localised with Rb795 both in foci and in the nucleoplasm (not shown).

Lamin A has been proposed to be involved in organisation and dynamics of splicing factor compartments (Jagatheesan *et al.,* 1999). To investigate whether in the absence of functional A-type lamins in Y259X fibroblasts splicing factor compartments show altered nuclear distribution, early **(p12)** and mid-passage **(p18)** Y259X fibroblasts were processed for double confocal microscopy using antibodies against SC-35 factor and Rb

isoform Rb795. In early passage (p12) Y259X fibroblasts **(Figure 4.16A (b) p12),** 20% of cells that showed distinct Rb795 foci also showed more pronounced SC-35 speckles, which completely co-localised with Rb795 foci. In these cells, Rb795 nucleoplasmic distribution was somewhat broader than that of SC-35. By mid passage p18 **(Figure 4.16A (b) p18)**, Y259X cells showed increased proportion of nuclei with distinct Rb795 foci (40%) and these cells showed large and pronounced SC-35 speckles which completely co-localised with large Rb795 foci. In these cells both SC-35 and Rb795 showed decreased nucleoplasmic distribution and lower foci number.

Splicing factor compartments are components of detergent/high salt insoluble nuclear matrix (Spector *et al.*, 1993). The focal distribution of Rb795 in late passage nuclei was particularly prominent after *in situ* nuclear matrix extraction. To investigate nuclear anchorage of Rb795 foci in relation to splicing factor compartments in late passage cells, early passage **(p7)** and late-passage **(p44)** fibroblasts were extracted *in situ* by detergent/nuclease/salt extraction and processed for double confocal microscopy using antibodies against SC-35 factor and Rb795 isoform. In early (p7) passage HDF after V stage extraction **(Figure 4.16B (a) p7)**, a majority of cells retained Rb795 strongly in the nucleoplasm in addition to prominent nuclear dots and these cells retained SC-35 strongly both in the nucleoplasm and in more prominent nuclear speckles. In these cells, Rb795 prominent dots and SC-35 speckles co-localised more often than before extraction. In contrast, in late (p44) passage HDF after V stage extraction **(Figure 4.16B (a) p44)**, a majority of cells retained bright nuclear foci of Rb795 and lacked nucleoplasmic distribution and these cells retained SC-35 in large nuclear speckles which completely co-localised with large Rb795 foci. In these cells, nucleoplasmic distribution of SC-35 was retained somewhat more intensely than that of Rb795.

To investigate whether absence of functional A-type lamins in Y259X laminopathy fibroblasts alters nuclear anchorage of splicing factor compartments, early **(p12)** and mid-passage **(p18)** Y259X fibroblasts were extracted *in situ* by detergent/nuclease/salt extraction and processed for double confocal microscopy using antibodies against splicing factor SC-35 and Rb isoform Rb795. In early (p12) passage Y259X cells after V stage extraction **(Figure 4.16B (b) p12)**, a majority of nuclei retained bright nuclear foci of Rb795 and these cells retained prominent SC-35 speckles. In these cells both SC-35 and Rb795 retained more intense nucleoplasmic distribution. In mid (p18)

passage Y259X cells after V stage extraction (**Figure 4.16B (b) p18**), a majority of cells retained bright nuclear foci of Rb795 and lacked nucleoplasmic distribution and in these cells SC-35 was retained in larger nuclear speckles which completely co-localised with larger Rb795 foci. In these cells, nucleoplasmic distribution of SC-35 was retained more intensely than that of Rb795.

## 4.14. Distribution and nuclear anchorage of splicing factor compartments and Rb795 during G1 phase of cell cycle in early passage wild-type fibroblasts

Interestingly, it was observed that 10% of early passage fibroblasts showed Rb795 in small nuclear dots that co-localised with SC-35 speckles. Hypophosphorylated Rb is known to bind to nuclear matrix protein p84 associated with speckle compartments during early G1 phase of cell cycle (Durfee *et al.*, 1994). This prompted me to examine Rb795 distribution in relation to speckle compartments during G1 phase of early passage cells. Early (p7) passage fibroblasts were grown in culture for 2 days and synchronised by serum starvation for 4 days. Cell cultures were serum re-stimulated for either 6, 12, 18 or 24 hours and processed for immunofluorescence microscopy using antibodies against splicing factor SC-35 and Rb 795 isoform.

During early G1 phase (6 hour post-restimulation) (**Figure 4.17A (a)**), 10-20 small dots of Rb795 were visible without nucleoplasmic distribution and these co-localised with bright speckles of SC-35 that showed markedly decreased nucleoplasmic meshwork. During early-mid G1 (12 hour post-restimulation) (**Figure 4.17A (b)**), Rb795 was present more brightly in nuclear dots and in the nucleoplasm and co-localised with SC-35 speckles and somewhat brighter nucleoplasmic meshwork. During mid-late G1 (18 hour post-restimulation) (**Figure 4.17A (c)**), Rb795 showed bright nucleoplasmic distribution with prominent nuclear dots that partially co-localised with bright SC-35 nuclear speckles and nucleoplasmic meshwork. During early S-phase (24 hour post-restimulation) (**Figure 4.17A (d)**), Rb795 showed bright granular nucleoplasmic distribution and lacked prominent nuclear dots whilst SC-35 remained in prominent nuclear speckles and nucleoplasmic meshwork.

The co-localisation of Rb795 isoform with splicing speckles during early to mid G1 phase of cell cycle suggests that Rb795 physically associates with splicing speckles

during this period, which could be involved in its nuclear tethering. To investigate this possibility, early (p7) passage quiescent fibroblasts were serum re-stimulated for either 6, 12, 18 or 24 hours, extracted *in situ* by detergent/nuclease/salt extraction and processed for double immunofluorescence microscopy using antibodies against splicing factor SC-35 and Rb 795 isoform.

During early G1 (6 hour post-restimulation) **(Figure 4.17B (a))**, Rb795 speckled distribution that co-localised with SC-35 speckles was retained after extraction. During early-mid G1 (12 hour post-restimulation) **(Figure 4.17B (b))**, Rb795 speckles and interconnected nucleoplasmic meshwork that co-localised with SC-35 splicing speckles and nucleoplasmic meshwork were resistant to extraction. During mid-late G1 (18 hour post-restimulation) **(Figure 4.17B (c))**, Rb795 prominent nuclear dots and bright nucleoplasmic meshwork were resistant to extraction although they did not significantly co-localise with SC-35 splicing speckles and bright nucleoplasmic meshwork. During early S phase (24 hour post-restimulation) **(Figure 4.17B (d))**, Rb795 nucleoplasmic meshwork was not retained whilst SC-35 splicing speckles and nucleoplasmic meshwork were retained after extraction.

## 4.15 Investigation of internal heterochromatin distribution and Rb795 foci in late passage wild type and Y259X laminopathy fibroblasts by confocal microscopy

In late passage dysmorphic nuclei, distribution of peripheral heterochromatin at the nuclear periphery is decreased or absent and instead late passage cells show condensed regions of chromatin located centrally in nuclei. These condensed regions of chromatin often correlated with A-type lamin accumulation in the nucleoplasm and LAP2α aggregation. By definition, regions of the chromatin that stain intensely and appear condensed correspond to heterochromatin (Taddei *et al.*, 1999). Interestingly, recent work showed that certain fibroblast cell types accumulate internal heterochromatin foci during senescence *in vitro*, which partially recruit Rb protein in repressing transcription at gene-specific E2F promoters. Therefore the internal chromatin distribution was investigated for the presence of heterochromatin foci in late passage nuclei in order to examine whether Rb795 nuclear foci represent Rb population recruited to heterochromatin foci. Early passage **(p7)** and late-passage **(p44)** fibroblasts were

processed for confocal microscopy using Rb795 antibody and a DNA-intercalating dye DAPI.

In early (p7) passage HDF **(Figure 4.18 (a) p7)**, DAPI staining showed a relatively uniform chromatin distribution in the nuclei and stained chromatin brightly at the nuclear periphery and inside the nuclei. Most nuclei contained condensed chromatin (heterochromatin) surrounding the nucleoli as expected (Taddei *et al.*, 1999). Internal chromatin foci were never observed. The uniform chromatin distribution in early (p7) passage nuclei correlated with a broader granular nucleoplasmic distribution of Rb795. Upon closer investigation of DAPI-stained chromatin in late (p44) passage nuclei, we did not observe that formation of heterochromatin foci was a general feature of senescent arrest in late passage fibroblasts we used. However, 10% of late passage nuclei had a more distinct distribution to their internal chromatin **(Figure 4.18 (a) p44)**. In these cells, DAPI staining of chromatin revealed a few focal areas of condensed internal chromatin and decreased chromatin distribution at the nuclear periphery. These focal areas of condensed chromatin partially co-localised with Rb795 nuclear foci. In these cells, nucleoplasmic distribution of Rb795 was absent.

Since laminopathy fibroblasts enter senescence prematurely and retain Rb795 foci, we investigated whether formation of heterochromatin foci accompanied premature senescent arrest in Y259X laminopathy fibroblasts. Early **(p12)** and mid-passage **(p18)** Y259X fibroblasts were processed for confocal microscopy using Rb795 antibody and a DNA-intercalating dye DAPI. In early (p12) passage Y259X cells **(Figure 4.18 (b) p12)**, DAPI staining of chromatin did not reveal internal heterochromatin foci in nuclei that showed distinct Rb795 foci. As observed before, DAPI staining showed decreased peripheral chromatin distribution and highly condensed regions of internal chromatin that correlated with appearance of Rb795 foci. By mid passage p18 **(Figure 4.18 (b) p18)**, Y259X cells showed increased proportion of nuclei with distinct Rb795 foci but only 6% of nuclei revealed focal areas of condensed internal chromatin which partially co-localised with Rb795 foci. In these cells, nucleoplasmic distribution of Rb795 was absent.

## 4.16. Cellular localisation of DNA damage foci and Rb795 foci in late passage wild type and Y259X fibroblasts by confocal microscopy

Senescent fibroblasts incur extensive DNA damage as a result of both telomere shortening and oxidative stress-induced random DNA damage (von Zglinicki *et al.*, 2005). These sites of DNA damage accumulate phospho-histone H2A.X proteins that form distinct nuclear foci. DNA repair proteins assemble at these foci indicating that foci represent active sites of DNA damage repair pathway (d'Adda di Fagagna *et al.*, 2003). Interestingly, active localisation of hypo-phosphorylated Rb on chromatin occurs in response to DNA damage (Avni *et al.*, 2003). These findings prompted me to examine whether hypo-phosphorylated Rb795 foci accumulate at the sites of DNA damage in late passage cells. Early passage **(p7)** and late-passage **(p44)** fibroblasts were processed for double confocal microscopy using antibodies against phospho-histone H2A.X (a marker for senescence-associated DNA damage foci) and Rb795 isoform.

In early (p7) passage HDF **(Figure 4.19 (a) p7)**, histone H2A.X foci were absent in most cells and only a few cells had one or two detectable histone foci. In these cells, Rb795 distribution was somewhat more granular and partially co-localised with one or two observed histone foci. In late (p44) passage cells **(Figure 4.19 (a) p44)**, phospho-histone H2A.X was present in distinct foci scattered inside the nucleus and around the nuclear periphery in most cells. These foci varied in size and number between cells most likely reflecting differences in the extent of DNA damage. Interestingly, Rb795 foci did not directly co-localise with phospho-histone foci but they showed a very distinct relationship to each other. Histone foci were always found at the periphery of commonly larger Rb795 foci and they sometimes showed a slight overlap. Histone foci were almost never seen without adjacent Rb795 foci although Rb795 foci were seen alone.

Laminopathy fibroblasts that enter premature senescent arrest do not show increased oxidative-stress related modifications to mutated lamins (Chapter 3). Apart from oxidative stress and telomere shortening, senescence-associated DNA damage signalling can be triggered by a loss of or dominant-negative assembly of telomere-binding proteins (von Zglinicki *et al.*, 2005). Therefore, it was hypothesized that increased aggregation of telomere-binding protein LAP2α in laminopathy fibroblasts

triggers DNA damage-induced premature senescence. To investigate whether premature senescent arrest in laminopathy cells engages DNA damage signalling, we examined whether laminopathy cells accumulate sites of DNA damage adjacent to Rb795 foci. Early passage **(p12)** and mid-passage **(p18)** Y259 laminopathy fibroblasts were processed for double confocal microscopy using antibodies against phospho-histone H2A.X and Rb795 isoform.

Surprisingly, in early (p12) passage Y259X cells **(Figure 4.19 (b) p12)**, 15% of nuclei displayed a significant number of phospho-histone H2A.X foci. Rb795 foci were seen in close proximity to histone foci and often showed overlap. By mid passage 18 **(Figure 4.19 (b) p18)**, 34% of Y259X nuclei displayed histone foci that increased in number and were scattered inside the nucleus and around the nuclear periphery. Histone foci were found at the periphery of larger Rb795 foci and were closely associated with them. In conclusion, since Rb795 foci appear in Y259X cells that show LAP2α aggregates and cell cycle arrest, the presence of histone foci in cells with Rb795 foci suggests that LAP2α aggregation may trigger DNA damage-induced premature senescent arrest.

## Discussion

In this chapter it was set out to explore whether hypo-phosphorylated Rb isoforms mediate senescent arrest and how A-type lamins and LAP2α may regulate Rb pathway in ageing and laminopathy fibroblasts.

### Senescent fibroblasts show a decreased expression of Rb780 and distinct foci of Rb795

Initially, I investigated protein expression of total Rb during ageing of fibroblasts *in vitro.* Consistent with other reports (Stein *et al.,* 1990, Stein *et al.,* 1999), aging fibroblasts show gradual decrease in expression of faster-migrating Rb species on SDS-PAGE although the total protein level of Rb remains constant. Therefore, during ageing of fibroblasts *in vitro* Rb protein becomes progressively de-phosphorylated with a subsequent accumulation of faster-migrating Rb species on SDS-PAGE. An accumulation of faster migrating Rb species in senescent fibroblasts can represent both un-phosphorylated and hypo-phosphorylated Rb species due to co-migration of un-phosphorylated and hypo-phosphorylated Rb species on SDS-PAGE (Ezhevsky *et al.,* 2000). This is because some phosphorylations of Rb during early G1 by cyclin D complexes do not introduce a shift in Rb mobility. Rb is hypo-phosphorylated on serine 780 and serine 795 during early G1 (Boylan *et al.,* 1999, Garnovskaya *et al.,* 2004, Kitigawa *et al.,* 1996) by cdk4/D1 complexes (Zarkowska and Mittnacht 1997, Connell-Crowley *et al.,* 1997, Pan *et al.,* 1998, Grafstrom *et al.,* 1999). Surprisingly, ageing fibroblasts show a decreasing phosphorylation of Rb on serine 780. On the other hand, although the level of nucleoplasmic Rb795 decreased considerably in 30% of late passage fibroblasts, this cell population contained Rb795 in distinct nuclear foci which were often larger in size and rounder in shape than Rb795 granules and dots seen in early passage fibroblasts. The presence of Rb795 in majority of late passage fibroblasts indicates that late passage cells contain a distinct population of hypo-phosphorylated Rb which contributes to accumulation of faster migrating Rb species on SDS-PAGE.

**Aberrant A-type lamins assembly and LAP2α aggregation in senescent fibroblasts correlate with a loss of Rb780 expression and appearance of distinct foci of Rb795**

In late passage fibroblasts, LAP2α and A-type lamins are aberrantly organised in the nucleus (Chapter 3). Since these proteins bind to hypo-phosphorylated Rb and can influence its cellular distribution (Markiewicz *et al.,* 2002a), I investigated how the observed changes in their nuclear organisation in senescent fibroblasts influence distribution and/or expression of hypo-phosphorylated Rb isoforms. Interestingly, late passage dysmorphic nuclei which contain lamin A/C herniations and/or honeycombs and accumulate intranuclear lamin A/C aggregates have a decreased or absent Rb780 expression. These dysmorphic nuclei also show a tendency of LAP2α to become heavily granulated and/or to aggregate (Chapter 3). In contrast, Rb795 lacked nucleoplasmic distribution in dysmorphic nuclei but remained present in distinct nuclear foci. Summarising the results obtained on relative proportions of LAP2α, Rb780 and Rb795 expression in senescent fibroblasts, 45% nuclei had all three proteins expressed, 20% of nuclei had LAP2α and Rb795 but not Rb780 and 10% of nuclei had Rb795 but not LAP2α or Rb780. Therefore, late passage fibroblasts show a deviation from a typical cell cycle dependent co-localisation between LAP2α and Rb isoforms seen in early passage proliferating cells.

**LAP2α aggregation and Rb795 nuclear foci correlate with premature senescent arrest in laminopathy fibroblasts**

To directly test the findings that aberrant assembly of A-type lamins in senescent fibroblasts affects distribution of LAP2α and hypo-phosphorylated Rb, I employed laminopathy fibroblasts with a homozygous Y259X non-sense mutation that are functionally null for A-type lamins. Y259X laminopathy fibroblasts accumulate nuclear abnormalities and undergo premature senescence (Chapter 3). In lamin A/C null fibroblasts, LAP2α is aberrantly mislocalised in the nucleus and tends to form aggregates. Lamin A/C null cells with LAP2α aggregates show a loss of proliferative potential. In addition, the increase in nuclear abnormalities and LAP2α aggregation in mid passage lamin A/C null laminopathy fibroblasts correlates with premature senescent arrest. In Y259X fibroblasts, LAP2α mislocalisation in the nucleus affected distribution of hypo-phosphorylated Rb isoforms in the nucleus. Cells with LAP2α

aggregates had a decreased or absent Rb780 expression, whilst expression of Rb795 became limited to distinct nuclear foci. LAP2α aggregation and altered distribution of hypo-phosphorylated Rb in laminopathy Y259X fibroblasts is reminiscent of senescent fibroblasts. Therefore abnormal LAP2α distribution in lamin A/C null fibroblasts disrupts distribution of hypo-phosphorylated Rb, which leads to premature senescent arrest. In addition, mid passage lamin A/C null fibroblasts showed a loss of expression of hyper-phosphorylated Rb and accumulation of faster-migrating Rb species on SDS-PAGE consistent with a premature entry into senescent state. Recently, it has been shown that in A-type lamin null mouse fibroblasts Rb protein level decreased because Rb became targeted for degradation by the proteosome (Johnson *et al.*, 2004). In contrast to lamin A/C null mouse fibroblasts, the total amount of Rb did not significantly change in lamin A/C null human fibroblasts, which indicates that Rb becomes targeted for de-phosphorylation.

**Late passage fibroblasts show a loss of nuclear anchorage of Rb780 but not of total Rb upon extraction**

The growth suppressing activity of hypo-phosphorylated Rb correlates with its nuclear matrix association during G1 phase of cell cycle (Mittnacht and Weinberg 1991). A-type lamins and LAP2α bind to hypo-phosphorylated Rb780 in the nucleus (Markiewicz *et al.*, 2002a) and are proposed to regulate its nuclear anchorage. My results show that in early passage fibroblasts, formation of detergent/salt resistant nucleoskeleton by A-type lamins and LAP2α stably anchors Rb780 in the nucleus. Senescent fibroblasts show increased solubility/instability of A-type lamins, which leads to a loss of LAP2α from nucleoskeleton upon nuclear matrix extraction (Chapter3). Consistent with this finding, A-type lamins and LAP2α do not support stable anchorage of Rb780 in the nucleus and consequently Rb780 is lost from the nucleoskeleton upon extraction. A loss of nuclear anchorage of LAP2α and Rb780 in late passage fibroblasts is supported by findings that LAP2α shows decreased binding to A-type lamins and that Rb780 isoform shows decreased binding to LAP2α in the nuclei of late passage cells. Nonetheless, some Rb protein does remain stably anchored in nucleoskeleton. My results reveal that hypo-phosphorylated isoform Rb795 remained anchored in the nucleus of late passage cells within distinct nuclear foci and would therefore contribute to nuclear anchorage of faster-migrating Rb protein on SDS-PAGE. Interestingly, *in situ* nuclear matrix

extraction uncovered more Rb795 antigens as higher intensity and more foci were seen. In addition, upon extraction of lamin A/C null fibroblasts *in situ*, stable retention of LAP2α in nucleoskeleton correlated with a stable retention of both hypo-phosphorylated isoforms Rb780 and Rb795 in the nucleoplasm. However, upon nuclear matrix extraction in majority of cells LAP2α tends to aggregate and shows a decreased or loss of retention in the nucleoskeleton, which correlates with a loss nuclear anchorage of hypo-phosphorylated Rb780. In contrast, although hypo-phosphorylated Rb795 shows a decreased retention in the nucleoplasm, Rb795 is retained in distinct nuclear foci. These results suggest that a loss of functional A-type lamins leads to a loss of nuclear anchorage of LAP2α and hypo-phosphorylated Rb780. Therefore binding of A-type lamins and LAP2α to hypo-phosphorylated Rb may be a requisite substrate for nuclear anchorage-dependent Rb phosphorylation.

What would be the mechanism behind Rb780 dephosphorylation? One clue to this question may come from the mechanism of Rb dephosphorylation during M phase by protein phosphatase PP1 (reviewed in Berndt *et al.,* 2003). Whilst the activity of this phosphatase is predicted to de-phosphorylate Rb to a hypo-phosphorylated form by interacting with hyper-phosphorylated Rb population, PP1 phosphatase preferentially interacts with hypo-phosphorylated forms and Rb780 is one of the four preferential sites of interaction (Tamrakar *et al.,* 1999). Moreover, at the end of mitosis, unlike other Rb isoforms, Rb780, Rb795 and Rb807 do not become de-phosphorylated but are increasingly phosphorylated (Tamrakar *et al.,* 2000). On the other hand, active PP1-mediated dephosphorylation of hypo-phosphorylated Rb occurs during hypoxic stress (Krtolica *et al.,* 1998). The mechanism behind Rb/PP1 binding is thought to involve other proteins that would facilitate their binding and regulate phosphatase activity. Interestingly mutant forms of Rb which are under-phosphorylated but do not become tethered in the nucleus, are also unable to become hyperphosphorylated (Mittnacht and Weinberg 1991). Thus it was suggested that Rb becomes a substrate for phosphorylation only when bound to its nuclear binding partners, which tether it to the nucleus. I propose that one such nuclear binding protein may be A-type lamins. Lamins are de-phosphorylated by PP1 phosphatase at the end of mitosis through G1 phase of cell cycle, which promotes lamina assembly (Thompson *et al.,* 1997). Binding of A-type lamins to Rb780/PP1 during G1 phase may prevent untimely dephosphorylation of Rb by PP1 and ensure timely progression through G1 phase.

**LAP2α knockdown in early passage proliferating fibroblasts causes cell cycle arrest and a loss of nuclear expression of Rb780**

Previous published work has shown that increasing LAP2α expression in serum-restimulated early passage quiescent fibroblasts correlates with an increased anchorage of hypo-phosphorylated Rb in the nucleus (Markiewicz *et al.,* 2002a). In order to directly investigate the role of LAP2α in cell proliferation and nuclear anchorage of hypo-phosphorylated Rb, I used small interfering RNA (sRNAi) to knock-down LAP2α expression in early passage fibroblasts. sRNAi is a sequence-specific post-transcriptional gene silencing mechanism which has been recently used to knock-down lamins in cells (Harborth *et al.,* 2001). My results show that LAP2α knockdown in early passage fibroblasts causes cell cycle arrest. This result is supported by the recent observation that cells with greater reductions of LAP2α after LAP2α knock-down exhibited impaired growth (Suzuki *et al.,* 2004, unpublished data). Knock-down of LAP2α expression in early passage proliferating fibroblasts caused down-regulation of hypo-phosphorylated Rb. Whilst hypo-phosphorylated Rb780 isoform showed a decreased or complete loss of expression in cells which showed decreased expression of LAP2α after LAP2α knock-down, Rb795 expression was decreased in the nucleoplasm with exception of small nuclear dots. These results suggest that in human fibroblasts LAP2α expression is required for expression and nuclear anchorage of hypo-phosphorylated Rb. Interestingly, the presence of Rb795 in a few small nuclear dots in LAP2α knock-down cells suggests that some expression of Rb795 does not depend on LAP2α expression. These Rb795 dots were significantly smaller and weaker than Rb795 foci seen in senescent fibroblasts.

**Rb795 nuclear foci co-localise with splicing compartments in senescent and lamin A/C null fibroblasts**

A distinct localisation pattern and a detergent/high salt-resistant nuclear anchorage of Rb795 foci in late passage fibroblasts are highly reminiscent of the nuclear splicing factor compartments. RNA splicing factors are present in high concentrations in the speckles called splicing factor compartments. Splicing factor compartments are located in the interchromatin regions and regions of low DNA density where actively transcribed chromatin is found (Carter *et al.,* 1991, Spector *et al.,* 1993, Fakan *et al.,*

1994). The transcription sites, active RNA polymerase II and splicing factor compartments are associated with a detergent/high salt insoluble nuclear matrix (Kimura *et al.,* 1999). One of the most studied components of splicing factor compartments is splicing factor SC-35 (Fu and Maniatis 1990) which is involved in the first step of splicing during 5' and 3' splice site selection of alternatively spliced mRNAs (Xiang-Ding *et al.,* 1992). My results show that in senescent nuclei splicing factor SC-35 tends to form large and round nuclear speckles. These speckles completely co-localised with Rb795 nuclear foci. Interestingly, N-terminal domain of hypo-phosphorylated Rb binds to nuclear matrix protein p84 associated with speckle compartments during early G1 phase of cell cycle (Durfee *et al.,* 1994). This result prompted me to examine whether Rb795 co-localises to speckle compartments during G1 phase in early passage proliferating cells. My results show that Rb795 revealed distinct localisation patterns during G1 phase of synchronously growing fibroblasts. Rb795 shows a significant co-localisation with SC-35 speckles during early-mid G1 but not during later stages of G1 phase or during S-phase. Since Rb795 speckles during early G1 show resistance to nuclear matrix extraction, it suggests that Rb795 may physically associate with splicing speckles during this period, which could be involved in its nuclear tethering. Rb795 speckles during early G1 are also reminiscent of Rb795 dots seen after knock-down of LAP2α in human fibroblasts, which indicates that LAP2α knock-down may cause cell cycle arrest in early G1.

Splicing factor compartments are involved in dynamic shuttling of splicing factors between the speckles and the nucleoplasm (Misteli *et al.,* 1997), and their size can change depending on RNA splicing and/or transcriptional levels in the cell; they become considerably enlarged due to a reduced disassociation of splicing factors from the speckles in the presence of transcriptional inhibitors (Spector *et al.,* 1993), in pathological conditions (Fakan and Puvion 1980), upon inhibition of splicing (O'Keefe *et al.,* 1994) or as a result of heat shock (Mintz *et al.,* 1999). In early passage cells, splicing factor compartments were present in smaller speckles and in the nucleoplasmic meshwork around speckles indicating a dynamic recruitment of splicing factor compartments in transcriptionally active early passage cells. Since in senescent cells SC-35 accumulates in enlarged speckles, it suggests that in senescent cells transcription and/or splicing activities in the cells may be reduced or altered. In addition, the presence of Rb795 in larger foci may also indicate that some Rb795 becomes redistributed from

the nucleoplasm to speckles that become enlarged. Interestingly, during early G1, transcriptional activity is the lowest and increases during cell cycle (Bregman *et al.,* 1995, Zeng *et al.,* 1997) concomitant with increased Rb phosphorylation. Therefore the mechanism of Rb association with splicing compartment during early G1 may depend on the level of Rb phosphorylation, which in turn may regulate the level of transcription. This interpretation is supported by the findings that hyper-phosphorylated Rb does not bind to speckle-associated p84 protein during late G1 or during S phase. Interestingly, in senescent cells, increased RNA accumulation (Schneider and Shorr 1975) and altered RNA distribution patterns (Johnson *et al.,* 1976) have been reported to occur due to defective RNA processing (Wolfe *et al.,* 1980, Schroder *et al.,* 1987, Muller *et al.,* 1993) and/or decreased mRNA transport (Maciera-Coelho *et al.,* 1966, Muller *et al.,* 1993). Therefore Rb795 may regulate post-transcriptional gene expression by inhibiting availability of splicing factors to certain sites of transcription and thus altering splicing patterns. Interestingly, viral oncoproteins that bind to and inactivate hypo-phosphorylated Rb, cause redistribution of SC-35 splicing factors and RNA polymerise from speckles to sites of transcription (Bridge *et al.,* 1993, Jimenez-Garcia and Spector 1993). This further suggests that Rb association with speckles may be one of the mechanisms by which dynamic redistribution of splicing factors occurs within speckles.

An important issue regarding spatial organisation of transcription and pre-mRNA splicing, concerns an involvement of underlying nuclear architecture. Using an energy transmission electron microscopy, it was demonstrated that the underlying protein architecture in speckles physically connects the relatively dispersed granules within the cluster (Henzdel *et al.,* 1999). Recently, lamin A has been found to co-localise with splicing speckles and was proposed to regulate their dynamics and organisation (Jagatheesan *et al.,* 1999). My results show that in absence of A-type lamins in lamin A/C null fibroblasts, splicing factors were enlarged but were still stably anchored in the nucleus. In line with this finding, it has been recently shown that splicing factor compartment formation and stability does not depend on A-type lamins as seen in lamin A/C null mouse fibroblasts (Vecerova *et al.,* 2004). However, our observations of enlarged speckles in human lamin A/C null fibroblasts argues that A-type lamins may indirectly influence organisation of splicing factor compartments by affecting RNA transcription. Interestingly, lamin mutants have recently been found to inhibit RNA pol

II transcription by sequestering a TATA binding protein (TBP) into aggregates that is necessary for formation of pre-initiation complexes on RNA pol II promoters containing TATA box (Spann *et al.,* 2002). In addition, N-deletion lamin A mutants caused a coordinate loss of internal lamin speckles and splicing speckles (Kumaran *et al.,* 2002). Moreover, fibroblasts from patients with lamin A/C mutations which show internal lamin A/C aggregates display enlarged splicing speckles and reduced RNA transcription (Cappani *et al.,* 2003). Interestingly, a recent report has shown that RNA pol II becomes mislocalised to nuclear aggregates at one pole of the nucleus in fibroblasts with lamin mutations (Reichart *et al.,* 2004). RNA pol II aggregation in cells with lamin mutations is highly reminiscent of the position of LAP2α aggregates in lamin A/C null cells. Altogether these results suggest that A-type lamins support stable association of RNA poll transcription in the nucleus. Similarly to splicing speckles, the presence and stability of Rb795 speckles in lamin A/C null fibroblasts is by implication also independent of A-type lamins. In addition, stable nuclear anchorage of Rb795 foci in the absence of A-type lamins' resistance to extraction in senescent fibroblasts supports the above argument. Interestingly, the ultrastructural studies have shown that Rb protein appears as granules of heterogeneous size over the interphase nuclei and that it was predominantly localised in euchromatic areas with low DNA density (Szekely *et al.,* 1991). The largest positive grains lined up on the heterochromatin/euchromatin boundary. Such a heterogeneous distribution of Rb is thought to be spatially organised by nuclear matrix scaffolding. These findings suggest that in the absence of A-type lamins or in due to its aberrant assembly, Rb795 distribution may be altered in a way that leads to its increased presence and/or association with splicing speckles.

**The mechanism of Rb795 growth-suppression during senescent arrest**

It has been shown that differential site-specific phosphorylation of Rb within functional domains may modulate Rb functional interactions involved in its growth-suppressing activities. The complexity of Rb hypo-phosphorylation has been overlooked since its first discovery (in Ezhevsky *et al.,* 2001). Two-dimensional polypeptide analysis of *in vivo* hypo-phosphorylated Rb showed that 13 out of 16 phospho sites are occupied suggesting that hypo-phosphorylated Rb may be compromised of a complex mixture of multiple phospho-isoforms containing a limited number of phosphates per Rb molecule (Mittnacht *et al.,* 1994). Interestingly, some hypo-phosphorylated isoforms have higher

affinities for binding to E2F than others, which suggests that hypo-phosphorylated Rb remains as both the active and passive repressor of E2F-responsive genes (Ezhevsky *et al.,* 2001). Rb795 has been shown to be a first serine site phosphorylated in smooth muscle cells upon mitogenic signalling which led to a 30% decrease in Rb/E2F binding (Garnovskaya *et al.,* 2004). Rb780 is also phosphorylated during early G1 *in vivo* but was not found in complexes with E2F (Kitigawa *et al.,* 1996). Moreover, mutation of ser795 to alanine did not abolish the E2F binding but prevented Rb from getting inactivated (Knudsen and Wang 1997, Connell-Crowley *et al.,* 1997). Given the heterogeneity of E2F regulated promoters Rb is thought to represses transcription in many different ways. Rb can indirectly repress transcription via either recruitment of histone deacetylases (Luo *et al.,* 1998, Brehm *et al.,* 1998) or heterochromatin binding protein HP1 (Nielsen *et al.,* 2001). Recent report has shown that in senescent fibroblasts Rb may repress transcription through recruitment of histone deacetylases and heterochromatin binding protein HP1 (Narita *et al.,* 2003). However, very small amount of Rb protein was found in complexes with these proteins. Previous reports have showed that in senescent cells E2F/Rb binding is essentially undetectable (Dimri and Campisi 1994) and that Rb may have targets other than E2F in senescent cells. This is because E2F has been found to regulate transcription of genes important for DNA damage signalling pathway, which is actively maintained in senescent cells (von Zglinicki *et al.,* 2005). Cells ectopically expressing E2F1 or 2 induce expression of DNA damage repair protein Rad51 by several fold (Ishida *et al.,* 2001). Moreover, Dimri and Campisi 1994 propose that Rb may inhibit transcription by interacting with TFIID or TFIID-associated proteins in senescent cells. Indeed, Rb can directly bind to TBP-associated factor TAFII250 that is a central player of TFIID basal transcriptional complex. Furthermore, although Rb growth-suppressing activity is dependent on the interactions with E2F through its C-terminal domains, N-terminal domain has also been implicated in growth-suppression function. Mutations in the N-terminal region disrupt the interaction with C-terminal domains that is important for Rb oligomerisation (Hensey *et al.,* 1994). All together the above reports suggest that Rb795 mechanism of growth-suppression in senescent fibroblasts may not occur directly through E2F signalling but more indirectly through its N-terminal association with splicing speckles.

**Senescent fibroblasts and lamin A/C null fibroblasts do not reveal internal heterochromatin foci but show areas of condensed internal chromatin**

It has been recently shown that during senescence of certain fibroblast types (IMR90 and WI38), internal chromatin forms heterochromatin foci (Narita *et al.,* 2003). These heterochromatin foci are proposed to form by Rb-mediated recruitment of histone deacetylases and other chromatin remodelling proteins to distinct chromatin sites. In such cells, Rb was found to partially co-localise with heterochromatin foci. In other fibroblast cell types (BJ and MEF), however, these foci were not detectible during senescence. Similarly, in fibroblast cells I used, formation of heterochromatin foci was not a general feature of senescent arrest. However, both senescent and laminopathy fibroblasts show condensed areas of internal chromatin which partially co-localise with Rb795 foci. Therefore a lack of heterochromatin foci during senescent arrest of some fibroblast types may occur due to Rb accumulation within splicing factor compartments rather than heterochromatin foci. Narita *et al.,* 2003 have raised a question whether the lack of heterochromatin foci in senescence of some fibroblast types would lead to a stable senescent arrest. Interestingly, senescent fibroblasts transfected with E1A viral oncoprotein do not enter proliferation whereas quiescent fibroblasts do (Narita *et al.,* 2003 unpublished data). E1A oncoprotein binds to the C-terminal domain of hypo-phosphorylated Rb which blocks phosphorylation on serine 795 (Zarkowska and Mittnacht 1997). Conversely, once Rb is phosphorylated on S795, the binding of this oncoprotein to Rb is inhibited. These results suggest that the presence of Rb795 isoform during senescence would lead to a stable senescent arrest that would permanently resist cell cycle activation by viral oncoproteins. On the other hand, the absence of Rb795 seen during quiescence (see Chapter 5) fits well with their observations that quiescent fibroblasts do not show resistance to virally induced proliferation. In addition, since a loss of retinoblastoma signalling pathways occurs in a wide variety of human tumours, this model may thus be of relevance to a proposed role of senescence as a tumour-suppressor mechanism (Campisi *et al.,* 2001). Wild-type Rb protein induces senescent-appearing cells in transfected cultures of Saos-2 cells, whilst mutant Rb is incapable to do so (Templeton *et al.,* 1991). Therefore, we could directly test the importance of Rb795 isoform in senescence by transfecting Saos-2 cells with Rb protein mutated at serine 795.

**DNA-damage associated phospho-histone foci accumulate in senescent and lamin A/C null fibroblasts and show a close association with Rb795 foci**

Senescing human cells and ageing mice accumulate DNA lesions with unrepairable double strand breaks (Sedelnikova *et al.*, 2004). These DNA lesions result from high levels of oxidative damage, telomere shortening or inefficient repair pathways (von Zglinicki *et al.*, 2005). The sites of DNA damage accumulate phospho-histone H2A.X and DNA repair proteins in distinct nuclear foci that are involved in active DNA damage signalling (d'Adda di Fagagna *et al.*, 2003). Rb protein plays an essential role in cell cycle arrest following DNA damage and is targeted by DNA damage checkpoint pathways (Harrington *et al.*, 1998). In senescent fibroblasts, although Rb795 foci did not completely overlap with phospho-histone foci, their foci were found adjacent to each other and showed a partial overlap. Rb is proposed to prevent re-replication of chromatin following DNA damage in cells (Cicchillitti *et al.*, 2003, Avni *et al.*, 2003). Interestingly, both histone H2A and other DNA-damage binding proteins have been purified from splicing factor speckles suggesting a link between DNA repair and RNA processing (Mintz *et al.*, 1999). Therefore, Rb795 may be recruited to nearby chromatin sites and speckles to prevent re-replication of damaged chromatin and/or to prevent recruitment of splicing factors to sites of transcription. Interestingly, lamin A/C null fibroblasts also accumulate DNA damage foci in cells that show Rb795 foci. This suggests that in the absence of functional A-type lamins in lamin A/C null human fibroblasts, chromatin may be more vulnerable to DNA damage and/or unable to repair the damage once it occurred. These results are supported by recently published work which showed that HGPS fibroblasts and mouse fibroblasts null for ZMPSTE protease show impaired DNA damage response (Liu *et al.*, 2005). Since laminopathy cells do not show increased oxidative modifications to A-type lamins (Chapter 3), it is unlikely that these DNA damage sites result from increased oxidative stress in laminopathy cells. However, senescence-associated DNA damage signalling can be triggered by a loss of telomere-binding proteins, which leads to telomere uncapping and premature senescence in the presence of normal telomere lengths (von Zglinicki *et al.*, 2005). Moreover, telomere dysfunction impairs DNA repair and DNA-repair-deficient human cell lines also senesce prematurely (Wong *et al.*, 2000). Therefore, I hypothesize that increased aggregation of telomere-binding protein LAP2α in lamin A/C null fibroblasts triggers DNA damage-induced premature senescence.

**Figure 4.1: During ageing of fibroblasts in vitro Rb protein becomes progressively de-phosphorylated with a subsequent accumulation of faster-migrating Rb species and a decreased expression of hypo-phosphorylated Rb780.** Primary cultures of human dermal fibroblasts were grown through serial passage (p) and the same number of cells was harvested after 3 days of growth in culture at early **(p7-p12)**, intermediate **(p17-p27)** and late **(p44)** passages. Whole cell extracts were blotted using antibodies against total Rb (IF8) and Rb isoform phosphorylated on ser 780 (Rb780). Arrowhead shows faster migrating Rb band of 110 kDa (un- and under-phosphorylated Rb species). Arrow shows slower-migrating Rb band of 115 kDa (hyper-phosphorylated Rb species).


HDF
passages p7 p12 p17 p22 p27 p44

# Figure 4.1

**Figure 4.2: Late passage fibroblasts that show epitope masking of IF8 antibody reveal distinct foci of Rb795 and no expression of Rb780 in the nuclei.** Human fibroblasts of early (**p7**) and late passage (**p44**) were seeded at an equal density, grown in culture for 3 days and processed for double immunofluorescence microscopy using antibodies against: (**a**) IF8 (total Rb) and Ki67, (**b**) IF8 and Rb780, and (**c**) IF8 and Rb795. Images were collected on a BioRad Radiance 2000 confocal microscope and projected as individual black and white or red/green colour merged micrographs in which IF8 is in red, and Rb780 and Rb795 are in green. Magnification: (**a**) & (**b**) **p7** 80x; (**a**) & (**b**) **p44** 120x.

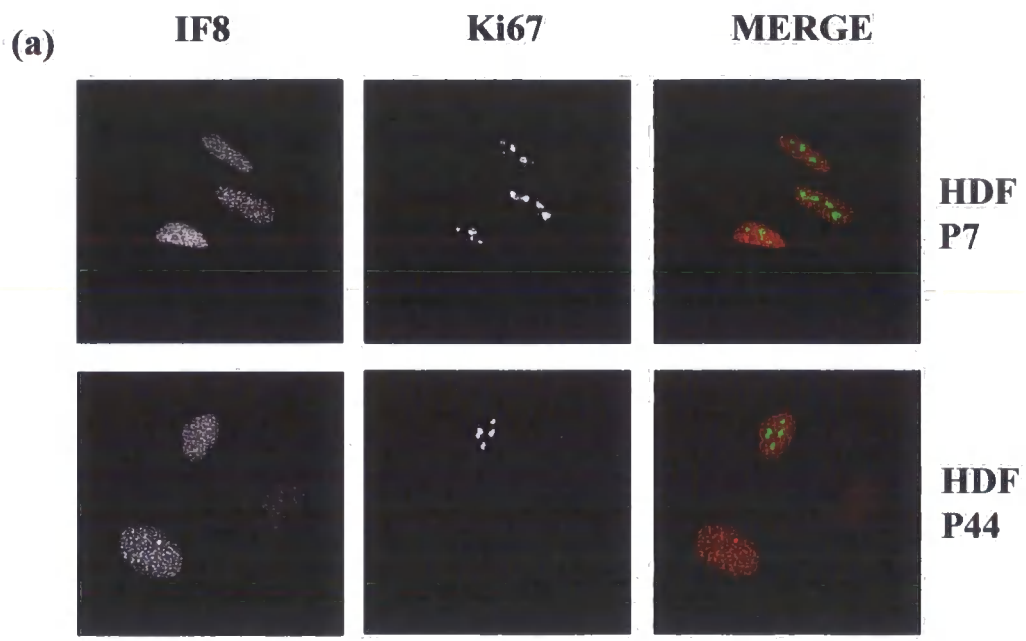


# Figure 4.2

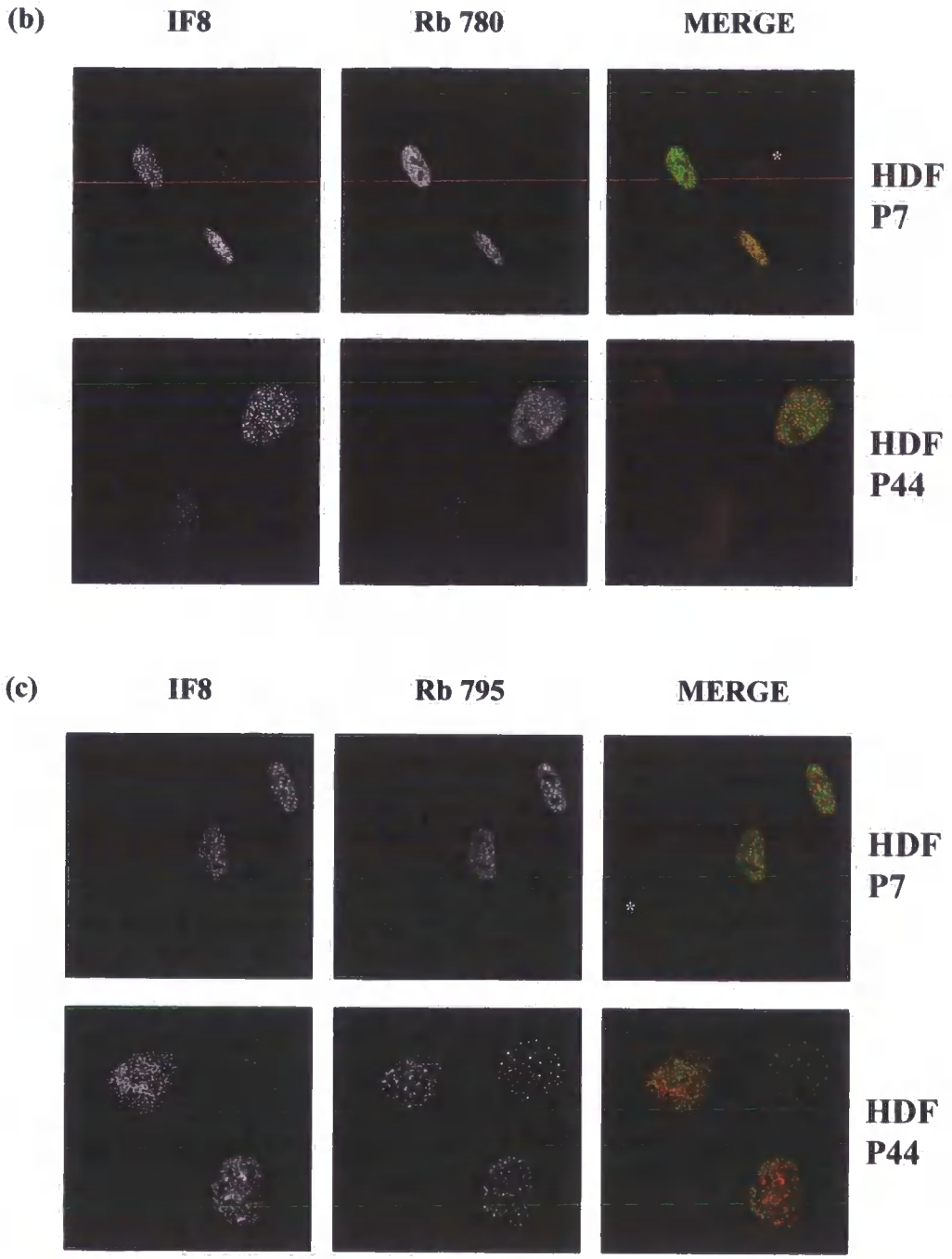
(b)
IF8
Rb 780
MERGE
HDF P7
HDF P44
(c)
IF8
Rb 795
MERGE
HDF P7
HDF P44

# Figure 4.2

**Figure 4.3: Late passage fibroblasts which show heavily granulated or aggregated LAP2α reveal distinct foci of Rb795 and no expression of Rb780 in the nuclei.** Human fibroblasts of early (**p7**) and late passage (**p44**) were seeded at an equal density, grown in culture for 3 days and processed for double immunofluorescence microscopy using antibodies against: (**a**) LAP2α and 780, and (**b**) LAP2α and Rb795. Images were collected on a BioRad Radiance 2000 confocal microscope and projected as individual black and white or red/green colour merged micrographs in which LAP2α is in red, and Rb780 and Rb795 are in green. Arrow points out nuclei with expected LAP2α distribution. Arrowhead points out nuclei with heavily granulated LAP2α. * points out nuclei with LAP2α aggregates. Magnification 80x.

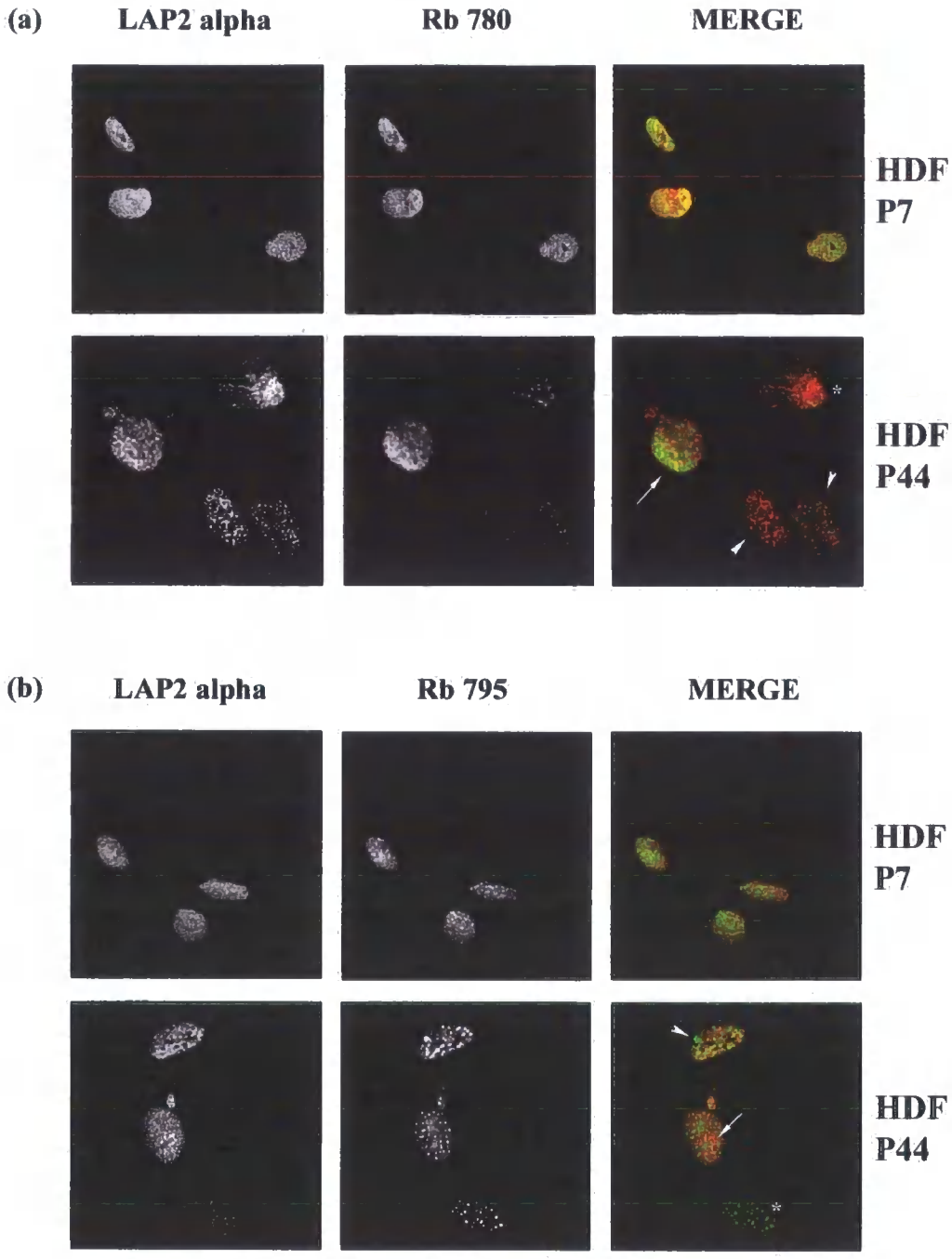
(a)
LAP2 alpha
Rb 780
MERGE
HDF P7
HDF P44
(b)
LAP2 alpha
Rb 795
MERGE
HDF P7
HDF P44

# Figure 4.3

**Figure 4.4: Late passage dysmorphic nuclei with lamin herniations and honeycombs show decreased expression of Rb780 but display distinct nuclear foci of Rb795.** Human fibroblasts of early **(p7)** and late passage **(p44)** were seeded at an equal density, grown in culture for 3 days and processed for double immunofluorescence microscopy using antibodies against: **(a)** lamin A/C and 780, and **(b)** lamin A/C and Rb795. DNA was stained using chromatin-staining dye DAPI. Images were collected on a Zeiss confocal microscope and projected as individual black and white or blue/red/green colour merged micrographs in which DAPI is in blue, lamin A/C is in red, and Rb780 and Rb795 are in green. Arrowheads point out lamin A/C distribution at the nuclear envelope and arrows point out lamin A/C distribution inside the nucleus in ovoid-shaped p7 nuclei and dysmorphic p44 nuclei. Note changes in peripheral and internal chromatin in p44 dysmorphic nuclei. * points out ovoid-shaped p44 nuclei. Magnification: **(a)** & **(b)** **p7** 80x; **(a)** & **(b)** **p44** 120x.

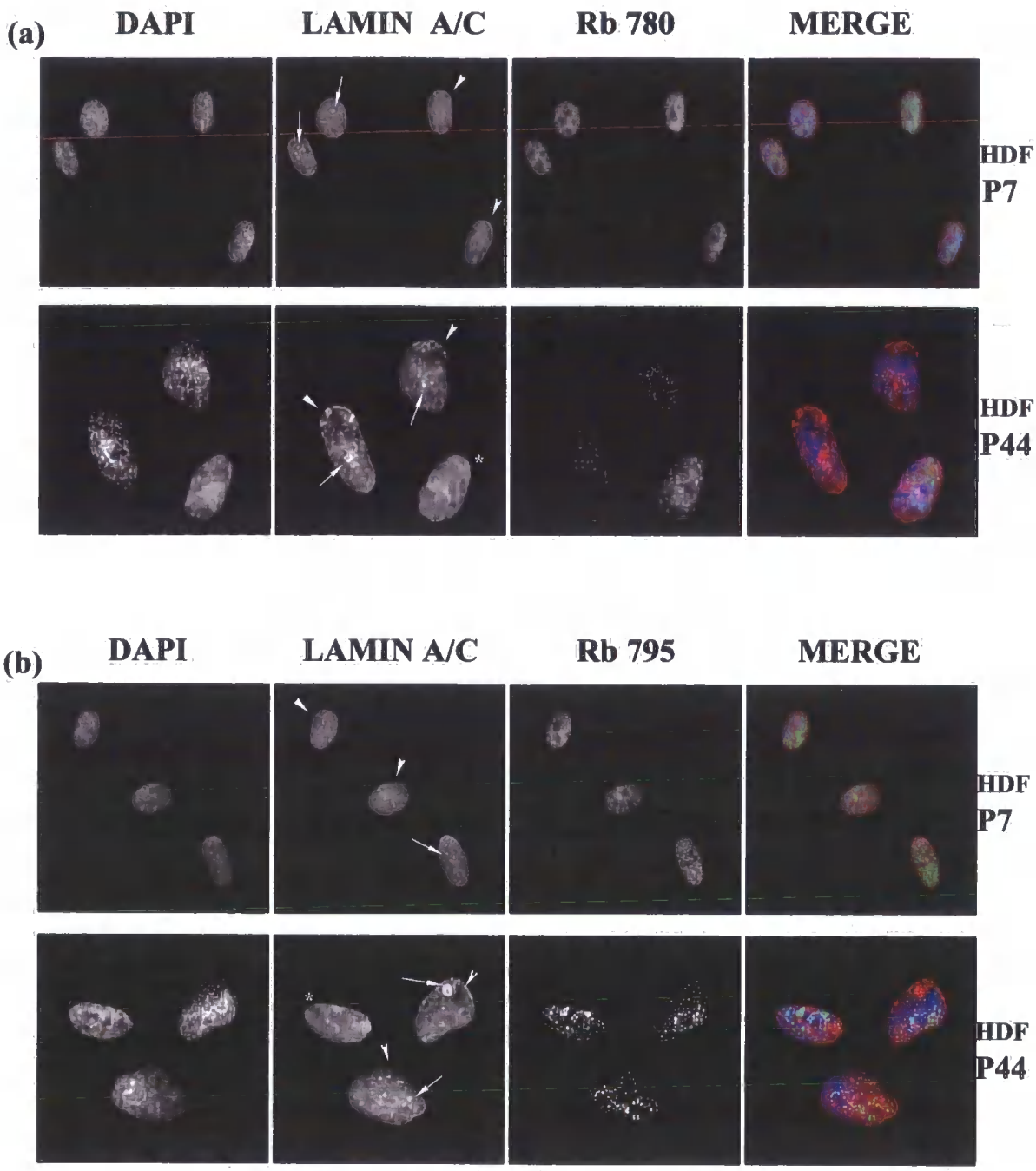
(a)
DAPI
LAMIN A/C
Rb 780
MERGE
HDF P7
HDF P44
(b)
DAPI
LAMIN A/C
Rb 795
MERGE
HDF P7
HDF P44

# Figure 4.4

**Figure 4.5: Dysmorphic nuclei of Y259X fibroblasts show increased incidence of LAP2α aggregates, which correlates with cell cycle arrest.** Early **(p12)** and mid passage **(p18)** Y259X fibroblasts were seeded at an equal density, grown in culture for 3 days and processed for double immunofluorescence microscopy using antibodies against: **(a)** lamin B2 and Ki67, and **(b)** LAP2α and Ki67. DNA was stained using chromatin-staining dye DAPI. Images were collected on a Zeiss confocal microscope and projected as individual black and white or blue/red/green colour merged micrographs in which DAPI is in blue, lamin B2 and LAP2α are in red, and Ki67 is in green. In DAPI micrographs, arrowheads point out peripheral chromatin distribution in dysmorphic nuclei. In LAP2α micrographs, arrows indicate nuclei with a tendency of LAP2α to aggregate and arrowheads indicate nuclei with LAP2α aggregates. In lamin B2 micrographs, arrows indicate nuclei with abnormal lamin B2 distribution at the nuclear envelope. Magnification 120x.

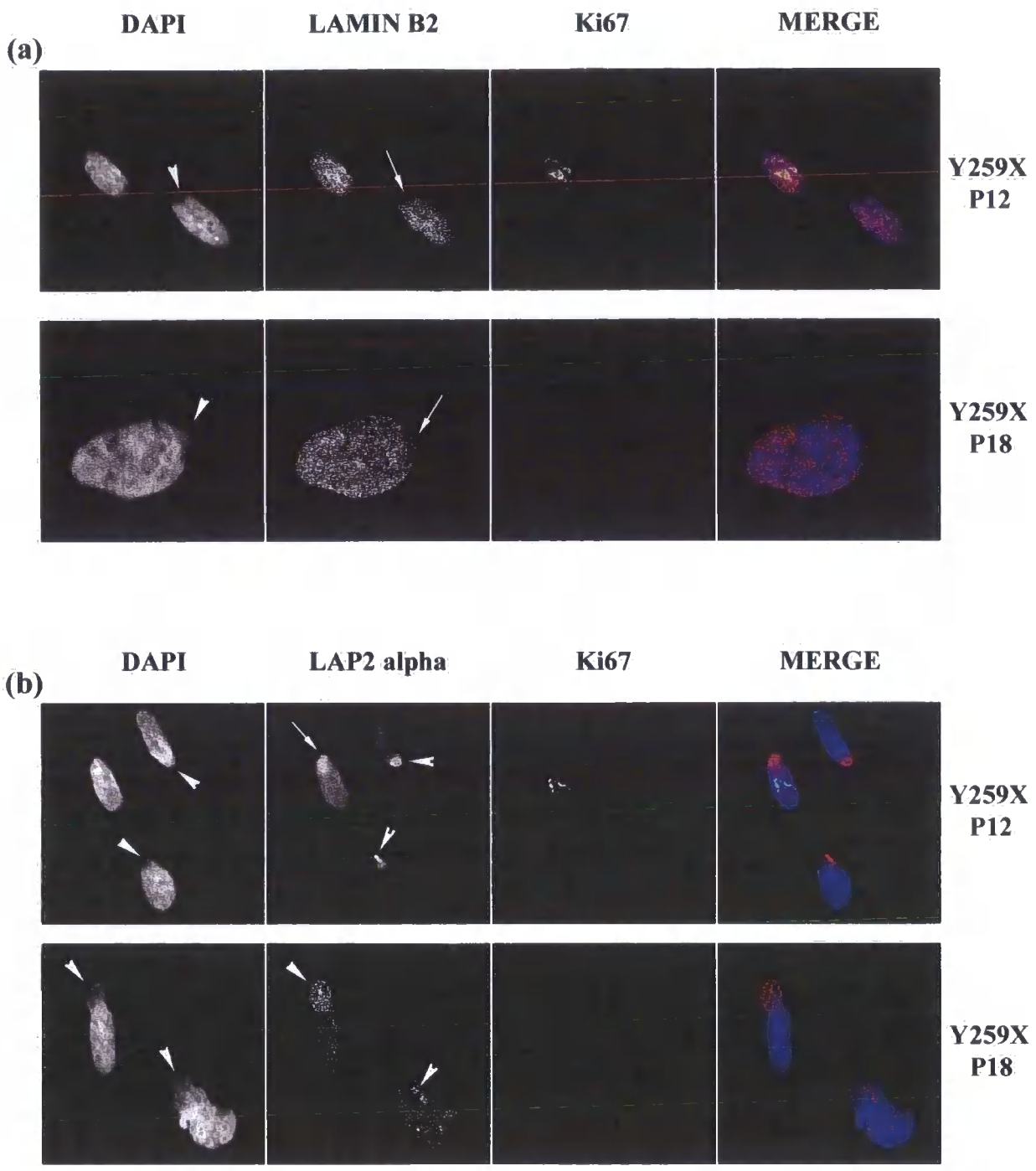
(a)
DAPI
LAMIN B2
Ki67
MERGE
Y259X P12
Y259X P18
(b)
DAPI
LAP2 alpha
Ki67
MERGE
Y259X P12
Y259X P18

# Figure 4.5

**Figure 4.6A: Y259X fibroblasts which show LAP2α aggregates display distinct nuclear foci of Rb795 and no expression of Rb780.** Early **(p12)** and mid passage **(p18)** Y259X fibroblasts were seeded at an equal density, grown in culture for 3 days and processed for double immunofluorescence microscopy using antibodies against: **(a)** LAP2α and Rb780, and **(b)** LAP2α and Rb795. DNA was stained using chromatin-staining dye DAPI. Images were collected on a Zeiss confocal microscope and projected as individual black and white or blue/red/green colour merged micrographs in which DAPI is in blue, LAP2α is in red, and Rb780 and Rb795 are in green. Arrows point out nuclei with a tendency of LAP2α to aggregate and arrowheads point out nuclei with LAP2α aggregates. * point out nuclei with expected LAP2α distribution. Magnification 80x.

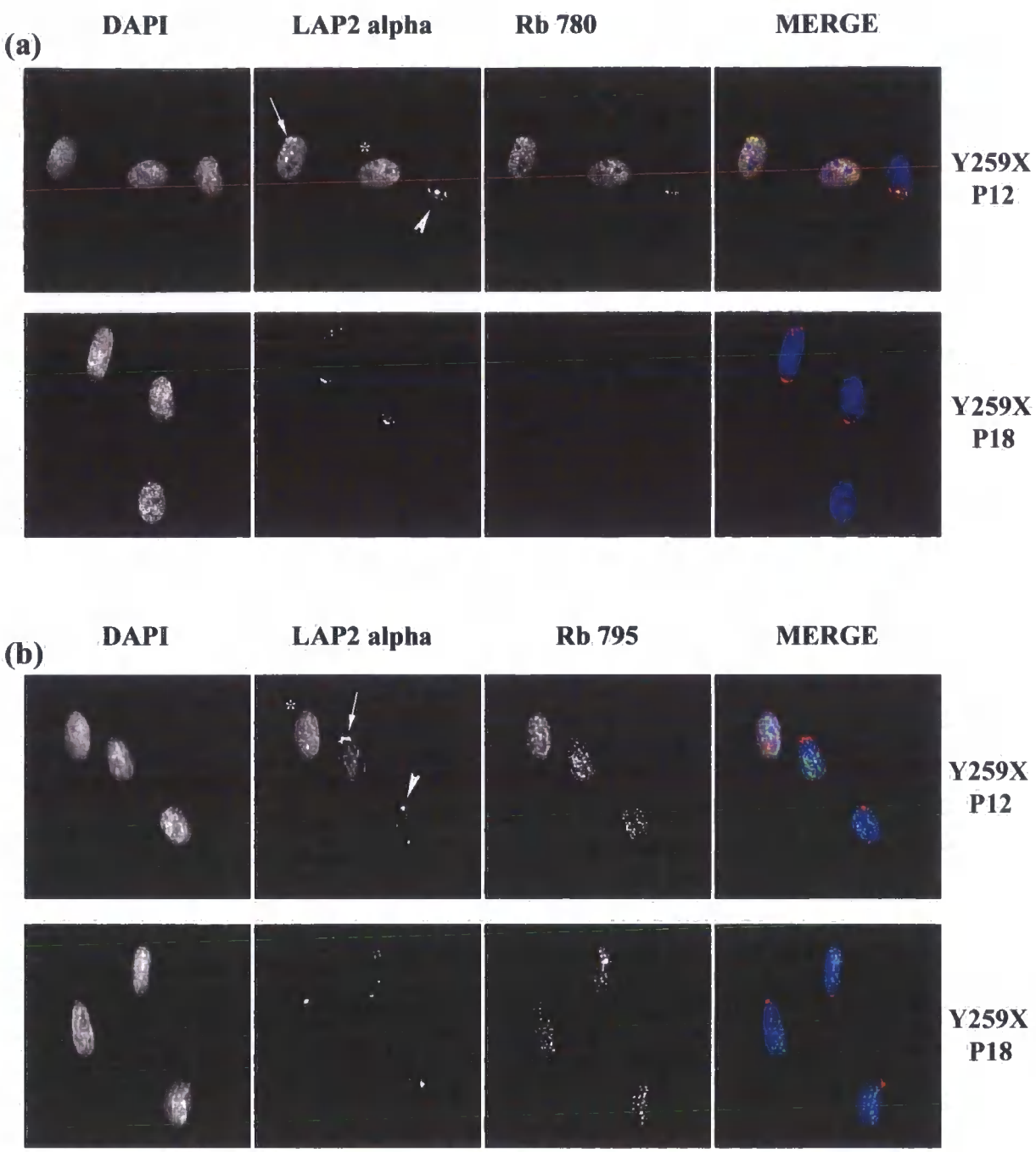
(a)
DAPI
LAP2 alpha
Rb 780
MERGE
Y259X P12
Y259X P18
(b)
DAPI
LAP2 alpha
Rb 795
MERGE
Y259X P12
Y259X P18

# Figure 4.6A

**Figure 4.6B: Loss of Rb780 expression in Y259X nuclei correlates with cell cycle arrest.** Early **(p12)** and mid passage **(p18)** Y259X fibroblasts were seeded at an equal density, grown in culture for 3 days and processed for double immunofluorescence microscopy using antibodies against: **(c)** IF8 Ki67, and **(d)** Rb780 and Ki67. DNA was stained using chromatin-staining dye DAPI. Images were collected on a Zeiss confocal microscope and projected as individual black and white or blue/red/green colour merged micrographs in which DAPI is in blue, IF8 is in red, and Rb780 is in green. Ki67 is in green in (a) and in red in (b). Magnification 80x.

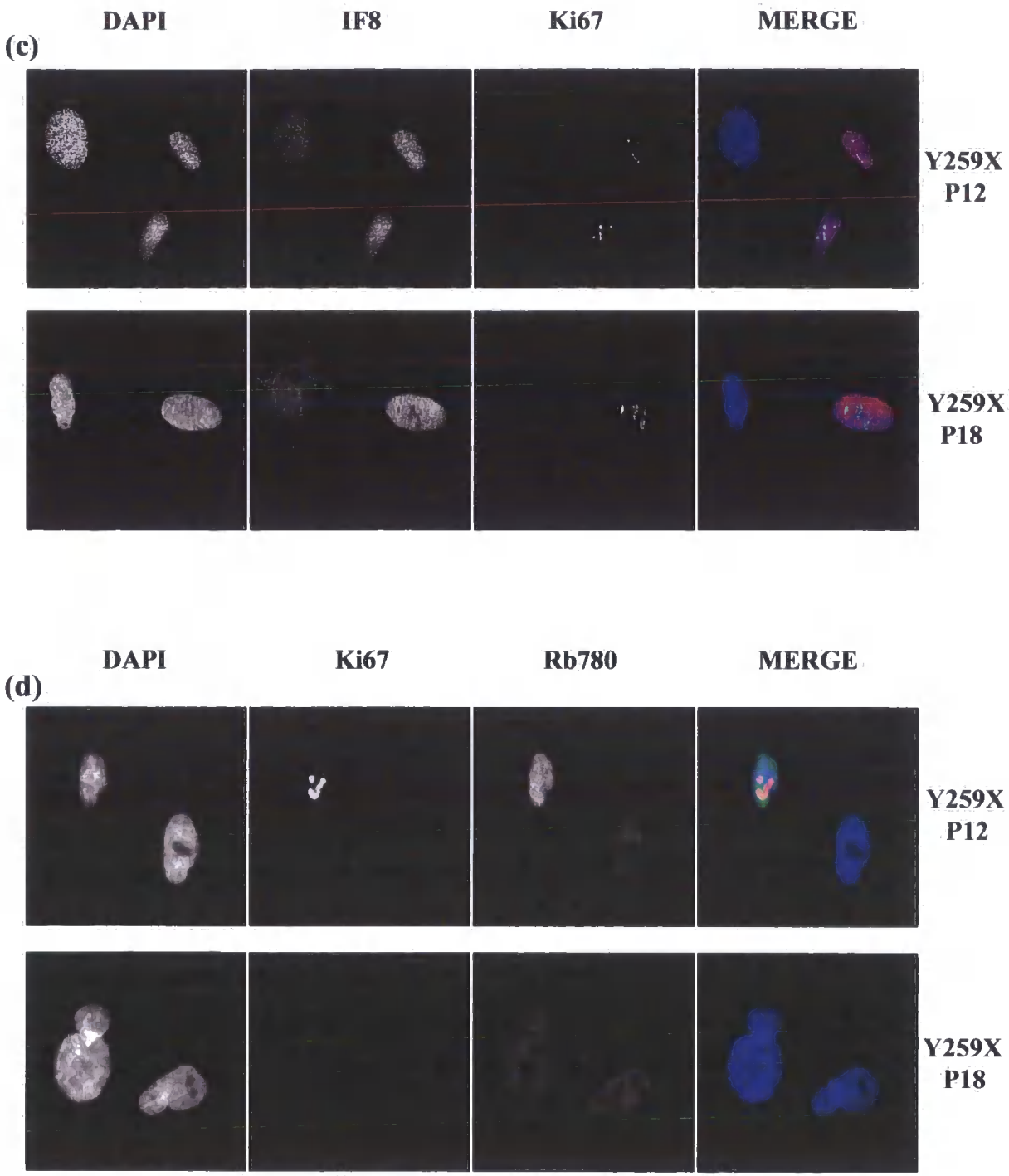
(c)
DAPI
IF8
Ki67
MERGE
Y259X P12
Y259X P18
(d)
DAPI
Ki67
Rb780
MERGE
Y259X P12
Y259X P18

# Figure 4.6B

**Figure 4.7: Mid passage Y259X fibroblasts which undergo premature senescent arrest show accumulation of faster-migrating Rb species and decreased protein expression of Rb780.** Early **(p12)** and mid **(p18)** passage Y259X laminopathy fibroblasts were grown in culture for 3 days and harvested. As a control, early **(p12)** and mid passage **(p18)** wild-type fibroblasts were grown in culture for 3 days and harvested. Whole cell extracts were prepared from the same number of cells and immunoblotted against total Rb (IF8) and Rb isoform phosphorylated on ser 780 (Rb780). Note the faster migrating Rb band of 110 kDa (un- and under-phosphorylated Rb species) and the slower-migrating Rb band of 115 kDa (hyper-phosphorylated Rb species).

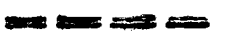

IF8 (total Rb)



phospho Rb780

| | | | | |
|---|---|---|---|---|
| **cell lines** | **HDF** | | **Y259X** | |
| **passages** | **p12** | **p18** | **p12** | **p18** |

# Figure 4.7

**Figure 4.8: Late passage fibroblasts show a loss of nuclear anchorage of Rb780 but not of total Rb upon extraction.** Early **(p7)** and late passage **(p44)** fibroblasts were submitted to a sequential extraction by CSK-Triton X100, RSB-Magic, chromatin digestion by DNAse1 and a final extraction by 0.25M ammonium sulphate. Whole cell extracts were prepared (P1) and soluble (S2, S3, S4, S5) and insoluble (P2, P3, P4, P5) fractions were immunoblotted with antibodies against Rb isoform phosphorylated on ser 780 (Rb780) and total Rb (IF8). Thin arrow points out slower migrating Rb band of 120 kDa (hyper-phosphorylated Rb). Arrowhead points out faster migrating Rb band of 110 kDa (hypo-phosphorylated Rb). Thick arrow points out Rb band of 115 kDa migrating at the intermediate level between the other two Rb bands (hypo-phosphorylated Rb).

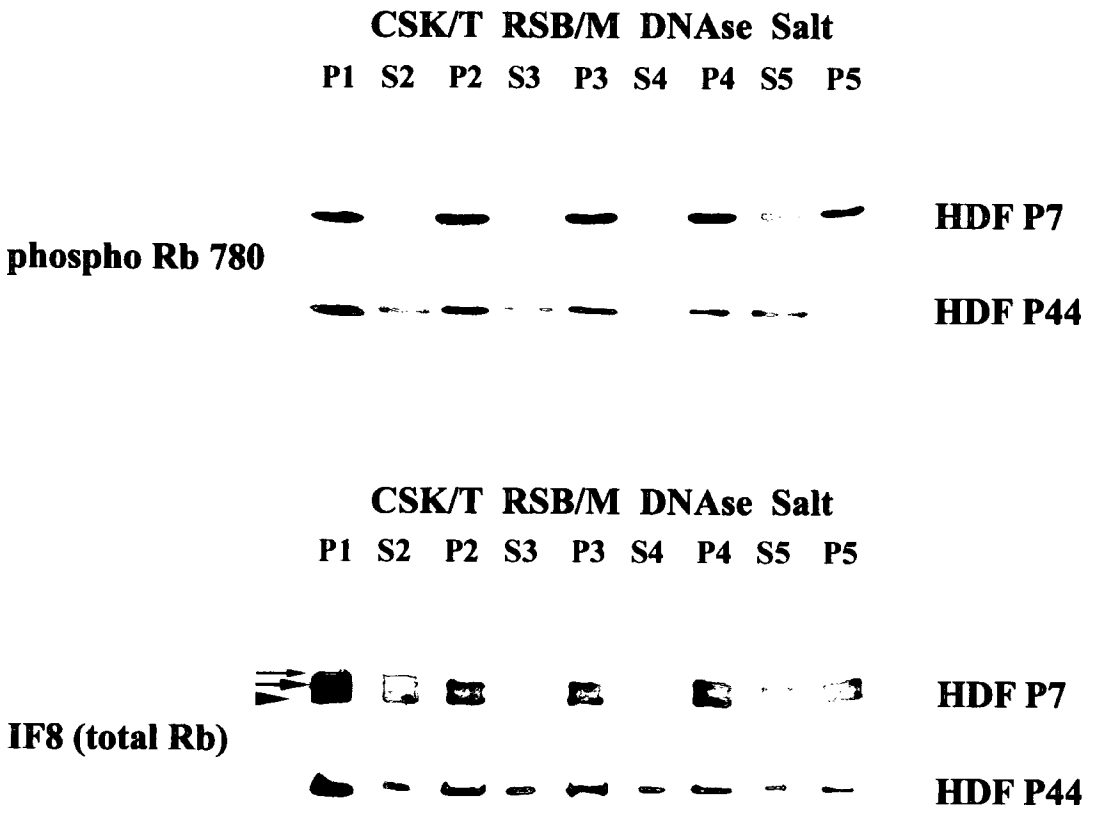
CSK/T RSB/M DNAse Salt
P1 S2 P2 S3 P3 S4 P4 S5 P5
phospho Rb 780
HDF P7
HDF P44
CSK/T RSB/M DNAse Salt
P1 S2 P2 S3 P3 S4 P4 S5 P5
IF8 (total Rb)
HDF P7
HDF P44

# Figure 4.8

**Figure 4.9: Late passage fibroblasts show prominent nuclear foci of Rb795 upon *in situ* nuclear matrix extraction.** Early (**p7**) and late passage (**p44**) fibroblasts were submitted to a nuclear matrix extraction *in situ* via five sequential treatments with CSK-Triton X100, RSB-Magic, DNAse1 digestion and 0.25M ammonium sulphate extraction and processed for immunofluorescence microscopy using antibodies against: (**a**) AB5 and Rb780 and, (**b**) AB5 and Rb795. (**a**) & (**b**) show cells after V stage (ammonium sulphate) extraction. Images were collected on a BioRad Radiance 2000 confocal microscope and projected as black and white or red/green colour merged micrographs in which AB5 is in red and Rb780 and Rb795 are in green. Magnification 120x.

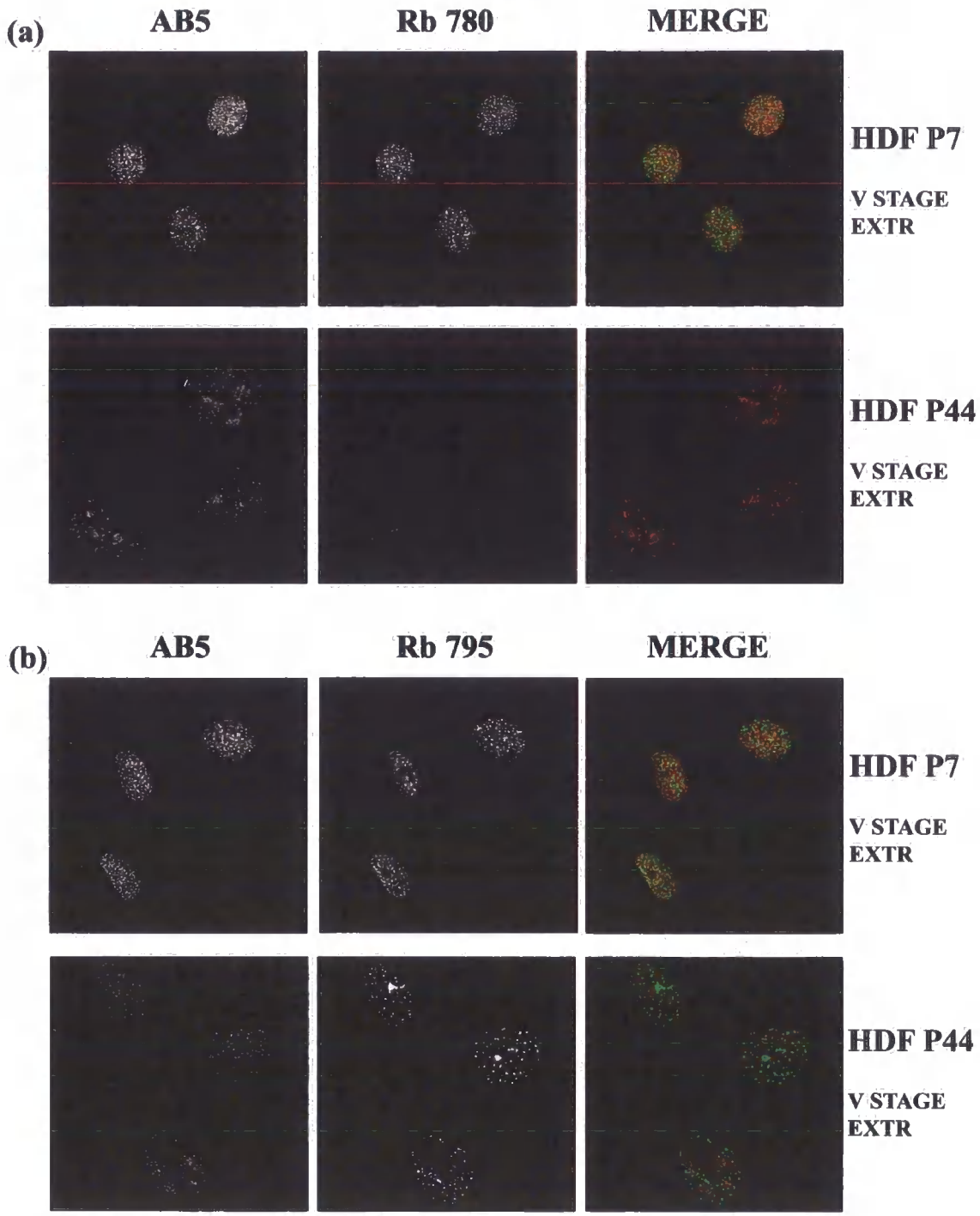
(a)
AB5
Rb 780
MERGE
HDF P7
V STAGE
EXTR
HDF P44
V STAGE
EXTR
(b)
AB5
Rb 795
MERGE
HDF P7
V STAGE
EXTR
HDF P44
V STAGE
EXTR

**Figure 4.9**

**Figure 4.10: Loss of nuclear anchorage of LAP2α in late passage fibroblasts correlates with a loss of nuclear anchorage of Rb780 but not speckle-associated Rb795.** Early **(p7)** and late passage **(p44)** fibroblasts were submitted to a nuclear matrix extraction *in situ* as described in Figure 4.9, fixed and processed for immunofluorescence microscopy using antibodies against: **(a)** LAP2α and Ki67, **(b)** LAP2α and Rb780, and **(c)** LAP2α and Rb795. **(a)** & **(c)** show cells after V stage (ammonium sulphate) extraction. **(b)** shows cells after II stage (CSK/Triton X100) extraction. Images were collected on a BioRad Radiance 2000 confocal microscope and projected as individual black and white or red/green colour merged micrographs in which LAP2α is in red, and Rb780 and Rb795 are in green. Magnification 120x.

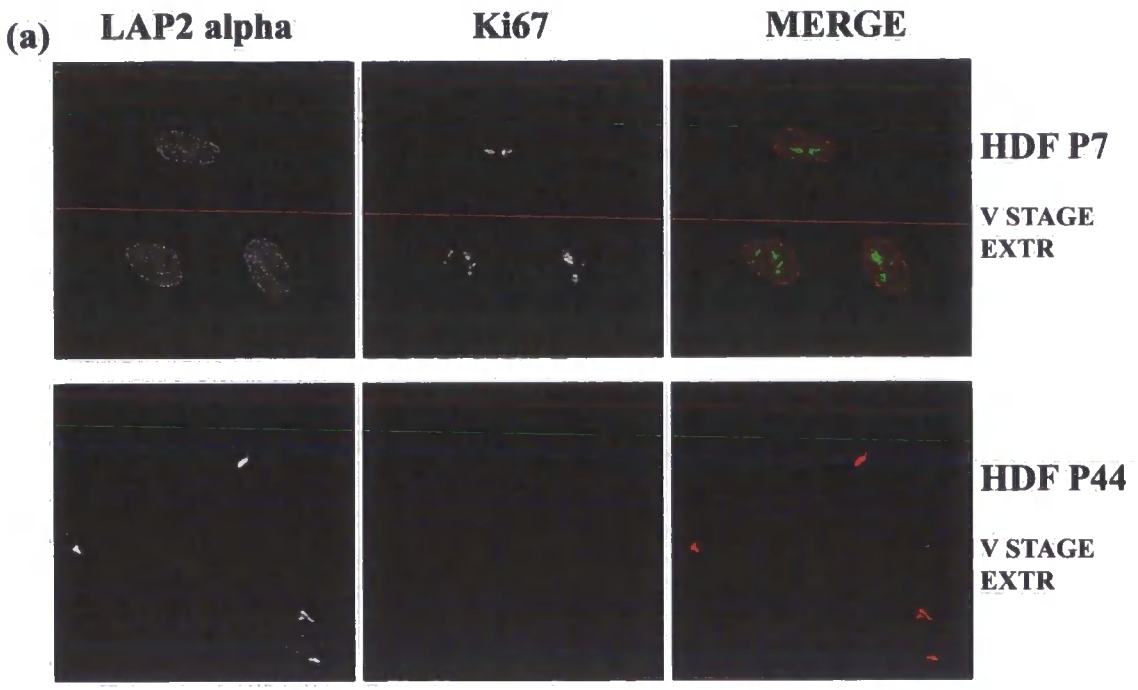
(a)
LAP2 alpha
Ki67
MERGE
HDF P7
V STAGE
EXTR
HDF P44
V STAGE
EXTR

Figure 4.10

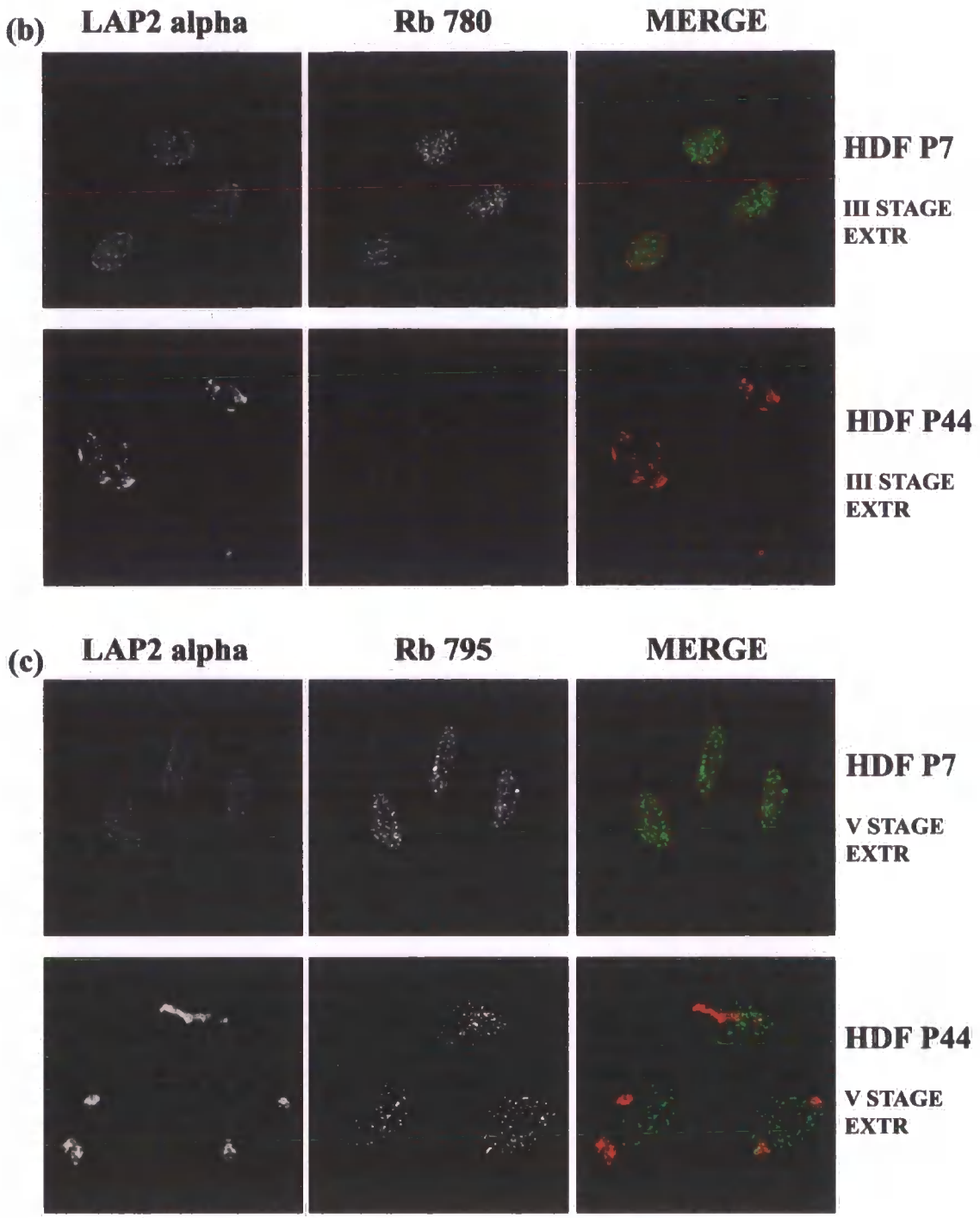
(b)
LAP2 alpha
Rb 780
MERGE
HDF P7
III STAGE
EXTR
HDF P44
III STAGE
EXTR
(c)
LAP2 alpha
Rb 795
MERGE
HDF P7
V STAGE
EXTR
HDF P44
V STAGE
EXTR

**Figure 4.10**

**Figure 4.11: Late passage fibroblasts show decreased presence of LAP2α/lamin C/Rb780 complexes in the nuclei.** Early **(p8)** and late passage **(p42)** cells were grown for 3 days in culture and the same number of cells was harvested for immunoprecipitation analysis. LAP2α was immuno-precipitated from nuclear extracts using LAP2α-specific antibody (LAP15) pre-incubated with Dynabeads. LAP2α immuno-precipitates were resolved on reducing SDS-PAGE and immunoblotted with antibodies against LAP2α (LAP15), lamin C (RαLC) and Rb phosphorylated on serine 780 (Rb780). The expected mobilities of the above proteins are: LAP2 α (75kDa), lamin C (65 kDa) and Rb780 (115 kDa). Under reducing conditions, heavy and light chains of IgGs are separated and heavy chains run at ~50 kDa (labelled IgG (h)). M shows mobility of molecular weight markers starting from the top: 208, 119, 94, 51 and 36 (kDa).

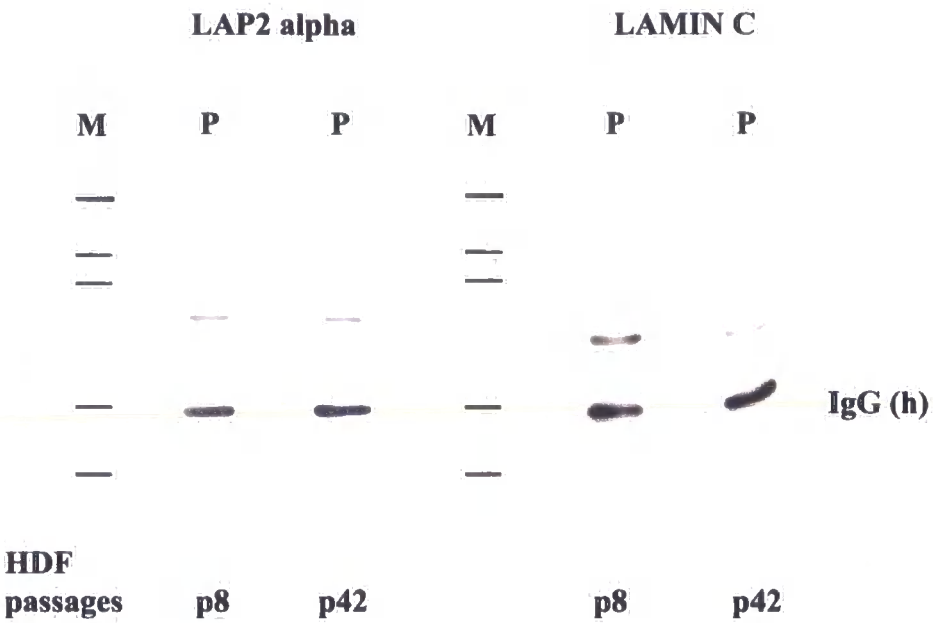
LAP2 alpha
LAMIN C
M
P
P
M
P
P
IgG (h)
HDF
passages
p8
p42
p8
p42

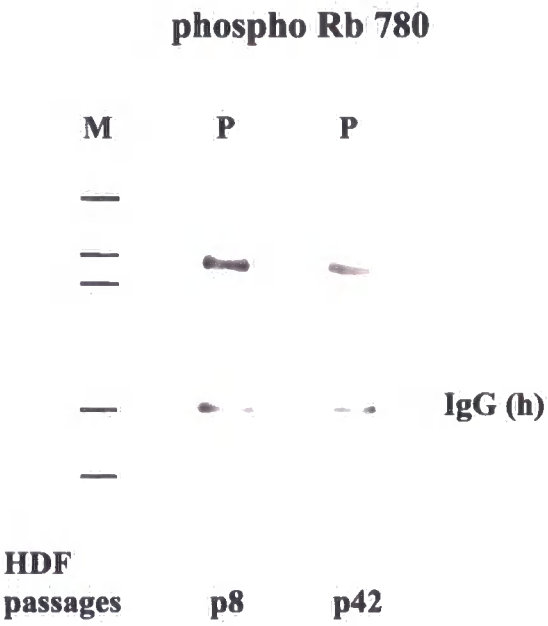
phospho Rb 780
M
P
P
IgG (h)
HDF
passages
p8
p42

# Figure 4.11

**Figure 4.12A: Y259X fibroblasts show decreased retention of lamin B2 and a loss/aggregation of LAP2α upon *in situ* nuclear matrix extraction.** Early **(p12)** passage Y259X fibroblasts were submitted to nuclear matrix extraction *in situ* via five sequential treatments with CSK, CSK-Triton X100, RSB-Magic, chromatin digestion by DNAse1 and 0.25 M ammonium sulphate and processed for immunofluorescence microscopy using antibodies against: **(a)** Lamin B2 and Ki67, and **(b)** LAP2α and Ki67. **(a)** & **(b)** show cells after V stage (ammonium sulphate) extraction. Images were collected on a BioRad Radiance 2000 confocal microscope and projected as individual black and white or red/green colour merged micrographs in which lamin B2 and LAP2α are in red, and Ki67 is in green. Arrow points out ovoid-shaped Ki67-positive nuclei. Arrowhead points out ovoid-shaped Ki67-negative nuclei. * points out dysmorphic Ki67-negative nuclei. Magnification 120x.

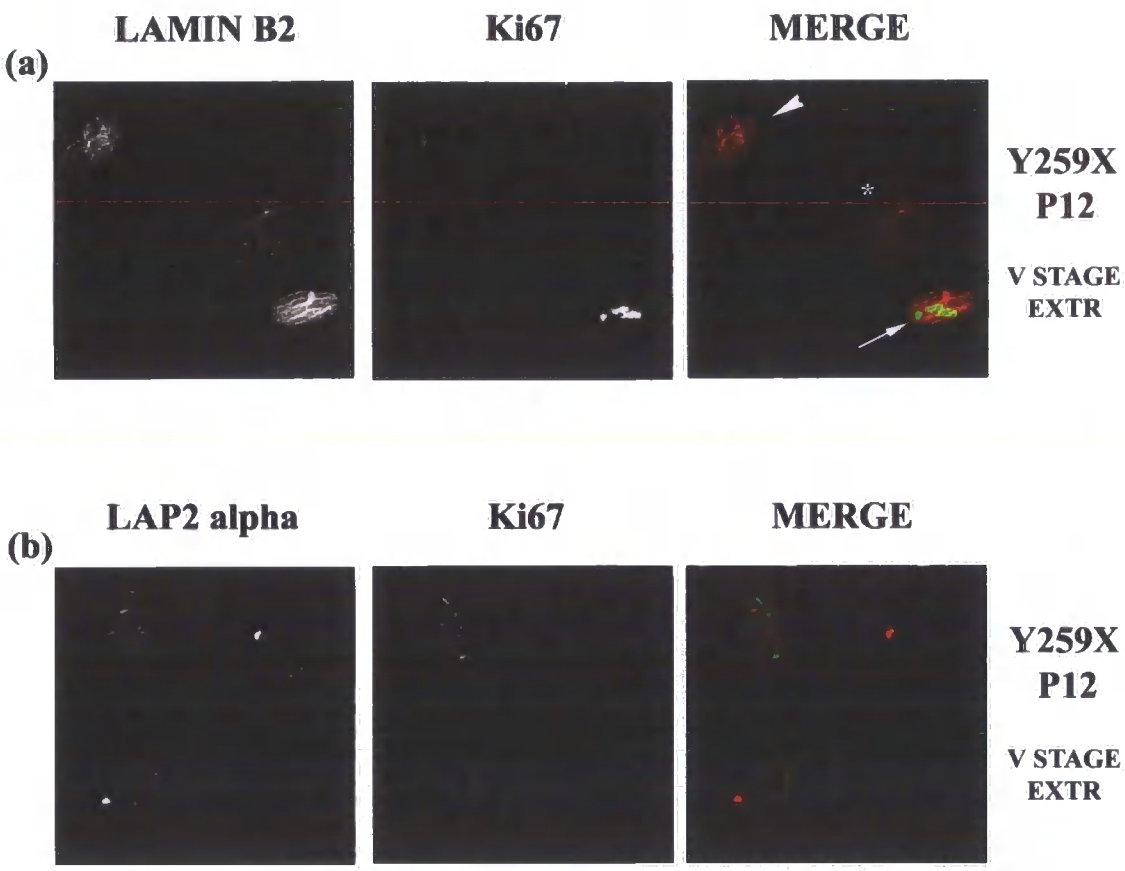
(a)
LAMIN B2
Ki67
MERGE
Y259X
P12
V STAGE
EXTR
(b)
LAP2 alpha
Ki67
MERGE
Y259X
P12
V STAGE
EXTR

**Figure 4.12A**

**Figure 4.12B: Y259X fibroblasts which show a loss/aggregation of LAP2α upon extraction do not retain Rb780 but retain distinct nuclear foci of Rb795.** Early **(p12)** or mid **(p18)** passage Y259X fibroblasts were submitted to nuclear matrix extraction *in situ* as described above and processed for immunofluorescence microscopy using antibodies against: **(c)** LAP2α and Rb780, and **(d)** LAP2α and Rb795. **(c)** shows cells after III stage (RSB/Magik) extraction & **(d)** shows cells after V stage (ammonium sulphate) extraction. Images were collected on a BioRad Radiance 2000 confocal microscope and projected as individual black and white or red/green colour merged micrographs in which LAP2α is in red, and Rb780 and Rb795 are in green. Magnification 120x.

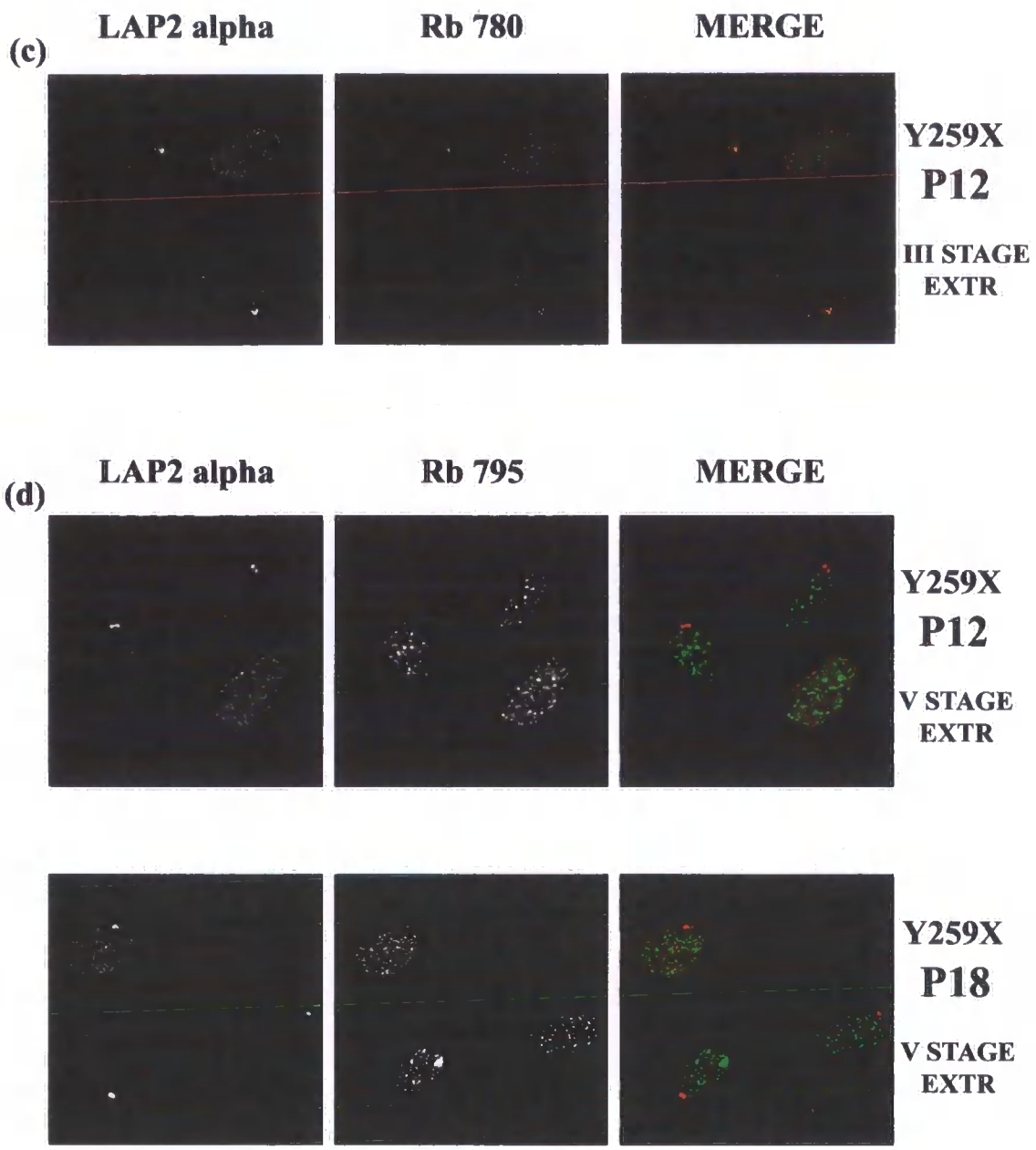
(c)
LAP2 alpha
Rb 780
MERGE
Y259X
P12
III STAGE
EXTR
(d)
LAP2 alpha
Rb 795
MERGE
Y259X
P12
V STAGE
EXTR
Y259X
P18
V STAGE
EXTR

**Figure 4.12B**

**Figure 4.13: Late passage fibroblasts retain some amount of total Rb which correlates with retention of distinct nuclear foci of Rb795.** Early **(p12)** or mid passage **(p18)** Y259X fibroblasts were submitted to a nuclear matrix extraction *in situ* as described in Figure 4.12 and processed for immunofluorescence microscopy using antibodies against: **(a)** AB5 and Rb780 and, **(b)** AB5 and Rb795. **(a)** & **(b)** show cells after V stage (ammonium sulphate) extraction. Images were collected on a BioRad Radiance 2000 confocal microscope and projected as black and white or red/green colour merged micrographs in which AB5 is in red and Rb780 and Rb795 are in green. Magnification 120x.

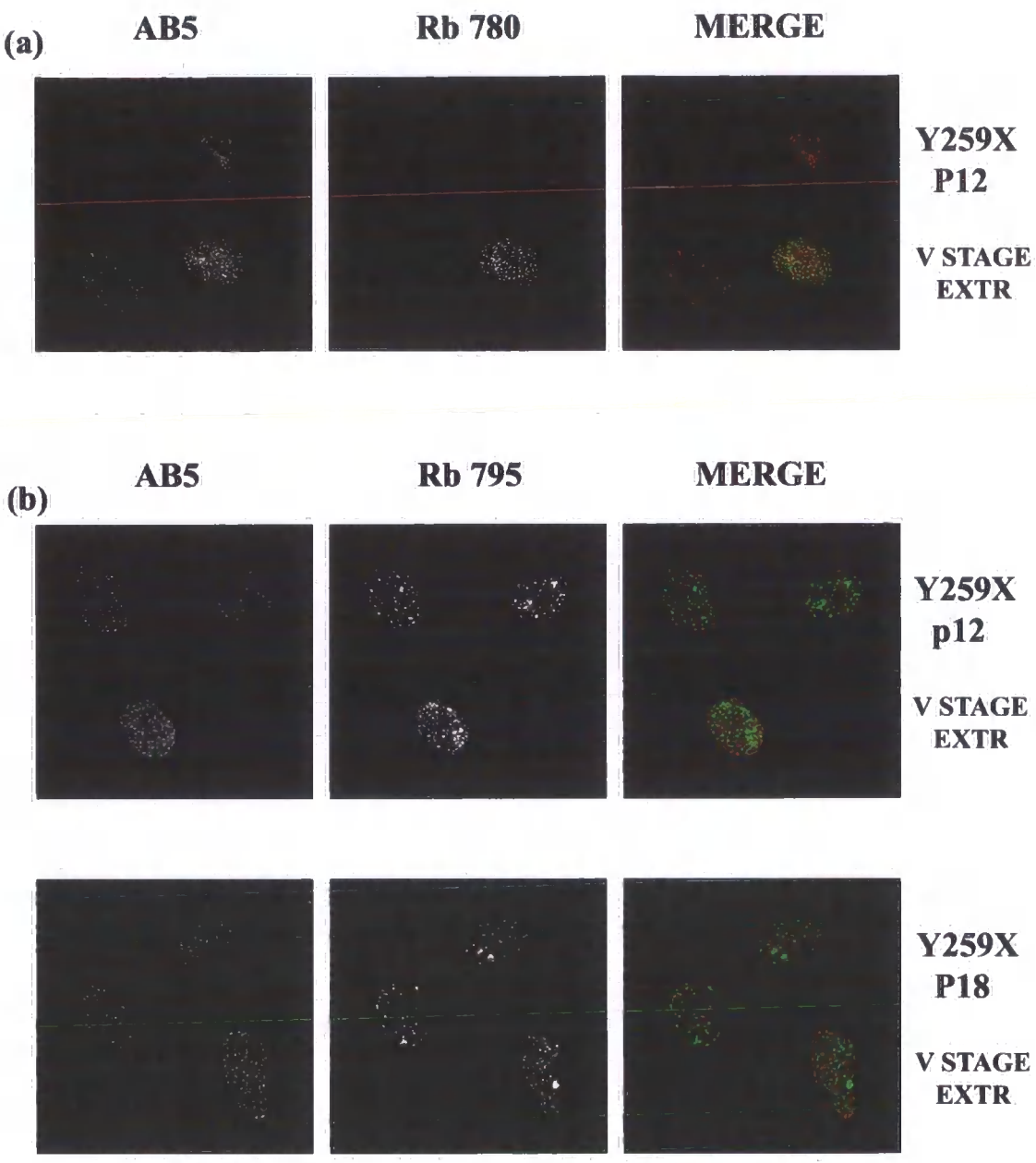
(a)
AB5
Rb 780
MERGE
Y259X
P12
V STAGE
EXTR
(b)
AB5
Rb 795
MERGE
Y259X
p12
V STAGE
EXTR
Y259X
P18
V STAGE
EXTR

**Figure 4.13**

**Figure 4.14A: LAP2α knockdown in early passage proliferating fibroblasts causes cell cycle arrest.** Early passage **(p8)** fibroblasts seeded at a medium density were grown in culture for one day and transfected with either RNA oligonucleotides designed to interfere against LAP2α-specific mRNA or control RNAi (GL2) oligonucleotides targeting Firefly luciferase. After 24 hours, transfected cultures were sub-cultured, grown in culture for another 48 hours and processed for double immunofluorescence microscopy using antibodies against: **(a)** LAP2α and Ki67, **(b)** LAP2β and Ki67. DNA was stained using chromatin-staining dye DAPI. Images were collected on a Zeiss confocal microscope and projected as black and white or blue/red/green colour merged micrographs, in which DAPI is in blue, LAP2α and LAP2β are in red and Ki67 is in green. Magnification 80x.

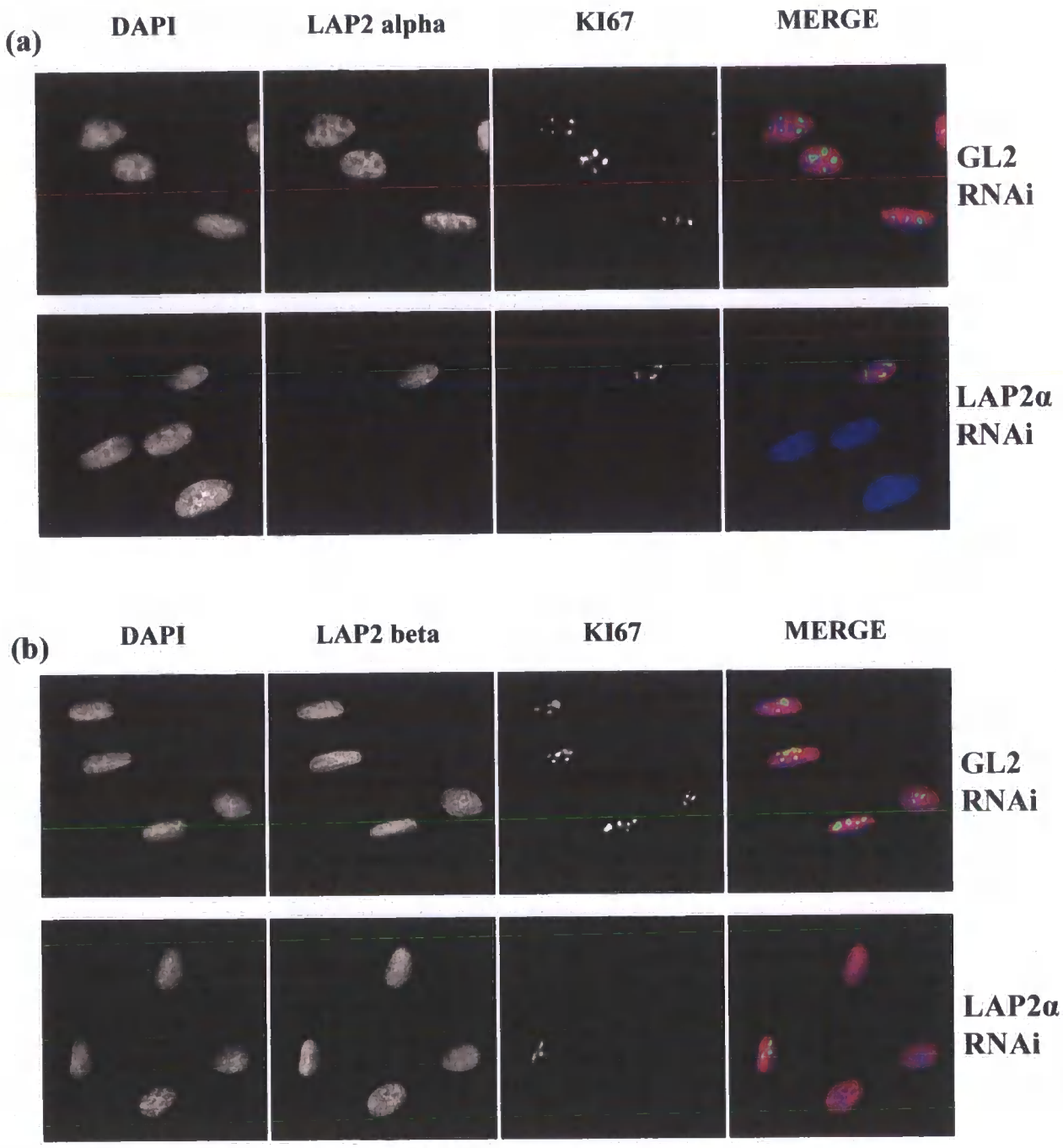
(a)
DAPI
LAP2 alpha
KI67
MERGE
GL2 RNAi
LAP2α RNAi
(b)
DAPI
LAP2 beta
KI67
MERGE
GL2 RNAi
LAP2α RNAi

**Figure 4.14A**

**Figure 4.14B: LAP2α knockdown in early passage fibroblasts leads to a loss of nuclear expression of Rb780 but not speckle-associated Rb795.** Early passage **(p8)** fibroblasts were transfected with either RNA oligonucleotides designed to interfere against LAP2α-specific mRNA or control RNAi (GL2) oligonucleotides targeting Firefly luciferase as described above and processed for double immunofluorescence microscopy using antibodies against: **(c)** LAP2α and Rb780, and **(d)** LAP2α and Rb795. DNA was stained using chromatin-staining dye DAPI. Images were collected on a Zeiss confocal microscope and projected as black and white or blue/red/green colour merged micrographs in which DAPI is in blue, LAP2α is in red and Rb780 and Rb795 are in green. Magnification 80x.

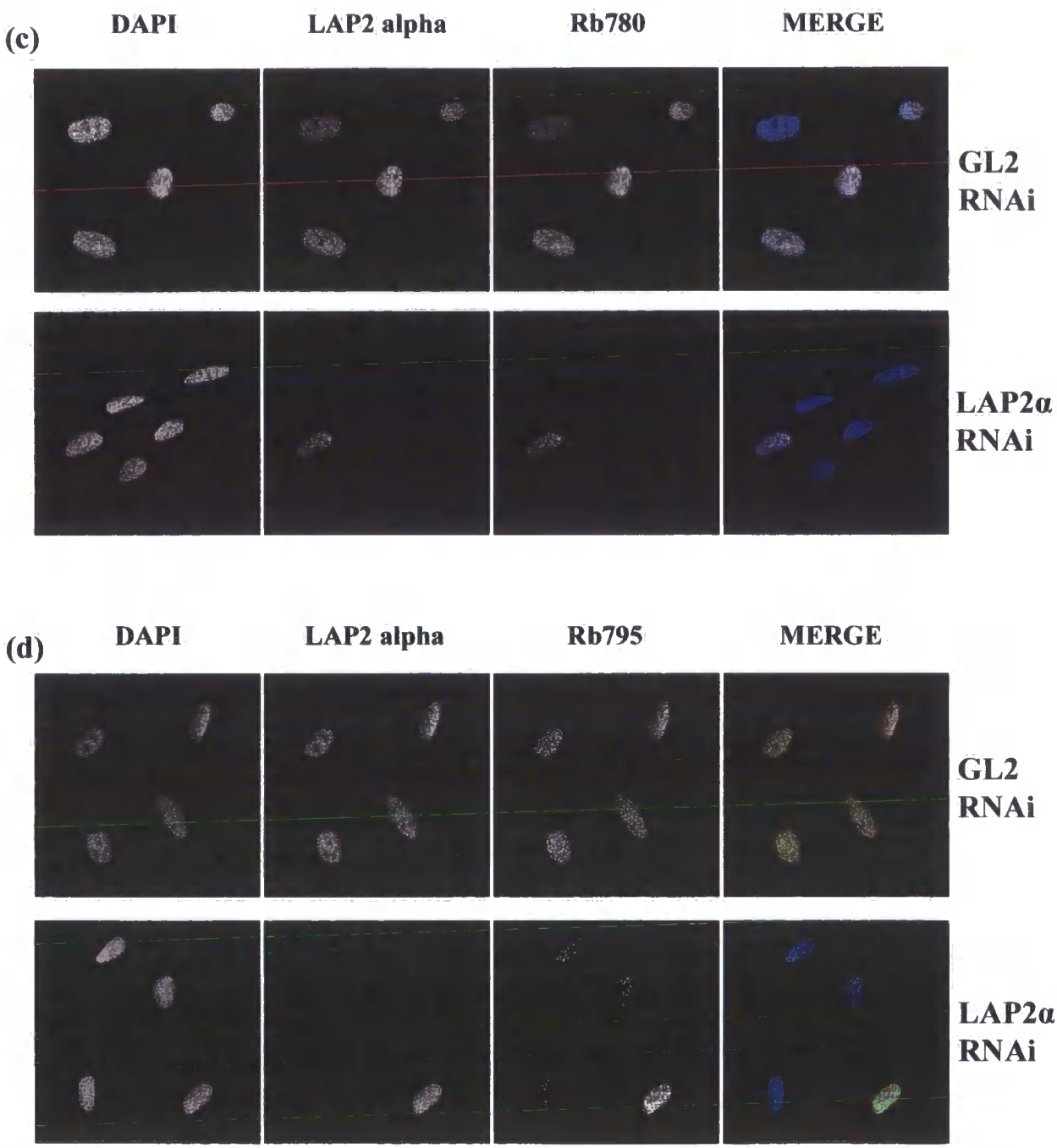
(c)
DAPI
LAP2 alpha
Rb780
MERGE
GL2 RNAi
LAP2α RNAi
(d)
DAPI
LAP2 alpha
Rb795
MERGE
GL2 RNAi
LAP2α RNAi

# Figure 4.14B

**Figure 4.15: LAP2α knockdown in early passage fibroblasts shows a significant down-regulation of LAP2α and Rb780 protein levels.** Early passage **(p8)** fibroblasts seeded at a medium density were grown in culture for one day and transfected with either RNA oligonucleotides designed to interfere against LAP2α-specific mRNA or control RNAi (GL2) oligonucleotides targeting Firefly luciferase. After 24 hours, transfected cultures were sub-cultured, grown in culture for another 48 hours and harvested. Whole cell extracts were prepared from the same number of cells for both transfected cultures and immunoblotted using antibodies against LAP2α (LAP15), LAP2β (LAP17), lamin A/C (JOL2) and Rb phosphorylated on serine 780 (Rb780). Molecular weight markers showed the expected mobility for the above proteins: LAP2α (75 kDa), LAP2β (55 kDa), lamin A & C (70 & 65 kDa) and Rb780 (115 kDa).

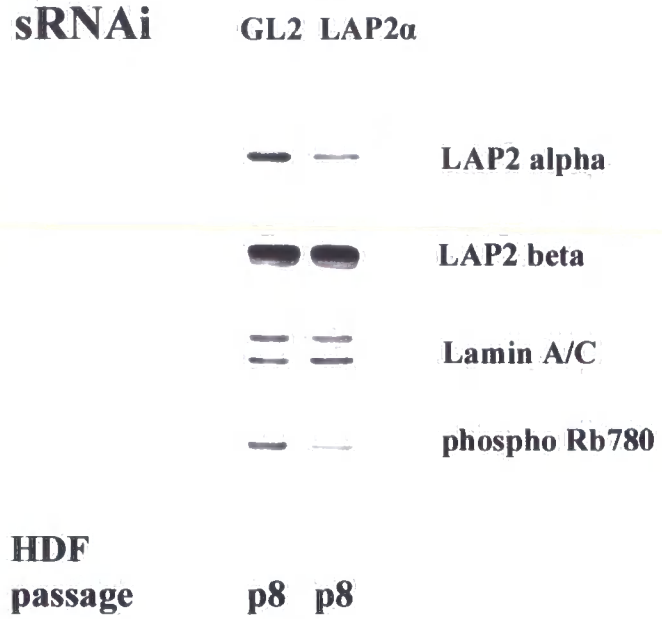
sRNAi
GL2
LAP2α
LAP2 alpha
LAP2 beta
Lamin A/C
phospho Rb780
HDF
passage
p8
p8

**Figure 4.15**

**Figure 4.16A: Rb795 nuclear foci co-localise with splicing compartments in late passage and Y259X fibroblasts.** **(a)** Early passage **(p7)** and late-passage **(p44)** fibroblasts were grown in culture for 3 days and processed for immunofluorescence microscopy using antibodies against SC-35 and Rb795. **(b)** Early **(p12)** and mid-passage **(p18)** Y259X fibroblasts were processed for immunofluorescence microscopy using antibodies against SC-35 and Rb795. Images were collected on a BioRad Radiance 2000 confocal microscope and projected as black and white or red/green colour merged micrographs in which SC-35 is in red and Rb795 is in green. Magnification 320x.

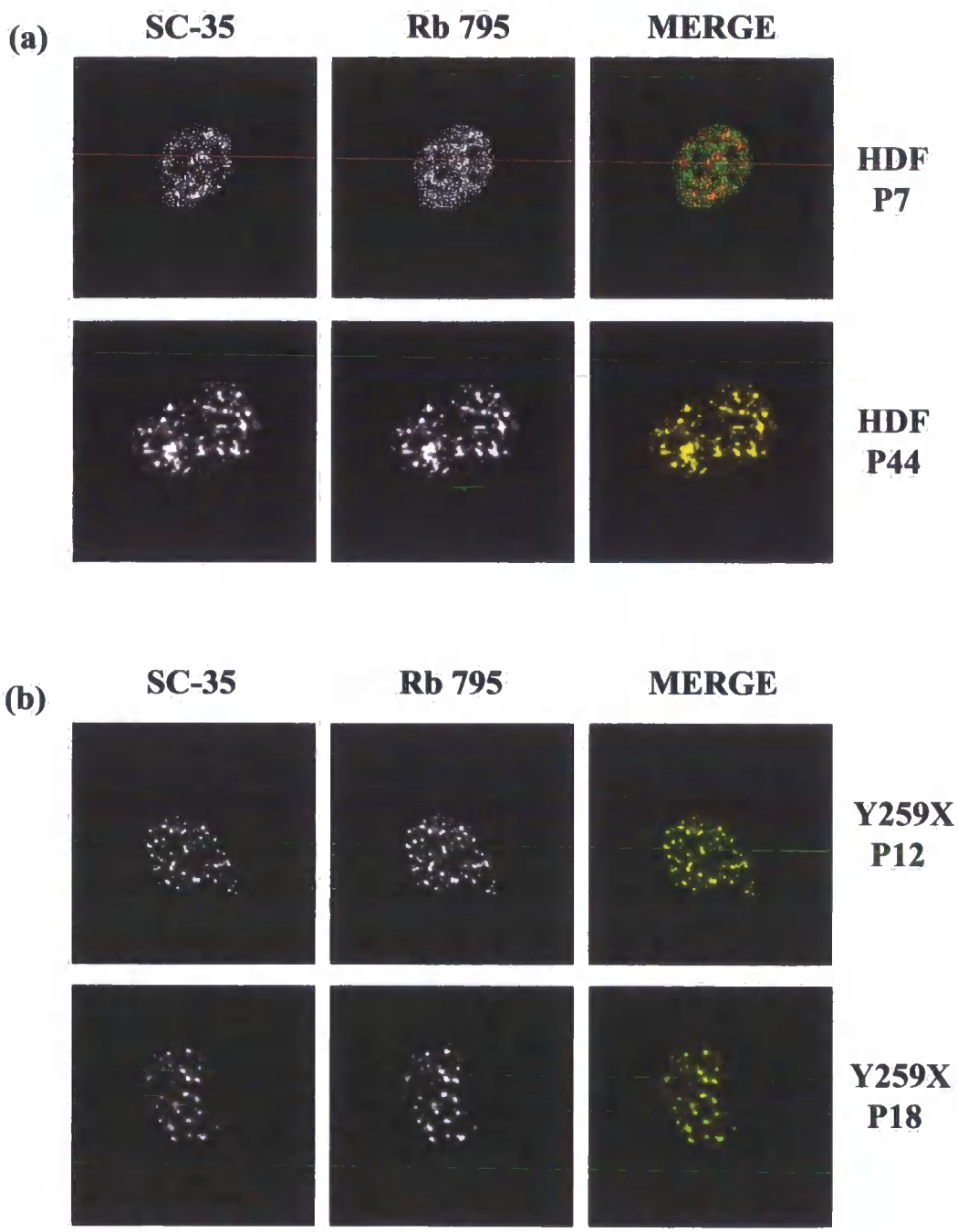
(a)
SC-35
Rb 795
MERGE
HDF
P7
HDF
P44
(b)
SC-35
Rb 795
MERGE
Y259X
P12
Y259X
P18

**Figure 4.16A**

**Figure 4.16B: Rb795 foci and splicing compartments are retained in the same speckled pattern upon extraction *in situ* of late passage and Y259X fibroblasts.**

**(a)** Early passage **(p7)** and late-passage **(p44)** fibroblasts were extracted *in situ* by detergent/nuclease/salt extraction and processed for double confocal microscopy using antibodies against SC-35 and Rb795. **(b)** Early **(p12)** and mid-passage **(p18)** Y259X fibroblasts were extracted *in situ* by detergent/nuclease/salt extraction and processed for double confocal microscopy using antibodies against SC-35 and Rb795. **(a)** & **(b)** show cells after V stage (ammonium sulphate) extraction. Images were collected on a BioRad Radiance 2000 confocal microscope and projected as black and white or red/green colour merged micrographs in which SC-35 is in red and Rb795 is in green. Magnification 320x.

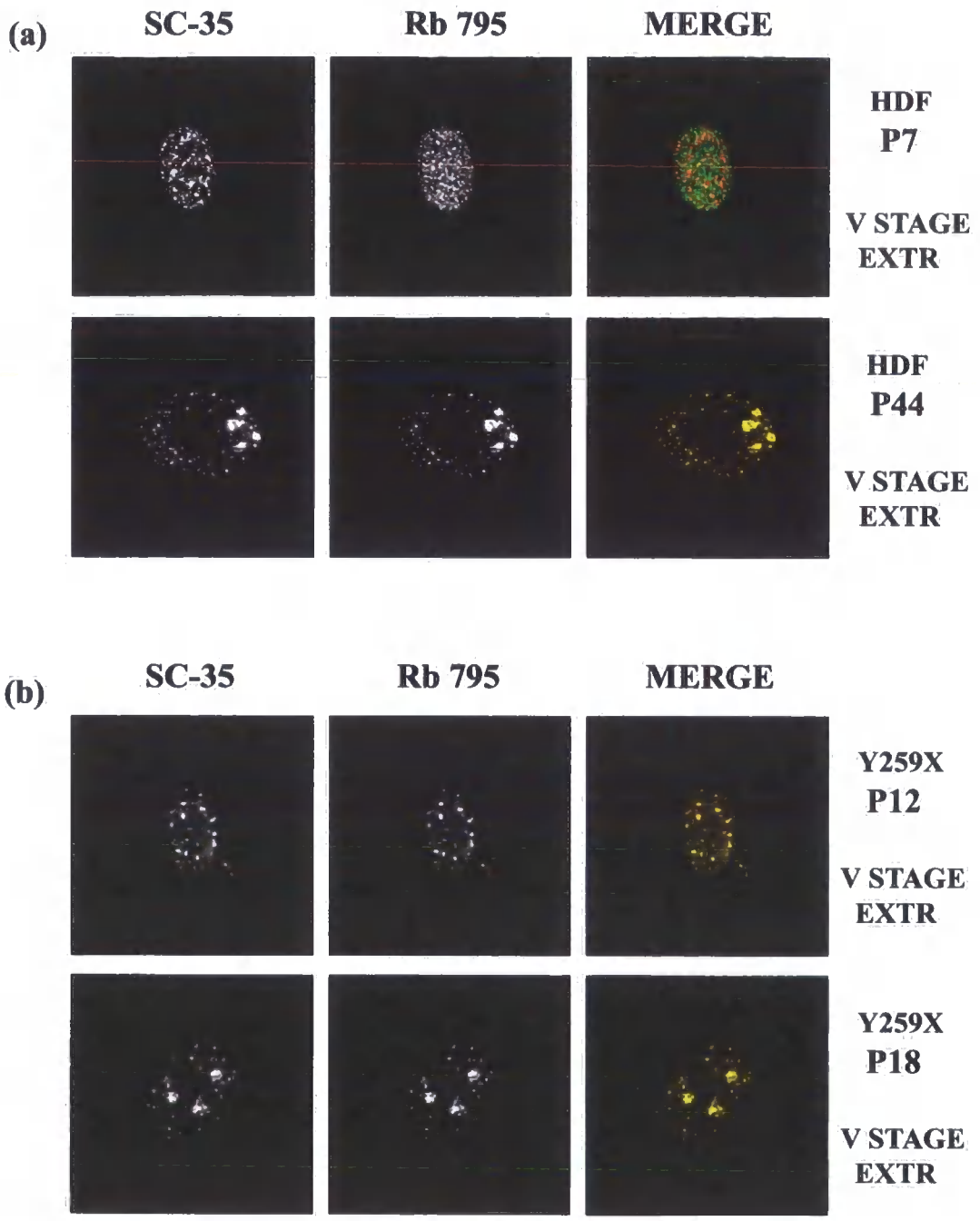
(a)
SC-35
Rb 795
MERGE
HDF
P7
V STAGE
EXTR
HDF
P44
V STAGE
EXTR
(b)
SC-35
Rb 795
MERGE
Y259X
P12
V STAGE
EXTR
Y259X
P18
V STAGE
EXTR

**Figure 4.16B**

**Figure 4.17A: Rb795 shows distinct localisation patterns during G1 phase of synchronously growing fibroblasts.** Early **(p8)** passage fibroblasts were grown for 2 days in culture and synchronised by serum starvation for 4 days. Cell cultures were re-stimulated for **6 (a), 12 (b), 18 (c)** and **24 (d)** hours and processed for immunofluorescence microscopy using antibodies against SC-35 and Rb780. Images were collected on a BioRad Radiance 2000 confocal microscope and projected as individual black and white or red/green colour merged micrographs in which SC-35 is in red, and Rb795 is in green. Magnification 120x.

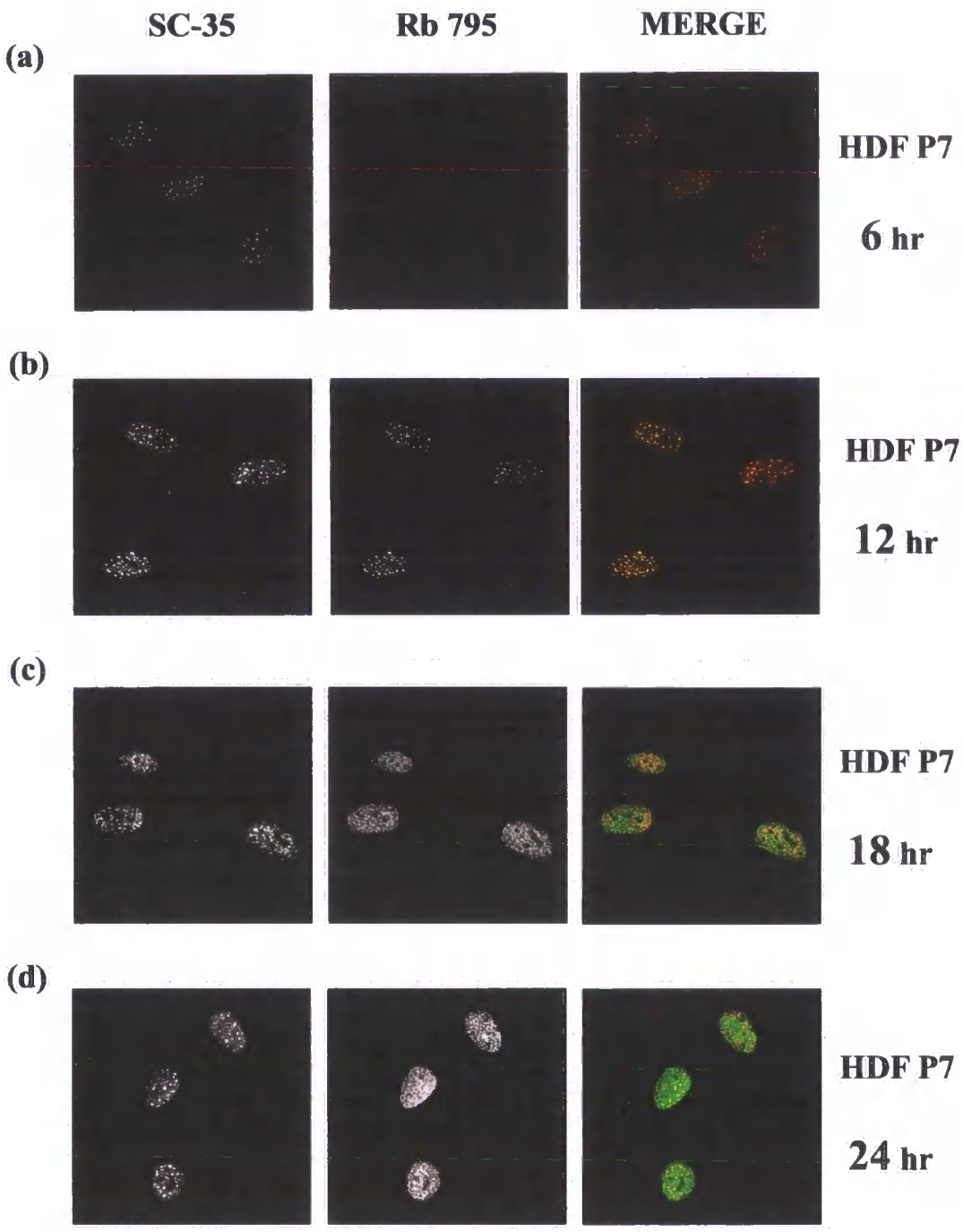
SC-35
Rb 795
MERGE
(a)
HDF P7
6 hr
(b)
HDF P7
12 hr
(c)
HDF P7
18 hr
(d)
HDF P7
24 hr

# Figure 4.17A

**Figure 4.17B: Localisation of Rb795 in splicing speckles during early G1 correlates with its nuclear anchorage.** Early **(p8)** passage fibroblasts were grown for 2 days in culture and synchronised by serum starvation for 4 days. Cell cultures were re-stimulated for **6 (a), 12 (b), 18 (c)** and **24 (d)** hours, extracted *in situ* by detergents/DNAse1/salts and processed for immunofluorescence microscopy using antibodies against SC-35 and Rb795. Images were collected on a BioRad Radiance 2000 confocal microscope and projected as individual black and white or red/green colour merged micrographs in which SC-35 is in red, and Rb795 is in green. Magnification 120x.

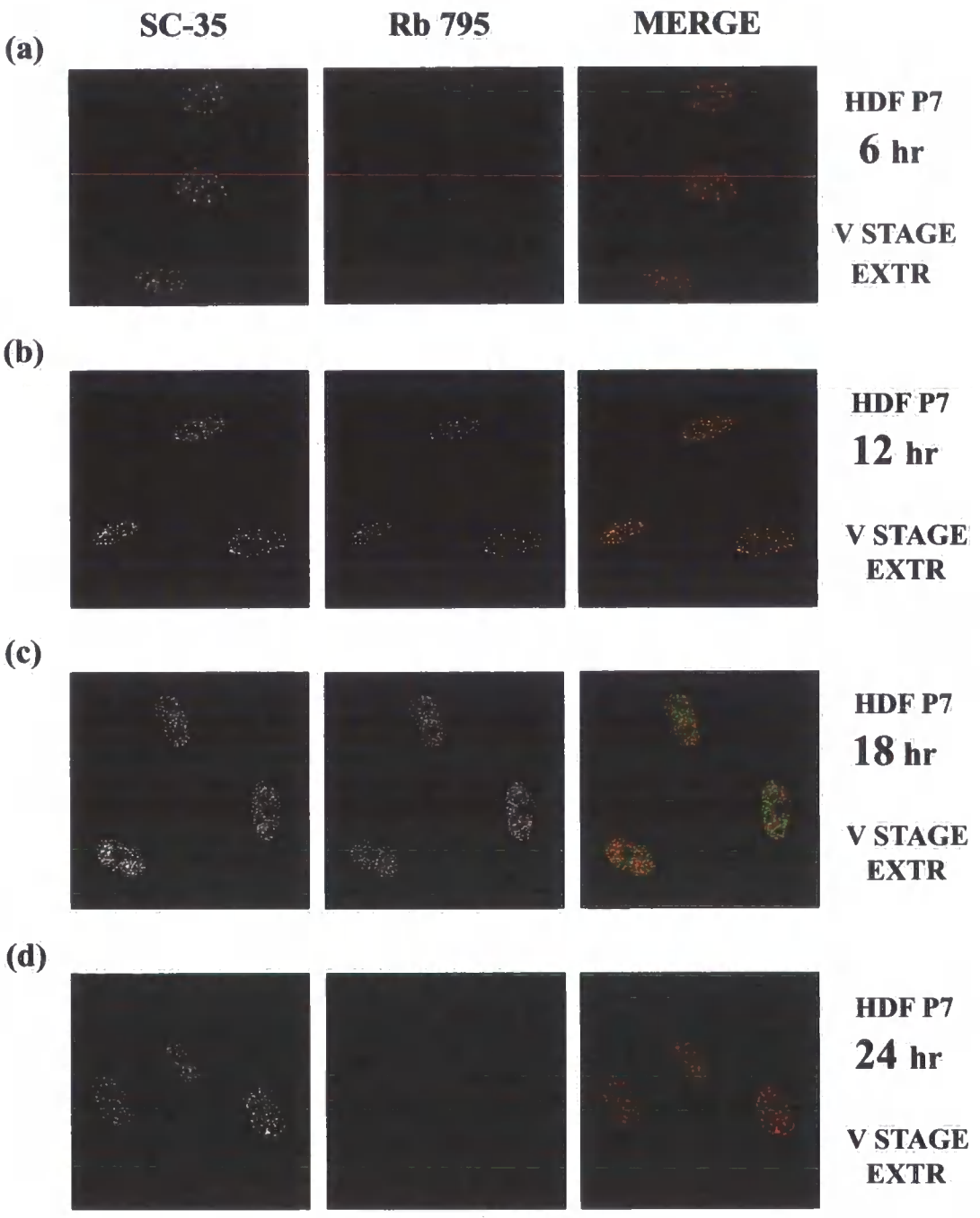
SC-35
Rb 795
MERGE
(a)
HDF P7
6 hr
V STAGE
EXTR
(b)
HDF P7
12 hr
V STAGE
EXTR
(c)
HDF P7
18 hr
V STAGE
EXTR
(d)
HDF P7
24 hr
V STAGE
EXTR

**Figure 4.17B**

**Figure 4.18: Wild-type fibroblasts of late passage and Y259X fibroblasts do not reveal internal heterochromatin foci but show focal areas of condensed chromatin that partially co-localise with Rb795 foci.** **(a)** Early passage **(p7)** and late-passage **(p44)** fibroblasts were processed for confocal microscopy using Rb795 antibody and a DNA-intercalating dye DAPI **(b)** Early **(p12)** and mid-passage **(p18)** Y259X fibroblasts were processed for confocal microscopy using Rb795 antibody and a DNA-intercalating dye DAPI. Images were collected on a Zeiss confocal microscope and projected as individual black and white or blue/green colour merged micrographs in which DAPI is in blue, and Rb795 is in green. Magnification 320x.

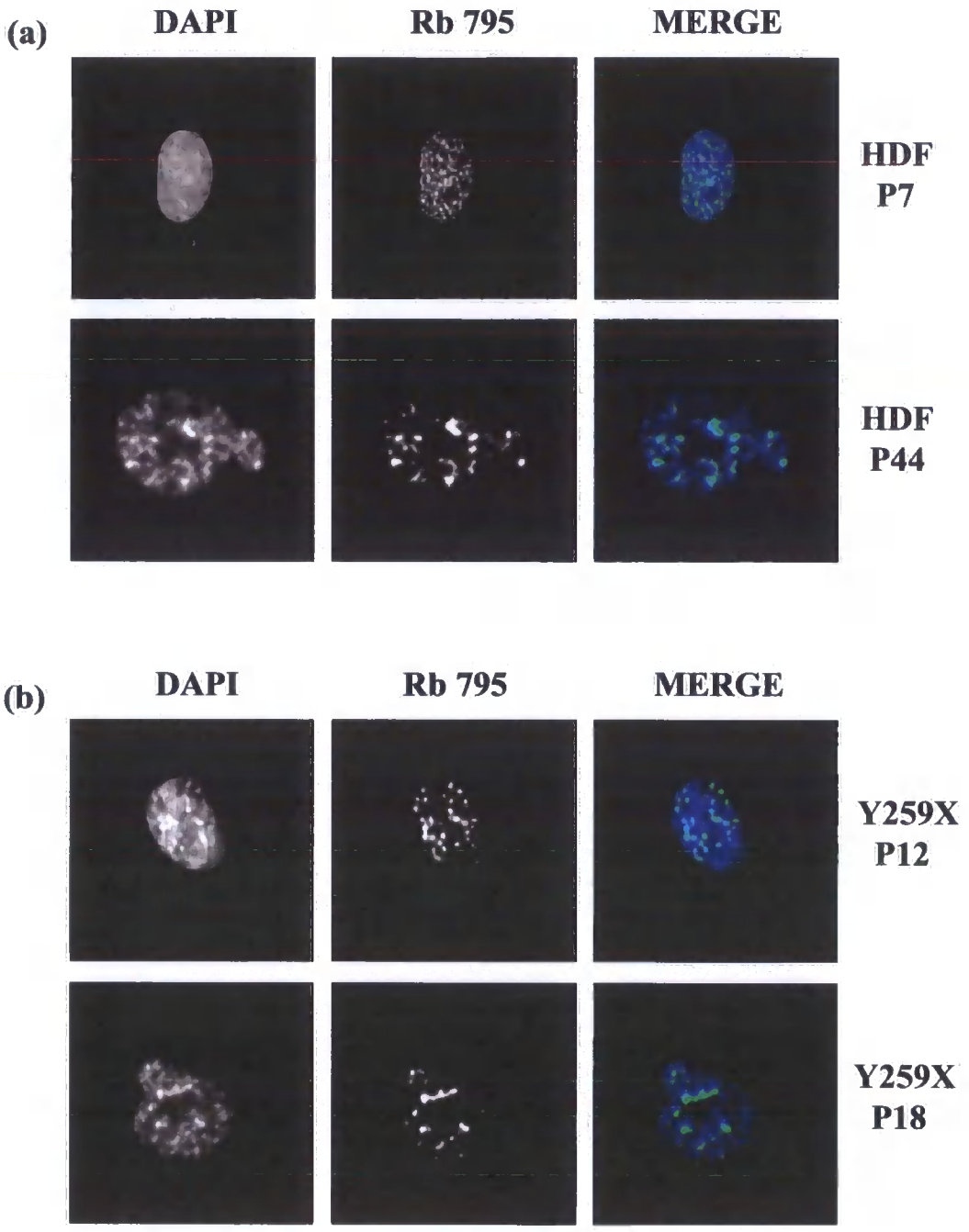
(a)
DAPI
Rb 795
MERGE
HDF
P7
HDF
P44
(b)
DAPI
Rb 795
MERGE
Y259X
P12
Y259X
P18

**Figure 4.18**

**Figure 4.19: DNA-damage associated phospho-histone foci accumulate in wild-type fibroblasts of late passage and Y259X fibroblasts and show a close association with Rb795 foci.** **(a)** Early passage **(p7)** and late-passage **(p44)** fibroblasts were processed for double confocal microscopy using antibodies against phospho-histone H2A.X and Rb795. **(b)** Early passage **(p12)** and mid-passage **(p18)** Y259 laminopathy fibroblasts were processed for double confocal microscopy using antibodies against phospho-histone H2A.X and Rb795. Images were collected on a Zeiss confocal microscope and projected as individual black and white or red/green colour merged micrographs in which H2A.X is in red, and Rb795 is in green. Magnification 360x.

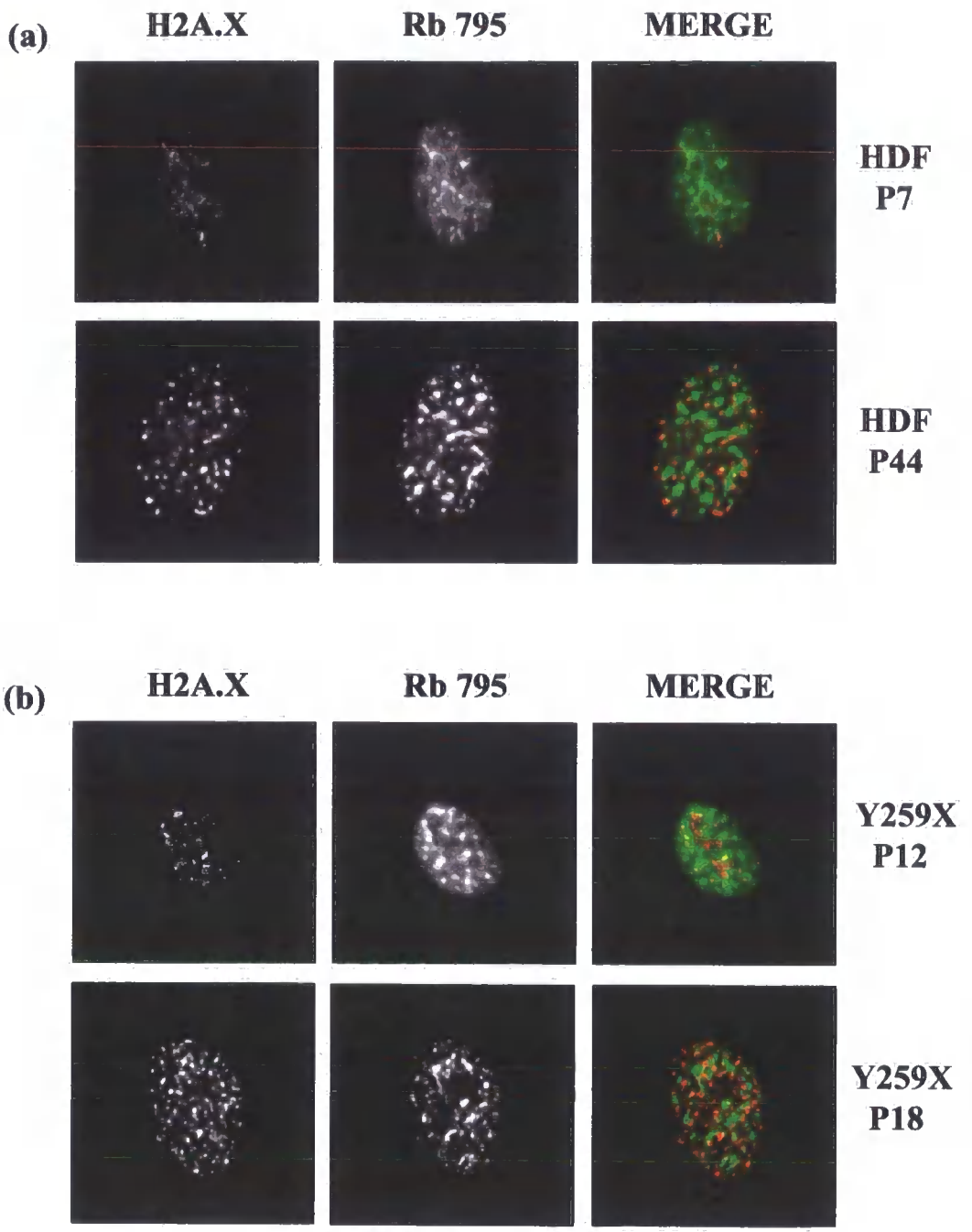
(a)
H2A.X
Rb 795
MERGE
HDF
P7
HDF
P44
(b)
H2A.X
Rb 795
MERGE
Y259X
P12
Y259X
P18

**Figure 4.19**

# CHAPTER 5-EXPRESSION, DISTRIBUTION AND SOLUBILITY PROPERTIES OF A-TYPE LAMINS, LAP2α AND RETINOBLASTOMA PROTEIN IN HUMAN FIBROBLASTS UNDERGOING QUIESCENCE

## Introduction

Growing primary cells in a limited amount of growth factors (serum) in their growth media or growing them to a high density induces quiescence ($G_0$ arrest) in otherwise proliferating cells (Lea *et al.*, 2003). Many different cell types in the human body are in a quiescent ($G_0$) state. Human dermal fibroblasts are one of the most popular primary cell models used for studying quiescence and cell cycle entry (Bridger *et al.*, 1993, Dyer *et al.*, 1997, Markiewicz *et al.*, 2002a). Unlike permanently arrested senescent fibroblasts, quiescent fibroblasts are only transiently arrested and are able to re-enter G1 phase of the cell cycle and divide upon exposure to mitogenic signals (growth factors in their media). Mitogenic stimulation of quiescent cells causes activation of a cascade of cyclin-dependent kinase (cdk)-cyclin complexes that initially hypo-phosphorylate and activate retinoblastoma protein (Rb) (Lees *et al.*, 1991). Hypophosphorylation of Rb is initiated by cdk6/4-cyclin D, and certain sites are known to be phosphorylated preferentially by different cdks, e.g., S780 and S795 by cdk4/6-cyclin D and T821 by cdk2-cyclin E. The hypo-phosphorylated Rb protein controls progression through G1 phase by inhibiting E2F transcription factor and thus negatively regulating late G1 phase restriction point and entry into S-phase (Chellappan *et al.*, 1991). During late G1, Rb protein is hyperphosphorylated by cdk-cyclin complexes, which inactivate its growth-suppressing function. The phosphorylation-dependent anchorage of Rb in the nucleus is essential for its growth-suppressing function during G1 phase of cell cycle (Mittnacht and Weinberg 1991, Mancini *et al.*, 1994).

During $G_1$-$G_0$ transition, Rb protein becomes un-phosphorylated (Ezhevsky *et al.*, 2001). Interestingly, un-phosphorylated Rb present in quiescent cells is not involved in active growth-suppression of E2F-regulated genes (Ezhevsky *et al.*, 2001). Instead, E2F genes are suppressed by Rb-related proteins p107 and p130 (Smith *et al.*, 1996). In addition to suppression of E2F-regulated genes, p130 is also involved in suppression of

metabolic genes during quiescent arrest. As a result, upon exposure to mitogenic signals, quiescent $G_0$ cells take longer to enter S-phase in the first cell cycle than in subsequent cell cycle. This is because during $G_0$-$G_1$ transition, there is a requirement in an increase in protein and RNA synthesis of metabolic genes necessary for entry into S-phase and a subsequent division. Thus, hypophosphorylated Rb actively suppresses S-phase genes but not metabolic genes. Interestingly, during senescent arrest, whilst E2F genes are actively suppressed, metabolic genes are still active. Therefore senescent fibroblasts do not rest in a true $G_0$ state but are arrested in G1 phase. Senescent arrest depends on sustained 'hyper-mitogenic' stimuli, which is different from 'hypo-mitogenic' arrest of quiescent cells (Blagosklonny *et al.*, 2003). Indeed, whilst quiescent fibroblasts lose hypo-phosphorylated Rb, senescent fibroblasts retain distinct nuclear foci of hypophosphorylated isoform Rb795 (chapter 4). These Rb foci are stably anchored in the nuclei of senescent cells, which is essential property for growth suppression. These investigations indicate that Rb795 foci in senescent fibroblasts may also depend on the presence of mitogenic stimuli.

Interestingly, LAP2α protein is expressed in a mitogen-dependent manner and its protein expression is absent in serum-deprived quiescent cells (Markiewicz *et al.*, 2002a). Following mitogenic stimulation of quiescent fibroblasts increasing expression of LAP2α coincides with an increased expression and nuclear anchorage of hypophosphorylated Rb. A-type lamins and LAP2α complexes bind to hypophosphorylated Rb during G1 phase of cell cycle and were proposed to regulate its nuclear anchorage. Indeed, RNAi knock-down of LAP2α in proliferating human fibroblasts led to decreased expression of hypophosphorylated Rb and cell cycle arrest despite the presence of mitogenic factors (chapter 4). These results suggest that nuclear anchorage of hypo-phosphorylated Rb is also required for proper progression through G1 phase of cell cycle. Although LAP2α expression is essential for nuclear anchorage of hypo-phosphorylated Rb, A-type lamins regulate nuclear anchorage of LAP2α that may in turn regulate nuclear anchorage of hypo-phosphorylated Rb during G1 phase. This is based on the findings that a lack of functional A-type lamins in laminopathy fibroblasts with Y259X mutation or RNAi knockdown of A-type lamins in human fibroblasts led to a loss of nuclear anchorage of both LAP2α and hypophosphorylated isoform Rb780 (chapter 4). Similarly, in senescent fibroblasts increased solubility/

instability of A-type lamins leads to a loss of nuclear anchorage of LAP2α and hypo-phosphorylated isoform Rb780.

In contrast to LAP2α, protein expression of A-type lamins is stable during quiescent arrest of human fibroblasts (Dyer *et al.*, 1997). Upon exposure of quiescent human fibroblasts to mitogenic signals, A-type lamins undergo N-terminal and C-terminal modifications which are thought to stabilise proliferation status of cells (Dyer *et al.*, 1997). Conversely, lack of these lamin modifications (Dyer *et al.*, 1997) may promote different lamin protein arrangements that promote stable quiescence. Increased protein stability of A-type lamins has also been proposed to support stable quiescent arrest in mouse fibroblasts (Pugh *et al.*, 1997). On the other hand, it has been reported that as fibroblasts age in culture they are increasingly incapable of entering quiescent arrest (Stein *et al.*, 1999). Since A-type lamins show aberrant assembly in senescent fibroblasts, this may prevent lamin protein rearrangements and/or modifications that allow entry into stable quiescent arrest.

Interestingly, although Rb protein levels do not become down-regulated during quiescent arrest, it is not known whether hypophosphorylated Rb becomes a target for degradation or dephosphorylation by a phosphatase (Ezhevsky *et al.*, 2001). The above results suggest that expression of hypo-phosphorylated Rb is at least in part regulated by its nuclear anchorage. In addition, the absence of growth-suppressing activity of un-phosphorylated Rb in quiescent cells may also be regulated by its nuclear anchorage. Therefore during $G_1$-$G_0$ transition of fibroblasts undergoing quiescence, changes in A-type lamins may regulate nuclear anchorage of LAP2α and hypo-phosphorylated Rb, which may lead to their eventual loss of protein expression during quiescent arrest.

In this chapter it was set out to explore how the mechanism of transient quiescent arrest may differ from permanent senescent arrest. In attempt to understand some of these differences, it was investigated how nuclear organisation, solubility properties and modifications of A-type lamins may differ in quiescence as opposed to senescence and whether these may regulate nuclear anchorage of LAP2α and hypo-phosphorylated Rb in fibroblasts undergoing quiescence. In addition, it was investigated how LAP2α expression and nuclear anchorage relate to expression and nuclear anchorage of hypo-phosphorylated Rb isoforms Rb780 and Rb795 in mitogen-restimulated quiescent

fibroblasts and whether LAP2α expression and Rb795 foci in senescent cells depend on mitogenic stimuli.

## Results

### 5.1. Protein expression of lamins, LAP2s and Rb in serum-starved (quiescent) and serum-re-stimulated quiescent fibroblasts as assessed by immunoblotting

LAP2α and hypo-phosphorylated Rb780 protein levels become down-regulated during quiescent arrest induced by serum-starvation (Markiewicz *et al.*, 2002a) and initially these results were confirmed by immunoblotting. Primary cultures of early passage (p8) human dermal fibroblasts were grown in complete medium (10% serum) for 2 days after which their media was replaced by serum-restricted medium (0.5% serum) in which cells were grown for 4 days to induce quiescence. As a proliferating control (P), cells were grown for 3 days in complete medium and harvested. Following growth in serum-restricted media, quiescent cultures (Q) were either immediately harvested or serum-re-stimulated for either 6 (R6), 12 (R12), 18 (R18) or 24 (R24) hours and subsequently harvested at those time-points. Whole cell extracts were prepared from the same number of cells and blotted using antibodies against LAP2α, LAP2β, lamins A/C, lamin B2, total Rb (IF8) and Rb isoform phosphorylated on ser 780 (Rb780).

These results confirm (**Figure 5.1**) that LAP2α expression became absent in quiescent fibroblasts (Q) as compared to proliferating fibroblasts (P). Following serum-restimulation of quiescent fibroblasts, LAP2α protein expression gradually increased (R6-18) and at 24 hours after re-stimulation (P24) reached a higher level than that of asynchronously growing fibroblasts (P). In contrast to LAP2α, LAP2β protein level did not significantly change between proliferating (P), quiescent (Q) or re-stimulated (R6-24) cultures. Similarly to LAP2β, no significant change was observed in protein expression levels of lamins A/C and lamin B2 between proliferating (P), quiescent (Q) or re-stimulated (R6-24) cultures. Immunoblotting against total Rb protein (IF8) showed that proliferating fibroblasts (P) had two populations of Rb protein- a slightly faster migrating band of 110 kDa that represents un- and under-phosphorylated Rb and a slower migrating band of 115 kDa that represents hyper-phosphorylated Rb. In proliferating cells (P), both hypo- and hyper-phosphorylated Rb species were present at

a similar level. In contrast, in quiescent cells (Q), the slower migrating hyper-phosphorylated Rb population was completely absent whilst the faster migrating Rb population was somewhat increased. On the other hand, in serum-re-stimulated cultures, hyper-phosphorylated Rb population progressively increased (R6-18) and at 24 hours after re-stimulation was present at higher level to that of asynchronously proliferating cells (P). The increase in hyper-phosphorylated Rb in R24 cultures was accompanied by a decrease in hypo-phosphorylated Rb level. Similarly to LAP2α, immunoblotting with a phospho-specific Rb antibody against hypo-phosphorylated isoform Rb780 confirmed that in quiescent cells (Q) Rb780 population was completely undetectable as compared to proliferating cells (P) but its protein expression gradually increased in re-stimulated cultures (R6-18) reaching a higher level to that of proliferating cells (P) after 24 hour-re-stimulation (R24). These results show that that in addition to a loss of hyper-phosphorylated Rb population, quiescent fibroblasts lose hypo-phosphorylated Rb780, which suggests that during quiescence the faster migrating Rb band detected by IF8 antibody represents un-phosphorylated Rb population as expected.

## 5.2. Cellular localisation and solubility properties of LAP2α and hypo-phosphorylated Rb isoforms during serum-re-stimulation of quiescent fibroblasts

The above results confirm that LAP2α and Rb780 protein expression increases following serum-restimulation of quiescent fibroblasts. Immunofluorescent microscopy showed that Rb795 expression also increases following serum-restimulation of quiescent fibroblasts, which is accompanied by distinct changes in its localisation patterns (Chapter 4). This prompted me to examine Rb780 and Rb795 distribution in relation to LAP2α expression during serum-restimulation of quiescent fibroblasts. Early (p8) passage cells were grown for 2 days in culture and synchronised by serum starvation for 4 days. Cell cultures were re-stimulated for 12, 18 and 24 hours and subsequently processed for immunofluorescence microscopy using antibodies against: 1) LAP2α and Rb780, and 2) LAP2α and Rb795.

During early-mid G1 phase (12 hours), LAP2α antibody showed that LAP2α expression appeared weakly in the nucleoplasm of most cells excluding nucleoli (**Figure 5.2A (a) LAP2α**). In cells where LAP2α began to appear weakly in the nucleus, Rb780 was also present as weakly in the nucleoplasm (**Figure 5.2A (a) Rb780**). In contrast, Rb795

appeared in bright nuclear dots in addition to weak nucleoplasmic distribution in cells that began to express LAP2α weakly in the nucleoplasm (**Figure 5.2A (a) Rb795**). During mid-late G1 (18 hours), LAP2α was present more brightly in the nucleoplasm of most cells (**Figure 5.2A (b) LAP2α**) and those cells showed brighter nucleoplasmic distribution of Rb780, which became somewhat more granular (**Figure 5.2A (b) Rb780**). In cells that expressed LAP2α more brightly in the nucleoplasm, Rb795 was also present more brightly in the nucleoplasm in addition to prominent nuclear dots (**Figure 5.2A (b) Rb795**). During S-phase (24 hours), LAP2α was present intensely in the nucleoplasm (**Figure 5.2A (c) LAP2α**) and in these cells Rb780 appeared intensely in the nucleoplasm (**Figure 5.2A (c) Rb780**). Rb795 also had a bright granular nucleoplasmic distribution and lacked prominent nuclear dots in cells which displayed intense LAP2α in the nucleoplasm (**Figure 5.2A (c) Rb795**). Both Rb780 and Rb795 nucleoplasmic distribution significantly co-localised with LAP2α distribution following 24 hour-serum-restimulation (**Figure 5.2A (c) MERGE**). These results show that upon serum-restimulation of quiescent fibroblasts an increased expression of LAP2α correlates with an increased expression of hypo-phosphorylated Rb isoforms. Whilst distribution pattern of Rb780 correlated significantly with LAP2α from early G1, Rb795 distribution correlated with LAP2α only after 18 hour post-restimulation (mid-late G1).

The nuclear anchorage of hypo-phosphorylated Rb increases with an increase in LAP2α expression (Markiewicz *et al.*, 2002a). Therefore the solubility properties of Rb780 and Rb795 were investigated in relation to LAP2α nuclear anchorage during serum-restimulation of quiescent fibroblasts. Early (p8) passage cells were synchronised by serum starvation for 4 days and re-stimulated for 12, 18 and 24 hours. Cell cultures were extracted *in situ* by detergent extraction (CSK/Triton X-100) and processed for double for immunofluorescence microscopy using antibodies against: 1) LAP2α and Rb780, and 2) LAP2α and Rb795.

Following Triton extraction of 12 hour-re-stimulated fibroblasts, LAP2α was retained very weakly in nuclei of most cells (**Figure 5.2B (a) LAP2α**) and Rb780 was retained very weakly in nuclei of these cells (**Figure 5.2B (a) Rb780**). In contrast, Rb795 was retained in small bright nuclear dots and only very weakly in the nucleoplasm in cells that retained weak LAP2α in the nucleus (**Figure 5.2B (a) Rb795**). After 18 hour-restimulation, LAP2α was retained more brightly in the nuclei (**Figure 5.2B (b)**

**LAP2α)** and those cells showed increased retention of Rb780 in the nucleus, which appeared as somewhat brighter and more granular staining after extraction **(Figure 5.2B (b) Rb780)**. Rb795 was also retained more brightly following extraction both in the nucleoplasm and in prominent nuclear dots in cells that retained brighter LAP2α in the nucleus **(Figure 5.2B (b) Rb795)**. Following Triton extraction of 24 hour-re-stimulated fibroblasts, LAP2α was retained intensely in the nucleus **(Figure 5.2B (c) LAP2α)** and in these cells neither Rb780 nor Rb795 was retained in the nucleus **(Figure 5.2B (c) Rb780 & Rb795)**. These results show that both Rb isoforms become increasingly anchored in the nuclei of cells in G1 phase of cell cycle that display an increased retention of LAP2α. In contrast, during S-phase when Rb becomes hyper-phosphorylated, Rb isoforms lost nuclear anchorage despite increased nuclear anchorage of LAP2α. Whilst Rb780 retention in the nucleoplasm correlated with an increased retention of LAP2α in the nucleus during G1 phase, Rb795 retention in the nucleoplasm correlated with LAP2α retention in the nucleus only after 18 hour post-restimulation (mid-late G1).

## 5.3. Protein expression of lamins, LAP2s and Rb in quiescent fibroblasts induced by contact-inhibition as assessed by immunoblotting

Primary cultures such as human dermal fibroblasts can also enter quiescent arrest by contact inhibition after reaching growth to a high density (confluence). It was therefore decided to investigate protein expression of LAP2α and Rb following quiescent arrest of fibroblasts induced by contact-inhibition by immunoblotting. Primary cultures of early passage (p8) human dermal fibroblasts were grown in complete medium (10% serum) for 7 days (confluent stage) or 10 days (post-confluent stage) without media change and harvested. As a proliferating control (P), cells were grown for 3 days in complete medium and harvested. Whole cell extracts were prepared from the same number of cells and blotted using antibodies against LAP2α, LAP2β, lamins A/C, lamin B2, total Rb (IF8) and Rb isoform phosphorylated on ser 780 (Rb780).

**Figure 5.3** shows that LAP2α protein expression became significantly decreased in confluent fibroblasts (C) as compared to proliferating fibroblasts (P). At post-confluent stage (PC), LAP2α protein expression became completely undetectable. In contrast to LAP2α, LAP2β protein level did not significantly change between proliferating (P),

confluent (C) and post-confluent (PC) cultures. In addition, protein levels of lamins A/C and lamin B2 remained constant between proliferating (P), confluent (C) and post-confluent (PC) cultures. Immunoblotting against total Rb protein (IF8) showed that proliferating cells (P) had two populations of Rb protein as expected: a slightly faster migrating band of 110 kDa which represents un- and under-phosphorylated Rb and a slower migrating band of 115 kDa which represents hyperphosphorylated Rb. In proliferating cells (P), both hypo- and hyper-phosphorylated Rb species were present at a similar level. In confluent fibroblasts (C), the slower migrating hyper-phosphorylated Rb population was significantly decreased and was completely absent in post-confluent cultures (PC). On the other hand, faster-migrating Rb population increased gradually in confluent cultures (C) and post-confluent cultures (PC). Immunoblotting with a phospho-specific Rb antibody against hypo-phosphorylated isoform Rb780 showed that in confluent cells (C) Rb780 protein level was significantly decreased and was completely absent in post-confluent (PC) cells. These results show that similarly to quiescent arrest induced by serum-starvation, quiescent arrest induced by contact inhibition is also accompanied by a gradual decline in the protein level of LAP2α and hypo-phosphorylated Rb 780.

### 5.4. Cellular localisation of lamins and LAP2s in quiescent fibroblasts as assessed by immunocytochemistry and confocal microscopy

Late passage fibroblasts which entered senescent arrest display changes in nuclear morphology which are accompanied by changes in lamin distribution at the nuclear envelope and aggregation of LAP2α in the nucleus (Chapter 3). To investigate how nuclear organisation of A-type lamins and LAP2α may differ during quiescent arrest as opposed to senescent arrest, the cellular localisation patterns of these proteins were examined using immunocytochemistry and confocal microscopy. Human dermal fibroblasts of early passage (p8) were induced to enter quiescent arrest by either serum-starvation or contact inhibition as described above. As a control, cells were grown for 3 days in complete medium to obtain proliferating cultures (not shown). Cultures were processed for double immunofluorescence microscopy using antibodies against: a) LAP2α and proliferating marker Ki67, b) LAP2α and lamin C, c) lamin B2 and Ki67, and d) LAP2β and Ki67. The same results were obtained for both serum-starved and contact-inhibited cultures. To avoid repetition, only images of serum-starved cultures

(Q) were shown which contained majority of non-proliferating quiescent cells and a minority of proliferating cells.

**Figure 5.4 (a)** shows serum-starved quiescent cultures of early passage (p8) in which more than 90% of cells stained negatively for proliferation marker Ki67 and these nuclei had a decreased or absent LAP2α staining in the nucleus. 10% of cells that stained brightly for Ki67 displayed bright nucleoplasmic distribution of LAP2α (excluding nucleoli). In Ki67 negative quiescent cells, we did not observe any LAP2α aggregation in the nucleus or in the cytoplasm. Next, in quiescent cells which showed decreased or absent LAP2α staining, lamin C showed a pronounced nuclear envelope distribution and a slightly decreased level in the nucleoplasm as compared to cells which displayed bright nucleoplasmic distribution of LAP2α **(Figure 5.4 (b))**. Similarly to Ki67-positive cells, in majority of quiescent cells (>95%), lamin C staining revealed ovoid nuclear shapes. In addition, in Ki67-negative quiescent nuclei, DNA-staining dye DAPI strongly overlapped with lamin C staining along the NE periphery (not shown).

In Ki67-negative quiescent nuclei, lamin B2 was present at both the nuclear envelope and in the nucleoplasm and at a similar intensity to a minority of Ki67 positive cells **(Figure 5.4 (c))**. Likewise, a B-type lamin binding partner, LAP2β was found at both the nuclear envelope and nucleoplasm in Ki67-negative quiescent cells and at a similar intensity to a minority of Ki67-positive cells **(Figure 5.4 (d)).** Both lamin B2 and LAP2β staining revealed ovoid-shaped nuclei in majority of Ki67-negative quiescent cells (>95%). These results demonstrate that changes which occur in nuclear morphology and distribution of lamins and LAP2s (and peripheral chromatin) during senescent arrest of late passage fibroblasts do not occur during quiescent arrest of early passage fibroblasts.

## 5.5. Cellular distribution of total Rb and hypo-phosphorylated isoforms in quiescent fibroblasts as assessed by immunofluorescence microscopy

Senescent fibroblasts show a decreased expression of Rb780 in the nucleus but retain distinct nuclear foci of Rb795 in LAP2α-negative or aggregated cells (Chapter 4). To investigate the possibility that LAP2α-negative quiescent cells still express Rb795 isoform, the cellular localisation patterns of total Rb protein and its hypo-

phosphorylated isoforms Rb780 and Rb795 were examined using immunocytochemistry and confocal microscopy. Human dermal fibroblasts of early passage (p8) were induced to enter quiescent arrest by either serum-starvation or contact inhibition as described above. As a control, cells were grown for 3 days in complete medium to obtain proliferating cultures (not shown). Cultures were processed for double immunofluorescence microscopy using antibodies against: a) IF8 (total Rb) and Ki67, b) AB5 (total Rb) and Ki67, c) IF8 and Rb780, d) IF8 and Rb795, e) LAP2α and Rb780 and f) LAP2α and Rb795. The same results were obtained for both serum-starved and contact-inhibited cultures. Below are described images of serum-starved cultures that contained majority of non-proliferating quiescent cells and a minority of proliferating cells.

**Figure 5.5 (a)** shows serum-starved quiescent cultures of early passage (p8) in which more than 90% of cells had a decreased or weak nucleoplasmic IF8 staining and those cells displayed weak or negative Ki67 staining respectively. 10% of cells that stained brightly for IF8 antibody displayed positive Ki67 staining. Since IF8 antibody did not detect any significant change in Rb protein level between quiescent (serum-starved or contact-inhibited) and proliferating cultures using immunoblotting, this result suggests that IF8 antibody shows epitope masking in non-proliferating cultures. Therefore, we stained quiescent cultures with another antibody that recognises total Rb (AB5). **Figure 5.5 (b)** shows that Ki67-negative serum-starved quiescent cells had a similar intensity of Rb staining in the nucleoplasm with AB5 antibody as the minority of cells which stained positively for Ki67 confirming that the total level of Rb protein does not significantly change in quiescent cells as compared to proliferating cells.

30% of late passage fibroblasts that show distinct nuclear foci of Rb795 display decreased nucleoplasmic staining with IF8 antibody (Chapter 4). Therefore the expression of Rb780 and Rb795 isoforms was investigated in relation to IF8 staining in quiescent cultures. **Figure 5.5 (c)** shows that in serum-starved quiescent cultures, cells which showed decreased or weak staining for IF8 displayed reduced or absent Rb780 staining in the nucleus respectively. In contrast, in a minority of cells that showed bright IF8 staining, bright nucleoplasmic expression of Rb780 was seen. Similarly to Rb780, serum-starved quiescent cells which showed decreased or weak staining for IF8 displayed decreased or absent staining of Rb795 in the nucleus (**Figure 5.5 (d)**). In

minority of cells that stained brightly for IF8, bright nucleoplasmic expression of Rb795 was seen. No quiescent cells that stained weakly for IF8 were observed to contain bright nuclear foci of Rb795.

Next, the expression of Rb isoforms was investigated in relation to LAP2α expression in quiescent cultures. In serum-starved quiescent cells in which nucleoplasmic staining of LAP2α was decreased or absent, Rb780 staining was also decreased or absent in the nucleoplasm (**Figure 5.5 (e)**). In minority of cells that displayed intense LAP2α staining in the nucleoplasm, Rb780 showed intense and somewhat granular nucleoplasmic staining. Similarly to Rb780, serum-starved quiescent cells showed a decreased or absent Rb795 staining in the nucleoplasm in cells that displayed decreased or absent LAP2α staining in the nucleus (**Figure 5.5 (f)**). A minority of cells showed a bright and granular nucleoplasmic staining of Rb795 and these cells stained intensely for LAP2α in the nucleoplasm. No LAP2α-negative quiescent cells were observed to contain bright nuclear foci of Rb795. Therefore, in serum-starved quiescent cells, down-regulation of LAP2α expression in the nucleus correlates with down-regulation in expression of both hypo-phosphorylated Rb isoforms in the nucleus.

## 5.6. Solubility properties of lamins, LAP2s and Rb in fibroblasts undergoing quiescence as assessed by biochemical fractionation and immunoblotting

LAP2α and Rb780 protein expression becomes gradually down-regulated within 4-5 days in serum-starved fibroblasts and within 7-10 days in contact-inhibited fibroblasts (see **section 5.1 and 5.3**). Since increased expression of LAP2α during serum-restimulation of quiescent fibroblasts leads to increased nuclear anchorage of hypo-phosphorylated Rb (Markiewicz *et al.*, 2002a), it was hypothesized that decreased anchorage of LAP2α and hypo-phosphorylated Rb in the nucleus precedes their loss of expression in quiescent nuclei. Ultimately, decreased nuclear anchorage of LAP2α and Rb780 may be regulated by changes in assembly properties of A-type lamins in fibroblasts undergoing quiescence. To investigate this possibility, the solubility properties of A-type lamins and their binding partners LAP2α and Rb780 were examined in fibroblasts undergoing quiescence using nuclear matrix extraction protocol. Human dermal fibroblasts of early passage (p8) were induced to enter quiescent arrest (Q) by either serum-starvation for 2 days or contact inhibition for 7 days as described

above. As a control, serum-starved quiescent fibroblasts were serum-re-stimulated for 48 hours to obtain proliferating cultures (P). The same number of cells in both cultures were harvested and submitted to a sequential extraction by CSK-Triton X100, RSB-Magic, chromatin digestion by DNAse1 and a final extraction by 0.25 M ammonium sulphate. The insoluble pellets P2, P3, P4 and P5 and the nuclear material solubilized after each step S2, S3, S4 and S5 were then analysed by immunoblotting. The whole cell pellet P1 was prepared as a control for both cultures. The same results were obtained for both serum-starved and contact-inhibited fibroblasts undergoing quiescence. Below are described immuno-blots of 2-day serum-starved fibroblasts and 2-day proliferating fibroblasts.

**Figure 5.6A lamin A/C** shows that in 2-day proliferating cells (P), A-type lamins (stained by JOL2 antibody) were present in all insoluble pellets after each step of the extraction. In addition, some amounts of lamin C and slightly less lamin A appeared in the soluble fractions after both DNAse1 treatment (S4) and ammonium sulphate extraction (S5). Similarly, in 2-day quiescing cells (Q), A-type lamins were present in the insoluble pellets after each step of extraction. However, lamin A never appeared in any of the soluble fractions, whilst only small amount of lamin C appeared in the soluble fraction after ammonium sulphate extraction (S5).

When immunoblotting the same extracts with LAP2α-specific antibody, in 2-day proliferating cells (P), A-type lamin binding partner, LAP2α, was only found in insoluble fractions throughout the extraction procedure albeit at decreasing levels **(Figure 5.6A LAP2α)**. In contrast, in 2 day-quiescing cells (Q), decreased amount of LAP2α was detected in the whole cell extract (P1), however, after extraction with CSK-Triton X100, the entire population of LAP2α present in the P1 pellet was found in the soluble fraction S2 and no LAP2α protein was detectable in the rest of the insoluble fractions.

Furthermore, the solubility properties of lamin B2 and its binding partner LAP2β were assessed. In 2-day proliferating HDF (P), lamin B2 was found in all the insoluble fractions during extraction. In addition, some amounts of lamin B2 appeared in the soluble fractions after both DNAse1 treatment (S4) and ammonium sulphate extraction (S5) **(Figure 5.6A lamin B2).** Similarly, in 2-day quiescing HDF (Q), lamin B2 was

present in all the insoluble fractions during extraction. However, no lamin B2 protein was detected in any of the soluble fractions. In 2-day proliferating cells (P), LAP2β was present in all the insoluble fractions during extraction procedure. In addition, LAP2β was slightly soluble after CSK/Triton extraction (S2) and following both DNAse1 digestion (S4) and ammonium sulphate extraction (S5) **(Figure 5.6A LAP2β)**. In contrast, in quiescing HDF (Q), although LAP2β was found in all the insoluble fractions, large amount of LAP2β population present in the whole cell pellet (P1) was solubilized after CSK/Triton extraction and was found in the soluble fraction S2. Following CSK/Triton extraction, the remaining population of LAP2β was only found in the insoluble fractions.

These results show that both A-type and B-type lamins become even more resistant to detergent/DNAse1/salt extraction in fibroblasts undergoing quiescence as opposed to proliferating fibroblasts. In contrast, both LAP2α and LAP2β became highly soluble after Triton extraction, which resulted in a complete loss of LAP2α and a decreased retention of LAP2β in the nucleoskeleton.

Next, the solubility properties of total Rb protein and hypo-phosphorylated Rb isoform Rb780 were assessed. **Figure 5.6B Rb780** shows that in 2-day proliferating cells (P), Rb780 was present in the insoluble pellets after each step of extraction whilst only some amounts appeared in the soluble fractions S2 and S5 resulting in the retention of a significant amount of Rb780 in a final insoluble pellet (P5). This result confirms that in proliferating cells, A-type lamins and LAP2α form a detergent/salt-resistant nucleoskeleton that stably anchors Rb780 in the nucleus. In contrast, in quiescing cells (Q), although some amount of Rb780 was detected in the whole cells extract (P1), after extraction with CSK-Triton X100, almost the entire population of Rb780 was found in the soluble fraction S2 and very little amount of Rb780 was detected in the insoluble fraction P2. No Rb780 was detected in the remaining insoluble fractions resulting in a loss of Rb780 from the nucleoskeleton. This result is consistent with the above data demonstrating that upon CSK/Triton extraction, quiescing cells show a complete loss of nucleoskeletal LAP2α and therefore would not support a stable anchorage of Rb780 in the nucleus.

Immunoblotting the same extracts with IF8 antibody showed that in 2-day proliferating cultures (P), Rb protein was present in all the insoluble fractions except for some amount of Rb protein being present in the soluble S2 fraction after CSK/Triton extraction and in the soluble fraction S5 after ammonium sulphate extraction (**Figure 5.6B IF8**). In contrast, in quiescing cells (Q), although increased amount of faster-migrating Rb protein was present in the whole cells extract P1, a large amount of Rb protein became soluble upon CSK/Triton X100 extraction and was found in the soluble fraction S2. This resulted in a very little amount of Rb present in the insoluble fraction P2, which decreased in the subsequent insoluble fractions P3 and P4 and was completely absent from the final insoluble fraction P5. Since IF8 antibody detects total Rb protein in cells, this result shows that no Rb protein is stably anchored in nucleoskeleton in fibroblasts undergoing quiescence.

## 5.7. Nuclear distribution and solubility properties of lamins and LAP2s upon *in situ* nuclear matrix extraction of fibroblasts undergoing quiescence

The presence of highly insoluble A-type in quiescent fibroblasts suggests their increased association with the lamina in quiescent nuclei. This interpretation is consistent with immunofluorescence data, which showed an increased presence of A-type lamins at the nuclear envelope (section 5.2). Therefore, a loss of LAP2α from nucleoskeleton in fibroblasts undergoing quiescence may stem from A-type lamin reorganisation from the nucleoplasm and increased assembly at the nuclear envelope, which may limit LAP2α binding sites. Likewise, increased association of B-type lamins with A-type lamins at the nuclear envelope may limit some LAP2β binding sites and lead to its decreased retention in the nucleus. In order to investigate nuclear distribution of lamins and LAP2s upon nuclear matrix extraction *in situ*, human dermal fibroblasts of early passage (p8) were induced to enter quiescent arrest by either serum-starvation for 2 days or contact inhibition for 7 days as described above. As a control, serum-starved quiescent fibroblasts were serum-re-stimulated for 48 hours to obtain proliferating cultures (not shown). Cell cultures were submitted to a sequential extraction by detergents, DNAse1 and salts as described above and processed for double immunofluorescence microscopy using antibodies against: a) LAP2α and Ki67, b) LAP2α and lamin C, c) lamin B2 and Ki67 and d) LAP2β and Ki67. The same results were obtained for both serum-starved and contact-inhibited fibroblasts undergoing

quiescence. Below are described images of 2-day serum-starved fibroblasts that contained majority of quiescing cells and a minority of proliferating cells.

**Figure 5.7 (a)** shows 2-day serum-starved quiescing cultures of early passage (p8) following II stage extraction (CSK/Triton) in which more than 80% of cells stained weakly or negatively for proliferation marker Ki67 and these nuclei did not retain any LAP2α in the nucleus. 20% of cells that stained brightly for Ki67 retained LAP2α relatively strongly in the nucleus. In Ki67 negative quiescing cells, we did not observe any LAP2α aggregation in the nucleus upon extraction. Following V stage extraction, quiescing cells that did not retain any LAP2α in the nucleus revealed intense lamin C retention at the nuclear envelope and decreased presence in the nucleoplasm **(Figure 5.7 (b))**. In contrast, 20% of cells which retained LAP2α weakly in the nucleus following V stage extraction retained lamin C strongly in the nucleus and did not reveal such intense presence at the nuclear envelope as was seen in nuclei which did not retain LAP2α in the nucleus. In quiescing cells that did not retain LAP2α in the nucleus, lamin C did not show any aggregation in the nucleus upon extraction.

Upon V stage extraction of Ki67-negative quiescing nuclei, lamin B2 revealed intense retention at the nuclear envelope and somewhat less intense presence in the nucleoplasm **(Figure 5.7 (c))**. 20% of cells that stained brightly for Ki67 also showed intense retention of lamin B2 at the nuclear envelope and somewhat more intense presence in the nucleoplasm as compared to Ki67-negative quiescing cells. Following II stage extraction of Ki67-negative quiescing cells, LAP2β was retained at the nuclear envelope and very weakly in the nucleoplasm as compared to Ki67-positive cells which retained LAP2β more strongly at both the nuclear envelope and in the nucleoplasm **(Figure 5.7 (d)).** Neither lamin B2 nor LAP2β revealed absence of staining at one pole of the nucleus upon extraction.

These results demonstrate that in fibroblasts undergoing quiescence, both A-type and B-type lamins revealed increased presence at the nuclear envelope following nuclear matrix extraction as compared to proliferating fibroblasts. This is in contrast to late passage fibroblasts that show increased solubility/instability of A-type lamins and a loss of B-type lamins from one pole of the nucleus. Interestingly, fibroblasts undergoing quiescence showed a loss of LAP2α from nucleoskeleton and a decreased retention of

LAP2β in the nucleoplasm despite the presence of highly insoluble lamins. Since both lamins revealed a decreased presence in the nucleoplasm upon extraction, this suggests that changes in assembly properties of lamins in the nucleus may limit the binding sites of their associated partners and influence their anchorage in nucleoskeleton.

### 5.8. Solubility properties of total Rb and hypophosphorylated isoforms as assessed by *in situ* nuclear matrix extraction and immunofluorescence microscopy

Fibroblasts undergoing quiescence displayed a loss of LAP2α and Rb780 upon mild detergent extraction confirming that nuclear anchorage of Rb780 depends on stably anchored LAP2α in the nucleus. In addition, the entire population of faster-migrating Rb present in quiescent fibroblasts was lost from nucleoskeleton upon extraction. This is in contrast to late passage fibroblasts that show some retention of faster-migrating Rb and Rb795 foci upon extraction. The focal distribution of Rb795 was particularly prominent after V stage nuclear matrix extraction of late passage fibroblasts. In order to investigate retention properties of Rb780 and Rb795 in relation to nuclear anchorage of LAP2α and total Rb in fibroblasts undergoing quiescence, 2-day serum-starved or contact-inhibited quiescing cultures of early passage (p8) were subjected to nuclear matrix extraction *in situ* as described above and prepared for immunofluorescence microscopy using antibodies against: a) AB5 and Rb780, b) AB5 and Rb795, c) LAP2α and Rb780 and d) LAP2α and Rb795. The same results were obtained for both serum-starved and contact-inhibited fibroblasts undergoing quiescence. Below are described images of 2-day serum-starved fibroblasts that contained majority of quiescing cells and a minority of proliferating cells.

**Figure 5.8 (a)** shows 2-day serum-starved quiescing cultures of early passage (p8) following II stage extraction (CSK/Triton) in which more than 80% of cells retained Rb very weakly in the nucleus as detected by AB5 antibody and those cells did not retain any Rb780 in the nucleus. 20% of cells that retained Rb (AB5) brightly in the nucleus also retained Rb780 brightly in the nucleus. Following V stage extraction, more than 80% of quiescing cells did not retain any Rb (AB5) in the nucleus and these cells did not reveal Rb795 foci upon extraction (**Figure 5.8 (b)**). A minority of cells that retained AB5 strongly in the nucleus also retained intense granular Rb795 staining in the nucleus.

Following II stage extraction of serum-starved quiescing cells, more than 80% of cells did not retain any LAP2α in the nucleus and those cells did not retain any Rb780 in the nucleus (**Figure 5.8 (c)**). 20% of cells that retained LAP2α brightly in the nucleus also retained Rb780 brightly in the nucleus. Similarly, following V stage extraction of quiescing cells, a majority of cells that did not retain any LAP2α in the nucleus did not retain any Rb795 in the nucleus (**Figure 5.8 (d)**). A minority of cells that retained LAP2α relatively strongly in the nucleus also retained intense granular staining of Rb795 in the nucleus. Therefore, in fibroblasts undergoing quiescence, a loss of retention of LAP2α in the nucleus correlates with a loss of nuclear anchorage of both hypo-phosphorylated isoforms in the nucleus. This is in contrast to senescent fibroblasts that show a loss of nuclear anchorage and aggregation of LAP2α and Rb780 but retention of distinct nuclear foci of Rb795 upon extraction.

## 5.9. C-terminal and N-terminal modifications of A-type lamins in quiescent and late passage fibroblasts as assessed by immunofluorescence microscopy

N-terminal domain of A-type lamins and C-terminal tail domain of lamin A have been shown to undergo modifications in a cell cycle-dependent manner which is proposed to support proliferation status of cells (Dyer *et al.*, 1997). These modifications include phosphorylations in N-terminal domain of A-type lamins and protein-protein or protein-chromatin interactions in lamin A tail domain. These modifications become reversed in quiescent fibroblasts and may therefore support stable quiescent arrest. Interestingly, as cells age in culture they show decreased ability to enter quiescent arrest (Stein *et al.*, 1999). Late passage fibroblasts show increased accumulation of unassembled A-type lamins and oxidative modifications in lamin A tail, which led to its proteolytic cleavage during nuclear extraction (Chapter 3). Therefore, it was hypothesized that changes in A-type lamins assembly in senescent fibroblasts may prevent A-type lamin modifications seen in early passage proliferating or quiescent fibroblasts. To investigate this possibility, lamin A tail-specific antibody (JOL4) and N-terminal lamin A/C antibody (JOL5) were utilised which show epitope masking in a growth-dependent manner (Dyer *et al.*, 1997).

Serum-starved or contact-inhibited quiescent fibroblasts of early passage (p8) and late passage (p44) fibroblasts grown in culture for 3 days were prepared for immunofluorescence microscopy using antibodies against 1) JOL4 and Ki67, 2) JOL4 and lamin C, 3) JOL5 and Ki67 and 4) JOL5 and lamin C. As a control, serum-starved quiescent fibroblasts were serum-re-stimulated for 48 hours to obtain proliferating cultures (data not shown). The same results were obtained for both serum-starved and contact-inhibited quiescent fibroblasts. Below are described images of serum-starved cultures that contained majority of non-proliferating quiescent cells and minority of proliferating cells.

Firstly, lamin A tail-specific modifications were investigated using JOL4 antibody. In serum-starved quiescent HDF of early passage (Q p8), >90% of cells stained negatively for proliferation marker Ki67 and those cells stained intensely for JOL4 antibody both at the nuclear envelope and in the nucleoplasm as expected **(Figure 5.9 (a) Q HDF p8)**. 10% of cells which stained positively for Ki67, stained weakly for JOL4 antibody. In late passage fibroblasts (p44), >80% of cells stained negatively for proliferation marker Ki67 and those cells showed unusual staining of lamin A with JOL4 antibody **(Figure 5.9 (a) HDF p44)**. Some Ki67-negative late passage cells showed lamin A at the nuclear envelope in addition to small dots and aggregates in the nucleoplasm whilst other cells displayed larger aggregates in the nucleoplasm and no staining at the nuclear envelope. These lamin A aggregates sometimes overlapped with the background Ki67 staining of nucleoli.

Late passage fibroblasts show accumulation of intranuclear lamin C in dots and fibers (Chapter 3). Since JOL4 antibody recognises lamin A, it was investigated whether cells with intranuclear lamin A aggregates also accumulate intranuclear lamin C. In serum-starved quiescent HDF of early passage (Q p8), majority of cells which stained brightly for JOL4 in the nucleus also stained brightly for lamin C at the nuclear envelope and somewhat weakly in the nucleoplasm **(Figure 5.9 (b) Q HDF p8).** In minority of cells that did not stain for JOL4 antibody typical of proliferating cells, lamin C stained brightly in the nucleus and somewhat less brightly at the nuclear envelope. In late passage fibroblasts (p44), cells which showed larger lamin A aggregates in the nucleoplasm with JOL4 antibody displayed increased presence of lamin C intranuclear dots and fibers and no staining at the nuclear envelope **(Figure 5.9 (b) HDF p44)**.

Lamin A and lamin C intranuclear structures did not significantly overlap although they appeared in cells together. On the other hand, late passage cells which showed some lamin A presence at the nuclear envelope and smaller aggregates in the nucleoplasm with JOL4 antibody also showed less accumulation of intranuclear lamin C dots and fibers. These results demonstrate that in early passage quiescent fibroblasts both lamins A and C showed increased assembly of at the nuclear envelope, whilst senescent fibroblasts accumulate intranuclear lamin C and aggregation of lamin A. In contrast, in proliferating cells, lamin A tail undergoes modifications that mask JOL4 epitope as expected.

Next, N-terminal phospho-modifications of lamins A/C were investigated using JOL5 antibody. In serum-starved quiescent HDF of early passage (Q p8), >90% of cells stained negatively for proliferation marker Ki67 and those cells stained intensely for JOL5 antibody both at the nuclear envelope and in the nucleoplasm as expected **(Figure 5.10A (a) Q HDF p8)**. 10% of cells which stained positively for Ki67, stained weakly for JOL5 antibody. In late passage fibroblasts (p44), >80% of cells stained negatively for proliferation marker Ki67 and those cells showed unusual staining of lamins A/C with JOL5 antibody **(Figure 5.10A (a) HDF p44)**. In some Ki67-negative late passage cells JOL5 staining of lamins A/C was restricted to multiple bright nucleoplasmic foci, and did not stain the nuclear envelope whilst in other cells JOL5 staining revealed widespread small nucleoplasmic foci and a few brightly-stained larger nucleoplasmic foci. Since JOL5 antibody recognises both lamins A and C, we investigated distribution of lamin C in cells that show nucleoplasmic lamin A/C foci with JOL5 antibody. In serum-starved quiescent HDF of early passage (Q p8), majority of cells which stained brightly for JOL5 in the nucleus also stained brightly for lamin C at the nuclear envelope and somewhat weakly in the nucleoplasm **(Figure 5.10A (b) Q HDF p8)**. In minority of cells that did not stain for JOL5 antibody typical of proliferating cells, lamin C stained brightly in the nucleus and somewhat less brightly at the nuclear envelope. In late passage fibroblasts (p44), cells that showed multiple lamin A/C nucleoplasmic foci with JOL5 antibody displayed less accumulation of intranuclear lamin C dots and more presence at the nuclear envelope. On the other hand, cells which showed widespread lamin A/C nucleoplasmic foci with JOL5 antibody displayed increased presence of intranuclear lamin C and no staining at the nuclear envelope **(Figure 5.10A (b) HDF p44)**.

Since mid passage laminopathy fibroblasts undergo premature senescent arrest (Chapter 3), it was investigated whether changes in N-terminal phosphorylation pattern of A-type lamins also accompany their premature senescent arrest. Mid passage (p24) laminopathy fibroblasts from a patient with E358K mutation (labelled F02) were grown in culture for 3 days and processed for immunofluorescence microscopy using antibodies against JOL5 and lamin C. **Figure 5.10A (b) F02 p24** shows that mid passage (p24) F02 fibroblasts showed three patterns of lamin A/C staining with JOL5 antibody. A majority of cells showed either a few or increased number of bright lamin A/C nucleoplasmic foci with JOL5 antibody and no staining at the nuclear envelope. Cells which displayed a limited number of nucleoplasmic lamin JOL5 foci showed lamin C more brightly at the nuclear envelope than cells which displayed increased number of nucleoplasmic JOL5 foci. A minority of cells stained weakly for JOL5 antibody typical of proliferating cells and these cells stained brightly for lamin for C in the nucleus and somewhat less brightly at the nuclear envelope.

Next, it was investigated whether lamin A/C nucleoplasmic foci detected by JOL5 antibody in late passage fibroblasts also display distinct nuclear foci of Rb795. Serum-starved quiescent fibroblasts of early passage (p8) and late passage (p44) fibroblasts were co-stained with JOL5 and Rb795 antibodies. In serum-starved quiescent HDF of early passage (Q p8), >90% of cells stained negatively for Rb795 and those cells stained intensely for JOL5 antibody both at the nuclear envelope and in the nucleoplasm as expected (**Figure 5.10A (c) Q HDF p8**). 10% of cells that showed bright granular nucleoplasmic distribution of Rb795 stained weakly for JOL5 antibody. In late passage fibroblasts (p44), cells that showed multiple lamin A/C nucleoplasmic foci with JOL5 antibody displayed brighter nucleoplasmic staining of Rb795 in addition to prominent nuclear foci. On the other hand, cells that showed widespread lamin A/C nucleoplasmic foci with JOL5 antibody displayed more distinct nuclear foci of Rb795 and decreased nucleoplasmic staining (**Figure 5.10A (c) HDF p44**). Interestingly, nucleoplasmic JOL5 foci and Rb795 foci partially co-localised especially in late passage cells that showed widespread staining of JOL5 foci. In these cells, multiple smaller nucleoplasmic JOL5 foci appeared to decorate larger Rb795 foci. In summary, these results confirm that A-type lamins in early passage quiescent fibroblasts show increased assembly at the nuclear envelope and uniform de-phosphorylation in their N-terminal domain during quiescent arrest. In contrast, late passage fibroblasts showed abnormal pattern of lamin

A/C N-terminal de-phosphorylation, which became more extensive in cells that accumulate unassembled lamins and Rb795 foci. Similarly, mid passage laminopathy fibroblasts that undergo premature senescent arrest also showed abnormal pattern of A-type lamin dephosphorylation in N-terminal domain reminiscent of late passage wild-type fibroblasts.

## 5.10. Protein expression of LAP2α and Rb780 in late passage fibroblasts grown in low serum conditions or grown to confluence as assessed by immunoblotting

Late passage fibroblasts that show >80% of non-proliferating cells do not down-regulate LAP2α expression (Chapter 3) as transiently arrested quiescent fibroblasts. Since late passage fibroblasts are cultured in the presence of mitotic stimuli (serum), LAP2α expression may still be induced upon induction of mitogenic signalling. Therefore, it was decided to investigate protein expression of LAP2α in late passage fibroblasts grown in low serum conditions or grown to confluence. Late passage (p42) fibroblasts were either grown for 3 days in complete medium and serum starved for 4 days (labelled SS) or grown in complete medium for 7 days with no media change (labelled C). As a control, late passage (p42) fibroblasts were grown for 3 days in complete medium (labelled S). Whole cell extracts were prepared from the same number of cells and blotted using antibodies against LAP2α, Rb780 and LAP2β.

**Figure 5.11** shows that LAP2α protein expression became significantly decreased in serum-starved late passage fibroblasts (SS) as compared to late passage fibroblasts grown in the presence of serum (S). Densitometry analysis showed that protein level of LAP2α in serum-starved late passage cells was 2.5X lower than that of late passage cells grown in presence of serum. Interestingly, late passage fibroblasts grown to confluence for 10 days (C) did not significantly down-regulate LAP2α protein as compared to cells grown in the presence of serum (S). In contrast to LAP2α, LAP2β protein level did not change in late passage fibroblasts grown in the presence of serum (S), to confluence (C) or in absence of serum (SS). Immunoblotting with a phospho-specific Rb antibody against hypo-phosphorylated isoform Rb780 showed that in both serum-starved late passage fibroblasts (SS) and in late passage fibroblasts grown to confluence (C), Rb780 protein was completely absent as compared to some Rb780 protein detected in late passage cells grown in presence of serum (S). These results

show that LAP2α and Rb780 expression in late passage fibroblasts depends on the presence of mitogenic stimuli in their growth media.

### 5.11. Cellular localisation of LAP2α and Rb isoforms in late passage wild-type and laminopathy fibroblasts grown in low serum conditions or to confluence

Senescent arrest in late passage cells depends on sustained mitogenic signalling and DNA damage signalling via phospho-histone foci is only fully activated upon mitogenic stimulation (Satyanarayana *et al.*, 2004). Since expression of LAP2α and Rb780 in late passage fibroblasts depend on mitogenic stimuli, it was investigated whether the presence of Rb795 foci also depends on mitogenic signalling. Late passage (p42) fibroblasts were serum-starved for 4 days or grown to confluence for 7 days as described above and prepared for immunofluorescence microscopy using antibodies against 1) LAP2α and Rb780, and 2) LAP2α and Rb795. As a control, late passage fibroblasts were grown in complete medium for 3 days (data not shown).

In serum-starved late passage fibroblasts (p42) **(Figure 5.12A (a))**, majority of cells showed decreased or absent LAP2α expression although such cells displayed high level of cytoplasmic LAP2α aggregates. In these late passage cells, Rb780 expression was lost **(Figure 5.12A (a) Rb780)**. Similarly, Rb795 foci became significantly down-regulated or absent **(Figure 5.12A (a) Rb780)**. On the other hand, in late passage (p42) fibroblasts grown to confluence **(Figure 5.12A (b))**, majority of cells did not down-regulated LAP2α expression and showed increased level of both nuclear and cytoplasmic aggregates. In these cells, Rb780 expression was lost **(Figure 5.12A (b) Rb780)** whilst Rb795 foci were still present **(Figure 5.12A (b) Rb795)**. Interestingly, Rb795 foci were only present in cells that showed LAP2α in the nucleus.

These results show that LAP2α expression and Rb795 foci in late passage fibroblasts depend on mitogenic stimuli present in their growth media although LAP2α still remained in cytoplasmic aggregates in low serum conditions. In contrast, in late passage cells grown to confluence neither LAP2α nor Rb795 foci became down-regulated whilst Rb780 expression was lost. This is in contrast to early passage fibroblasts grown to confluence that show a correlated down-regulation of LAP2α and both Rb780 and Rb795 isoforms. Since laminopathy fibroblasts with Y259X mutation display LAP2α

aggregates and Rb795 foci, their expression was investigated in laminopathy cells grown to confluence. Early (p12) and mid passage (p18) laminopathy fibroblasts from a patient with Y259X mutation were grown in complete medium for 7 days with no media change to induce confluence and prepared for immunofluorescence microscopy using the following antibodies: (a) LAP2α and Rb780, and (b) LAP2α and Rb795.

In early (p12) passage Y259X laminopathy fibroblasts grown to confluence, majority of cells (70%) showed decreased or absent LAP2α expression which often extended into cytoplasm and 30% of cells showed LAP2α aggregates at one pole of the nucleus and no nucleoplasmic staining **(Figure 5.12B (a) & (b) Y259X p12)**. In all these cells Rb780 expression was lost **(Figure 5.12B (a))**. Whilst Rb795 expression was lost in cells that did not contain any LAP2α, it was present in bright nuclear foci in cells that contained LAP2α aggregates at one pole of the nucleus **(Figure 5.12B (b) Y259X p12)**. In comparison to early (p12) passage Y259X fibroblasts, mid passage (p18) Y259X fibroblasts grown to confluence arrested at much lower density. Majority of mid passage Y259X cells grown to confluence (55%) showed LAP2α aggregates at one pole of the nucleus and 45% of cells had absent LAP2α staining **(Figure 5.12B (b) Y259X p18)**. In all these cells Rb780 expression was lost (data not shown). On the other hand, Rb795 was present in bright nuclear foci in cells that retained LAP2α aggregates and was absent in cells that did not contain any LAP2α **(Figure 5.12B (b) Y259X p18)**. These results show that both early and mid passage Y259X fibroblasts showed increased incidence of LAP2α aggregates following 7-day growth in culture (confluence) as compared to 3-day growth in culture (Chapter 4). Interestingly, whilst both Rb780 and Rb795 became down-regulated in Y259X fibroblasts, which completely lacked LAP2α, nuclear foci of Rb795 remained in cells that showed LAP2α aggregates whilst Rb780 expression was lost.

Late passage fibroblasts grown to confluence for 7 days did not down-regulate LAP2α expression. Since late passage fibroblasts arrest their growth at sub-confluent level, LAP2α expression was investigated in late passage fibroblasts seeded at a high density. Late passage (p42) fibroblasts were seeded at a high density and grown in complete medium for 3 days and processed for immunofluorescent microscopy using antibodies against: (a) LAP2α and lamin C, and (b) lamin B2 and lamin C.

Interestingly, in late (p42) passage fibroblasts grown at high density, a striking feature occurred in nuclei of many cells manifested by a crescent staining of LAP2α and lamin C which corresponded to a hyper-condensation of chromatin (DAPI) against one side of the nucleus (**Figure 5.12C (a)**). Similarly, lamin B2 also displayed crescent nuclear staining in cells that showed hyper-condensation of chromatin (**Figure 5.12C (b)**). This feature of chromatin staining is typical of apoptotic response (reviewed in Rogalinska *et al.*, 2002). This result indicates that late passage fibroblasts fail to adequately respond to mechanical stimuli triggered by a cell-cell contact at high density, which then activates apoptotic pathway.

## Discussion

In this chapter it was set out to explore how different nuclear organisation of A-type lamins may regulate quiescent as opposed to senescent arrest and how quiescent-associated changes in A-type lamins may regulate nuclear anchorage of LAP2α and hypo-phosphorylated Rb in fibroblasts undergoing quiescence.

### LAP2α and hypo-phosphorylated Rb780 become down-regulated in quiescent fibroblasts induced by mitogen-starvation or contact-inhibition

My results confirm that during quiescent arrest induced by mitogen-starvation, protein levels of A-type lamins do not change, which is contrast to their binding partners LAP2α and Rb780 whose protein expression becomes absent. The loss of protein expression of slower-migrating hyperphosphorylated Rb species confirms that cells were indeed not cycling and entered quiescent arrest. Following mitogen-stimulation of quiescent fibroblasts, LAP2α and Rb780 expression gradually increases reaching the highest level in S-phase during the first cell cycle. Similarly, the level of hyperphosphorylated Rb is highest during S-phase when the level of hypo-phosphorylated Rb is somewhat decreased. Interestingly, the appearance of slower-migrating Rb species occurs in early G1 suggesting that some hypo-phosphorylated Rb species can also introduce a shift in Rb mobility on SDS-PAGE. This is consistent with the previous findings (Ezhevsky *et al.*, 2001). In addition, the protein levels of B-type lamins and its binding partner LAP2β are stable during quiescence and mitogen-stimulation, and like A-type lamins, do not show a mitogen-dependent regulation of their protein levels. Interestingly, expression of LAP2α and hypo-phosphorylated Rb780 becomes significantly down-regulated in fibroblasts induced to enter quiescence by contact-inhibition followed by a complete absence of their expression at post-confluent stage. In contrast, expression of lamins and LAP2β is constant in both confluent and post-confluent quiescent fibroblasts. Therefore LAP2α protein expression is regulated in a both mitogen-dependent and cell-contact-regulated manner.

**Mitogen-stimulated quiescent fibroblasts show a correlated increase in expression and nuclear anchorage of LAP2α and hypophosphorylated Rb780 and Rb795**

Following mitogen-stimulation, quiescent fibroblasts take longer to enter S-phase in the first cell cycle than in subsequent cell cycle. Using S-phase proliferation marker PCNA (proliferating cell nuclear antigen), it was determined that most cells entered S-phase by 30 hours post-restimulation (data not shown). My results show that upon mitogen-stimulation, expression of LAP2α in the nucleus increases in a cell-cycle dependent manner reaching the highest level of nuclear expression in S-phase cells of the first cell cycle. The increase in LAP2α expression in the nucleus correlates with an increase in expression of both Rb isoforms in the nucleus and their distribution almost completely co-localised during S-phase of first cell cycle. Interestingly, whilst Rb780 isoform showed somewhat granular nuclear distribution that co-localised with LAP2α in the nucleus from early G1 to S-phase, Rb795 distribution varied in its co-localisation to LAP2α during G1 phase of the first cell cycle. During early G1 (12 hours) when LAP2α expression was relatively weak in the nuclei, Rb795 was present in small bright nuclear speckles and only weakly in the nucleoplasm and did not significantly co-localise with LAP2α. In contrast, although Rb795 was still present in prominent nuclear speckles during mid G1 (18 hours), Rb795 distribution in the nucleoplasm significantly co-localised with LAP2α. Correlated with its increase in nuclear expression, LAP2α also shows an increase in nuclear anchorage reaching the highest level of retention in S-phase cells of the first cell cycle. With an increased retention of LAP2α in the nuclei of G1 phase cells, both hypo-phosphorylated Rb isoforms become increasingly anchored in the nuclei. However, coincident with hyperphosphorylation of Rb during late G1 and S-phase, both Rb780 and Rb795 lose their nuclear anchorage whilst LAP2α showed maximal retention during S-phase. These results are consistent with findings that hyperphosphorylation of Rb during late G1 phase and S-phase weakens nuclear anchorage of Rb (Mittnacht and Weinberg 1991) and their binding to A-type lamins (Mancini *et al.*, 1994). On the other hand, LAP2α binds to A-type lamins throughout interphase (Dechat *et al.*, 1998) and would therefore still be anchored in the nucleus when Rb loses its nuclear anchorage. Interestingly, whilst increased Rb780 retention in the nucleoplasm during G1 phase correlated with an increased retention of LAP2α in the nucleus, increased Rb795 retention in the nucleoplasm correlated with LAP2α retention in the nucleus only during mid-late G1 (18 hours). During early G1 (6 hours) when

LAP2α and Rb780 expression is almost absent (data not shown), Rb795 was retained in small bright nuclear speckles (chapter 4). Rb795 localisation and nuclear anchorage significantly co-related with splicing factor SC-35 during early-mid G1 (6-12 hours) and less so during mid-late G1 (18 hours). These results suggest that during entry into cell cycle, Rb may be first hypo-phosphorylated on serine 795 that is anchored in the nucleus via association with splicing speckles. This is consistent with other report that showed that Rb becomes hypo-phosphorylated on serine 795 within ten minutes following mitogen-stimulation. During early G1, hypo-phosphorylated Rb has been shown to bind to nuclear matrix protein p84 associated with nuclear speckles. On the other hand, LAP2α and A-type lamin binding to Rb may occur once Rb has become hypo-phosphorylated on serine 780. Since Rb becomes phosphorylated sequentially, it would be expected that A-type lamins and LAP2α bind to Rb795 at some point during G1. This is supported by the finding that increased Rb795 retention in the nucleoplasm correlates with LAP2α retention in the nucleus during mid-late G1 (18 hours). However, evidence also suggests that Rb may exist as different singly phosphorylated species during G1 and therefore A-type lamins and LAP2α may show different binding affinities to Rb780 and Rb795. Alternatively, since our results indicate that nuclear anchorage of hypo-phosphorylated Rb is also required for proper progression through G1 phase (chapter 4), sequential binding of A-type lamins and LAP2α to different hypo-phosphorylated isoforms may ensure their nuclear anchorage and execution of differential functions during progression through G1 phase.

**Quiescent arrest of fibroblasts induced by mitogen-starvation or contact inhibition is not characterised by dysmorphic nuclear morphology and LAP2α aggregation**

Late passage fibroblasts which entered senescent arrest display a range of dysmorphic nuclear phenotypes which are accompanied by changes in lamin distribution at the nuclear envelope and LAP2α aggregation in the nucleus and/or cytoplasm (Chapter 3). My results show that quiescent arrest of human fibroblasts induced by either mitogen-starvation or contact-inhibition is characterised by ovoid nuclear shapes and regular nuclear size similar to those in proliferating fibroblasts. In quiescent arrest, down-regulation of LAP2α in fibroblasts occurs in the absence of aggregation in either nucleus or in cytoplasm. In contrast to proliferating fibroblasts, A-type lamins show increased presence at the nuclear envelope than in the nucleoplasm in quiescent

fibroblasts. In addition, no A-type lamin nuclear dots and fibers seen in G1 phase proliferating fibroblasts appear in quiescent fibroblasts, which is consistent with previous findings (Bridger *et al.*, 1993, Dyer *et al.*, 1997, Pugh *et al.*, 1997). This is also in contrast to senescent fibroblasts that show increased presence of A-type lamins in the nucleoplasm and accumulation of nuclear dots and fibers (chapter 3). Unlike senescent fibroblasts, quiescent fibroblasts show uniform distribution of B-type lamins and LAP2β at the nuclear envelope and peripheral chromatin is always strongly associated with the nuclear lamina. These results demonstrate that different nuclear organisation of A-type lamins, LAP2α and peripheral chromatin accompanies quiescent as opposed to senescent arrest of fibroblasts.

**Fibroblasts undergoing quiescence show a correlated down-regulation of expression of LAP2α and hypo-phosphorylated isoforms Rb780 and Rb795**

In senescent fibroblasts, although LAP2α protein level remains stable, cells show a decreased expression of Rb780 in the nucleus. In addition, senescent nuclei retain distinct foci of Rb795 in cells that show aggregated LAP2α or down-regulated LAP2α expression (Chapter 4). These Rb795 foci become particularly prominent after nuclear matrix extraction of senescent fibroblasts. In contrast, during quiescent arrest, no LAP2α-negative fibroblasts contained nuclear foci of Rb795. This is also confirmed by *in situ* nuclear matrix extraction of quiescent fibroblasts that did not reveal Rb795 foci in quiescent nuclei. Moreover, quiescent arrest was accompanied by a correlated down-regulation in expression of LAP2α and both hypo-phosphorylated isoforms Rb780 and Rb795 in the nucleus. These results are consistent with the findings that Rb is un-phosphorylated in quiescent fibroblasts (Ezhevsky *et al.*, 2001). Senescent fibroblasts that contain distinct nuclear foci of Rb795 show decreased nucleoplasmic staining of Rb with IF8 antibody (Chapter 4). Similarly, in quiescent fibroblasts Rb is only weakly detected by IF8 antibody *in situ*. Since IF8 antibody shows stable protein levels of Rb in both quiescent and senescent fibroblasts using immunoblotting, this suggests that IF8 antibody most likely shows epitope masking of Rb (pocket A) in non-proliferating cultures. In contrast, mitogen-stimulated quiescent fibroblasts show a cell-cycle dependent increase in the intensity of IF8 staining during the first cell cycle (data not shown). This suggests that intensity of IF8 staining correlates with increase in cell cycle-dependent Rb phosphorylation which may prevent epitope masking of Rb pocket

A. The epitope masking of Rb pocket A may occur due to protein-protein interactions as progressive phosphorylation of Rb during G1 is known to weaken binding of many different proteins to Rb (Zarkowska and Mittnacht 1997). Therefore, a lack of phosphorylation of Rb pocket A in both quiescent and senescent fibroblasts most likely permits protein-protein interactions, which lead to epitope masking.

**A-type and B-type lamins, but not their binding partners LAP2α and LAP2β, become more insoluble in fibroblasts undergoing quiescence**

In fibroblasts undergoing quiescence induced by either mitogen-starvation or contact-inhibition, both A-type and B-type lamins become even more resistant to nuclear matrix extraction than actively proliferating fibroblasts. The presence of highly insoluble A-type and B-type lamins in quiescent fibroblasts most likely reflects their increased association with the nuclear lamina. This is supported by observations that A-type and B-type lamins reveal increased assembly at the nuclear envelope upon *in situ* nuclear matrix extraction of quiescing fibroblasts. This is in contrast to senescent fibroblasts that show increased solubility/instability properties of A-type lamins in the nucleus and decreased assembly at the nuclear envelope. In senescent fibroblasts, increased solubility and aberrant assembly of A-type lamins in the nucleus led to a loss of nuclear anchorage of LAP2α upon nuclear matrix extraction. Interestingly, in contrast to lamins, both LAP2s show increased solubility properties in fibroblasts undergoing quiescence. Whilst LAP2β shows decreased retention in the nucleus following *in situ* nuclear matrix extraction, LAP2α is completely lost from nucleoskeleton following mild detergent extraction. Therefore, although LAP2β expression is not regulated in a cell-cycle dependent manner, its solubility properties are. This most likely reflects changes in B-type lamin organisation in quiescing cultures. On the other hand, in senescent fibroblasts, B-type lamins and LAP2β solubility properties were essentially similar to early passage proliferating fibroblasts. I propose that during quiescence changes in assembly properties of A-type and B-type lamins leads to their increased assembly at the nuclear envelope and possibly limits the binding sites for their associated partners and thus their anchorage in nucleoskeleton. These results suggest that different organisation of A-type and B-type lamins may provide different mechanism by which fibroblasts regulate quiescence, senescence or active proliferation.

**Quiescing fibroblasts show a correlated loss of nuclear anchorage of LAP2α and hypo-phosphorylated isoforms Rb780 and Rb795 upon nuclear matrix extraction**

Interestingly, LAP2α and both hypo-phosphorylated isoforms Rb780 and Rb795 show a loss of resistance to mild detergent extraction in fibroblasts undergoing quiescence. Since fully quiescent fibroblasts cultures completely down-regulate expression of LAP2α and hypo-phosphorylated Rb, my results support the hypothesis that nuclear anchorage of these proteins may at least in part regulate their protein stability and expression. I propose that A-type lamin reorganisation from the nucleoplasm and increased assembly at the nuclear envelope in fibroblasts undergoing quiescence may limit LAP2α binding sites on lamin filament in the nucleus and lead to a loss of its nuclear anchorage. This in turn would lead to a loss of hypo-phosphorylated Rb in the nucleus. Alternatively, a direct modification of LAP2α during G1-G0 transition may affect its binding to A-type lamins and lead to a loss of its anchorage in the nucleus. LAP2α-specific C-terminal domain binds to A-type lamins and chromosomes (Dechat *et al.*, 1998, Vlcek *et al.*, 1999). Binding of LAP2α to chromosomes is regulated in a phosphorylation-dependent manner. Recently, a LAP2α mutant has been created with mutations in all phosphorylation sites in its C-terminal domain (Gajewsky *et al.*, 2004). Although these mutations conferred the ability of LAP2α to bind to chromosomes throughout mitosis, they did not affect mitosis or nuclear disassembly. These results suggest that LAP2α interaction with A-type lamins is not controlled by LAP2α phosphorylation but may involve lamin modifications. It has been proposed that lamin reorganisation occurs during progression to proliferating state to provide attachment sites that accommodate lamin-protein interactions (Dyer *et al.*, 1997). Therefore, I propose that A-type lamins rearrangements in the nucleus, possibly triggered by a lack of proliferation-associated modifications, regulate nuclear anchorage of LAP2α and hypo-phosphorylated Rb during quiescence. Recent reports have showed that only hypo-phosphorylated Rb has an active growth-suppressing role whilst neither hyper- nor un-phosphorylated Rb has a role in growth-suppression (Ezhevsky *et al.*, 2001). During quiescent arrest, Rb is un-phosphorylated and other Rb-related proteins p130 and p107 actively suppress E2F-stimulated genes. The growth-suppressing role of Rb depends on its nuclear anchorage. My results support the above findings as I show that un-phosphorylated Rb present in quiescent fibroblasts is not stably anchored in the nucleus. This is contrast to senescent fibroblasts that still retain some faster-migrating

Rb in the nucleoskeleton, which argues that senescent arrest is actively maintained by growth-suppressing activity of hypo-phosphorylated Rb.

**Aberrant assembly of A-type lamins in senescent and laminopathy fibroblasts prevents lamin rearrangements seen in proliferating and quiescent fibroblasts**

A-type lamin rearrangements during quiescent arrest may be triggered by a lack of interactions with other nuclear components or a lack of lamin phosphorylations (Dyer *et al.*, 1997). Human dermal fibroblasts show growth-dependent epitope masking in C-terminal tail of lamin A, which is proposed to be involved in protein-protein or protein-chromatin interactions and in N-terminal region of lamins A/C which occurs due to phosphorylations. Using lamin A tail-specific antibody (JOL4), I show that senescent cells do not assemble lamin A at the nuclear envelope and instead accumulate lamin A foci and aggregates in the nucleoplasm. These changes in lamin A assembly in senescent cells occur together with intranuclear accumulation of lamin C dots and fibers. In senescent fibroblasts C-terminal tail in lamin A shows oxidative modifications that prevent formation of higher order structures under non-reducing SDS-PAGE (Chapter 3). This suggests that oxidative damage in lamin A tail in senescent cells prevents lamin A assembly at the nuclear envelope and tail-specific modifications that occur in proliferating cells. In addition, proper lamina assembly is required for lamin phosphorylations that regulate nuclear envelope growth (Ottaviano and Gerace 1985). Upon insulin stimulation, quiescent fibroblasts undergo rapid phosphorylation of lamins A and C. Lamins are phosphorylated during interphase and hyper-phosphorylated during mitosis (Gerace and Blobel 1980). In contrast, senescent cells accumulate multiple nucleoplasmic foci of lamins A/C as detected by N-terminal lamin A/C specific antibody (JOL5), which increase in number and become widespread within the nucleoplasm of some cells. The presence of A-type lamins in these foci is increased in senescent cells that show unassembled lamins and Rb795 foci. This suggests that unassembled A-type lamins in senescent cells become gradually de-phosphorylated in their N-terminal domain most likely because they would not be able to interact with kinases targeted at the NE. Interestingly I have observed accumulation of similar lamin A/C nucleoplasmic foci in laminopathy fibroblasts with E358K mutation. Similarly to senescent fibroblasts, E358K laminopathy fibroblasts that accumulate nucleoplasmic JOL5 foci undergo cell cycle arrest and retain Rb795 foci (data not shown). Recently

insulin stimulus has been shown to induce N-terminal phosphorylation of lamin A (Cenni *et al.*, 2005). This phosphorylation remains during both proliferation and differentiation myoblasts into muscle cells but not in quiescent myoblasts. Interestingly these authors observed that lamin A phosphorylation was reduced in laminopathy myoblasts and muscle fibers but not in interstitial fibroblasts.

**A model for different lamin and LAP2 organisation in fibroblasts undergoing quiescence as opposed to proliferation**

A-type and B-type lamin assembly at the nuclear envelope differs mainly due to their different post-translational processing which influences their solubility properties during mitosis (Foisner and Gerace 1993). Additional mechanisms that influence their different assembly include specific membrane receptors and specific assembly characteristics. B-type lamins have specific receptors at the nuclear envelope that facilitate their membrane association such as LBR (Ye and Worman 1994). Integral membrane proteins that specifically interact with A-type lamins have also been identified (LAP1C, emerin, MAN1) and emerin has been shown to be important for lamin C association at the nuclear envelope (Vaughan *et al.*, 2001). Another important factor for A-type lamins assembly is its preference for heterotypic interactions with B-type lamins (Krohne *et al.*, 1987, Georgatos *et al.*, 1988, Ye and Worman 1995), which assists incorporation of A-type lamins into the lamina (Dyer *et al.*, 1996). Interestingly, recent work has showed that B-type lamins, B1 and B2 significantly differ in the strength of their binding interactions. Unlike lamin B1, lamin B2 homotypic binding interactions are much weaker than those of lamin A, and heterotypic interactions between lamin A and lamin B2 or lamin C monomers significantly increases their insolubility (Schirmer *et al.*, 2004). In the light of these findings, my results suggest that lamin A heterotypic interactions with lamin C and lamin B2 increase during quiescence of fibroblasts, which results in their increased resistance to extraction. Increased interactions of A-type lamins with B-type lamins would lead to their increased assembly at the nuclear envelope (Hutchison 2002). In contrast, in proliferating cells, homotypic interactions of lamin C and lamin B2 may occur in addition to heterotypic interactions, which would increase lamin B2 and lamin C solubility. Decreased heterotypic interactions of lamin C would also lead to its increased presence in the nucleoplasm. Previous work has shown that the presence of intranuclear lamins in proliferating

fibroblasts depends on lamin C levels and that A-type lamin assembly becomes more efficient if it occurs via hetero-oligomeric complexes of lamin A and C rather than lamin C homo-oligomeric complexes (Pugh *et al.*, 1997). The question arises to as how binding of A-type and B-type lamin associated partners influences their assembly properties? In proliferating cells, growth of the lamina may be driven by changes in conformation of assembled lamins, by insertion of new lamin subunits and modulation by LAPs (Gerace and Burke 1988, Yang *et al.*, 1997). Since quiescent nuclei often appear more compact than proliferating nuclei, during quiescence, lamin associations promoting lamina filament width may occur at the expense of associations promoting lamina growth. In proliferating cells, LAP2β binds to lamin B1 rod domain in vitro, which is required for nuclear growth after mitosis and S-phase progression (Furukawa and Kondo 1998). Interestingly, it is thought that LAP2β interaction may modulate lamin B polymerisation and thus formation of higher order filament structures (Furukawa *et al.*, 1998), as the region in lamin B rod domain involved in binding to LAP2β is important for lamin B dimerisation (Ye and Worman 1995). Recently, it has been shown that LAP2β mediates interactions between polymers of A- and B-type lamins (Lang and Krohne 2003) and increased lamin B2 solubility has been proposed to support proliferation status of cells (Schirmer *et al.*, 2004). Based on these findings, I propose that in fibroblasts undergoing quiescence weakening of LAP2β binding to lamin B in localised regions of the lamina may modify pathway of lamina organisation by promoting lamin A binding to lamin B at the nuclear envelope, which may subsequently diminish A-type lamin binding to LAP2α in the nucleus. Alternatively, changes in A-type lamin modifications during quiescence may initially decrease binding to LAP2α and release a population of A-type lamins free to compete for lamin B binding at the nuclear envelope and displace LAP2β.

**Senescent and laminopathy fibroblasts arrest at lower cell density with increased incidence of LAP2α aggregates and a loss of Rb780**

As cells age in culture they show decreased ability to enter quiescent arrest by contact-inhibition (Stein *et al.*, 1999). If fibroblasts are grown at constant density and left to reach confluence for two weeks, regardless of their age, cells arrest at the end of the 2-week period. However, whilst early passage fibroblasts reversibly arrest at high cell density, as cells age, their density in quiescence declines (Stein *et al.*, 1999). My results

show that early passage fibroblasts reversibly arrest at high cell density with correlated down-regulation of LAP2α and both Rb780 and Rb795 isoforms. In contrast, in senescent fibroblasts, although their density at confluence declined, the protein expression of Rb780 was lost. In contrast, LAP2α expression and Rb795 foci did not become down-regulated in late passage fibroblasts grown to confluence. Similarly, laminopathy fibroblasts arrest at a lower density than wild type fibroblasts and display increased incidence of LAP2α aggregates and Rb795 foci when grown to confluence. These results suggest that exit of cell cycle at lower cell density and a loss of Rb780 in senescent and laminopathy fibroblasts may be joint consequences of LAP2α aggregation. In addition, since down-regulation of Rb780 expression is reversible by sub-cultivation or serum-stimulation of early passage wild-type quiescent fibroblasts, age-related decrease in Rb780 is not reversible and therefore the cell cycle arrest at confluence would become progressively less reversible. Interestingly, when late passage fibroblasts are grown at high density, in many cells the chromatin together with LAP2α and lamins adopts striking half-moon distribution as it condenses against only one side of the nucleus typical of apoptotic response (reviewed in Rogalinska *et al.*, 2002). Laminopathy fibroblasts also become highly disorganised in relation to each other when grown at high density as observed by light microscopy. This indicates a lack of adaptive response to mechanical stimuli triggered by cell-cell contact in senescent and laminopathy fibroblasts. Cell-cell contact at high density is a form of mechanical stress to which fibroblasts respond by contracting their cell volume and assuming a highly elongated spindle shape. This is consistent with other reports of impaired mechano-signalling in laminopathy fibroblasts (Broers *et al.*, 2005, Lammerding *et al.*, 2004).

**LAP2α expression and Rb795 foci depend on mitogenic stimuli in senescent fibroblasts**

Senescent cells activate full DNA damage signalling only upon mitogenic stimulation (Satyanarayana *et al.*, 2004). My results show that Rb795 foci also depend on the presence of mitogenic stimuli in the growth media of late passage fibroblasts. During low serum conditions, senescent cells significantly down-regulate LAP2α expression although many cells still show cytoplasmic aggregates of LAP2α. This is in contrast to early passage quiescent fibroblasts which completely down-regulate LAP2α expression in the absence of aggregation. It has been shown that serum-starved or confluent

cultures undergo much higher protein proteolysis than serum-sufficient early passage fibroblasts (Cockle and Dean 1984). Therefore, LAP2α protein expression may be regulated, at least in part, at the level of protein stability during quiescence. On the other hand, senescent fibroblasts have a diminished capacity to enhance catabolism during serum starvation (Dice *et al.*, 1982). Protein proteolysis by the proteosome is selectively impaired in senescent fibroblasts due to its inhibition by abnormally aggregated proteins (Grune *et al.*, 1997). The accumulation of aggregated proteins in senescent cells is a consequence of irreversible oxidative damage to proteins by which they become resistant to proteolytic removal by competitively inhibiting the proteosome (Friguet *et al.*, 1994). Since LAP2α becomes oxidatively modified in senescent fibroblasts (Chapter 3), some LAP2α protein may incur irreversible oxidative damage and become resistant to protein degradation. The inability to completely down-regulate LAP2α may also prohibit senescent fibroblasts from entering a true $G_0$ state.

**Functional implications of A-type lamin rearrangements during quiescent arrest**

Fibroblasts are not terminally differentiated cells and studying fibroblasts can provide insights into a developmental programme that can not be appreciated by studying more classic pre-adipocyte and myoblast models. Interestingly, the model of cellular quiescence in mouse 3T3 fibroblasts mimics the first stages of differentiation when cells exit cell cycle and show a significant increase in A-type lamin protein expression (Pugh *et al.*, 1997). Therefore, A-type lamins are thought to assist differentiation by facilitating growth arrest. This is also supported by the findings that two markers of cellular quiescence, BU31 antigen and statin, recognise lamins A and C (Coates *et al.*, 1992). Apart from an increase in A-type lamin expression, other researchers have noted that rearrangement of endogenous A-type lamin assemblies is sufficient to induce differentiation in human promyelocytic leukaemia HL-60 cells (Collard *et al.*, 1992). Similarly, it has been shown that remodelling of the nuclear lamina is required for skeletal muscle differentiation in vitro (Markiewicz *et al.*, 2005). Therefore, increased organisation of A-type lamins at the nuclear envelope in quiescent human fibroblasts may help to stabilize cells that have exited cell cycle prior to their embarking on differentiation pathway. Since ageing and laminopathy fibroblasts show aberrant assembly of A-type lamins and impaired ability to enter quiescent arrest by contact inhibition, one could predict that these cells would show an impaired differentiation

pathway. Indeed, human fibroblasts with mutations in lamins fail to differentiate into adipocyte cells (Vergnes *et al.*, 2004) and mouse myoblasts transfected with mutated lamins fail to differentiate into muscle cells (Markiewicz *et al.*, 2005, Favreau *et al.*, 2004). Myoblasts transfected with lamin mutants show incomplete withdrawal from cell cycle and inappropriately dephosphorylated Rb upon differentiation stimuli, which suggests that A-type lamins may induce quiescence in differentiating myoblasts by sequestering Rb (Favreau *et al.*, 2004). Other researchers have also reported that proper regulation of Rb pathway is essential during muscle cell differentiation (Markiewicz *et al.*, 2005, Mariappan and Parnaik 2005). Since my results show that changes in A-type lamin organisation in early passage fibroblasts undergoing quiescence led to a loss of nuclear anchorage of entire pool of hypo-phosphorylated Rb which did not occur in senescent and laminopathy fibroblasts, they also suggest an aberrant mechanism of Rb regulation in latter cells and further support the above findings.

**Figure 5.1: LAP2α and hypo-phosphorylated Rb780 become down-regulated in quiescent fibroblasts induced by mitogen-starvation whilst expression of lamins and LAP2β remains constant.** Primary cultures of early passage **(p8)** human dermal fibroblasts were grown in complete medium (10% serum) for 2 days after which their media was replaced by serum-restricted media (0.5% serum) in which cells were grown for 4 days to induce quiescence **(Q)** and harvested. Alternatively, quiescent cultures were serum-re-stimulated for either 6 **(R6)**, 12 **(R12)**, 18 **(R18)** or 24 **(R24)** hours and harvested at those time-points. As a proliferating control **(P)**, cells were grown for 3 days in complete medium and harvested. Whole cell extracts were prepared from the same number of cells and immunoblotted using antibodies against LAP2α (LAP15), LAP2β (LAP17), lamins A/C (JOL2), lamin B2 (LN43), total Rb (IF8) and Rb isoform phosphorylated on ser 780 (Rb780). Molecular weight markers showed the expected mobility for the above proteins: lamin A & C (70 & 65 kDa), lamin B2 (68 kDa), LAP2α (75 kDa) and LAP2β (55 kDa).

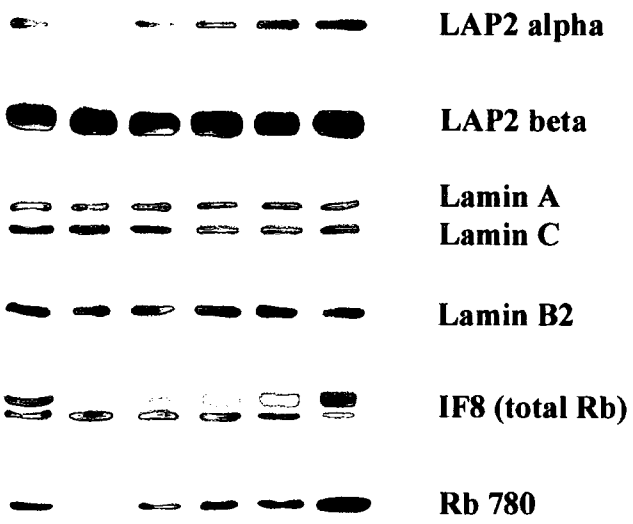
LAP2 alpha
LAP2 beta
Lamin A
Lamin C
Lamin B2
IF8 (total Rb)
Rb 780
HDF extracts
P
Q
R6
R12
R18
R30
passage
P8
P8
P8
P8
P8
P8

# Figure 5.1

**Figure 5.2A: Mitogen-stimulated quiescent fibroblasts show a correlated increase in expression of LAP2α and hypophosphorylated Rb780 and Rb795.** Early **(p8)** passage wild-type fibroblasts were grown for 2 days in culture and synchronised by serum starvation for 4 days. Cell cultures were re-stimulated for **12 (a)**, **18 (b)** and **24 (c)** hours and processed for immunofluorescence microscopy using antibodies against: **(1)** LAP2α and Rb780, and **(2)** LAP2α and Rb795. Images were collected on a BioRad Radiance 2000 confocal microscope and projected as individual black and white or red/green colour merged micrographs in which LAP2α is in red, and Rb780 and Rb795 are in green. Magnification 63x.

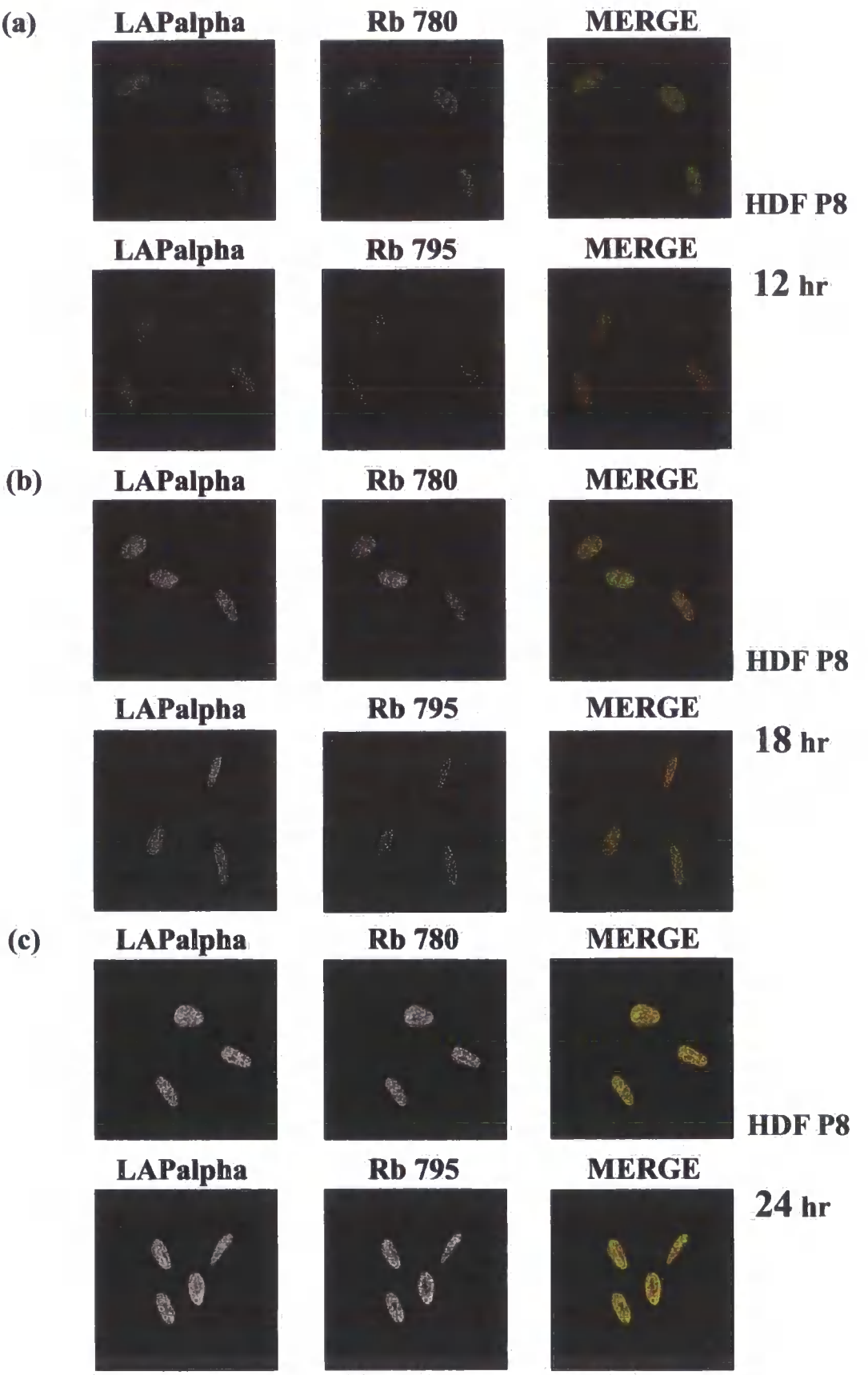
(a)
LAPalpha
Rb 780
MERGE
HDF P8
LAPalpha
Rb 795
MERGE
12 hr
(b)
LAPalpha
Rb 780
MERGE
HDF P8
LAPalpha
Rb 795
MERGE
18 hr
(c)
LAPalpha
Rb 780
MERGE
HDF P8
LAPalpha
Rb 795
MERGE
24 hr

**Figure 5.2A**

**Figure 5.2B: Increased nuclear anchorage of LAP2α correlates with an increase in nuclear anchorage of both hypophosphorylated isoforms Rb780 and Rb795 during G1 phase of mitogen-stimulated quiescent fibroblasts.** Early **(p8)** passage wild-type fibroblasts were grown for 2 days in culture and synchronised by serum starvation for 4 days. Cell cultures were re-stimulated for **12 (a)**, **18 (b)** and **24 (c)** hours, extracted with CSK/Triton and subsequently processed for immunofluorescence microscopy using antibodies against: **(1)** LAP2α and Rb780, and **(2)** LAP2α and Rb795. Images were collected on a BioRad Radiance 2000 confocal microscope and projected as individual black and white or red/green colour merged micrographs in which LAP2α is in red, and Rb780 and Rb795 are in green. Magnification 63x.

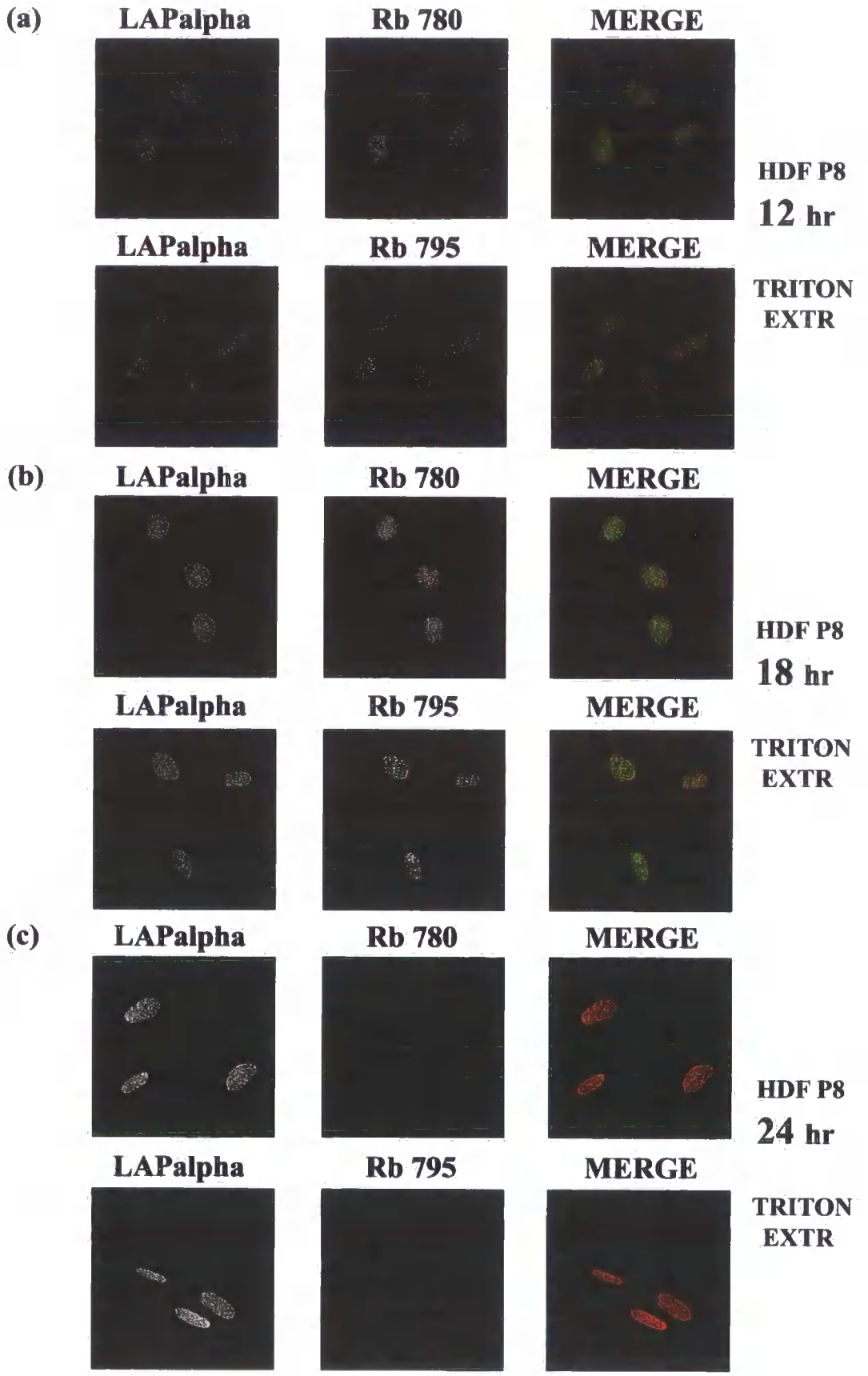
(a)
LAPalpha
Rb 780
MERGE
HDF P8
12 hr
LAPalpha
Rb 795
MERGE
TRITON
EXTR
(b)
LAPalpha
Rb 780
MERGE
HDF P8
18 hr
LAPalpha
Rb 795
MERGE
TRITON
EXTR
(c)
LAPalpha
Rb 780
MERGE
HDF P8
24 hr
LAPalpha
Rb 795
MERGE
TRITON
EXTR

**Figure 5.2B**

**Figure 5.3: Expression of LAP2α and hypo-phosphorylated Rb780 becomes significantly down-regulated in fibroblasts induced to enter quiescence by contact-inhibition followed by a complete absence of their expression at post-confluent stage.** Wild-type fibroblasts of early passage **(p8)** were grown in complete medium (10% serum) for 7 days (confluent stage-**C**) or 10 days (post-confluent stage-**PC**) and harvested. As a proliferating control **(P)**, cells were grown for 3 days in complete medium and harvested. Whole cell extracts were prepared from the same number of cells and blotted using antibodies against LAP2α (LAP15), LAP2β (LAP17), lamins A/C (JOL2), lamin B2 (LN43), total Rb (IF8) and Rb isoform phosphorylated on ser 780 (Rb780). Molecular weight markers showed the expected mobility for the above proteins: LAP2α (75 kDa), LAP2β (55 kDa), lamins A/C (70 & 65 kDa), lamin B2 (68 kDa), IF8 (110-115 kDa) and Rb780 (115).

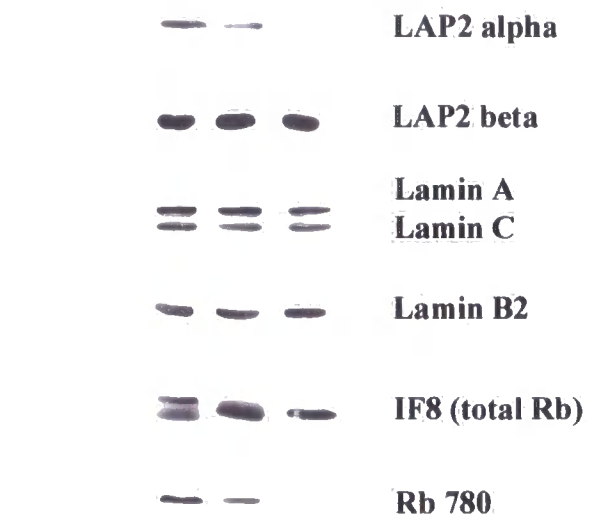
LAP2 alpha
LAP2 beta
Lamin A
Lamin C
Lamin B2
IF8 (total Rb)
Rb 780
HDF status
P
C
PC
passage
P8
P8
P8

# Figure 5.3

**Figure 5.4: Quiescent arrest of fibroblasts induced by mitogen-starvation or contact inhibition is not characterised by dysmorphic nuclear morphology and LAP2α aggregation.** Wild-type fibroblasts of early passage (**p8**) were induced to enter quiescent arrest (**Q**) by either serum-starvation or contact inhibition as described above. Cultures were processed for double immunofluorescence microscopy using antibodies against: (**a**) LAP2α and Ki67, (**b**) LAP2α and lamin C, (**c**) Lamin B2 and Ki67, and (**d**) LAP2β and Ki67. The same results were obtained for both serum-starved and contact-inhibited cultures. Only images of serum-starved cultures were shown which contained majority of non-proliferating quiescent cells and a minority of proliferating cells. Images were collected on a BioRad Radiance 2000 confocal microscope and projected as individual black and white or red/green colour merged micrographs in which LAP2α, lamin B2 and LAP2β are in red, and Ki67 and lamin C are in green. Magnification 63x.

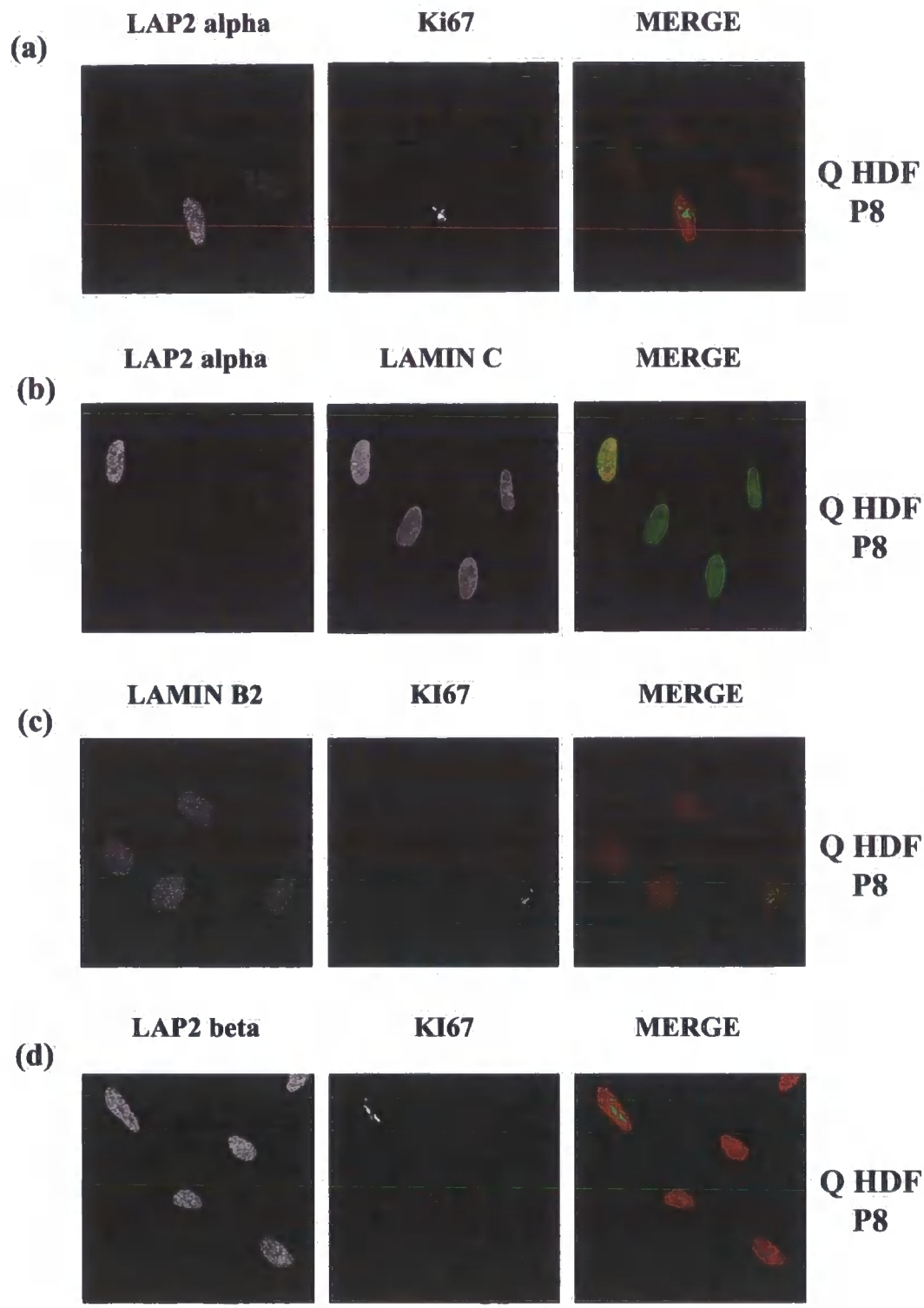
(a)
LAP2 alpha
Ki67
MERGE
Q HDF P8
(b)
LAP2 alpha
LAMIN C
MERGE
Q HDF P8
(c)
LAMIN B2
KI67
MERGE
Q HDF P8
(d)
LAP2 beta
KI67
MERGE
Q HDF P8

# Figure 5.4

**Figure 5.5: Fibroblasts undergoing quiescence show epitope masking of Rb pocket A (IF8) and a correlated down-regulation in expression of LAP2α and hypo-phosphorylated isoforms Rb780 and Rb795.** Wild-type fibroblasts of early passage **(p8)** were induced to enter quiescent arrest **(Q)** by either serum-starvation or contact inhibition as described above. Cultures were processed for double immunofluorescence microscopy using antibodies against: **(a)** Rb (IF8) and Ki67, **(b)** Rb (AB5) and Ki67, **(c)** Rb (IF8) and Rb780, **(d)** Rb (IF8) and Rb795, **(e)** LAP2α and Rb780, and **(f)** LAP2α and Rb795. The same results were obtained for both serum-starved and contact-inhibited cultures. Only images of serum-starved cultures were shown which contained majority of non-proliferating quiescent cells and a minority of proliferating cells. Images were collected on a BioRad Radiance 2000 confocal microscope and projected as individual black and white or red/green colour merged micrographs in which IF8, AB5 and LAP2α are in red, and Ki67, Rb780 and Rb795 are in green. Magnification 63x.

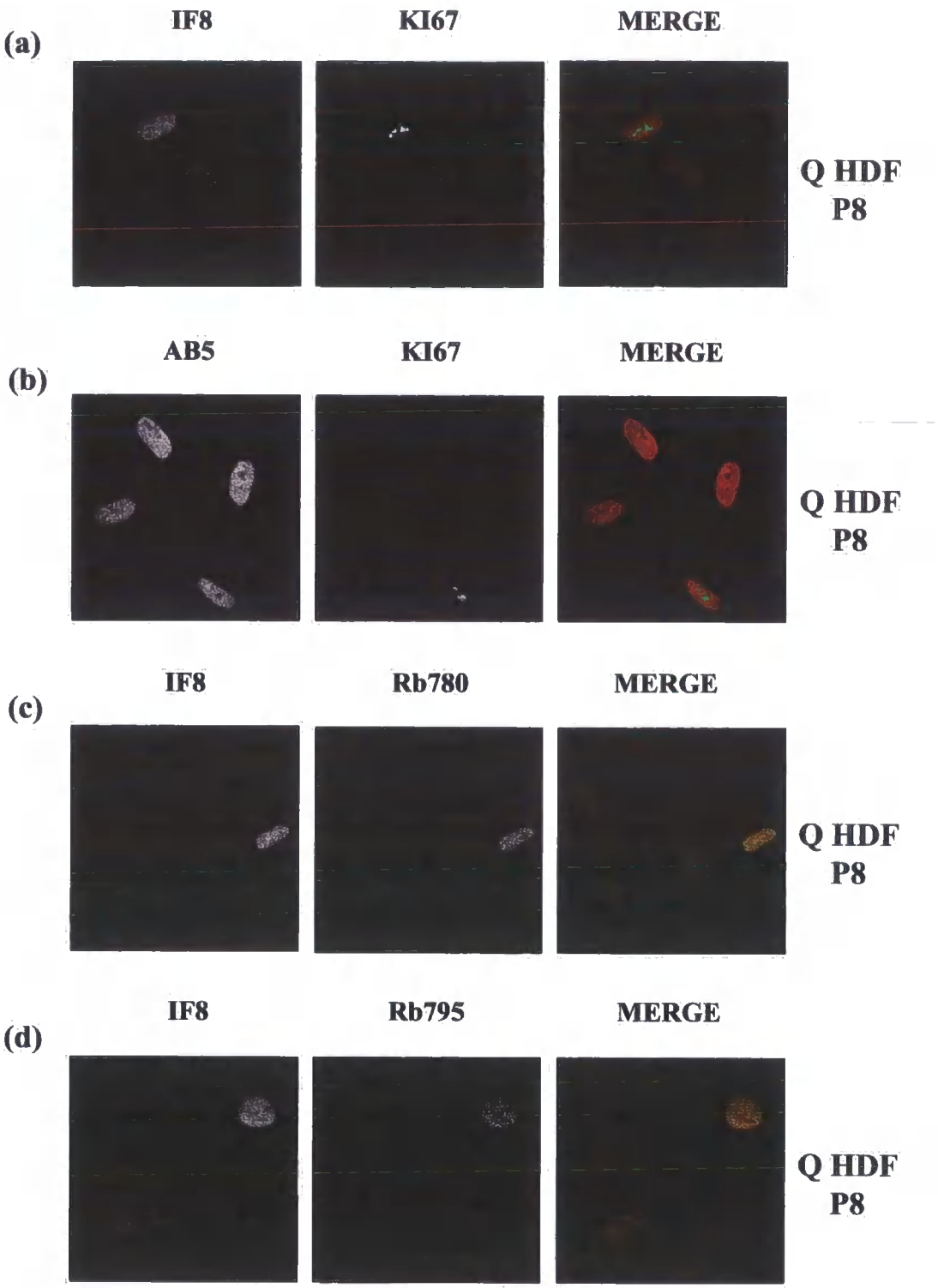
(a)
IF8
KI67
MERGE
Q HDF P8
(b)
AB5
KI67
MERGE
Q HDF P8
(c)
IF8
Rb780
MERGE
Q HDF P8
(d)
IF8
Rb795
MERGE
Q HDF P8

# Figure 5.5

**Figure 5.6A: A-type and B-type lamins, but not their binding partners LAP2α and LAP2β, become more insoluble in fibroblasts undergoing quiescence.** Wild-type fibroblasts of early passage **(p8)** were induced to enter quiescent arrest **(Q)** by either serum-starvation for 2 days or contact inhibition for 7 days as described above. As a control, serum-starved quiescent fibroblasts were serum-re-stimulated for 48 hours to obtain proliferating cultures **(P)**. The same number of cells in both cultures were harvested and submitted to a sequential extraction by CSK-Triton X100, RSB-Magic, chromatin digestion by DNAse1 and a final extraction by 0.25M ammonium sulphate. Whole cell extracts were prepared (P1) and soluble (S2, S3, S4, S5) and insoluble (P2, P3, P4, P5) fractions were immunoblotted with antibodies against lamin A/C (JOL2), LAP2α (LAP15), Lamin B2 (LN43) and LAP2β (LAP17). The same results were obtained for both serum-starved and contact-inhibited fibroblasts undergoing quiescence. Only immuno-blots of 2-day serum-starved **(Q)** and 2-day proliferating **(P)** fibroblasts are shown. Molecular weight markers showed the expected mobility for the above proteins: lamin A/C (70 & 65 kDa), LAP2α (75 kDa), lamin B2 (68 kDa) and LAP2β (55 kDa).

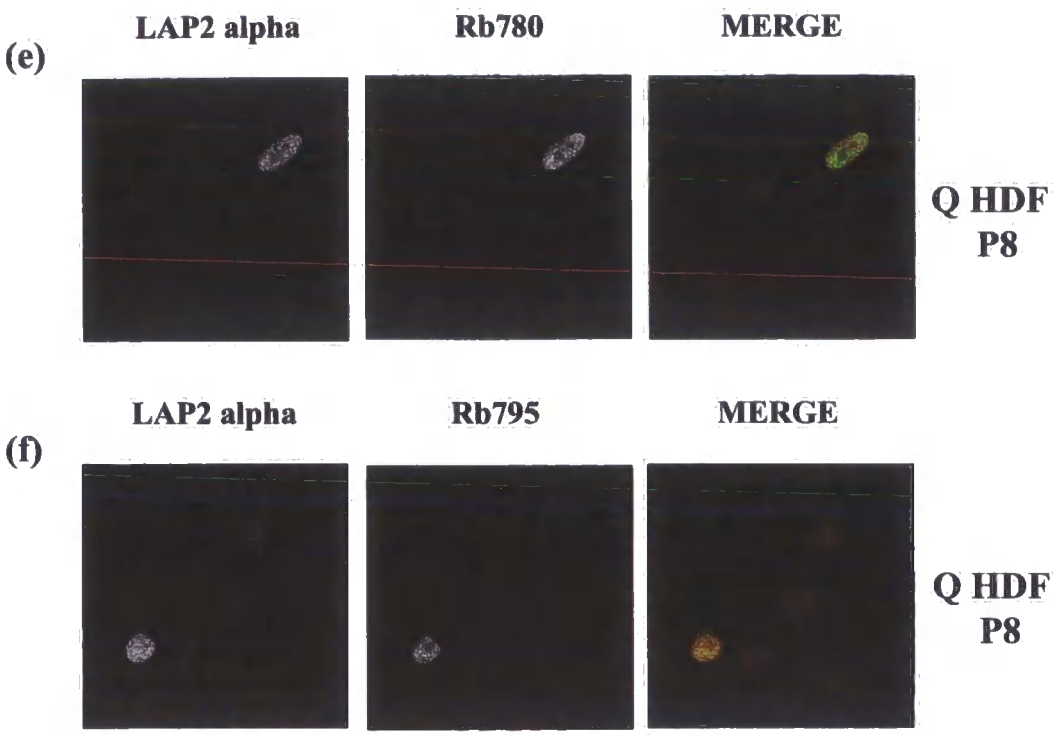
(e)
LAP2 alpha
Rb780
MERGE
Q HDF
P8
(f)
LAP2 alpha
Rb795
MERGE
Q HDF
P8

# Figure 5.5

**Figure 5.6B: Fibroblasts undergoing quiescence show a loss of nuclear anchorage of both hypo-phosphorylated Rb780 and un-phosphorylated Rb upon nuclear matrix extraction.** 2-day serum-starved **(Q)** and 2-day proliferating **(P)** wild-type fibroblasts of early passage **(p8)** were extracted sequentially as described in Figure 6A. S and P fractions were immunoblotted with antibodies against Rb isoform phosphorylated on ser 780 (Rb780) and total Rb (IF8). Molecular weight markers showed the expected mobility for the above proteins: Rb780 (115 kDa) and IF8 (110-115 kDa).

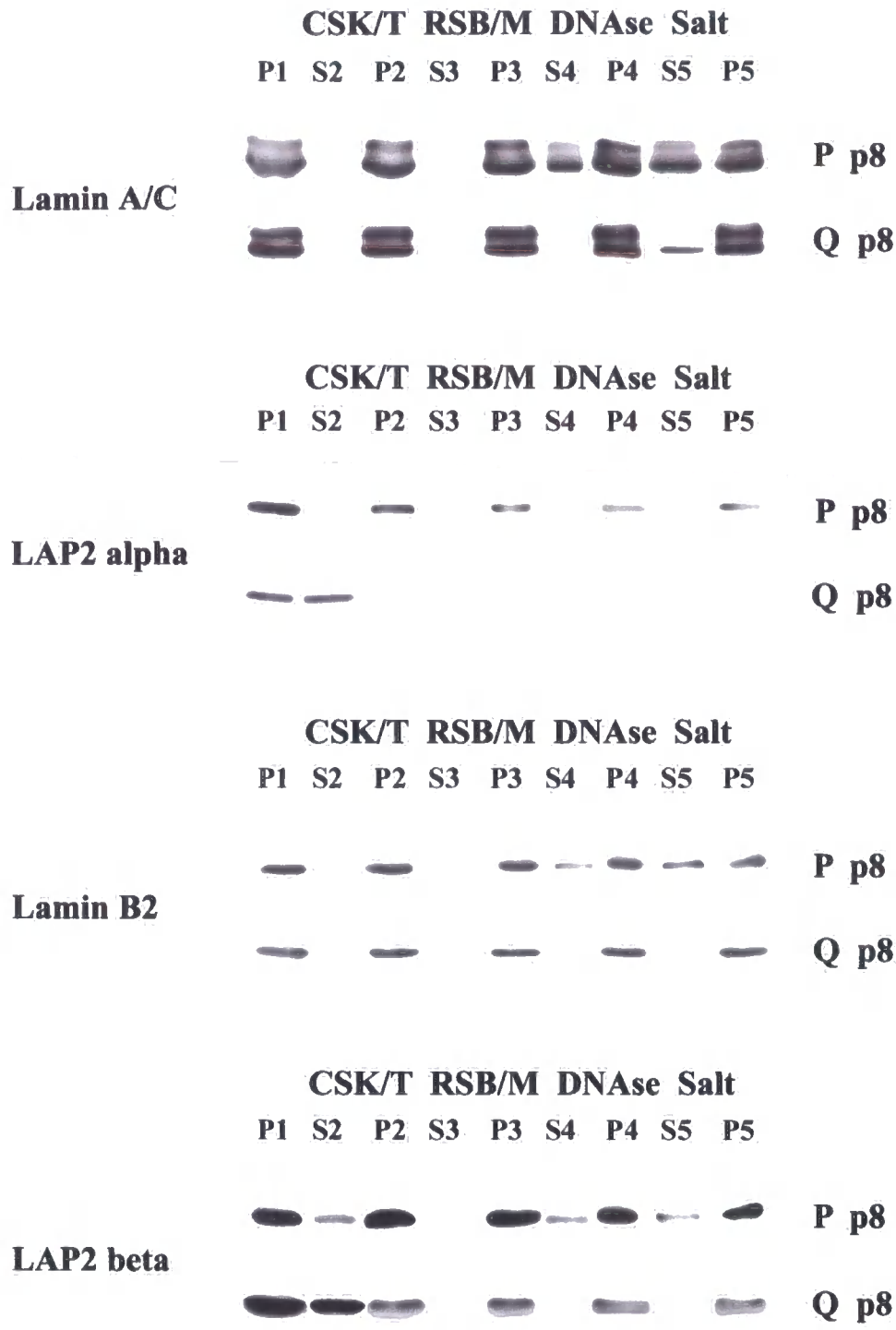
CSK/T RSB/M DNAse Salt
P1 S2 P2 S3 P3 S4 P4 S5 P5
Lamin A/C
P p8
Q p8
CSK/T RSB/M DNAse Salt
P1 S2 P2 S3 P3 S4 P4 S5 P5
LAP2 alpha
P p8
Q p8
CSK/T RSB/M DNAse Salt
P1 S2 P2 S3 P3 S4 P4 S5 P5
Lamin B2
P p8
Q p8
CSK/T RSB/M DNAse Salt
P1 S2 P2 S3 P3 S4 P4 S5 P5
LAP2 beta
P p8
Q p8

# Figure 5.6A

**Figure 5.7: LAP2α does not aggregate upon *in situ* nuclear matrix extraction of fibroblasts undergoing quiescence and lamin C reveals increased assembly at the nuclear envelope.** 2-day serum-starved **(Q)** and 2-day proliferating **(P)** wild-type fibroblasts of early passage **(p8)** were extracted sequentially *in situ* as described in Figure 6A, fixed and processed for immunofluorescence microscopy with antibodies against: **(a)** LAP2α and Ki67, **(b)** LAP2α and lamin C, **(c)** Lamin B2 and Ki67, and **(d)** LAP2β and Ki67. **(b)** & **(c)** show cells after V stage (ammonium sulphate) extraction. **(a)** & **(d)** show cells after II stage (CSK/Triton X100) extraction. Images were collected on a BioRad Radiance 2000 confocal microscope and projected as black and white or red/green colour merged micrographs in which LAP2α, lamin B2 and LAP2β are in red and lamin C and Ki67 are in green. Magnification 63x.

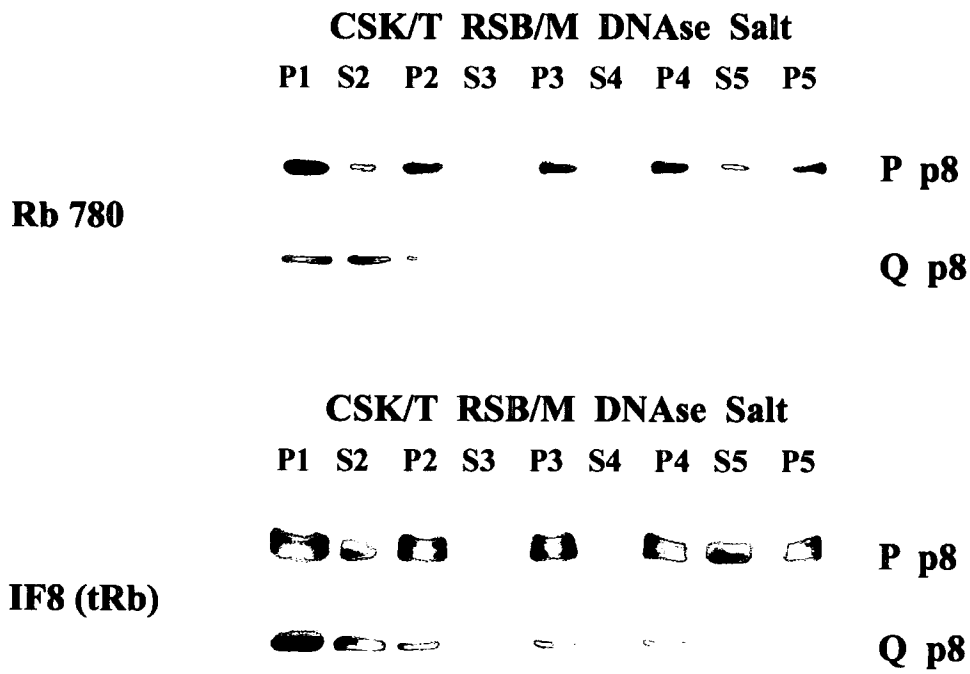
CSK/T RSB/M DNAse Salt
P1 S2 P2 S3 P3 S4 P4 S5 P5
P p8
Rb 780
Q p8
CSK/T RSB/M DNAse Salt
P1 S2 P2 S3 P3 S4 P4 S5 P5
P p8
IF8 (tRb)
Q p8

# Figure 5.6B

**Figure 5.8: Quiescing fibroblasts show a correlated loss of nuclear anchorage of LAP2α and hypo-phosphorylated isoforms Rb780 and Rb795 upon nuclear matrix extraction *in situ*.** 2-day serum-starved (**Q**) and 2-day proliferating (**P**) wild-type fibroblasts of early passage (**p8**) were extracted sequentially *in situ* as described in Figure 6A, fixed and processed for immunofluorescence microscopy with antibodies against: (**a**) Rb (AB5) and Rb780, (**b**) Rb (AB5) and Rb795, (**c**) LAP2α and Rb780, and (**d**) LAP2α and Rb795. (**a**) & (**c**) show cells after II stage (CSK/Triton X100) extraction. (**b**) & (**d**) show cells after V stage (ammonium sulphate) extraction. Images were collected on a BioRad Radiance 2000 confocal microscope and projected as individual black and white or red/green colour merged micrographs in which IF8 and LAP2α are in red, and Rb780 and Rb795 are in green. Magnification 63x.

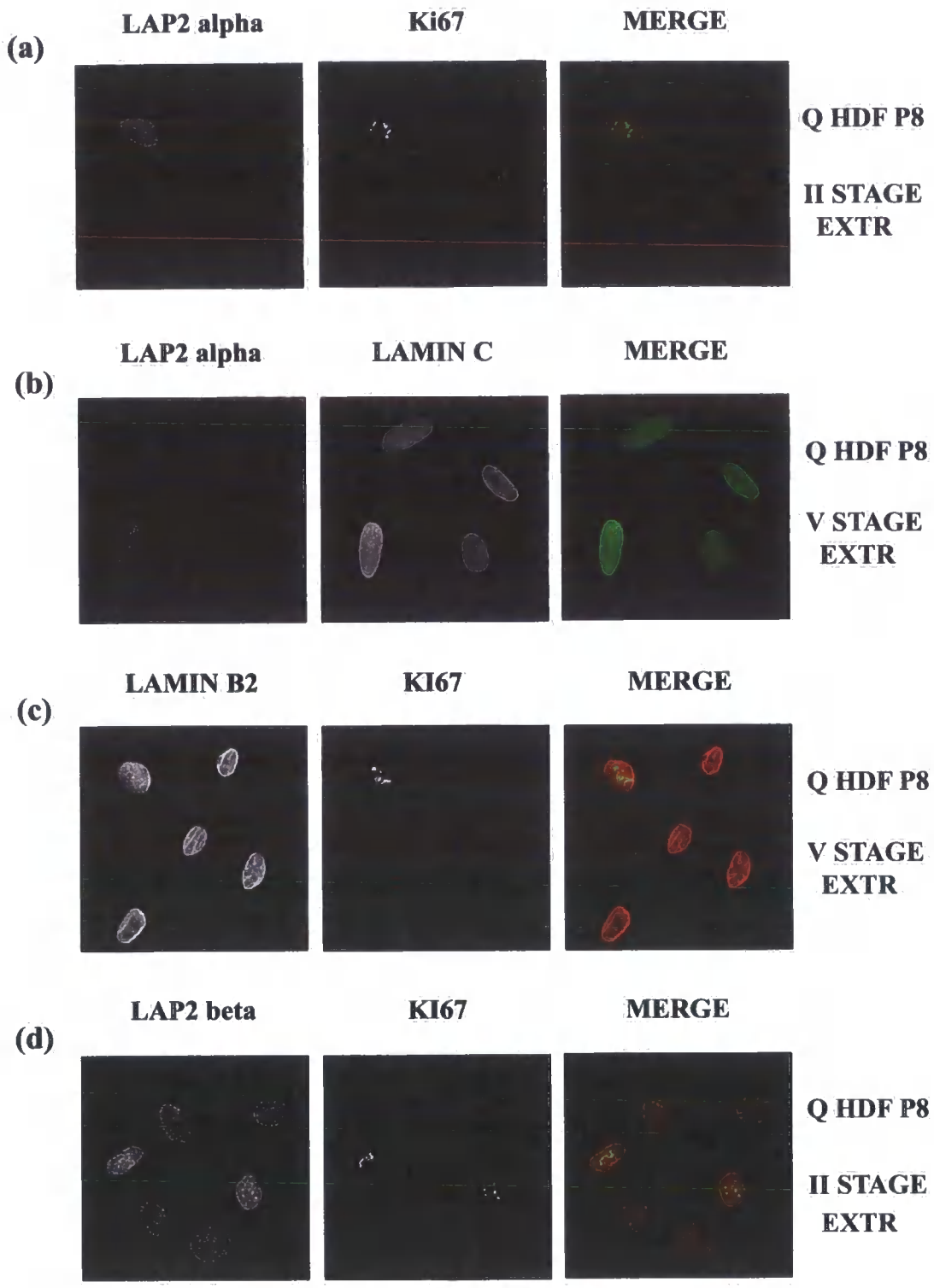
(a)
LAP2 alpha
Ki67
MERGE
Q HDF P8
II STAGE EXTR
(b)
LAP2 alpha
LAMIN C
MERGE
Q HDF P8
V STAGE EXTR
(c)
LAMIN B2
KI67
MERGE
Q HDF P8
V STAGE EXTR
(d)
LAP2 beta
KI67
MERGE
Q HDF P8
II STAGE EXTR

# Figure 5.7

**Figure 5.9: Senescent fibroblasts show a decreased assembly of lamin A at the nuclear envelope and accumulate lamin A foci and aggregates in the nucleoplasm which occur together with intranuclear accumulation of lamin C dots and fibers.** Serum-starved or contact-inhibited quiescent fibroblasts of early passage **(Q p8)** and late passage **(p44)** fibroblasts grown in culture for 3 days were prepared for immunofluorescence microscopy using following antibodies: **(a)** JOL4 (lamin A tail) and Ki67, and **(b)** JOL4 and lamin C. The same results were obtained for both serum-starved and contact-inhibited quiescent fibroblasts. Images of serum-starved early passage (Q p8) and late passage fibroblasts (p44) are shown. Images were collected on a BioRad Radiance 2000 confocal microscope and projected as individual black and white or red/green colour merged micrographs in which JOL4 is in red, and Ki67 and lamin C are in green. Magnification 120x.

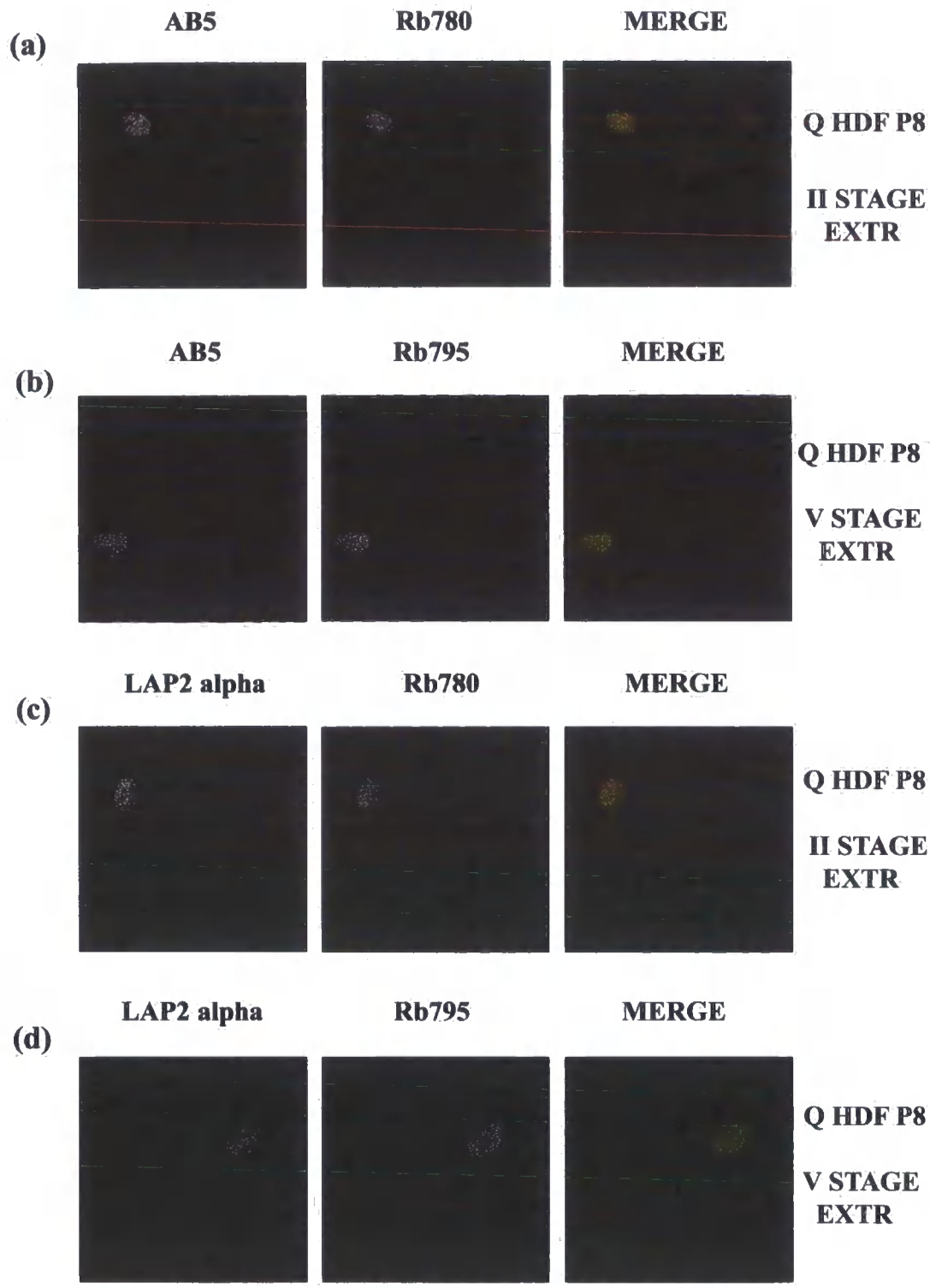
(a)
AB5
Rb780
MERGE
Q HDF P8
II STAGE EXTR
(b)
AB5
Rb795
MERGE
Q HDF P8
V STAGE EXTR
(c)
LAP2 alpha
Rb780
MERGE
Q HDF P8
II STAGE EXTR
(d)
LAP2 alpha
Rb795
MERGE
Q HDF P8
V STAGE EXTR

# Figure 5.8

**Figure 5.10A: Senescent and laminopathy fibroblasts accumulate multiple nucleoplasmic foci of un-phosphorylated A-type lamins which become widespread in cells which show decreased assembly of lamins at the nuclear envelope.** Serum-starved quiescent wild-type fibroblasts of early passage **(Q p8)** or late passage **(p44)** wild-type and mid passage **(p24)** fibroblasts from a patient with E358K mutation **(F02)** grown in culture for 3 days were prepared for immunofluorescence microscopy using following antibodies: **(a)** JOL5 (N-terminal lamin A/C) and Ki67, and **(b)** JOL5 and lamin C. Images were collected on a BioRad Radiance 2000 confocal microscope and projected as individual black and white or red/green colour merged micrographs in which JOL5 is in red, and Ki67 and lamin C are in green. Magnification 120x.

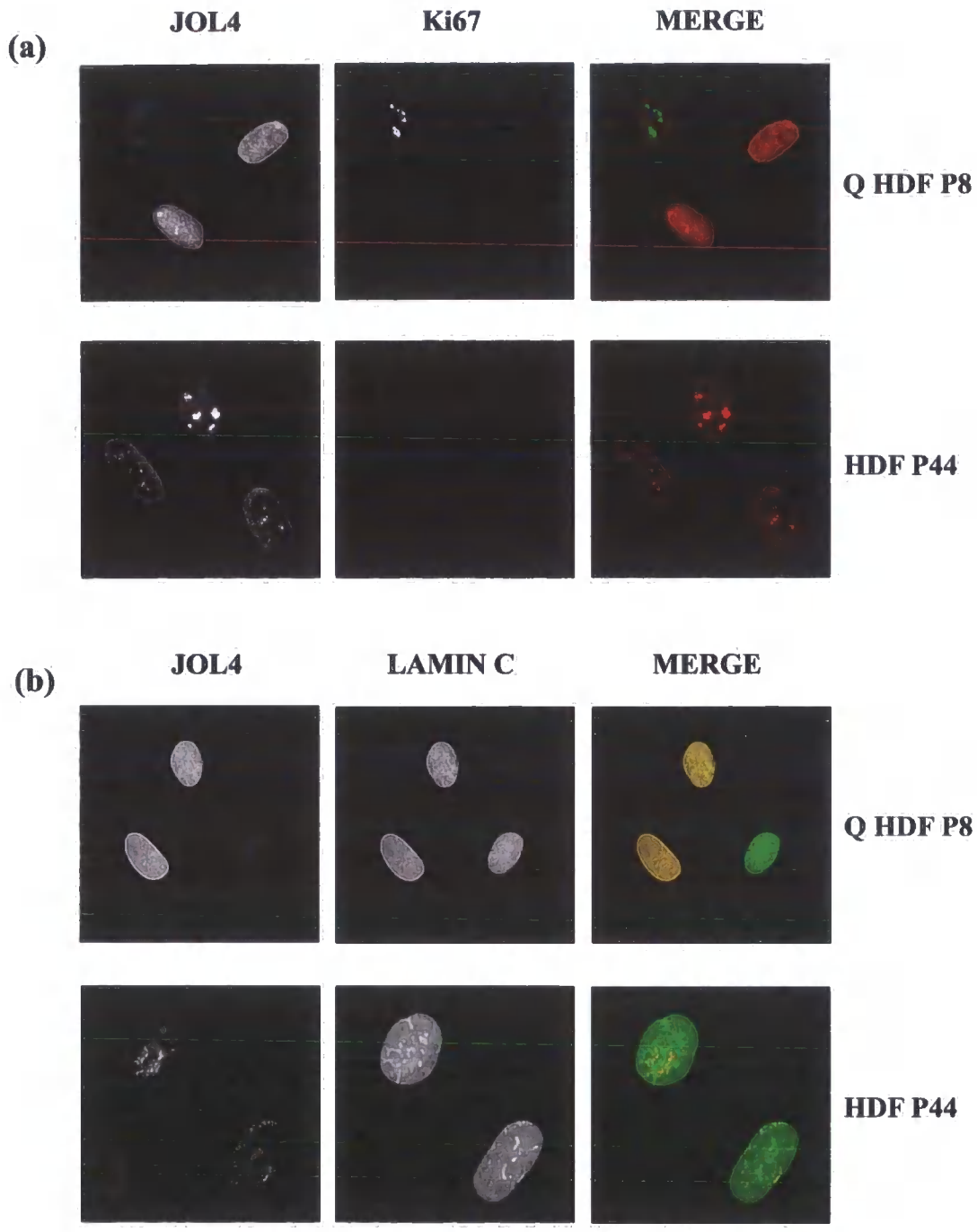
(a)
JOL4
Ki67
MERGE
Q HDF P8
HDF P44
(b)
JOL4
LAMIN C
MERGE
Q HDF P8
HDF P44

# Figure 5.9

**Figure 5.10B: Nucleoplasmic foci of un-phosphorylated A-type lamins accumulate in senescent fibroblasts which show distinct nuclear foci of Rb795.** Serum-starved early passage **(Q p8)** or late passage **(p44)** wild-type fibroblasts grown in culture for 3 days were prepared for immunofluorescence microscopy using antibodies: **(c)** JOL5 (N-terminal lamin A/C) and Rb795. Images were collected on a BioRad Radiance 2000 confocal microscope and projected as individual black and white or red/green colour merged micrographs in which JOL5 is in red, and Rb795 is in green. Magnification 120x.

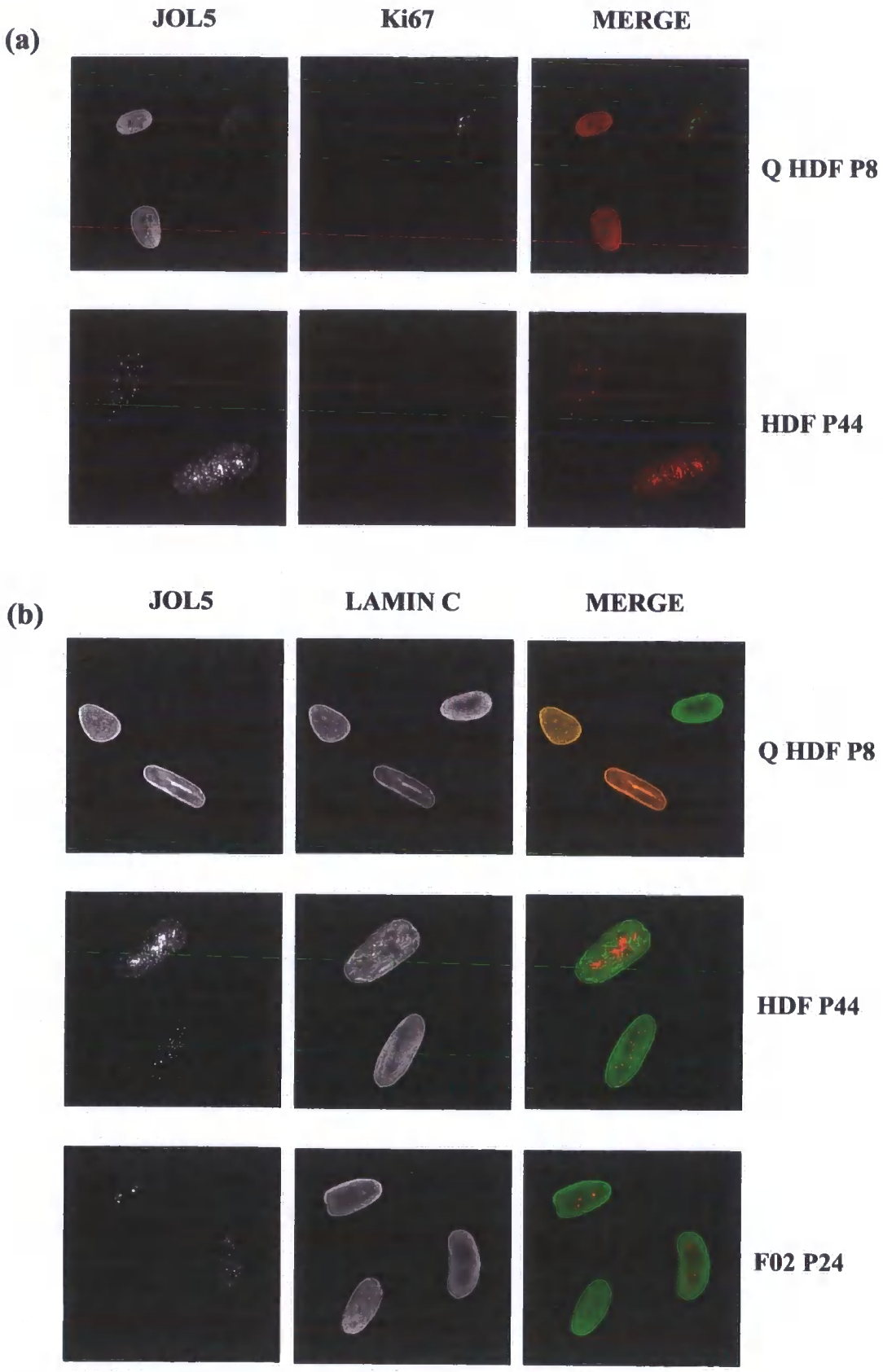
(a)
JOL5
Ki67
MERGE
Q HDF P8
HDF P44
(b)
JOL5
LAMIN C
MERGE
Q HDF P8
HDF P44
F02 P24

# Figure 5.10A

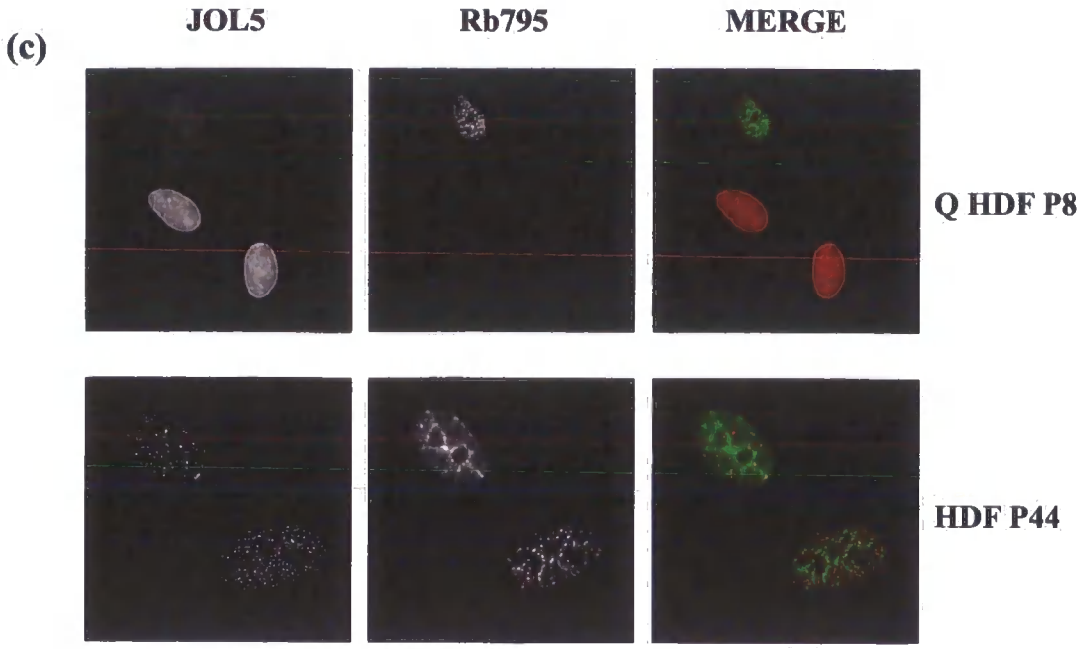


# Figure 5.10B

**Figure 5.11: Senescent fibroblasts grown in low serum conditions but not to confluence significantly down-regulate LAP2α and lose Rb780 expression under both growth conditions.** Wild-type fibroblasts of late passage **(p42)** were either grown for 3 days in complete medium and serum starved for 4 days **(SS)** or grown in complete medium for 7 days **(C)**. As a control, late passage (p42) fibroblasts were grown for 3 days in complete medium **(S)**. Whole cell extracts were prepared from the same number of cells and blotted using antibodies against LAP2α (LAP15), Rb isoform phosphorylated on ser 780 (Rb780) and LAP2β (LAP17). Molecular weight markers showed the expected mobility for the above proteins: LAP2α (75 kDa), Rb780 (115 kDa) and LAP2β (55 kDa).

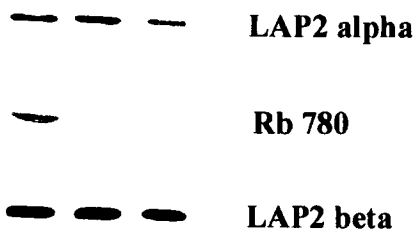


| HDF status | S | C | SS |
|---|---|---|---|
| passage | P42 | P42 | P42 |

# Figure 5.11

**Figure 5.12A: LAP2α expression and Rb795 foci depend on the presence of mitogenic stimuli in senescent fibroblasts.** Wild-type fibroblasts of late passage **(p42)** were either serum starved for 4 days **(SS)** or grown in complete medium for 7 days **(C)** and prepared for immunofluorescence microscopy using antibodies against: **(1)** LAP2α and Rb780, and **(2)** LAP2α and Rb795. Images were collected on a BioRad Radiance 2000 confocal microscope and projected as individual black and white or red/green colour merged micrographs in which LAP2α is in red, and Rb780 and Rb795 are in green. Magnification 120x.

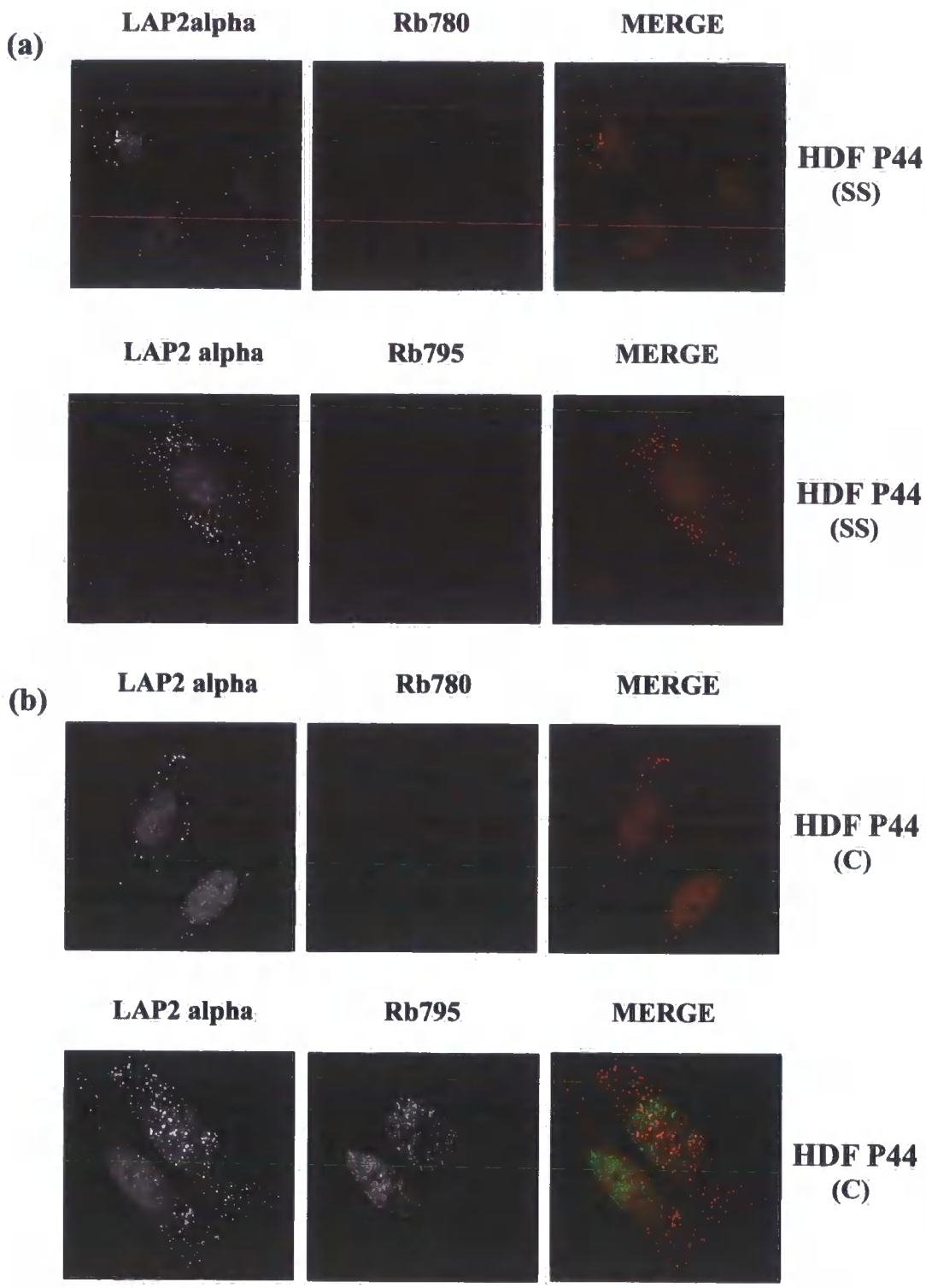
(a)
LAP2alpha
Rb780
MERGE
HDF P44
(SS)
LAP2 alpha
Rb795
MERGE
HDF P44
(SS)
(b)
LAP2 alpha
Rb780
MERGE
HDF P44
(C)
LAP2 alpha
Rb795
MERGE
HDF P44
(C)

**Figure 5.12A**

**Figure 5.12B: Y259X fibroblasts arrest at lower cell densities with an increased incidence of LAP2α aggregates and Rb780 loss but retain Rb795 foci.** Early **(p12)** and mid passage **(p18)** fibroblasts from a patient with Y259X mutation were grown in complete medium for 7 days to induce confluence and prepared for immunofluorescence microscopy using antibodies against: **(a)** LAP2α and Rb780, and **(b)** LAP2α and Rb795. DNA was stained using chromatin-staining dye DAPI. Images were collected on a Zeiss confocal microscope and projected as individual black and white or blue/red/green colour merged micrographs in which DAPI is in blue, LAP2α is in red, and Rb780 and Rb795 are in green. Magnification 63x.

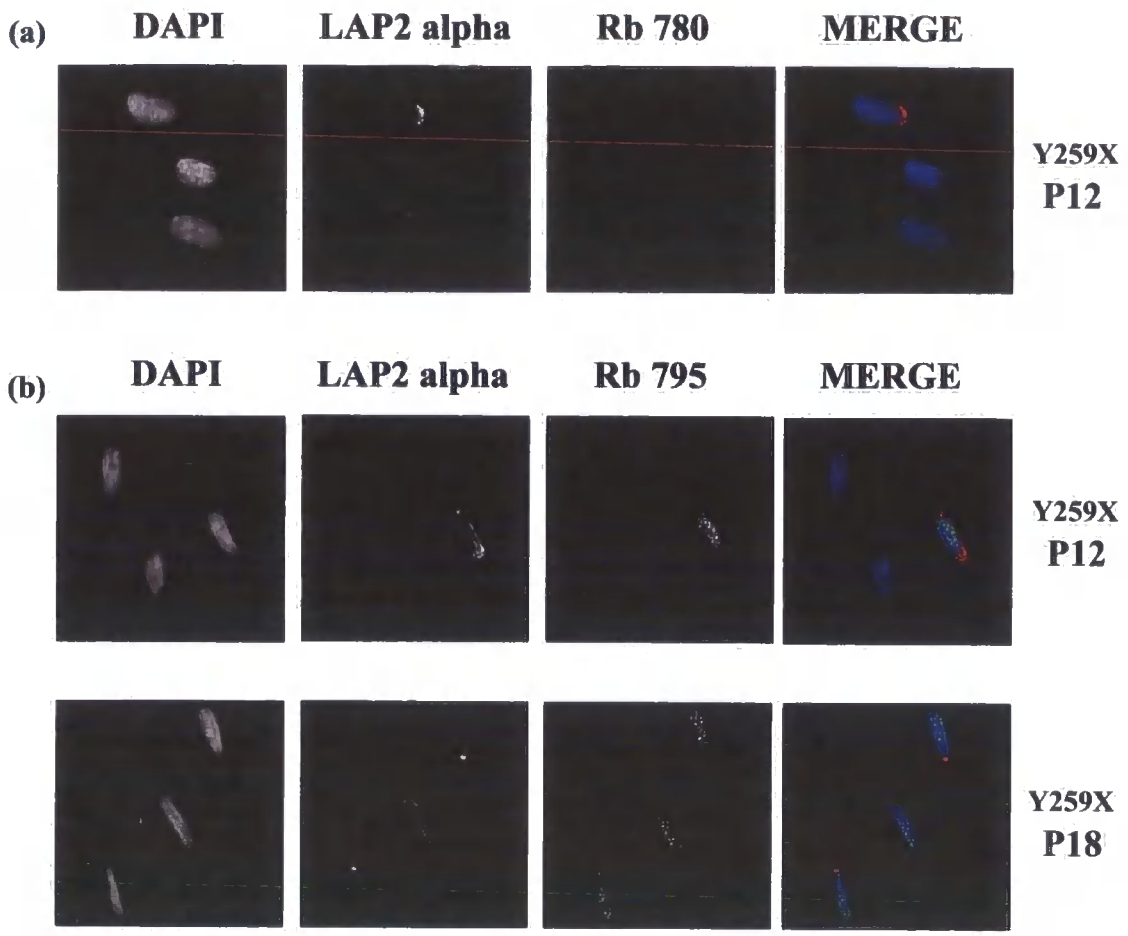
(a)
DAPI
LAP2 alpha
Rb 780
MERGE
Y259X
P12
(b)
DAPI
LAP2 alpha
Rb 795
MERGE
Y259X
P12
Y259X
P18

# Figure 5.12B

**Figure 5.12C: In senescent fibroblasts grown at high density, chromatin together with LAP2α and lamins adopts striking half-moon morphology typical of apoptotic response.** Wild-type fibroblasts of late passage (**p42**) were grown at high density for 3 days in complete medium and prepared for immunofluorescence microscopy using antibodies against: **(a)** LAP2α and lamin C, and **(b)** Lamin B2 and lamin C. DNA was stained using chromatin-staining dye DAPI. Images were collected on a Zeiss confocal microscope and projected as individual black and white or blue/red/green colour merged micrographs in which DAPI is in blue, LAP2α and lamin B2 are in red, and lamin C is in green. Magnification 120x.

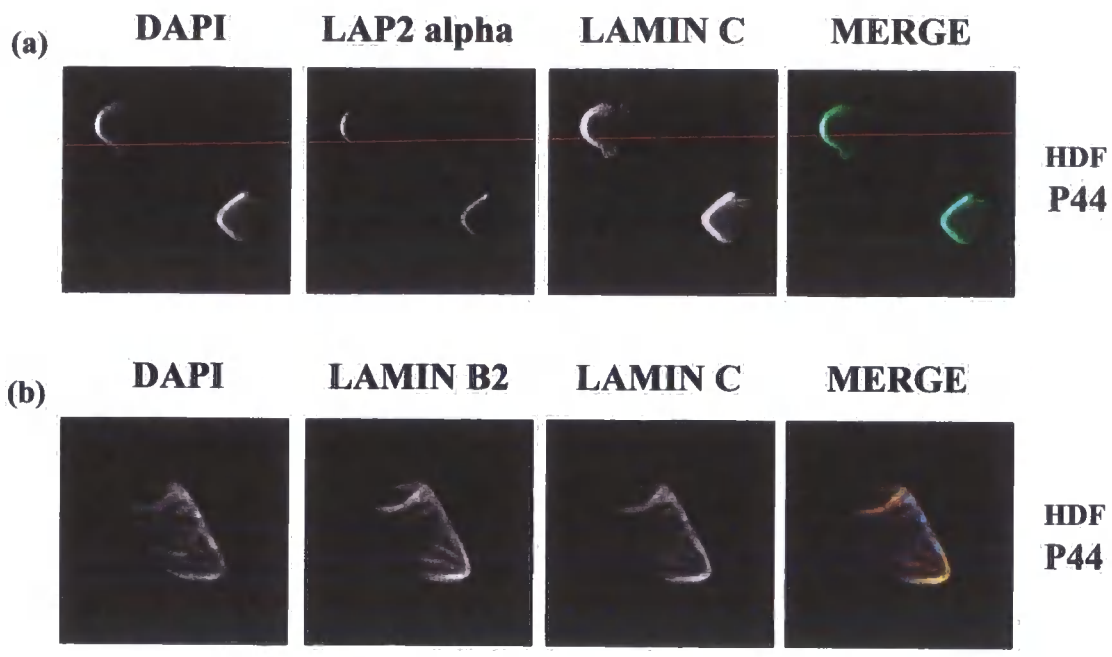
(a)
DAPI
LAP2 alpha
LAMIN C
MERGE
HDF
P44
(b)
DAPI
LAMIN B2
LAMIN C
MERGE
HDF
P44

# Figure 5.12C

# CHAPTER 6-GENERAL DISCUSSION

Mutations in A-type lamins have been found to cause a number of tissue-specific diseases and two premature ageing syndromes, collectively termed laminopathies (reviewed in Hutchison 2002). Recently, it has been shown that some lamin mutations cause tissue-specific diseases that also show many clinical features of premature ageing syndromes (Caux *et al.*, 2003, Navarro *et al.*, 2004). These findings suggest that mutations in A-type lamins may be linked to premature ageing. In this thesis, I investigated the hypothesis that lamin mutations are linked to premature ageing and that A-type lamins play a role in normal ageing of cells.

To begin to investigate how nuclear organisation of lamins may change as fibroblasts age in culture, I initially investigated their protein expression during ageing. Interestingly protein expression of A-type and B-type lamins or their binding partners did not change during ageing of fibroblasts. Nonetheless, fibroblasts aged in culture acquire changes in nuclear morphology reminiscent of laminopathy and progeroid fibroblasts. In laminopathy fibroblasts, these nuclear phenotypes arise due to a poor and/or aberrant assembly of mutant A-type lamins at the nuclear envelope (Raharjo *et al.*, 2001, Favreau *et al.*, 2003, Ostlund *et al.*, 2001, Bechert *et al.*, 2003) and lamin C is consistently found mislocalised to the nucleoplasm (Hutchison 2002). Similarly, in senescent fibroblasts, these dysmorphic nuclear phenotypes are accompanied by aberrant nuclear localisation of lamin C and LAPα. The presence of these nuclear abnormalities and aggregation of LAP2α correlates with a loss of proliferative potential in both senescent and laminopathy fibroblasts tested. The incidence of LAP2α aggregation and dysmorphic nuclear phenotypes is increased in mid passage laminopathy fibroblasts as compared to their age-matched controls. Consistent with this finding, all laminopathy cell lines, irrespective of the position of the lamin mutation, entered senescence prematurely between mid passages 20 and 26, demonstrating that lamin mutations are linked to premature ageing *in vitro*. Interestingly, emerin mutations have also been shown to affect LAP2α localisation in the nucleus (Markiewicz *et al.*, 2002b). The observation that some early passage Y259X laminopathy fibroblasts still had a normal distribution of LAP2α in the nucleus is consistent with the view that other proteins such as emerin could also stabilise LAP2α localisation in the nucleus. Indeed, although emerin is mislocalised to the ER in most Y259X human fibroblasts (Muchir *et*

*al.*, 2003) or lamin A/C null mouse fibroblasts (Sullivan *et al.*, 1999), it is also partially localised to nuclear envelope in some cells. Similarly, in senescent fibroblasts, emerin is mainly mislocalised to the nucleoplasm (data not shown).

Senescent fibroblasts show a broad range of nuclear dysmorphic phenotypes including herniations, honeycombs, chromatin detachments, aberrant chromatin bridges and micronuclei. B-type lamins and LAP2β become absent from large areas of lobules in dysmorphic lamin null (Muchir *et al.*, 2003, Sullivan *et al.*, 1999) or lamin mutant cells (Vigouroux *et al.*, 2001, Goldman *et al.*, 2004). In senescent nuclei with herniations and honeycombs, lamin B and LAP2β were often missing from one pole of the nucleus. Other reports have also shown that senescent cells and premature ageing cells accumulate high DNA contents and karyotypic changes including aneuploid and polyploid nuclei, chromosome aberrations and micronuclei and mitotic misregulation has been implicated in chromosomal pathologies associated with the ageing process (Ly *et al.*, 2000). One of the most striking nuclear phenotypes in senescent cells is 'cut' phenotype characterised by lamin bridges and mitotic-like chromatin. Similar phenotype was reported after microinjection of lamin antibodies during mitosis (Benavente and Krohne 1986) or RNAi knockdown of Ce-lamin in C.elegans cells (Liu *et al.*, 2001). Many mitotic mutants of the fission yeast *Schizosaccharomyces pombe* have been originally found to produce a so-called cut phenotype and contained telomeric DNA on chromatin bridges (Funabiki *et al.*, 1996). Cut-like phenotype can also be induced in human cells by a loss of telomere-binding proteins that lead to telomere instability (Veldman *et al.*, 2004, van Steensel *et al.*, 1998). Interestingly, LAP2α transiently binds to telomeres during anaphase/telophase and was proposed to be involved in telomere positioning (Dechat *et al.*, 2004). The aggregation of telomere-binding protein LAP2α in cytoplasmic granules around chromatin bridges in senescent cells may therefore be linked to telomere instability and cut-like phenotypes in senescent cells.

Mislocalisation of lamin C in the nucleoplasm in laminopathy cells results in increased mobility and solubility upon nuclear extraction (Broers *et al.*, 2005, Markiewicz *et al.*, 2002b). Upon nuclear extraction, senescent fibroblasts show a loss of lamin C and LAP2α from nucleoskeleton. Lamin A, on the other hand, became altered in a manner that makes it unstable and shows a partial proteolysis within its specific C-terminal tail.

Interestingly, other authors have reported a cysteine protease-dependent proteolytic activity to be elevated during extraction preparation of senescent cells which results in a limited cleavage of proteins such as telomere-binding protein Ku86 (Jeng *et al.*, 1999). *In vitro* studies have shown that enhanced susceptibility to degradation by intracellular cysteine proteases is often employed as a criterion of unfolding which occurs in oxidised proteins (Grune *et al.*, 1997). Lamin A contains three cysteines in its C-terminal-specific tail and shares one cysteine residue with lamin C in the common C-terminal domain whilst LAP2α contains ten cysteines in α-specific C-terminal domain. Interestingly, cleavage of lamin A around Cys 588-590 would generate a proteolytic product similar in size to the one generated during extraction of senescent nuclei.

Glutathione is the most abundant cellular thiol that is essential for normal regeneration of oxidized protein sulfhydryl groups (Eaton *et al.*, 2002). During ageing, levels of reduced glutathione are significantly decreased which correlates with an increase in the rate of formation of S-glutathiolated proteins and protein disulphides (Thomas and Mallis 2001). We show that lamins A/C and LAP2α become significantly S-glutathiolated in senescent cells. This is consistent with a previous report that showed that lamin A/C undergoes S-glutathiolation as a result of oxidative stress during renal ischemia (Eaton *et al.*, 2003). Since S-glutathiolation can be a reversible process during recovery of cellular redox, it can be regarded as a protective mechanism that guards against irreversible protein thiol oxidation (Dean *et al.*, 1986, Davies *et al.*, 1993). However, if the glutathiolated cysteine residues are functionally critical, S-glutathiolation will render the protein inactive and compromise cellular function (Eaton *et al.*, 2002). This, on the other hand, may cause permanent loss of replicative or divisional competence (Davies *et al.*, 1999). S-glutathiolation of proteins can inhibit disulphide bonding within or between protein cysteines (Cumming *et al.*, 2004). Lamin A and to a lesser extent lamin C can form non-native disulphide cross-links upon nuclear isolation during non-reducing conditions (Kaufmann *et al.*, 1983). We show that lamin A and LAP2α readily form intra- and/or inter- molecular disulphides in early passage cells under non-reducing conditions, whilst they accumulate in monomeric form in senescent cells. Formation of disulphide cross-links in lamin A and LAP2α depends on their free reactive cysteine sulfhydryl groups and therefore glutathiolation of these proteins in senescent cells prevents their formation. Cysteine residues can serve at least three structural functions in proteins: formation of disulphide bonds, hydrogen

bonding and coordinate bonds formation with metal ions (McDuffee *et al.*, 1997). On the other hand, cysteine oxidation produces protein destabilization and disordered conformation (Freeman *et al.*, 1995, McDufee *et al.*, 1997). Therefore, the inability of lamin A and LAP2α to form higher-order disulphide structures under non-reducing conditions in senescent cells suggests that the glutathiolated monomers may affect their higher order assembly in the nucleus. This is also supported by findings that lamin A-tail specific antibody failed to detect lamin A at the nuclear envelope and revealed many intranuclear aggregates. Other reports have shown that lamin A specific tail mutants do not assemble properly at the nuclear envelope (Loewinger and McKeon 1988). Interestingly, the C-terminal tail of lamins A/C binds to LAP2α. LAP2α interaction with lamins A/C occurs via its C-terminal specific domain (Dechat *et al.*, 1998) and this binding region in LAP2α contains three cysteine residues. We show that LAP2α shows decreased binding to A-type lamins. Therefore oxidative modifications in the C-terminal tails of A-type lamins and LAP2α may directly affect their binding. C-terminal domain in LAP2α is also a nuclear targeting domain essential for its binding to telomeres and chromosomes (Vlcek *et al.*, 1999) and this chromosomes binding region contains seven cysteine residues. Therefore, aberrant targeting of LAP2α to telomeres may lead to telomere instability and chromosome segregation defects seen in ageing cells. Interestingly, laminopathy cells do not enter premature senescence as a result of abnormally increased oxidative modifications of cysteines in mutated lamins. Lamin mutations, on the other hand, have been directly shown to affect higher order filament assembly (Krimm *et al.*, 2002, Strelkov *et al.*, 2004). Therefore, lamin mutations may cause premature senescence by affecting higher order lamina assembly. This in turn may lead to aberrant assembly of LAP2α and premature senescent arrest.

A-type lamins and LAP2α bind to hypo-phosphorylated Rb during G1 phase of cell cycle (Markiewicz *et al.*, 2002a). In contrast, senescent fibroblasts and lamin A/C null fibroblasts show dramatic de-phosphorylation of Rb protein with a subsequent accumulation of faster-migrating Rb species. Rb is hypo-phosphorylated on serine 780 and serine 795 during early G1 by cyclin D/cdk complexes (Pan *et al.*, 1998, Grafstrom *et al.*, 1999). Senescent and lamin A/C null fibroblasts showed a decreased expression of hypo-phosphorylated Rb on serine 780. On the other hand, although the level of nucleoplasmic Rb795 decreased, Rb795 was seen in distinct nuclear foci, which were often large and round indicating that these cells contain a distinct population of hypo-

phosphorylated Rb that mediates senescent arrest. Dysmorphic senescent nuclei that contain lamin A/C herniations and/or honeycombs had a decreased or absent Rb780 expression and showed a tendency of LAP2α to aggregate. In contrast, Rb795 lacked nucleoplasmic distribution in dysmorphic nuclei but remained present in distinct nuclear foci. Similarly, LAP2α mislocalisation in the nucleus of both senescent and lamin A/C null fibroblasts affected distribution of hypo-phosphorylated Rb isoforms correlated with a loss of expression of Rb780 but not Rb795. My results show that A-type lamins and LAP2α form a strong detergent/salt-resistant nucleoskeleton that stably anchors Rb780 in the nucleus of early passage cells. In contrast, A-type lamins and LAP2α do not stably anchor Rb780 in the nucleus in senescent fibroblasts. Similarly, in the absence of A-type lamins in lamin A/C null fibroblasts, LAP2α and hypo-phosphorylated Rb780 were not properly anchored in the nucleus. Loss of nuclear anchorage of Rb780 in late passage fibroblasts is consistent with decreased binding of this Rb isoform to A-type lamin/LAP2α complexes in the nucleus. Previous published work has shown that increasing LAP2α expression in serum re-stimulated early passage quiescent fibroblasts correlates with an increased anchorage of hypo-phosphorylated Rb in the nucleus (Markiewicz *et al.*, 2002a). In order to directly investigate the role of LAP2α in cell proliferation and nuclear anchorage of hypo-phosphorylated Rb, I used small interfering RNA (sRNAi) to knockdown LAP2α expression in early passage fibroblasts. sRNAi is a sequence-specific post-transcriptional gene silencing mechanism that is triggered by introducing double-stranded RNA into cells (Harborth *et al.*, 2001). Knockdown of LAP2α expression in early passage proliferating fibroblasts caused down-regulation of hypo-phosphorylated Rb and cell cycle arrest demonstrating that LAP2α expression is essential for proliferation.

In contrast to Rb780, hypo-phosphorylated isoform Rb795 remains stably anchored in the nucleus of senescent and lamin A/C null fibroblasts within distinct nuclear foci. A distinct localisation pattern and a detergent/high salt-resistant nuclear anchorage of Rb795 foci in late passage fibroblasts are reminiscent of nuclear splicing factor compartments. Splicing factor compartments correspond to speckled clusters found in interchromatin regions and on perichromatin fibrils (Spector *et al.*, 1993, Fakan *et al.*, 1994). My results demonstrate that Rb795 foci in senescent and lamin A/C null fibroblasts show a significant co-localisation with splicing speckles. Hypophosphorylated Rb is known to bind to nuclear matrix protein associated with

speckle compartments during early G1 phase of cell cycle (Durfee *et al.*, 1994). Interestingly, in early passage cells Rb795 shows distinct changes in localisation patterns during G1 and significantly co-localised with splicing factor compartments during early G1 phase. The co-localisation of Rb795 isoform with splicing speckles during early G1 phase was correlated with stable anchorage of Rb795 within speckles which suggests that localisation of Rb795 to speckles may be involved in its nuclear tethering in early G1. On the other hand, the increase in LAP2α expression in the nucleus correlates with an increase in expression of both Rb isoforms in the nucleus. Interestingly, whilst Rb780 isoform co-localised with LAP2α in the nucleus from early G1 to S-phase, Rb795 showed a significant co-localisation with LAP2α during mid-late G1 phase. These results suggest that Rb795 localisation and nuclear anchorage during early G1 is not dependent on LAP2α expression.

Decreased assembly of lamin C at the nuclear envelope of senescent nuclei was correlated with a loss of heterochromatin at the nuclear periphery. This suggests that the lamina in senescent nuclei no longer ensures the tight connections between the chromatin and the nuclear envelope. Interestingly, senescent fibroblasts undergo relocation of heterochromatin from the nuclear periphery to more internal sites in the nucleus (Bridger *et al.*, 2000) and exhibit loss of silencing of peripheral heterochromatin (Imai *et al.*, 1997). In addition, certain fibroblast cell types accumulate internal heterochromatin foci during senescence *in vitro*, which partially co-localise with Rb protein (Narita *et al.*, 2003). I did not observe that formation of distinct heterochromatin foci was a general feature of senescent arrest in late passage fibroblasts I used although accumulation of condensed chromatin regions was common inside senescent nuclei. Senescent fibroblasts incur extensive DNA damage as a result of both telomere shortening and oxidative stress-induced random DNA damage (Zglinicki *et al.*, 2005). These sites of DNA damage accumulate phospho-histone H2A.X proteins that form distinct nuclear foci. DNA repair proteins assemble at these foci indicating that foci represent active sites of DNA damage repair signalling (d'Adda di Fagagna *et al.*, 2003). Senescent cells activate full DNA damage signalling only upon mitogenic stimulation (Satyanarayana *et al.*, 2004). My results show that Rb795 foci also depend on the presence of mitogenic stimuli in the growth media of late passage fibroblasts. Interestingly, active localisation of hypo-phosphorylated Rb on chromatin occurs in response to DNA damage (Avni *et al.*, 2003). Rb795 foci appeared in cells together

with histone foci and although they did not directly co-localise their foci showed a very close inter-relationship. In addition, senescence-associated DNA damage signalling can be triggered by a loss of or dominant-negative assembly of telomere-binding proteins (von Zglinicki *et al.*, 2005). Importantly, lamin A/C null fibroblasts showed an increased occurrence of histone foci in early and particularly in mid passage cells which underwent senescent arrest. Interestingly, a recent report has shown that Zmpste24 null mouse cells and HGPS accumulate increased DNA damage and chromosome aberrations due to compromised DNA repair in the absence of telomere shortening (Liu *et al.*, 2005). Therefore, I hypothesize that increased aggregation of telomere-binding protein LAP2α in laminopathy fibroblasts triggers DNA damage-induced premature senescence.

The unchanged protein level of LAP2α in senescent fibroblasts was a surprising result. This is because in early passage fibroblasts LAP2α protein expression is exclusively correlated with cell proliferation. Since senescent cells are cultured in the presence of mitotic factors (serum), LAP2α expression may still be induced in senescent cells upon induction of mitogenic signalling. I indeed show that LAP2α expression in senescent fibroblasts is mitogen-dependent. Other authors have demonstrated that the upstream mitogenic signalling still occurs in senescent cultures but it is blocked at the downstream pathways (Seshadri and Campisi 1990, Kim *et al.*, 2003) and many genes remain mitogen-inducible (Campisi *et al.*, 2001). However, LAP2α did not become completely down-regulated in senescent fibroblasts in low serum conditions and tended to aggregate in cytoplasmic granules. Given that LAP2α is oxidatively modified in late passage cells, it most likely that some population becomes resistant to proteolytic degradation. Senescent fibroblasts have been show to down-regulate protein degradation during serum-starvation due to inhibition of proteosome by accumulation of aggregated protein (Friguet *et al.*, 1994). Therefore, in senescent cells, LAP2α protein expression is may still be induced upon mitogenic signalling but its expression may become uncoupled from cell cycle due to its loss of nuclear anchorage.

In contrast to senescent fibroblasts, quiescent arrest of human fibroblasts induced by either mitogen-starvation or contact-inhibition is characterised by ovoid nuclear shapes and regular nuclear size similar to those in proliferating fibroblasts. In quiescent arrest, down-regulation of LAP2α in fibroblasts occurs in the absence of aggregation in either

nucleus or in cytoplasm. In fibroblasts undergoing quiescence, both A-type and B-type lamins become even more resistant to nuclear matrix extraction than actively proliferating fibroblasts. The presence of highly insoluble A-type and B-type lamins in quiescent fibroblasts most likely reflects their increased association with the nuclear lamina. In senescent fibroblasts, increased solubility and aberrant assembly of A-type lamins in the nucleus led to a loss of nuclear anchorage of LAP2α. In contrast, both LAP2s show increased solubility properties in fibroblasts undergoing quiescence. Whilst LAP2β shows decreased retention in the nucleus following *in situ* nuclear matrix extraction, LAP2α is completely lost from nucleoskeleton following mild detergent extraction. The increased LAP2 solubility most likely results from changes in assembly properties of A-type and B-type lamins. In contrast to proliferating fibroblasts, A-type lamins show increased presence at the nuclear envelope in quiescent fibroblasts. Increased assembly of lamins at the nuclear envelope may limit the binding sites for their associated partners and lead to their decreased anchorage in nucleoskeleton. These results are in line with previous findings which showed that LAP2β binding to B-type lamins may modulate its polymerisation which is necessary to promote S-phase progression (Furukawa *et al.*, 1998) and that increased lamin B2 solubility may support proliferation status of cells (Schirmer *et al.*, 2004).

Cell growth, differentiation and gene expression are all coupled to mechanical stimuli, which are sensed through changes in protein shape (e.g. protein folding and conformation) and motion (e.g. flexibility) (Ingber 1997). Recently, it has been proposed that the lamina network has properties of mechanical stability and flexibility, which facilitates transmission of mechanical signals across the nuclear envelope (Dahl *et al.*, 2004). Interestingly, the intracellular environment of muscle cells undergoes changes in redox environment during mechanical activity, which leads to modulation of protein activities involved in muscle contraction via cysteine oxidation through ROS. This is the case with the Ig domains of the giant muscle protein titin which forms reversible disulphide bridges predicted to modulate elasticity and conformational flexibility of Ig domains under mechanical stress conditions by restricting their motion and contributing to increasing sarcomeric resistance (Mayans *et al.*, 2001). Conversely, in the resting state of muscle cells, muscle proteins such as titin carry out their function in a reducing environment that is unfavourable to disulphide bridge formation. Interestingly, molecular modelization favours the occurrence of disulphide bond

between Ig-like domains of lamin A/C molecules from anti-parallel protofilaments of adjacent protofibrils (Stierle *et al.*, 2003). I therefore propose that changes in assembly properties of A-type lamins during quiescent arrest may involve disulphide formation between its Ig-like domains (Cys 580), which would increase mechanical stability and compaction of the lamina.

Recent reports have showed that only hypo-phosphorylated Rb has an active growth-suppressing role whilst neither hyper- nor un-phosphorylated Rb has a role in growth-suppression (Ezhevsky *et al.*, 2001). During quiescent arrest, Rb is un-phosphorylated and other Rb-related proteins p130 and p107 actively suppress E2F-stimulated genes. The growth-suppressing role of Rb depends on its nuclear anchorage (Mittnacht and Weinberg, 1990). My results support the above findings as we show that un-phosphorylated Rb present in quiescent fibroblasts is not stably anchored in the nucleus and would therefore not be involved in active growth-suppression. This is contrast to senescent fibroblasts that still retain distinct foci of hypo-phosphorylated Rb795, which argues that senescent arrest is actively maintained by growth-suppressing activity of hypo-phosphorylated Rb.

Lamin phosphorylation during interphase regulates nuclear envelope growth and occurs only on assembled lamins (Ottaviano and Gerace 1985). Senescent cells accumulate multiple nucleoplasmic foci of lamins A/C as detected by N-terminal lamin A/C specific antibody (JOL5), which shows phospho-dependent epitope masking in proliferating fibroblasts (Dyer *et al.*, 1997). The presence of A-type lamins in these foci is increased in senescent cells that show unassembled lamins and Rb795 foci. This suggests that unassembled A-type lamins in senescent cells become gradually de-phosphorylated in their N-terminal domain most likely because they would not be able to interact with kinases targeted at the NE. Interestingly I have observed accumulation of similar lamin A/C nucleoplasmic foci in laminopathy fibroblasts with E358K mutation. N-terminal phosphorylation of lamin A is also reduced during differentiation of laminopathy myoblasts into muscle fibers (Cenni *et al.*, 2005). A-type lamins are thought to assist differentiation by facilitating growth arrest (Pugh *et al.*, 1997) and remodelling of the nuclear lamina is required for skeletal muscle differentiation *in vitro* (Markiewicz *et al.*, 2005). Increased association of A-type lamins with the nuclear lamina in quiescent human fibroblasts suggests that lamins may stabilize quiescent

arrest. This is supported by the findings that ageing and lamin A/C null fibroblasts show an impaired ability to enter quiescent arrest by contact-inhibition.

Sensing of cellular concentrations of oxygen is an essential mechanism in many tissues because of the risk of oxidative damage from excess $O_2$ levels (hyperoxia) and of metabolic demise from insufficient $O_2$ levels (hypoxia) (Semenza *et al.*, 2001). Oxygen level beyond the 'perceived normoxic range' is a significant stressor leading to growth arrest due to a high level of production of ROS (Packer *et al.*, 1977). In response to oxidative stress, mammalian cells increase expression of antioxidant enzymes and activate protective genes (von Zglinicki *et al.*, 2001). To defend against DNA damage induced by oxidation, proliferating cells trigger DNA damage checkpoint response, which arrests their growth in order to prevent the damaged DNA being replicated. This allows cells to repair DNA damage and mount an adaptive response to prevent further oxidative damage. According to whether or not damaged DNA is repaired, cells resume cell growth or enter a state of permanent growth arrest (senescence). If A-type lamins sense changes in oxidative stress levels via S-glutathiolation in human fibroblasts, they may also be a part of this adaptive response pathway, which leads to Rb-mediated cell cycle arrest (see **Figure 6.1**). I propose that in response to redox imbalance in proliferating cells, A-type lamins become glutathiolated, which leads to altered interaction with LAP2α and nucleoplasmic forms of Rb (Rb780) which in turn leads to cell cycle arrest via speckle-associated forms of Rb (Rb795). If cells regenerate their redox status and/or repair their damaged DNA, A-type lamins become de-glutathiolated and capable of binding to LAP2α and nucleoplasmic Rb (Rb780/795), which allows cell cycle progression. On the contrary, persistent levels of high oxidative stress and/or chronic DNA damage leads to accumulation of irreversibly oxidised A-type lamins and permanent cell cycle arrest (senescence). In laminopathy cells, mutated lamins assemble aberrantly which leads to aggregation of LAP2α and a loss of nucleoplasmic (Rb780) but not speckle-associated forms of Rb (Rb795). Aggregation and/or loss of LAP2α would lead to destabilisation and/or fusions of telomeres, which would then signal DNA damage checkpoint arrest. I suggest that lamin A/C mutations may trigger abnormal generation of DNA damage, and thus activation of DNA damage signalling pathway, which in turns leads to premature senescence.

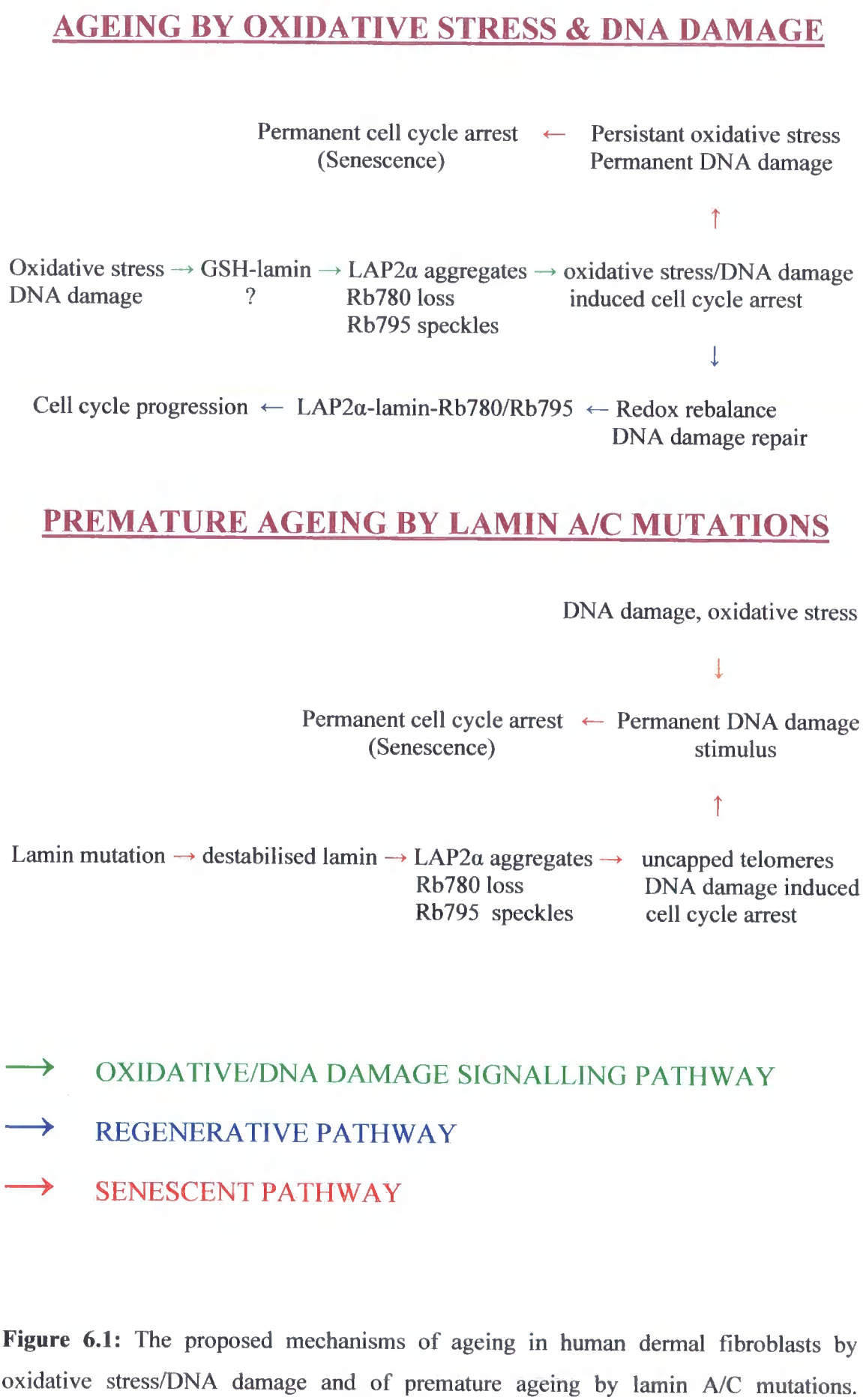


**Figure 6.1:** The proposed mechanisms of ageing in human dermal fibroblasts by oxidative stress/DNA damage and of premature ageing by lamin A/C mutations.

# Bibliography

Agarwal, A. K., J. P. Fryns, et al. (2003). "Zinc metalloproteinase, ZMPSTE24, is mutated in mandibulo-acral dysplasia." Hum Mol Genet **12**(16): 1995-2001.

Allison, S. J. and J. Milner (2003). "Loss of p53 has site-specific effects on histone H3 modification, including serine 10 phosphorylation important for maintenance of ploidy." Cancer Res **63**(20): 6674-9.

Allsopp, R. C., H. Vaziri, et al. (1992). "Telomere length predicts replicative capacity of human fibroblasts." Proc Natl Acad Sci U S A **89**(21): 10114-8.

Alsheimer, M., and R. Benavente. (1996). "Change of karyoskeleton during mammalian spermatogenesis: expression pattern of nuclear lamin C2 and its regulation." Exp Cell Res **228**: 181-8.

Alsheimer, M., E. Fecher, et al. (1998). "Nuclear envelope remodelling during rat spermiogenesis: distribution and expression pattern of LAP2/thymopoietins." J Cell Sci **111** (15): 2227-34.

Alsheimer, M., B. Liebe, et al. (2004). "Disruption of spermatogenesis in mice lacking A-type lamins." J Cell Sci **117**(7): 1173-8.

Alvarez-Reyes, M. (2004). "Interactions between nuclear lamins and their binding partners in EDMD fibroblasts." PhD thesis. University of Durham

Apel, E. D., R. M. Lewis, et al. (2000). "Syne-1, a dystrophin- and Klarsicht-related protein associated with synaptic nuclei at the neuromuscular junction." J Biol Chem **275**(41): 31986-95.

Arora, P., B. Muralikrishna, et al. (2004). "Cell-type-specific interactions at regulatory motifs in the first intron of the lamin A gene." FEBS Lett **568**(1-3): 122-8.

Artandi, S. E., S. Chang, et al. (2000). "Telomere dysfunction promotes non-reciprocal translocations and epithelial cancers in mice." Nature **406**(6796): 641-5.

Ashery-Padan, R., N. Ulitzur, et al. (1997). "Localization and posttranslational modifications of otefin, a protein required for vesicle attachment to chromatin, during Drosophila Melanogaster development." Mol Cell Biol **17**(7): 4114-23.

Avni, D., H. Yang, et al. (2003). "Active localization of the retinoblastoma protein in chromatin and its response to S phase DNA damage." Mol Cell **12**(3): 735-46.

Bakala, H., E. Delaval, et al. (2003). "Changes in rat liver mitochondria with aging. Lon protease-like reactivity and N (epsilon)-carboxymethyllysine accumulation in the matrix." Eur J Biochem **270**(10): 2295-302.

Barbie, D. A., B. A. Kudlow, et al. (2004). "Nuclear reorganization of mammalian DNA synthesis prior to cell cycle exit." Mol Cell Biol **24**(2): 595-607.

Barton, R. M. and H. J. Worman (1999). "Prenylated prelamin A interacts with Narf, a novel nuclear protein." J Biol Chem **274**(42): 30008-18.

Bechert, K., M. Lagos-Quintana, et al. (2003). "Effects of expressing lamin A mutant protein causing Emery-Dreifuss muscular dystrophy and familial partial lipodystrophy in HeLa cells." Exp Cell Res **286**(1): 75-86.

Beck, L. A., T. J. Hosick, et al. (1988). "Incorporation of a product of mevalonic acid metabolism into proteins of Chinese hamster ovary cell nuclei." J Cell Biol **107**(4): 1307-16.

Beck, L. A., T. J. Hosick, et al. (1990). "Isoprenylation is required for the processing of the lamin A precursor." J Cell Biol **110**(5): 1489-99.

Beer, S. M., E. R. Taylor, et al. (2004). "Glutaredoxin 2 catalyzes the reversible oxidation and glutathionylation of mitochondrial membrane thiol proteins: implications for mitochondrial redox regulation and antioxidant DEFENSE." J Biol Chem **279**(46): 47939-51.

Belmont, A. S., Y. Zhai, et al. (1993). "Lamin B distribution and association with peripheral chromatin revealed by optical sectioning and electron microscopy tomography." J Cell Biol **123**(6 Pt 2): 1671-85.

Benavente, R., G. Krohne, et al. (1985). "Cell type-specific expression of nuclear lamina proteins during development of Xenopus laevis." Cell **41**(1): 177-90.

Benavente, R. and G. Krohne (1986). "Involvement of nuclear lamins in postmitotic reorganization of chromatin as demonstrated by microinjection of lamin antibodies." J Cell Biol **103**(5): 1847-54.

Bergo, M. O., B. Gavino, et al. (2002). "Zmpste24 deficiency in mice causes spontaneous bone fractures, muscle weakness, and a prelamin A processing defect." Proc Natl Acad Sci U S A **99**(20): 13049-54.

Berndt, N. (2003). "Roles and regulation of serine/threonine-specific protein phosphatases in the cell cycle." Prog Cell Cycle Res **5**: 497-510.

Bione, S., E. Maestrini, et al. (1994). "Identification of a novel X-linked gene responsible for Emery-Dreifuss muscular dystrophy." Nat Genet **8**(4): 323-7.

Blagosklonny, M. V. (2003). "Cell senescence and hypermitogenic arrest." EMBO Rep **4**(4): 358-62.

Blasco, M. A., S. M. Gasser, et al. (1999). "Telomeres and telomerase." Genes Dev **13**(18): 2353-9.

Bodnar, A. G., M. Ouellette, et al. (1998). "Extension of life-span by introduction of telomerase into normal human cells." Science **279**(5349): 349-52.

Bonne, G., M. R. Di Barletta, et al. (1999). "Mutations in the gene encoding lamin A/C cause autosomal dominant Emery-Dreifuss muscular dystrophy." Nat Genet **21**(3): 285-8.

Boylan, J. F., D. M. Sharp, et al. (1999). "Analysis of site-specific phosphorylation of the retinoblastoma protein during cell cycle progression." Exp Cell Res **248**(1): 110-4.

Boyle, S., S. Gilchrist, et al. (2001). "The spatial organization of human chromosomes within the nuclei of normal and emerin-mutant cells." Hum Mol Genet **10**(3): 211-9.

Brandriff, B. F., L. A. Gordon, et al. (1994). "Human chromosome 19p: a fluorescence in situ hybridization map with genomic distance estimates for 79 intervals spanning 20 Mb." Genomics **23**(3): 582-91.

Bregman, D. B., L. Du, et al. (1995). "Transcription-dependent redistribution of the large subunit of RNA polymerase II to discrete nuclear domains." J Cell Biol **129**(2): 287-98.

Brehm, A., E. A. Miska, et al. (1998). "Retinoblastoma protein recruits histone deacetylase to repress transcription." Nature **391**(6667): 597-601.

Bridge, E., M. Carmo-Fonseca, et al. (1993). "Nuclear organization of splicing small nuclear ribonucleoproteins in adenovirus-infected cells." J Virol **67**(10): 5792-802.

Bridger, J. M., S. Boyle, et al. (2000). "Re-modelling of nuclear architecture in quiescent and senescent human fibroblasts." Curr Biol **10**(3): 149-52.

Bridger, J. M. and I. R. Kill (2004). "Aging of Hutchinson-Gilford progeria syndrome fibroblasts is characterised by hyperproliferation and increased apoptosis." Exp Gerontol **39**(5): 717-24.

Bridger, J. M., I. R. Kill, et al. (1993). "Internal lamin structures within G1 nuclei of human dermal fibroblasts." J Cell Sci **104**(2): 297-306.

Broers, J. L., Y. Raymond, et al. (1993). "Nuclear A-type lamins are differentially expressed in human lung cancer subtypes." Am J Pathol **143**(1): 211-20.

Broers, J. L., N. M. Bronnenberg, et al. (2002). "Partial cleavage of A-type lamins concurs with their total disintegration from the nuclear lamina during apoptosis." Eur J Cell Biol **81**(12): 677-91.

Broers, J. L., H. J. Kuijpers, et al. (2005). "Both lamin A and lamin C mutations cause lamina instability as well as loss of internal nuclear lamin organization." Exp Cell Res **304**(2): 582-92.

Broers, J. L., B. M. Machiels, et al. (1997). "A- and B-type lamins are differentially expressed in normal human tissues." Histochem Cell Biol **107**(6): 505-17.

Broers, J. L., B. M. Machiels, et al. (1999). "Dynamics of the nuclear lamina as monitored by GFP-tagged A-type lamins." J Cell Sci **112**(20): 3463-75.

Broers, J. L., E. A. Peeters, et al. (2004). "Decreased mechanical stiffness in LMNA-/- cells is caused by defective nucleo-cytoskeletal integrity: implications for the

development of laminopathies." Hum Mol Genet **13**(21): 2567-80.

Brown, K. (1999). "Nuclear structure, gene expression and development." Crit Rev Eukaryot Gene Expr **9**(3-4): 203-12.

Brown, K. C. and T. Kodadek (2001). "Protein cross-linking mediated by metal ion complexes." Met Ions Biol Syst **38**: 351-84.

Buchkovich, K., L. A. Duffy, et al. (1989). "The retinoblastoma protein is phosphorylated during specific phases of the cell cycle." Cell **58**(6): 1097-105.

Buendia, B., A. Santa-Maria, et al. (1999). "Caspase-dependent proteolysis of integral and peripheral proteins of nuclear membranes and nuclear pore complex proteins during apoptosis." J Cell Sci **112 (Pt 11)**: 1743-53.

Burke, B. and L. Gerace (1986). "A cell free system to study reassembly of the nuclear envelope at the end of mitosis." Cell **44**(4): 639-52.

Burke, B. and C. L. Stewart (2002). "Life at the edge: the nuclear envelope and human disease." Nat Rev Mol Cell Biol **3**(8): 575-85.

Burkle, A. (2002). "In memoriam Bernard Strehler--genomic instability in ageing: a persistent challenge." Mech Ageing Dev **123**(8): 899-906.

Cai, M., Y. Huang, et al. (2001). "Solution structure of the constant region of nuclear envelope protein LAP2 reveals two LEM-domain structures: one binds BAF and the other binds DNA." EMBO J **20**(16): 4399-407.

Cao, H. and R. A. Hegele (2000). "Nuclear lamin A/C R482Q mutation in Canadian kindreds with Dunnigan-type familial partial lipodystrophy." Hum Mol Genet **9**(1): 109-12.

Caldwell, G. A., F. Naider, et al. (1995). "Fungal lipopeptide mating pheromones: a model system for the study of protein prenylation." Microbiol Rev **59**(3): 406-22.

Campisi, J. (2001). "From cells to organisms: can we learn about aging from cells in culture?" Exp Gerontol **36**(4-6): 607-18.

Campisi, J. (2001). "Cellular senescence as a tumour-suppressor mechanism." Trends Cell Biol **11**(11): S27-31.

Cao, H. and R. A. Hegele (2003). "LMNA is mutated in Hutchinson-Gilford progeria (MIM 176670) but not in Wiedemann-Rautenstrauch progeroid syndrome (MIM 264090)." J Hum Genet **48**(5): 271-4.

Capanni, C., V. Cenni, et al. (2003). "Failure of lamin A/C to functionally assemble in R482L mutated familial partial lipodystrophy fibroblasts: altered intermolecular interaction with emerin and implications for gene transcription." Exp Cell Res **291**(1): 122-34.

Carlin, C., P. D. Phillips, et al. (1994). "Cleavage of the epidermal growth factor

receptor by a membrane-bound leupeptin-sensitive protease active in nonionic detergent lysates of senescent but not young human diploid fibroblasts." J Cell Physiol **160**(3): 427-34.

Cartegni, L., M. R. di Barletta, et al. (1997). "Heart-specific localization of emerin: new insights into Emery-Dreifuss muscular dystrophy." Hum Mol Genet **6**(13): 2257-64.

Carter, K. C., K. L. Taneja, et al. (1991). "Discrete nuclear domains of poly (A) RNA and their relationship to the functional organization of the nucleus." J Cell Biol **115**(5): 1191-202.

Caux, F., E. Dubosclard, et al. (2003). "A new clinical condition linked to a novel mutation in lamins A and C with generalized lipoatrophy, insulin-resistant diabetes, disseminated leukomelanodermic papules, liver steatosis, and cardiomyopathy." J Clin Endocrinol Metab **88**(3): 1006-13.

Cenni, V., P. Sabatelli, et al. (2005). "Lamin A N-terminal phosphorylation is associated with myoblast activation: impairment in Emery-Dreifuss muscular dystrophy." J Med Genet **42**(3): 214-20.

Chellappan, S., V. B. Kraus, et al. (1992). "Adenovirus E1A, simian virus 40 tumour antigen, and human papilloma virus E7 protein share the capacity to disrupt the interaction between transcription factor E2F and the retinoblastoma gene product." Proc Natl Acad Sci USA **89**(10): 4549-53.

Chellappan, S. P., S. Hiebert, et al. (1991). "The E2F transcription factor is a cellular target for the RB protein." Cell **65**(6): 1053-61.

Chelsky, D., C. Sobotka, et al. (1989). "Lamin B methylation and assembly into the nuclear envelope." J Biol Chem **264**(13): 7637-43.

Chen, J. H., K. Stoeber, et al. (2004). "Loss of proliferative capacity and induction of senescence in oxidatively stressed human fibroblasts." J Biol Chem **279**(47): 49439-46.

Chen, L., L. Lee, et al. (2003). "LMNA mutations in atypical Werner's syndrome." Lancet **362**(9382): 440-5.

Chen, P. L., P. Scully, et al. (1989). "Phosphorylation of the retinoblastoma gene product is modulated during the cell cycle and cellular differentiation." Cell **58**(6): 1193-8.

Cheutin, T., M. F. O'Donohue, et al. (2003). "Three-dimensional organization of pKi-67: a comparative fluorescence and electron tomography study using FluoroNanogold." J Histochem Cytochem **51**(11): 1411-23.

Cicchillitti, L., P. Fasanaro, et al. (2003). "Oxidative stress induces protein phosphatase 2A-dependent dephosphorylation of the pocket proteins pRb, p107, and p130." J Biol Chem **278**(21): 19509-17.

Clarke, S. (1992). "Protein isoprenylation and methylation at carboxyl-terminal cysteine

residues." Annu Rev Biochem **61**: 355-86.

Clements, L., S. Manilal, et al. (2000). "Direct interaction between emerin and lamin A." Biochem Biophys Res Commun **267**(3): 709-14.

Cockle, S. M. and R. T. Dean (1984). "Distinct proteolytic mechanisms in serum-sufficient and serum-restricted fibroblasts. Transformed 3T3 cells fail to regulate proteolysis in relation to culture density only during serum-sufficiency." Biochem J **221**(1): 53-60.

Cohen, M., K. K. Lee, et al. (2001). "Transcriptional repression, apoptosis, human disease and the functional evolution of the nuclear lamina." Trends Biochem Sci **26**(1): 41-7.

Collard, J. F., J. L. Senecal, et al. (1992). "Redistribution of nuclear lamin A is an early event associated with differentiation of human promyelocytic leukaemia HL-60 cells." J Cell Sci **101**(3): 657-70.

Collas, I. and J. C. Courvalin (2000). "Sorting nuclear membrane proteins at mitosis." Trends Cell Biol **10**(1): 5-8.

Collas, P., L. Thompson, et al. (1997). "Protein kinase C-mediated interphase lamin B phosphorylation and solubilization." J Biol Chem **272**(34): 21274-80.

Columbaro, M., E. Mattioli, et al. (2001). "Staurosporine treatment and serum starvation promote the cleavage of emerin in cultured mouse myoblasts: involvement of a caspase-dependent mechanism." FEBS Lett **509**(3): 423-9.

Connell-Crowley, L., J. W. Harper, et al. (1997). "Cyclin D1/Cdk4 regulates retinoblastoma protein-mediated cell cycle arrest by site-specific phosphorylation." Mol Biol Cell **8**(2): 287-301.

Corrigan, D. P., D. Kuszczak, et al. (2005). "Prelamin A endoproteolytic processing in vitro by recombinant Zmpste24." Biochem J **387**(1): 129-38.

Cross, T., G. Griffiths, et al. (2000). "PKC-delta is an apoptotic lamin kinase." Oncogene **19**(19): 2331-7.

Csoka, A. B., S. B. English, et al. (2004). "Genome-scale expression profiling of Hutchinson-Gilford progeria syndrome reveals widespread transcriptional misregulation leading to mesodermal/mesenchymal defects and accelerated atherosclerosis." Aging Cell **3**(4): 235-43.

Cumming, R. C., N. L. Andon, et al. (2004). "Protein disulfide bond formation in the cytoplasm during oxidative stress." J Biol Chem **279**(21): 21749-58.

Dabauvalle, M. C., K. Loos, et al. (1991). "Spontaneous assembly of pore complex-containing membranes ("annulate lamellae") in Xenopus egg extract in the absence of chromatin." J Cell Biol **112**(6): 1073-82.

Dabauvalle, M. C., E. Muller, et al. (1999). "Distribution of emerin during the cell

cycle." Eur J Cell Biol **78**(10): 749-56.

d'Adda di Fagagna, F., M. P. Hande, et al. (1999). "Functions of poly (ADP-ribose) polymerase in controlling telomere length and chromosomal stability." Nat Genet **23**(1): 76-80.

Dahl, K. N., S. M. Kahn, et al. (2004). "The nuclear envelope lamina network has elasticity and a compressibility limit suggestive of a molecular shock absorber." J Cell Sci **117**(20): 4779-86.

Dalle-Donne, I., D. Giustarini, et al. (2003). "Reversible S-glutathionylation of Cys 374 regulates actin filament formation by inducing structural changes in the actin molecule." Free Radic Biol Med **34**(1): 23-32.

Dalle-Donne, I., A. Milzani, et al. (1999). "The tert-butyl hydroperoxide-induced oxidation of actin Cys-374 is coupled with structural changes in distant regions of the protein." Biochemistry **38**(38): 12471-80.

Davies, S. L., J. R. Jenkins, et al. (1993). "Human cells express two differentially spliced forms of topoisomerase II beta mRNA." Nucleic Acids Res **21**(16): 3719-23.

De Sandre-Giovannoli, A., R. Bernard, et al. (2003). "Lamin a truncation in Hutchinson-Gilford progeria." Science **300**(5628): 2055.

De Sandre-Giovannoli, A., M. Chaouch, et al. (2002). "Homozygous defects in LMNA, encoding lamin A/C nuclear-envelope proteins, cause autosomal recessive axonal neuropathy in human (Charcot-Marie-Tooth disorder type 2) and mouse." Am J Hum Genet **70**(3): 726-36.

Dean, R. T., S. Fu, et al. (1997). "Biochemistry and pathology of radical-mediated protein oxidation." Biochem J **324**(1): 1-18.

Dean, R. T., S. M. Thomas, et al. (1986). "Oxidation induced proteolysis and its possible restriction by some secondary protein modifications." Biomed Biochim Acta **45**(11-12): 1563-73.

DeCaprio, J. A., Y. Furukawa, et al. (1992). "The retinoblastoma-susceptibility gene product becomes phosphorylated in multiple stages during cell cycle entry and progression." Proc Natl Acad Sci USA **89**(5): 1795-8.

DeCaprio, J. A., J. W. Ludlow, et al. (1989). "The product of the retinoblastoma susceptibility gene has properties of a cell cycle regulatory element." Cell **58**(6): 1085-95.

Dechat, T., A. Gajewski, et al. (2004). "LAP2alpha and BAF transiently localize to telomeres and specific regions on chromatin during nuclear assembly." J Cell Sci **117**(25): 6117-28.

Dechat, T., J. Gotzmann, et al. (1998). "Detergent-salt resistance of LAP2alpha in interphase nuclei and phosphorylation-dependent association with chromosomes early in nuclear assembly implies functions in nuclear structure dynamics."

EMBO J **17**(16): 4887-902.

Dechat, T., B. Korbei, et al. (2000). "Lamina-associated polypeptide 2alpha binds intranuclear A-type lamins." J Cell Sci **113 Pt 19**: 3473-84.

Dechat, T., S. Vlcek, et al. (2000). "Review: lamina-associated polypeptide 2 isoforms and related proteins in cell cycle-dependent nuclear structure dynamics." J Struct Biol **129**(2-3): 335-45.

Dhe-Paganon, S., E. D. Werner, et al. (2002). "Structure of the globular tail of nuclear lamin." J Biol Chem **277**(20): 17381-4.

Di Leonardo, A., S. P. Linke, et al. (1994). "DNA damage triggers a prolonged p53-dependent G1 arrest and long-term induction of Cip1 in normal human fibroblasts." Genes Dev **8**(21): 2540-51.

Dice, J. F. (1982). "Altered degradation of proteins microinjected into senescent human fibroblasts." J Biol Chem **257**(24): 14624-7.

Dimri, G. P. and J. Campisi (1994). "Altered profile of transcription factor-binding activities in senescent human fibroblasts." Exp Cell Res **212**(1): 132-40.

Dimri, G. P., K. Itahana, et al. (2000). "Regulation of a senescence checkpoint response by the E2F1 transcription factor and p14 (ARF) tumour suppressor." Mol Cell Biol **20**(1): 273-85.

Dimri, G. P., X. Lee, et al. (1995). "A biomarker that identifies senescent human cells in culture and in aging skin in vivo." Proc Natl Acad Sci U S A **92**(20): 9363-7.

Ding, X. Z. and I. Mocchetti (1992). "Regulation of cholecystokinin mRNA content in rat striatum: a glutamatergic hypothesis." J Pharmacol Exp Ther **263**(1): 368-73.

Dou, Q. P., P. J. Markell, et al. (1992). "Thymidine kinase transcription is regulated at G1/S phase by a complex that contains retinoblastoma-like protein and a cdc2 kinase." Proc Natl Acad Sci U S A **89**(8): 3256-60.

Dreger, M., L. Bengtsson, et al. (2001). "Nuclear envelope proteomics: novel integral membrane proteins of the inner nuclear membrane." Proc Natl Acad Sci U S A **98**(21): 11943-8.

Dreger, M., H. Otto, et al. (1999). "Identification of phosphorylation sites in native lamina-associated polypeptide 2 beta." Biochemistry **38**(29): 9426-34.

Dreuillet, C., J. Tillit, et al. (2002). "In vivo and in vitro interaction between human transcription factor MOK2 and nuclear lamin A/C." Nucleic Acids Res **30**(21): 4634-42.

Duband-Goulet, I., J. C. Courvalin, et al. (1998). "LBR, a chromatin and lamin binding protein from the inner nuclear membrane, is proteolyzed at late stages of apoptosis." J Cell Sci **111 ( Pt 10)**: 1441-51.

Duband-Goulet, I. and J. C. Courvalin (2000). "Inner nuclear membrane protein LBR preferentially interacts with DNA secondary structures and nucleosomal linker." Biochemistry **39**(21): 6483-8.

Durfee, T., K. Becherer, et al. (1993). "The retinoblastoma protein associates with the protein phosphatase type 1 catalytic subunit." Genes Dev **7**(4): 555-69.

Durfee, T., M. A. Mancini, et al. (1994). "The amino-terminal region of the retinoblastoma gene product binds a novel nuclear matrix protein that co-localizes to centres for RNA processing." J Cell Biol **127**(3): 609-22.

Dyer, J.A. (1996). "An immunological investigation of human lamin A associations in vivo and in vitro." PhD thesis. University of Durham.

Dyer, J. A., I. R. Kill, et al. (1997). "Cell cycle changes in A-type lamin associations detected in human dermal fibroblasts using monoclonal antibodies." Chromosome Res **5**(6): 383-94.

Dyer, J. A., B. E. Lane, et al. (1999). "Investigations of the pathway of incorporation and function of lamin A in the nuclear lamina." Microsc Res Tech **45**(1): 1-12.

Earnshaw, W. C. (1995). "Nuclear changes in apoptosis." Curr Opin Cell Biol **7**(3): 337-43.

Eaton, P., H. L. Byers, et al. (2002). "Detection, quantitation, purification, and identification of cardiac proteins S-thiolated during ischemia and reperfusion." J Biol Chem **277**(12): 9806-11.

Eaton, P., W. Fuller, et al. (2002). "S-thiolation of HSP27 regulates its multimeric aggregate size independently of phosphorylation." J Biol Chem **277**(24): 21189-96.

Eaton, P., M. E. Jones, et al. (2003). "Reversible cysteine-targeted oxidation of proteins during renal oxidative stress." J Am Soc Nephrol **14** (8, Suppl 3): S290-6.

Eggert, M., N. Radomski, et al. (1993). "Identification of novel phosphorylation sites in murine A-type lamins." Eur J Biochem **213**(2): 659-71.

Eggert, M., N. Radomski, et al. (1991). "Identification of phosphorylation sites on murine nuclear lamin C by RP-HPLC and microsequencing." FEBS Lett **292**(1-2): 205-9.

Ellis, D. J., H. Jenkins, et al. (1997). "GST-lamin fusion proteins act as dominant negative mutants in Xenopus egg extract and reveal the function of the lamina in DNA replication." J Cell Sci **110**(20): 2507-18.

Ellis, J. A., C. A. Brown, et al. (2000). "Two distal mutations in the gene encoding emerin have profoundly different effects on emerin protein expression." Neuromuscul Disord **10**(1): 24-30.

Ellis, J. A., M. Craxton, et al. (1998). "Aberrant intracellular targeting and cell cycle-dependent phosphorylation of emerin contribute to the Emery-Dreifuss muscular

dystrophy phenotype." J Cell Sci **111**(6): 781-92.

Eriksson, M., W. T. Brown, et al. (2003). "Recurrent de novo point mutations in lamin A cause Hutchinson-Gilford progeria syndrome." Nature **423**(6937): 293-8.

Esposito, F., F. Cuccovillo, et al. (1998). "A new p21waf1/cip1 isoform is an early event of cell response to oxidative stress." Cell Death Differ **5**(11): 940-5.

Esposito, F., L. Russo, et al. (2000). "Retinoblastoma protein dephosphorylation is an early event of cellular response to pro-oxidant conditions." FEBS Lett **470**(2): 211-5.

Ezhevsky, S. A., A. Ho, et al. (2001). "Differential regulation of retinoblastoma tumour suppressor protein by G (1) cyclin-dependent kinase complexes in vivo." Mol Cell Biol **21**(14): 4773-84.

Ezhevsky, S. A., H. Nagahara, et al. (1997). "Hypo-phosphorylation of the retinoblastoma protein (pRb) by cyclin D:Cdk4/6 complexes results in active pRb." Proc Natl Acad Sci U S A **94**(20): 10699-704.

Fairley, E. A., J. Kendrick-Jones, et al. (1999). "The Emery-Dreifuss muscular dystrophy phenotype arises from aberrant targeting and binding of emerin at the inner nuclear membrane." J Cell Sci **112**(15): 2571-82.

Fairley, E. A., A. Riddell, et al. (2002). "The cell cycle dependent mislocalisation of emerin may contribute to the Emery-Dreifuss muscular dystrophy phenotype." J Cell Sci **115**(Pt 2): 341-54.

Fakan, S. and E. Puvion (1980). "The ultrastructural visualization of nucleolar and extranucleolar RNA synthesis and distribution." Int Rev Cytol **65**: 255-99.

Fakan, S. (1994). "Perichromatin fibrils are in situ forms of nascent transcripts." Trends Cell Biol **4**(3): 86-90.

Faragher, R. G. and D. Kipling (1998). "How might replicative senescence contribute to human ageing?" Bioessays **20**(12): 985-91.

Fatkin, D., C. MacRae, et al. (1999). "Missense mutations in the rod domain of the lamin A/C gene as causes of dilated cardiomyopathy and conduction-system disease." N Engl J Med **341**(23): 1715-24.

Favreau, C., E. Dubosclard, et al. (2003). "Expression of lamin A mutated in the carboxyl-terminal tail generates an aberrant nuclear phenotype similar to that observed in cells from patients with Dunnigan-type partial lipodystrophy and Emery-Dreifuss muscular dystrophy." Exp Cell Res **282**(1): 14-23.

Favreau, C., D. Higuet, et al. (2004). "Expression of a mutant lamin A that causes Emery-Dreifuss muscular dystrophy inhibits in vitro differentiation of C2C12 myoblasts." Mol Cell Biol **24**(4): 1481-92.

Ferraro, A., M. Eufemi, et al. (1989). "Glycosylated forms of nuclear lamins." FEBS Lett **257**(2): 241-6.

Fidzianska, A. and I. Hausmanowa-Petrusewicz (2003). "Architectural abnormalities in muscle nuclei. Ultrastructural differences between X-linked and autosomal dominant forms of EDMD." J Neurol Sci **210**(1-2): 47-51.

Fidzianska, A., D. Toniolo, et al. (1998). "Ultrastructural abnormality of sarcolemmal nuclei in Emery-Dreifuss muscular dystrophy (EDMD)." J Neurol Sci **159**(1): 88-93.

Finkel, T. (2003). "Oxidant signals and oxidative stress." Curr Opin Cell Biol **15**(2): 247-54.

Fitzgerald, J., D. Kennedy, et al. (2000). "UNCL, the mammalian homologue of UNC-50, is an inner nuclear membrane RNA-binding protein." Brain Res **877**(1): 110-23.

Foisner, R. and L. Gerace (1993). "Integral membrane proteins of the nuclear envelope interact with lamins and chromosomes, and binding is modulated by mitotic phosphorylation." Cell **73**(7): 1267-79.

Freeman, M. L., M. J. Borrelli, et al. (1995). "Characterization of a signal generated by oxidation of protein thiols that activates the heat shock transcription factor." J Cell Physiol **164**(2): 356-66.

Fricker, M., M. Hollinshead, et al. (1997). "Interphase nuclei of many mammalian cell types contain deep, dynamic, tubular membrane-bound invaginations of the nuclear envelope." J Cell Biol **136**(3): 531-44.

Friedman, D. L. and R. Ken (1988). "Insulin stimulates incorporation of 32Pi into nuclear lamins A and C in quiescent BHK-21 cells." J Biol Chem **263**(3): 1103-6.

Friend, S. H., R. Bernards, et al. (1986). "A human DNA segment with properties of the gene that predisposes to retinoblastoma and osteosarcoma." Nature **323**(6089): 643-6.

Friguet, B., E. R. Stadtman, et al. (1994). "Modification of glucose-6-phosphate dehydrogenase by 4-hydroxy-2-nonenal. Formation of cross-linked protein that inhibits the multicatalytic protease." J Biol Chem **269**(34): 21639-43.

Frippiat, C., Q. M. Chen, et al. (2001). "Subcytotoxic H2O2 stress triggers a release of transforming growth factor-beta 1, which induces biomarkers of cellular senescence of human diploid fibroblasts." J Biol Chem **276**(4): 2531-7.

Fu, X. D. and T. Maniatis (1990). "Factor required for mammalian spliceosome assembly is localized to discrete regions in the nucleus." Nature **343**(6257): 437-41.

Funabiki, H., I. Hagan, et al. (1993). "Cell cycle-dependent specific positioning and clustering of centromeres and telomeres in fission yeast." J Cell Biol **121**(5): 961-76.

Funabiki, H., K. Kumada, et al. (1996). "Fission yeast Cut1 and Cut2 are essential for

sister chromatid separation, concentrate along the metaphase spindle and form large complexes." EMBO J **15**(23): 6617-28.

Furukawa, K. (1999). "LAP2 binding protein 1 (L2BP1/BAF) is a candidate mediator of LAP2-chromatin interaction." J Cell Sci **112**(15): 2485-92.

Furukawa, K., C. E. Fritze, et al. (1998). "The major nuclear envelope targeting domain of LAP2 coincides with its lamin binding region but is distinct from its chromatin interaction domain." J Biol Chem **273**(7): 4213-9.

Furukawa, K. and Y. Hotta (1993). "cDNA cloning of a germ cell specific lamin B3 from mouse spermatocytes and analysis of its function by ectopic expression in somatic cells." EMBO J **12**(1): 97-106.

Furukawa, K., H. Inagaki, et al. (1994). "Identification and cloning of an mRNA coding for a germ cell-specific A-type lamin in mice." Exp Cell Res **212**(2): 426-30.

Furukawa, K. and T. Kondo (1998). "Identification of the lamina-associated-polypeptide-2-binding domain of B-type lamin." Eur J Biochem **251**(3): 729-33.

Furukawa, K., N. Pante, et al. (1995). "Cloning of a cDNA for lamina-associated polypeptide 2 (LAP2) and identification of regions that specify targeting to the nuclear envelope." EMBO J **14**(8): 1626-36.

Furukawa, K., S. Sugiyama, et al. (2003). "Barrier-to-autointegration factor plays crucial roles in cell cycle progression and nuclear organization in Drosophila." J Cell Sci **116**(Pt 18): 3811-23.

Furukawa, Y., J. A. DeCaprio, et al. (1990). "Expression and state of phosphorylation of the retinoblastoma susceptibility gene product in cycling and noncycling human haematopoietic cells." Proc Natl Acad Sci USA **87**(7): 2770-4.

Gajewski, A., E. Csaszar, et al. (2004). "A phosphorylation cluster in the chromatin-binding region regulates chromosome association of LAP2alpha." J Biol Chem **279**(34): 35813-21.

Gant, T. M., C. A. Harris, et al. (1999). "Roles of LAP2 proteins in nuclear assembly and DNA replication: truncated LAP2beta proteins alter lamina assembly, envelope formation, nuclear size, and DNA replication efficiency in Xenopus laevis extracts." J Cell Biol **144**(6): 1083-96.

Garg, A., R. A. Speckman, et al. (2002). "Multisystem dystrophy syndrome due to novel missense mutations in the amino-terminal head and alpha-helical rod domains of the lamin A/C gene." Am J Med **112**(7): 549-55.

Garnovskaya, M. N., Y. V. Mukhin, et al. (2004). "Mitogen-induced rapid phosphorylation of serine 795 of the retinoblastoma gene product in vascular smooth muscle cells involves ERK activation." J Biol Chem **279**(23): 24899-905.

Georgatos, S. D., J. Meier, et al. (1994). "Lamins and lamin-associated proteins." Curr Opin Cell Biol **6**(3): 347-53.

Georgatos, S. D., A. Pyrpasopoulou, et al. (1997). "Nuclear envelope breakdown in mammalian cells involves stepwise lamina disassembly and microtubule-drive deformation of the nuclear membrane." J Cell Sci **110 ( Pt 17)**: 2129-40.

Georgatos, S. D., C. Stournaras, et al. (1988). "Heterotypic and homotypic associations between the nuclear lamins: site-specificity and control by phosphorylation." Proc Natl Acad Sci USA **85**(12): 4325-9.

Gerace, L. and G. Blobel (1980). "The nuclear envelope lamina is reversibly depolymerized during mitosis." Cell **19**(1): 277-87.

Gerace, L. and B. Burke (1988). "Functional organization of the nuclear envelope." Annu Rev Cell Biol **4**: 335-74.

Gerace, L., C. Comeau, et al. (1984). "Organization and modulation of nuclear lamina structure." J Cell Sci Suppl **1**: 137-60.

Glass, C. A., J. R. Glass, et al. (1993). "The alpha-helical rod domain of human lamins A and C contains a chromatin binding site." EMBO J **12**(11): 4413-24.

Goldberg, M., H. Jenkins, et al. (1995). "Xenopus lamin B3 has a direct role in the assembly of a replication competent nucleus: evidence from cell-free egg extracts." J Cell Sci **108 (Pt 11)**: 3451-61.

Goldberg, M., H. Lu, et al. (1998). "Interactions among Drosophila nuclear envelope proteins lamin, otefin, and YA." Mol Cell Biol **18**(7): 4315-23.

Goldberg, M. W. and T. D. Allen (1995). "Structural and functional organization of the nuclear envelope." Curr Opin Cell Biol **7**(3): 301-9.

Goldman, R. D., Y. Gruenbaum, et al. (2002). "Nuclear lamins: building blocks of nuclear architecture." Genes Dev **16**(5): 533-47.

Goldman, A. E., R. D. Moir, et al. (1992). "Pathway of incorporation of microinjected lamin A into the nuclear envelope." J Cell Biol **119**(4): 725-35.

Goldman, R. D., D. K. Shumaker, et al. (2004). "Accumulation of mutant lamin A causes progressive changes in nuclear architecture in Hutchinson-Gilford progeria syndrome." Proc Natl Acad Sci U S A **101**(24): 8963-8.

Goldstein, G. (1974). "Isolation of bovine thymin: a polypeptide hormone of the thymus." Nature **247**(435): 11-4.

Goldstein, S. (1990). "Replicative senescence: the human fibroblast comes of age." Science **249**(4973): 1129-33.

Gorbunova, V., A. Seluanov, et al. (2002). "Expression of human telomerase (hTERT) does not prevent stress-induced senescence in normal human fibroblasts but protects the cells from stress-induced apoptosis and necrosis." J Biol Chem **277**(41): 38540-9.

Goss, V. L., B. A. Hocevar, et al. (1994). "Identification of nuclear beta II protein kinase C as a mitotic lamin kinase." J Biol Chem **269**(29): 19074-80.

Gotzmann, J., S. Vlcek, et al. (2000). "Caspase-mediated cleavage of the chromosome-binding domain of lamina-associated polypeptide 2 alpha." J Cell Sci **113**(21): 3769-80.

Grafstrom, R. H., W. Pan, et al. (1999). "Defining the substrate specificity of cdk4 kinase-cyclin D1 complex." Carcinogenesis **20**(2): 193-8.

Gribbon, C., R. Dahm, et al. (2002). "Association of the nuclear matrix component NuMA with the Cajal body and nuclear speckle compartments during transitions in transcriptional activity in lens cell differentiation." Eur J Cell Biol **81**(10): 557-66.

Gruber, J., T. Lampe, et al. (2005). "RNAi of FACE1 protease results in growth inhibition of human cells expressing lamin A: implications for Hutchinson-Gilford progeria syndrome." J Cell Sci **118**(4): 689-96.

Gruenbaum, Y., Y. Landesman, et al. (1988). "Drosophila nuclear lamin precursor Dm0 is translated from either of two developmentally regulated mRNA species apparently encoded by a single gene." J Cell Biol **106**(3): 585-96.

Gruenbaum, Y., K. K. Lee, et al. (2002). "The expression, lamin-dependent localization and RNAi depletion phenotype for emerin in C. elegans." J Cell Sci **115**(5): 923-9.

Grune, T., T. Reinheckel, et al. (1997). "Degradation of oxidized proteins in mammalian cells." Faseb J **11**(7): 526-34.

Guillemin, K., T. Williams, et al. (2001). "A nuclear lamin is required for cytoplasmic organization and egg polarity in Drosophila." Nat Cell Biol **3**(9): 848-51.

Haas, M. and E.Jost (1993) "Functional analysis of phosphorylation sites in human lamin A controlling lamin disassembly, nuclear transport and assembly." Eur J Cell Biol **62**(2): 237-247

Haddad, J. J. (2004). "Oxygen sensing and oxidant/redox-related pathways." Biochem Biophys Res Commun **316**(4): 969-77.

Hannan, K. M., B. K. Kennedy, et al. (2000). "RNA polymerase I transcription in confluent cells: Rb downregulates rDNA transcription during confluence-induced cell cycle arrest." Oncogene **19**(31): 3487-97.

Haraguchi, T., J. M. Holaska, et al. (2004). "Emerin binding to Btf, a death-promoting transcriptional repressor, is disrupted by a missense mutation that causes Emery-Dreifuss muscular dystrophy." Eur J Biochem **271**(5): 1035-45.

Haraguchi, T., T. Koujin, et al. (2001). "BAF is required for emerin assembly into the reforming nuclear envelope." J Cell Sci **114**(24): 4575-85.

Harborth, J., S. M. Elbashir, et al. (2001). "Identification of essential genes in cultured mammalian cells using small interfering RNAs." J Cell Sci **114**(Pt 24): 4557-65.

Harman, D. (1956). "Aging: a theory based on free radical and radiation chemistry." J Gerontol **11**(3): 298-300.

Harman, D. (2001). "Aging: overview." Ann N Y Acad Sci **928**: 1-21.

Harrington, E. A., J. L. Bruce, et al. (1998). "pRB plays an essential role in cell cycle arrest induced by DNA damage." Proc Natl Acad Sci U S A **95**(20): 11945-50.

Harris, C. A., P. J. Andryuk, et al. (1994). "Three distinct human thymopoietins are derived from alternatively spliced mRNAs." Proc Natl Acad Sci USA **91**(14): 6283-7.

Harris, C. A., P. J. Andryuk, et al. (1995). "Structure and mapping of the human thymopoietin (TMPO) gene and relationship of human TMPO beta to rat lamin-associated polypeptide 2." Genomics **28**(2): 198-205.

Hayflick, L. (1965). "The Limited in Vitro Lifetime of Human Diploid Cell Strains." Exp Cell Res **37**: 614-36.

Hayflick, L. (1998). "How and why we age." Exp Gerontol **33**(7-8): 639-53.

Hayflick, L. and P. S. Moorhead (1961). "The serial cultivation of human diploid cell strains." Exp Cell Res **25**: 585-621.

Heald, R. and F. McKeon (1990). "Mutations of phosphorylation sites in lamin A that prevent nuclear lamina disassembly in mitosis." Cell **61**(4): 579-89.

Heitlinger, E., M. Peter, et al. (1991). "Expression of chicken lamin B2 in *Escherichia coli*: characterization of its structure, assembly, and molecular interactions." J Cell Biol **113**(3): 485-95.

Heitlinger, E., M. Peter, et al. (1992). "The role of the head and tail domain in lamin structure and assembly: analysis of bacterially expressed chicken lamin A and truncated B2 lamins." J Struct Biol **108**(1): 74-89.

Hellemans, J., O. Preobrazhenska, et al. (2004). "Loss-of-function mutations in LEMD3 result in osteopoikilosis, Buschke-Ollendorff syndrome and melorheostosis." Nat Genet **36**(11): 1213-8.

Hennekes, H. and E. A. Nigg (1994). "The role of isoprenylation in membrane attachment of nuclear lamins. A single point mutation prevents proteolytic cleavage of the lamin A precursor and confers membrane binding properties." J Cell Sci **107 (Pt 4)**: 1019-29.

Hennekes, H., M. Peter, et al. (1993). "Phosphorylation on protein kinase C sites inhibits nuclear import of lamin B2." J Cell Biol **120**(6): 1293-304.

Hensey, C. E., F. Hong, et al. (1994). "Identification of discrete structural domains in the retinoblastoma protein. Amino-terminal domain is required for its

oligomerization." J Biol Chem **269**(2): 1380-7.

Hocevar, B. A., D. J. Burns, et al. (1993). "Identification of protein kinase C (PKC) phosphorylation sites on human lamin B. Potential role of PKC in nuclear lamina structural dynamics." J Biol Chem **268**(10): 7545-52.

Hoffmann, K., C. K. Dreger, et al. (2002). "Mutations in the gene encoding the lamin B receptor produce an altered nuclear morphology in granulocytes (Pelger-Huet anomaly)." Nat Genet **31**(4): 410-4.

Hoger, T. H., G. Krohne, et al. (1991). "Interaction of Xenopus lamins A and LII with chromatin in vitro mediated by a sequence element in the carboxy terminal domain." Exp Cell Res **197**(2): 280-9.

Holaska, J. M., A. K. Kowalski, et al. (2004). "Emerin caps the pointed end of actin filaments: evidence for an actin cortical network at the nuclear inner membrane." PLoS Biol **2**(9): E231.

Holaska, J. M., K. K. Lee, et al. (2003). "Transcriptional repressor germ cell-less (GCL) and barrier to autointegration factor (BAF) compete for binding to emerin in vitro." J Biol Chem **278**(9): 6969-75.

Holtz, D., R. A. Tanaka, et al. (1989). "The CaaX motif of lamin A functions in conjunction with the nuclear localization signal to target assembly to the nuclear envelope." Cell **59**(6): 969-77.

Hozak, P., A. M. Sasseville, et al. (1995). "Lamin proteins form an internal nucleoskeleton as well as a peripheral lamina in human cells." J Cell Sci **108**(2): 635-44.

Hozak, P., C. Schofer, et al. (1993). "A study on nucleolar DNA: isolation of DNA from fibrillar components and ultrastructural localization of different DNA probes." J Cell Sci **104 (Pt 4)**: 1199-205.

Hu, Q. J., N. Dyson, et al. (1990). "The regions of the retinoblastoma protein needed for binding to adenovirus E1A or SV40 large T antigen are common sites for mutations." EMBO **9**(4): 1147-55.

Huang, H. J., J. K. Yee, et al. (1988). "Suppression of the neoplastic phenotype by replacement of the RB gene in human cancer cells." Science **242**(4885): 1563-6.

Hutchison, C. and I. Kill (1989). "Changes in the nuclear distribution of DNA polymerase alpha and PCNA/cyclin during the progress of the cell cycle, in a cell-free extract of Xenopus eggs." J Cell Sci **93**(4): 605-13.

Hutchison, C. J. (2002). "Lamins: building blocks or regulators of gene expression?" Nat Rev Mol Cell Biol **3**(11): 848-58.

Hutchison, C. J., M. Alvarez-Reyes, et al. (2001). "Lamins in disease: why do ubiquitously expressed nuclear envelope proteins give rise to tissue-specific disease phenotypes?" J Cell Sci **114**(1): 9-19.

Hutchison, C. J., D. Brill, et al. (1989). "DNA replication and cell cycle control in Xenopus egg extracts." J Cell Sci Suppl **12**: 197-212.

Hutchison, C. J., R. Cox, et al. (1988). "The control of DNA replication in a cell-free extract that recapitulates a basic cell cycle in vitro." Development **103**(3): 553-66.

Hutchison, C. J. and H. J. Worman (2004). "A-type lamins: guardians of the soma?" Nat Cell Biol **6**(11): 1062-7.

Imai, S., S. Nishibayashi, et al. (1997). "Dissociation of Oct-1 from the nuclear peripheral structure induces the cellular aging-associated collagenase gene expression." Mol Biol Cell **8**(12): 2407-19.

Ingber, D. E. (1997). "Tensegrity: the architectural basis of cellular mechanotransduction." Annu Rev Physiol **59**: 575-99.

Ishida, R., R. Takashima, et al. (2001). "Mitotic specific phosphorylation of serine-1212 in human DNA topoisomerase II alpha." Cell Struct Funct **26**(4): 215-26.

Iwasa, H., J. Han, et al. (2003). "Mitogen-activated protein kinase p38 defines the common senescence-signalling pathway." Genes Cells **8**(2): 131-44.

Izumi, M., O. A. Vaughan, et al. (2000). "Head and/or CaaX domain deletions of lamin proteins disrupt preformed lamin A and C but not lamin B structure in mammalian cells." Mol Biol Cell **11**(12): 4323-37.

Jagatheesan, G., S. Thanumalayan, et al. (1999). "Colocalization of intranuclear lamin foci with RNA splicing factors." J Cell Sci **112**(24): 4651-61.

Jang, G. F., K. Yokoyama, et al. (1993). "A prenylated protein-specific endoprotease in rat liver microsomes that produces a carboxyl-terminal tripeptide." Biochemistry **32**(36): 9500-7.

Jeng, Y. W., H. C. Chao, et al. (1999). "Senescent human fibroblasts have elevated Ku86 proteolytic cleavage activity." Mutat Res **435**(3): 225-32.

Jenkins, H., T. Holman, et al. (1993). "Nuclei that lack a lamina accumulate karyophilic proteins and assemble a nuclear matrix." J Cell Sci **106**(1): 275-85.

Jimenez-Garcia, L. F. and D. L. Spector (1993). "In vivo evidence that transcription and splicing are coordinated by a recruiting mechanism." Cell **73**(1): 47-59.

Johnson, B. R., R. T. Nitta, et al. (2004). "A-type lamins regulate retinoblastoma protein function by promoting subnuclear localization and preventing proteasomal degradation." Proc Natl Acad Sci USA **101**(26): 9677-82.

Johnson, L. F., R. Levis, et al. (1976). "Changes in RNA in relation to growth of the fibroblast. IV. Alterations in the production and processing of mRNA and rRNA in resting and growing cells." J Cell Biol **71**(3): 933-8.

Kapiloff, M. S., R. V. Schillace, et al. (1999). "mAKAP: an A-kinase anchoring protein

targeted to the nuclear membrane of differentiated myocytes." J Cell Sci **112** (**Pt 16**): 2725-36.

Karantza, V., A. Maroo, et al. (1993). "Overproduction of Rb protein after the G1/S boundary causes G2 arrest." Mol Cell Biol **13**(11): 6640-52.

Kaufmann, S. H., W. Gibson, et al. (1983). "Characterization of the major polypeptides of the rat liver nuclear envelope." J Biol Chem **258**(4): 2710-9.

Kennedy, B. K., D. A. Barbie, et al. (2000). "Nuclear organization of DNA replication in primary mammalian cells." Genes Dev **14**(22): 2855-68.

Kilic, F., M. B. Dalton, et al. (1997). "In vitro assay and characterization of the farnesylation-dependent prelamin A endoprotease." J Biol Chem **272**(8): 5298-304.

Kill, I. R., R. G. Faragher, et al. (1994). "The expression of proliferation-dependent antigens during the lifespan of normal and progeroid human fibroblasts in culture." J Cell Sci **107**(2): 571-9.

Kill, I. R. and C. J. Hutchison (1995). "S-phase phosphorylation of lamin B2." FEBS Lett **377**(1): 26-30.

Kim, K. H., G. T. Park, et al. (2004). "Expression of connective tissue growth factor, a biomarker in senescence of human diploid fibroblasts, is up-regulated by a transforming growth factor-beta-mediated signalling pathway." Biochem Biophys Res Commun **318**(4): 819-25.

Kim, S. J., K. Y. Kim, et al. (1992). "Inhibition of protein phosphatases blocks myogenesis by first altering MyoD binding activity." J Biol Chem **267**(21): 15140-5.

Kim, S. J., H. D. Lee, et al. (1991). "Regulation of transforming growth factor beta 1 gene expression by the product of the retinoblastoma-susceptibility gene." Proc Natl Acad Sci USA **88**(8): 3052-6.

Kim, S. J., K. Park, et al. (1992). "Post-transcriptional regulation of the human transforming growth factor-beta 1 gene." J Biol Chem **267**(19): 13702-7.

Kirkwood, T. B. (1996). "Human senescence." Bioessays **18**(12): 1009-16.

Kitten, G. T. and E. A. Nigg (1991). "The CaaX motif is required for isoprenylation, carboxyl methylation, and nuclear membrane association of lamin B2." J Cell Biol **113**(1): 13-23.

Kobberling, J. and M. G. Dunnigan (1986). "Familial partial lipodystrophy: two types of an X linked dominant syndrome, lethal in the hemizygous state." J Med Genet **23**(2): 120-7.

Knudsen, E. S. and J. Y. Wang (1997). "Dual mechanisms for the inhibition of E2F binding to RB by cyclin-dependent kinase-mediated RB phosphorylation." Mol Cell Biol **17**(10): 5771-83.

Krimm, I., C. Ostlund, et al. (2002). "The Ig-like structure of the C-terminal domain of lamin A/C, mutated in muscular dystrophies, cardiomyopathy, and partial lipodystrophy." Structure (Camb) **10**(6): 811-23.

Krohne, G., I. Waizenegger, et al. (1989). "The conserved carboxy-terminal cysteine of nuclear lamins is essential for lamin association with the nuclear envelope." J Cell Biol **109**(5): 2003-11.

Krtolica, A. and J. Campisi (2002). "Cancer and aging: a model for the cancer promoting effects of the aging stroma." Int J Biochem Cell Biol **34**(11): 1401-14.

Krtolica, A., N. A. Krucher, et al. (1998). "Hypoxia-induced pRB hypophosphorylation results from down-regulation of CDK and upregulation of PP1 activities." Oncogene **17**(18): 2295-304.

Krtolica, A., S. Parrinello, et al. (2001). "Senescent fibroblasts promote epithelial cell growth and tumorigenesis: a link between cancer and aging." Proc Natl Acad Sci USA **98**(21): 12072-7.

Kruhlak, M. J., M. A. Lever, et al. (2000). "Reduced mobility of the alternate splicing factor (ASF) through the nucleoplasm and steady state speckle compartments." J Cell Biol **150**(1): 41-51.

Kumaran, R. I., B. Muralikrishna, et al. (2002). "Lamin A/C speckles mediate spatial organization of splicing factor compartments and RNA polymerase II transcription." J Cell Biol **159**(5): 783-93.

Laemmli, U. K. (1970). "Cleavage of structural proteins during the assembly of the head of bacteriophage T4." Nature **227**(5259): 680-5.

Laliberte, J. F., A. Dagenais, et al. (1984). "Identification of distinct messenger RNAs for nuclear lamin C and a putative precursor of nuclear lamin A." J Cell Biol **98**(3): 980-5.

Lamb, N. J., J. C. Cavadore, et al. (1991). "Inhibition of cAMP-dependent protein kinase plays a key role in the induction of mitosis and nuclear envelope breakdown in mammalian cells." EMBO J **10**(6): 1523-33.

Lammerding, J., P. C. Schulze, et al. (2004). "Lamin A/C deficiency causes defective nuclear mechanics and mechanotransduction." J Clin Invest **113**(3): 370-8.

Lamond, A. I. and W. C. Earnshaw (1998). "Structure and function in the nucleus." Science **280**(5363): 547-53.

Lang, C. and G. Krohne (2003). "Lamina-associated polypeptide 2beta (LAP2beta) is contained in a protein complex together with A- and B-type lamins." Eur J Cell Biol **82**(3): 143-53.

Lattanzi, G., V. Cenni, et al. (2003). "Association of emerin with nuclear and cytoplasmic actin is regulated in differentiating myoblasts." Biochem Biophys Res Commun **303**(3): 764-70.

Lazebnik, Y. A., A. Takahashi, et al. (1995). "Studies of the lamin proteinase reveal multiple parallel biochemical pathways during apoptotic execution." Proc Natl Acad Sci U S A **92**(20): 9042-6.

Lea, N., S. Orr, et al. (2003). "Commitment Point during G0→G1 That Controls Entry into the cell cycle." Mol Cell Biol **23**(7): 2351-2361

Lebel, S., C. Lampron, et al. (1987). "Lamins A and C appear during retinoic acid-induced differentiation of mouse embryonal carcinoma cells." J Cell Biol **105**(3): 1099-104.

Lee, K. K., Y. Gruenbaum, et al. (2000). "C. elegans nuclear envelope proteins emerin, MAN1, lamin, and nucleoporins reveal unique timing of nuclear envelope breakdown during mitosis." Mol Biol Cell **11**(9): 3089-99.

Lee, K. K., T. Haraguchi, et al. (2001). "Distinct functional domains in emerin bind lamin A and DNA-bridging protein BAF." J Cell Sci **114**(24): 4567-73.

Lee, K. K., D. Starr, et al. (2002). "Lamin-dependent localization of UNC-84, a protein required for nuclear migration in Caenorhabditis elegans." Mol Biol Cell **13**(3): 892-901.

Lee, W. H., R. Bookstein, et al. (1987). "Human retinoblastoma susceptibility gene: cloning, identification, and sequence." Science **235**(4794): 1394-9.

Lee, W. H., J. Y. Shew, et al. (1987). "The retinoblastoma susceptibility gene encodes a nuclear phosphoprotein associated with DNA binding activity." Nature **329**(6140): 642-5.

Lees, J. A., K. J. Buchkovich, et al. (1991). "The retinoblastoma protein is phosphorylated on multiple sites by human cdc2." EMBO J **10**(13): 4279-90.

Lehner, C. F., G. Furstenberger, et al. (1986). "Biogenesis of the nuclear lamina: in vivo synthesis and processing of nuclear protein precursors." Proc Natl Acad Sci USA **83**(7): 2096-9.

Li, J., M. Gorospe, et al. (2001). "Transcriptional induction of MKP-1 in response to stress is associated with histone H3 phosphorylation-acetylation." Mol Cell Biol **21**(23): 8213-24.

Lin, C. W. and A. Engelman (2003). "The barrier-to-autointegration factor is a component of functional human immunodeficiency virus type 1 preintegration complexes." J Virol **77**(8): 5030-6.

Lin, F., D. L. Blake, et al. (2000). "MAN1, an inner nuclear membrane protein that shares the LEM domain with lamina-associated polypeptide 2 and emerin." J Biol Chem **275**(7): 4840-7.

Lin, F., J. M. Morrison, et al. (2005). "MAN1, an integral protein of the inner nuclear membrane, binds Smad2 and Smad3 and antagonizes transforming growth factor-beta signalling." Hum Mol Genet **14**(3): 437-45.

Lin, F. and H. J. Worman (1993). "Structural organization of the human gene encoding nuclear lamin A and nuclear lamin C." J Biol Chem **268**(22): 16321-6.

Lin, F., D. Xiao, et al. (2000). "Unique anti-activator protein-1 activity of retinoic acid receptor beta." Cancer Res **60**(12): 3271-80.

Lin, H. F. and M. F. Wolfner (1991). "The Drosophila maternal-effect gene fs (1)Ya encodes a cell cycle-dependent nuclear envelope component required for embryonic mitosis." Cell **64**(1): 49-62.

Liu, J., K. K. Lee, et al. (2003). "MAN1 and emerin have overlapping function(s) essential for chromosome segregation and cell division in Caenorhabditis elegans." Proc Natl Acad Sci U S A **100**(8): 4598-603.

Liu, J., T. Rolef Ben-Shahar, et al. (2000). "Essential roles for Caenorhabditis elegans lamin gene in nuclear organization, cell cycle progression, and spatial organization of nuclear pore complexes." Mol Biol Cell **11**(11): 3937-47.

Lloyd, D. J., R. C. Trembath, et al. (2002). "A novel interaction between lamin A and SREBP1: implications for partial lipodystrophy and other laminopathies." Hum Mol Genet **11**(7): 769-77.

Loewinger, L. and F. McKeon (1988). "Mutations in the nuclear lamin proteins resulting in their aberrant assembly in the cytoplasm." EMBO J **7**(8): 2301-9.

Lourim, D. and J. J. Lin (1989). "Expression of nuclear lamin A and muscle-specific proteins in differentiating muscle cells *in ovo* and *in vitro*." J Cell Biol **109**(2): 495-504.

Lourim, D. and J. J. Lin (1992). "Expression of wild-type and nuclear localization-deficient human lamin A in chick myogenic cells." J Cell Sci **103**(3): 863-74.

Luderus, M. E., A. de Graaf, et al. (1992). "Binding of matrix attachment regions to lamin B1." Cell **70**(6): 949-59.

Luderus, M. E., J. L. den Blaauwen, et al. (1994). "Binding of matrix attachment regions to lamin polymers involves single-stranded regions and the minor groove." Mol Cell Biol **14**(9): 6297-305.

Ludlow, J. W., J. A. DeCaprio, et al. (1989). "SV40 large T antigen binds preferentially to an under-phosphorylated member of the retinoblastoma susceptibility gene product family." Cell **56**(1): 57-65.

Luo, J., J. A. Lang, et al. (1998). "Transforming growth factor beta1 regulates the expression of cyclo-oxygenase in cultured cortical astrocytes and neurons." J Neurochem **71**(2): 526-34.

Lundberg, A. S. and R. A. Weinberg (1998). "Functional inactivation of the retinoblastoma protein requires sequential modification by at least two distinct cyclin-cdk complexes." Mol Cell Biol **18**(2): 753-61.

Lutz, R. J., M. A. Trujillo, et al. (1992). "Nucleoplasmic localization of prelamin A:

implications for prenylation-dependent lamin A assembly into the nuclear lamina." Proc Natl Acad Sci U S A **89**(7): 3000-4.

Ly, D. H., D. J. Lockhart, et al. (2000). "Mitotic misregulation and human aging." Science **287**(5462): 2486-92.

Ma, H., A. J. Siegel, et al. (1999). "Association of chromosome territories with the nuclear matrix. Disruption of human chromosome territories correlates with the release of a subset of nuclear matrix proteins." J Cell Biol **146**(3): 531-42.

Machiels, B. M., A. H. Zorenc, et al. (1996). "An alternative splicing product of the lamin A/C gene lacks exon 10." J Biol Chem **271**(16): 9249-53.

Macieira-Coelho, A., J. Ponten, et al. (1966). "The division cycle and RNA-synthesis in diploid human cells at different passage levels in vitro." Exp Cell Res **42**(3): 673-84.

Maison, C., A. Pyrpasopoulou, et al. (1997). "The inner nuclear membrane protein LAP1 forms a native complex with B-type lamins and partitions with spindle-associated mitotic vesicles." EMBO J **16**(16): 4839-50.

Mallette, F. A., S. Goumard, et al. (2004). "Human fibroblasts require the Rb family of tumour suppressors, but not p53, for PML-induced senescence." Oncogene **23**(1): 91-9.

Mancini, M. A., B. Shan, et al. (1994). "The retinoblastoma gene product is a cell cycle-dependent, nuclear matrix-associated protein." Proc Natl Acad Sci U S A **91**(1): 418-22.

Manilal, S., T. M. Nguyen, et al. (1996). "The Emery-Dreifuss muscular dystrophy protein, emerin, is a nuclear membrane protein." Hum Mol Genet **5**(6): 801-8.

Manilal, S., C. A. Sewry, et al. (1997). "Diagnosis of X-linked Emery-Dreifuss muscular dystrophy by protein analysis of leucocytes and skin with monoclonal antibodies." Neuromuscul Disord **7**(1): 63-6.

Mansharamani, M. and K. L. Wilson (2005). "Direct binding of nuclear membrane protein MAN1 to emerin in vitro and two modes of binding to barrier-to-autointegration factor." J Biol Chem **280**(14): 13863-70.

Mariappan, I. and V. K. Parnaik (2005). "Sequestration of pRb by cyclin D3 causes intranuclear reorganization of lamin A/C during muscle cell differentiation." Mol Biol Cell **16**(4): 1948-60.

Markiewicz, E., M. Ledran, et al. (2005). "Remodelling of the nuclear lamina and nucleoskeleton is required for skeletal muscle differentiation in vitro." J Cell Sci **118**(Pt 2): 409-20.

Markiewicz, E., T. Dechat, et al. (2002) "Lamin A/C Binding Protein LAP2α Is Required for Nuclear Anchorage of Retinoblastoma Protein." Mol Biol Cell **13**: 4401-4413

Markiewicz, E., R. Venables, et al. (2002). "Increased solubility of lamins and redistribution of lamin C in X-linked Emery-Dreifuss muscular dystrophy fibroblasts." J Struct Biol **140**(1-3): 241-53.

Martelli, A. M., R. Bortul, et al. (2002). "Molecular characterization of protein kinase C-alpha binding to lamin A." J Cell Biochem **86**(2): 320-30.

Martin, G. M. and J. Oshima (2000). "Lessons from human progeroid syndromes." Nature **408**(6809): 263-6.

Martin, L., C. Crimaudo, et al. (1995). "cDNA cloning and characterization of lamina-associated polypeptide 1C (LAP1C), an integral protein of the inner nuclear membrane." J Biol Chem **270**(15): 8822-8.

Martins, S., S. Eikvar, et al. (2003). "HA95 and LAP2 beta mediate a novel chromatin-nuclear envelope interaction implicated in initiation of DNA replication." J Cell Biol **160**(2): 177-88.

Martins, S. B., T. Eide, et al. (2000). "HA95 is a protein of the chromatin and nuclear matrix regulating nuclear envelope dynamics." J Cell Sci **113**(21): 3703-13.

Mayans, O., J. Wuerges, et al. (2001). "Structural evidence for a possible role of reversible disulphide bridge formation in the elasticity of the muscle protein titin." Structure (Camb) **9**(4): 331-40.

McDuffee, A. T., G. Senisterra, et al. (1997). "Proteins containing non-native disulfide bonds generated by oxidative stress can act as signals for the induction of the heat shock response." J Cell Physiol **171**(2): 143-51.

McKeon, F. D., D. L. Tuffanelli, et al. (1983). "Autoimmune response directed against conserved determinants of nuclear envelope proteins in a patient with linear scleroderma." Proc Natl Acad Sci U S A **80**(14): 4374-8.

Meier, J., K. H. Campbell, et al. (1991). "The role of lamin LIII in nuclear assembly and DNA replication, in cell-free extracts of Xenopus eggs." J Cell Sci **98**(3): 271-9.

Meier, J. and S. D. Georgatos (1994). "Type B lamins remain associated with the integral nuclear envelope protein p58 during mitosis: implications for nuclear reassembly." EMBO J **13**(8): 1888-98.

Mercuri, E. and F. Muntoni (2001). "What's new in neuromuscular disorders? Nuclear envelope and Emery-Dreifuss muscular dystrophy." Eur J Paediatr Neurol **5**(1): 3-5.

Mical, T. I. and M. J. Monteiro (1998). "The role of sequences unique to nuclear intermediate filaments in the targeting and assembly of human lamin B: evidence for lack of interaction of lamin B with its putative receptor." J Cell Sci **111 ( Pt 23)**: 3471-85.

Mintz, P. J., S. D. Patterson, et al. (1999). "Purification and biochemical characterization of interchromatin granule clusters." EMBO J **18**(15): 4308-20.

Mislow, J. M., J. M. Holaska, et al. (2002). "Nesprin-1alpha self-associates and binds directly to emerin and lamin A in vitro." FEBS Lett **525**(1-3): 135-40.

Mislow, J. M., M. S. Kim, et al. (2002). "Myne-1, a spectrin repeat transmembrane protein of the myocyte inner nuclear membrane, interacts with lamin A/C." J Cell Sci **115**(1): 61-70.

Misteli, T. and D. L. Spector (1996). "Serine/threonine phosphatase 1 modulates the subnuclear distribution of pre-mRNA splicing factors." Mol Biol Cell **7**(10): 1559-72.

Mittnacht, S. (1998). "Control of pRB phosphorylation." Curr Opin Genet Dev **8**(1): 21-7.

Mittnacht, S., J. A. Lees, et al. (1994). "Distinct sub-populations of the retinoblastoma protein show a distinct pattern of phosphorylation." EMBO J **13**(1): 118-27.

Mittnacht, S. and R. A. Weinberg (1991). "G1/S phosphorylation of the retinoblastoma protein is associated with an altered affinity for the nuclear compartment." Cell **65**(3): 381-93.

Moir, R. D., A. D. Donaldson, et al. (1991). "Expression in Escherichia coli of human lamins A and C: influence of head and tail domains on assembly properties and paracrystal formation." J Cell Sci **99**(2): 363-72.

Moir, R. D., M. Montag-Lowy, et al. (1994). "Dynamic properties of nuclear lamins: lamin B is associated with sites of DNA replication." J Cell Biol **125**(6): 1201-12.

Moir, R. D., T. P. Spann, et al. (2000). "Disruption of nuclear lamin organization blocks the elongation phase of DNA replication." J Cell Biol **149**(6): 1179-92.

Moir, R. D., T. P. Spann, et al. (2000). "Review: the dynamics of the nuclear lamins during the cell cycle-- relationship between structure and function." J Struct Biol **129**(2-3): 324-34.

Morris, G. E. (2000). "Nuclear proteins and cell death in inherited neuromuscular disease." Neuromuscul Disord **10**(4-5): 217-27.

Morris, G. E. (2001). "The role of the nuclear envelope in Emery-Dreifuss muscular dystrophy." Trends Mol Med **7**(12): 572-7.

Mossakowska, M., J. Moraczewska, et al. (1993). "Proteolytic removal of three C-terminal residues of actin alters the monomer-monomer interactions." Biochem J **289**(3): 897-902.

Mounkes, L. C., B. Burke, et al. (2001). "The A-type lamins: nuclear structural proteins as a focus for muscular dystrophy and cardiovascular diseases." Trends Cardiovasc Med **11**(7): 280-5.

Mounkes, L. C., S. Kozlov, et al. (2003). "A progeroid syndrome in mice is caused by defects in A-type lamins." Nature **423**(6937): 298-301.

Mounkes, L. C. and C. L. Stewart (2004). "Aging and nuclear organization: lamins and progeria." Curr Opin Cell Biol **16**(3): 322-7.

Muchir, A., G. Bonne, et al. (2000). "Identification of mutations in the gene encoding lamins A/C in autosomal dominant limb girdle muscular dystrophy with atrioventricular conduction disturbances (LGMD1B)." Hum Mol Genet **9**(9): 1453-9.

Muchir, A., B. G. van Engelen, et al. (2003). "Nuclear envelope alterations in fibroblasts from LGMD1B patients carrying nonsense Y259X heterozygous or homozygous mutation in lamin A/C gene." Exp Cell Res **291**(2): 352-62.

Mukherjee, A. B. and C. Costello (1998). "Aneuploidy analysis in fibroblasts of human premature aging syndromes by FISH during in vitro cellular aging." Mech Ageing Dev **103**(2): 209-22.

Muller, W. E., P. S. Agutter, et al. (1993). "[Age-dependent changes in mRNA transport (nucleus-cytoplasm)]." Z Gerontol **26**(4): 221-31.

Muralikrishna, B., J. Dhawan, et al. (2001). "Distinct changes in intranuclear lamin A/C organization during myoblast differentiation." J Cell Sci **114**(22): 4001-11.

Muralikrishna, B. and V. K. Parnaik (2001). "SP3 and AP-1 mediate transcriptional activation of the lamin A proximal promoter." Eur J Biochem **268**(13): 3736-43.

Nagano, A., R. Koga, et al. (1996). "Emerin deficiency at the nuclear membrane in patients with Emery-Dreifuss muscular dystrophy." Nat Genet **12**(3): 254-9.

Narita, M., S. Nunez, et al. (2003). "Rb-mediated heterochromatin formation and silencing of E2F target genes during cellular senescence." Cell **113**(6): 703-16.

Nath, J., J. D. Tucker, et al. (1995). "Y chromosome aneuploidy, micronuclei, kinetochores and aging in men." Chromosoma **103**(10): 725-31.

Navarro, C. L., A. De Sandre-Giovannoli, et al. (2004). "Lamin A and ZMPSTE24 (FACE-1) defects cause nuclear disorganization and identify restrictive dermopathy as a lethal neonatal laminopathy." Hum Mol Genet **13**(20): 2493-503.

Newport, J. W., K. L. Wilson, et al. (1990). "A lamin-independent pathway for nuclear envelope assembly." J Cell Biol **111**(1): 2247-59.

Nielsen, S. J., R. Schneider, et al. (2001). "Rb targets histone H3 methylation and HP1 to promoters." Nature **412**(6846): 561-5.

Nigg, E. A. (1989). "The nuclear envelope." Curr Opin Cell Biol **1**(3): 435-40.

Nikolakaki, E., G. Simos, et al. (1996). "A nuclear envelope-associated kinase phosphorylates arginine-serine motifs and modulates interactions between the lamin B receptor and other nuclear proteins." J Biol Chem **271**(14): 8365-72.

Nikolova, V., C. Leimena, et al. (2004). "Defects in nuclear structure and function

promote dilated cardiomyopathy in lamin A/C-deficient mice." J Clin Invest **113**(3): 357-69.

Nili, E., G. S. Cojocaru, et al. (2001). "Nuclear membrane protein LAP2beta mediates transcriptional repression alone and together with its binding partner GCL (germ-cell-less)." J Cell Sci **114**(Pt 18): 3297-307.

Nixon, R. A. (2003). "The calpains in aging and aging-related diseases." Ageing Res Rev **2**(4): 407-18.

Notredame, C., D. G. Higgins, et al. (2000). "T-Coffee: A novel method for fast and accurate multiple sequence alignment." J Mol Biol **302**(1): 205-17

Novelli, G. and M. R. D'Apice (2003). "The strange case of the "lumper" lamin A/C gene and human premature ageing." Trends Mol Med **9**(9): 370-5.

Oberhammer, F. A., K. Hochegger, et al. (1994). "Chromatin condensation during apoptosis is accompanied by degradation of lamin A+B, without enhanced activation of cdc2 kinase." J Cell Biol **126**(4): 827-37.

O'Keefe, R. T., A. Mayeda, et al. (1994). "Disruption of pre-mRNA splicing in vivo results in reorganization of splicing factors." J Cell Biol **124**(3): 249-60.

Okumura, K., K. Nakamachi, et al. (2000). "Identification of a novel retinoic acid-responsive element within the lamin A/C promoter." Biochem Biophys Res Commun **269**(1): 197-202.

Oliver, C. N. (1990). "Measurement of oxidized proteins in systems involving activated neutrophils or HL-60 cells." Methods Enzymol **186**: 575-9.

Ostlund, C., G. Bonne, et al. (2001). "Properties of lamin A mutants found in Emery-Dreifuss muscular dystrophy, cardiomyopathy and Dunnigan-type partial lipodystrophy." J Cell Sci **114**(24): 4435-45.

Ottaviano, Y. and L. Gerace (1985). "Phosphorylation of the nuclear lamins during interphase and mitosis." J Biol Chem **260**(1): 624-32.

Otto, H., M. Dreger, et al. (2001). "Identification of tyrosine-phosphorylated proteins associated with the nuclear envelope." Eur J Biochem **268**(2): 420-8.

Ozaki, T., M. Saijo, et al. (1994). "Complex formation between lamin A and the retinoblastoma gene product: identification of the domain on lamin A required for its interaction." Oncogene **9**(9): 2649-53.

Packer, L. and K. Fuehr (1977). "Low oxygen concentration extends the lifespan of cultured human diploid cells." Nature **267**(5610): 423-5.

Padan, R., S. Nainudel-Epszteyn, et al. (1990). "Isolation and characterization of the Drosophila nuclear envelope otefin cDNA." J Biol Chem **265**(14): 7808-13.

Padmakumar, V. C., S. Abraham, et al. (2004). "Enaptin, a giant actin-binding protein, is an element of the nuclear membrane and the actin cytoskeleton." Exp Cell Res

**295**(2): 330-9.

Pan, D., L. D. Estevez-Salmeron, et al. (2005). "The integral inner nuclear membrane protein MAN1 physically interacts with the R-Smad proteins to repress signalling by the transforming growth factor-{beta} superfamily of cytokines." J Biol Chem **280**(16): 15992-6001.

Pan, W., T. Sun, et al. (1998). "Defining the minimal portion of the retinoblastoma protein that serves as an efficient substrate for cdk4 kinase/cyclin D1 complex." Carcinogenesis **19**(5): 765-9.

Paulin-Levasseur, M., A. Scherbarth, et al. (1988). "Lack of lamins A and C in mammalian haemopoietic cell lines devoid of intermediate filament proteins." Eur J Cell Biol **47**(1): 121-31.

Pendas, A. M., Z. Zhou, et al. (2002). "Defective prelamin A processing and muscular and adipocyte alterations in Zmpste24 metalloproteinase-deficient mice." Nat Genet **31**(1): 94-9.

Peter, M., E. Heitlinger, et al. (1991). "Disassembly of in vitro formed lamin head-to-tail polymers by CDC2 kinase." EMBO J **10**(6): 1535-44.

Peter, M., J. Nakagawa, et al. (1990). "In vitro disassembly of the nuclear lamina and M phase-specific phosphorylation of lamins by cdc2 kinase." Cell **61**(4): 591-602.

Plasilova, M., C. Chattopadhyay, et al. (2004). "Homozygous missense mutation in the lamin A/C gene causes autosomal recessive Hutchinson-Gilford progeria syndrome." J Med Genet **41**(8): 609-14.

Polioudaki, H., N. Kourmouli, et al. (2001). "Histones H3/H4 form a tight complex with the inner nuclear membrane protein LBR and heterochromatin protein 1." EMBO Rep **2**(10): 920-5.

Powell, L. and B. Burke (1990). "Internuclear exchange of an inner nuclear membrane protein (p55) in heterokaryons: in vivo evidence for the interaction of p55 with the nuclear lamina." J Cell Biol **111**(6 Pt 1): 2225-34.

Prufert, K., C. Winkler, et al. (2004). "The lamina-associated polypeptide 2 (LAP2) genes of zebrafish and chicken: no LAP2alpha isoform is synthesised by non-mammalian vertebrates." Eur J Cell Biol **83**(8): 403-11.

Pugh, G. E., P. J. Coates, et al. (1997). "Distinct nuclear assembly pathways for lamins A and C lead to their increase during quiescence in Swiss 3T3 cells." J Cell Sci **110 ( Pt 19)**: 2483-93.

Quinlan, R., C. Hutchison, et al. (1995). "Intermediate filament proteins." Protein Profile **2**(8): 795-952.

Raharjo, W. H., P. Enarson, et al. (2001). "Nuclear envelope defects associated with LMNA mutations cause dilated cardiomyopathy and Emery-Dreifuss muscular dystrophy." J Cell Sci **114**(24): 4447-57.

Raju, G. P., N. Dimova, et al. (2003). "SANE, a novel LEM domain protein, regulates bone morphogenetic protein signalling through interaction with Smad1." J Biol Chem **278**(1): 428-37.

Rao, L., D. Perez, et al. (1996). "Lamin proteolysis facilitates nuclear events during apoptosis." J Cell Biol **135**(1): 1441-55.

Reichart, B., R. Klafke, et al. (2004). "Expression and localization of nuclear proteins in autosomal-dominant Emery-Dreifuss muscular dystrophy with LMNA R377H mutation." BMC Cell Biol **5**: 12.

Riemer, D. and K. Weber (1994). "The organization of the gene for Drosophila lamin C: limited homology with vertebrate lamin genes and lack of homology versus the Drosophila lamin Dmo gene." Eur J Cell Biol **63**(2): 299-306.

Reimer, R. A., S. Glen, et al. (1998). "Proglucagon and glucose transporter mRNA is altered by diet and disease susceptibility in 30-day-old biobreeding (BB) diabetes-prone and normal rats." Pediatr Res **44**(1): 68-73.

Rober, R. A., H. Sauter, et al. (1990). "Cells of the cellular immune and hemopoietic system of the mouse lack lamins A/C: distinction versus other somatic cells." J Cell Sci **95**(4): 587-98.

Rogalinska, M. (2002). "Alterations in cell nuclei during apoptosis." Cell Mol Biol Lett **7**(4): 995-1018.

Rolls, M. M., P. A. Stein, et al. (1999). "A visual screen of a GFP-fusion library identifies a new type of nuclear envelope membrane protein." J Cell Biol **146**(1): 29-44.

Roy, S., S. Khanna, et al. (2003). "Oxygen sensing by primary cardiac fibroblasts: a key role of p21(Waf1/Cip1/Sdi1)." Circ Res **92**(3): 264-71.

Rzepecki, R., S. S. Bogachev, et al. (1998). "In vivo association of lamins with nucleic acids in Drosophila melanogaster." J Cell Sci **111**(1): 121-9.

Samper, E., F. A. Goytisolo, et al. (2000). "Mammalian Ku86 protein prevents telomeric fusions independently of the length of TTAGGG repeats and the G-strand overhang." EMBO Rep **1**(3): 244-52.

Sarkar, P. K. and R. A. Shinton (2001). "Hutchinson-Guilford progeria syndrome." Postgrad Med J **77**(907): 312-7.

Sasseville, A. M. and Y. Langelier (1998). "In vitro interaction of the carboxy-terminal domain of lamin A with actin." FEBS Lett **425**(3): 485-9.

Sasseville, A. M. and Y. Raymond (1995). "Lamin A precursor is localized to intranuclear foci." J Cell Sci **108**(1): 273-85.

Satyanarayana, A., R. A. Greenberg, et al. (2004). "Mitogen stimulation cooperates with telomere shortening to activate DNA damage responses and senescence signalling." Mol Cell Biol **24**(12): 5459-74.

Scaffidi, P. and T. Misteli (2005). "Reversal of the cellular phenotype in the premature aging disease Hutchinson-Gilford progeria syndrome." Nat Med **11**(4): 440-5.

Schirmer, E. C. and L. Gerace (2004). "The stability of the nuclear lamina polymer changes with the composition of lamin subtypes according to their individual binding strengths." J Biol Chem **279**(41): 42811-7.

Schirmer, E. C., T. Guan, et al. (2001). "Involvement of the lamin rod domain in heterotypic lamin interactions important for nuclear organization." J Cell Biol **153**(3): 479-89.

Schmidt, M. and G. Krohne (1995). "In vivo assembly kinetics of fluorescently labelled Xenopus lamin A mutants." Eur J Cell Biol **68**(4): 345-54.

Schneider, E. L. and S. S. Shorr (1975). "Alteration in cellular RNAs during the in vitro lifespan of cultured human diploid fibroblasts." Cell **6**(2): 179-84.

Schroder, H. C., R. Messer, et al. (1987). "Superoxide radical-induced loss of nuclear restriction of immature mRNA: a possible cause for ageing." Mech Ageing Dev **41**(3): 251-66.

Sedelnikova, O. A., I. Horikawa, et al. (2004). "Senescing human cells and ageing mice accumulate DNA lesions with unrepairable double-strand breaks." Nat Cell Biol **6**(2): 168-70.

Seluanov, A., D. Mittelman, et al. (2004). "DNA end joining becomes less efficient and more error-prone during cellular senescence." Proc Natl Acad Sci U S A **101**(20): 7624-9.

Semenza, G. L. (2001). "Hypoxia-inducible factor 1: oxygen homeostasis and disease pathophysiology." Trends Mol Med **7**(8): 345-50.

Serrano, M. and M. A. Blasco (2001). "Putting the stress on senescence." Curr Opin Cell Biol **13**(6): 748-53.

Serrano, M., A. W. Lin, et al. (1997). "Oncogenic Ras provokes premature cell senescence associated with accumulation of p53 and p16INK4a." Cell **88**(5): 593-602.

Seshadri, T. and J. Campisi (1990). "Repression of c-fos transcription and an altered genetic program in senescent human fibroblasts." Science **247**(4939): 205-9.

Shackleton, S., D. J. Lloyd, et al. (2000). "LMNA, encoding lamin A/C, is mutated in partial lipodystrophy." Nat Genet **24**(2): 153-6.

Shelton, K. R., V. H. Guthrie, et al. (1980). "On the variation of the major nuclear envelope (lamina) polypeptides." Biochem Biophys Res Commun **93**(3): 867-72.

Shimi, T., T. Koujin, et al. (2004). "Dynamic interaction between BAF and emerin revealed by FRAP, FLIP, and FRET analyses in living HeLa cells." J Struct Biol **147**(1): 31-41.

Shirodkar, S., M. Ewen, et al. (1992). "The transcription factor E2F interacts with the retinoblastoma product and a p107-cyclin A complex in a cell cycle-regulated manner." Cell **68**(1): 157-66.

Shoeman, R. L. and P. Traub (1990). "The in vitro DNA-binding properties of purified nuclear lamin proteins and vimentin." J Biol Chem **265**(16): 9055-61.

Shultz, L. D., B. L. Lyons, et al. (2003). "Mutations at the mouse ichthyosis locus are within the lamin B receptor gene: a single gene model for human Pelger-Huet anomaly." Hum Mol Genet **12**(1): 61-9.

Shumaker, D. K., K. K. Lee, et al. (2001). "LAP2 binds to BAF.DNA complexes: requirement for the LEM domain and modulation by variable regions." Embo J **20**(7): 1754-64.

Simos, G. and S. D. Georgatos (1992). "The inner nuclear membrane protein p58 associates in vivo with a p58 kinase and the nuclear lamins." Embo J **11**(11): 4027-36.

Simos, G., H. Tekotte, et al. (1996). "Nuclear pore proteins are involved in the biogenesis of functional tRNA." EMBO J **15**(9): 2270-84.

Sinensky, M., K. Fantle, et al. (1994). "The processing pathway of prelamin A." J Cell Sci **107**(1): 61-7.

Sinensky, M., T. McLain, et al. (1994). "Expression of prelamin A but not mature lamin A confers sensitivity of DNA biosynthesis to lovastatin on F9 teratocarcinoma cells." J Cell Sci **107**(8): 2215-8.

Smith, E. D., B. A. Kudlow, et al. (2005). "A-type nuclear lamins, progerias and other degenerative disorders." Mech Ageing Dev **126**(4): 447-60.

Smith, J. R. and O. M. Pereira-Smith (1996). "Replicative senescence: implications for in vivo aging and tumour suppression." Science **273**(5271): 63-7.

Smogorzewska, A. and T. de Lange (2002). "Different telomere damage signalling pathways in human and mouse cells." EMBO J **21**(16): 4338-48.

Smythe, C., H. E. Jenkins, et al. (2000). "Incorporation of the nuclear pore basket protein nup153 into nuclear pore structures is dependent upon lamina assembly: evidence from cell-free extracts of Xenopus eggs." EMBO J **19**(15): 3918-31.

Spann, T. P., A. E. Goldman, et al. (2002). "Alteration of nuclear lamin organization inhibits RNA polymerase II-dependent transcription." J Cell Biol **156**(4): 603-8.

Spann, T. P., R. D. Moir, et al. (1997). "Disruption of nuclear lamin organization alters the distribution of replication factors and inhibits DNA synthesis." J Cell Biol **136**(6): 1201-12.

Spector, D. L., S. Landon, et al. (1993). "Organization of RNA polymerase II transcription and pre-mRNA splicing within the mammalian cell nucleus." Biochem Soc Trans **21**(4): 918-20.

Steen, R. L., M. Beullens, et al. (2003). "AKAP149 is a novel PP1 specifier required to maintain nuclear envelope integrity in G1 phase." J Cell Sci **116**(11): 2237-46.

Steen, R. L. and P. Collas (2001). "Mistargeting of B-type lamins at the end of mitosis: implications on cell survival and regulation of lamins A/C expression." J Cell Biol **153**(3): 621-6.

Steen, R. L., S. B. Martins, et al. (2000). "Recruitment of protein phosphatase 1 to the nuclear envelope by A-kinase anchoring protein AKAP149 is a prerequisite for nuclear lamina assembly." J Cell Biol **150**(6): 1251-62.

Stein, G. H., M. Beeson, et al. (1990). "Failure to phosphorylate the retinoblastoma gene product in senescent human fibroblasts." Science **249**(4969): 666-9.

Stein, G. H., L. F. Drullinger, et al. (1999). "Differential roles for cyclin-dependent kinase inhibitors p21 and p16 in the mechanisms of senescence and differentiation in human fibroblasts." Mol Cell Biol **19**(3): 2109-17.

Stewart, C. and B. Burke (1987). "Teratocarcinoma stem cells and early mouse embryos contain only a single major lamin polypeptide closely resembling lamin B." Cell **51**(3): 383-92.

Stick, R. (1992). "The gene structure of Xenopus nuclear lamin A: a model for the evolution of A-type from B-type lamins by exon shuffling." Chromosoma **101**(9): 566-74.

Stick, R. (1994). "The gene structure of B-type nuclear lamins of Xenopus laevis: implications for the evolution of the vertebrate lamin family." Chromosome Res **2**(5): 376-82.

Stick, R. and P. Hausen (1985). "Changes in the nuclear lamina composition during early development of Xenopus laevis." Cell **41**(1): 191-200.

Stierle, V., J. Couprie, et al. (2003). "The carboxyl-terminal region common to lamins A and C contains a DNA binding domain." Biochemistry **42**(17): 4819-28.

Strelkov, S. V., J. Schumacher, et al. (2004). "Crystal structure of the human lamin A coil 2B dimer: implications for the head-to-tail association of nuclear lamins." J Mol Biol **343**(4): 1067-80.

Strouboulis, J. and A. P. Wolffe (1996). "Functional compartmentalization of the nucleus." J Cell Sci **109**(8): 1991-2000.

Stuurman, N., S. Heins, et al. (1998). "Nuclear lamins: their structure, assembly, and interactions." J Struct Biol **122**(1-2): 42-66.

Sullivan, T., D. Escalante-Alcalde, et al. (1999). "Loss of A-type lamin expression compromises nuclear envelope integrity leading to muscular dystrophy." J Cell Biol **147**(5): 913-20.

Suzuki, Y., H. Yang, et al. (2004). "LAP2alpha and BAF collaborate to organize the

Maloney murine leukaemia virus preintegration complex." EMBO J **23**(23): 4670-8.

Szekely, L., E. Uzvolgyi, et al. (1991). "Subcellular localization of the retinoblastoma protein." Cell Growth Differ **2**(6): 287-95.

Taddei, A., D. Roche, et al. (1999). "Duplication and maintenance of heterochromatin domains." J Cell Biol **147**(6): 1153-66.

Takahashi, A., E. S. Alnemri, et al. (1996). "Cleavage of lamin A by Mch2 alpha but not CPP32: multiple interleukin 1 beta-converting enzyme-related proteases with distinct substrate recognition properties are active in apoptosis." Proc Natl Acad Sci USA **93**(16): 8395-400.

Tamrakar, S., E. Rubin, et al. (2000). "Role of pRB dephosphorylation in cell cycle regulation." Front Biosci **5**: D121-37.

Taniura, H., C. Glass, et al. (1995). "A chromatin binding site in the tail domain of nuclear lamins that interacts with core histones." J Cell Biol **131**(1): 33-44.

Templeton, D. J., S. H. Park, et al. (1991). "Non-functional mutants of the retinoblastoma protein are characterized by defects in phosphorylation, viral oncoprotein association, and nuclear tethering." Proc Natl Acad Sci USA **88**(8): 3033-7.

Thomas, J. A. and R. J. Mallis (2001). "Aging and oxidation of reactive protein sulfhydryls." Exp Gerontol **36**(9): 1519-26.

Thompson, L. J., M. Bollen, et al. (1997). "Identification of protein phosphatase 1 as a mitotic lamin phosphatase." J Biol Chem **272**(47): 29693-7.

Thompson, L. J. and A. P. Fields (1996). "beta II protein kinase C is required for the G2/M phase transition of cell cycle." J Biol Chem **271**(25): 15045-53.

Tiwari, B., B. Muralikrishna, et al. (1998). "Functional analysis of the 5' promoter region of the rat lamin A gene." DNA Cell Biol **17**(11): 957-65.

Tiwari, B. and V. K. Parnaik (1999). "Identification of altered DNA-protein interactions at the lamin A proximal promoter in quiescent hepatocytes." Cell Mol Biol (Noisy-le-grand) **45**(6): 865-75.

Todorova, A., B. Halliger-Keller, et al. (2003). "A synonymous codon change in the LMNA gene alters mRNA splicing and causes limb girdle muscular dystrophy type 1B." J Med Genet **40**(10): e115.

Toussaint, O., E. E. Medrano, et al. (2000). "Cellular and molecular mechanisms of stress-induced premature senescence (SIPS) of human diploid fibroblasts and melanocytes." Exp Gerontol **35**(8): 927-45.

Traub, P., A. Scherbarth, et al. (1988). "Differential sensitivity of vimentin and nuclear lamins from Ehrlich ascites tumor cells toward Ca2+ -activated neutral thiol proteinase." Eur J Cell Biol **46**(3): 478-90.

Traub, P., A. Scherbarth, et al. (1988). "Large scale co-isolation of vimentin and nuclear lamins from ehrlich ascites tumour cells cultured in vitro." Prep Biochem **18**(4): 381-404.

Tunnah, D., C.A. Sewry, et al. (2005) "The apparent absence of lamin B1 and emerin in many tissue nuclei is due to epitope masking." J Mol Histol **36**(5): 337-344

Van Hooser, A., D. W. Goodrich, et al. (1998). "Histone H3 phosphorylation is required for the initiation, but not maintenance, of mammalian chromosome condensation." J Cell Sci **111**(23): 3497-506.

Vandre, D. D. and V. L. Wills (1992). "Inhibition of mitosis by okadaic acid: possible involvement of a protein phosphatase 2A in the transition from metaphase to anaphase." J Cell Sci **101**(1): 79-91.

van Steensel, B., A. Smogorzewska, et al. (1998). "TRF2 protects human telomeres from end-to-end fusions." Cell **92**(3): 401-13.

Vaughan, A., M. Alvarez-Reyes, et al. (2001). "Both emerin and lamin C depend on lamin A for localization at the nuclear envelope." J Cell Sci **114**(Pt 14): 2577-90.

Vecerova, J., K. Koberna, et al. (2004). "Formation of nuclear splicing factor compartments is independent of lamins A/C." Mol Biol Cell **15**(11): 4904-10.

Veldman, T., K. T. Etheridge, et al. (2004). "Loss of hPot1 function leads to telomere instability and a cut-like phenotype." Curr Biol **14**(24): 2264-70.

Venables, R. S., S. McLean, et al. (2001). "Expression of individual lamins in basal cell carcinomas of the skin." Br J Cancer **84**(4): 512-9.

Vergnes, L., M. Peterfy, et al. (2004). "Lamin B1 is required for mouse development and nuclear integrity." Proc Natl Acad Sci U S A **101**(28): 10428-33.

Vigouroux, C., M. Auclair, et al. (2001). "Nuclear envelope disorganization in fibroblasts from lipodystrophic patients with heterozygous R482Q/W mutations in the lamin A/C gene." J Cell Sci **114**(Pt 24): 4459-68.

Vlcek, S., T. Dechat, et al. (2001). "Nuclear envelope and nuclear matrix: interactions and dynamics." Cell Mol Life Sci **58**(12-13): 1758-65.

Vlcek, S., H. Just, et al. (1999). "Functional diversity of LAP2alpha and LAP2beta in postmitotic chromosome association is caused by an alpha-specific nuclear targeting domain." EMBO J **18**(22): 6370-84.

von Zglinicki, T., A. Burkle, et al. (2001). "Stress, DNA damage and ageing -- an integrative approach." Exp Gerontol **36**(7): 1049-62.

von Zglinicki, T., G. Saretzki, et al. (1995). "Mild hyperoxia shortens telomeres and inhibits proliferation of fibroblasts: a model for senescence?" Exp Cell Res **220**(1): 186-93.

von Zglinicki, T., G. Saretzki, et al. (2005). "Human cell senescence as a DNA damage

response." Mech Ageing Dev **126**(1): 111-7.

Vorburger, K., G. T. Kitten, et al. (1989). "Modification of nuclear lamin proteins by a mevalonic acid derivative occurs in reticulocyte lysates and requires the cysteine residue of the C-terminal CXXM motif." EMBO J **8**(13): 4007-13.

Wagner, M., G. Brosch, et al. (2001). "Histone deacetylases in replicative senescence: evidence for a senescence-specific form of HDAC-2." FEBS Lett **499**(1-2): 101-6.

Wang, S. M., C. Nishigori, et al. (1991). "Reduced DNA repair in progeria cells and effects of gamma-ray irradiation on UV-induced unscheduled DNA synthesis in normal and progeria cells." Mutat Res **256**(1): 59-66.

Wang, X., S. Xu, et al. (2002). "Barrier to autointegration factor interacts with the cone-rod homeobox and represses its transactivation function." J Biol Chem **277**(45): 43288-300.

Ward, G. E. and M. W. Kirschner (1990). "Identification of cell cycle-regulated phosphorylation sites on nuclear lamin C." Cell **61**(4): 561-77.

Waterham, H. R., J. Koster, et al. (2003). "Autosomal recessive HEM/Greenberg skeletal dysplasia is caused by 3 beta-hydroxysterol delta 14-reductase deficiency due to mutations in the lamin B receptor gene." Am J Hum Genet **72**(4): 1013-7.

Wilkinson, F. L., J. M. Holaska, et al. (2003). "Emerin interacts in vitro with the splicing-associated factor, YT521-B." Eur J Biochem **270**(11): 2459-66.

Wilson, K. L. (2000). "The nuclear envelope, muscular dystrophy and gene expression." Trends Cell Biol **10**(4): 125-9.

Wolfe, J. (1980). "A possible skeletal substructure of the macronucleus of Tetrahymena." J Cell Biol **84**(1): 160-71.

Wolffe, A. P. (1991). "Implications of DNA replication for eukaryotic gene expression." J Cell Sci **99 ( Pt 2)**: 201-6.

Wright, W. E. and J. W. Shay (2001). "Cellular senescence as a tumour-protection mechanism: the essential role of counting." Curr Opin Genet Dev **11**(1): 98-103.

Wydner, K. L., J. A. McNeil, et al. (1996). "Chromosomal assignment of human nuclear envelope protein genes LMNA, LMNB1, and LBR by fluorescence in situ hybridization." Genomics **32**(3): 474-8.

Xu, L., Y. Kang, et al. (2002). "Smad2 nucleocytoplasmic shuttling by nucleoporins CAN/Nup214 and Nup153 feeds TGFβ signalling complexes in the cytoplasm and nucleus." Mol Cell **10**(2): 271-82.

Yalon, M., S. Gal, et al. (2004). "Sister chromatid separation at human telomeric regions." J Cell Sci **117**(10): 1961-70.

Yan, T., S. Li, et al. (1999). "Altered levels of primary antioxidant enzymes in progeria skin fibroblasts." Biochem Biophys Res Commun **257**(1): 163-7.

Yang, L., T. Guan, et al. (1997). "Integral membrane proteins of the nuclear envelope are dispersed throughout the endoplasmic reticulum during mitosis." J Cell Biol **137**(6): 1199-210.

Yang, L., T. Guan, et al. (1997). "Lamin-binding fragment of LAP2 inhibits increase in nuclear volume during the cell cycle and progression into S phase." J Cell Biol **139**(5): 1077-87.

Ye, Q. and H. J. Worman (1995). "Protein-protein interactions between human nuclear lamins expressed in yeast." Exp Cell Res **219**(1): 292-8.

Yeakley, J. M., H. Tronchere, et al. (1999). "Phosphorylation regulates in vivo interaction and molecular targeting of serine/arginine-rich pre-mRNA splicing factors." J Cell Biol **145**(3): 447-55.

Yuan, J., G. Simos, et al. (1991). "Binding of lamin A to polynucleosomes." J Biol Chem **266**(14): 9211-5.

Zarkowska, T. and S. Mittnacht (1997). "Differential phosphorylation of the retinoblastoma protein by G1/S cyclin-dependent kinases." J Biol Chem **272**(19): 12738-46.

Zastrow, M. S., S. Vlcek, et al. (2004). "Proteins that bind A-type lamins: integrating isolated clues." J Cell Sci **117**(7): 979-87.

Zeng, C., E. Kim, et al. (1997). "Dynamic relocation of transcription and splicing factors dependent upon transcriptional activity." EMBO J **16**(6): 1401-12.

Zhang, Q., J. N. Skepper, et al. (2001). "Nesprins: a novel family of spectrin-repeat-containing proteins that localize to the nuclear membrane in multiple tissues." J Cell Sci **114**(24): 4485-98.

Zhao, K., A. Harel, et al. (1996). "Binding of matrix attachment regions to nuclear lamin is mediated by the rod domain and depends on the lamin polymerisation state." FEBS Lett **380**(1-2): 161-4.

Zhen, Y. Y., T. Libotte, et al. (2002). "NUANCE, a giant protein connecting the nucleus and actin cytoskeleton." J Cell Sci **115**(15): 3207-22.

Zheng, R., R. Ghirlando, et al. (2000). "Barrier-to-autointegration factor (BAF) bridges DNA in a discrete, higher-order nucleoprotein complex." Proc Natl Acad Sci U SA **97**(16): 8997-9002.

response." Mech Ageing Dev **126**(1): 111-7.

Vorburger, K., G. T. Kitten, et al. (1989). "Modification of nuclear lamin proteins by a mevalonic acid derivative occurs in reticulocyte lysates and requires the cysteine residue of the C-terminal CXXM motif." EMBO J **8**(13): 4007-13.

Wagner, M., G. Brosch, et al. (2001). "Histone deacetylases in replicative senescence: evidence for a senescence-specific form of HDAC-2." FEBS Lett **499**(1-2): 101-6.

Wang, S. M., C. Nishigori, et al. (1991). "Reduced DNA repair in progeria cells and effects of gamma-ray irradiation on UV-induced unscheduled DNA synthesis in normal and progeria cells." Mutat Res **256**(1): 59-66.

Wang, X., S. Xu, et al. (2002). "Barrier to autointegration factor interacts with the cone-rod homeobox and represses its transactivation function." J Biol Chem **277**(45): 43288-300.

Ward, G. E. and M. W. Kirschner (1990). "Identification of cell cycle-regulated phosphorylation sites on nuclear lamin C." Cell **61**(4): 561-77.

Waterham, H. R., J. Koster, et al. (2003). "Autosomal recessive HEM/Greenberg skeletal dysplasia is caused by 3 beta-hydroxysterol delta 14-reductase deficiency due to mutations in the lamin B receptor gene." Am J Hum Genet **72**(4): 1013-7.

Wilkinson, F. L., J. M. Holaska, et al. (2003). "Emerin interacts in vitro with the splicing-associated factor, YT521-B." Eur J Biochem **270**(11): 2459-66.

Wilson, K. L. (2000). "The nuclear envelope, muscular dystrophy and gene expression." Trends Cell Biol **10**(4): 125-9.

Wolfe, J. (1980). "A possible skeletal substructure of the macronucleus of Tetrahymena." J Cell Biol **84**(1): 160-71.

Wolffe, A. P. (1991). "Implications of DNA replication for eukaryotic gene expression." J Cell Sci **99 ( Pt 2)**: 201-6.

Wright, W. E. and J. W. Shay (2001). "Cellular senescence as a tumour-protection mechanism: the essential role of counting." Curr Opin Genet Dev **11**(1): 98-103.

Wydner, K. L., J. A. McNeil, et al. (1996). "Chromosomal assignment of human nuclear envelope protein genes LMNA, LMNB1, and LBR by fluorescence in situ hybridization." Genomics **32**(3): 474-8.

Xu, L., Y. Kang, et al. (2002). "Smad2 nucleocytoplasmic shuttling by nucleoporins CAN/Nup214 and Nup153 feeds TGFβ signalling complexes in the cytoplasm and nucleus." Mol Cell **10**(2): 271-82.

Yalon, M., S. Gal, et al. (2004). "Sister chromatid separation at human telomeric regions." J Cell Sci **117**(10): 1961-70.

Yan, T., S. Li, et al. (1999). "Altered levels of primary antioxidant enzymes in progeria skin fibroblasts." Biochem Biophys Res Commun **257**(1): 163-7.

Yang, L., T. Guan, et al. (1997). "Integral membrane proteins of the nuclear envelope are dispersed throughout the endoplasmic reticulum during mitosis." J Cell Biol **137**(6): 1199-210.

Yang, L., T. Guan, et al. (1997). "Lamin-binding fragment of LAP2 inhibits increase in nuclear volume during the cell cycle and progression into S phase." J Cell Biol **139**(5): 1077-87.

Ye, Q. and H. J. Worman (1995). "Protein-protein interactions between human nuclear lamins expressed in yeast." Exp Cell Res **219**(1): 292-8.

Yeakley, J. M., H. Tronchere, et al. (1999). "Phosphorylation regulates in vivo interaction and molecular targeting of serine/arginine-rich pre-mRNA splicing factors." J Cell Biol **145**(3): 447-55.

Yuan, J., G. Simos, et al. (1991). "Binding of lamin A to polynucleosomes." J Biol Chem **266**(14): 9211-5.

Zarkowska, T. and S. Mittnacht (1997). "Differential phosphorylation of the retinoblastoma protein by G1/S cyclin-dependent kinases." J Biol Chem **272**(19): 12738-46.

Zastrow, M. S., S. Vlcek, et al. (2004). "Proteins that bind A-type lamins: integrating isolated clues." J Cell Sci **117**(7): 979-87.

Zeng, C., E. Kim, et al. (1997). "Dynamic relocation of transcription and splicing factors dependent upon transcriptional activity." EMBO J **16**(6): 1401-12.

Zhang, Q., J. N. Skepper, et al. (2001). "Nesprins: a novel family of spectrin-repeat-containing proteins that localize to the nuclear membrane in multiple tissues." J Cell Sci **114**(24): 4485-98.

Zhao, K., A. Harel, et al. (1996). "Binding of matrix attachment regions to nuclear lamin is mediated by the rod domain and depends on the lamin polymerisation state." FEBS Lett **380**(1-2): 161-4.

Zhen, Y. Y., T. Libotte, et al. (2002). "NUANCE, a giant protein connecting the nucleus and actin cytoskeleton." J Cell Sci **115**(15): 3207-22.

Zheng, R., R. Ghirlando, et al. (2000). "Barrier-to-autointegration factor (BAF) bridges DNA in a discrete, higher-order nucleoprotein complex." Proc Natl Acad Sci U SA **97**(16): 8997-9002.